The Effects of Physical Inactivity on Skeletal Muscle Metabolic Function

---

A dissertation submitted for the degree of Ph.D by

John Noone, B.Sc.

Under the supervision of
Dr. Donal J. O'Gorman

Faculty of Science and Health, School of Health and Human Performance,
Dublin City University, Dublin 9, Ireland

Submitted to Dublin City University
September, 2021

Declaration

I hereby certify that this material, which I now submit for assessment on the programme of study leading to the award of Doctor of Philosophy is entirely my own work, and that I have exercised reasonable care to ensure that the work is original, and does not to the best of my knowledge breach any law of copyright, and has not been taken from the work of others save and to the extent that such work has been cited and acknowledged within the text of my work.

Signed: _____

(Candidate) ID Number: 16213522

Date: 07/09/2021

Publications

Publications (in chronological order):

O'Donoghue, G., Kennedy, A., Andersen, G., Carr, B., Cleary, S., Durkan, E., Davis, H., Faerch, K., Fitzpatrick, P., Kenny, H., McCaffrey, N., Monedero, J., Murphy, E., **Noone, J.**, Suvitaival, T., Thybo, T., Wheeler, M., Vistisen, D., Nolan, J. J., O'Gorman, D.J. (2019). **Phenotypic Responses to a Lifestyle Intervention Do Not Account for Inter-Individual Variability in Glucose Tolerance for Individuals at High Risk of Type 2 Diabetes**. *Frontiers in Physiology, Exercise Physiology*. **10** (317)

Damiot, A., Demangel, R., **Noone, J.**, Chery, I., Zahariev, A., Normand, S., Brioche, T., Crampes, F., de Glisezinski, I., Lefai, E., Bareille, M.P., Chopard, Drai, J., Collin-Chavagnac, D., Heer, M., Gauquelin-Koch, G., Prost, M., Simon, P., Py, G., Blanc, S., Simon, C., Bergouignan, A., O'Gorman, D.J. (2019). **A Nutrient Cocktail Prevents Lipid Metabolism Alterations Induced by 20 Days of Daily Steps Reduction and Fructose Overfeeding: Result from a Randomized Study**. *Journal of Applied Physiology*. **126** (1)

Publications in Preparation:

Noone, J., O'Gorman, D.J., Kenny, H. **Mitochondrial Dynamics and the Role and Regulation of Optic Atrophy 1 (OPA1) in Skeletal Muscle and Cardiac Pathophysiology**. Trends in Endocrinology and Metabolism (TEM). Expected submission September 2021

Oral Presentations (in chronological order):

Noone, J., O'Gorman, D.J. **A Cocktail to Prevent the Metabolic Effects of Physical Inactivity.** Biological Research Society, Dublin City University, Dublin, Ireland, January 26th 2018

Noone, J., O'Gorman, D.J. **Managing the Skeletal Muscle Alterations Due to Space Flight.** School of Health and Human Performance Research Showcase, Dublin City University, Dublin, Ireland, February 12th 2018

Noone, J., O'Gorman, D.J. **A Nutrient Cocktail to Counteract Skeletal Muscle Mitochondrial Respiratory Adaptations Induced by Prolonged Bed Rest.** Irish Postgraduate Research Conference 2018. Dublin City University, Dublin, Ireland, November 9th 2018

Noone, J., O'Gorman, D.J. **The Effect of Prolonged Bed Rest on Human Skeletal Muscle Metabolism**. Exercise, Bioenergetics and Aging Program, AdventHealth Translational Research Institute for Metabolism and Diabetes, Orlando, Florida, USA, December 4th 2020

Poster Presentations (in chronological order):

Noone, J., Damiot, A., Demangel, R., Chery, I., Zahariev, A., Normand, S., Brioche, T., Crampes, F., de Glisezinski, I., Lefai, E., Chopard, A., Drai, J., Colin-Chavagnac, D., Heer, M., Gauquelin-Koch, G., Prost, M., Simon, P., Pr, G., Bergouignan, A., Simon, C., Blanc, S., O'Gorman, D.J. **A Cocktail of Dietary Anti-Oxidants and Omega-3 Fatty Acids to Prevent Metabolic Deterioration Within the Skeletal Muscle Induced by Inactivity**. Biological Research Society, Dublin City University, Dublin, Ireland, January 26th 2018

Noone, J., Damiot, A., Crampes, F., Bergouignan, A., Blanc, S., O'Gorman, D.J. **A Nutrient Cocktail to Counteract Skeletal Muscle Mitochondrial Respiratory Adaptations Induced by Prolonged Bed Rest.** Cell Symposia, Aging and Metabolism. Sitges, Spain, September 23-25th 2018

Noone, J., Damiot, A., Crampes, F., Bergouignan, A., Blanc, S., O'Gorman, D.J. **A Nutrient Cocktail to Counteract Skeletal Muscle Mitochondrial Respiratory Adaptations Induced by Prolonged Bed Rest.** Biological Research Society, Dublin City University, Dublin, Ireland, January 25th 2019

Noone, J., O'Gorman, D.J. ***In-vitro*** **Electrical Pulse Stimulation to Mimic an Acute Exercise Bout in C_2C_{12} Myotubes Regulates Mitochondrial Fission and Fusion Pathways.** Cell Symposia, Exercise Metabolism, Sitges, Spain, May 5-7th 2019

***Noone, J.**, Damiot, A., Crampes, F., Bergouignan, A., Blanc, S., Kenny, H., O'Gorman, D.J. **The Role of Resistance Vibration Exercise (RVE) on Pathways of Mitochondrial Fusion-Fission Following 21 Days of Bed Rest.** Royal Academy of Medicine, Ireland student research medal and awards. Royal College of Physicians Ireland. October 14th 2019

*Shortlisted for student research medal award

***Noone, J.**, Damiot, A., Crampes, F., Bergouignan, A., Blanc, S., Kenny, H., O'Gorman, D.J. **The Role of Resistance Vibration Exercise (RVE) on Pathways of Mitochondrial Fusion-Fission Following 21 Days of Bed Rest.** Copenhagen Bioscience Conference - Metabolism in Action, Novo Nordisk, Favrholm Campus, Hillerød, Denmark. October 27-31st 2019

*Novo Nordisk Fonden bursary award recipient

Table of Contents

List of Figures

*All unattributed figures are prepared by the candidate and are his own work. Subsequently, no source reference is indicated. In cases where candidate has adapted the work of another, the initial source is referenced.

List of Tables

Acknowledgements

I wish to recognise and thank the following people for their support and contribution to this thesis:

My supervisor, Dr. Donal O'Gorman, for not only providing me with this opportunity but for his guidance, mentorship and the high standards he sets. I have been very lucky to gain so many invaluable experiences under his tutelage. From hibernating bears in Sweden to bed rest studies within the European Space Agency. I have learned an awful lot, both as a scientist and a person, from his supervision. I am extremely grateful.

Dr. Helena Kenny who provided me with her expertise, experience and level head. She was always there to answer any question I had even from all the way across the pond.

Prof. Stéphane Blanc, Dr. Audrey Bergouignan, Dr. François Crampes, Prof. Cédric Moro, Dr. Claire Laurens and Dr. Marie-Pierre Bareille for all of their help throughout the bed rest study in Toulouse. I am lucky in the friendships I've gained from this work in Anthony and Will. I would like to extend my thanks to them and all of the team for their facilitation and humour throughout these demanding experimental days and beyond.

All of the participants of the bed rest studies. Without their efforts and willingness, none of this would have been possible.

DCU and the project funders, Enterprise Ireland and the European Space Agency PRODEX programme.

Those within the Energy Metabolism Research Group, the PRODEX study group and all of the staff and students of the National Institute for Cellular Biotechnology for their help and facilitation throughout my PhD. Particular thanks go to Joanne, Finbarr and Laura for their assistance in the lab, and of course to Mairead for answering any admin problem I had, be that big or small.

All of the members of the Toxicology lab and first floor open office, specifically Nicola and Ali, I would have been lost without your support and camaraderie.

Head of School, Dr. Sarahjane Belton, and all the staff and students within the School of Health and Human Performance. Particular thanks go to Aishling and Javier their great support, listening to all of my ramblings and helping me in whatever way they could.

Those within the Faculty of Science and Health beyond my own school but particularly to Keith and Rob for all of the good times, from animal face-off and Scone Thursday's to the laboratory techniques you taught me along the way.

My mother and father, Sheila and Greg, for their unwavering support and shared values in education and life. You have encouraged my ambition to pursue these aspirations of mine and taught me the value and contentment in hard work.

My sister, Emma, who has always been there for me through thick and thin. She is an inspiration in her own pursuit of fulfilment which is endorsed by her vocation as a veterinarian.

My friends who have reassured and spurred me on along the way but notably to Des who I am indebted to for his patience and understanding throughout this journey.

All of these people and experiences combined have shaped me to become the researcher and person I am today, but none more so than my family. I would like to dedicate this thesis them.

Abbreviations

△△**Ct** – Delta Delta Cycle Threshold
△**Ct** – Delta Cycle Threshold
△**P** – Proton Gradient
ACAT2 - Acetyl-CoA acetyltransferase 2
ACC – Acetyl-CoA Carboxylase
AceCS2 - Acetyl-CoA synthase 2
ACTC1 - Actin Alpha Cardiac Muscle 1
ADOA – Autosomal Dominant Optic Atrophy
ADP – Adenosine Diphosphate
AICAR - 5-Aminoimidazole-4-carboxamide ribonucleotide
Ama – Antimycin A
AMP- Adenosine monophosphate
AMPK – AMP-activated protein kinase
ANOVA – Analysis of Variance
ANT – Adenine Nucleotide Translocase
AP – Alkaline Phosphate
ARED – Advanced Resistance Exercise Devices
AS160 - Akt substrate of 160 kDa
ATGL – Adipose Triglyceride Lipase
Atgs – Autophagy related genes
ATP – Adenosine Triphosphate
BAP31 – B-cell receptor-associated protein 31
BBR – Berlin Bed Rest Study
BCAA – Branch Chain Amino Acids
BCL2-L13 – B-cell lymphoma 2-Like protein 13
BDC – Baseline Data Collection
BM – Body Mass
BMD - Bone Mineral Density
BMI – Body Mass Index
BNIP3 - BCL-2/Adenovirus E1B Interacting Protein 3
BP – Blood Pressure
BR – Bed Rest
BSA – Bovine Serum Albumin
Ca^{2+} - Calcium
CaMK - Calmodulin-Dependent Protein Kinase
cAMP – cyclic Adenosine Monophosphate
CD36 – Cluster of Differentiation 36
CD38 – Cluster of Differentiation 38
CDK – Cyclin-Dependent Kinase
CDK1 - Cyclin-Dependent-Kinase 1
cDNA – Complementary Deoxyribonucleic Acid
CHO – Carbohydrate
CI – Complex one
CII – Complex two
CIV – Complex four

Ckm – Creatine kinase muscle

CMT2A – Charcot-Marie-Tooth Type 2A

CNRS – The French National Centre for Scientific Research

CoA – Coenzyme A

CONT – Control

COXIV – Cytochrome C Oxidase Subunit 4

CPT – Carnitine Palmitoyltransferase

CSA – Cross Sectional Area

Ct – Cycle Threshold

DAG – Diacylglycerol

DEPC – Diethyl Pyrocarbonate

DEXA – Dual Energy X-Ray Absorptiometry

DHA - Docosahexaenoic Acid

DLR – Institute for Aerospace Medicine

DMSO – Dimethylsulphoxide

DNA – Deoxyribonucleic Acid

DNM2 – Dynamin 2

Drp1 – Dynamin Related Protein 1

DTT – Dithiothreitol

EAA – Essential Amino Acids

ECL – Engaged Chemiluminescence

EGTA - Ethylene Glycol Tetraacetic Acid

EMG – Electromyography

EPA - Eicosapentaenoic Acid

ER – Endoplasmic Reticulum

ERMCS– Endoplasmic Reticulum Mitochondrial Contact Sites

ERR – Estrogen-Related Receptor

ESA – European Space Agency

ETC – Electron Transport Chain

ETS - Electron Transport System

FA – Fatty Acids

FAD – Flavin Adenine Dinucleotide

$FADH_2$ - Reduced form of Flavin Adenine Dinucleotide

FAO – Fatty Acid Oxidation

FATPs – Fatty Acids Transport Proteins

FCCP - Carbonyl cyanide p-trifluoro-methoxyphenyl hydrazine

FFA – Free Fatty Acids

FFM – Fat-Free Mass

FGF21 – Fibroblast Growth Factor 21

Fis1 – Mitochondrial fission protein 1

FOXO1 - Forkhead box protein O1

Fzo – Fuzzy Onion Protein

G6P – Glucose-6-Phosphate

G6PD – Glucose-6-Phosphate Dehydrogenase

GABP – GA-binding Protein

GAPdh – Glyceraldehyde 3-phosphate dehydrogenase

GAPPA – Global Action Plan on Physical Activity

GDH - Glutamate Dehydrogenase

GLUT1/4 – Glucose Transporter Type 1/4

GTP – Guanosine-5'-Triphosphate

GTPase – Guanosine Triphosphatase
H - Hydrogen
H_2O - Water
H_2O_2 - Hydrogen peroxide
HCL – Hydrochloric acid
HDAC – Histone Deacetylase
HDL – High Density Lipoprotein
HDT – Head Down Tilt
HIF-1α – Hypoxia-inducible factor 1-alpha
HIIT – High Intensity Interval Training
HR – Heart Rate
HR2 – Heptad-Repeated Domain 2
HRR – High-Resolution Respirometry
HSL – Hormone Sensitive Lipase
HSM – Human Skeletal Muscle
IGF – Insulin-Like Growth Factor
IL-6 - Interleukin 6
IMF – Intermyofibrillar
IMM – Inner Mitochondrial Membrane
IMMT – Inner Membrane Mitochondrial Protein
IMS – Industrial Methylated Spirits
IMS – Intermembrane Space
InsP3 – Inositol Triphosphate
INT – Intervention
iRED – interim Resistance Exercise Device
IRS – Insulin Receptor Substrate
kDa – kilodalton
Kg – Kilogram
LC3b – Light Chain 3b
LD – Lipid Droplet
LDL – Low Density Lipoprotein
L-OPA1 – long isoform Optic Atrophy 1
LPL – Lipoprotein Lipase
M -meter
MARF – Mitochondrial Assembly Regulatory Factor
MCD – Malonyl-CoA Decarboxylase
MCU – Mitochondrial Calcium Uniporter
MET – Metabolic Equivalents
Mff-1 – Mitochondrial fission factor-1
Mfn1 – Mitofusin 1
Mfn2- Mitofusin 2
MHC 1 – Myosin Heavy Chain 1
MHC 2a – Myosin Heavy Chain 2a
MHC 2b – Myosin Heavy Chain 2b
MHC 2x – Myosin Heavy Chain 2x
MIB – Mitochondrial Intermembrane Space Bridging Complex
MICOS – Mitochondrial Contact Site and Cristae Organizing System
MiD49 - Mitochondrial dynamics protein 49
MiD51 - Mitochondrial dynamics protein 51
MiNA – Mitochondrial Network Analysis

MIQE - Minimum Information for Publication of Quantitative Real-Time PCR Experiments
MiR05 - Mitochondrial Respiration Medium
MitoNEET - CDGSH iron-sulfur domain-containing protein 1
MK167 – Antigen KI-67
mmHg – millimetre of mercury
Mna – Malonic Acid
MPB - Muscle Protein Breakdown
MPC – Mitochondrial Pyruvate Carrier
MPP – Mitochondrial Processing Peptidase
MPS – Muscle Protein Synthesis
mRNA – messenger Ribonucleic Acid
MT_ATP6 – ATP Synthase Membrane Subunit 6
MT_CO4 – Cytochrome C Oxidase Subunit 4
MTFP1 – Mitochondrial Fission Process Protein 1
mTORC1 - mammalian Target of Rapamycin Complex 1
Murf-1 – Muscle RING-finger protein-1
MVPA – Moderate to Vigorous Intensity Physical Activity
MYL2 – Myosin Light Chain 2
MYOD1 – Myoblast Determination Protein 1
MYOG – Myogenin
Na_3VO_4 – Sodium Orthovanadate
NAD – Nicotinamide Adenine Dinucleotide
NAM- Nicotinamide
NAMPT – Nicotinamide Phosphoribosyltransferase
NCHS – National Center for Health Statistics
NDUFA4 – NADH dehydrogenase subunit IV
NDUFS1 – NADH-ubiquinone oxidoreductase 75 kDa subunit, mitochondrial
NEFA – Non-Esterified Fatty Acid
NF- kβ - Nuclear Factor kappa-light-chain-enhancer of activated B cells
NHANES – National Health and Nutrition Examination Survey
NPRQ - Non-Protein Respiratory Quotient
NR4A3 – Nuclear Receptor Subfamily 4 Group A Member 3
NRF – Nuclear Respiratory Factor
O_2 – Oxygen
OGTT - Oral Glucose Tolerance Test
OMA1 - Metalloendopeptidase
OMM – Outer Mitochondrial Membrane
OPA1 – Optic Atrophy 1
OXPHOS – Oxidative Phosphorylation
p62 – Sequestosome-1
p70-S6 K - Ribosomal protein S6 kinase
PA – Phosphatidic Acid
PAL – Physical Activity Level
PalM – Palmitate and Malate
PARK2 – Parkin
PARL – Presenilin-Associated Rhomboid-Like Protein
PAX7 – Paired Box Protein 7
PBS – Phosphate Buffered Saline
PDH – Pyruvate Dehydrogenase
PDK – Pyruvate Dehydrogenase Kinase

pDrp1^{s600} – phosphorylated Dynamin Related Protein 1 serine 600
pDrp1^{s616} - phosphorylated Dynamin Related Protein 1 serine 616
pDrp1^{s637} – phosphorylated Dynamin Related Protein 1 serine 637
PGC1 - Pparg coactivator 1
Pi – Inorganic Phosphate
PI3K - Phosphoinositide 3-kinases
PICP – Osteocalcinin and Type 1 Procollagen Propeptide
PINK1 – PTEN-Induced Kinase 1
PKA – Protein Kinase A
PKB/ Akt – Protein Kinase B
PKC – Protein Kinase C
PM – Pyruvate and Malate
PMSF – Phenylmethylsulfonyl fluoride
PMT – Photomultiplier Tube
POLG – Polymerase Gamma Accessory Subunit
PPAR – Peroxisome Proliferator-Activated Receptor
Ppp3 – Calcineurin
PTH – Parathyroid Hormone
PVDF – Polyvinylidene Difluoride
Q - Cardiac Output
R+ - Recovery Period
RAC1 – Ras-related C3 Botulinum Toxin Substrate 1
RER – Respiratory Exchange Ratio
RMR – Resting Metabolic Rate
RNAi - RNA interference
RNS – Reactive Nitrogen Species
ROS – Reactive Oxygen Species
ROX – Residual Oxygen Consumption
RPM – Revolutions Per Minute
RQ – Respiratory Quotient
RSV – Resveratrol
RT - Resistance Training
RT-qPCR – Real Time-quantitative Polymerase Chain Reaction
RVE – Resistance Vibration Exercise
SAM – Sorting and Assembly Machinery Subunit
SD – Standard Deviation
SDS - Sodium Dodecyl Sulfatepolyacrilamide
SDS-PAGE – Sodium Dodecyl Sulphate–Polyacrylamide Gel Electrophoresis
SE – Standard Error
SiF – Stress-induced Fission
siRNA – small interfering RNA
SIRT – Sirtuin
s-OPA1 – short isoform Optic Atrophy 1
SSM – Subsarcolemmal
STX – Syntaxin
SUIT – Substrate-Uncoupler Inhibitor Titration
SV – Stroke Volume
TAG – Triglyceride
TBC1D15/17 - TBC1 Domain Family Member 15/17
TBS – Tris Buffered Saline

TCA – Tricarboxylic Acid
TF - Transcription Factor
Tfam – Mitochondrial transcription factor A
Thio – Thioglycolate
TIM – Translocase of the Inner Membrane
TMPD - N,N,N',N'-Tetramethyl-p-phenylenediamine dihydrochloride
TNF-α – Tumour Necrosis Factor Alpha
TNN1 – Troponin 1
TOM – Translocase of the Outer Membrane
tRNA – transfer Ribonucleic Acid
TSB - tryptone soya broth
UL – Upper Limit
UQ – Ubiquinnone
UQH2 – Ubiquinol
VDAC1 –Voltage-Dependent Anion-Selective Channel 1
VE – Ventilatory Efficiency
VL – Vastus Lateralis
VLCAD - Very Long-Chain Acyl-CoA Dehydrogenase
VLDL – Very Low-Density Lipoprotein
VO_2 max – Maximal aerobic capacity
VO_2 peak – Peak oxygen uptake capacity
W - Watts
WBV – Whole Body Vibration
WHA - World Health Assembly
WHO – World Health Organization
XXS-2A-BR2 – Polyphenol Compound
YME1L - i-AAA protease ATP-dependent zinc metalloprotease
α-KG – α-Ketoglutarate

Abstract

The Effects of Prolonged Inactivity on Skeletal Muscle Metabolic Function

John Noone

Bed rest leads to multiple adverse physiological consequences, comparable to the effects of physical inactivity. The role of cellular metabolism in the regulation of these physiological changes during bed rest has not been studied in detail.

The aim of this study was to test if prolonged bed rest decreases mitochondrial function, muscle mass and impacts upon mitochondrial dynamics in healthy young men. We also evaluated the impact a micronutrient cocktail supplement had in mitigating these changes.

60 days bed rest resulted a number of anthropometric changes including reduction in lean muscle mass (p<0.05) and an increase in fat mass (p<0.05). These changes were accompanied by an increase in RQ indicative of a switch from fat to carbohydrate oxidation at rest (p<0.05). Mitochondrial respiration, expressed per mg of wet muscle weight, was lower during ETS (CI), ETS (CII) and CII respiration following 60 days of bed rest (p<0.05), a change which was not evident when normalised to mitochondrial content. We concluded that the adaptations in the regulators of mitochondrial density/amount may explain these changes. In particular, we observed a significant decrease in mitochondrial fusion marker, OPA1 and fission marker, Drp1 (p<0.05). Our intervention mitigated these changes, increasing OPA1:Drp1 ratio (p<0.05) suggesting our intervention increased mitochondrial elongation. A comparison between our 60-day study and a previously conducted 21-day bed rest study emphasised the important role OPA1 may be having throughout bed rest epitomised by a shift in mitochondrial dynamics over time from a fragmented phenotype (21-day BR) to a rebalancing of fusion-fission (60-day BR).

Further *in-vitro* analysis uncovered the novel role SIRT4 has on these processes with knockdown increasing OPA1-mediated mitochondrial fusion while increasing ADP-stimulated OXPHOS (p<0.05) indicative of SIRT4s regulation of free fatty acid oxidation.

Bed rest leads to a series of adverse physiological and cellular adaptations which may be limited by micronutrient supplementation. Although further clarification is needed, SIRT4 may have a role in this regard with mechanisms linking mitochondrial dynamics and function.

Chapter I: Introduction

Introduction

Only until very recently has the detrimental impact of physical inactivity been distinguished. This research has demonstrated both the direct and the indirect effect physical inactivity on multiple risk factors for diseases such as obesity, hypertension, insulin resistance, inflammation and dyslipidemia. In fact, Booth & Lees, [52], reference that physical inactivity increases relative risk of coronary artery disease by 45%, stroke by 60%, hypertension by 30%, type 2 diabetes by 50% and osteoporosis by 59% [259,52].

There is ample evidence in the literature to support the beneficial role of acute and chronic exercise on broader physiological outcomes and improving health [202]. However, little is known about the mechanisms underlying the physiological responses to physical inactivity. It has been accepted for many years now that an average weekly volume of 150–300 min of moderate intensity or 75–150 min of vigorous intensity, or an equivalent combination of MVPA is sufficient to reduce the risk non-communicable, chronic disease [70]. While there is clear evidence to demonstrate an inverse relationship between physical activity and all-cause mortality [56,211,279,45], further evidence is required to clarify whether there is a cause-effect relationship between physical inactivity and chronic disease development or whether this is just a simple correlation.

Physical inactivity results in an increased accumulation of visceral and subcutaneous fat, accompanied by an increased loss of skeletal muscle mass and bone mineral density when energy balance is not maintained. Such adverse effects can increase the risk of insulin resistance, cardiovascular disease, osteoporosis/osteopenia and obesity [27,33]. There is growing evidence to suggest that some of the mechanisms underpinning these adverse adaptations to physical inactivity are interlinked. First proposed by Kelley et al. [261], metabolic flexibility is defined as the ability of an organism to respond or adapt according to changes in metabolic or energy demand as well as the prevailing conditions or activity [261,188]. A dysregulation in this response, termed ‘metabolic inflexibility’, occurs in times of prolonged inactivity, such as bed rest, and is associated with muscle atrophy, risk of obesity, insulin resistance and type 2 diabetes. The mechanisms leading to these adverse changes are understudied and incompletely understood to

date [33,452]. Further research into these processes can help to increase our understanding of this behaviour which will address ways to counteract such adverse changes.

Statement of the Problem

The majority of our understanding to date stems from indirect measurements based on exercise training in sedentary individuals or animal models of hind limb suspension [78,190,461]. It has been widely accepted that exercise training results in positive physiological adaptations. However, the role of metabolism and specifically mitochondrial function with physical inactivity has not been studied in-depth. Mitochondrial dynamics impact greatly on mitochondrial function [539]. However, little is known about the impact prolonged bed rest may have on the regulation of mitochondrial dynamics and if these changes could help explain the physiological changes.

Bergouignan et al. [33], illustrated how gaps in our knowledge in understanding the physiological impact of physical inactivity may be due to the difficulty implementing longer term physical inactivity interventions in healthy subjects [33]. Bed rest has been shown to lead to many of the recognized physiological changes observed with sedentary behaviour. Independent of energy balance, bed rest induces muscle atrophy, a shift in muscle fiber type from slow to fast twitch and a switch in preferred substrate oxidation at rest from fat to carbohydrate. Additionally, the limited work to date measuring mitochondrial function suggests adaptations in mitochondrial bioenergetics following bed rest [263,488]. Whether these adaptations persist over time or whether they are acute, adjustable changes is still up for debate with longer termed bed rest studies necessary to answer such a question. To our knowledge there has been no work to date measuring mitochondrial function or dynamics after such a long period in bed.

Along with developing a greater understanding of the intricate adaptations which occur following prolonged bed rest, an important aspect of these studies is in the assessment of novel countermeasures and their ability to mitigate the adverse effects of bed rest. It is accepted that interventions combining exercise and nutrition are most likely to be successful in preventing some of the adverse effects of bed rest. However, due to their complexity, limited combinational research studies have been conducted to date to illustrate this possible beneficial effect.

As such, alternative countermeasures should be considered. Due to their motility and proven benefit to our overall health (i.e. maintaining redox balance, decreasing proteolysis), supplementation of antioxidants and anti-inflammatory agents may be useful agents to help negate the adverse changes observed with physical inactivity [194,407,410,337]. The majority of

our understanding into the impact antioxidant/anti-inflammatory supplementation may have on metabolism is limited to animal models of hind-limb suspension, but what limited work there is on humans indicates some protective effect which they may have.

Many different and intricate ideas have been considered to help mitigate the effects of physical inactivity, most of which have proved inadequate. As such there is a need to further investigate and optimize countermeasures to physical inactivity. This optimization can only be achieved by understanding the physiological responses to physical inactivity and the impact countermeasures may be having at a cellular level. Subsequently, bed rest studies provide not only a simulation model to test potential countermeasures but also provide a platform that can allow us to investigate human physiology in the setting of physical inactivity.

In summary, we are currently unclear on the impact prolonged physical inactivity has on skeletal muscle mitochondrial function and if any changes may be explained through adaptations in mitochondrial dynamics. A greater understanding in this regard could help in the design and execution of an effective countermeasure to alleviate the effects of physical inactivity. This thesis will address this problem by investigating changes in mitochondrial function and dynamics following a 60-day bed rest study in healthy, young males.

Significance

The most recently published World Health Organization (WHO) report highlights the increasing trend in individuals failing to meet the minimum recommendations for physical activity. As of 2020 it was reported that one in four adults (27.5%) and more than 80% of adolescents fail to adhere to the minimum recommendations of 30 minutes of moderate to vigorous intensity physical activity (MVPA) per day [199,70,200]. Consequently, the World Health Assembly (WHA) approved the Global Action Plan on Physical Activity (GAPPA) 2018-2030 aimed to reduce physical inactivity by 15% by 2030. Not only are such aims crucial for the health of the global population, given physical inactivity has been reported to lead to 5.2 million deaths and 6-10% of all major non-communicable diseases annually worldwide [303], they are also paramount financially, given on average $117 billion is spent annually on health care costs due to inadequate physical activity [402]. Given the financial and health burden inactivity appears to have, more research is necessary to fully determine its impact.

Of the limited research conducted into physical inactivity to date much of the proteomic and transcriptomic evidence points to adaptations in skeletal muscle metabolic control, however this

has so often been neglected from study [456,122,264]. Putting clarity to the metabolic adaptations occurring following prolonged bed rest may provide more of an insight into how and why the alterations we are aware of transpire.

Aim, Hypotheses, Objectives

Aim: The aim of this thesis is to determine the effect prolonged bed rest has on whole body and skeletal muscle metabolic function in healthy young men.

Hypotheses

1. Physical inactivity, through the model of bed rest, will result in a shift in substrate metabolism from fatty acid to carbohydrate and a decrease in muscle mass which will progressively become more apparent with a greater time spent in bed rest.
2. Physical inactivity will result in a decrease in mitochondrial function, increasing markers indicative of mitochondrial fragmentation which will progressively become more apparent with a greater time spent in bed rest.
3. Supplementation of an antioxidant/anti-inflammatory cocktail will mitigate the effect of bed rest on mitochondrial function and muscle mass.

Objectives

1. To measure and compare changes in whole body physiological responses and skeletal muscle metabolic responses to 60-days of bed rest.
2. To determine if supplementation with a micronutrient cocktail could mitigate the physiological and/or cellular metabolic changes during bed rest
3. To determine the time-course of these changes by comparing the physiological and skeletal muscle metabolic responses with a previously conducted 21-day bed rest study.
4. To further investigate novel upstream regulators of mitochondrial dynamics through *in-vitro* cell culture methods to help explain the changes, if any, in mitochondrial function, dynamics, substrate oxidation and muscle mass.

Experimental Overview

To test our hypothesis a 2-armed randomly assigned, 60-day bed rest study was designed. 10 subjects were randomly assigned to the control group (CONT) and 10 were randomly assigned to the intervention group (INT). The control (CONT) consisted of 60-days bed rest and the intervention (INT) consisting of the same bed rest protocol as the CONT trial but with supplementation of a micronutrient cocktail (Intervention - INT) composed of a polyphenol

compound mix (XXS-2A-BR2), Vitamin E, Selenium and Omega-3 fatty acids consisting of 6 pills per day: two at breakfast, two at lunch and two at dinner. Multiple tests were performed before and after the intervention. Given this study was conducted in conjunction with the European Space Agency, all tests and measurements were conducted at -6° head down tilt (HDT) in order to simulate the physiological impacts of microgravity on the body. Energy balance was monitored throughout and energy intake was adjusted to ensure subjects would remain in energy balance. Muscle biopsies were obtained before and after each period of bed rest and skeletal muscle analysis aided in the measurement of mitochondrial function using high-resolution respirometry (HRR).

To assess the possible impact time in bed may be having on skeletal muscle mitochondrial function and dynamics, we compared the changes observed following 60 days of bed rest within our control group to control muscle biopsy samples collected from a previously complete, comparable 21-day -6° HDT European Space Agency study stored within our biobank.

Finally, further *in-vitro* cell culture investigation into the mechanisms regulating the changes observed with both 21 and 60 days bed rest was conducted. These efforts evolved our understanding on the mitochondrial adaptations ensuing with bed rest while also identifying a novel pathway relating to mitochondrial dynamics.

Conclusion

This thesis was designed to investigate the impact of physical inactivity, induced by bed rest, on whole body and skeletal muscle metabolism. This study was conducted alongside a number of collaborators with specific expertise. Prof. Stephane Blanc (CNRS, Strasbourg, France) and Asst. Prof. Audrey Bergouignan (CNRS, Strasbourg, France and University of Colorado, Denver, USA) have extensive experience in whole body metabolism with particular emphasis on stable isotopes and body weight control. The design of the present bed rest study, and the comparable 21-day bed rest study, allows us to have control over energy regulation and timing of the measurements we wish to conduct, providing us with well-controlled studies to investigate skeletal muscle physiology. Further *in-vitro* experimentation into the mechanisms regulating these changes in their essence are well controlled enabling us to have a more detailed picture of the adaptations occurring to skeletal muscle in response to bed rest. In order to establish a justification for this thesis a detailed review of the existing literature was embarked upon.

Chapter II: Review of Literature

Introduction

Physical inactivity is among the leading modifiable risk factors for the development of chronic non-communicable diseases such as cardiovascular disease, obesity and type 2 diabetes [295]. Physical inactivity is an ever-growing problem within today's society particularly with the advancement in communication technology and other labour-saving innovations, increasing the likelihood that the opportunities for sedentary behaviour that currently exist will become even more prevalent in the future [136].

Subsequently, between 2001 and 2016 National Center for Health Statistics (NCHS), National Health and Nutrition Examination Survey (NHANES) explored this impact within the United States. This country-wide survey of 51,895 individuals highlighted an increase in sitting time from 7 to 8.2 hours per day among adolescents and 5.5 to 6.4 hours per day among adults throughout the study. Investigators also found this increased sedentary behaviour to be strongly correlated to time spent sitting in front of the television/computer on an average day [558].

Given the impact sedentary behaviour such as physical inactivity has on our physiology and its increased prevalence, a greater understanding into the early physiological changes which occur due to prolonged inactivity is necessary in order to put clarity to the complex adaptations which occur.

Physiological Changes with Bed Rest

Bed rest is considered one of the most robust models for studying the extreme physiological effects of inactivity [208]. It has also been identified as a model to mimic the effects of microgravity on earth and the European Space Agency (ESA) has adopted an anti-orthostatic -6° head down tilt (HDT) bed rest (BR) model for its human spaceflight research. Unlike lifelong sedentary behaviour and aging, the physiological changes during bed rest are transient and reversible. However, research in this area still provide insight to changes in disease related risk factors (e.g. decreased insulin sensitivity and decreased glucose tolerance) [495,93,404,385,90]. Further research in this area can help grow our understanding of the physiological limits of the body and ensure the safety of the patient in bed in a highly controlled environment. Subsequently,

-6° HDT bed rest has become one of the most common methods for measuring extreme physiological adaptations of the body [33].

In an upright position the body counteracts the effect of gravity. However, with bed rest (and spaceflight), the body adapts in an attempt to function optimally by modifying afferent signalling from the various stressors. These physiological adaptations have been investigated extensively over the past 50 years, with particular focus on the sensorimotor, cardiovascular, neuromuscular and musculoskeletal systems [358]. Bed rest leads to changes in balance and gait, cardiovascular deconditioning, loss in muscle mass, muscle deconditioning and musculoskeletal strength. These changes are highly associated with postural control dysfunction (specifically noted following spaceflight) and chronic bed-confinement following major trauma and surgery (particularly in the elderly population) which can lead to problematic functional issues upon readjustment to an upright position [207,22].

Body Compositional Changes with Bed Rest

Numerous body compositional adaptations have been shown to arise from prolonged bed rest. However, these changes are relative to the study design. The European Space Agency human spaceflight programme has embraced designs aimed at controlling energy balance in bed rest studies. In these studies, fat mass remains constant while body weight decreases, unlike other studies that maintain body mass. In both designs bed rest leads to a decrease in skeletal muscle mass and bone mineral density [365,272]. Therefore, when controlling for energy balance, the decrease in muscle mass will lead to a proportional decrease in body weight [125,454,546] but when body weight is maintained the decrease in skeletal muscle mass is counterbalanced by an increase in fat mass [39,129]. For this reason, it is important to consider the study design when comparing to other bed rest studies, particularly, when considering metabolic responses as fat accumulation is a confounding factor on these outcomes.

Cardiovascular Alterations with Bed Rest

There are numerous cardiovascular alterations as a result of the orthostatic stress posed by the -6°HDT bed rest model resulting in deconditioning to the cardiovascular system, particularly the heart and blood vessels, subsequently leading to orthostatic intolerance. Orthostatic intolerance is an intolerance to the stress of standing upright but the exact cause of this intolerance has yet to be uncovered. However, it has been proposed that the redistribution of central plasma volume, due to fluid shift toward the head while at -6°HDT, results in hypovolemia as a consequence of the

increased diuresis and natriuresis, could be the primary factor leading to this intolerance [240,389,22].

There are multiple adverse cardiovascular changes which can lead to orthostatic intolerance. These include reduced cardiac vagal nerve activity, increased adrenergic receptor reactivity, increased R-R interval variability, a reduction in red blood cell mass, decreased systolic blood pressure and reduced mean arterial blood pressure [157,389,434,358]. However, the most noteworthy change appears with the remodelling and atrophy of the heart, with a noted ~15% and ~14% reduction in left ventricular volume and mass following 60-day -6°HDT bed rest [548]. This is particularly significant as cardiac remodelling has been shown to affect a multitude of cardiovascular processes due to the hearts central role in the cardiovascular system. The role that loss of hydrostatic gradient has on heart remodelling is extrapolated further in Figure 2.1. One of the most noteworthy changes is to the its effects on oxygen uptake.

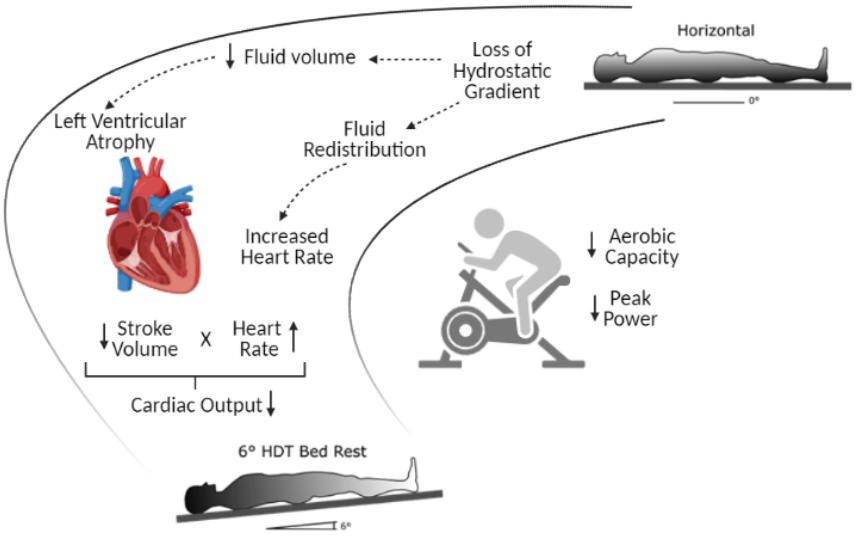

Figure 2. 1. Schematic representation of the effect of -6° HDT bed rest on aerobic capacity

Oxygen uptake is the product of systemic blood flow (cardiac output) and systemic oxygen extraction (arterial venous oxygen difference). Cardiac remodelling impacts this by reducing cardiac output (Q). This is supported by an observed reduction in stroke volume and heart rate (Q=HR x SV) during maximal exercise. This is opposed to what occurs at rest, where heart rate is increased to maintain Q due to the impact -6°HDT bed rest has on cardiac structure. Skeletal muscle maximal oxygen consumption capacity (VO_2 max) has been shown to significantly decrease with prolonged bed rest, a decrease proven to level off as bed rest duration continues with no association noted between decline in VO_2 max and the decline in total body weight and lean body mass [191,277,434]. Work by Greenleaf et al. [191], as presented below in Figure 2.2, highlights

that following 30 days of bed rest there is an 18.2% decrease in relative aerobic capacity ($ml \cdot kg \cdot min^{-1}$) and a 12.6% decrease in absolute aerobic capacity ($L \cdot min^{-1}$). These figures have subsequently been supported by further evidence from within the field [125].

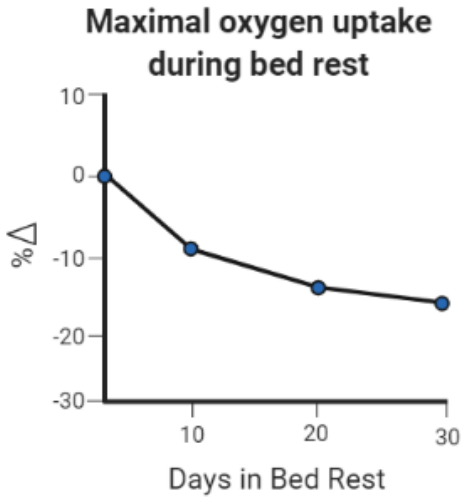

Figure 2. 2. Reduction in maximal oxygen uptake throughout bed rest. Adapted from *Greenleaf et al.* [191]

As cardiorespiratory fitness is an independent predictor of cardiovascular health, quantification of the decrease in VO_2 max (absolute and relative) during or following bed rest provides us with a concise measure of the impact bed rest has on our cardiovascular system both centrally (cardiac output) and peripherally (arterial venous difference, AVO_2 diff).

Bone Alterations with Bed Rest

Bed rest decreases the gravity related loading on the skeleton and the dynamic mechanical force during movement but bone remodelling can also result from nutritional and hormonal changes, the biochemical effect of imbalance in anabolic/catabolic markers of bone structure and the individual's age, sex and ethnicity [442,468,229,425].

The mechanical unloading of microgravity has been shown to have a significant adverse effect upon the skeletal system. LeBlanc et al. [300], tracked multiple cosmonauts (men and women) aboard the Mir Space Station between 4-14.4 months and reported a significant reduction in bone integrity supported by demineralization in bones specific to the lumbar spine, femoral neck, the hip and the bones of the lower extremities (preferentially affecting the trabecular bone within these regions) [300]. These changes are consistent in bed rest research, most likely due to their role in postural control and weight unloading [385].

Although we see significant skeletal muscle and bone loss with bed rest, the rate of change differs, with muscle mass reducing at an ~3% greater rate than the loss of bone. LeBlanc et al. [299], pointed to just a 1% reduction in bone density within the vertebral column after 1 week of immobility, something subsequently supported by further work [289]. Beller et al. [29], reported that 60 days of bed rest led to a 3.4% loss in bone mineral density (BMD) of the proximal femur, and a 2.8% loss at the distal tibia in healthy, young women. This may not seem significant, but after comparing these changes to those experienced by elderly women, who are at increased risk of osteoporosis/osteopenia, and who show a 0.7-1.0% loss in proximal femur BMD and a 2-4% loss of BMD at the distal tibia each year, the adverse effects of prolonged bed rest on bone metabolism are put into context. Additionally, Smith et al. [480], highlighted how it takes 2.5 times longer to regain bone than it does to lose it, with different skeletal regions representing different rates of change.

Due to the significant loss in BMD with prolonged bed rest/microgravity, much work in this field to date has been focused on identifying the histochemical markers which can help explain these adaptations. At present, histomorphometric bone analysis points to an imbalance between bone resorption and formation, specifically an increased bone resorption (i.e. increased activity of osteoclasts) and reduction in bone formation, as can be seen in Figure 2.3. Smith et al. [480], supported this, noting reductions in a multitude of bone formation markers following 3 months of space flight. This work pointed specifically to a reduction in alkaline phosphate (AP), osteocalcinin and type 1 procollagen propeptide (PICP). Zerwekh et al. [573], reported increases in bone resorption markers such as pyridinoline, deoxypyridinoline, and N-telopeptide following 12 weeks bed rest, to explain this change in bone metabolism with prolonged weightlessness [327,298,481,573,480,526,178].

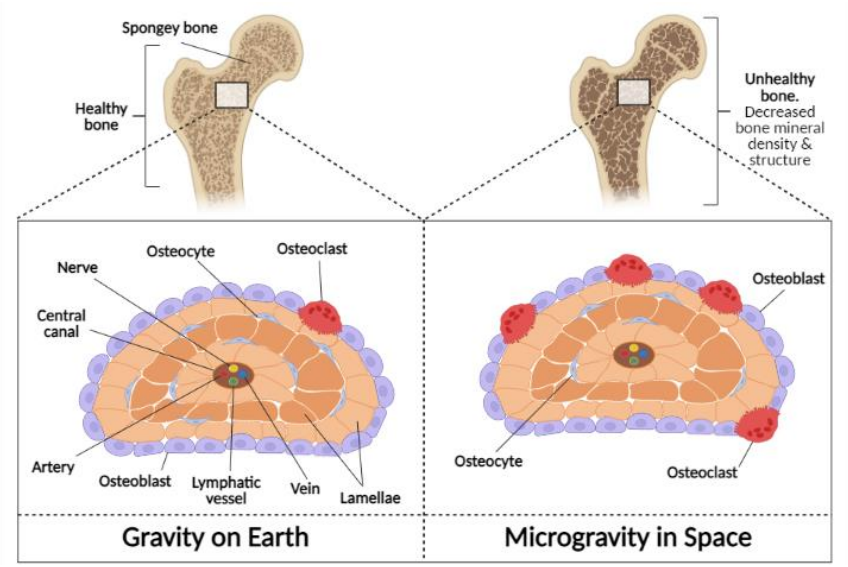

Figure 2. 3. Schematic representation comparing bone structure with gravity and microgravity

In addition, the regulation of calcium homeostasis has also been considered as there are reductions in Vitamin D (aid in calcium absorption), calcitonin (inhibits osteoclast activity) and parathyroid hormone (PTH) (regulates calcium levels in blood) [75,479]. As bone loss begins almost immediately following unloading, supported by a sustained increase in calcium excretion (140mg/day during space flight) [480], there is a greater risk of cardiac arrhythmia and kidney stones [287,413]. Therefore, that alterations to our skeletal system as a result of prolonged bed rest/microgravity has multiple integrated effects on our overall health.

Combining the adverse effects bed rest/microgravity on bone structure with the aforementioned effects on our cardiovascular system alone, irrespective of the other changes observed, greatly increases our risk for fractures and future morbidity and mortality. Supporting that while this thesis will not focus on these aspects in great detail, they are vitally important, integrated physiological systems for overall health maintenance.

Neuromuscular Alterations and Regulation with Bed Rest

Bed rest has been shown to have a significant impact on the skeletal muscle system with particular structural and subsequent adverse functional adaptations, all of which are relative to time in bed/microgravity. A reduction in mechanical loading leads to decreases in muscular strength, muscular endurance, maximal explosive power and neuromotor function. Given the effect both -6° HDT and microgravity have in reducing blood flow to the lower extremities, anti-gravity muscles such as the leg and trunk musculature are preferentially affected by the loss of mechanical loading,

predominantly our extensor muscles, compared to hand and upper limb musculature [275,359,385,125].

Bed rest has a significant impact on skeletal muscle functional capacity, with a noted linear regression with time in bed. This can be seen through significant reductions in torque ranging from 15-40% depending on bed rest duration [32,20,277]. The reductions in muscle strength due to prolonged bed rest/microgravity has been shown to occur over two phases as can be seen in Figure 2.4, an initial phase of rapid decline in muscular strength followed by a slower, more gradual decline thereafter. This initial rapid decrease has been principally linked to a reduction in neuromotor function, be this through specific alterations to the motor unit or to a change in their recruitment pattern [85,22].

Another reason for this link to neuromotor functional change is due to a non-proportional reduction in muscle force to muscle mass. Adams et al. [2], found that peak isometric force of the legs was reduced by 17% following 90-180 days of space flight while the corresponding muscle mass was reduced by just 11%. These observations are more apparent with shorter bouts of bed rest/microgravity as 20 days of bed rest resulted in a ~10% drop in maximal knee extension force in comparison to just an ~8% decrease in muscle cross-sectional area [260]. In conclusion, inactivity has a greater, independent impact on neuromuscular function to muscle mass, particularly in the initial phase of inactivity.

Loss of muscular endurance capacity and maximal explosive power has been strongly linked to time in bed, with the greater losses seen following more prolonged periods of bed rest/microgravity [430,156,429]. The loss of endurance capacity and explosive power are two of the first adaptations to occur in the skeletal muscle within the first few days of bed rest.

Another acute response by the muscle to bed rest is the loss in muscle volume. This decrease in volume can be quite drastic, and as with loss in force, correlated strongly with the gradual decrease in muscular strength. Relatively short periods of bed rest (7 days) lead to a decrease in thigh muscle mass of ~3% [125] and a further 20 days sees an ~8% decrease in thigh muscle cross sectional area [260]. A review by Philips et al. [396], reported an average loss in CSA of 0.6% per day over the first 30-days [179,180,147,560,47,48,184,518], a loss which continues beyond the initial phases of bed rest but trends similarly to what is observed with maximal oxygen consumption during maximal exercise. This increase in muscle atrophy with progressing bed rest is also supported by negative nitrogen balance data demonstrating an imbalance between protein synthesis and protein degradation in skeletal muscle.

The endurance capacity and explosive power of the skeletal muscle is related to neuromuscular capacity and fiber type composition. The skeletal muscle is composed of oxidative, slow-twitch and glycolytic, fast-twitch, fibers which are reduced both in expression and in CSA as bed rest/microgravity progresses [495]. As anti-gravity musculature is generally composed of myosin heavy chain type 1 fibers (MHC 1) (characterized by higher proportion of mitochondria and myoglobin), the consensus has been that such fibers appear more susceptible to atrophy. This thinking is accentuated by an increased expression/enlargement of the other myosin heavy chain (MHC) isoforms such myosin heavy chain 2X (MHC 2X) following prolonged stints of inactivity [153,536]. Animal models of immobilization support this theory, presenting clear differences in atrophy between fiber types following hindlimb suspension (reduced MHC1, increased MHC 2A/B) [30]. In human muscle this is a far more controversial topic. With the limitations in methodology it is debatable whether the changes in muscle composition following bed rest are representative as some believe the changes reflect sampling from different fibers while others acknowledge the limitation in the method but accept that the biopsy is representative of the muscle as a whole [225,560]

It is thought that the reasoning for these compositional changes can be explained by protein turnover rate. In humans the rate of protein turnover is much more homogenous between fiber types than it is in animals [396]. The decreases noted in MHC isoforms with prolonged bed rest in human muscle are clear mechanistic explanations for the aforementioned reduction in muscular endurance (MHC type I) and explosive power (type IIa, IIx). Another mechanistic explanation for this functional observation is the initial reduction in MHC fiber cross sectional area with reduced activity. A systematic review and meta-analysis of 42 studies and 451 participants by Vikne et al. [536], supported this, highlighting an initial reduction in MHC1 and maintenance of MHC 2x cross sectional area with reduced ambulation. As with the reduction in muscle strength, this reduction plateaus after 3 weeks of bed rest with a more gradual decrease thereafter, supporting the importance of muscle fiber composition and functional performance.

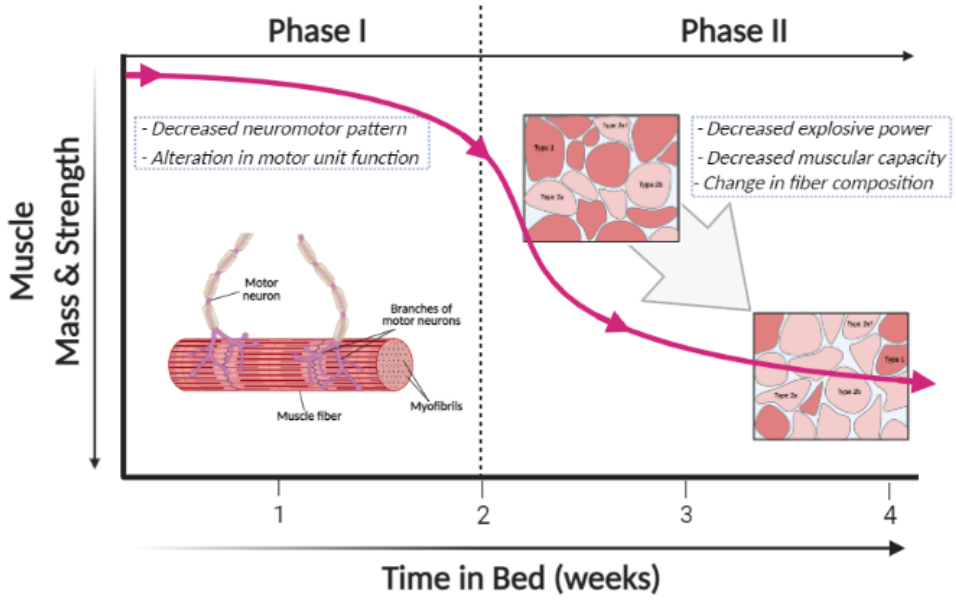

Figure 2. 4. Schematic representation of the neuromuscular adaptations due to bed rest

Prolonged bed rest leads to decrements in skeletal muscle mass and strength correlated to reductions in MHC isoform composition. These changes significantly impact on the skeletal muscle endurance capacity, force output and neuromotor function, all of which can be regained with appropriate resistance and aerobic training within weeks of disuse.

Other General Health Challenges Accompany Extended Periods of Bed Rest

In addition to the multiple physiological alterations resulting from extended periods of bed rest comparative to microgravity there are also numerous more general health challenges accompanying such prolonged periods of bed rest. These challenges include gastrointestinal, dermatological, genitourinary and psychological complications impacting greatly upon overall health. The most prominent gastrointestinal condition associated with extensive periods of bed rest relate to constipation, with reduced activity such as that noted with bed rest commonly considered a relevant determinant [236]. Although the symptoms associated with constipation are often intermittent and mild, they can difficult to treat and can be debilitating at times [310].

Urinary incontinence is common in patients undergoing extensive periods of bed rest. This is because it is more difficult to void in a supine position which can predispose individuals to develop kidney stones due to excessive calcium in the urine (hypercalciuria) which is widely reported to occur with bed rest [375]. Along with being extremely painful, this can be problematic leading to severe kidney infection, hypertension and end-stage renal disease [265].

Dermatologically, bed rest has been shown to lead to the development of pressure sores (decubitus ulcers) as a result of the sustained pressure placed on the skin from immobilization. The strategy for prevention of ulcers include reducing pressure, friction and shear forces and preserving the integrity of the skin through frequent turning and positioning [509]. This is of vital importance considering how the most common complications related to pressure ulcers include osteomyelitis and sepsis, increasing individual's mortality.

In addition to the multiple effects bed rest has on individual's physical health it has also been proven to have a significant impact on overall mental health. Cognitive and psychosocial complications of bed rest and sedentary behaviour include depression, neurosis, helplessness and fatigue. It has been considered that these adverse effects stem from a lack of aerobic physical activity, strengthening the argument on the importance of exercise not only for physical but mental health also [319,550].

Counteracting some of the general physical and mental health challenges accompanying bed rest studies is complex. However, most of these issues are reduced by 24/7 patient care, reducing subject discomfort as best as is possible without jeopardising the integrity of the research study.

Countermeasures and Bed Rest

Given the multiple adverse adaptations to prolonged bed rest, the development of novel preventative medicines, therapeutic interventions, clinical care and rehabilitation programmes to attempt to mitigate these adverse changes have been subject to investigation for many years [93]. These different interventions are also known as countermeasures. Bed rest is a well-controlled model to test and refine countermeasure hardware and protocols prior to use in microgravity while providing a valuable insight into the development of efficient strategies to counteract the effects of physical inactivity [306,33]. As can be seen in Figure 2.5, these countermeasures have varied from pharmacological, nutritional and technological countermeasures to exercise protocols, some of which have now become standard practice stemmed from successful interventional studies, aimed to mitigate the deleterious adaptations to the effects of microgravity and physical inactivity. Although such interventions have proven to be effective in certain circumstances, many have not been capable of sufficiently preventing/delaying the adverse physiological changes [438].

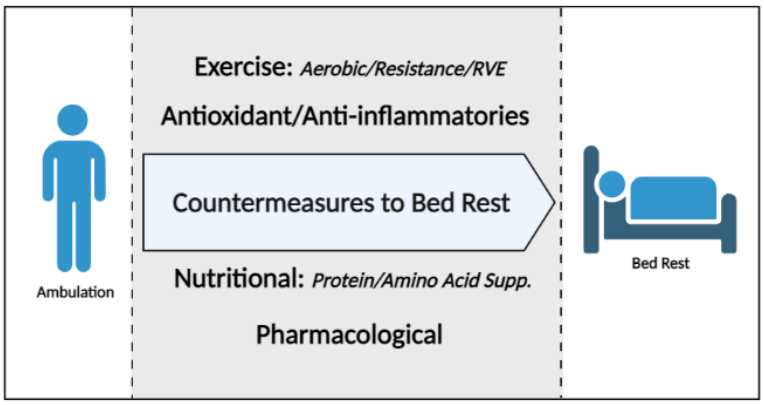

Figure 2. 5. Schematic representation of the multiple different types of countermeasures to counter the effects of bed rest

Exercise Countermeasures

Ever since the 28- to 84-day Skylab missions in the 1970s, exercise programs have been implemented to counteract the negative effects of microgravity. Throughout these missions, astronauts were required to cycle (treadmill running has since been implemented), and perform multiple resistance exercise regimes in an attempt to maintain cardiovascular, skeletal muscle, and overall health. These programs are split into 3 phases, (i) the Adaptation Phase (2-3 weeks), (ii) the Main Phase and (iii) the Preparation for Re-entry Phase (3-4 weeks) all of which incorporate resistance exercise (lower extremity focused) and aerobic exercise with ever increasing loads

based on individual capacity and mission length. The overall goal is to ensure 1.5 hours of exercise training everyday per week [93]. However, although such strict regimes are aimed at maintaining crewmember health, which is the case of cardiovascular capacity, crewmembers have observed significant decreases in both CSA and function of muscle within the lower extremities [517]. Subsequently, research has focused on optimising the program to protect against decreases in body mass, muscle strength and bone mineral density while maintaining aerobic capacity; a difficult task considering the operational constrains on the International Space Station (ISS) [394].

Aerobic Exercise

Without effective countermeasures, there is a noted reduction in aerobic capacity with prolonged bed rest. The cardiovascular adaptations to prolonged bed rest occur in two separate phases, an initial, rapid loss of aerobic capacity paralleled with a loss of plasma volume which is then followed by a more prolonged phase of reduction in aerobic capacity influenced by both central and peripheral adaptations [306]. The complexity of the adaptations are very much dependent on the duration of bed rest with greater reductions noted with increased time in bed.

Aerobic exercise has been used as a countermeasure but the optimal protocol has yet to be devised. The measurement of maximal aerobic capacity (VO_2 max) is regarded as the best single indicator of maximal endurance and aerobic physical fitness and is the most widely reported [154,55]. However, as body weight changes following bed rest the use and interpretation of absolute (i.e. the total change in maximal aerobic capacity irrespective of a person's mass) or relative changes should be carefully interpreted. During the first 30 days of bed rest, aerobic capacity decreases at an average rate of 0.8-0.9% per day [306]. This change is more apparent during the first 1 to 2 weeks and become more gradual thereafter. Greenleaf et al. [191], reported a 12.6% decrease in absolute aerobic capacity and an 18.2% decrease in relative capacity following 30 days in bed. Due to the adaptations which occur with bed rest and the differences between the absolute and relative VO_2 max responses, both should be referenced, this is not always the case [494,521].

Unfortunately, moderate intensity aerobic exercise is not effective in preventing the loss of absolute or relative maximal aerobic capacity [494,500]. However, the adaptations to exercise training are dependent on the intensity, duration and frequency of the stimulus [471,441,72]. Shibasaki et al. [471], showed that -6°HDT exercise training (cycling) at 75% of pre-bed rest heart rate for 90 minutes significantly mitigated the adverse effects of 18 days -6° HDT on aerobic capacity (ml/kg/min). This is supported by Crandall et al. [104] and Dorfman et al. [128], who also

highlight the positive impact on preserving plasma volume, thermoregulatory response and diastolic function. Given the proven beneficial effects of high intensity interval training (HIIT) on aerobic capacity, it is not surprising to see that shorter exercise bouts of higher intensity (90% pre-bed rest heart rate) at -6° HDT prove to have significant effects in preventing the reductions in aerobic capacity and plasma volume [191]. Aerobic exercise, particularly at a high intensity, proves beneficial in preventing the adverse effects prolonged inactivity can have on our aerobic capacity. However, maintaining aerobic exercise capacity needs to be accompanied by interventions that prevent the loss in muscle mass.

Resistance Exercise

As noted earlier prolonged bed rest leads to significant increases in muscle atrophy and reductions in muscle strength and power and aerobic exercise does not provide enough impetus to reduce these adverse changes in the skeletal muscle. Considerable efforts have been focused on resistance exercise during bed rest, given the impact on increasing protein synthesis, insulin sensitivity and mitochondrial and cellular function [282,482,284,132].

Similar to high intensity aerobic exercise, high intensity muscle loading (resistive and explosive) has proven to be most encouraging in reducing muscle loss, mitigating some of the losses in strength, size and skeletal muscle function observed during prolonged bed rest [3,282,439]. Akima et al. [3] and Kawakami et al. [260] proposed the beneficial effect of different lower extremity resistance exercise protocols on maintaining skeletal muscle size and function during 20 days of bed rest. Alkner & Tesch [8] subsequently prevented knee extensor muscle atrophy, electromyography (EMG) activity and task-specific force and power of the knee extensor and plantar flexor during 90 days of bed rest. A protocol coupling maximal concentric and eccentric actions in the supine squat (4 sets of 7 repetitions) with calf presses (4 sets of 14 repetitions) every 3 days' mitigated changes in muscle volume, torque and EMG activity in knee extensor and platar flexor muscles [8].

Trappe et al. [519] added to the findings of Alkner and Tesch,[8] by measuring specific changes skeletal muscle fiber composition following 84 days of bed rest. Bamman and colleagues had previously measured these changes but after 14 days [20]. Trappe et al. observed a shift in MHC isoforms from MHCI to MHC I/IIa (in both control and intervention) and MHC II/IIx (in control only), an observation seen in many studies before. They also noted reductions in control MHC1 and MHC IIa fiber size (-15%), strength (-46%) and speed of contraction, changes which were not apparent within the resistance exercise group [519]. Studies such as these prove the beneficial effect of

resistance training in mitigating the adverse changes in the skeletal muscle associated with prolonged bed rest and space flight.

Although the adverse phenotypic adaptations to bed rest are offset by resistance exercise, less is known about the mechanisms underlying this protective effect. Resistance exercise has been shown to prevent the bed rest-induced decrease in muscle protein synthesis [147] and down regulate transcription factors contributing to muscle wasting [238]. However, its effect on muscle protein balance (i.e. protein synthesis versus breakdown) is still unknown [452]. In addition to this, resistance exercise has been shown to only partially prevent the metabolic alterations induced by bed rest [34,67,196]. Further muscle genome-wide studies measuring the effectiveness of resistance training support these concerns [145] as transcripts related to proteasome degradation, the cell cycle and nucleotide metabolism do not respond.

Resistance and aerobic exercise have exhibited specific, independent benefits on muscle function, structure and overall health but are still ineffective countermeasures on their own. Studies combining both have therefore been proposed to manage the changes observed during muscle-unloaded induced by bed rest [121,405]. These studies, although beneficial in the prevention of muscle alterations induced by bed rest, irrespective of exercise type, duration, intensity or frequency, did not protect against the adverse metabolic outcomes [455,518,35,276]. Subsequently, more work is necessary to identify an effective countermeasure to offset these changes.

Resistance Vibration Exercise

Sanders [459] and Whedon et al. [549] were the first to identify the use of vibration as a therapy, using oscillating motorized beds to counteract the cardiovascular and musculoskeletal effects of deconditioning. Whedon et al. [549] noted the influence whole body vibration (WBV) appeared to have on bone health, with reductions in subject's urinary phosphorus and calcium. This advancement kindled much interest into the role vibration could have as a therapy for bone health, investigation which naturally began with the use of animal models [250,189,233]. Due to successful outcomes in increasing bone thickness in rats, theorized to be due to the vibration signals effect in activating the mechanosensors in the osteoclast and osteocyte cells [172,293,386], experimentation into the possible benefits WBV had in humans was initiated. Unfortunately, unlike the benefits seen in the rodent model, WBV in humans has not been proven to have any overall positive effect on bone health and therefore doesn't appear to be an effective countermeasure in this regard [245].

Nevertheless, there has been some beneficial effects of vibration on skeletal muscle function. Nazarok & Spirak, 1985, were the first to apply vibration to athletes and observed specific improvements in muscular strength. Vibration has been identified to have a specific role in enhancing muscular power during and immediately following exercise [117,97,437]. However, when used as a countermeasure to the adverse effects of bed rest [571,17], it was not effective in preventing the losses in muscle volume imposed by 14 days -6° HDT bed rest [44].

The Berlin Bed Rest Study (BBR) was designed to assess the synergistic role WBV may have in combination with lower extremity resistance exercise, resistance vibration exercise (RVE), throughout 60 days of bed rest [28]. A schematic representation of RVE can be seen in Figure 2.6. After taking skeletal muscle biopsies, Blottner et al. [46] reported that RVE maintained the myofiber size in the vastus lateralis and soleus. This was in contrast to the control group that shifted from slow to fast twitch muscle phenotype. This shift has been observed before but what is intriguing is the capability of RVE in maintaining its slow-twitch characteristics irrespective of the prolonged bed rest.

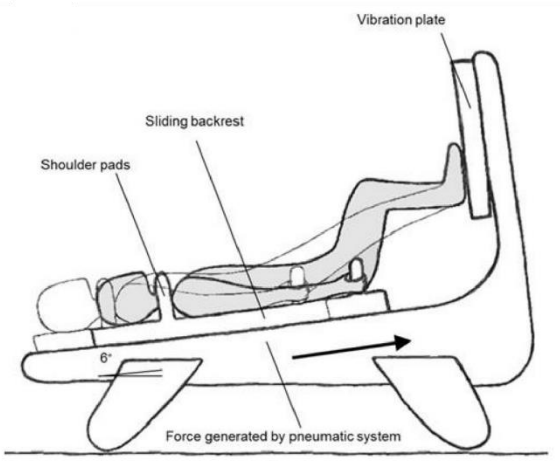

Figure 2. 6. Schematic representation of the squatting exercise performed on the Galileo "Space Exercise device" with subjects lying in bed at -6° head down tilt. *Liphardt et al.* [317]

Due to the success of this study, a second BBR study was implemented, the Berlin Bed Rest Study-2 (BBR-2) [28]. This study consisted of three groups, the control group, the RVE group and a resistance training (RT) group. Their findings supported the ability of RVE to preserve thigh CSA and maximal voluntary contraction torque, an observation comparable to what was noted with RT on its own [360]. Additionally, Kenny et al. [263], advanced this field further referencing how RVE may also have a beneficial effect on muscle metabolism, particularly noting its ability to preserve skeletal muscle insulin sensitivity and mitochondrial respiration in comparison to their control group following 21 days of -6°HDT. These results prove the value RVE has on overall health

maintenance and possibly athletic performance, while also strongly supporting the effects a combination of vibration exercise and resistance exercise have in furthering this beneficial effect.

Nutritional Countermeasures

Recently, there has been increased focus on the development of nutritional countermeasures to mitigate the negative effects of bed rest. Some attempt to counteract the changes by inducing protein synthesis, subsequently preventing muscle loss, while others attempt to prevent some of the other adverse changes through antioxidant and anti-inflammatory supplementation. Unfortunately, the results to date have been ambiguous with inconsistencies in study design, particularly related the maintenance of energy balance, or not, as well as the impact of caloric restriction on protein metabolism [40].

Another point to note in studies measuring the beneficial effects of supplementation is the difference between human and animal models. Rodents have a greater rate of protein turnover in comparison to humans, spending the majority of their life in the growing phase, signified by a greater increase in protein synthesis to degradation (most studies on rodents are complete in the growing phase) [323]. These differences underline the scrutiny required to fully understand and to advance the field of nutritional countermeasures to prevent the adverse changes associated with inactivity.

Protein and Amino Acid Supplementation

Protein supplementation as a countermeasure for inactivity has been of interest for many years due to the role dietary protein has in protein synthesis. In just 14 days of bed rest protein synthesis can decrease by up to 50%, with no change in protein degradation [146]. The primary role of protein supplementation is to level the imbalance between synthesis and degradation in an attempt to maintain skeletal muscle mass and reduce atrophy. Whey protein appears to be the most beneficial as it maintains skeletal muscle protein synthesis, due to its high concentration of essential amino acids (EAAs) in comparison to other vegetable sources such as soy, corn, gluten or wheat protein [116].

In spite of this, there is no beneficial effect of whey protein supplementation on metabolic flexibility in healthy young men following 21 days of -6 ° HDT bed rest. Similar losses in fat-free mass (FFM) and reductions in metabolic flexibility have been seen in comparison to those without

supplementation [454]. This is in agreement with previous work by Blottner et al. [46], referencing similar losses in FFM and reductions in metabolic flexibility to what was observed in their control group.

Other studies focused on supplementation with specific amino acids, particularly branch chain amino acids (BCAA). Leucine has been the focus of much of this work as it has been shown to be a potent stimulator of protein synthesis both *in-vivo* and *in-vitro* [332,551,95] but a leucine-enriched high protein diet does not appear to have beneficial effects during bed rest [520,518]. The work by Trappe et al. [520,518] reported a similar degree of muscle atrophy in the soleus muscle between the control (-29%) and the nutritional countermeasure (-28%), explained by specific decreases in MHC I fibers (-14%). Although bed rest duration was shorter, these adaptations are in contrast to that by English et al. [142]. This work suggested a partial protective effect on muscle mass and function during 14 days of bed rest with leucine supplementation. Subsequently, leucine supplementation may be of benefit during the initial days of bed rest but ineffective thereafter. These data do not support the use of a high-protein countermeasure, alone, to prevent the deleterious effects of more prolonged bed rest on skeletal muscle.

Antioxidant & Anti-Inflammatory Supplementation

It has been well established that resting and exercising skeletal muscle produce both low and high levels of reactive oxygen species (ROS), respectively [24,427,428,362,533]. The purpose of these changes in ROS are still under debate but are thought to be a normal physiological response by the body to changes in the cellular environment and part of the early adaptive response to exercise. Prolonged skeletal muscle disuse has also been shown to significantly increase the production ROS, with the mitochondria considered to be the main source, however there is still some debate in this regard [209,343,333,409,59,291]. The increased ROS has been noted to disturb redox balance (equilibrium between pro-oxidant molecules and anti-oxidant defences) effecting the signalling pathways controlling both proteolysis and protein synthesis in the inactive skeletal muscle [510,273]. The disturbed redox signalling, particularly in the early phase of bed rest, is considered to be a factor in the increased muscle loss and decreased muscle function relating to disuse [111,66,407,410].

Due to the affects ROS appear to have in disturbing redox-signalling, antioxidant and anti-inflammatory agents have been established to prevent induced oxidative stress. The most prominent antioxidant is Vitamin E, which also acts as an anti-inflammatory due to its ability to inhibit NF-κB [231,247,266], but others such as selenium (in combination with Vitamin E) and

polyphenols (such as resveratrol) all show promise as possible protectors against the adverse effect of prolonged inactivity. However, the current literature is limited and more research is needed to build on these preliminary findings, particularly with human studies.

Vitamin E and Selenium

Vitamin E is a major lipid-soluble antioxidant found in the cell membrane [244,544,543] and although much of the work supporting the benefits of Vitamin E to date has been conducted on rodents, evidence does suggest a potential protective effect of Vitamin E supplementation on skeletal muscle disuse [274,11,118,470]. Due to its structure, Vitamin E has been shown to accumulate within the mitochondria of the cell, passing through its lipid bilayer protecting against oxidative damage induced by excessive reactive oxygen and nitrogen species [478,361]. To date, there is no evidence on the role of Vitamin E in counteracting the adverse effects of bed rest in humans but the evidence in animal studies of immobilization, particularly relating to its ability to modulate genes corresponding to proteolysis, provides a justification for examining in human trials.

As with Vitamin E, little to no work to date has been conducted on the effect selenium may have in protecting against the changes associated with physical inactivity in humans. Yet, preliminary evidence suggests a possible beneficial role in boosting the efficacy of Vitamin E by acting as a scavenger for reactive oxygen and nitrogen species (ROS and RNS), alleviating oxidative stress [387,38].

Omega-3 Fatty Acids

The anti-inflammatory Omega-3 fatty acids (ω-3), found in fish oils and dietary supplements, has been studied with physical inactivity, given the favourable effects on immune function, cognition and bone health [141,83,76]. There has been evidence to support the beneficial effect of Omega-3 FA in skeletal muscle, particularly eicosapentaenoic acid (EPA 20:5*n*-3) and docosahexaenoic acid (DHA 22:6*n*-3), which act by incorporating themselves into the membrane phospholipids of the sarcolemma and intracellular organelles [336]. The current recommendation of EPA and DHA is between 250-500mg/day in combination [512].

EPA and DHA exert independent biological actions and therefore should be examined both together and separately. Much of the work has shown that EPA has a greater influence on muscle protein turnover [256,246] than DHA, which appears to be heavily involved in neuromuscular function [457]. Although the exact mechanism has yet to be uncovered, there is clear evidence

linking Omega-3 FA, and particularly EPA, to enhanced skeletal muscle protein synthesis due to enhancement of $mTOR^{ser62448}$ and p70-S6 K^{Th389}, key regulatory proteins in muscle protein synthesis [120,476,477]. Rodacki et al. [445] support these findings, pointing particularly to the synergistic effect Omega 3-FA (fish oils) and resistance exercise on skeletal muscle strength, a process known to act on both mTOR and p70-S6 K1 signalling.

Due to the impact Omega-3 FA supplementation has on muscle protein synthesis, muscle protein breakdown and inflammation in multiple scenarios as can be seen in Figure 2.7, it has been considered as a strategy to counteract against muscle disuse. One of the few studies assessing this to date by McGlory et al. [337] noted that supplementation of EPA and DHA, 4 weeks before and throughout 2-weeks of unilateral leg immobilization, attenuated the decline in muscle mass in young women. However, it is unknown if Omega-3 FA feeding protects muscle loss during periods of disuse in older men and women. More work is necessary in this area but preliminary findings show their value.

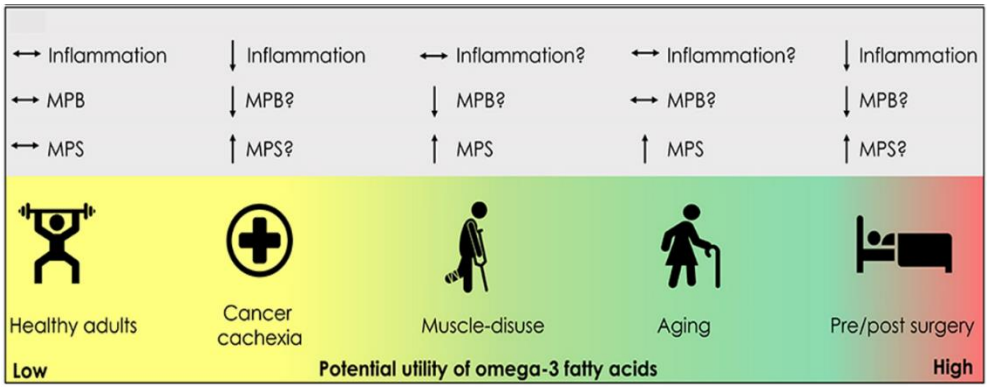

Figure 2. 7. Schematic representation of the potential clinical scenarios for the use of omega-3 fatty acid supplementation to promote and/or mitigate losses in skeletal muscle mass. *McGlory et al.* [336]

Polyphenols

Polyphenols are naturally formed (although some may also be synthetically synthesised), plant-based compounds [222] that constitute a large group of bioactive phytochemicals which include multiple sub-classes such as flavonoids, stilbenes, phenolic acids, and lignans [158]. Due to the differing sub-classes, they have been proposed to have multiple effects throughout the body, particularly in the vasculature, the skeletal muscle and in substrate metabolism.

Flavonoids

Originally much of the work in this area focused on flavonoids, commonly found in fruits, vegetables, grains, bark, roots, stems, flowers, tea and wine. With over 5000 flavonoid compounds identified to date, flavonoids were originally observed to progressively increase flow mediated dilation in the vasculature following short-term intake [464,216] as they have a specific effect on endothelial function by increasing nitric oxide availability and vasodilation [50,106]. Like most polyphenols, flavonoids have antioxidant and anti-inflammatory properties acting to scavenge free radicals, protect oxidants and increase expression and activity of anti-oxidant enzymes [186,414,267]. Additionally, flavonoid supplementation has been touted as a potential therapeutic for treating muscle atrophy relating to disuse [86,380,562,204]. However, much of the evidence to date has been conducting using animal hindlimb suspension, immobilization or denervation studies [357,356,577]. Further clinical application of flavonoid use for muscle atrophy in humans is necessary as the only evidence to date reporting epicatechin (a flavanol subclass) supplementation for 7 days increased grip strength by 7% in elderly participants [201].

Stilbenoids

Resveratrol (RSV), a member of the stilbenoids sub-family of polyphenols, is commonly found in the skin of grapes, green plants and peanuts [26,4]. This widely available nutritional supplement has been linked with changes in metabolic gene expression, protein synthesis/degradation, antioxidant activity, glucose disposal and inflammation. For this reason, resveratrol has widely been considered as an “exercise mimetic” due to such poly-pharmacologic action particularly within the cardiovascular, skeletal muscle systems and the liver [331,206].

The antioxidant properties of resveratrol appear stronger in *in-vitro* experiments due to poor bioavailability *in-vivo* [167,37,383]. Regardless, evidence suggests RSV supplementation *in-vivo* is efficacious, with the majority of its impact on gene expression, particularly those involved in ROS production and inflammation [175,62,176]. Timmers et al. [513] supported this, highlighting how resveratrol supplementation (150mg/day) in obese men during a double-blind cross-over study for 30 days led to significant improvements in resting metabolic rate, blood pressure, glucose control along with reductions in ROS and markers of inflammation (IL-6, TNF-α). They concluded that these reductions in ROS where elucidated by improvements in mitochondrial activity, referencing increased protein expression of specific markers of cellular metabolism regulating mitochondrial biogenesis.

Momken et al. [347], used 400mg/kg/day of resveratrol supplementation to demonstrate a positive effect on muscle mass loss and protein balance during 15 days of hindlimb suspension in rats. Translated into human doses, this represents a daily intake of 4.5 g/d, a dose that far exceeds those used in clinical trials and which will require testing for side effects [330]. The dose-response may explain why Bennett et al. [30], found that 125mg/kg/day resveratrol supplementation was unable to attenuate the decreases in plantaris muscle weight during 14-day hindlimb suspension. Although these results emphasise the positive impact resveratrol supplementation had in animal models, there is limited evidence on the beneficial effect resveratrol supplementation has in humans. In fact, human studies suggest supplementation of 250mg/d resveratrol may have a blunting effect on the outcomes of exercise training in humans [183,376]. This does not imply that resveratrol supplementation would have an adverse effect during bed rest in humans but due to the scarcity of literature on this topic at present it is still up for debate. There is little data at present in the context of 'normal' intakes of resveratrol and whether past research findings are influenced by the energy status of the animal/person prior to supplementation, subsequently more work in this field is needed. Such an emphasis on the above will not only to remove the ambiguity around dosing but also to put clarity as to whether the positive effects observed in animal models can be translated to human trials.

There is so much still to investigate with polyphenols like resveratrol and flavonoids but it is clear that they have a positive impact with regards to their anti-inflammatory and antioxidant capacity in particular. One of the challenges is that many of these micronutrients are investigated individually in order to understand the mechanisms of action. This helps to put clarity into the possible antagonistic-agonistic effects supplements may have on each other when co-administered possibly leading to an overall benefit to humans, helping to to overcome the inactivity induced changes in skeletal muscle metabolism. At present very little data exists on the role these may have in the context of prolonged bed rest in humans, with little to nothing on the possible role they may have in combination. There is great potential for this new, emerging area.

Metabolic Changes with Bed Rest

Prolonged bed rest results in adverse changes to our cardiovascular, skeletal muscle, bone and neural systems among others. Skeletal muscle adaptations are quite substantial, with a referenced 0.6% loss per day over the first 30 days of bed rest [396]. The cause for these adaptations are still under debate, with considerable changes to multiple cellular processes, such as to protein synthesis/degradation, proposed to be of most importance.

However, recent transcriptomic and proteomic skeletal muscle profiling following bed rest/microgravity emphasize why the study of the metabolic adaptations to bed rest is an emerging field of interest. Although most of these studies reference the changes in regulators of protein synthesis/degradation, the majority of the changes appear to occur to metabolic/mitochondrial related targets, indicative of a shift in substrate oxidation from lipid to carbohydrate [491,505,145,403]. Kenny et al. [264] supported this by reporting that 21 days of bed rest decreased the expression of mitochondrial proteins involved in fatty acid oxidation.

Given these findings, investigating the metabolic adaptations occurring during bed rest could prove beneficial by helping to explain the changes in skeletal muscle but also in ways to counteract these changes.

Metabolism

Metabolism is a term that is used to describe all chemical reactions involved in maintaining the living state of the cells and the organism and is central to understanding the phenotypic characteristics of all living organisms [508]. It is a process converting food to energy in order to conduct cellular processes, to aid protein, lipid, nucleic acid and carbohydrate synthesis and the removal of nitrogenous wastes. Many of these processes become altered with prolonged bed rest, generally referred to as “metabolic inflexibility”. Bergouignan et al. [33] described this as a high variance in insulinemia associated with a low variance in non-protein respiratory quotient (NPRQ) [261,33,188], variances which are independent of other observed alterations with prolonged bed rest as is extrapolated further in Figure 2.8. Figure 2.8 represents how physically active women (*n*=8) subjected to 2 months of bed rest [35], and trained men (*n*=10) were asked to stop both structured and spontaneous physical activity for 1 month. Bergouignan et al. [33] showed that metabolically flexible subjects will greatly increase carbohydrate oxidation (i.e., high variation in NPRQ) after the consumption of a meal despite a low increase in plasma insulin concentration (i.e., low variation in insulin). A metabolically inflexible individual, i.e. a person who also displays

insulin resistance/desensitivity, will display a low increase in carbohydrate oxidation (i.e., low changes in NPRQ) despite a marked elevation in insulin secretion (i.e., high variation in insulin). It can be observed from Figure 2.8 that variances in NPRQ and insulin are linearly distributed along a continuum of physical activity level. These variances are associated with reductions in insulin sensitivity [42,7,125,263], glucose tolerance, hyperinsulinemia and hypertriglyceridemia in healthy individuals [318,34]. In its essence, metabolic inflexibility is the reduction in one's ability to use fat as a source of energy, in conjunction with an impaired ability to oxidise carbohydrate during feeding/insulin stimulated conditions.

These adaptations in substrate oxidation are strongly correlated to to muscle atrophy, a shift in muscle fibre type towards glycolytic, fast-twitch fibers and an increase in ectopic fat storage; all characteristics of phenotypic changes during prolonged bed rest.

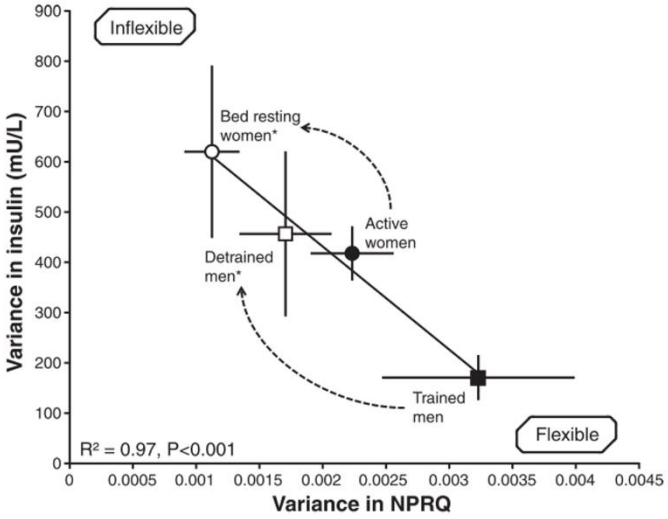

Figure 2. 8. Metabolic flexibility is the relationship between daily individual intraindividual variances of plasma insulin concentrations and nonprotein respiratory quotient (NPRQ), *Bergouignan et al.* [33]

Carbohydrate Metabolism

Carbohydrates and free fatty acids (FFA) are the preferred fuel source of the skeletal muscle. The preferred source of carbohydrate in the human body, glucose, is a highly controlled polymer ranging between 70-170mg/dL in normal, healthy individuals.

Glucose is a hydrophilic molecule which subsequently cannot pass through the cell membrane without the aid of a membrane transporter. The principal insulin stimulated GLUT isoform in the skeletal muscle is GLUT4 while GLUT1 is involved during fasting [258] The activity of GLUT4 is

dependent on the two factors, insulin and the contraction of the muscle which are represented schematically in Figure 2.9.

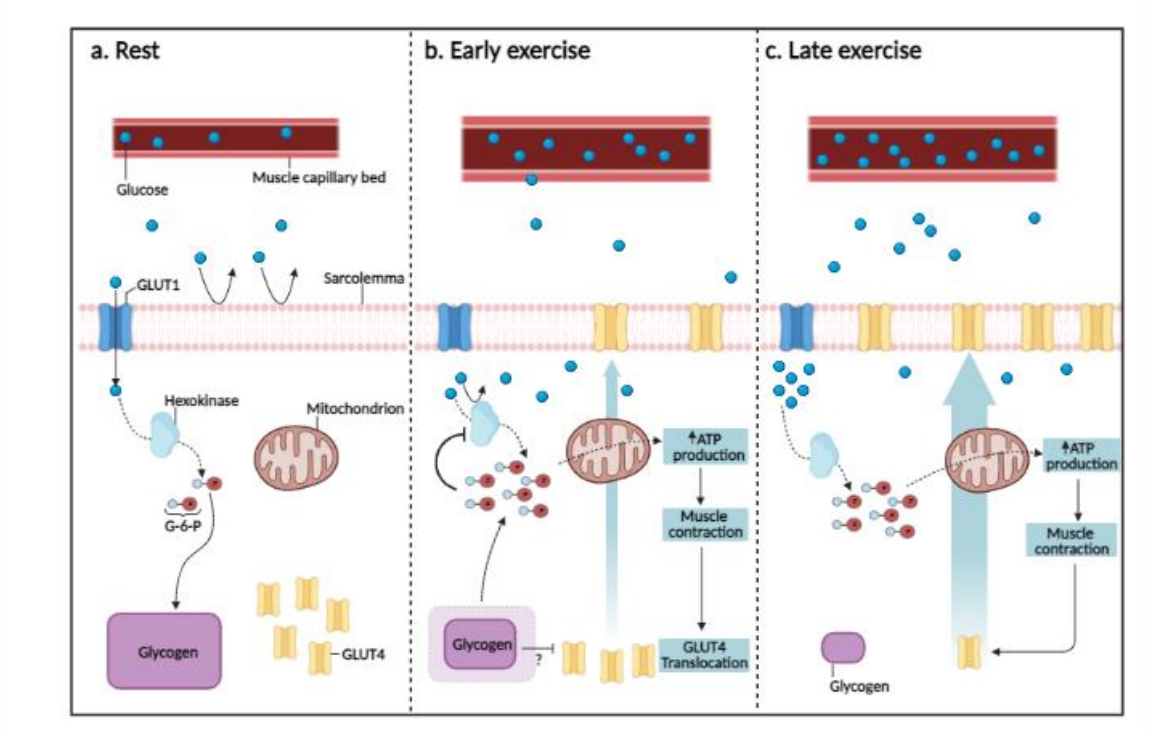

Figure 2. 9. Schematic representation of the action of GLUT1 & GLUT4 for glucose transport into the muscle cell at rest and during exercise. Adapted from *Sylow et al.* [501]

Insulin, an endocrine peptide, anabolic hormone, is secreted from the pancreatic β-cells and increases glucose uptake into the skeletal muscle cell by signal transduction via a series of protein phosphorylation cascades [258]. These cascades result in the translocation of GLUT4 from its intracellular storage depot to the surface membrane of the skeletal muscle cell, a process known as insulin-dependent glucose transport [432,351,393]. Additionally, glucose can be taken up into the skeletal muscle independent of insulin, a process known as insulin-independent glucose transport. Skeletal muscle contraction acts to translocate GLUT4 to the surface membrane, a physiological adaptation of our muscle to ensure the uptake of energy in demanding circumstances such as high-intensity exercise [372,432,340]. Both insulin-dependent and insulin-independent glucose transport are further represented in Figure 2.10.

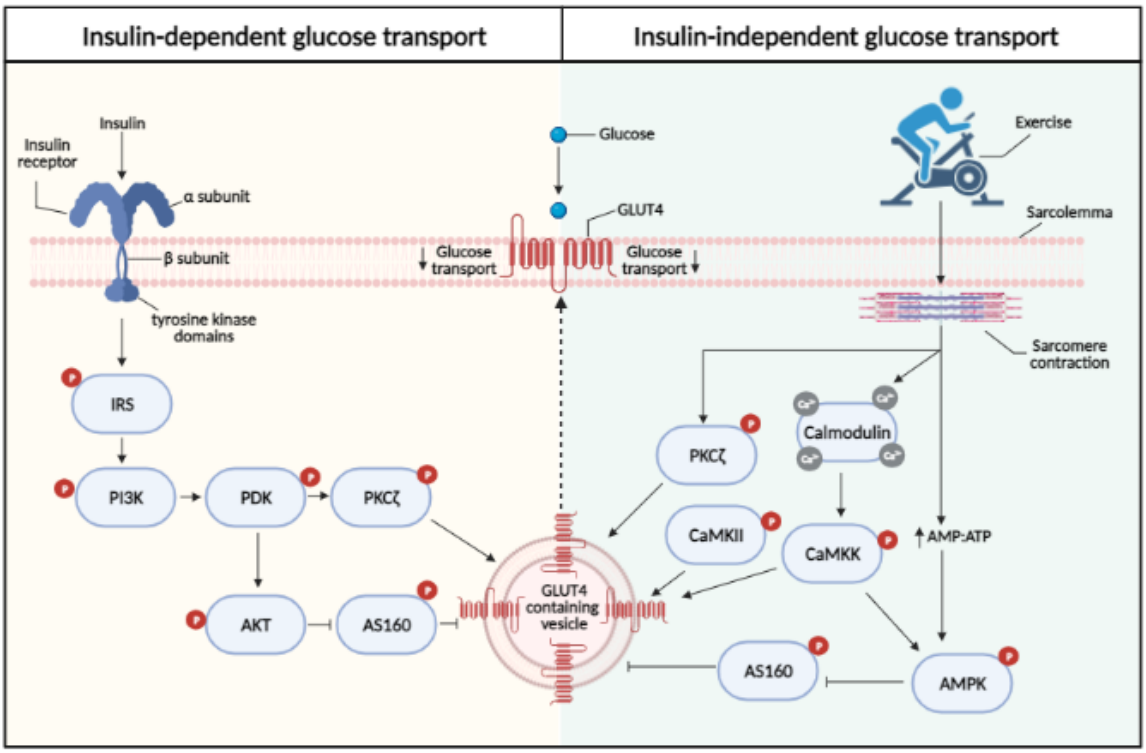

Figure 2. 10. Schematic representation of insulin-dependent and insulin-independent glucose transport into the muscle cell. Adapted from *Di Meo et al.* [340]

The amount of GLUT4 that is present in the cell membrane at any given time reflects the amount of glucose uptake into the cell, and is the rate limiting step. Once into the skeletal muscle cell, glucose undergoes glycolysis, generating pyruvic acid, or is stored as glycogen. Under aerobic conditions pyruvic acid is transformed to Acetyl-CoA that is further metabolized in the citric acid cycle within the mitochondria, ultimately leading to the generation of chemically bound energy in form of ATP. Alternatively, under anaerobic conditions the generated pyruvic acid ferments to produce lactic acid [258].

The inability of a target tissue, such as skeletal muscle, to mount a coordinated glucose-lowering response to suppress endogenous glucose production, decrease lipolysis, reduce cellular uptake of plasma glucose and net glycogen synthesis at a normal plasma insulin level leads the progression of a metabolic abnormality known as insulin resistance [254,253,255]. Bed rest has been used as a model to study the mechanistic alterations resulting in insulin resistance. Due to the reduction in energy expenditure while at -6°HDT bed rest and the positive correlation acute overfeeding has in increasing metabolic dysfunction, studies measuring the metabolic adaptations to bed rest should be conducted with subjects in stable energy balance (energy intake = energy expenditure) [454].

As far back as the 1970s oral glucose tolerance tests (OGTT), have supported the fact that 10-14 days of bed rest leads to a reduction in glucose tolerance and hyperinsulinemia [318,126]. It has been proposed that this is due to an impairment in peripheral glucose uptake, possibly due to a reduction in insulin sensitivity, and is not due to a deficiency in insulin production. These findings have been supported in recent work by Bergouignan et al. [36] and Blanc et al. [42] and with the euglycemic-hyperinsulinemic clamp technique. Dirks et al. [125] who also used this technique found that changes in glucose uptake occur within 7 days of bed rest. This is a common trend during prolonged bed rest models (14-21 days) which have noted a similar reduction in insulin sensitivity and carbohydrate oxidation [263]. Considering our 'normal' diet is very high in carbohydrate at approximately 50% energy intake and the impact bed rest has on carbohydrate metabolism, it has been proposed that a reduction in dietary carbohydrate intake as a percentage of total energy intake during bed rest may help to reflect the loss of carbohydrate oxidation capacity with reduced activity.

The mechanistic investigation of insulin resistance can shine further light on how and why such changes occur during bed rest. However, the problem identifying the primary defect in this cascade is challenging as there is a balance between changes in insulin sensitivity and insulin secretion. Bed rest as a model of inactivity has proven to be ideal for gathering a greater understanding into carbohydrate metabolism and the metabolic condition of insulin resistance [33,393]. On-going examination into the mechanistic explanations for these changes will shed further light onto our understanding of carbohydrate metabolism.

Lipid Metabolism

FFA are one of the preferred fuel sources of energy for the skeletal muscle. However, the use of FFA is highly dependent on a balance between lipid uptake, lipid storage and lipid breakdown, actions which in themselves are dependent on substrate availability.

Following uptake into the body (i.e. a meal), fatty acids (FA) move from the plasma into the skeletal muscle via fatty acid transport proteins. Once into the skeletal muscle cell, FAs can either be used directly for energy or stored, both of which are highly dependent on the metabolic status of the cell.

When the rate of skeletal muscle FA uptake increases beyond FA oxidation, lipids are stored. Cell oxidative stress can ensue if this influx of FA becomes too great. However, this can also lead to the generation of lipid droplets (LDs) [325]. Physiologically, LDs are high-energy pools for the skeletal muscle to use during times of need (i.e. exercise). However, lipid use is subject to LD

composition (“the athletes paradox”), with a higher percentage of lipotoxic species (ceramides, diacylglycerides) in the LD of those suffering from metabolic disorders such as obesity and type 2 diabetes [198,133,10]. In times of energy demand, these stored TAGs are broken down for energy by a process of lipolysis.

In the mitochondria the process of FA oxidation (β-oxidation) is initiated to generate acetyl-CoA, which enters the citric acid cycle and the electron transport to produce ATP [351]. Lipolysis and β-oxidation are slower processes than carbohydrate oxidation, but the net ATP yield is greater (Yield of ATP per mole of glucose: ~27-29 ATP (glucose shuttle dependent), Yield of ATP per mole of palmitate: 96.5 ATP) [58]. The activity of lipolytic enzymes is increased with exercise training and reduced with aging, particularly in slow-twitch, oxidative muscle fibers (type 1) given their increased mitochondrial density [12,525], supporting the positive impact exercise has in managing our metabolic flexibility.

Prolonged bed rest leads to the development of metabolic inflexibility, insulin resistance and a subsequent decrease in lipid oxidation and increased ectopic lipid storage. However, Dirks et al. [125] found no change in skeletal muscle lipid content following 1-wk bed rest in healthy males, but they did note a decrease in insulin sensitivity (29±5%). The trending increase in lipid droplet size and FFA content within the slow-twitch, oxidative fibers supports that accumulation of lipotoxic species, such as diacylglycerides (DAGs), ceramides and acylcarnitine, may be a product of disease progression and not an instigating factor in the development of insulin resistance, an observation supported by other studies [217,218]. Additional work examining the metabolic response in the muscle during bed rest proposes a decrease in activity and expression of key mitochondrial free fatty acid transporters, such as CPT1 which acts to move long chain fatty acids into the mitochondria for β-oxidation [35,488]. Thus, the changes to fat stores as a result of bed rest could be explained by reductions in free fatty acid oxidation leading to this increase in FFA content.

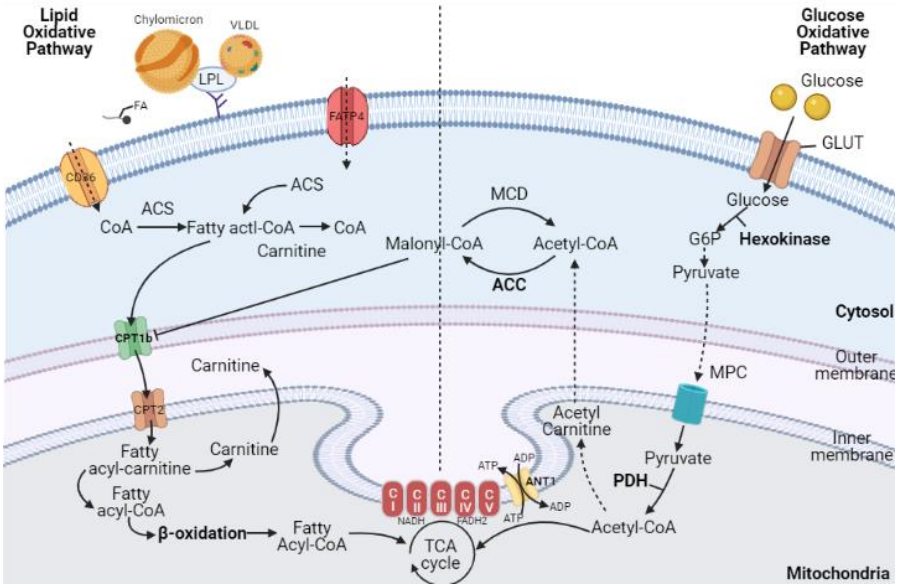

Figure 2. 11. Schematic comparison between the lipid and the glucose oxidative pathways

As there is a cross-over in the oxidation of lipids and carbohydrates, which are represented further within Figure 2.11, the storage of these two substrates also depend on overall utilisation. Therefore, a more integrated approach to the adaptations which occur to our metabolism with prolonged bed rest is required.

Carbohydrate and Lipid Metabolism

Under normal circumstances the switch in carbohydrate and lipid oxidation depends on the type and the amount of nutrient available for oxidation within the cell regulated through specific metabolic pathways, a concept coined as the Randle Cycle [423]. Randle et al. [423] proposed that under postprandial conditions an increase in free fatty acids (FFA) would lead to an increase in fatty acid oxidation while inhibiting phosphofructokinase and pyruvate dehydrogenase. Such inhibition leads to an accumulation of glucose-6-phosphate which acts to inhibit hexokinase, resulting in an increase in intracellular glucose concentration (a negative feedback loop for glucose uptake). These signalling cascades are represented clearly within Figure 2.12, with high fatty acid oxidation (FAO) on the left and high glycolysis on the right.

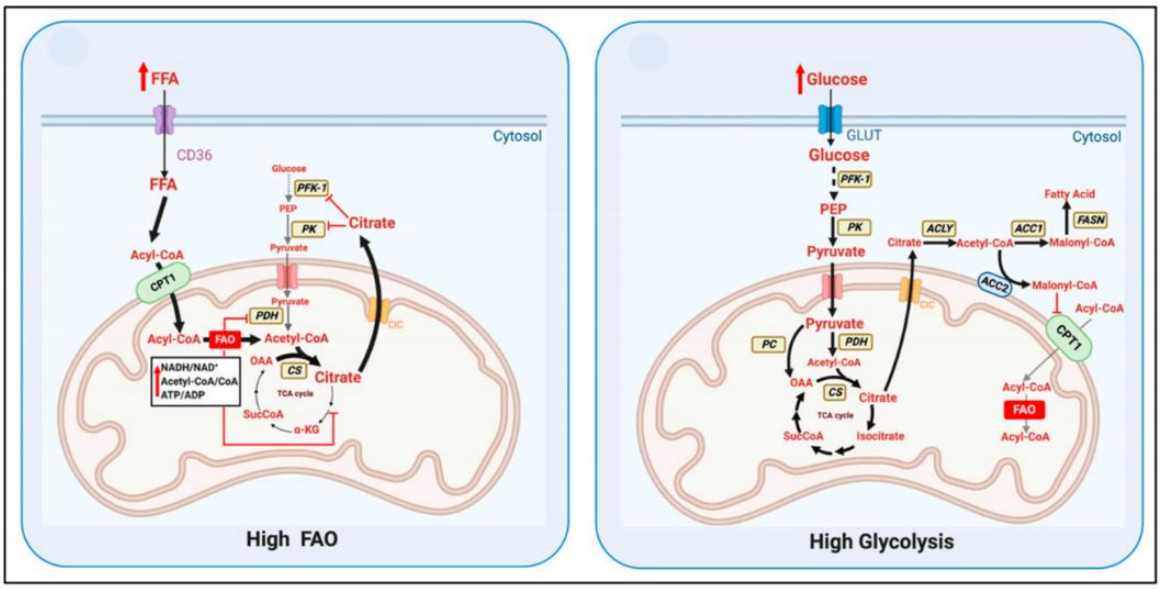

Figure 2. 12. Schematic representation of the Randle Cycle. *De Oliveria et al.* [377]

Bed rest is known to reverse this cycle (reverse Randle Cycle), shifting fuel preferences in favour of carbohydrate metabolism, an effect which has been correlated to an inhibition in FA oxidation, independent of energy availability [42,262,492,34]. A metabolic impairment in the capacity to increase fat oxidation results in a build-up of non-esterified fatty acids (NEFA). These are subsequently stored as ectopic fat in the liver, bone and/or skeletal muscle and/or stored centrally/peripherally within the adipose tissue, a metabolic change noticed in individuals with insulin resistance and metabolic disease [42,103,105,307].

When taken together, these findings suggest that prolonged inactivity leads to an adverse integrated, systematic response from our body. Such negative effects occur to our insulino-

sensitive organs such as our musculature, adipose tissue and the liver affecting their sensitivity to insulin and fuel oxidation, dampening overall systemic metabolic flexibility.

Protein Metabolism

Although an important substrate for overall energy metabolism, protein metabolism only accounts for ~10-15% of total energy. Proteins are made of monomers, known as amino acids, which can be divided into non-essential (9) and essential amino acids (11) based on the ability of our body to endogenously produce them. These amino acids can be used by the liver or sent from the liver to other organs, such as the skeletal muscle, for protein synthesis. Protein synthesis is a process of transcription within the nucleus to generate the mRNA for translation with the tRNA in the ribosome situated in the cytoplasm. Translation, regulated by the activity of mTORC1 (mammalian target of rapamycin complex 1), of the tRNA with mRNA creates a polypeptide chain of these amino acids bound together via peptide bonds [545,451]. Most natural polypeptide chains contain between 50-2000 amino acid residues and are commonly referred to as proteins.

Protein degradation is the process of breaking down of protein into smaller polypeptides and amino acids. This process is initiated with the binding of ubiquitin to the lysine residue of the target protein. The ubiquitin tagging of the protein signals the action of proteasomes which subsequently degrades the protein into peptides and amino acids [252]. At normal physiological pH (7.35-7.45) amino acids are composed of a carbon back-bone, an amine group (containing nitrogen) and an R group.

As eluded to previously, whole body lean mass significantly decreases during bed rest, characterized by dramatic increases in skeletal muscle atrophy [33,125]. Animal models of disuse, such as models of hindlimb suspension or denervation suggest an initial decrease in protein synthesis followed by a predominant increase in protein degradation [511,408,77]. Interestingly, this is in contrast to what is seen in human models of disuse with inherent species differences helping to explain this. Total protein turnover in adult rats is 3-to 4-fold greater than in humans, while adult rat muscle protein synthesis rates are ~2.5-fold greater [396]. Thus, consideration must be given to the differences between models when making comparisons or generalisations. Studies of protein metabolism in bed rest support an initial increase protein degradation in the first few days of bed rest (~4 days) followed by a substantial decline in muscle protein synthesis (MPS) [146,47,498,397].

Moderate feeding at rest is one of the key stimulators of MPS, doubling its activity as can be seen in Figure 2.13. This dose-response relationship has been proposed to be mainly due to the increase

of in amino acid concentration [49,345]. By increasing MPS, the muscle net balance (muscle protein breakdown (MPB) > MPS) is reversed. Interestingly, after 14 days of bed rest there is a reduced rate of MPS, even in response to an increased amino acid provision [49]. Consequently, bed rest has a particular detrimental effect on protein metabolism, notably MPS, and is difficult to reverse.

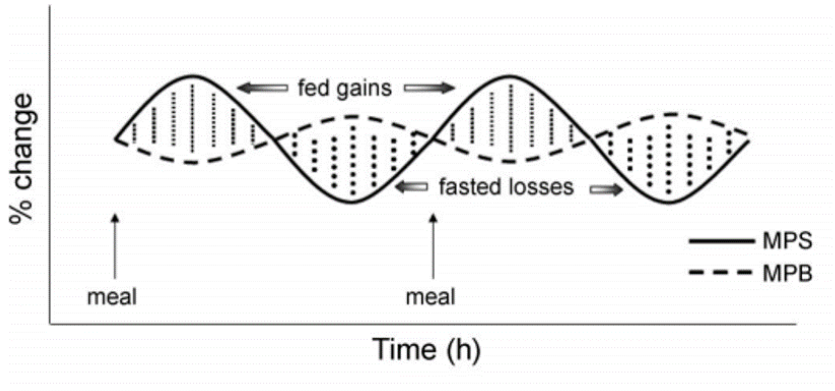

Figure 2. 13. Schematic representing percent change in muscle protein synthesis (MPS) and muscle protein breakdown (MPB) in response to feeding and starvation. *Burd et al.* [71]

Prolonged bed rest has been shown to significantly impair our antioxidant defence system (reduction in superoxide dismutase 1) and mitochondrial function. Increased oxidative stress with prolonged bed rest has been strongly considered as a potential trigger to the observed decline in protein synthesis and increase protein degradation This is represented clearly in Figure 2.14 (increased Murf-1, Astrogen-1, ATGs, FOXO1, NF-kβ) [66]. Animal models have identified a reduction in protein translation, and a subsequent decrease in protein synthesis, due to a reduced activity of mTORC1, to be one of the major drivers of skeletal muscle atrophy with disuse [563]. This is an interesting observation, given the regulatory role reactive oxygen species (ROS) appear to have on mTORC1 activity [314,169]. These findings complement the work by Drummond et al. [132] who concluded that 7 days of bed rest significantly blunted muscle protein synthesis, mTORC1 signalling, and amino acid transporter protein content in response to acute essential amino acid ingestion in healthy, older adults. Such adaptations suggest that a reduction in protein translation, due to reduced mTORC1 signalling, could be a major factor in the decreased protein synthesis observed during -6°HDT bed rest in humans.

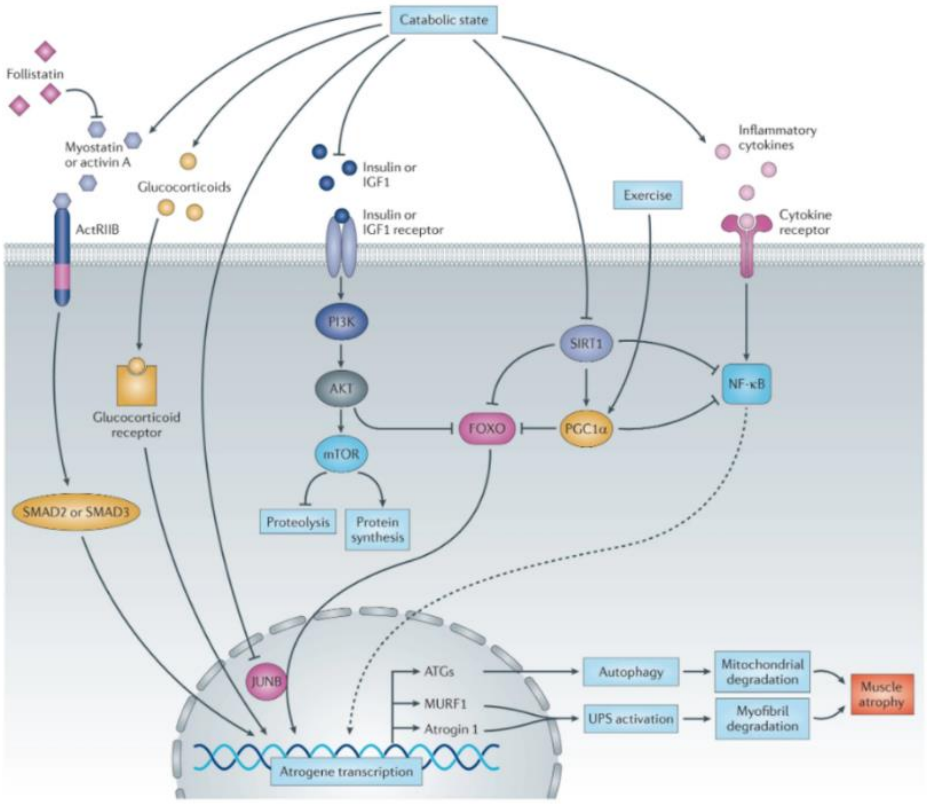

Figure 2. 14. Schematic representation of the multiple intracellular signalling pathways activated through muscle atrophy, including mTOR signalling. *Cohen et al.* [100]

Although its supply of ATP is significantly less to that of carbohydrate and lipid metabolism, protein metabolism has an extremely important role in substrate metabolism. Thus, protein metabolism should be taken into consideration when deducing the adverse effects prolonged bed rest has on skeletal muscle metabolism.

Conclusion

Bed rest results in a series of adverse physiological effects on skeletal muscle, comparable to what occurs in microgravity. These adaptations are represented not only by a decrease in muscle mass, strength and function but also by the shift in substrate oxidation at rest from fat to carbohydrate, along with the accumulation of lipid species and gradual intolerance to glucose. Given multiple studies have signified that changes in our metabolism may be the instigating factor for such adverse adaptations, a greater understanding of how metabolism is regulated and the role the mitochondria may have following bed rest is required.

Mitochondrial Function and Regulation of Energy Metabolism

Mitochondria in Brief

Discovered by Albert Von Kolliker in 1857, the mitochondria are highly specialised organelles, abundantly present in all mammalian cells, with the exception of mature erythrocytes, having multiple responsibilities within the cell. The mitochondria play a key role in energy metabolism via the production of energy in the form of adenosine tri-phosphate (ATP) in response to the energy demands of the cell [60]. This energy is generated from the ability of the mitochondria to convert nutrient equivalents into readily available energy equivalents, a process known as oxidative phosphorylation [418]. As discussed previously, prolonged bed rest has been shown to lead to significant alterations in fuel metabolism supported through decreased lipid oxidation, and decreased glucose tolerance. Subsequently, it is of importance to consider the structure and function of the mitochondria with respect to alternative environmental stressors, be that exercise or prolonged physical inactivity.

Mitochondrial Structure and Function

The mitochondria are double-stranded organelles composed of four distinct regions, the outer mitochondrial membrane (OMM), the intermembrane space, the inner mitochondrial membrane (IMM) and the mitochondrial matrix (see Figure 2.15). The OMM is a lipid rich, smooth and highly fluid layer, porous for small molecules (<10kDa) to freely pass through it, rendering the intermembrane space chemically similar to the cytosol [223]. In contrast, the IMM is protein rich, folded and compartmentalised [155]. The folding's of the IMM make up the mitochondrial matrix which is the location for five complexes forming the respiratory chain where oxidative phosphorylation takes place to generate energy in the form of adenosine triphosphate (ATP).

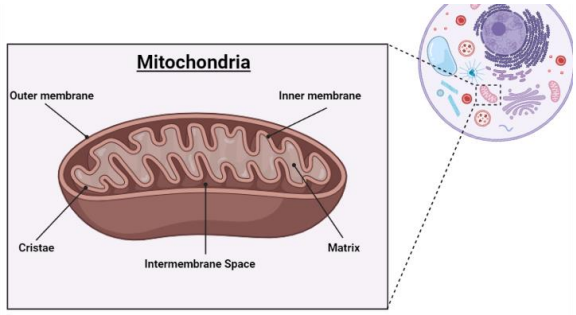

Figure 2. 15. Schematic representation of the structure of the mitochondria

Mitochondrial size and content is under dynamic regulation and is higher in those performing exercise training [261,436,348] while lower in those with type 2 diabetes [57,419,290]. This adaptive process is organised by a balance between mitochondrial dynamics, mitochondrial biogenesis and mitochondrial breakdown. The perpetual, cyclical process of mitochondrial dynamics enables the mitochondria to form larger or smaller mitochondria based on the energy demands in the cell and is a vital process to help maintain overall mitochondrial function. Exercise has been shown to increase mitochondrial size by inhibiting processes of mitochondrial fission, while increasing pathways relating to fusion [569,15,503]. This balance between fusion and fission allows the mitochondria to organize into a dynamic network within the cell, known as a reticulum resulting in a more efficient distribution of energy within the cell [270,335].

This network of elongated mitochondria becomes fragmented when there is an imbalance in dynamics. An example of this occurs with muscle atrophy as a consequence of physical inactivity, resulting in a reduced expression of mitochondrial transcripts relating to fusion [506]. This is comparable to what occurs to type 2 diabetics, which could explain the decrease in mitochondrial size as mentioned previously [582,453], and could be an integral step towards the changes in substrate metabolism linked to physical inactivity.

The skeletal muscle is composed of two distinct mitochondrial subpopulations, both of which are characterised by their location in the cell which are underlined in Figure 2.16. These are the intermyofibrillar (IMF) and subsarcolemmal mitochondria (SSM) [99] and have distinct functions based on their composition and cellular location. The intermyofibrillar mitochondria contains a greater amount of proteins associated with oxidative phosphorylation coupled with higher respiratory chain complex activity while the subsarcolemmal mitochondria are involved in actions associated with signal transduction and substrate transport [149]. Considering these distinct differences it has been observed that SSM decrease by up to 33% following immobilisation and

IMF mitochondria decrease by just 20% [370]. These differences emphasise the plasticity and efficiency of the skeletal muscle with regards to energy metabolism but also signify a possible hierarchy within the mitochondrial subpopulations adaptation to reduced activity.

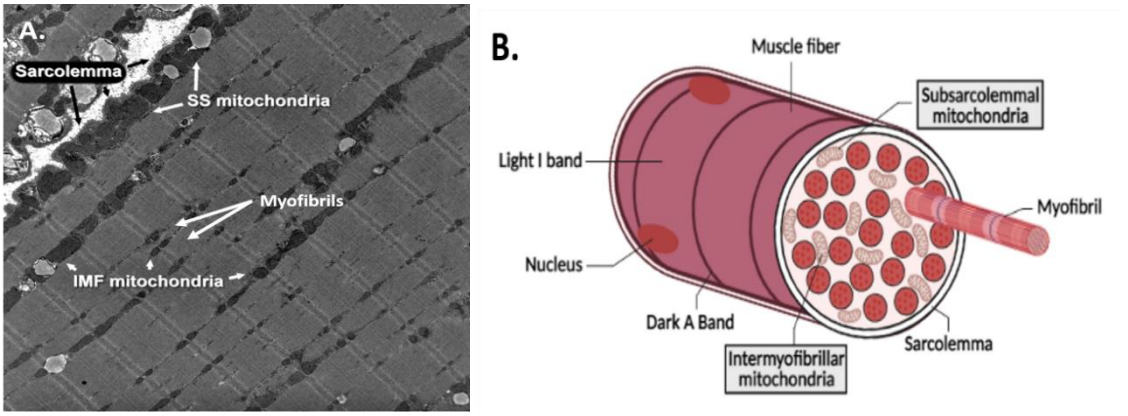

Figure 2. 16. (A) Micrograph (x 11,400 magnification) of a skeletal muscle cell illustrating intermyofibrillar (IMF) and subsarcolemmal (SS) mitochondria [92] & (B) Schematic representation of muscle fiber with labelled IMF & SS mitochondria location within the muscle cell

The mitochondria are highly specialised, dynamic organelles within the cell, adapting to the cellular demands. Increasing our understanding of the mitochondria and ways to counteract its dysfunction in response to different environmental stimuli such as physical inactivity, has been a priority in the field of aging and health for many years.

Oxidative Phosphorylation

Oxidative phosphorylation (OXPHOS) refers to the process of storing energy in the form of ATP generated by the mitochondria. The process of ATP generation is a coordinated series of redox reactions catalysed by the respiratory chain and electron shuttles in the mitochondrial intermembrane space (flavoproteins, iron-sulphur protein, ubiquinone and cytochome) [283]. Electrons derived from metabolic reducing equivalents (NADH and $FADH_2$) are fed into the ETC through complex I or II and eventually pass to molecular O_2 at complex IV to form H_2O. As electrons are transferred through the respiratory chain, protons are ejected from the mitochondrial matrix through complexes I, III, and IV to the intermembrane space, establishing a proton gradient ($\triangle P$). The generation of the proton gradient ($\triangle P$) across the inner membrane through the process of oxidative phosphorylation is coupled to ATP synthesis, a process first proposed by Peter Mitchell in 1961 (the chemiosmotic theory) as represented in Figure 2.17. $\triangle P$ dissipates when protons move back in, mainly through the large F_0/F_1 ATP synthase.

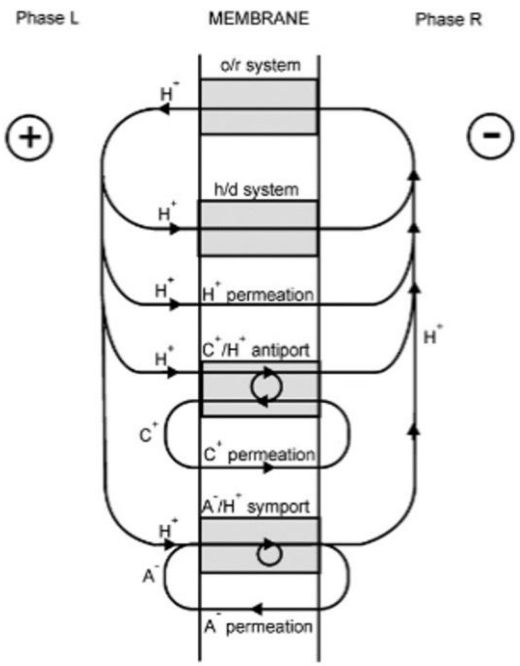

Figure 2. 17. Peter Mitchell's 'coupling through proton circuits' from Mitchell's first 'little grey book' [369]

The activity of ATP synthase catalysis the generation of ATP from the previously created ADP and inorganic phosphate (Pi). For each NADH from the krebs cycle (tricarboxylic acid (TCA)) that enters the ETC, 3 pairs of protons are pumped out of the mitochondrial matrix. The process of proton pumping and ATP generation is, for the most part, coupled. However, proton leak back through the membrane and into the mitochondrial matrix is responsible for uncoupling substrate oxidation and ATP synthesis. Each complex is oxidised when it passes an electron and is reduced when it receives an electron. This consistent movement along the chain, and not backwards, is due to the fact that each complex further along the chain has a greater affinity for an electron in comparison to the previous complex. The location and role of the mitochondrial respiratory chain for ATP generation is further eluded to in Figure 2.18. The capacity of each complex on this respiratory chain to function optimally is of crucial importance for overall oxidative capacity of the mitochondria.

Given this role, it is of no surprise that reactive oxygen and nitrogen species (ROS & RNS), by-products of oxidative phosphorylation, have been proposed to lead to mitochondrial dysfunction. ROS, RNS and superoxides are formed in the electron transport chain, particularly with the Q cycle when transferring an electron between complex I and III or/and complex I to complex II to QH_2. In normal circumstances the activity of superoxide dismutase (SOD) acts on these superoxides, converting them to hydrogen peroxide. Increases in ROS and RNS (i.e. when the above does not

occur efficiently) have been proposed as one of the leading causes of “secondary aging” due to the damaging role high levels of ROS and RNS have been proposed to have [51,408,426].

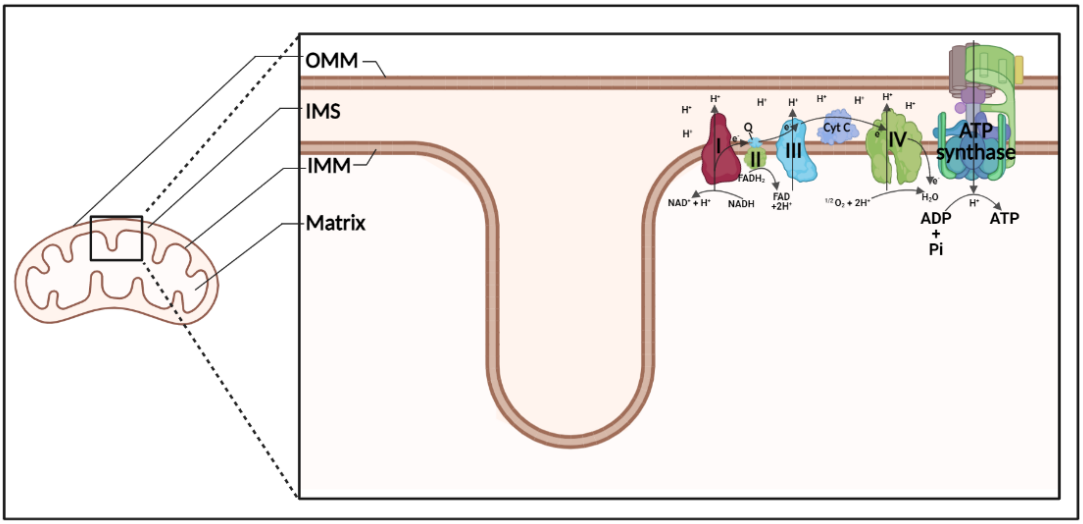

Figure 2. 18. Schematic representation of the components of the mitochondrial respiratory chain for ATP generation

Mitochondrial Regulation

In order to achieve its overall aim and function in cellular respiration and energy metabolism, the mitochondria are regulated by a series of interlinked, continually adapting processes within the mitochondrial life cycle (see Figure 2.19). This is regulated by mitochondrial biogenesis, mitochondrial fusion-fission dynamics and mitochondrial breakdown (mitophagy). Mitochondrial function is largely dependent on their number and size, which are principally determined by the balance between these complex processes. These highly conserved, innate processes facilitate a network of organelles well-adapted to requirements imposed upon them by their external environment.

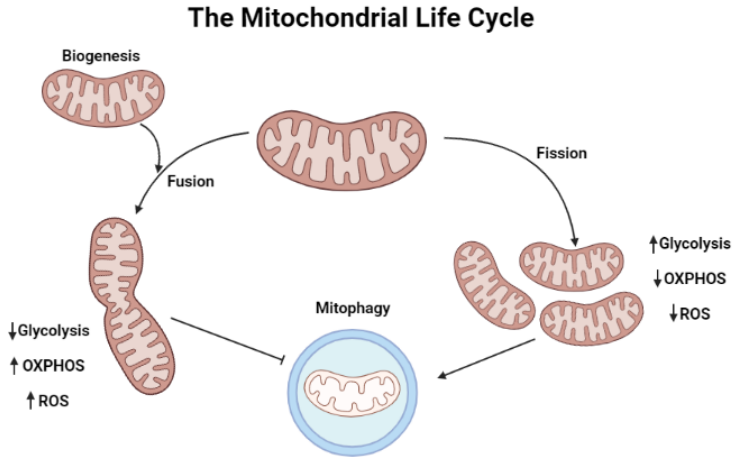

Figure 2. 19. The mitochondrial life cycle and the inter-relationship between biogenesis, dynamics and mitophagy. Adapted from *Bordi et al.* [53]

Mitochondrial Biogenesis

Mitochondrial biogenesis is the synthesis and expansion of mitochondrial networks in response to the cellular demands [268]. For mitochondrial biogenesis to occur there is a need for the coordination of nuclear and mitochondrial genomes (given that all but 22 mitochondrial proteins are nuclear-encoded) [249]. The management and coordination of these genomes is regulated by peroxisome proliferator-activated receptor (PPAR) gamma coactivator-1 (PGC-1) as can be seen in Figure 2.20. Also known as the "master regulator", PGC-1 co-activates a wide range of transcription factors which serve to coordinate the regulation of mitochondrial and nuclear genomes. These include nuclear respiratory factor 1 and 2 (NRF-1/2), peroxisome proliferator-activated receptor γ (PPARγ), estrogen-related receptors (ERRs) and mitochondrial DNA-specific transcription factor A, transcription factor A of the mitochondria (Tfam) [268,302]. PGC-1 has two isoforms, PGC-1α and PGC-1β, both of which have overlapping and differing effects [355]. PGC-1α

has been extensively studied in the literature. Less can be said for PGC-1β but, like PGC-1α, it is necessary for mitochondrial activity, by increasing mitochondrial uncoupling, and biogenesis, through its regulation of mitochondrial volume [484,581].

Given the importance of this transcription coactivator in skeletal muscle mitochondrial content and activity and its sensitivity to a series of stimuli such as Ca^{2+}, reactive oxygen species (ROS) and imbalances in energy, it is highly relevant in the field of metabolism relating to both activity and inactivity. One of the first changes following aerobic exercise training is an increase in mtDNA:nDNA ratio, a primary step in mitochondrial biogenesis supported by enhanced PGC-1α expression in the skeletal muscle. While physical activity increases mitochondrial biogenesis, physical inactivity has the opposite effect as demonstrated by significant reductions in PGC-1α expression and the mtDNA:nDNA ratio following bed rest [435,66,235,264,488].

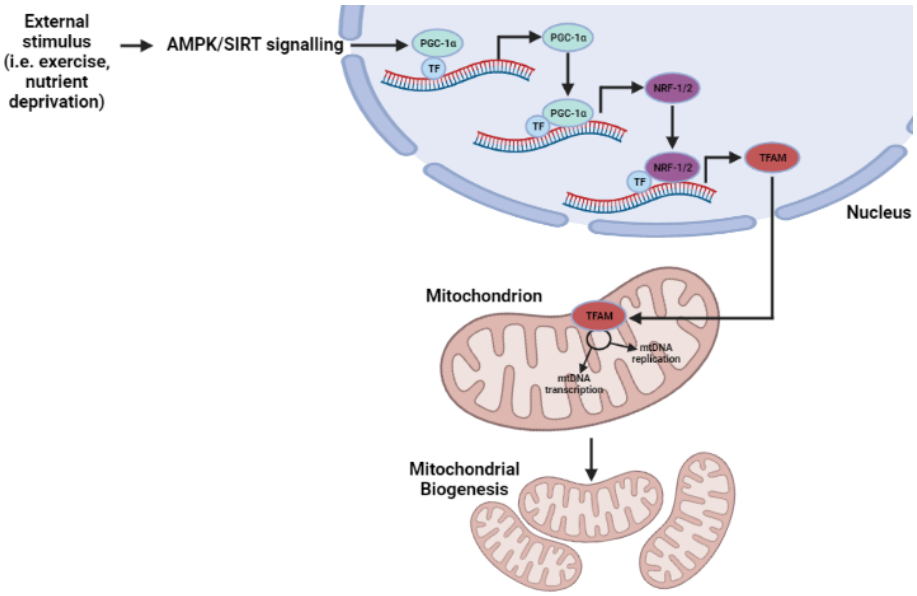

Figure 2. 20. Schematic representation of the regulation of mitochondrial biogenesis. Adapted from *Picca et al.* [398]

As PGC-1α has not only been described as a master regulator of biogenesis but also a metabolic sensor, changes in its expression/activity in response to environmental stimuli, such as inactivity, demonstrate its importance to mitochondrial content and cellular bioenergetics. Two other metabolic sensors, AMP-activated protein kinase (AMPK) and NAD^+-deacetylases and ADP-ribosyltransferases from the sirtuin family (except for SIRT7), have been described to directly impact PGC-1α activity and expression [79,382,127,280,69,61,532,87].

AMPK is one of the main sensors of cellular energy status activated in response to stress (i.e. exercise, AICAR, metformin) and is involved in multiple pathways, as can be seen in Figure 2.21. By sensing increases in the AMP:ATP and ADP:ATP ratios [164,212,171], AMPK restores energy balance by inhibiting ATP-consuming biosynthetic pathways, while promoting catabolic pathways that regenerate ATP through the breakdown of macromolecules such as those relating to glucose/lipid oxidation [220]. Less is known about AMPK's response to bed rest [433,73]. Although, considering its direct phosphorylation and activation of PGC-1α [243], and PGC-1α's decreased expression in response to bed rest, it would be logical to assume AMPK would decrease in expression/activity. Despite this, proteomic analysis of skeletal muscle biopsies following 24 days of bed rest indicates no change in AMPK signalling proteins [66]. Thus, PGC-1α's response to bed rest has been touted to be independent of this, although AMPK protein changes do not necessarily reflect enzymatic activity.

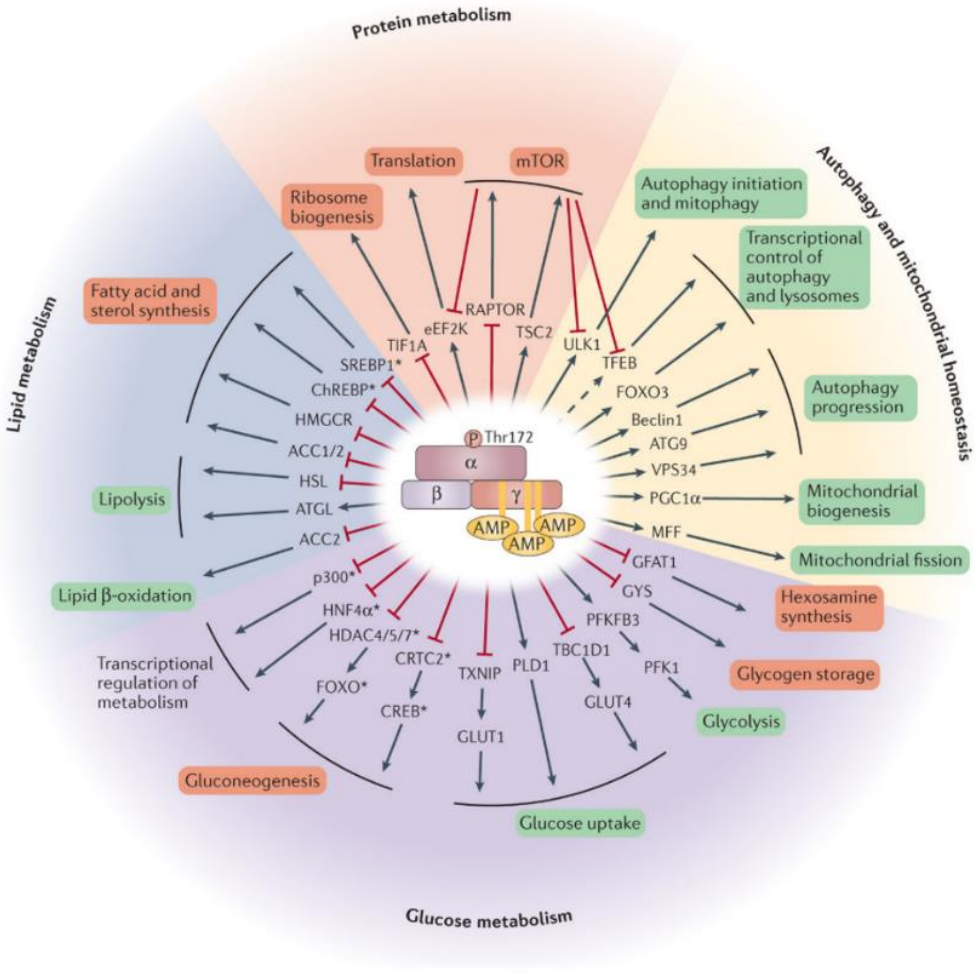

Figure 2. 21. AMPK regulates a variety of metabolic processes, [220]

Sirtuins are a group of seven highly conserved NAD^+-dependent histone deacetylases and ADP-ribosyltransferases (see Figure 2.22 for more information) involved in many biological processes, particularly in the regulation of energy metabolism [294,81,215,102,195]. The requirement of NAD^+ and ADP-ribose in sirtuin catalyzed reactions is fundamental to their regulation and enables sirtuins to directly respond to changes in intracellular metabolism, promoting ATP synthesis. Given the majority of mitochondrial metabolic enzymes are differentially acetylated according to the nutritional state of the cell, there is much to suggest that acetylation regulates cellular metabolism and coordinates substrate switching [542,579,557].

As AMPK is the energy sensor in the cell, there is evidence to support that it regulates members of the sirtuin family [570,382,497,221,315,499,107,552,574]. While there is further evidence to support that AMPK may be SIRT-dependent, particularly SIRT1, SIRT3 and SIRT5 [166,80,69,575,232], creating an argument for an AMPK-SIRT cycle. Although still a matter of debate, evidence in the literature support this, particularly considering its direct regulation of

PGC-1α, akin to AMPK. In spite of this, both AMPK and member of the SIRT family could have different responses to different environmental stimuli [367,64,9,535,226]. There is insufficient evidence to date to determine the other members of the SIRT family involved in the regulation of AMPK but what is available supports that they are AMPK-dependent.

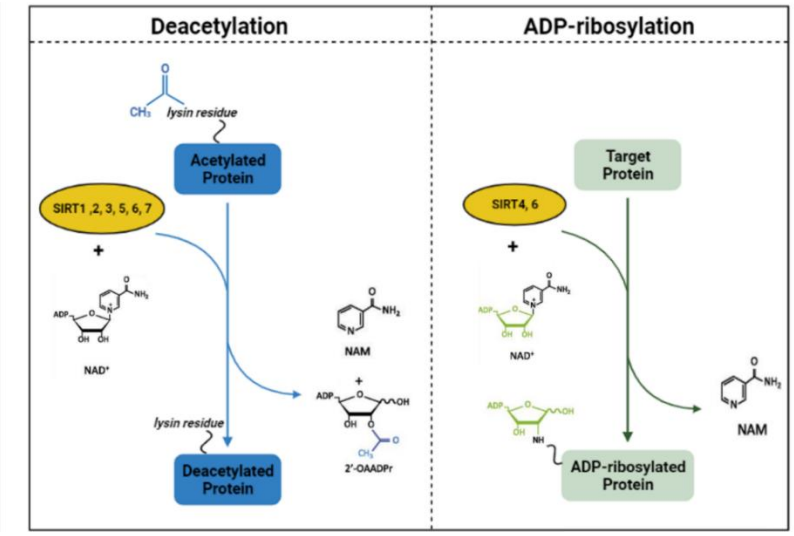

Figure 2. 22. Sirtuins are a family of NAD+ histone deacetylases and ADP-ribosyltransferases. Adapted from *Morigi et al.* [353]

As with AMPK, there is limited work on the impact of bed rest on skeletal muscle SIRT expression, although one study in particular by Ringholm et al. [435], reported a significant decrease in SIRT1 expression following 7 days of bed rest. This was supported by Brocca et al. [66] who did not find a change in AMPK activity but did observe a significant reduction in PGC-1α. Buso et al. [73] also reported a sirtuin dependence of PGC-1α following bed rest, reporting a decrease in SIRT3 expression, a mitochondrial sirtuin known to be sensitive to energy demanding stimuli such as exercise [382,61,532].

This evidence suggests an AMPK-SIRT-PGC-1α axis which adapts differently based on the environmental stimulus in order to regulate mitochondrial biogenesis and cellular metabolism. The literature strongly supports the role that PGC-1α has in regulating mitochondrial biogenesis in skeletal muscle, characterized by increased oxidative phosphorylation and overall muscle performance with exercise and opposing responses throughout bed rest.

Mitochondrial Quality Control (Mitophagy)

Mitophagy is the mitochondrial equivalent to autophagy (i.e. lysosome-dependent degradation of organelles and macromolecules). It is a quality control measure to ensure the removal and breakdown of poorly functioning, damaged mitochondria from the cell. [346,528,555,565].

Damaging events, such as when mitochondria are exposed to high levels of reactive oxygen species (ROS) during oxidative phosphorylation or through natural mitochondrial protein mutation lead to mitochondrial removal. This process of degradation is similar to the removal of damaged cells in that the target, being the damaged mitochondria in this circumstance, is initially recognized by the phagophore. The phagophore subsequently goes through a process of elongation to engulf the damaged mitochondria creating an autophagosome surrounding the target. The autophagosomes subsequently fuse with lysosomes containing hydrolases creating an autophagolysosome. Once mature, this autophagolysosome containing the damaged mitochondria is removed and degraded [14,130].

In addition to the clustering of LC3b II there is an accumulation and activation of the serine/threonine kinase PTEN-induced putative kinase 1 (PINK1) to the mitochondrial outer membrane. Under normal conditions, PINK1 is imported through the TOM complex of the OMM and into the TIM complex of the IMM where it is cleaved by the mitochondrial processing peptidase (MPP) [400] and presenilin-associated rhomboid-like protein (PARL), an inner mitochondrial membrane protein. However, when the mitochondria become uncoupled and damaged, identified by a low or collapsed mitochondrial membrane potential, PARL is unable to cleave PINK1 [96,565] leading to an accumulation of PINK1 on the OMM. PINK1 acts as a flag of mitochondrial damage/degradation to the rest of the cell, signalling the recruitment of Parkin, a cytosolic E3-ubiquitin ligase, and a polyubiquitin chain into the cytosol. The subsequent activation of Parkin leads to the ubiquitination of outer mitochondrial membrane proteins (such as mitofusins 1 and 2, preventing mitochondrial fusion) [182,91]. This Parkin-mediated ubiquitin binding flags the damaged mitochondria for phagophore recruitment.

The formation of the phagophore is initially triggered by a cascade of signalling events, beginning with the activation of a family of proteins known as the Atgs (autophagy related genes), of which there are 5 members (Atg1, Atg5, Atg 6, Atg 7, and Atg14) [555,130]. While it enters its final stage of activation LC3b II becomes cleaved from the phagophore membrane along with p62/SQSTM1 to facilitate the recruitment of damaged mitochondria to the phagophore. LC3b II subsequently interacts with BCL-2/adenovirus E1B interacting protein 3 (BNIP3) or by p63/SQMT1-dependent clustering of ubiquitinated mitochondria [465] locking the phagophore to the damaged mitochondria leading to the eventual proteasomal degradation of outer mitochondrial membrane proteins and mitochondrial engulfment [368,5]. This process of mitophagy is represented schematically in Figure 2.23.

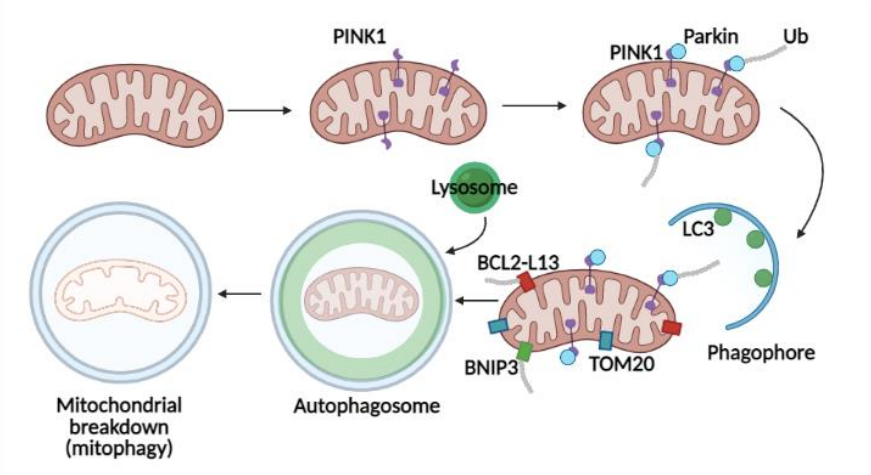

Figure 2. 23. Schematic representation of the process of mitochondrial breakdown and removal (mitophagy)

Given the importance of maintaining healthy mitochondria for overall cellular function, the process of mitophagy is continually occurring with the half-life of mitochondria varying from tissue to tissue [561]. Dysregulation of this finely balanced system can occur from alterations to many systems within the cell from dysfunctional dynamics [529,553] to alterations in energy metabolism. As with biogenesis, defects to members of the sirtuin family have been identified as key players in that regard, particularly SIRT1 [460,554], SIRT2 [311,320,472], SIRT3 [114,417,567] and SIRT5 [406,540] all of which have been shown to regulate PINK1-Parkin mediated mitophagy.

Neurological disorders such as Parkinson's disease, Alzheimer's disease and Huntington's disease are states strongly linked to dysfunctional regulation of mitophagy [89,14,368,487,561]. In making such a point, mitophagy has also been associated with cancer, with metabolic-reprogramming in cancer cells being associated with decreased mitophagy and increased mitochondrial biogenesis [131], cardiovascular disease, with mitophagy factors proving to be both protective and damaging, and renal dysfunction [63,561].

Subsequently, the process of mitophagy is intimately linked with mitochondrial biogenesis, impacting upon its overall function. However, another regulator of mitochondrial function, mitochondrial dynamics, is imperative in maintain an overall healthy mitochondrial environment.

Mitochondrial Fission/Fusion (Dynamics)

Mitochondria constantly undergo biogenesis but also undergo a process of reshaping and phenotypic modification that is critical to the regulation of mitochondrial integrity, number and their distribution in the cell; these processes are important in the control of skeletal muscle mass and function [565,341,444,450]. The dynamic, repetitive, morphological adaptations to the

mitochondria are highly controlled, in fine balance and are instigated by two opposing processes on the inner and outer mitochondrial membranes: mitochondrial fusion (binding of mitochondria together) and fission (dividing of mitochondria into multiple segments) [565,486].

Mitochondrial Fission

Mitochondrial fission, of which there are two forms, mitochondrial partitioning and mitochondrial pinching (see Figure 2.24), is a multifaceted process of mitochondrial division. Pinching and partitioning, of mitochondria take place throughout the muscle fiber (subsarcrolemmal/intermyofibrillar), something which is not the case in all tissues. Partitioned mitochondria are solely found among the subsarcolemmal mitochondria (SSM), and pinching predominating in the intermyofibrillar (IMF) mitochondria in skeletal muscle and cardiac tissue [504]. Both SS and IMF mitochondria have been discussed previously under section 'Mitochondrial Structure and Function'.

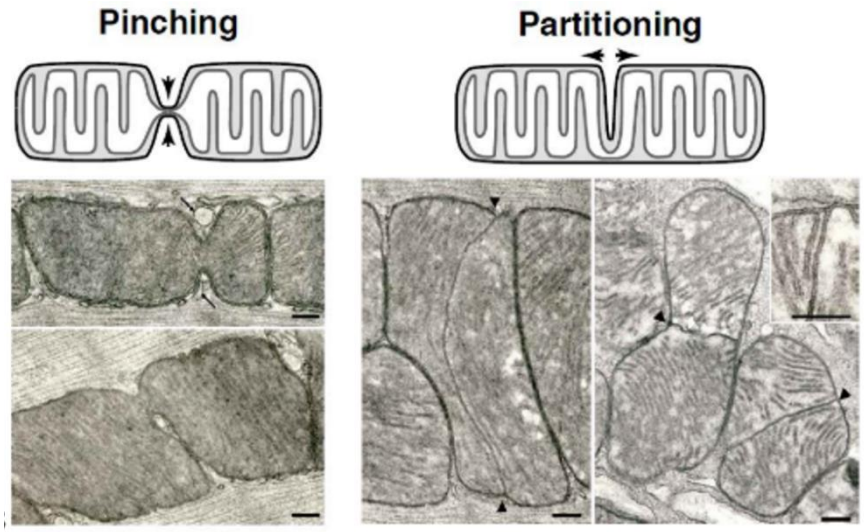

Figure 2. 24. Mitochondrial fission proceeds through two alternative mechanisms termed pinching and portioning. *Tandler et al.* [504]

Mitochondrial fission has been compared to a mitochondrial "stress test", a vital contributor to the mitochondrial quality control (mitophagy) process in the cell. Following a fission event, when one mitochondrion is divided into two daughter mitochondria, one of these daughters in most circumstances is transiently hyperpolarized (with an accumulation of debris) and the other is in a steady state. Mitophagy-mediated mitochondrial removal of damaged, hyperpolarized mitochondria is triggered ("selective disposal theory) [528,565] and so the process of dynamics and removal are intertwined for maintaining cellular health and optimal mitochondrial function.

The process of mitochondrial fission is initiated by Drp1 (Dynamin related protein 1) in the cytosol and a number of proteins located on either the IMM or OMM, including Fis1 (mitochondrial fission protein 1), Mff-1 (mitochondrial fission factor-1), MiD49 (Mitochondrial dynamics protein 49 also known as Mitochondrial elongation factor 2), MiD51 (Mitochondrial dynamics protein 51 also known as Mitochondrial elongation factor 1) [504], all of which are represented schematically in Figure 2.25.

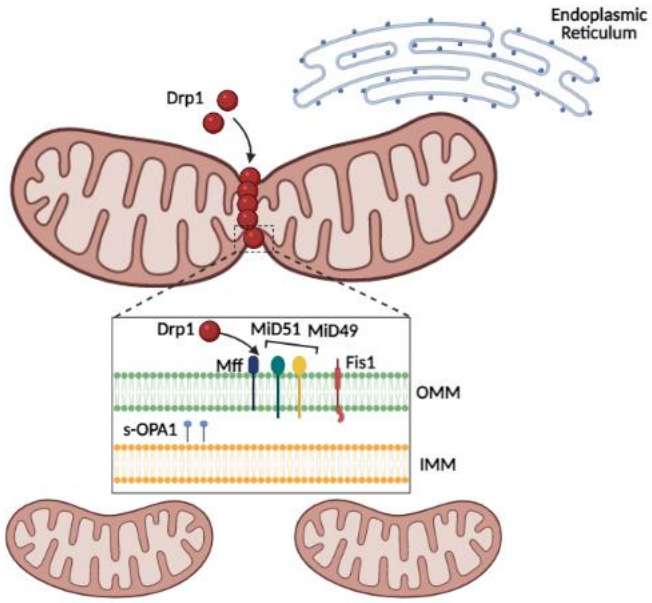

Figure 2. 25. Schematic representation of mitochondrial fission and its instigators. Adapted from Wai & Langer [539]

Environmental stressors such as physical activity, physical inactivity and nutritional excess are the main instigators of the mitochondrial fission process [539]. However, the initial factors in mitochondrial fission appear more complex. Limited work has been completed on such initial factors of inner mitochondrial membrane fission within the human model.

Dynamin related protein 1 (Drp1)

Drp1 is a protein containing four domains; the N terminal GTP binding site, the middle, the insert B and the C-terminal Guanosine Triphosphatase (GTPase) effector (GED) [228]. Insert B, also known as the variable domain, has been identified as the critical domain for mitochondrial fission as this is the site for binding of the target membrane. Importantly, none of these domains are membrane localizing, transmembrane or membrane anchoring and therefore Drp1 needs to be actively recruited to the mitochondrial surface, and anchored to receptors on the OMM, in order to execute its function [568]. The action of Drp1-dependent mitochondrial fission can be divided into: 1) translocation of Drp1 to the outer mitochondrial membrane (OMM) from the cytosol

where it resides, 2) subsequent higher-order assembly, 3) GTP hydrolysis, and ultimately disassembly [228].

The recruitment of Drp1 occurs when the mitochondrial fission process protein 1 (MTFP1 also known as mitochondrial fission process 1,18 kDa (MTFP18)) (de)phosphorylates Drp1, resulting in its translocation from the cytosol to the OMM [354]. Mff, miD49 and miD51 are anchored along the OMM and recruit Drp1 to the mitochondrial surface where it oligomerizes into ring-like structures at future sites of division binding [568]. Drp1 leads to the constriction process but not the cleavage during division. The mitochondrial abscission has yet to be understood however most research seem to point to another GTPase, dynamin 2 (DNM2), and/or the action of the endoplasmic reticulum (ER-mitochondria contact sites – ERMCS) as the mediators completing the fission process, which are represented in Figure 2.26 [379,161,305,415,539,278,537,504].

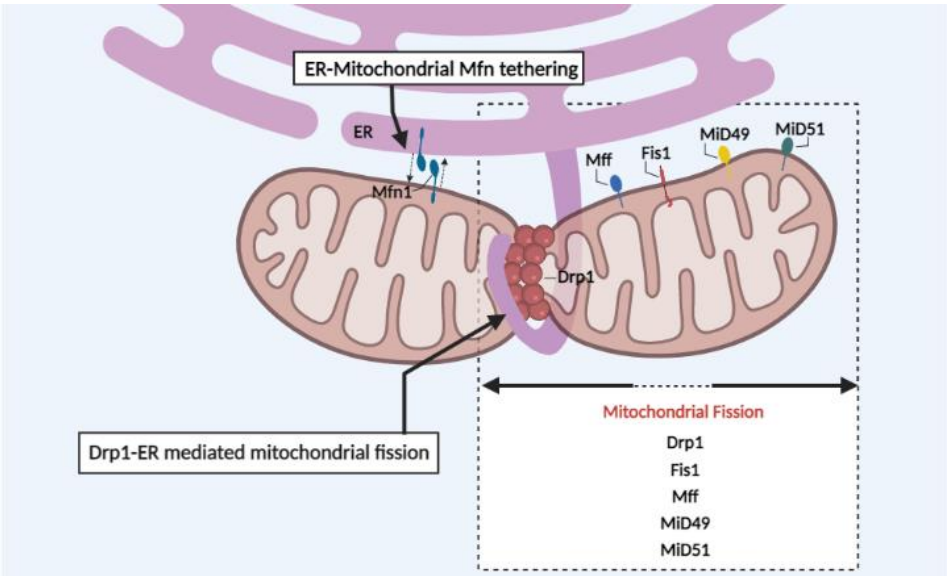

Figure 2. 26. Schematic representation of ER-mediated mitochondrial fission. Adapted from *Sebastian et al.* [467]

Drp1 has three phosphorylation sites related to mitochondrial fission, serine 600, serine 616 and serine 637 all of which are independently regulated. Drp1 increases mitochondrial fission when phosphorylated at serine 600 ($pDrp1^{ser600}$) by calmodulin-dependent protein kinase Iα (CaMKIα) or serine 616 ($pDrp1^{ser616}$) by cyclin-dependent-kinase 1 (CDK1). Phosphorylation at serine 637 ($pDrp1^{ser637}$) by protein kinase A (PKA) decreases fission activity and the dephosphorylation of Drp1 at serine 637($pDrp1^{ser637}$) by calcineurin (Ppp3) will increase mitochondrial fission [203,583,173]. Thus, CaMKIα, CDK1, PKA and Ppp3 are all physiological regulators of mitochondrial dynamics and in particular mitochondrial fission. However, other pathways such as

those relating to SIRT3-FOXO3, SIRT4 and p53 mediated apoptotic pathways, among others have also been noted to induce Drp1 expression [524,151,163].

The majority of the work examining the regulation of Drp1 has focused on Calcineurin, a ubiquitously expressed calcium-sensitive serine-threonine phosphatase. As Ppp3 is activated by an influx of intracellular calcium, it is therefore considered a key signalling node conveying environmental stimuli into an adaptive response. Ablation of calcineurin [395] leads to hyperphosphorylation of pDrp1^{s637} (inhibiting Drp1 activity) resulting in an increase in mitochondrial elongation and increased complex IV and ATP synthase activity in skeletal muscle. This is similar to the response when PKA-dependent phosphorylation of Drp1^{ser637} is activated by nutrient deprivation [187,421,354].

This hyperfusion is in contrast to the effect of skeletal muscle Drp1 overexpression which leads to a decrease in mitochondrial area and swelling in the tibialis anterior muscle, mediated by pDrp1^{s616} [576]. This is associated with multiple mitochondrial functional defects, accelerated mitochondrial breakdown and increased FGF21, a common marker of mitochondrial disease and highly correlated with metabolic disease such as type 2 diabetes and obesity [516,181], emphasising the importance of a balance in fusion and fission. Under normal circumstances, the action of Drp1 is thought to be protective in order to prevent excessively high/low calcium concentrations from having a detrimental effect on mitochondrial homeostasis.

Drp1 is an extremely important factor in overall mitochondrial homeostasis due to its function in mitochondrial fission. However, it is clear that there are many other Drp1 independent mitochondrial fission mechanisms including Fis1.

Fis1, MiD49, MiD51 & Mff

Another mitochondrial fission protein, mitochondrial fission protein 1 (Fis1), is situated on the OMM. This is joined by several other mitochondrial fission proteins such as MiD49, MiD51, and Mff. The role of Fis1 is currently a matter of debate. In yeast, Fis1 has been shown to recruit Drp1 to initiate Drp1-mediated mitochondrial fission. Although Fis1 is evolutionarily conserved from yeast to humans, in mammalian cells it has been suggested that Fis1 plays a greater role than just recruitment of Drp1. A number of studies have shown that Fis1 appears to compete for Drp1 binding [228,316], while others show that Fis1 blocks mitochondrial fusion [566] and has a distinct role from fission by increasing mitophagy, apoptosis, mitochondrial motility and inter-organelle communication, all of which can be seen schematically in Figure 2.27 [241,379,234].

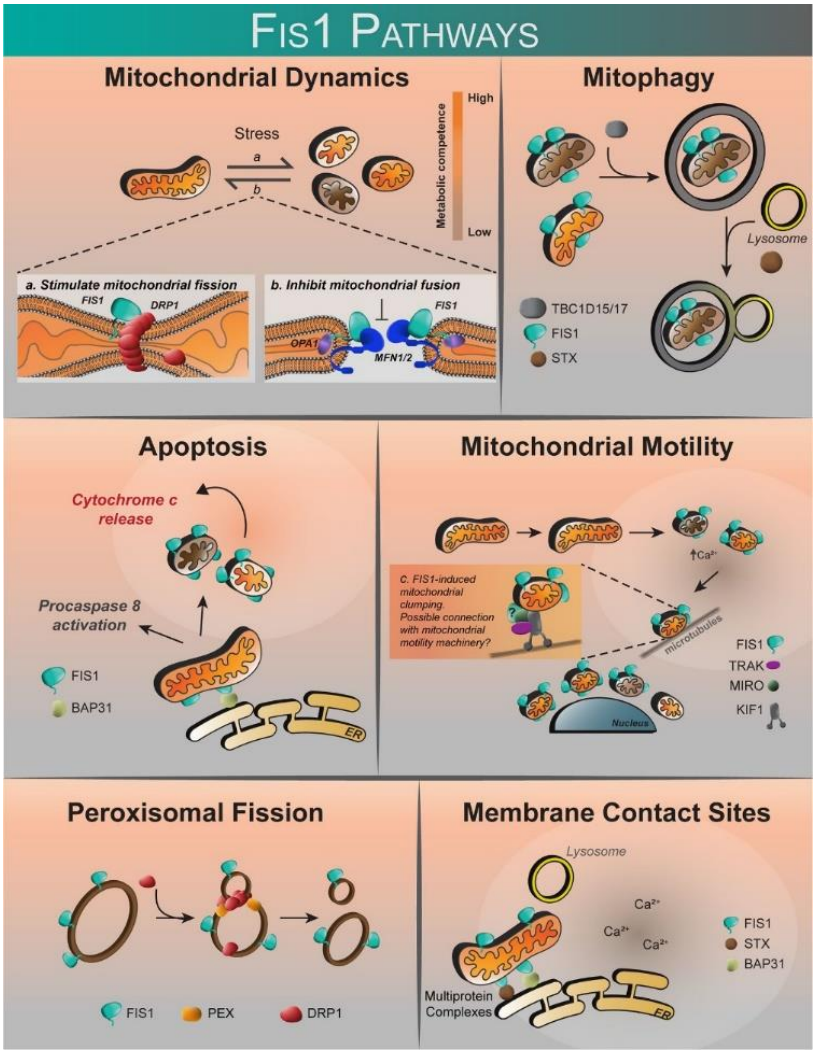

Figure 2. 27. Fis1 is proposed to have multiple regulatory roles within the cell. *Inhenacho et al.* [234]

Some argue that this multi-functional role is due to the fact that there are numerous mitochondrial fission proteins which, when present, elevate Fis1 from its original Drp1 recruitment role, to binding and inhibiting the GTPase activity of certain mitochondrial fusion regulators. Fis 1 over expression leads to increased mitochondrial division initiated by an imbalance in fusion and fission [566]. Fis1 conditional knockout animal models result in type 1 skeletal muscle (mitochondrial dense) mitochondrial hyperfusion/elongation, defects in the mitochondrial respiratory chain (impaired OXPHOS capacity and decreased Complex 1 function), and an increase in mitophagy, supported by excessive LC3 accumulation [566,576].

Mff, MiD49 and MiD51 have also been proven critical in the regulation of mitochondrial dynamics by recruiting Drp1 from the cytosol to initiate mitochondrial division. However, which of the three (Mff, MiD49/51) is of most importance (if any) is still up for debate. It is speculated that each are

present on the OMM of all cell types but the importance of their role is very much cell-type specific [326].

Mitochondrial fission plays an integral role in overall cellular homeostasis, increasing mitochondrial number to contributing to mitochondrial quality control. However, the process of mitochondrial division is in fine balance with the other regulator of mitochondrial dynamics, mitochondrial fusion. An imbalance in this tightly controlled process can lead to significant cellular disruption and metabolic disease.

Mitochondrial Fusion

Fusion of the mitochondria is an intricate two-step process where the outer and inner mitochondrial membranes fuse by separate events through regulation of Mitofusin 1 (Mfn1), Mitofusin 2 (Mfn2) and Optic Atrophy 1 (OPA1) (see Figure 2.28). Such activity of the mitochondria is said to ensure maximal oxidative capacity and is therefore a vital process for overall cellular metabolism and mitigation of cellular stress (through mixing of contents of partially damaged mitochondria) [565,395]. In addition to its essential role in energy provision, fusion between mitochondria may also act to rescue mitochondria with mutations by cross-complementation. Such fusion between poorly functional mitochondria can act to mitigate the effects of environmental damage through the exchange of proteins and lipids between mitochondria. This mitochondrial component sharing is thought to be a compensatory mechanism to maintain cellular homeostasis, as long as the mutation load within fusing mitochondria remains below 80-90% per cell [565]. For this reason, mitochondrial fusion has a multifaceted role from maintaining a mitochondrial reticulum to cellular homeostasis.

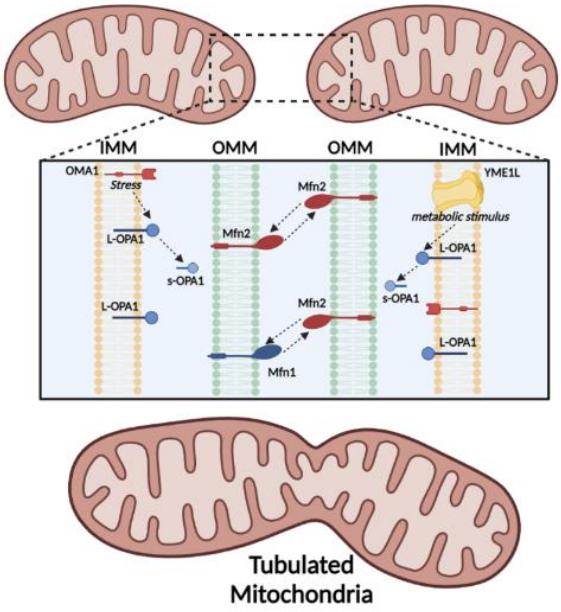

Figure 2. 28. Schematic representation of mitochondrial fusion and its main instigators. Adapted from Wai & Langer [539]

Outer Mitochondrial Membrane Fusion

Mitofusin 1 and 2 (Mfn1 and Mfn2) are highly conserved dynamin-like GTPases of the outer mitochondrial membrane, vital for the overall integrity of the mitochondrial structure acting as regulator proteins in the biogenesis and maintenance of the mitochondrial networks [84,444]. Both Mfn1 and Mfn2 are homologs of the fuzzy onion protein (fzo) sharing a 63% identity to each other, with the same relevant functional domains [583]. Their full function is imperative for the two step process of mitochondrial fusion, initiated by the tethering of two adjacent mitochondria on their membranes by specific Mfn1/Mfn2 domains followed by the GTPase docking of both membranes prior to final fusion.

Mitofusin 1 (Mfn1)

Mitofusin 1 is a transmembrane GTPase protein with two separate and well conserved domains, the HR2 (heptad-repeat domain 2) and the HR1 domain, also known as the GTPase domain. Both the HR2 and the GTPase domains are exposed to the cytosol anchored to the OMM. The HR2 domain has been proposed to be involved in tethering to adjacent mitochondria while the fusion between the adjacent mitochondria depends on the activity of the GTPase domain. An inhibition of the GTPase activity leads to a reduced capability of the mitochondria to elongate and fuse while reduction in the activity of the HR2 domain results in reduced mitochondrial tethering [583]. The

purpose of Mfn1 and Mfn2 are not fully understood considering both appear to have very similar physiological functions. Studies in mice suggest that Mfn2 is of more importance than Mfn1 with regards to overall mortality and pathology with Mfn1 function only considered of importance for placenta development during gestation [565]. Mutation of Mfn1 is highly correlated with the development of both optic atrophy and 3-methylglutaconic aciduria type 3, a neuro ophthalmologic syndrome.

Mitofusin 2 (Mfn2)

Originally called, mitochondrial assembly regulatory factor (MARF), mitofusin 2 has the same functional domains as Mfn1 but has lower GTPase activity and a higher affinity for GTP in comparison to Mfn1 [583]. The function of Mfn2 is similar to that of Mfn1 but it is expressed on the OMM and the ER and therefore appears to have more than just a role in mitochondrial fusion [65].

Mfn2 has been proposed to contribute to the maintenance and operation of the mitochondrial network. Inhibition/knockout studies highlight how repression of Mfn2 results in significant functional alterations in the mitochondria, such as reduced glucose oxidation, a reduction in mitochondrial membrane potential, a reduction in cell respiration, and an increase in mitochondrial proton leak [16,583]. Given Mfn2 also appears to tether the ER to the mitochondria, knockout disrupts the ER morphology, loosening the ER-mitochondrial interaction, increasing the distance between both organelles and subsequently decreasing mitochondrial calcium uptake by reduced Inositol trisphosphate (InsP3) mediated calcium signalling (supporting the ER-mitochondrial calcium microdomains theory - when distance between the two organelles is increased uptake during InsP3 mediated calcium signalling is lower) [65]. In addition to functional changes Mfn2 knockout/inhibition results in unimpeded mitochondrial division [539].

These adaptations are apparent in humans who suffer from Charcot-Marie-Tooth type 2A (CMT2A) disease, an axonal peripheral sensorimotor neuropathy particularly in the lower and upper limbs resulting in severe progressive muscle weakness, motor deficits, and peripheral neuropathy [444]. In skeletal muscle, Mfn2 expression is decreased in obese and type 2 diabetic individuals as is mitochondrial size and mitochondrial network volume [16]. Mfn2 ablation studies point to the importance of Mfn2 in the regulation of metabolic signalling. Overexpression studies support the previously discussed role Mfn2 plays in tethering ER-mitochondria. An increase in Mfn2 appears to strengthen the bond between ER and mitochondria leading to increased mitochondrial elongation but also to increased mitochondrial breakdown, possibly due to

excessive calcium transfer into the mitochondria [65]. This work highlights the interlink between dynamics and mitophagy but also the significance of Mfn2 in overall mitochondrial homeostasis.

Inner Mitochondrial Membrane Fusion

Optic Atrophy 1 (L-OPA1 & s-OPA1)

Optic atrophy 1 (OPA1) a specialised dynamin-like GTPase on the inner mitochondrial membrane (IMM) where its GTP-binding and GTPase effector domains are exposed to the IMM space [538,539,341]. In addition to its role in fusion, OPA1 also plays an important role in maintaining cristae morphology and protecting against the release of cytochrome C and onset of apoptosis. OPA1 is regulated by two proteases, metalloendopeptidase, OMA1, and i-AAA protease ATP-dependent zinc metalloprotease, YME1L, which cleave the IMM bound long-OPA1 (L-OPA1) to the soluble short-OPA1 (s-OPA1) [140,328,308].

The proteolytic actions of YME1L have been shown to respond to metabolic stimuli, while OMA1 is activated by a change in the electrical charge on the mitochondrial membrane which occurs during dysfunction (stress-induced fission, SiF), reducing the activity of OPA1 [463,96,239,483,580,583,329,150]. Much like Mfn1 and Mfn2, it has been proposed that those involved in regulating mitophagy (i.e. PINK1) and it's GTPase activity, such as the sirtuin NAD^+-deacetylases, may have a role in reducing OPA1 [269,458,288,556]. Samant et al. [458], indicated that SIRT3 may deacetylate and activate OPA1 during stressful conditions in an attempt maintain fitness of the mitochondrial population, increasing mitochondrial tubulation. A predominance of L-OPA1 is associated with mitochondrial fusion which is in contrast to an increase in the activity of OMA1 and YME1L which activate L-OPA1 proteolysis resulting in s-OPA1, fewer L-OPA1 forms and overall mitochondrial fission [523,329]. The interaction of OPA1 with other proteins including members of the SIRT family can be seen in Figure 2.29.

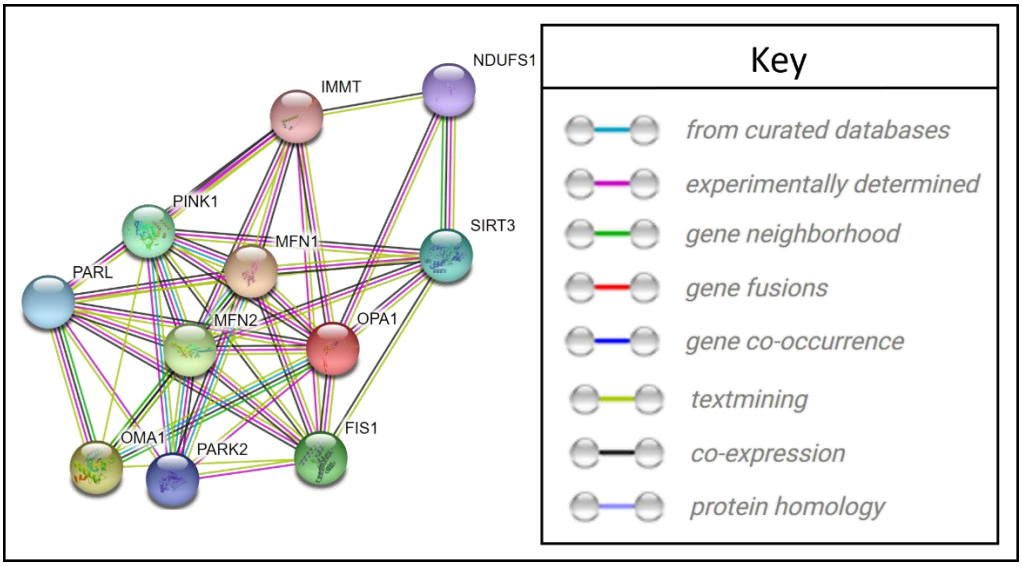

Figure 2. 29. Node diagram illustrating OPA1 interactions with other proteins including members of the sirtuin family, *STRING database*, v11.0

OPA1 mediated mitochondrial fusion occurs once Mfn1/2 tether and fuse to the OMM of an adjacent mitochondrion. L-OPA1, which is tethered to the inner membrane space and facing the intermembrane space binds to another L-OPA1 on the inner mitochondrial membrane of the adjacent mitochondrion [523]. This fusion process leads to mitochondrial enlargement, mixing the compartments within the mitochondria.

The action of Mfn1/2 and OPA1 fusion proteins is assisted by scaffolding proteins on the outer mitochondrial membrane (OMM). MitoNEET (CDGSH iron-sulfur domain-containing protein 1) is known to form intermitochondrial junction tethering between adjacent mitochondria, forming mitochondrial tubular networks (also known as mitochondrial nanotunnels) (see Figure 2.30). This is an important process as these tubular networks aid mitochondria-to-mitochondria communication allowing for more efficient calcium transmission and apoptotic signals across mitochondria [537]. It is debated, whether these mitochondrial nanotunnels are merely a result of stalled or incomplete fission events. Another theory is that nanotunnels are projections from single, isolated mitochondria as this is apparent in bacteria. These observations have been made in IMF mitochondria (as opposed to SS or perinuclear) in skeletal muscle, due to the restricted motility of IMF mitochondria, enabling effective mitochondria-mitochondrial communication.

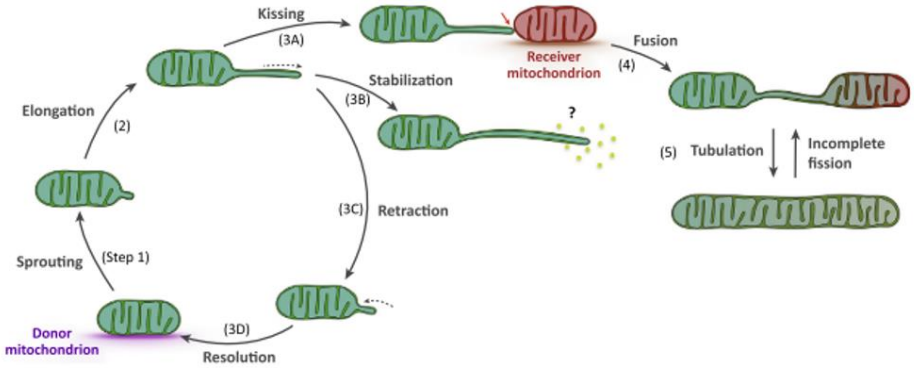

Figure 2. 30. Schematic representation of the lifecycle of the mitochondrial nanotunnel as depicted by *Vincent et al.* [537]

In addition to the mitochondrial fusion, OPA1 stabilizes the cristae junction, IMM-IMM and IMM-OMM contact sites. In the intermembrane space (IMS), large protein complexes, MICOS (mitochondrial contact site and cristae organizing system), as can be seen in Figure 2.31, act to fuse/tether the OMM to the IMM at the cristae junctions. A direct interaction with both OPA1 and cardiolipin at the cristae junctions is proposed to help give the cristae its curvature, subsequently allowing for the greater distribution of oxidative phosphorylation proteins (OXPHOS) in the cristae.

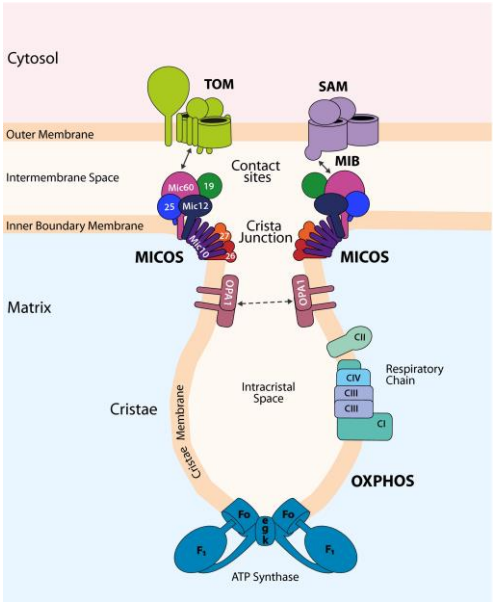

Figure 2. 31. Schematic representation of the determinants of mitochondrial cristae architecture and dynamics, *Colina-Tenorio et al.* [101]

From a mitochondrial functional perspective, the MICOS-OPA1-cardiolipin interaction is important in the formation of respiratory supercomplexes by generating greater surface area and helping to

enhance ETS/OXPHOS activity by decreasing the diffusion distances of substrates and electron transfer [523,329]. Loss of OPA1 leads to widening of the cristae lumen and junction, a reduction in IMM potential, an increase in basal mitochondrial calcium level and an induction of apoptosis.

Skeletal muscle OPA1 knockout and over expression studies, highlight the importance of OPA1 on mitochondrial bioenergetics, the mitochondrial network and overall skeletal muscle health. Romanello et al. [450] reported that OPA1 knockout in adult mice, although ultimately leading to premature death and excessive mitochondrial fragmentation, presented a phenotype of sarcopenia and unhealthy aging. Such observations were strongly correlated with the upregulation of markers associated with ER stress. OPA1 overexpression studies [531], reinforce the knockout work, illustrating OPA1's role in preventing muscle denervation induced muscle atrophy.

Mitochondrial fusion is regulated by a series of interlinked processes vitally important for increased mitochondrial size in the cell. An increased mitochondrial size provides the cell with a greater ATP supply to meet the cellular demands, shifting the cells preferred energy source from carbohydrates to fat oxidation epitomised by the increased OXPHOS in more elongated mitochondria [399,572]. With these beneficial effects in mind, increases in size need to be achieved through homeostatic regulation between both mitochondrial fusion and fission factors among many others. Concomitant abrogation of both mitochondrial fusion and fission support this. Such studies represent how a re-balance in mitochondrial dynamics act as a compensatory mechanism to alleviate the detrimental effects that changes in either fusion or fission may have, improving mitochondrial respiration, mitophagy and thereby mitochondrial function [450].

Adaptations of Mitochondrial Dynamics to Environmental Stress

Physical Inactivity

The discussion on mitochondrial plasticity is often interwoven with mitochondrial adaptations to physical inactivity and ageing [224,350,6,263,431]. The limited literature on mitochondrial function support the interpretation that prolonged inactivity has detrimental effects on cellular metabolism [73,522,488]. Kenny et al. [263] highlighted this fact by demonstrating that 21-days of bed rest significantly decreased skeletal muscle oxidative capacity and its proton conductance but also mitochondrial content. Subsequently, the dysfunction in the mitochondria may in fact be an adaptation of the organelle to the 'new' energy state (i.e. less energy requirement due to physical inactivity), reflecting a change in mitochondrial function and number.

As discussed previously, skeletal muscle is composed of multiple different fiber types (MHC 1, MHC 2A/X). It is important to keep this in mind as due to methodological limitations in biopsy acquirement following bed rest the majority of these studies solely focus on the expression of markers within the vastus lateralis (VL), which under normal circumstances are composed of more oxidative than glycolytic fibers. As such, the changes we reference here are related to the VL only.

In addition to the direct impact of physical inactivity on mitochondrial function, there is strong transcriptomic and proteomic evidence supporting alterations to mitochondrial function [491,505,145,264,403]. Alibegovic et al. [6] reported that 9 days of physical inactivity led to alterations in the expression of ~4,500 genes and downregulation of up to 34 pathways predominantly associated with mitochondrial biogenesis. While Buso et al., [73], emphasised these changes could also be translational, highlighting a significant reduction in targets of mitochondrial biogenesis following 14 days of bed rest.

There is limited evidence of the impact of physical inactivity on mitochondrial dynamics in human trials. Animal models of disuse indicate significant decreases the expression of proteins involved in the regulation of fusion [237,78,257,338]. These adaptations are yet to be fully elucidated within the human bed rest model. However, other models of sedentary behaviour, such as that by Tezze et al. [506] who compared sedentary individuals with aged-matched, exercising counterparts, found sedentary people have a reduced expression of mitochondrial fusion transcripts, OPA1, Mfn1 and Mfn2. While mild overexpression of such transcripts (OPA1) has been shown to prevent muscle denervation induced muscle atrophy. Taken together, OPA1 and other regulators of mitochondrial fusion, could be an important regulators of muscle atrophy and metabolic disease.

There are no reports, to our knowledge, of changes in mitochondrial fission proteins following bed rest. However, animal models of denervation and Drp1-overexpression/knockdown have signified how regulators of mitochondrial fission may contribute to skeletal muscle atrophy and remodelling [448,373,516,135]. Romanello et al. [450] reiterated this but also noted how inhibition of these pathways, while also inhibiting regulators of mitochondrial fusion, protected against muscle wasting by blocking the activation of markers associated with muscle atrophy, emphasising the importance in fusion-fission balance. Whether these changes in muscle atrophy are direct or consequential requires further study but evidence points to a strong correlation to a with reduced expression of FGF21 levels in the muscle and so could signify a direct relationship.

Adaptations in pathways of mitophagy following bed rest-induced muscle atrophy are less clear. Most of our understanding to date stems from both *in-vitro* and animal models, indicating that reductions in PINK1/Parkin result in significant muscle atrophy [388]. Borgia et al. [54] further reported that patients with muscular atrophy have increased PINK1 protein expression in mitochondria isolated from skeletal muscle [466]. Considering ubiquitination of Parkin results in the reduced expression of OMM proteins such as Mfn1 and Mfn2 [182,91], and inactivity has been suggested to increase mitophagy in skeletal muscle, the changes observed in the mitochondria following inactivity could be explained by the integrated response of mitophagy and mitochondrial dynamics.

Physical Activity

Acute exercise and exercise training regimes have been shown to have significant and sometimes different effects on markers of mitochondrial dynamics, specifically those relating to fission and fusion. While there isn't evidence to state a direct effect of exercise on these markers there is enough research to support that exercise may regulate their expression.

Aerobic exercise training increases the translocation of PGC-1α to the mitochondria and nuclei, where it functions as a co-activator for both mitochondrial and nuclear transcription factors, such as Mfn1 and Mfn2, regulators of the mitochondrial fusion process [31]. Consequently, upregulation of mitochondrial biogenesis is strongly associated with increased mitochondrial fusion [237,13]. The upregulation in mitochondrial fusion following exercise is consistently supported in the literature, either by increased expression of targets related to mitochondrial fusion, such as Mfn1, Mfn2 or OPA1, or decreased activity of regulators of mitochondrial fission [15,19,349,475].

Fealy et al. [144] illustrated that aerobic exercise training may impact on dynamics by decreasing fission activity, supported by a reduction in pDrp1^{s616}. This work, along with that of others, suggests that exercise training leads to an increased transcription of mitochondrial fission and fusion targets [84,391,139,144,13,19]. This adaptation with exercise training suggests that skeletal muscle mitochondrial dynamics are most likely intertwined with mitochondrial biogenesis, increasing overall mitochondrial content and quality intended to maintain cellular homeostasis [555].

The question as to whether these adaptations are acute or chronic was explained in research by Egan et al. [139]. This work identified that the adaptations to dynamics as highlighted previously following exercise training are not consistent with an acute bout of exercise. This time-course

analysis over 14-days supported the training-induced alterations in skeletal muscle regulators of fission (Drp1) and fusion (Mfn2). However, after just one exercise bout, Drp1 expression dramatically increased. This study suggests an adaptive response to exercise training epitomised by a dysregulation in mitochondrial fission following just one acute exercise bout, leading to a rebalancing in fusion-fission as training progresses [123,391].

In addition to the training bout, subject training status should be considered when evaluating the effects exercise. Arribat et al. [13] suggest that such changes may be age and training status specific. Sedentary individuals between the age of 60-80 years who were recruited into the 16-week aerobic exercise training study showed an enhancement in protein expression of fusion (Mfn2, OPA1) and an inhibition of fission (Drp1) in comparison to life-long exercisers. This work suggests that the enhancement of mitochondrial fusion was to support the need for an increased mitochondrial content posed by the metabolic demands of exercise. Interestingly, when we compare these changes to what was noted in models of reduced activity [506], regulators of mitochondrial fusion, particularly OPA1, appear to be highly sensitive to changes imposed by the environmental demands, be that exercise or inactivity.

Physical activity appears to have a specific effect on mitochondrial fusion-fission dynamics. However, training status, age and training bout have been shown to lead to alternative adaptations in dynamics, supporting the malleability of the mitochondria to maintain cellular homeostasis in a stressful environment such as with exercise training.

Nutritional Excess and Restriction

Nutritional excess is the main contributor to increased lipid accumulation in tissues, particularly skeletal muscle. This increased skeletal muscle lipid accumulation is associated with metabolic disease such as insulin resistance, type 2 diabetes and obesity and in turn significantly reduces mitochondrial oxidative enzyme capacity [213]. Additional to alterations in mitochondrial function, mitochondrial dynamics are strongly impacted by such behaviour. Kelley et al. [261] first recognized that mitochondrial area was significantly decreased (a 35% reduction) as a result of obesity. Unfortunately, researchers at the time were unaware that this could be due to alterations in mitochondrial dynamics. Since then, evidence has emerged that obesity could be inducing mitochondrial fragmentation in skeletal muscle and causing the previously observed reduction in mitochondrial respiratory capacity. Houzelle et al. [227] recognized a similar trend with disconnected, smaller, circular and more isolated mitochondria in obese individuals in comparison to their lean counterparts. This study attributed these phenotypical changes to alterations in both

OPA1 and Fis1, both of which significantly reduced in protein expression in the obese cohort. A decreased expression of OPA1 would explain these observed changes. While the decreased Fis1 expression could be indicative of decreased mitochondrial fission and reduced mitochondrial quality control, given the interrelationship between dynamics and mitophagy. In that event, decreased Fis1 expression could explain the reduction in mitochondrial oxidative phosphorylation, resulting in smaller, more fragmented and poorer functioning mitochondria. Animal work [16] further supported that the increased fragmentation could be orchestrated by adverse alterations in the regulators of fusion dynamics, indicating decreased expression of skeletal muscle Mfn2 in inherently obese, male Zucker rats. As with work by Houzelle et al. [227], this observation was concomitant with significant alteration to the mitochondrial network and a reduction in oxidative phosphorylation.

The changes with long-term over-feeding appear clear, whereby a decrease in fusion leads to increased mitochondrial fragmentation which results in reduced mitochondrial size and oxidative phosphorylation. These changes are similar to what is observed with severe nutrient deprivation with accelerated mitochondrial fission and a promotion in cell apoptosis in an attempt to preserve energy for neighbouring cells [110], a complete contrast to what occurs with mild nutrient deprivation.

Nutritional deprivation induces mitochondrial fusion and increases energy-producing efficiency to compensate the energy demand for growth. The activity of mammalian target of rapamycin (mTOR) (mTORC1 & mTORC2) has been shown to play a key role in relation to mitochondrial fission dynamics in particular. *In-vitro* inhibition/conditional knockdown studies have shown that reduced expression of mTOR leads to activation of pDrp1^{ser637} and inactivation of pDrp1^{ser616} preventing Drp1 translocation resulting in mitochondrial elongation [354]. This consequent increased fusion and mitochondrial elongation is in synch with what occurs during mild nutrient deprivation where we see a decrease in the activation of mTOR and ribosomal protein S6K (p70 S6 K), the purpose of which is thought to enhance the mitochondria's most basic function, the synthesis of ATP [187,421,565,138].

Given calorie restriction/fasting impacts greatly upon cellular energy status, the other pathways regulating energy within the cell are significantly upregulated. Unlike the response of mTOR, fasting/calorie restriction increases cAMP, AMPK and SIRT1/3 (via an increase in NAD^+) activity and expression, upregulating core autophagy machinery (Atgs) through the activation of Forkhead Box O (FoxO) transcription factors [304]. Such increases, accelerate autophagy, providing more potential energy for the energy deprived cell. This is helped further by calorie restriction/fasting

induced-mitochondrial fusion mediated by the increase in cAMP and AMPK. The increase in cAMP and AMPK has been shown to phosphorylate and inactivate Drp1-mediated mitochondrial fission, in times of nutrient deprivation, similar to what occurs with decreased expression of mTOR [168,313,507].

The actions of AMPK, insulin and mTOR signalling on mitochondrial morphology with starvation and excess nutrition are represented clearly in Figure 2.32.

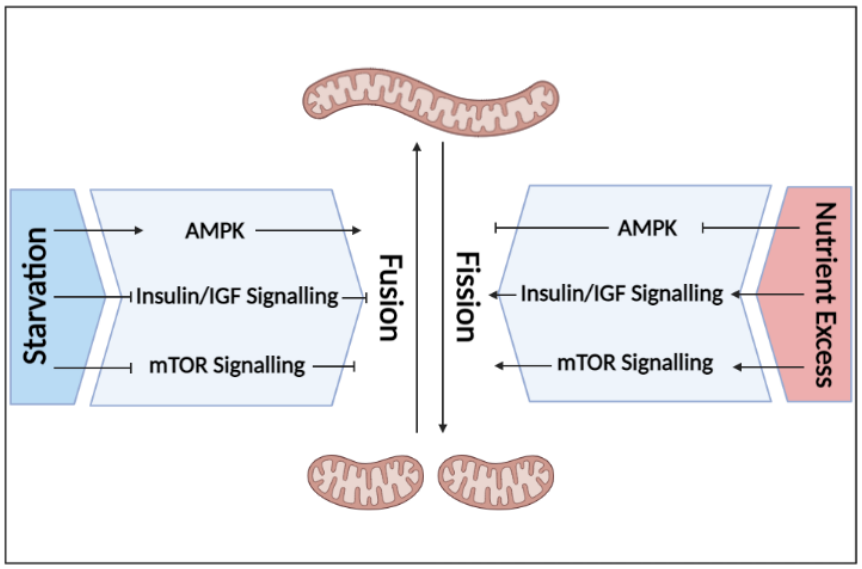

Figure 2. 32. Schematic representation on the role of starvation and nutrient excess on mitochondrial dynamics. Adapted from *Liu et al.* [322]

The mitochondria are dynamic subcellular organelles, convert nutrient intermediates into readily available energy equivalents. However, in times of nutritional excess/deprivation the mitochondria adapt in an attempt to preserve its prime function, oxidative phosphorylation. This adaptation is a highly controlled system coordinated by mitochondrial fusion and fission dynamics.

Conclusion

The reduction in exercise capacity with confinement and bed rest is well established with reduced plasma volume reducing cardiac filling pressure, stroke volume and cardiac output. Skeletal muscle fibre size and density are reduced, as is bone mass resulting in profound changes in functional capacity. Bed rest also causes metabolic alterations, inducing insulin resistance, decreased fat oxidation and ectopic fat storage all lending to overall metabolic dysfunction. Metabolic dysfunction is strongly associated with reductions in mitochondrial function regulated

a coordinated response in biogenesis, mitophagy and dynamics. Mitochondrial dynamics is a highly plastic process firmly impacted by the surrounding environment our bodies are subjected to, be that during exercise, nutrient excess/deprivation or physical inactivity. The role mitochondrial dynamics may have in the progression of metabolic dysfunction induced by physical inactivity poorly investigated within the human model. Having a greater understanding of the complex adaptations skeletal muscle mitochondria undergo and how they change with physical inactivity will allow us to develop appropriate countermeasures to counteract the negative impact of physical inactivity.

Chapter III: Methodology

Brief Summary of Measurements and Techniques Used

A 60-day -6° head down tilt (HDT) bed rest study was conducted aimed to measure the effectiveness of a nutritional supplement (micronutrient cocktail) in counteracting the adverse physiological (Table 3.1) and skeletal muscle cellular response (Table 3.2) to 60 days -6° HDT bed rest. The following is a summary of the measurements assessed and techniques used for their quantification:

Physiological Response to Bed Rest:

Table 3. 1 Measurements and techniques used to assess the physiological response to bed rest

Measurement	Technique Used
Height	Stadiometer
Weight	Weighing trolley
Other anthropometrics (fat-free mass, fat mass, body fat %)	Dual Energy X-ray Absorptiometry
Heart rate & Blood pressure	Digital blood pressure cuff
Resting Metabolic Rate & Respiratory Quotient	Canopy dilution indirect calorimetry
Aerobic capacity	Cycle ergometer, monitored using indirect calorimetry
Peak Heart Rate	12-lead Electrocardiogram

Cellular Response to Bed Rest:

Table 3. 2. Measurements and techniques used to assess the cellular response to bed rest

Measurement	Technique Used
Skeletal muscle biopsy	Bergstrom technique
Mitochondrial content	RT-qPCR
Mitochondrial respiration	Oroboros O2k High Resolution Respirometry (carbohydrate SUIT)
Transcriptional expression	RT-qPCR
Translational expression	Western blot

In order to determine the time-course effect of some of these physiological and cellular responses to bed rest we quantified and analysed new data from the control arm of a previously conducted -6°HDT 21-day bed rest study. The same methods used for the 60-day study (Table 3.2) were used for the 21-day study and compared against the changes we observed following 60-days -6° HDT bed rest within our control group.

We subsequently used *in-vitro* cell culture methods to further investigate novel upstream regulators of mechanisms observed to change following both 21 and 60 days -6° HDT bed rest. These measurements were optimised using C_2C_{12} myotubes (see Appendices Section E & G) with techniques then applied to primary human skeletal muscle myotubes (ATCC PCS-950-010^{TM}) in culture. Table 3.3 is a summary of the measurements taken and the technique used:

Table 3. 3. Measurements and techniques used *in-vitro*

Measurement	Technique Used
Sirtuin 4 knockdown	siRNA knockdown with transfection reagent
Transcriptional expression	RT-qPCR
Translational expression	Western blot
Mitochondrial respiration	Oroboros O2k High Resolution Respirometry (fatty acid SUIT)
Mitochondrial and Nuclei probing	Immunofluorescence labelling with confocal microscopy

Experimental Overview of the 60-day Bed Rest Study

This study was a randomized controlled, parallel design, study funded by the European Space Agency and conducted at the MEDES clinic, Clinique de l'Espace (CHU Rangueuil, Toulouse, France. The first campaign was conducted between January and April 2017 and the second campaign between September and December 2017. All subjects remained at -6° head down tilt (HDT) for the entire study duration (60 days in bed), to simulate cardiovascular changes in microgravity, whether assigned to the control (CONT) or Nutritional Supplement group (intervention - INT). The experimental schedule was broken into three periods (i) A baseline ambulatory period of 14 days (baseline data collection, BDC) followed by (ii) 60 days at -6° bed rest (HDT) and then (iii) 14 days of a recovery period (R+). During the first baseline data collection (BDC) and last (R+) periods, subjects remained in the bed rest facility at MEDES.

A clear representation of the 60-day bed rest study design can be found below in Figure 3.1 which will be further within this section.

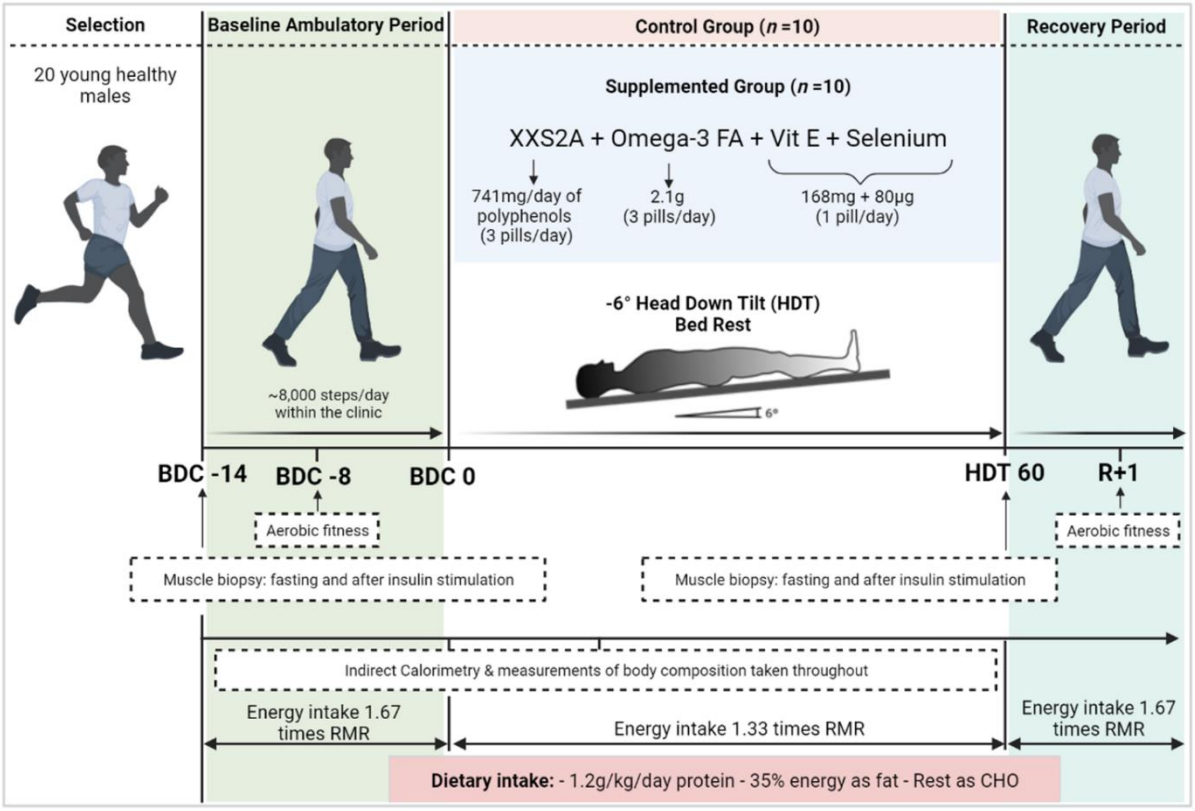

Figure 3. 1. 60-day bed rest study design

Subject Selection

A total of 20 men were selected to partake in the bed rest study following a selection process that included a review of their lifestyle, a medical history and examination as well as physical, biological and psychological assessments. An information document was provided to each candidate and they had the opportunity to ask any questions. Once satisfied, they signed the specific Information and Consent Form. These volunteers were then notified of a selection visit at MEDES to check if they did (or did not) meet the requirements of the inclusion and non-inclusion criteria. The study was approved by the appropriate Ethics Committee (Comite de Protection des Personnes / CPP Sud – Ouest Outre-Mer I) and the French Health Authorities (Agence Francaise de Securite Sanitaire des Produits de Sante).

Sample Size

This study was conducted by the European Space Agency human spaceflight programme and directed to their records. The cocktail study was the first study to investigate the effects of an antioxidant and anti-inflammatory micronutrient cocktail on different physiological systems in bed rest, and is therefore considered an exploratory study. Thus, no power analysis was performed.

Table 3. 4. List of inclusion and exclusion criteria for the 60-day bed rest study

Inclusion criteria	Exclusion criteria
Healthy male	Past record of orthostatic intolerance
Aged 20-45	Cardiac rhythm disorders
BMI between 20-25	Chronic back pains
Between 158-190cm in height	History of hiatus hernia or gastro-esophageal reflux
No personal nor family past record of chronic or acute disease or psychological disturbances which could affect the physiological data and/or create a risk for the subject during the experiment	History of thyroid dysfunction, renal stones, diabetes, migraines
Fitness: < 35 years: 35 ml/min./kg < VO_2max < 60ml/min/kg > 35 years: 30 ml/min./kg < VO_2max < 60ml/min/kg	Past record of thrombophlebitis, family history of thrombosis or positive response in thrombosis screening procedure
Active and free from any orthopedic, musculoskeletal and cardiovascular disorders	Abnormal result for lower limbs echo-Doppler
Non-smokers, no alcohol, no drug dependence and no medical treatment	History or active claustrophobia
Covered by a Social Security system	History of genetic muscle and bone diseases of any kind Bone mineral density: T-score ≤ -1.5
Free of any engagement during the three study planned periods	Osteosynthesis material, presence of metallic implants
	History of knee problems or joint surgery/broken leg
	Poor tolerance to blood sampling
	Having given blood (more than 8ml/kg) in a period of 8 weeks or less before the start of the experiment
	Special food diet, vegetarian or vegan
	History of intolerance to lactose or food allergy
	Positive reaction to any of the following tests: HVA IgM (hepatitis A), HBs antigen (hepatitis B), anti-HVC antibodies (hepatitis C), anti-HIV1+2 antibodies
	Echocardiography: inappropriate thoracic acoustic window
	Subject already participating or in the exclusion period of a clinical research
	Refusal to give permission to contact his general practitioner
	Incarcerated persons
	Subject who, in the judgment of the investigator, is likely to be non-compliant during the study, or unable to cooperate because of a language problem or poor mental development
	Subject who has received more than €4,500 within 12 months for being a research subject
	Subject under guardianship or trusteeship

Table 3.5 represents a breakdown of the number of volunteers in campaign 1 and 2 which completed their medical screening and psychological screening and those who were finally selected (along with a back-up) for these bed rest trials.

Table 3. 5. Number of volunteers in 60-day bed rest study

Number of volunteers	Campaign 1	Campaign 2
Medical Screening	35	29
Psychological Screening	18	19
Final Selection	10 + 4 back up	10 + 5 back up

Physical Activity During the Baseline Ambulatory Period

Habitual physical activity was objectively measured in free living conditions over a period of ten consecutive days by self-reported questionnaires and quantification of subject's daily step count and intensity of activity. The goal was to maintain habitual physical activity of the subjects while they were staying at the clinic in confined conditions during the baseline ambulatory period, and thus prevent any deconditioning prior to the bed rest.

A hip-worn triaxial accelerometer (Actigraph GT3x+, Actigraph™, USA) was used for 10 days before the start of the bed rest to quantify daily steps and intensity of activity. The accelerometer was taped to a stretch belt and hip-worn on the right iliac crest. Each subject received a logbook and was instructed to record specific activities or events. Physical activity level (PAL), defined as the ratio between daily total energy expenditure and resting metabolic rate (RMR) was estimated for each participant. RMR was estimated according to the WHO equations [143,424]. From the habitual PAL value and the estimated RMR, physical activity energy expenditure was estimated for each subject in order to develop an individual physical activity program.

About 30% of habitual activity energy expenditure was expended while in the facility during structured exercise session. Each participant performed 4 walking/running sessions on a treadmill and 4 biking sessions on a bicycle over 8 days during the BDC period. The exact duration of the running bout and the bike resistance were adjusted to achieve 30% of habitual activity energy expenditure. The remaining 70% of habitual activity energy expenditure was reached by walking in the facility. Participants were asked to reach about 8000 steps/day in order to guarantee a maximal shift in activity at the start of the bed-rest. Participants were equipped with a wrist-worn activity tracker bracelet (Polar Loop, Polar®, Finland) in order to record/save daily physical activity

and have a real-time visual feedback. The number of daily steps each day were assessed to help the participants reach the targeted number of steps.

Bed Rest Safety Measures

To ensure safety and well-being of subjects, a 24h/day medical and paramedical care was provided. As part of this standardized procedure, general health indicators such as blood pressure and heart rate were assessed daily (Intellivue MMS X2, Philips Ltd., Best, The Netherlands) in the fasting state, immediately following the scheduled wake-up at 6:30 AM (lights off at 11PM). Body mass (BM) was assessed daily following the first urine void of the day (DVM 5703, Sartorius Ltd., Goettingen, Germany). 24h urine volume pools were also assessed daily. Safety parameters (from blood and urine samples) were periodically assessed by an independent medical doctor, who additionally monitored the subjects' health status during daily ward rounds

Blood and Urine Samples Analyses

Plasma glucose (Abbott Ltd.), NEFA (FUJIFILM, Wako Ltd.), triglycerides (Randox Ltd.) and insulin (Roche Ltd.) were measured by colorimetric assays and chemiluminescence methods, according to the manufacturer's instructions. The ratio between low-density lipoprotein (LDL) and high-density lipoprotein (HDL) cholesterol was determine by polyacrylamide gradient electrophoresis (SPIRAGEL® 1.5-25%). The urine was analyzed for nitrogen content according to the Dumas method (RapidN Cube ®, Elementar, Germany).

Dietary Intake

Diet was tightly controlled during the study by registered dieticians and provided by the MEDES Clinical Team. For all ESA bed rest studies, the aim is to maintain fat mass while accepting the fat free mass will decrease. Fat mass is clamped by ensuring the total energy intake matches energy expenditure. This is achieved by measuring resting metabolic rate and body composition and adjusting the diet accordingly. Participants were fed conventional foods calculated to provide 1.2 g/kg/day of protein, 35% of energy as fat and the rest as carbohydrates. Energy intake was calculated to provide 1.67 times the resting metabolic rate during the control and recovery periods and 1.33 during the best rest. Food ingested was weighted and energy ingested was calculated using the NUTRILOG software (Version 3.11b). No extra food was allowed between the three daily meals taken at set times. All leftovers on the tray were weighted by the staff of the Metabolic kitchen.

Micronutrient Cocktail Supplementation

The supplemented group received a polyphenol nutrient cocktail derived from the following sources: Liliaceae, Vernenaceae, Lamiaceae, Vitaceae, Rubiaceae, Theaceae and Rutaceae, and consisting of Allium cepa, Lippia citriodora, Ajuga reptans, Vitis vinifera, coffearobusta, Camellia sinensis, and Citrus aurantium. The cocktail is referred to as XXS-2A and was designed by Spiral Company (Dijon, France). The daily dose was achieved by the ingestion of six pills (two at breakfast, lunch and dinner) to reach a total dose of 741 mg/d of polyphenols that was composed of 323.4mg/d flavonols (including quercetin 135mg), 78.0mg/d oligostilbens (including resveratrol 21mg), 96.0mg/d hydroxycinnamic acids (including chlorogenic acid 42mg), 135.6mg/d flavanols (including epigallocatechin gallate 60mg) and 108.0mg/d flavanones (including naringin 30mg). As there are no dietary references intake (DRI) available for polyphenols, the ~500 mg/d dose was based on several reviews on the bioavailability and bioefficacy of polyphenols in humans and other studies that tested the effects of polyphenols on exercise performance and oxidative stress. The 3g daily dose of ω-3 fatty acids (Omacor, Pierre Fabre Laboratories, Toulouse France) was based on French pharmacopeia recommendations for hypolipemic effects (2-4 g/day) and was provided as a single pill per meal. It comprised of 1.1 g of eicosapentaenoic acid (EPA) and 1 g of docosahexaenoic acid (DHA). Vitamin E and selenium were given as a single daily pill providing 168mg of vitamin E associated with 80µg of selenium (Solgar, Marne la Vallée, France). The daily recommended intake for Vitamin E is set at 15mg/d. The tolerable upper limit (UL) for intake is set at 1 g in adults, therefore the dose from the commercially available pill was 6 times lower than the UL but 11 times higher than the DRI. To capitalize on the cocktail effect, the dose of vitamin E was two-fold lower than the doses that were previously reported to provide positive effects on metabolism and muscle. Regarding selenium, the intake reported in most countries presents a large variability. DRI and UL are respectively set at 55 µg and 400 µg per day. The selected dose provided a daily supplement that set the daily intake at 135 µg/d which is 3 times lower than the UL and lower than the dose reported in previous studies. The control group did not receive any supplementation or placebo.

Physiological Assessments

These methods were performed by a clinical team based within clinic and shared with all research groups involved in the study.

Anthropometrics

Height (m) was measured to the nearest centimeter using a stadiometer and body mass (kg) was measured to the nearest 0.1 kg at baseline and the first thing every morning during bedrest on a weighing trolley. This allowed them to roll from the bed to the weighing scales.

Dual Energy X-Ray Absorptiometry (DEXA)

The measurement of body composition using DEXA (Hologic®, DXA, QDR4500C, USA) is achieved from the differential absorption of x-rays of two different intensities. This calculation allows for the quantification of overlying soft tissue. It is possible to obtain values for fat and fat free mass using a whole-body scan and using instrument specific algorithms [547]. For the total body scan, subjects were centered and squared in the middle of the table with ankles and knees taped together and the scanner laser light was positioned 3cm above the subject's head. The scanner arm moved down over the subject's body obtaining sliced images. Fat mass and fat free mass were calculated. The radiation exposure is extremely low (0.001mSv) (www.radiologyinfo.org). DEXA used 8 times throughout the study – Two measurements were taken during baseline data collection (BDC-13 and BDC-3), four during bed rest (HDT13, HDT30, HDT45, HDT60) and two during recovery (R+7, R+14).

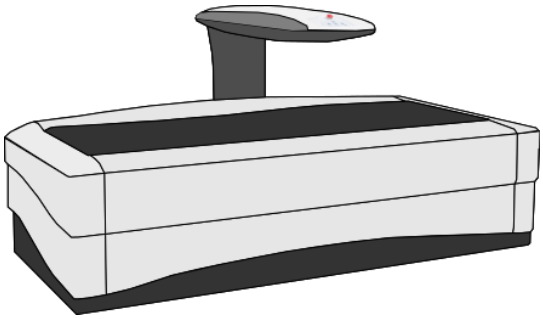

Figure 3. 2. Dual X-Ray Absorptiometry was used to measure body composition through bed rest

Aerobic Capacity

Peak oxygen uptake capacity (VO_2peak) during cycling was measured using a cycle ergometer (Lode, B.V., Groningen, The Netherlands), once before bed rest (BDC-8) and once after bed rest (R+1). After an initial 5 minutes of seated rest, subjects were instructed to start and maintain a

cadence of 75 rpm while the load was increased every minute in steps of 25 W (starting from 3 min at 50 W) until volitional exhaustion despite strong verbal encouragement. Breath-by-breath oxygen uptake and carbon dioxide production was monitored using the Innocor™ system (Innovision, Odense, Denmark) and heart rate was continuously monitored by 12-lead ECG (PADSY, Medset Medizintechnik GmbH, Germany). The spiroergometry data was filtered by taking the median of 5 breaths and subsequently a moving average over 30 seconds. Afterwards, the peak values for the following parameters were extracted: VO_2, heart rate, respiratory exchange rate, and ergometer power. If the peak respiratory exchange rate was below 1.10, the trial was deemed not exhaustive and not considered for further analyses.

Resting Metabolic Rate

Subjects lay in bed with respiratory quotient (RQ - carbohydrate and fat oxidation rates) and resting metabolic rate (RMR) calculated using canopy dilution respirometry (Quark, Cosmed, Italy) (see Figure 3.3) with the classical equation of indirect calorimetry corrected for urinary nitrogen excretion [160,148]. Resting metabolic rate was performed on all subjects following an overnight fast and prior to breakfast on baseline data collection (BDC) days 14, 10 and 2 before head down tilt (HDT). This same procedure was then performed on all subjects during HDT on days 4, 25, 39, 49 and 58.

Figure 3. 3. Indirect calorimetry under the canopy hood performed using the Quark, Cosmed

Skeletal Muscle Biopsies

Prior to and just before the end of the 60-day bed rest period (BDC-6 and HDT56) skeletal muscle specimens were obtained by muscle biopsy from the vastus lateralis while subjects where in the fasted state (see Figure 3.4). An area of skin was anaesthetized (2% w/v lidocaine HCl) and a small

(0.5 cm) incision was made. A sterilized Bergstrom skeletal muscle biopsy needle was inserted into the muscle and approximately 200 mg of tissue was removed while applying suction. Pressure was maintained on the wound for 10 minutes and the incision was closed with steristrip tape and wrapped tightly in a crepe bandage.

Figure 3. 4. Vastus lateralis skeletal muscle biopsy performed on all subjects pre and post bed rest using the Bergstrom technique

Skeletal Muscle Biopsy Analysis

The muscle biopsy samples were either frozen in liquid nitrogen for nucleic acid and protein analysis or put into a preservation medium, BIOPS solution (in mM; 2.77CaK^2 EGTA, 7.23 K^2 EGTA, 20 immidazole, 20 taurine, 6.65 MgCl^2, 5.77 ATP, 3.95 phosphocreatine, 0.5 dithiothreitol, 50 K-MES, pH 7.1 at 0˚C) and prepared immediately for analysis of mitochondrial function using the High-Resolution Respirometery, O2k Oroboros (Oroboros Instruments GmbH).

Cell Culture Methods

Cryopreservation (freezing and thawing)

Freezing Working Stocks

Cells in the middle of exponential phase where trypsinized, pelleted and resuspended in Cryo-SFM (Promocell GmbH, C-29912). Once suspended, cells where aliquoted into 1ml pre-chilled and labelled cryovials (Greiner Bio-one GmbH, 121278). These where immediately placed in a Mr. Frosty™ Freezing Container (Thermo Fisher Scientific Inc., 5100-0001) (see Figure 3.5) which was placed into a -80°C freezer until frozen. This was to ensure cells were gradually cooled a rate of -1°C/minute. Once frozen, cells were removed from Mr. Frosty container and the vials were lowered into the liquid nitrogen at -196°C for storage. All cells where counted and a viability assay was complete before they were frozen. Human skeletal muscle myoblasts where frozen at a minimum of $4x10^5$ per cryovial.

Figure 3. 5. Mr.Frosty™ container used for initial cell cryopreservation

Thawing Frozen Stocks

Fresh growth media was warmed at 37°C in a water bath and a 5 ml aliquot of this media was placed in a 30 ml white capped universal. The cryovial was removed from the liquid nitrogen tank and rapidly placed into a 37°C water bath, making sure the lid did not get in contact with the water to maintain sterility. When the cell suspension was thawed, the cryovial was sterilized with diluted industrial methylated spirits (IMS) and the cells were transferred to the pre-warmed media inside a laminar flow cabinet. Cells were then centrifuged at 1,400rpm for 13 minutes for human skeletal muscle primary cells (ATCC PCS-950-010™) in order to remove the toxic Cryo-SFM. The supernatant was carefully discarded and the cell pellet was resuspended into 1 ml pre-warmed growth media. A cell viability count was performed and cells were subsequently suspended in a culture flask with pre-warmed media. The flask was then labelled and placed into a CO_2 incubator.

Primary Skeletal Muscle Cell Maintenance

Primary Skeletal Muscle Cell Growth

Media for Growth of Primary Skeletal Muscle Cells: A Primary Skeletal Muscle Growth Kit (ATCC PCS-950-040™), consisting of L-glutamine (10mM), rh EGF (5ng/ml), dexamethasone (10µM), rh FGF-b (5 ng/mL), rh insulin (25µg/mL), stem cell qualified FBS (4%), was added to Mesenchymal Stem Cell Basal Medium (ATCC PCS-500-030) to grow human primary skeletal muscle myoblasts. Media was heated to 37°C for 15 minutes prior to use.

Trypsin Solution: Sterile trypsin solution was made up using autoclaved PBS, 0.25% trypsin (Gibco™) and autoclaved 0.01% EDTA (Sigma-Aldrich) solution stored in aliquots at -20°C. Solution was heated to 37°C for 15 minutes prior to use.

Subculture of Primary Human Skeletal Muscle Cells: Primary human skeletal muscle cells (ATCC PCS-950-010™) (see Figure 3.6) where maintained in conditions as mentioned previously and sub-cultured when the cells reached 70-80% confluence in order to maintain them in mid-exponential phase of their growth cycle. Further information on these cells can be found within the Appendices (Section H). Culture media was removed from the flask (T25, T75, T175) and discarded in a glass waste bottle. The flask was rinsed with 1 ml trypsin (based off the size of the flask) to remove any residual media. Then, 2-3 ml of trypsin was added to the flask, which was then incubated at 37°C until almost all the cells had detached from the bottom of the flask (approximately 2-3 minutes). The detachment of cells was monitored under a microscope to prevent over-exposure to trypsin. Once the cells were detached, a volume of growth media equivalent to that of trypsin was added to the flask in order to neutralise the effect of the trypsin, and the media, trypsin and cellular solution was transferred to a 20 ml sterile universal tube and centrifuged at 1,400 rpm for 13 minutes. The supernatant was discarded, and the pellet was resuspended in 2 ml of growth media. Following resuspension, cells where counted using trypan blue viability method.

Once counted, appropriate amount of cells where then seeded into T25/T75/T175 and 6 well plates. Cells were fed every 3-4 days until passaged once 70-80% confluent again. Cells were passaged just 4-5 times to prevent any unwanted characteristic changes, after this cells were cryopreserved.

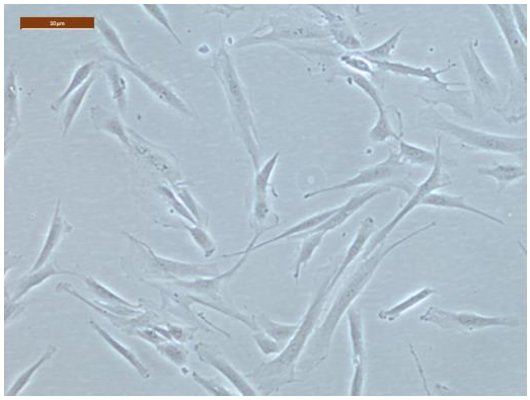

Figure 3. 6. Human Skeletal Muscle myoblasts, ATCC® PCS-950-010

Human Skeletal Muscle Cell Differentiation

Once myoblasts reached 80-90% confluence (3-4 days), growth media was removed and discarded into waste. Cells where washed with phosphate buffered saline (PBS). Human skeletal muscle myoblasts were then incubated in differentiation media (skeletal differentiation tool, ATCC PCS-950-050™) (2ml per well of a 6 well plate) at 37°C and 0.5% CO_2. Cells were differentiated for 10-12 days until cells differentiated into myotubes with media replacement occurring on day 3, day 6 and day 9 (see Figure 3.7). Media replacement consisted of removing current media, discarding it into waste, washing each well with PBS before incubating once again in differentiation media. Media was heated to 37°C for 15 minutes prior to use.

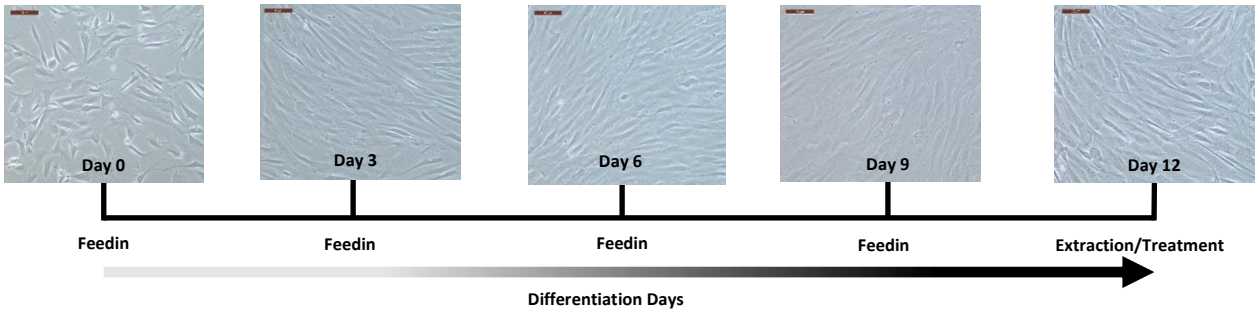

Figure 3. 7. Schematic representation of the differentiation of human skeletal muscle myotubes over 12 days

Cell Counting & Viability

Following centrifugation of cells and resuspension of these into new growth media, cells were counted and tested for viability. 20µl of resuspended cells were incubated with 20µl trypan blue solution (0.4%) (Sigma-Aldrich, T8154) to make a 1:1 solution in a 1.75ml eppendorf for 5 minutes. 10µl of this suspension was then counted using a haemocytometer (this was completed twice and an average of both was taken). Live cells equated to those which were not blue (i.e. viable cells)

and non-viable those which were blue. The haemocytometer was cleaned before and after each use with IMS.

Cell count: [(count 1 total/4) + (count 2 total/4)]/2 = cells x 10^4

Cell viability: Total viable cells/Total cells (viable and dead) x 100

Viable cells per ml: Average viable count per square x Dilution factor x 10^4

Total viable cells per sample: Viable cells/ml x Original volume of fluid from which the cell sample was removed

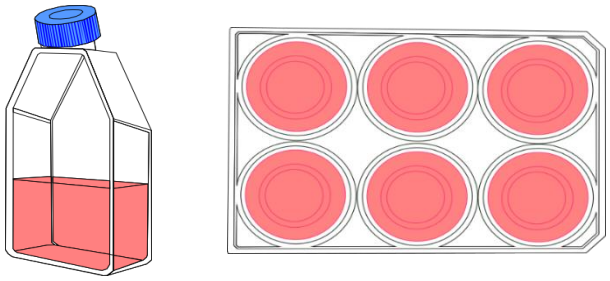

Figure 3. 8. T75/T175 flasks were used for sub-culturing human skeletal muscle cells before seeding into 6 well plates

Sterility checks

Sterility checks were regularly performed in the media and their additives. A 1ml volume sample of the liquid being tested was added to 9ml of tryptone soya broth (TSB) to check growth of yeasts and aerobes. Thioglycolate (Thio) broth was used to identify the presence of aerobic and anaerobic bacteria. This media maintains a gradual reduced oxygen concentration along its depth due to the presence of sodium thioglycolate, which removes oxygen from the media. A 1ml of sample media was added to the top of Thio to assess aerobic bacterial contamination whereas for anaerobic growth, 1ml was added to the bottom of the media contained in a 30ml universal (Greiner Bio-one GmbH, 201152), where no/low oxygen concentration is found. The three samples were incubated at 37°C for 7 days and then checked for turbidity, which would indicate contamination.

Mycoplasma testing

Routine mycoplasma examinations were carried out on the cell lines used in this study by a trained in-house technician. Media samples were collected from cultures that had been subcultured at least three times in media without the presence of antibiotics or selective agents. Culture media

was collected at day three of the culture and centrifuged at 1000 rpm for 5 min to remove any cell debris. The conditioned media (5 ml minimum) was then stored at -20°C until tested.

Briefly, the test was based on the Hoechst DNA staining method. NRK cells (normal rat kidney fibroblasts) were used as a testing cell line due to their resistance to fixation. These cells were seeded and grew in coverslips overnight. The conditioned media to be tested was then added and the cells were incubated at 37°C. When 20-50% confluence was observed (usually at day 4-5), the cells were fixed and stained with Hoechst 33258 dye. This dye stains all DNA present in the cell culture, including the NRK nuclear DNA as well as the mycoplasma DNA. The stains were then observed under a fluorescent microscope. Presence of small fluorescent bodies outside the cells indicated mycoplasma infection.

Primary Human Skeletal Muscle Myotube siRNA Transfection

RNA interference (RNAi) using small interfering RNA (siRNA) transfection was conducted on primary human skeletal muscle myotubes differentiated between days 10-12. Primary human skeletal muscle myotubes were transfected using Invitrogen Silencer Select Pre-designed siRNA to SIRT4 (5nmol) (Thermo Fisher Scientific Inc., s23764 and s23765) and a silencer select siRNA negative control (5nmol) (scramble, Thermo Fisher Scientific Inc., 4390843). s23764 and s23765 silencer select pre-designed siRNA to SIRT4 (5nmol) and silencer select siRNA negative control (4390843) (5nmol) were made to 100µM using sterile nuclease free water in sterile conditions. From this 100µM stock solution all siRNA silencer selects were made to 10µM using sterile nuclease free water in sterile conditions. This 10µM solution was used for all siRNA experiments.

Primary Human Skeletal Muscle Myotube Optimal siRNA Transfection Reagent

Four separate transfection reagents were assessed for optimal siRNA SIRT4 knockdown in primary human skeletal muscle myotubes, MirusIT-TKO®(Mirus Bio LLC., MIR 2154), DharmaFECT™ 1 (Dharmacon Inc., T-2001-S), DharmaFECT™ 3 (Dharmacon Inc., T-2003-S) and Lipofectamine 3000 (Invitrogen™, L3000001). Each transfection reagent was assessed at three separate concentrations (2µl, 4µl and 6µl per 50µl Gibco™ Opti-MEM, Reduced Serum Medium, Thermo Fisher Scientific Inc., 31985047) in all conditions. Six separate 12 well plates were seeded with primary human skeletal muscle myoblasts ($1x10^5$ per well). Once myoblasts reached 90% confluence, growth media (Mesenchymal Stem Cell Basal Medium (ATCC PCS-500-030™)) was removed, cells were washed with PBS and cells were incubated in differentiation media to help them form into myotubes (skeletal differentiation tool, ATCC PCS-950-050™). Cells were fed on days 2, 4, 6 and 8. On day 10 primary human skeletal muscle myotubes were assessed for optimal

siRNA transfection reagent. Media was removed from wells and cells were washed with PBS. Cells were then incubated in 900µl Opti-MEM I Reduced Serum Medium (Gibco™, 31985047). 25nM of siRNA silencer select s23764, s23765 and silencer select siRNA negative control (4390843) were used for all transfection reagent conditions. For each well condition an eppendorf consisting of 2.5µl of 10µM siRNA silencer select stock in 47.5µl Opti-MEM was made (making a 50nM siRNA) (see Table 3.6 for siRNA concentration preparation). Each 50nM siRNA was incubated with a specific transfection reagent (2µl, 4µl, 6µl transfection reagent in 50µl Opti-MEM) of the same volume (making it a 25nM siRNA) for manufacturers specified time (indicated in Table 3.7).

Table 3. 6. SIRT4 siRNA concentration for identifying optimal siRNA transfection reagent

siRNA Target (10µM)	***siRNA Concentration (10µM)***	***siRNA Volume (10µM)***		***Opti-MEM***
s23764/s23765/Scramble	25nM	2.5µl		47.5 µl
		s23764	**s23765**	
Duplex siRNA	25nM	1.25µl	1.25µl	47.5µl

Table 3. 7. Multiple siRNA transfection reagents were used to assess for optimum SIRT4 knockdown

Transfection Reagent	***Complex Formation Time***
Lipofectamine 3000	5 minutes
DharmaFECT 1	20 minutes
DharmaFECT 3	20 minutes
MirusIT-TKO	20 minutes

siRNA transfection reagent and siRNA silencer select complex solution (100µl) were carefully pipette into 900µl of Opti-MEM already pipette onto cells within their wells. Cells were then incubated with specific complexes (see Table 3.8 and Figure 3.9 for conditions per plate) for 24 hours at 37°C and 0.5% CO_2.

Table 3. 8. siRNA transfection reagent optimisation plate setup

12 well plate #	***Condition***
1	siRNA silencer select s23764 (SIRT4)
2	siRNA silencer select s23765 (SIRT4)
3	siRNA silencer select duplex (s23764 and s23765) (SIRT4)
4	silencer select siRNA negative control (4390843)
5	Transfection reagent only (no siRNA silencer select)
6	Control (no siRNA silencer select and no transfection reagent)

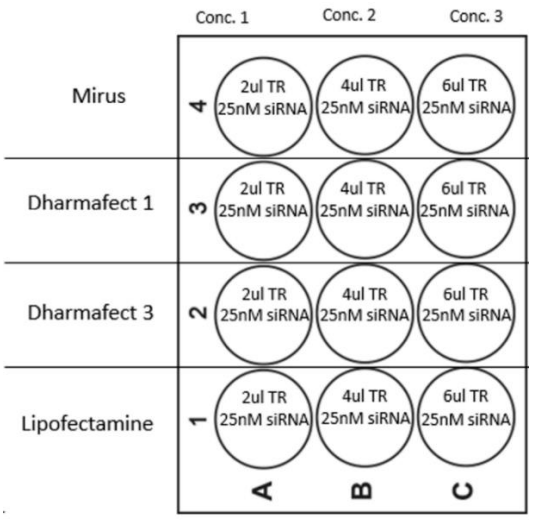

Figure 3. 9. Example plate setup for optimal siRNA transfection reagent experiment

Following 24-hour incubation, siRNA complexes were removed and disposed of. Cells were washed with PBS and re-incubated in differentiation media for another 24 hours. Following 24-hour incubation in differentiation media, media was removed, cells were washed with PBS and cells were extracted using Tri reagent (0.5ml per well). Cells were then stored within labelled eppendorfs at -80°C until ready to perform RNA extraction and subsequent RT-qPCR for presence of the Sirtuin 4 (SIRT4) gene.

Primary Human Skeletal Muscle Myotube Optimal siRNA Concentration

Following optimisation of the transfection reagent and its concentration, the optimal siRNA silencer select concentration was determined. Primary human skeletal muscle myoblasts ($1x10^5$ per well) were grown until confluent in 12 well plates, differentiated using differentiation media for 10 days, feeding cells on days 2, 4, 6 and 8. On day 10, media was removed, cells were washed using PBS and cells were incubated again in 900µl Opti-MEM per well. Four different concentrations of siRNA silencer select were made (25nM, 50nM, 75nM and 100nM). These were all incubated in 6µl lipofectamine 3000 in 50µl Opti-MEM per well for 5 minutes to create a complex before being carefully pipette into their specific wells in drops (see Figure 3.10, Table 3.9, 3.10 and 3.11 for specificities in plating, preparation and testing of different siRNA concentrations on SIRT4 expression).

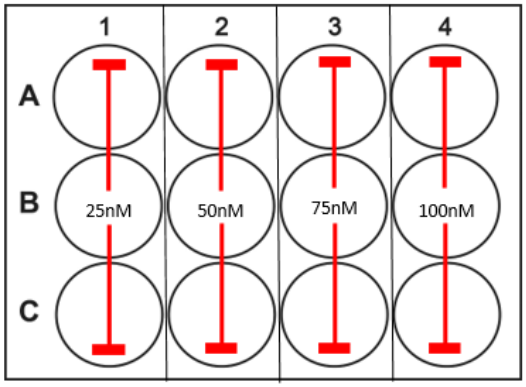

Figure 3. 10. Example of plate setup with 4 different concentrations of SIRT4 siRNA silencer select and set concentration of transfection reagent for optimal siRNA concentration experiment

Table 3. 9. Different concentrations of SIRT4 siRNA were used in optimisation

siRNA Concentration	*siRNA s23764/ s23765/Scramble (10µM)*	*Opti-MEM*
25nM	2.5µl	47.5µl
50nM	5µl	45µl
75nM	7.5µl	42.5µl
100nM	10µl	40µl

Table 3. 10. Different concentrations of SIRT4 siRNA Duplex were used in optimisation

siRNA Concentration	*siRNA s23764 (10µM)*	*siRNA s23765 (10µM)*	*Opti-MEM*
25nM	1.25µl	1.25µl	47.5µl
50nM	2.5µl	2.5µl	45µl
75nM	3.75µl	3.75µl	42.5µl
100nM	5µl	5µl	40µl

Table 3. 11. Representing the different conditions used to test for the optimal SIRT4 siRNA concentration

12 well plate #	*Condition*
1	siRNA silencer select s23764 (SIRT4)
2	siRNA silencer select s23765 (SIRT4)
3	siRNA silencer select duplex (s23764 and s23765) (SIRT4)
4	silencer select siRNA negative control (4390843)
5	Transfection reagent only (no siRNA silencer select)
6	Control (no siRNA silencer select and no transfection reagent)

Cells were incubated with each complex for 24 hours at 37°C, 0.5% CO_2. After 24-hours media was removed and cells were washed with PBS. Cells were then re-incubated in differentiation media for a further 24 hours. Following this 24-hour incubation media was removed, cells were washed in PBS and cells were extracted from wells using Tri reagent. Tri reagent extracts were then stored

within eppendorfs at -80°C until ready to perform RNA extraction and subsequent RT-qPCR for presence of the Sirtuin 4 (SIRT4) gene.

Primary Human Skeletal Muscle Myotubes Optimal siRNA Transfection Time

The next step was to optimise the incubation time to knockdown SIRT4 by examining the changes following 0-, 1-, 24-, 48- and 72-hours. Primary human skeletal muscle myoblasts were grown until confluent in 12 well plates and differentiated as described above. 3.75µl siRNA silencer select s23764 and 3.75µl siRNA silencer select s23765 were added to 42.5µl Opti-MEM to create a duplex siRNA at 75nM. This complex was then incubated with a solution of 6µl lipofectamine 3000 in 50µl Opti-MEM per well for 5 minutes. 7.5µl silencer select siRNA negative control (4390843) (scramble) was added to 42.5µl Opti-MEM. This was incubated in a solution of 6µl lipofectamine 3000 in 50µl Opti-MEM for 5 minutes and as with the duplex sample, the scramble sample (4390843) was added to its specific well in drops. Cells were incubated with each complex for 24 hours at 37°C, 0.5% CO_2. After 24-hours media was removed and cells were washed with PBS.

Cells were then either re-incubated in differentiation media for a further 60 minutes, 24 hours, 48 hours or 72 hours or extracted using Tri reagent for time point 0 minutes (see Figure 3.11). Following incubation, media was removed, cells were washed in PBS and cells were extracted from wells using Tri reagent. Tri reagent extracts were then stored within eppendorfs at -80°C until ready to perform RNA extraction and subsequent RT-qPCR for presence of the Sirtuin 4 (SIRT4) gene.

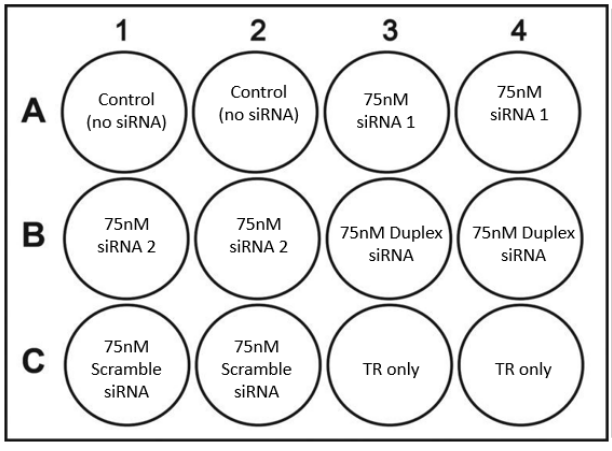

Plate set up for primary human skeletal muscle myotube optimal siRNA transfection time
Cells extracted following 24-hours siRNA incubation:

- 0 minutes
- 60 minutes
- 24 hours
- 48 hours
- 72 hours

Figure 3. 11. Example of plate setup for optimal siRNA transfection time

MitoTraker Green FM Mitochondrial Content Probing

MitoTraker Green FM (Invitrogen™, M7514) (MW: 671.88) was prepared to 1mM using sterile dimethyl sulfoxide (DMSO) as per manufacturer's instructions to assess mitochondrial content. MitoTraker Green was wrapped in tinfoil and stored at -20°C due to light sensitivity and stock solutions were replaced every 2-weeks. Following optimization of MitoTraker Green FM concentration and the time of incubation using C_2C_{12} myotubes (see Appendix Section G), 150nM MitoTraker Green FM was prepared in differentiation medium (ATCC PCS-950-050™). Primary HSM myotubes, grown and differentiated for 10 days on 35mm imaging dishes with a polymer coverslip bottom (Ibidi GmbH, µ-Dish 35mm, 81156), were prepared for this assay by removing media and washing in PBS twice. Cells were subsequently incubated in 150nM of MitoTraker Green in differentiation media at 37°C, 0.5% CO_2 in darkness (sensitive to light) for 30 minutes. Following incubation, media was removed and cells were washed with PBS twice. Cells were then suspended in differentiation medium before counter staining for nuclei content to aid in the analysis of mitochondrial content and tubulation using confocal microscopy (Leica Microsystems, DM IRE2).

Nuclear Content Probing

NucBlue Live Stain (Thermo Fisher Scientific Inc., Hoechst 33342 dye, R37605) was used to probe cell nuclei for live cell imaging. Prior to nuclei staining (and following mitochondrial content staining), the media was removed and cells were washed with PBS before reincubation in the relevant cell media and 2 drops of NucBlue Live Stain (R37605) per milliliter of cell media. NucBlue Live Stain was incubated for 20 minutes at 37°C and the cells were washed with fresh PBS before reincubation in human skeletal muscle differentiation medium (ATCC PCS-950-050™). Cells were then assessed for nuclear staining using confocal microscopy (Leica Microsystems, DM IRE2).

Confocal Microscopy

Live scan confocal microscopy experiments were conducted using a Leica DM IRE2 confocal microscope. 35mm imaging dishes with a polymer coverslip bottom (Ibidi GmbH, µ-Dish 35mm, 81156) were used for all cell culture experiments requiring confocal microscopy. The microscope stage was maintained at 37°C with humidified 5% CO_2 air during imaging. All cell imaging planes were standardized, capturing a maximum of 2 elongated myotubes per image, to limit bias in analysis. Care was taken to shield samples from confocal laser as much as possible prior to acquisition in order to prevent bleaching of the fluorophore and a reduction in image quality. Once the ideal image was attained, focus was set to 4X zoom in order to measure mitochondrial

tubulation per cell between stacks in series. Photomultiplier Tube 1 (PMT1) was set between 405nm and 488nm for nuclei imaging, while PMT2 was set between 500nm and 550nm for mitochondrial imaging. Deconvolution of all attained images was subsequently undergone using MetaMorph Imaging System prior to image analysis.

Mitochondrial Network Analysis (MiNA)

Mitochondrial networks were analysed using the Mitochondrial Network Analysis (MiNA) toolset in ImageJ as per Valente et al., A simple ImageJ macro tool for analyzing mitochondrial network morphology in mammalian cell culture [530]. This toolset recognizes two distinct object types; individuals (structures with no junctions) and networks (structures with at least one junction). Networks are broken into; branch, junctions, slabs, and end-points. See below for graphical representation of the image preparation process within ImageJ and terminology used (Figure 3.12).

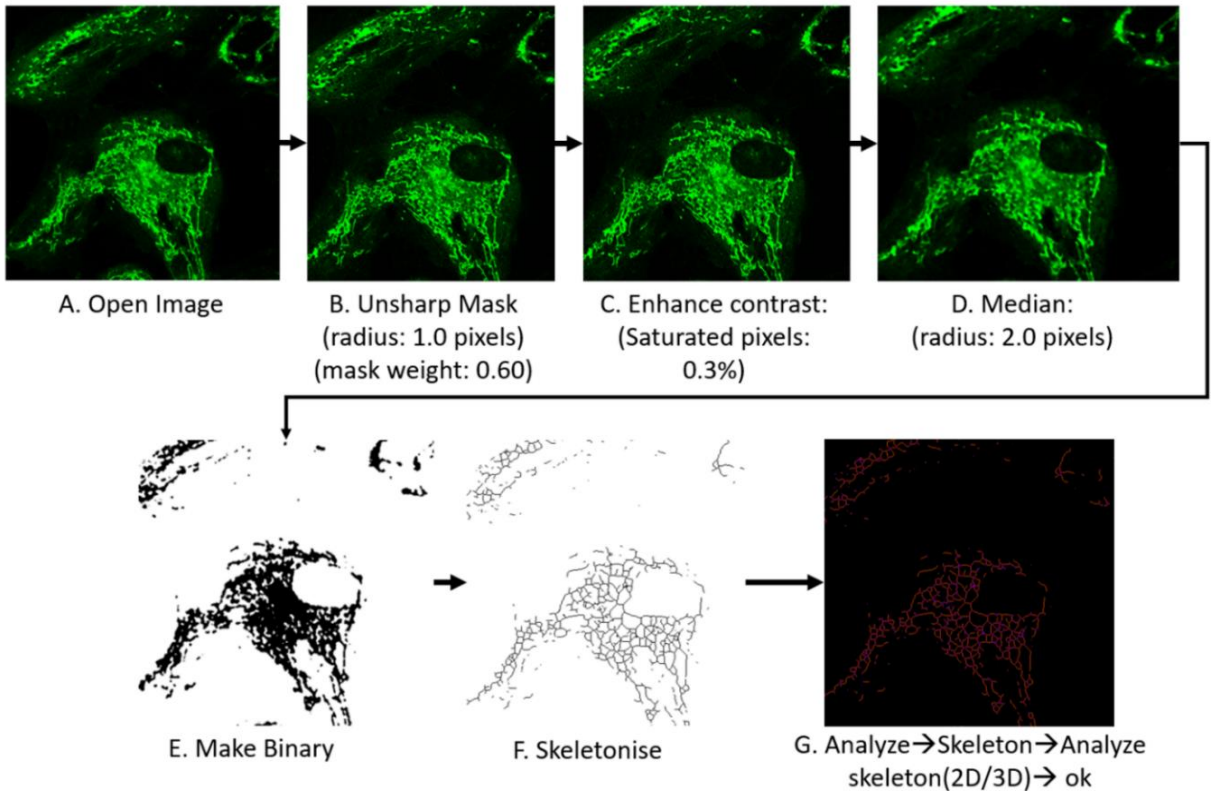

Figure 3. 12. Analysis of mitochondrial networks using MiNA

(Preparation of an image of a primary human skeletal muscle cell probed with MitoTraker Green FM for mitochondrial network feature analysis. and (D) median. The image is then (E) binarized and (F) skeletonised before (G) analysis of its networks) following A-G)

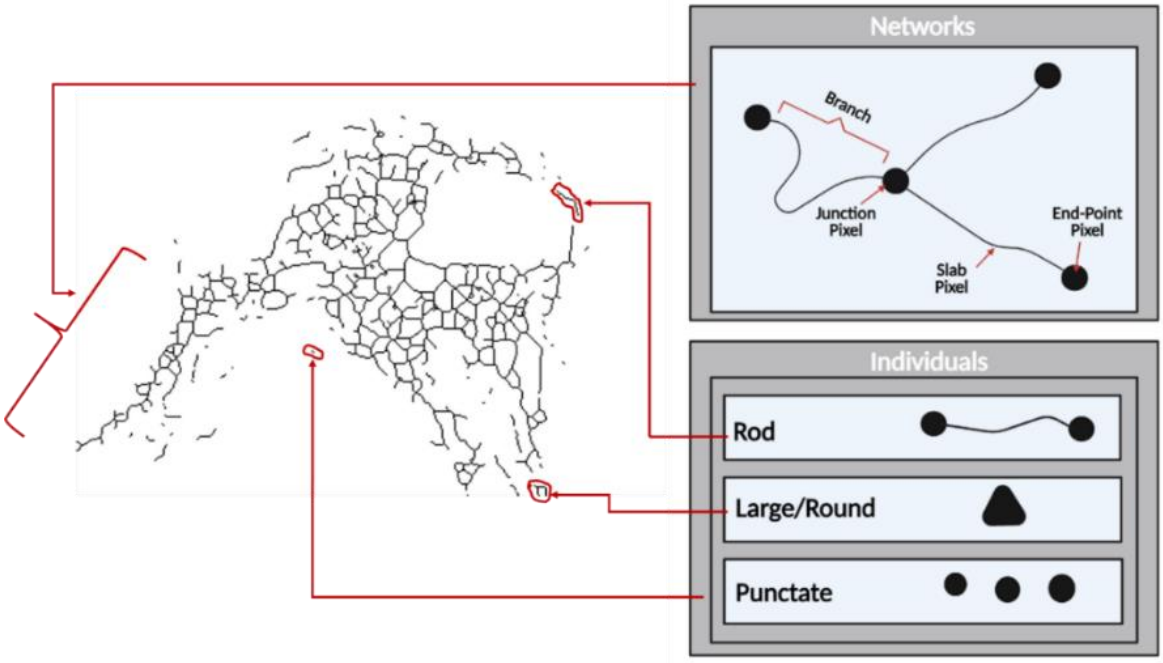

Examples of common mitochondrial network features. MiNA will recognize only two types of mitochondrial structures in a skeletonized image: networks and individuals. Individuals are punctate (a single pixel in the skeletonized image), rods (unbranched structures with two or more pixels in the skeletonized image), and large/round structures (which are reduced to rods, or occasionally small networks, during skeletonization). Networks are mitochondrial structures with at last a single node and three branches. As per Valente et al. [530]

Sample Analysis

Mitochondrial Substrate-Uncoupler-Inhibitor Titration (SUIT) Respiration Assays

Respiration was measured at 37˚C in each chamber containing 2ml MiR05. Oxygen concentration within each chamber was set at 200nmol O_2/ml. The software DatLab (Oroboros Instruments GmbH, Innsbruck, Austria) was used for data acquisition at 2 second time intervals [392]. The carbohydrate (CHO) substrate-uncoupler-inhibitor-titration (SUIT) protocol for high resolution respirometry was applied following stabilization to all human skeletal muscle biopsy samples, while the fatty acid (FA) SUIT protocol for high-resolution respirometry was applied following stabilization to all human skeletal muscle cell culture samples. The Oroboros-O2k chambers were calibrated to the respiration medium, MiR05, prior to both the CHO and FA SUIT protocols with air calibrations (R1) performed prior to every experiment and zero calibrations (R0) were performed weekly. K-Lactobionic, CaK_2EGTA, and K_2EGTA stocks prepared in advance of making BIOPS and MIR05 solutions. MiR05 (EGTA 0.5 mM, $MgCl_2.6H_2O$ 3 mM, taurine 20 mM, KH_2P0_4 10 mM, HEPES 20 mM, BSA 1 g $liter^{-1}$, potassium-lactobionate 60 mM, mannitol 110 mM, dithiothreitol 0.3 mM, pH 7.1, adjusted with 5M KOH) was made in advance of all experiments [286,392].

Human Skeletal Muscle Fibre Preparation

Following biopsy of the human vastus lateralis approximately 8mg of muscle tissue was immediately placed the ice-cold BIOPS solution (CaK_2EGTA 2.77 mM, K_2EGTA 7.23nM, Na_2ATP 5.77mM, $MgCl_2.6H_2O$ 6.56mM, taurine 20nM, Na_2Phosphocreatine 15mM, Imidazole 20nM, DTT 0.5nM, MES hydrate 50nM, pH 7.1, adjusted with 5M KOH). After rapid manual separation of the muscle fibres, with two very sharp forceps on a petri dish in BIOPS under a microscope (see Figure 3.13), the fibres were quickly placed in a BIOPS solution supplemented with 50ul/ml saponin and gently agitated at 4˚C for 30 minutes. Saponin specifically removes the sarcolemma and leaves the intracellular structures intact [534,285]. The muscle fibres were then washed in respiration medium, MiR05. Fibres were blotted, weighed and immediately placed in the two chambers for respirometry measurements [185].

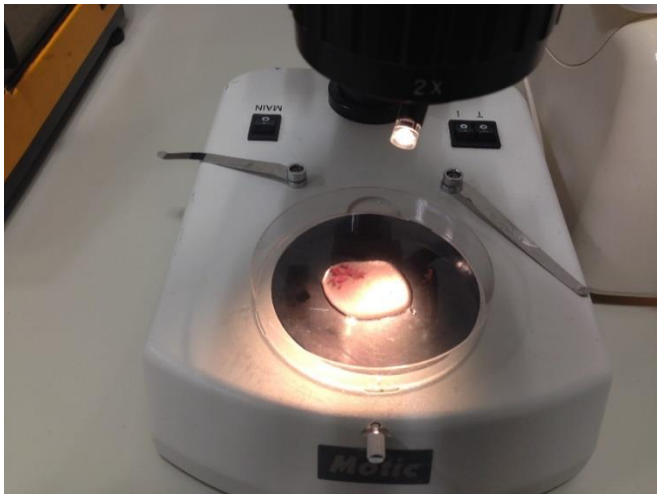

Figure 3. 13. Mechanical separation of human skeletal muscle biopsy within BIOPS for preparation for high- resolution respirometry

Cell Culture Preparation

Following siRNA SIRT4 knockdown of human skeletal muscle myotubes, cells were prepared for their Oroboros-O2k SUIT protocol. In sterile conditions media was removed from the skeletal muscle myotubes grown, differentiated and treated in culture. Cells were subsequently incubated in trypsin at 37°C and 0.5% CO_2 until cells detached from their plate. Following myotube detachment, trypsin was neutralized using skeletal muscle differentiation media (ATCC PCS-950-050™). Cells were then suspended within a 20 ml sterile universal tube before being centrifuged at 1,000rpm for 5 minutes. Following centrifugation, the supernatant was removed and cells before they were resuspended in 5ml MiR05 before cells were counted in trypan blue. Following cell count, 2.5ml of counted cells suspension were pipette into the two empty Oroboros-O2k chambers, calibrated with MiR05, for experimentation.

Carbohydrate (CHO) SUIT – Human Skeletal Muscle Biopsies

Substrate combinations were used for electron transport through complex I (CI) and complex II (CII) of the electron transport chain for the CHO SUIT. Oroboros-O2k chambers were calibrated in MiR05. Prepared biopsy sample was placed into chamber with calibrated MiR05. Following the stabilization of ROUTINE respiration, LEAK respiration was measured in the presence of pyruvate and malate (PM) and in the absence of adenosine diphosphate (ADP). LEAK respiration refers to the proton flux through the inner mitochondrial membrane [392]. It is mainly controlled by and compensating for the proton leak across the inner mitochondrial membrane. Oxidative phosphorylation (OXPHOS) was then measured with the addition of ADP. OXPHOS refers to the oxidative phosphorylation capacity at saturating ADP concentrations and it is the measure of the oxygen consumption coupled to the phosphorylation of ADP to ATP. Glutamate was then added as an additional substrate to generate NADH (PMG). Uncoupler titrations of Carbonyl cyanide p-trifluoro-methoxyphenyl hydrazine (FCCP) were performed in the ADP activated state, to achieve Complex I linked electron transport system (ETS CI) capacity (non-coupled). Maximal ETS capacity with convergent electrons flow from complex I and II was reached after addition of succinate (Complex I & II linked ETS capacity). Complex I was inhibited by the titration of rotenone (R) to measure respiration through CII only. Malonic acid (Mna) and Antimycin A (Ama) were then titrated to inhibit complex II and III, respectively (residual oxygen consumption - ROX) (see Table 3.12 for full breakdown of the CHO SUIT products, concentrations and volumes used). ROX remains even after the inhibition of the ETS. All mitochondrial respiratory states were corrected for ROX which accounts for non-mitochondrial cellular oxygen consuming processes.

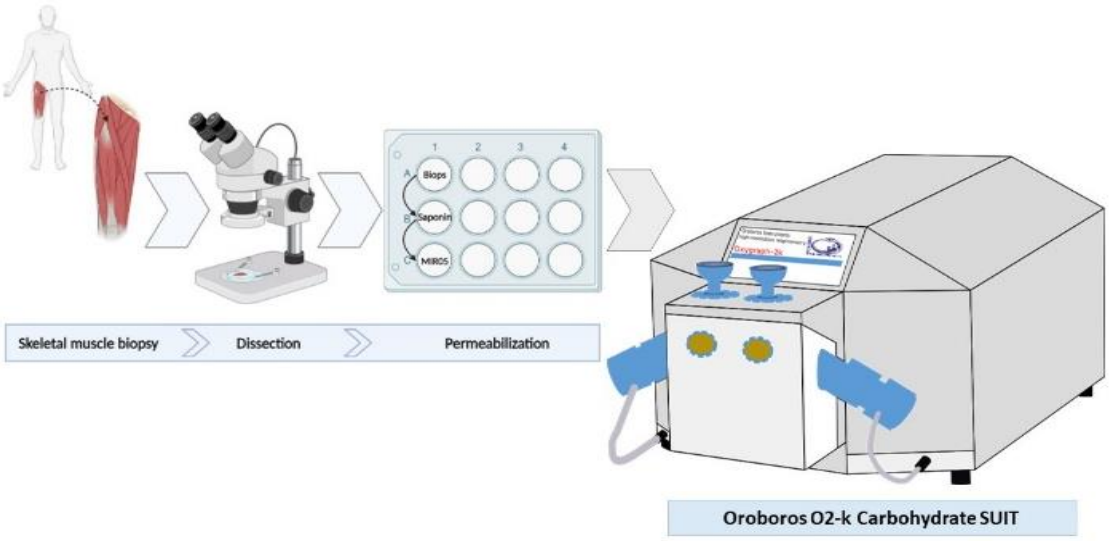

Figure 3. 14. Schematic representation of the process of human skeletal muscle biopsy mitochondrial respiration

Table 3. 12. Carbohydrate SUIT using the Oroboros Oxygraph O2k

Products	*Stock Solution (M)*	*Chamber (mM)*	*Syringe Volume (µL)*
Pyruvate	2	5	5
Malate	0.8	5	12.5
ADP	0.5	2.5	10
Glutamate	2	10	10
FCCP	0.001	0.001	1
Succinate	1	10	20
Rotenone	0.001	0.005	10
Malonate	2	5	5
Antimycin A	0.005	0.0025	1
Ascorbate	0.8	2	5
TMPD	0.2	0.5	5

Fatty Acid (FA) SUIT – Cell culture

Respiration of human skeletal muscle myotubes were measured at 37 ˚C with approximately $4x10^5$ cells per ml in each chamber containing 2ml MiR05. As with the CHO SUIT, ROUTINE respiration was measured following stabilization of oxygen flux within the chamber. However, unlike the CHO SUIT, LEAK respiration was measured by the addition of palmitate and malate (PalM). Oxidative phosphorylation (OXPHOS) was then measured with the addition of ADP. The experiment proceeded with the addition of malonic acid (Mna) and Antimycin A (Ama) to inhibit complex II and III for the calculation of ROX. As with the CHO SUIT, all mitochondrial respiratory states were corrected for ROX. See Table 3.13 for full breakdown of the fatty acid SUIT products, concentrations and volumes used.

Table 3. 13. Fatty Acid SUIT using the Oroboros Oxygraph O2k

Products	***Stock Solution (M)***	***Chamber (mM)***	***Syringe Volume (µL)***
Palmitoyl-carnitine	0.01	0.04	8
Malate	0.8	5	12.5
ADP	0.5	2.5	10
Malonate	2	5	5
Antimycin A	0.005	0.0025	1

Protein Extraction & Quantification

Lyophylisation - Human Skeletal Muscle Biopsies

Muscle which had been stored at -80°C was cut under liquid nitrogen into pieces ~25-30 mg. Samples were lyophilised (Christ Alpha 1-2 LD Plus) (see Figure 3.15) for 16 hours and a further 2-hour final dry to ensure all moisture was removed from the muscle. Following lyophilisation muscle was quickly dissected under a microscope with two sterile tweezers to remove any connective tissue and excess blood. Samples were weighed once again and placed into a new eppendorf.

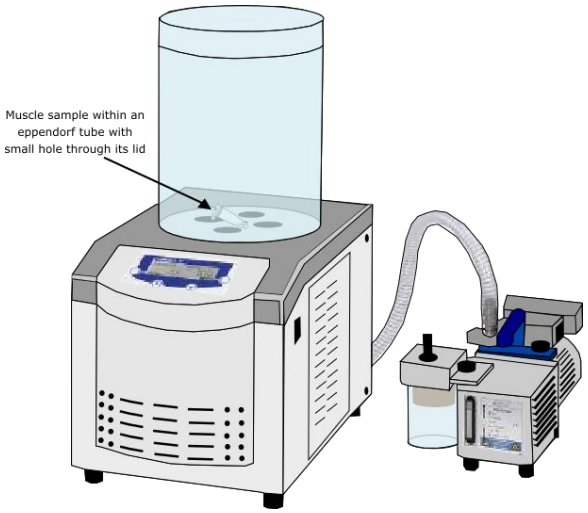

Figure 3. 15. Schematic representation of the Christ Alpha 1-2 LD Plus, lyophyliser used to freeze dry skeletal muscle sample

Protein Extraction – Human Skeletal Muscle Biopsies

Lyophilised samples were homogenized using a hand-held homogenizer (Kinematica AG, Dispersing and Mixing Technology) for approximately 3x20 seconds at 25,000rpm (max) in homogenization buffer (Okadiac buffer (200uM), protease inhibitor (50X prepared with ultrapure water) (Sigma Aldrich, P8340), DTT (100mM), sodium orthovanadate (100mM), PMSF (100mM). Samples were then left on ice for 10 minutes, centrifuged (Thermo Fisher Scientific Ltd., Sorvak Legend Micro21R centrifuge) at 14,000 rpm for 20 minutes at 4°C and the supernatant was used for protein quantification. See Figure 3.16 for a schematic representation of protein extraction from lyophilised skeletal muscle.

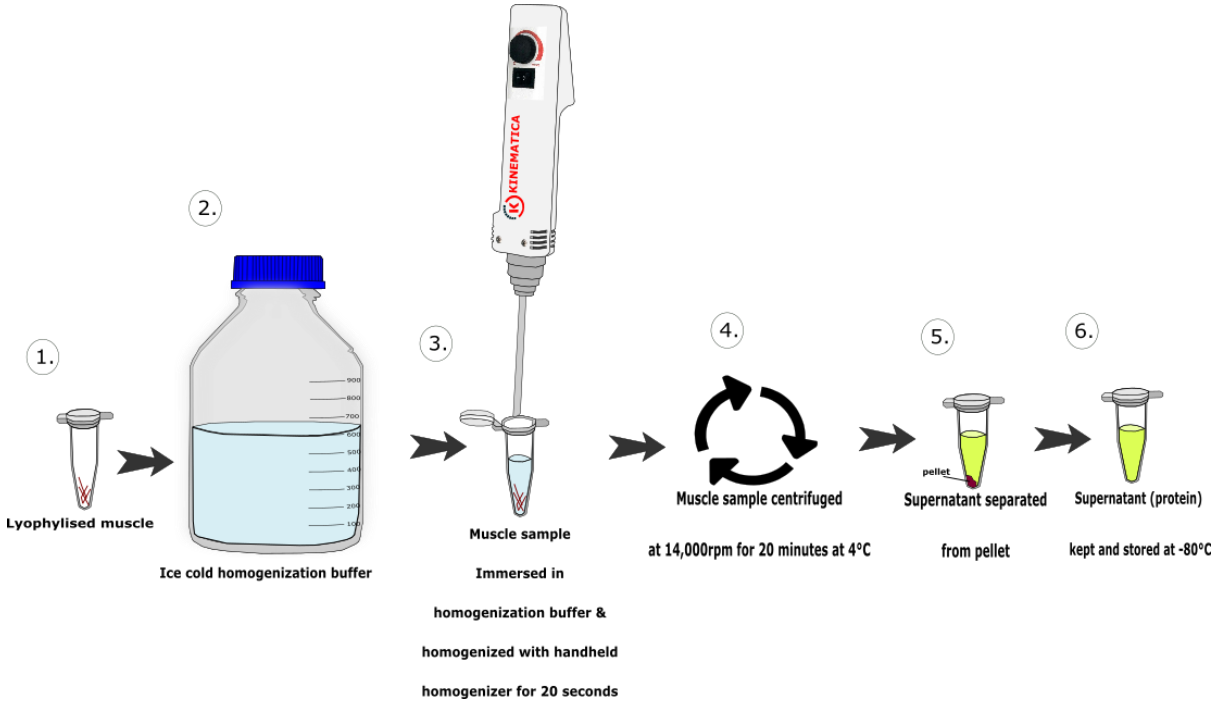

Figure 3. 16. Schematic representation of the process to isolate human skeletal muscle protein

Protein Extraction – Cell culture

NP40 Lysis buffer supplemented with 1 × protease inhibitor cocktail (50x prepared with ultrapure water) (Sigma Aldrich, P8340), 1 × PMSF (100mM), 1x Na_3VO_4 (100mM), 1 × DTT (100mM) was used for protein extraction of primary human skeletal muscle cells. Media was removed from the cell line, washed with PBS and suspended the NP40 lysis buffer supplemented solution (40-70µl per well of 6 well plate depending on cell concentration). Cells were scraped off well using cell scraper and pipette into a 2ml eppendorf tube, all extraction process took place on ice. Cells were incubated in lysis buffer at 4°C for 30 minutes on a stirrer, then centrifuged at 14,000 rpm for 20 minutes at 4°C using a microcentrifuge (Thermo Fisher Scientific Ltd., Sorvak Legend Micro21R centrifuge). The protein containing supernatant was stored in a fresh, pre-chilled and labelled eppendorf at -80°C. See Figure 3.17 for a schematic representation of protein extraction from cell lines.

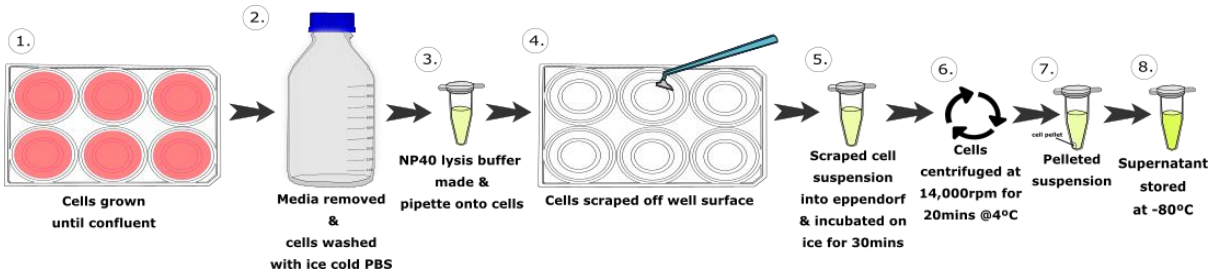

Figure 3. 17. Schematic representation of the process of protein extraction from cells in culture

Protein Quantification using the Bradford Assay

For protein quantification, a Bradford assay was used based on the Bio-Rad protein assay kit (Bio-Rad Inc., 500-0006). Before starting, the Bradford reagent (Quick Start Bradford 1x Dye Reagent, Bio-Rad Inc., 500-0205) was removed from the fridge (4°C) to let the solution warm up to room temperature. A standard protein curve (1.0, 0.5, 0.25, 0.125, 0mg/ml) was prepared by diluting bovine serum albumin (BSA) (2mg/ml) (Quick Start Bovine Serum Albumin Standard, Bio-Rad Inc., 500-0206) in UHP water. Samples were also diluted (1:10) in UHP. In a 96-well plate, 5µl of each dilution (testing sample and standard curve) was added in triplicate. Using a multi-channel pipette, 200 µl of Bradford reagent was added to each well. Absorbance was read at 595nm using the BioTek Synergy HT plate reader. A standard curve was generated to quantify protein in the muscle samples, based on the known protein concentrations and the given absorbance, using the equation of the line (Y=m*X+C) and its linear regression (R^2).

Sample Preparation - Sodium Dodecyl Sulfatepolyacrilamide Gel (SDS-PAGE)

SDS-PAGE - Human Skeletal Muscle Biopsies

Protein samples extracted from human skeletal muscle biopsies were made to equal protein concentrations within a buffer containing protein sample, homogenization buffer and 5x Laemmle buffer for SDS-PAGE.

SDS-PAGE - Cell Culture

Protein samples extracted from myotubes grown in cell culture were made to equal protein concentrations within a buffer containing protein sample, NP40 lysis buffer and 5x Laemmle buffer for SDS-PAGE.

Sodium Dodecyl Sulfatepolyacrilamide Gel (SDS-PAGE)

Following sample preparation, samples were heated at 70°C for 10 minutes to denature protein enzymes using a Thermo Scientific Hybaid Px2 PCR heating block. Ready-to-use SDS gels (Life technologies Bis-Tris 4-12% Bolt 12 well (Thermo Fisher Scientific Inc., NW04122BOX), NOVEX WW 4-20% TG Gel 12 well, Thermo Fisher Scientific Inc., XP04202BOX) were placed in the SDS rig along with approximately 800ml 1x MES buffer/gel (20X Bolt MOPS/MES SDS Running Buffer, Thermo Fischer Scientific Inc., B0001/B0002). Once prepared, SDS gels were ran at 150V for 10 minutes within the rig before any sample was loaded into gels. Following pre-run, molecular weight marker (SeeBlue Plus2 Pre-Stained Protein Standard (Thermo Fisher Scientific Inc., LC5925)/ Spectra Multicolor High Range Protein Ladder (Thermo Fisher Scientific Inc., 26625)) (5µl) was loaded into the appropriate well. An equal amount of protein sample was then loaded into the appropriate SDS gel well to allow for correct comparison of the results. Once loaded, protein samples were separated using electrophoresis at the appropriate voltage for the specific set of time depending on weight of protein of interest (i.e. 150V for 1.5 hours). See Figure 3.18 for a schematic representation of the full process of SDS-PAGE. Following sample separation in gel, SDS gels were transferred onto either polyvinylidene difluoride (PVDF) or nitrocellulose membranes, depending on protein of interest.

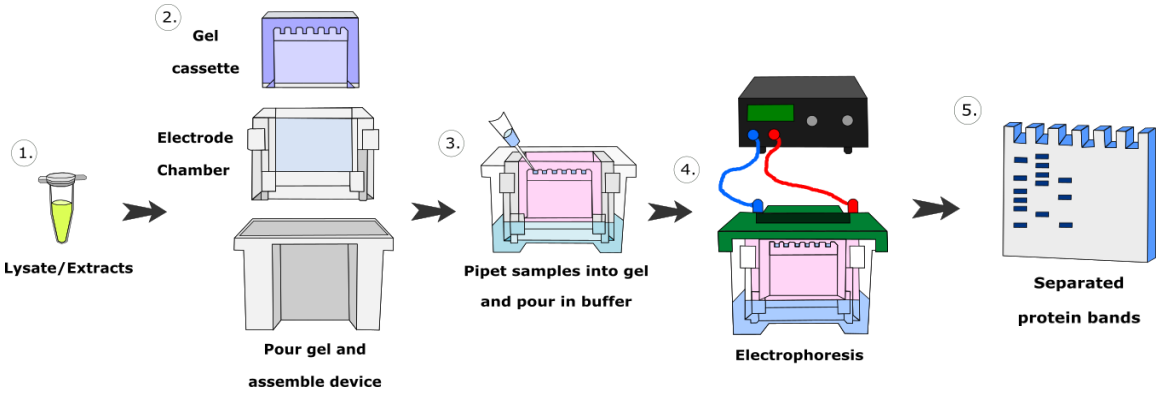

Figure 3. 18. Schematic representation of the process of SDS-PAGE using extracted protein

Western Blot

Protein Transfer

Protein was transferred onto a nitrocellulose membrane (trans-blot turbo nitrocellulose Bio-Rad, 1704159 or regular size, nitrocellulose (IB301001)/Polyvinylidene fluoride (IB401031), Invitrogen™ iBlot™ Transfer Stacks) using the TurboBlot (Bio-Rad Trans-Blot Turbo Transfer System) or the iBlot1 (Invitrogen™) (see Figure 3.19) transfer systems.

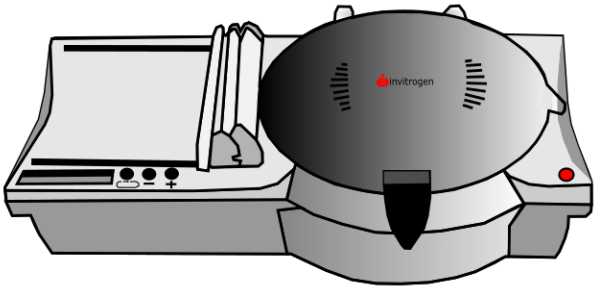

Figure 3. 19. Schematic representation of iBlot 1, Invitrogen used to transfer protein from gel onto nitrocellulose and PVDF membranes

Determination of Protein Transfer

Following transfer, nitrocellulose membranes were immersed in Ponceau stain (neat) for 30 seconds to ensure that the protein had transferred. All Ponceau was washed off using TBS-tween (tween: Sigma-Aldrich, Tween20 p1379) 30 seconds after immersion (Ponceau stain was not performed when looking at phosphorylated proteins).

Gels transferred onto PVDF membranes (and nitrocellulose membranes looking at phosphorylated proteins) were immersed briefly in Brilliant Blue G (Sigma-Aldrich, B0770) to ensure that the protein of interest had correctly transferred onto the membrane.

This was performed as follows:

The gel was submerged in a fixing solution for 1 hour (7% glacial acetic acid in 40% methanol). It was subsequently immersed in Coomassie Brilliant Blue G solution (4 parts Brilliant Blue G, 1-part methanol) for 2 hours. The gel was then placed in 10% acetic acid, 25% methanol solution for 30 seconds, rinsed with 25% methanol. Gel was then read for presence/absence of protein using a light box.

Antibody Incubation

Membranes were then blocked in TBS Li-Cor Odyssey blocking buffer (Li-Cor, 927-50000) or 5% milk (Bio-Rad, 170-6404) in TBS (1X) for 2 hours before incubation in primary antibody of target proteins, which was prepared in the Odyssey blocking buffer and our own antibody dilution buffer (100% Tris-Buffered Saline, 0.1% sodium azide, 0.1% bovine serum albumin), overnight at 4^{o}C. See Table 3.14 for a full list of antibodies and positive controls directed against target proteins for immunoblot assays. Following primary incubation overnight, the membrane was washed six times using Belly Dancer orbital shaker, for 10 minutes each time, in TBS-tween. The membrane was incubated with Li-Cor secondary antibody (donkey anti-rabbit 800CW (Li-Cor, 925-32213)/donkey anti-mouse 800CW (Li-Cor, 925-32212) or donkey anti-rabbit 680 RD (Li-Cor, 925-68073)/donkey anti-mouse 680RD (925-68072) prepared within Odyssey blocking buffer only) or a goat anti-rabbit/mouse IgG (H + L)- Horseradish peroxidase (HRP) conjugate secondary (Bio-Rad, Cat:170-6515 & 170-6516) for 2 hours in darkness. Information on cell lines grown to assist in the probing of protein targets (positive controls) are extrapolated further within the Appendix (Section F).

Table 3. 14. Antibodies & positive controls directed against target proteins for immunoblot assays

Target	*Supplier*	*Product*	*kDa*	*Host*	*Monoclonal/ Polyclonal*	*Positive Control*
Alpha-Tubulin	Cell Signalling Technology Inc.	DM1A #3873	50	Mouse	Monoclonal	HeLa
AMPK	Cell Signalling Technology Inc.	23A3 #2603	62	Rabbit	Monoclonal	293T
ANT1	Abcam plc.	ab180715	33	Rabbit	Polyclonal	HepG2
BCL2-L13	Abcam plc.	ab27795	55-60	Rabbit	Polyclonal	Jurkat cell lysate
BNIP3	Cell Signalling Technology Inc.	D7U1T. 44060	50-55	Rabbit	Monoclonal	HeLa
CPT1b	Abcam plc.	Ab134988	88	Rabbit	Polyclonal	Human skeletal muscle
Drp1	Cell Signalling Technology Inc.	D6C7. 8570	78-82	Rabbit	Monoclonal	HeLa, C_2C_{12}
Fis1	Santa Cruz Inc.	B-5 (sc-376447)	18	Mouse	Monoclonal	HeLa, SK-BR-3
GAPdh	Cell Signalling Technology Inc.	5174	37	Rabbit	Monoclonal	HeLa
Hexokinase II	Cell Signalling Technology Inc.	C64G5 #2867	102	Rabbit	Monoclonal	HeLa
HIF-1α	Cell Signalling Technology	3716	120	Rabbit	Monoclonal	Raji
LC3B	Cell Signalling Technology Inc.	2775	16	Rabbit	Monoclonal	HeLa
MCU	Cell Signalling Technology Inc.	14997S	30	Rabbit	Monoclonal	PANC-1
Mfn1	Cell Signalling Technology Inc.	D6E2S. 14739	82	Rabbit	Monoclonal	HeLa
Mfn2	Cell Signalling Technology Inc.	9482	80	Rabbit	Monoclonal	HEK293T
mTOR	Cell Signalling Technology Inc.	2972	289	Rabbit	Monoclonal	HEK293
NR4A3/NOR1	Novus Biologicals plc.	OTI5C2	85	Mouse	Monoclonal	HEK293
OMA1	Abcam plc.	ab154949	59	Rabbit	Polyclonal	Rat heart tissue lysate
OPA1	Cell Signalling Technology Inc.	D6U6N. 80471	80-100	Rabbit	Monoclonal	MEFs
pACC(Ser79)	Cell Signalling Technology Inc.	3661	280	Rabbit	Monoclonal	HEK293
pAMPK (Thr172)	Cell Signalling Technology Inc.	2535	62	Rabbit	Monoclonal	C_2C_{12}
Pan-Calcineurin A	Cell Signalling Technology Inc.	2614	59	Rabbit	Monoclonal	MCF7
Parkin	Cell Signalling Technology Inc.	2132	52	Rabbit	Monoclonal	C6
pDrp1 (s616)	Cell Signalling Technology Inc.	3455	78-82	Rabbit	Monoclonal	HeLa
pDrp1 (s637)	Cell Signalling Technology Inc.	4867	78-82	Rabbit	Monoclonal	PC-12

Target	*Supplier*	*Product*	*kDa*	*Host*	*Monoclonal/ Polyclonal*	*Positive Control*
PGC-1alpha	Calbiochem/Millipore KGaA	777-797. 516557	92	Rabbit	Polyclonal	C_2C_{12}
PINK1	Cell Signalling Technology Inc.	D8G3. 6946	63	Rabbit	Monoclonal	293T
Pyruvate Dehydrogenase	Cell Signalling Technology Inc.	C54G1 #3205S	43	Rabbit	Monoclonal	HepG2, HeLa
SIRT1	Cell Signalling Technology Inc.	9475	120	Rabbit	Monoclonal	HeLa
SIRT4	Sigma-Aldrich	HPA029691	36	Rabbit	Polyclonal	HepG2, Rat kidney lysate
TOM20	Santa Cruz Inc.	F-10. SC-17764	20	Mouse	Monoclonal	HeLa, Raji
VDAC1	Cell Signalling Technology Inc.	D73D12 #4661	32	Rabbit	Monoclonal	HEK293
YME1L	Abcam plc.	ab170123	90	Rabbit	Polyclonal	HepG2, HeLa

Protein Detection

Following secondary incubation, blots were washed six times as before using TBS-tween. Proteins were visualized using the Odyssey Infrared Imaging System (Figure 3.20) at either an intensity of 680RD (red/700nm channel) or 800CW (green/800nm channel) (based on secondary antibody used) (Li-Cor, BioSciences).

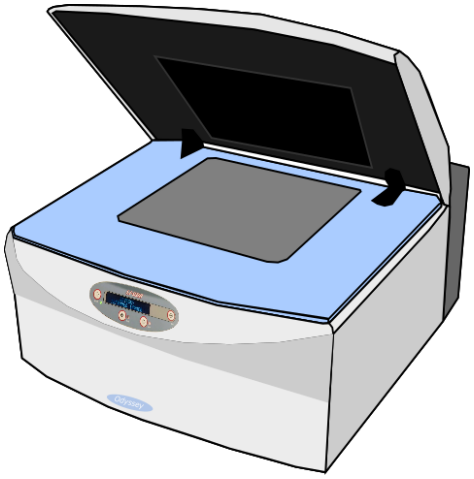

Figure 3. 20. Schematic representation of the Odyssey Infrared Imaging System, Li-Cor, used to detect protein expression

Some proteins with a high molecular weight or sample with low protein concentration following extraction were visualized using engaged chemiluminescence (ECL), detected in a dark room using fixing and developing solutions before being quantified by densitometry.

Densitometry Analysis

Relative protein abundance was quantified using densitometry using the TotalLab Quant software (v1.0). Samples were controlled against a biological control and a housekeeping protein (GAPdh rabbit mAb 14C10, 1:5000, Cell Signaling Technology, 2118 or Alpha-Tubulin mouse mAb, 1:5000, Sigma-Aldrich, T9026). The molecular weight of each protein was compared to a positive control, following the manufacturers suggestions (see positive control table for more information).

Stripping Nitrocellulose Membranes

Some nitrocellulose membranes were stripped and reprobed. Following TBS-tween washing, membranes were incubated in stripping buffer (Thermo Fisher Scientific Inc. Restore™ PLUS Western Blot Stripping Buffer, 46430) for 5 minutes and washed in TBS-tween 3 times (10 minutes each). Membranes were then blocked in Odyssey Blocking Buffer (TBS) (Li-Cor, 927-50000) for 45 minutes before being incubated for 1 hour in the secondary horse radish peroxidase (HRP) of

relevance. Following incubation in secondary antibody the blot was washed 3 times (10 minutes each) in TBS-tween before being assessed using the Odyssey Infrared Imaging System (Li-Cor). The absence of protein bands following 2-15 minutes of incubation in ECL substrate and subsequent detection of protein through Ponceau staining (Sigma-Aldrich, P7170-1L) (30 seconds per membrane) confirmed the stripping was successful.

mRNA Analysis

All Ribonucleic acid (RNA) was isolated and manipulated in an RNase-free environment as it is fragile and easily degraded. Thus, measures to avoid this potential hazard were avoided. All areas were sprayed down with RNaseZap® decontamination solution (Invitrogen™, AMA9780) prior to extraction to remove RNase contamination from surfaces. Tri reagent (guanidinium thiocyanate-phenol-chloroform extraction) (Sigma-Aldrich, T9424) was used for all RNA extraction. RNA was extracted for the purposes of investigating gene expression.

mRNA Extraction – Human Skeletal Muscle Biopsies

Lyophilised samples were placed on ice and 1ml Tri reagent (Sigma-Aldrich, T9424) and homogenized using a hand-held homogenizer (Kinematica AG, Dispersing and Mixing Technology) for approximately 20 seconds at 25,000rpm (max), three times (see Figure 3.21 for schematic representation). Sample was then centrifuged at 1,000rpm for 5 minutes before supernatant was removed and pipette into RNase free tube. Samples were stored at -80°C until RNA isolation procedure.

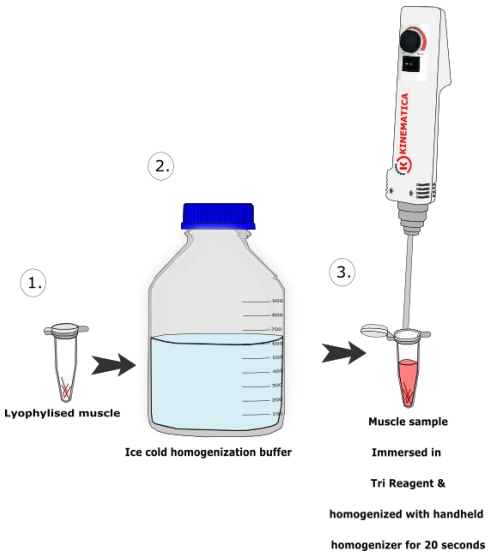

Figure 3. 21. Schematic representation of process of isolating skeletal muscle RNA expression following lyophilisation using Tri reagent

mRNA Extraction – Cell culture

RNA was extracted from myotubes grown in cell culture using Tri Reagent (Sigma-Aldrich, T9424). Differentiation media was removed from cells and wells were washed using pre-chilled PBS. 1ml Tri reagent was pipette per well on a 6 well plate. Cells were scraped using a scraper to gather as much sample as possible. Tri reagent was suspended and re-pipette in order to extract all cells from well. Cells were quickly pipette into a cooled eppendorf before being moved directly into -80°C until RNA isolation.

mRNA Isolation

Samples prepared in Tri Reagent were taken out of -80°C and let stand at ambient temperature for 5 minutes. Molecular biology grade chloroform (Sigma-Aldrich, 496189) was added to each sample (to make a concentration of 80% Tri reagent, 20% chloroform). Sample was shaken vigorously for 15 minutes and incubated at ambient temperature for 15 minutes. Sample was subsequently centrifuged at 13,000rpm for 20 minutes at 4°C. The upper aqueous phase (RNA phase) was transferred into a new eppendorf. Molecular biology grade isopropanol (2-propanol) (Sigma-Aldrich, I9516) was subsequently added to this (0.5 the total volume of tri reagent started with i.e. generally 0.5ml) (see Figure 3.22 for schematic representation of phase separation and isopropanol precipitation). Sample was introverted 7-8 times before leaving to stand at 4°C for 10 minutes. RNA was then centrifuged at 13,000rpm at 4°C for 10 minutes, the supernatant was

removed, and the RNA pellet was washed with 1ml 75% ethanol (RNase-free). Sample was vortexed and then once again centrifuged at 13,000rpm for 10 minutes at 4°C. Supernatant was removed carefully before RNA pellet was dried at room temperature for 5-10 minutes. Pellet was then resuspended in nuclease-free water (50ul per tube). Tubes where then incubated at 60°C in a thermocycler for 10 minutes and immediately kept on ice before quantification using the NanoDrop® ND-1000 system (used in conjunction with operating software v3.8.1) manufactured by Thermo Fisher Scientific Ltd. Samples were then stored at -80°C before transcription into complimentary DNA (cDNA).

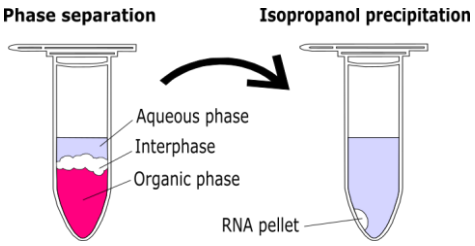

Figure 3. 22. Schematic representation of the phase separation and RNA pellet following isopropanol precipitation

Quantification of RNA by NanoDrop ND-1000 Spectrophotometer

RNA concentration was determined in each sample using a Nanodrop ND-1000 spectrophotometer (Thermo Fisher Scientific Inc.). Following selection of the correct measurement criteria using the software settings (RNA-40), the instrument was calibrated and blanked using 1.5µl RNase-free water. 1.5µl of sample were subsequently pipette on the measurement pedestal and sample absorbance was read at wavelengths of 260/280nm and 260/230nm and the ratio between each was analysed.

260/280 nm: A ratio of ~ 2.0 is regarded as highly purified RNA

260/230 nm: Another measurement of nucleic acid purity; a ratio of 1.8-2.2 was regarded as highly purified RNA.

RNA concentration (ng/µL) was calculated using Beer-Lambert law, based on absorbance at

260 nm:

$$\text{Absorbance} = (E)\,(b)\,(c)$$

Where E is the molar absorptivity coefficient (or extinction coefficient) with units of l/mol-cm, b is the path length (0.1 cm), and c is the analyte concentration in Moles.

Reverse Transcription

RNA samples were converted from single-stranded RNA into double-stranded complimentary DNA (cDNA) using reverse transcription. This was conducted using the High Capacity cDNA Reverse Transcription Kit 200 Rxn (Thermo Fisher Scientific Inc., 4368814). An equal amount of reverse transcription mastermix (see Table 3.15) was added to an equal amount of RNA (1:1 solution).

Table 3. 15. Reverse transcription reaction mix and volumes

RT reaction mix component	*Volume required per 1 reaction (µl)*
Multiscribe	1
Nuclease Free Water	4.2
Random Primers	2
NTPs	0.8
Buffer	2
Total	10

Samples where then reverse transcribed in the PCR thermocycler (Bio-Rad, USA) using the following protocol (Table 3.16):

Table 3. 16. Reverse transcription procedure using PCR thermocycler

Stage	*Temperature (°C)*	*Duration (min.)*
Cycle (40)	25	10
	37	120
Hold	85	5
Hold	4	∞

Once complete the now cDNA samples were quantified using the NanoDrop® ND-1000 system. All samples were made to an equal concentration (i.e. 200ng/µl) using nuclease free water. cDNA was stored at -20°C until needed.

Real-Time Quantitative Polymerase Chain Reaction (RT-qPCR)

Real-Time quantitative Polymerase chain reaction (RT-qPCR) was used to amplify the target gene for measurement of the cycle threshold (Ct), the number of amplification curves and melting peaks. A mastermix for RT-qPCR (see Table 3.17) was created for each gene of interest using cDNA sample of interest.

Table 3. 17. RT-qPCR mastermix per reaction

Component	***1 Reaction (µl)***	***2.5 Reactions (pipetting error) (µl)***
Syber Green (FastStart Essential DNA Green Master, Roche, 06402712001)	6	15
Forward Primer (10µM)	1	2.5
Reverse Primer (10µM)	1	2.5
Nuclease free water	2	5
cDNA	2	5

12µl of mastermix was pipette into each required well of a 96 well plate (LightCycler®480 plates 96 well, Roche, 04729692001) in duplicate. Plates were sealed using supplied LightCycler® sealant and RT-qPCR reaction ran using the LightCycler® 96 (see Figure 3.23 for schematic representation of the Lightcycler® 96 and Table 3.18 for RT-qPCR run overview).

Figure 3. 23. Schematic representation of the LightCycler® 96 Instrument, Roche

Table 3. 18. RT-qPCR LightCycler 96 ®run overview

LightCycler 96 RT-qPCR Run Overview			
	Cycles	**Temperature (°C)**	**Time (seconds)**
Reincubation	1	95	600
3 Step Amplification	45	95	10
		60	10
		72	10
Melting	1	95 65 97	10 60 1

RT-qPCR Gene Analysis

Cycle threshold (Ct) values were analysed using the standard delta-delta Ct method (△△Ct) and consistency between experiments was managed by maintaining Minimum Information for Publication of Quantitative Real-Time PCR Experiments (MIQE) guideline standards [74]. Initially the average Ct value of each duplicate was calculated. Duplicates <0.2 cycles apart from each other were disregarded. Delta Ct (△Ct) was calculated by normalising the Ct gene of interest to the Ct value of the endogenous control (Ct average between duplicates of gene of interest – Ct average between duplicates of endogenous control). Delta Delta Ct (△△Ct) for each gene was calculated across two groups (experimental and control). △△Ct = △Ct (experimental) - △Ct (control). Fold change for each gene from each group was calculated as $2^{(-\triangle\triangle Ct)}$. If fold change was greater than 1 then the result was reported as an up-regulation.

Agarose Gel Electrophoresis

One gram of agarose (Sigma-Aldrich, A9539) was dissolved in 100ml 1x TAE buffer (Sigma-Aldrich, 11666690001) when boiled. Following cooling of buffer, 2µl of Sybr Safe DNA Gel stain (Invitrogen™, S33102) was added per 100ml 1x TAE buffer. Buffer was then solidified into a gel within a gel cassette in darkness (as gel is light sensitive). As gel is setting carefully pipette 2µl 6x loading buffer (6x sucrose + bromophenol blue) per well of amplified RT-qPCR sample (sample will turn blue in presence of DNA). Prepare molecular weight marker for gel using 1µl 100 base pair DNA ladder (Invitrogen™, 15628019), 1µl 6x loading buffer and 4µl nuclease free water. Once agarose gel is set pipette 6µl molecular weight marker and 6µl sample per well to gel. Allow samples to run for approximately 1.5 hours at 100 volts. Analyze gel for the presence/absence of bands and refer to its base pair using the G box system (Syngene - Syber Safe - Epi short wave - UV mode).

Mitochondrial DNA to Nuclear DNA Ratio (mtDNA:nDNA)

Several biochemical measures of mitochondrial components are used as biomarkers of mitochondrial content. The most common methods include citrate synthase activity, cardiolipin content, mitochondrial DNA content, complex I-V protein and complex I-V activity. Mitochondrial DNA to nuclear DNA ratio (mtDNA:nDNA) was used in this regard to normalize all skeletal muscle respirometry data to mitochondrial content. Two mitochondrial (MT_ATP6 and NDUFA4) and three nuclear (MT_CO4, COXIV and POLG) DNA primers were developed to help in this analysis (see Table 3.19 for mtDNA and nDNA targets). Following reverse transcription, both mitochondrial and nuclear DNA targets were analysed using RT-qPCR. As before, the average Ct value of each duplicate was calculated. Delta Ct (△Ct) was calculated by normalizing the Ct gene of interest to the Ct value of the control (e.g. NDUFA4 Ct average between duplicates of sample of interest – NDUFA4 Ct average between duplicates of control). Delta Delta Ct (△△Ct) was subsequently calculated by subtracting mitochondrial DNA △Ct from the nuclear DNA △Ct (e.g. NDUFA4 △Ct – POLG△Ct). The fold change for each was subsequently calculated as $2^{(-\triangle\triangle Ct)}$. Finally, skeletal muscle respirometry data was normalised for mtDNA:nDNA (mitochondrial content) by dividing the ROX-muscle wet weight normalised data by the previously calculated mtDNA:nDNA ratio (pmol[s*ml^{-1}]mg^{-1}mtDNA:$nDNA^{-1}$). All primer combinations were analysed but it was decided to use data controlling skeletal muscle respiration against NDUFA4:POLG (all additional information in this regard can be found in the Appendix Section C).

Table 3. 19. Mitochondrial and nuclear DNA targets

Mitochondrial DNA Targets	***Nuclear DNA Targets***
ATP synthase membrane subunit 6 (MT_ATP6) - *mitochondrial gene for mitochondrial product*	Cytochrome C oxidase subunit 4 (MT_CO4) – *nuclear gene for mitochondrial product*
NADH dehydrogenase subunit IV (NDUFA4) - *mitochondrial gene for mitochondrial product*	Cytochrome C oxidase subunit 4 (COXIV) –*nuclear gene for mitochondrial product*
	Polymerase Gamma Accessory Subunit (POLG) – *nuclear gene for nuclear product*

Primer Design and Optimization

Primers were made MIQE guideline compliant using the following simplified seven step process:

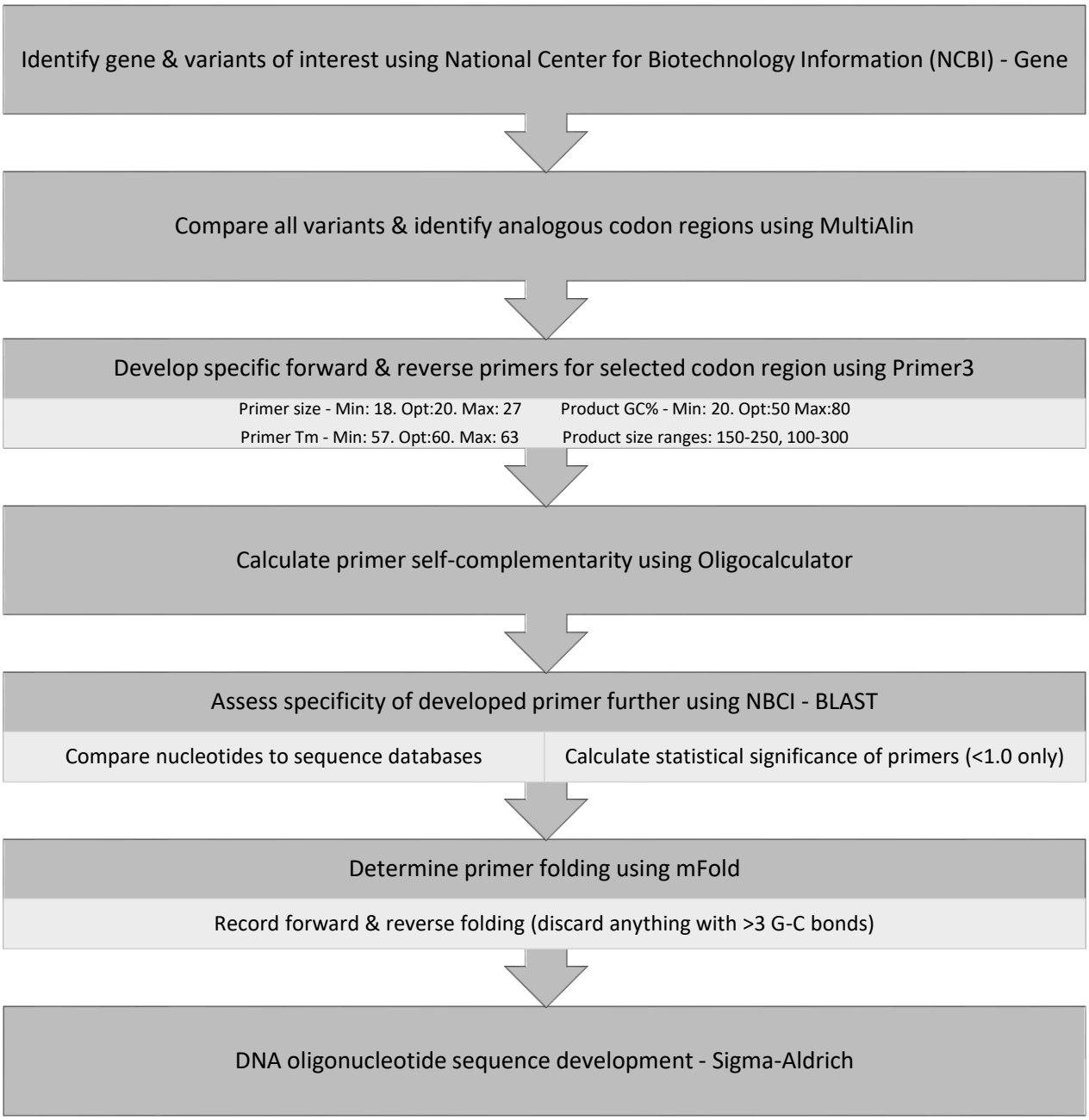

Once a forward and reverse primer passed MIQE guideline criteria, DNA oligonucleotide sequences were generated and purchased from Sigma-Aldrich. All primers where made to 100µM using nuclease-free water (not DEPC-treated) (Thermo Fisher Scientific Inc., AM9932) in an environment clear of RNases by using RNaseZap® decontamination solution (Invitrogen™, AMA9780).

Genes were analyzed for expression using the LightCycler® 96 RT-qPCR reaction. The resulting amplified gene (12µl) was diluted in nuclease free water (1:1000). A serial dilution (1:10) of this 1:1000 amplified primer was conducted to measure the efficiency of the primer at lower concentrations (see Table 3.20 for serial dilutions made for primer optimisation). Each dilution was made up into a mastermix for a RT-qPCR reaction using the LightCycler® 96.

Table 3. 20. Serial dilution of amplified gene for primer optimisation

Dilution	***Concentration***
1	1:1,000
2	1:10,000
3	1:100,000
4	1:1,000,000
5	1:10,000,000
6	1:100,000,000
7	1:1,000,000,000

Primer efficiency was calculated from the resulting slope and R^2 of the line based on the Cycle threshold (Ct) results of the serial dilution experiments. Primer efficiency was only accepted if between 90-110%.

Table 3.21 highlights all primers designed with their forward and reverse nucleotide sequences. Primer base pair, e-value (the closer this to zero, the less potential for a false positive), mfold structure, self-complementarity, agarose gel bands, amplification curves and melting peaks are also referenced. These steps ensured our primers were MIQE guideline compliant, designed and optimized to instill confidence in RT-qPCR outputs. Further primer optimization along with primer amplification curves, melt curves and efficiency curves can be found within the Appendix (Section I).

Table 3. 21. List of primers with base pairs, forward, reverse and efficiency data

Primer	*Base Pairs (100-300)*	*Forward primer (5'-3')*	*Forward M-fold structures*	*Reverse Primer (3'-5')*	*Reverse M-fold structures*	*Self-Comp.*	*Bands. Agarose Gel*	*Amp. curves*	*Melting peaks*	*Efficiency (%)*
ACAT2	220	atggaacgggaacagtcacc	6	tcttccagtgaccaacctgc	2	No	1	1	2	103.87
Acetyl-CoA Carboxylase	248	gccatgttattgctgctcgg	1	accccgaatagacagctcct	1	No	1	1	1	95.81
ACTC1	229	ccagagcaagagaggcatcc	2	cacgtacatggcagggacat	5	No	1	1	1	99.14
AMPK alpha 1	130	acagaagccaaatcagggac	3	ggagaagagtcaagtgaggtca	5	No	1	1	1	101.66
AMPK alpha 2	196	cgcctctagtcctccatctg	3	tcggattccaagatgccact	6	No	1	1	1	103.91
ANT1	227	agttctggcgctactttgct	4	gccttggacagagacgttga	4	No	1	1	1	95.16
ANT2	167	gttgccgggttgacttccta	7	acattggaccatgcaccctt	3	No	1	1	1	101.34
CD38	242	tcagttcacacaggtccagc	3	tactgcgggatccattgagc	5	No	1	1	1	98.25

Primer	*Base Pairs (100-300)*	*Forward primer (5'-3')*	*Forward M-fold structures*	*Reverse Primer (3'-5')*	*Reverse M-fold structures*	*Self-Comp.*	*Bands. Agarose Gel*	*Amp. curves*	*Melting peaks*	*Efficiency (%)*
CKM	175	ttaagaaagctggccacccc	4	gtacccctcttctgcagacg	4	No	1	1	1	104
COXIV	154	accggctccagttcaatgag	2	aaggtgatcggctttggagg	5	No	1	1	2	98.85
CPT1b	150	atcaagaagtgccggaccag	1	acaggaacgcacagtctcag	2	No	1	1	2	102.15
DRP1	155	tcagagtgagctagtaggcca	2	gagtctcccggatttcagca	7	No	1	1	1	90.19
Fis1	179	caaggaggaacagcgggatt	5	tgcccacgagtccatctttc	3	No	1	1	1	93.56
G6PD	198	gaggctgcagttccatgatg	2	tcagggagcttcacgttctt	2	No	1	1	1	92.26
GAPdh	187	tccagaacatcatccctgcc	4	gcctgcttcaccaccttctt	4	No	1	1	1	95.44
IGF-1	168	gctggtggatgctcttcagt	8	ttgaggggtgcgcaatacat	2	No	1	1	1	101.57
Malonyl-CoA Decarboxylase	247	tccagcaacatccaggcaat	2	agttcagaagccccagaagc	2	No	1	1	1	95.20

Primer	*Base Pairs (100-300)*	*Forward primer (5'-3')*	*Forward M-fold structures*	*Reverse Primer (3'-5')*	*Reverse M-fold structures*	*Self-Comp.*	*Bands. Agarose Gel*	*Amp. curves*	*Melting peaks*	*Efficiency (%)*
Mff	117	tgaaagaccactagattttctggattt	4	cgaacagcattttcactcatagacc	3	No	1	1	1	90.66
Mfn1	193	acgccttagtgcttcagacc	3	gaagaccagcccagggaaaa	3	No	1	1	1	112.41
Mfn2	193	ctctcccggccaaacatctt	7	cgttgagcacctccttagca	2	No	1	1	1	95.83
MiD49	148	tctacgacgggctgcagg	7	gtccctcgccacagtgtc	4	No	1	1	1	93.65
MiD51	159	gtgacagctgaccacatcca	2	gtcccagtaactgctcccac	2	No	1	1	1	103.03
MK167	210	tcgaccctacagagtgctca	1	gtggggagcagaggttcttc	6	No	1	1	1	92.42
MT_ATP6	168	agatgtctctgttgctccgc	3	cagacacatcaccagcctgt	4	No	1	1	1	96.94
MT_CO4	128	gttgtatcgcattaagttcaagga	7	gcttctgccacatgataacga	1	No	1	1	1	94.6
mTOR	248	ttatgggcagcaacggacat	2	cttctccctgtagtcccgga	5	No	1	1	1	95.97

Primer	*Base Pairs (100-300)*	*Forward primer (5'-3')*	*Forward M-fold structures*	*Reverse Primer (3'-5')*	*Reverse M-fold structures*	*Self-Comp.*	*Bands. Agarose Gel*	*Amp. curves*	*Melting peaks*	*Efficiency (%)*
MYH1	160	ggtcttctggggctcctaga	3	aggcacggacattgtactgg	4	No	1	1	1	93.62
MYH2	241	atcaatgacctgactgcgca	1	cctcctcatactgttcccgc	3	No	0	1	1	91.28
MYH4	241	ggaggaggaaatcgaggcag	2	atctgcgtgcttcttccgaa	2	No	1	1	1	107.19
MYH7	234	gaccttcaagcgggagaaca	4	cgctcgatctctgccttgat	2	No	1	1	2	106.52
MYL2	221	aagcaaagaagagagccggg	1	gttaattggacccggagcct	2	No	1	1	1	99.16
MYOD1	181	atccgctatatcgagggcct	4	tgtagtccatcatgccgtcg	7	No	1	1	1	102.24
MYOG	195	tgccatccagtacatcgagc	7	gtgagcagatgatcccctgg	1	No	1	1	1	93.01
Nampt	225	agggttacaagttgctgcca	4	agacgttaatcccaaggcca	3	No	1	1	1	108.68
NDUFA4	246	atgctccgccagatcatcg	5	ccagtttgttccagggctct	8	No	1	1	1	98.6

Primer	*Base Pairs (100-300)*	*Forward primer (5'-3')*	*Forward M-fold structures*	*Reverse Primer (3'-5')*	*Reverse M-fold structures*	*Self-Comp.*	*Bands. Agarose Gel*	*Amp. curves*	*Melting peaks*	*Efficiency (%)*
NR4A3	176	acaagagacgtcgaaaccga	3	tggaggagaaggtggagagg	2	No	1	1	1	95.94
OMA1	162	ttgcatcctctaagccctgc	3	tgcctgccaccatttcctta	5	No	1	1	1	109.34
OPA1	220	tggaatgactttgcggagga	6	cacactgttcttgggtccga	10	No	1	1	1	101.82
Parkin	231	cacaccccacctctgacaag	3	ccacacaaggcagggagtag	7	No	1	1	1	103.45
PAX7	182	gaaggccaaacacagcatcg	1	ctgggtagtgggtcctctca	11	No	1	1	1	100.83
PGC-1alpha	236	caagcaaagggagaggcaga	1	acctgcgcaaagtgtatcca	13	No	1	1	1	96.58
PINK1	159	aacatctcggcaggttcctc	6	gatgatgttggggtgagggg	7	No	1	1	1	92.3
POLG	249	gttgaaagccatggtgcagg	1	ccatagatgcggccgtagtt	4	No		1	1	90.12

Primer	*Base Pairs (100-300)*	*Forward primer (5'-3')*	*Forward M-fold structures*	*Reverse Primer (3'-5')*	*Reverse M-fold structures*	*Self-Comp.*	*Bands. Agarose Gel*	*Amp. curves*	*Melting peaks*	*Efficiency (%)*
Pyruvate Dehydrogenase-α	161	tcgctatggaatgggaacgt	5	gccccttcccagatctacaa	1	No	1	1	1	95.23
Pyruvate Dehydrogenase-β	160	accatagaagccagtgtcatga	3	ggacatcagcaccagtgaca	1	No	1	1	1	102.11
RAC1	197	cactgtcccaacactcccat	2	aacactgtcttgaggcctcg	5	No	1	1	1	96.89
SIRT1	205	cattttccatggcgctgagg	3	cccaaatccagctcctccag	2	No	1	1	1	90.17
SIRT3	103	cgttgtgaagcccgacattg	7	cccaaggatgagcagcagat	3	No	1	1	1	94.53
SIRT4	210	caagtccggagctttcaggt	2	gagcttcttctcccaggcag	2	No	1	1	1	94.65
SIRT5	175	acgtcgtgtggtttggagaa	3	tccgtgttaaattcagccactg	2	No	1	1	1	90.3
SIRT6	105	tgtttgtggaagaatgtgcca	2	ccttagccacggtgcagag	1	No	1	1	1	93.86

Primer	*Base Pairs (100-300)*	*Forward primer (5'-3')*	*Forward M-fold structures*	*Reverse Primer (3'-5')*	*Reverse M-fold structures*	*Self-Comp.*	*Bands. Agarose Gel*	*Amp. curves*	*Melting peaks*	*Efficiency (%)*
TNN1	192	ggtggatgaggagcgatacg	1	cgcagatccatggacacctt	3	No	1	1	1	102.45
YME1L	185	ggagccacaaacttcccaga	2	aagccaacagtacctcgagc	5	No	1	1	1	93.14

Statistical Analysis

In order to determine if the data was normally distributed the Shapiro-Wilk and Kolmogorov-Smirnov test of normal distribution were used and accepted with a *p*-value greater than 0.05 allowing for parametric analysis. If samples were not normally distributed a non-parametric analysis of the data was conducted. Homogeneity of variance was measured using a Levene's test and accepted with a *p*-value greater than 0.05. If *p* was less than 0.05 homogeneity of variance was violated and a non-parametric Kruskal-Wallis test was used to conduct analysis.

Physiological & Human Skeletal Muscle Data

Due to inter-individual variation between subjects, the bed rest data (physiological, protein and mRNA expression) are presented as mean ± standard error (SE). Two-way (treatment x time) mixed analysis of variance (ANOVA) with pair-wise comparisons was used to determine differences between the intervention and control groups for the 60 days bed rest study. Where a main effect was found, the student Bonferroni post-hoc test was used to determine where the difference existed. An independent samples t-test was subsequently used to measure difference between BDC (pre) muscle protein expression due to inevitable inter-individual variation between subjects. An unpaired student's t-test was used to analyse the difference between the 21-day bed rest BDC (pre) and HDT (post) and the same was used to analyse the difference between the 60-day bed rest control BDC and HDT. As these were between-subjects study designs with different subjects completing the 21-day trial to the 60-day trial we did not statistically compare the changes between the two but we did recognize similar trending changes with both trials. All measurements obtained for high resolution respirometry of the muscle biopsies attained within the 60-day bed rest study were normalised for the wet weight of the muscle fibres and for wet weight plus mtDNA:nDNA ratio. Therefore, absolute respiratory rates (oxygen flux) are expressed as picomoles of oxygen per milligram of wet weight per second (pmol/(s*ml)) normalised for ROX and subsequently normalised for mtDNA:nDNA ratio ($pmol[s*ml^{-1}]mg^{-1}/mtDNA:nDNA^{-1}$). All western blot and RT-qPCR data was normalised against a loading control (GAPdh/Alpha-Tubulin) and then subsequently against a biological (internal) control. All phosphorylated proteins were normalised against loading control, then the internal control before being normalised to total protein expression which had undergone the same process. All statistical analysis was performed using GraphPad Prism with significance accepted at $p<0.05$.

Cell Culture Data

Data is presented as a mean ± standard deviation (SD) for all cell culture experiments. One-way ANOVA with pair-wise comparisons was used to determine the differences between the untreated (control) and treated (Duplex/Scramble) for cell culture experiments. Where a main effect was found, the student Bonferroni post-hoc test was used to determine where the difference existed. Were no scramble is presented, analysis of difference in the means between control and treated groups was calculated using a paired student's t-test. As with the 60-day and 21-day bed rest trials, all western blot and RT-qPCR data was normalised against a loading control (GAPdh/α-Tubulin) and then subsequently against a biological (internal) control. All phosphorylated proteins were normalised against loading control, then the internal control before being normalised to total protein expression which had undergone the same process. All statistical analysis was performed using GraphPad Prism with significance set at $p<0.05$.

Chapter IV: Physiological Response to Bed Rest

Overview – 60-Day Bed Rest

In total, 20 healthy males aged 34.15±1.75 years with BMI of 23.92±0.43 (kg/M^2) took part in the 60-day bed rest study. All subjects completed all trials however, 'subject I' did not complete a post muscle biopsy. Subjects were randomly assigned to the control trial (CONT) (*n*=10) and the intervention (INT) trial (*n*=10). We hypothesized that 60 days of bed rest would lead to multiple anthropometric changes such as a decrease in fat free mass and weight. These changes would be in conjunction to change in resting metabolic rate, respiratory quotient and decreases in parameters of aerobic fitness.

Anthropometric and Body Composition

The body composition before (BDC-2), during (HDT25) and at the end of the bed rest study (HDT58) are presented in Table 4.1. There was a significant reduction in weight (kg), lean muscle mass (whole body and leg) (kg) at HDT25 and at the end of bed rest (HDT58) as an effect of time in the control and intervention group (p<0.0005). Due to the reduction in lean muscle mass, there was a significant increase in body fat percentage and fat mass (whole body and leg) (kg) with 60 days of -6° HDT bed rest within both groups (p<0.0005).

Table 4. 1. Control and intervention anthropometric data, before, during & following 60 days of bed rest

	Control (n=10)			***Intervention (n=10)***			
	Pre (BDC-2)	**HDT 25**	**Post (HDT 58)**	**Pre (BDC -2)**	**HDT 25**	**Post (HDT 58)**	**Sig. effect of time**
Weight (kg)	73.69±2.68	72.35±2.64	71.60±2.56	72.09±1.81	71.07±1.78	70.75±1.79	p<0.0005
Body Fat (%)	25.37±1.03	26.53±1.02	27.48±2.56	27.06±1.29	28.23±1.22	29.64±1.28	p<0.0005
WB FFM (kg)	54.89±1.83	53.06±1.79	51.81±1.68	52.49±1.23	50.91±1.13	49.6±1.05	p<0.0005
WB FM (kg)	18.80±1.23	19.30±1.23	19.79±1.29	19.60±1.25	20.16±1.22	21.09±1.32	p<0.0005
Arm fat (kg)	2.45±0.17	2.42±0.16	2.51±0.17	2.45±0.16	2.48±0.20	2.55±0.19	-
Arm lean (kg)	7.58±0.33	7.36±0.34	7.48±0.31	6.70±0.26	6.54±0.23	6.45±0.20	-
Leg fat (kg)	6.55±0.52	6.73±0.50	7.04±0.57	6.62±0.51	6.79±0.49	7.06±0.56	p<0.0005
Leg lean (kg)	17.72±0.59	16.87±0.64	15.96±0.52	17.16±0.59	16.11±0.57	15.18±0.53	p<0.0005

(WB FFM – whole body fat free mass, WB FM – whole body fat mass. No significant difference between control and intervention but significant differences between BDC and HDT as an effect of time for weight (kg), body fat (%), whole body free-fat mass (kg), whole body fat mass, leg lean mass (kg) and leg fat mass (kg) (p<0.0005). Data is presented as mean ±SE)

Heart Rate and Blood Pressure

Heart rate, diastolic and systolic blood pressure throughout 60 days bed rest are presented in Table 4.2. These variables were measured twice a day between BDC-14 and HDT 58, once in the morning before breakfast and once in the evening before dinner. The results in Table 4.2 represent measurements taken on BDC -2, HDT 25 and HDT 58 in the morning and in the evening.

There was a no significant difference in heart rate between control and intervention groups but there was a significant effect of time in morning and evening heart rate following 60 days of bed rest (p<0.0005). There was no significant difference in morning systolic or diastolic blood pressure between control and intervention groups. However, there was a significant increase over time (p<0.0005). Additionally, there was no significant difference between evening systolic or diastolic blood pressure between the control and intervention groups, with no effect of time. Mean morning and mean evening blood pressure significantly increased over time (p<0.05) but there was no effect of trial. Following -6°HDT subjects will exhibit symptoms of orthostatic intolerance, which can be represented by an increase in heart rate and a decrease in stroke volume. Such adaptations can significantly impact subject's cardiovascular health, particularly their maximal aerobic capacity.

Table 4. 2. Control and intervention heart rate and blood pressure data before, during & after 60 days of bed rest

	Control (n=10)			***Intervention (n=10)***			
	Pre (BDC-2)	**HDT 25**	**Post (HDT 58)**	**Pre (BDC -2)**	**HDT 25**	**Post (HDT 58)**	**Sig. effect of time**
Morning HR (BPM)	57.90±2.55	59.60±1.83	64.20±2.18	55.80±2.87	58.50±2.12	64.40±2.44	p<0.0005
Evening HR (BPM)	67.10±4.11	64.70±2.53	67.60±2.59	61.00±2.99	61.70±2.17	66.20±2.36	p<0.0005
Morning SBP (mmHg)	115±1.52	116.30±2.2	109.30±3.37	108.80±2.79	112.30±3.62	112.80±2.41	p<0.0005
Morning DBP (mmHg)	64.80±2.24	67.30±2.37	66.70±2.13	63.80±1.76	67.00±2.35	68.50±1.92	p<0.0005
Mean Morning BP (mmHg)	83.00±2.08	84.70±1.37	82.10±2.37	78.60±2.49	82.70±2.63	83.50±2.07	p<0.0005
Evening SBP (mmHg)	119.90±3.1	122.70±3.6	121.80±3.67	122.10±3.96	118.00±2.80	119.30±3.23	-
Evening DBP (mmHg)	71.10±2.09	70.30±2.45	71.30±3.12	70.40±2.04	71.20±1.88	71.60±1.59	-
Mean Evening BP (mmHg)	86.90±1.71	88.00±2.44	90.00±2.73	88.40±2.43	87.20±1.99	88.60±2.47	p<0.05

(Heart rate, beats per minute (BPM), systolic blood pressure (SBP) and diastolic blood pressure (DBP) measurements taken in the morning and in the evening on baseline data collection (BDC) -2, head down tilt (HDT) 25 and HDT 58 for the control (n=10) and intervention groups (n=10). No significant difference between control and intervention but significant differences between BDC and HDT as an effect of time for morning HR, evening HR, morning SBP, morning DBP, mean morning BP and mean evening BP (p<0.05). Data is presented as mean ±SE)

Resting Energy Metabolism

Resting energy expenditure was measured in the post absorptive state, twelve hours after the last evening meal and an overnight fast (Figure 4.1). Eight measurements of resting energy metabolism were complete before and during the bed rest study. There was a significant decrease in resting metabolic rate (RMR) as an effect of time in the control and intervention groups (p<0.005) with no difference between groups. There was a significant increase in respiratory quotient (RQ) as an effect of time in both the control and the intervention trials (p<0.005), with no difference between groups.

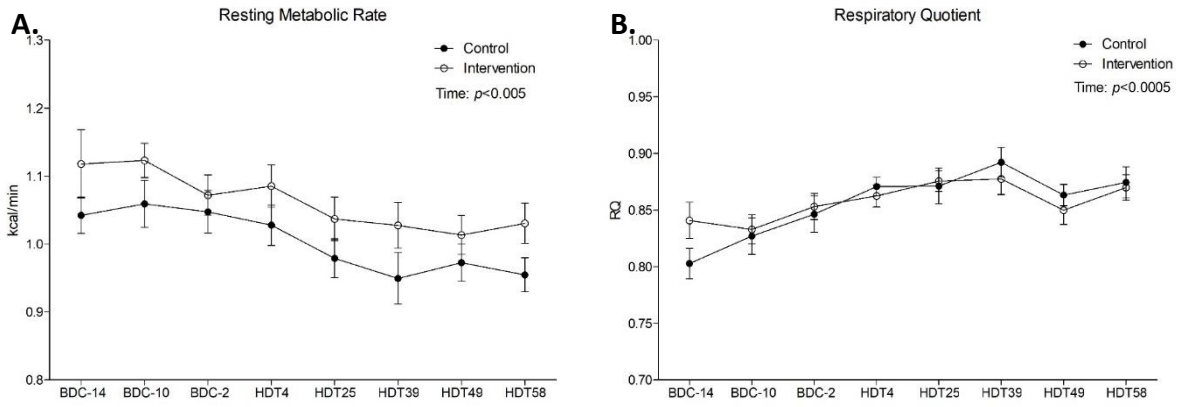

Figure 4. 1. Resting metabolic rate and substrate utilization throughout 60 days of bed rest

(Resting metabolic rate (RMR) (A) and substrate utilization (RQ) (B) throughout bed rest. BDC, baseline data collection, HDT, head down tilt. Significant effect of time noted at p<0.005 for RMR and p<0.0005 for RQ. Data is expressed as mean ± SE)

Aerobic Fitness

Aerobic fitness was assessed prior to bed rest on BDC-8 and following bed rest on R+1 (Figure 4.2). There was a significant decrease in absolute ($L \cdot min^{-1}$) and relative ($ml \cdot kg^{-1} \cdot min^{-1}$) VO_2 peak following 60 days of bed rest (p<0.0005). The deconditioning effect of bed rest resulted in a significant increase in peak respiratory exchange ratio (RER) in both control and intervention groups (p<0.05), while there was a significant increase in peak heart rate (HR) within both groups following bed rest (p<0.05). At maximal exercise intensity, ventilation (VE) (p<0.05) and peak power was significantly lower than before bed rest in both groups (p<0.0005).

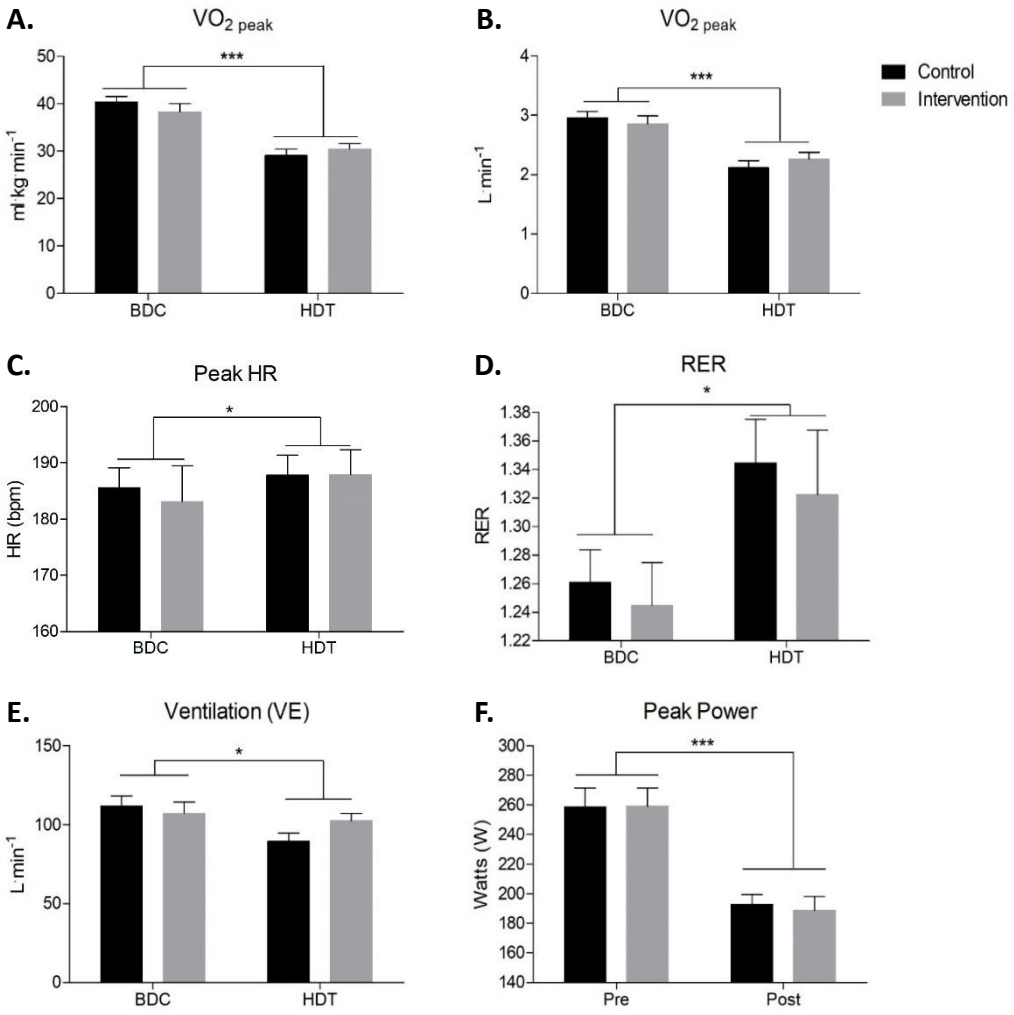

Figure 4. 2. Measurements of aerobic fitness before & following 60 days of bed rest

(Maximal exercise response before and after bed rest. Measured parameters include (A) relative VO_2 peak ($ml \cdot kg \cdot min^{-1}$), (B) absolute VO_2 peak ($L \cdot min^{-1}$), (C) peak heart rate (HR), (D) respiratory exchange ratio (RER), (E) Ventilatory Efficiency ($L \cdot min^{-1}$) & (F) peak power (Watts). Data are presented as mean ± SE. **significantly different to BDC as an effect of time, p<0.005, ***significantly different to BDC as an effect of time, p<0.0005)

Comparison of 60-Day Bed Rest Physiological Measurements with 21-Day of Bed Rest

In order to determine if there was an effect of time on the changes in protein expression involved in mitochondrial regulation we compared the physiological and metabolic results from the control group of this 60-day bed rest trial with the control group from the 21-day bed rest study previously conducted by our group [263]. 21-day bed rest experimental study design and overview can be found in the Appendix (Section A).

A total of eleven healthy male subjects (aged 33.67±2.45) volunteered to participate in the 21-day bed rest study (height (M) 1.77±0.02, weight (kg) 72.55±3.04, BMI (kg/M^2) 22.44±0.50). We understand there are slight physical differences between subject's baseline data from the 60-day and the 21-day bed rest studies (with an increase in baseline FM in those within the 60-day trial) but the main focus is on the muscle protein differences in Chapter V. As they are separate studies we compare the within-group differences following bed rest.

Body Composition 21 and 60-day Bed Rest

Anthropometric data such as weight (kg), body fat percentage (%), fat-free mass (kg) and fat mass (kg) were compared following the 21-day and the 60-day bed rest study control groups (Figure 4.3) (further changes to body composition within the 21-day bed rest study can be found in Appendix Section A). There was a significant decrease in weight (A) in both the 21-day and 60-day bed rest study (p<0.005). There was a significant increase in body fat percent (B) with 21 days and 60 days bed rest (p<0.05). Fat-free mass (C) significantly decreased in both the 21- and 60-day bed rest trials (p<0.05). Finally, there was a significant increase in fat mass (D) with 60 days of bed rest but not with 21 days bed rest (p<0.05).

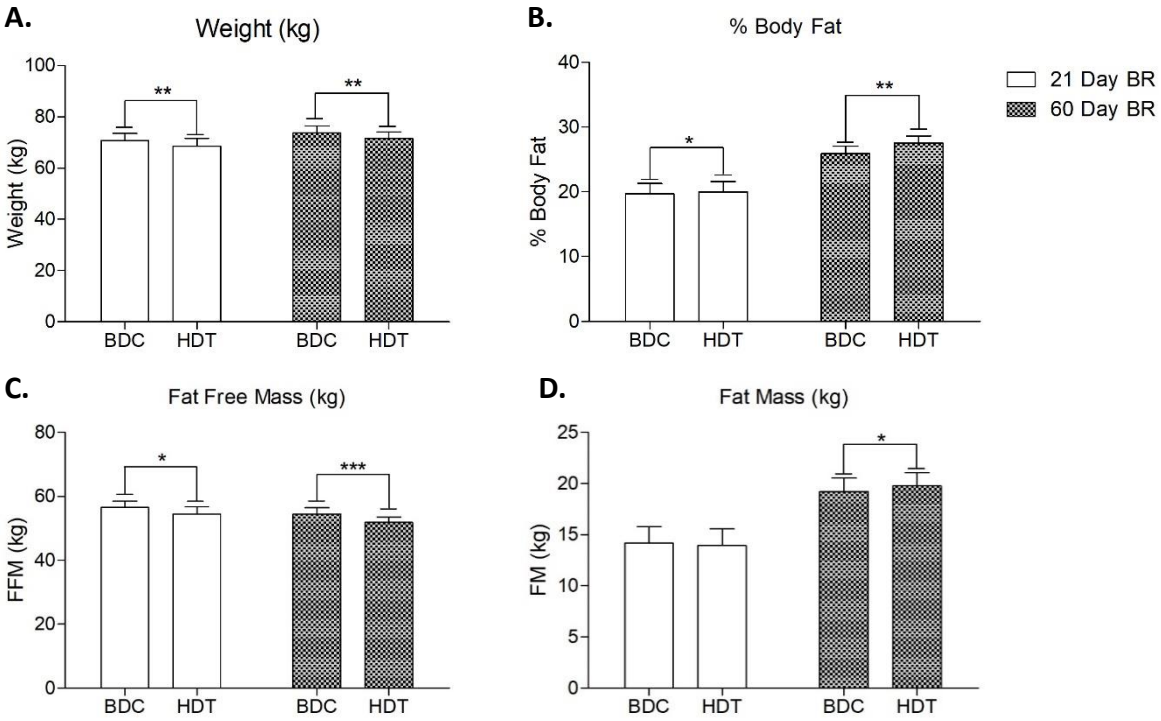

Figure 4. 3. Anthropometric changes observed before & following 21 & 60 days of bed rest

(Weight (kg)(A), body fat (%)(B), fat free mass (C) and fat mass (kg)(D) before and after 21 and 60 days of bed rest. Data are presented as mean ± SE, ** p<0.005, *** p<0.0005)

Aerobic Fitness 21 and 60-day Bed Rest

Aerobic fitness was assessed prior to bed rest and following both bed rest trials (Figure 4.4). There was a significant decrease in relative ($ml \cdot kg^{-1} \cdot min^{-1}$) (A) and absolute ($L \cdot min^{-1}$) (B) maximal aerobic capacity following both 21 and 60 days of bed rest (p<0.0005). The deconditioning effect of bed rest resulted in a significant increase in respiratory exchange ratio (RER) (D), although significance was only observed following 60 days bed rest (p<0.05). At maximal exercise intensity, peak power (F) was significantly lower than before bed rest in both groups (p<0.0005). There was also a significant reduction in ventilation (E) in both the 21 and 60-day bed rest trials (p<0.005). There was no significant increase in peak heart rate (HR) (C) during the aerobic fitness test following both 21 and 60 days of bed rest (p>0.05).

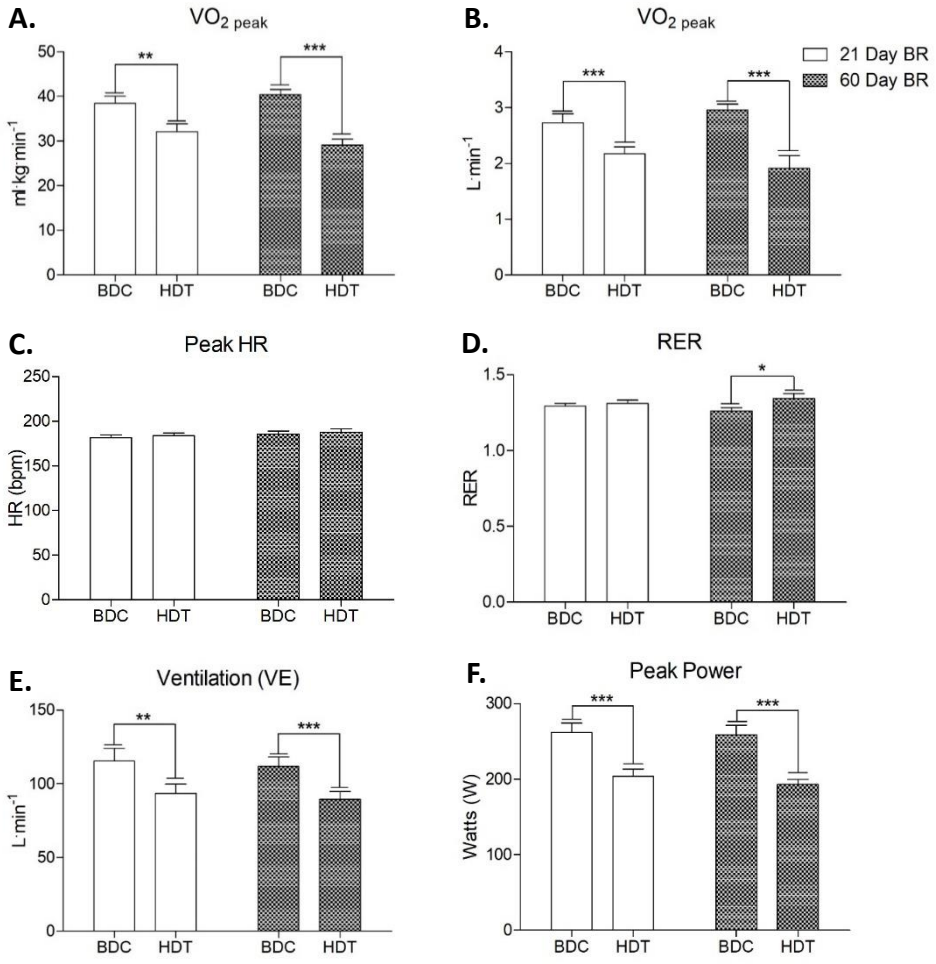

Figure 4. 4. Measurements of aerobic fitness before & following 21 & 60 days of bed rest

(Maximal exercise response before and after bed rest. Measured parameters include (A) relative VO_2 peak ($ml \cdot kg \cdot min^{-1}$), (B) absolute VO_2 peak ($L \cdot min^{-1}$), (C) peak heart rate (HR), (D) respiratory exchange ratio (RER), (E) Ventilatory Efficiency ($L \cdot min^{-1}$) & (F) peak power (Watts). Data are presented as mean ± SE. * p<0.05, ** p<0.005, *** p<0.0005)

Discussion on the Physiological Effects of Bed Rest

The results presented in this chapter highlight the impact prolonged bed rest on body composition, cardiovascular function and energy metabolism significantly influencing overall aerobic fitness and functional capacity. Consistent with previously published bed rest studies [263,434,454], our results highlight a significant decrease in resting metabolic rate and an increase in respiratory quotient suggesting a shift from fat to carbohydrate oxidation at rest. The adaptations observed in aerobic fitness support previously published studies with a reduction in VO_2 peak (absolute and relative), ventilation efficiency (VE), peak power and an increase in peak heart rate and respiratory exchange ratio (RER). Additionally, we observed a decrease in weight and fat free mass coinciding with an increase in fat mass and body fat percent. Finally, -6°HDT bed rest also resulted in a significant increase in heart rate and decrease in blood pressure typical in all -6° HDT bed rest studies.

Energy Regulation

The 60-day and 21-day bed rest studies were designed to maintain subject energy balance during bed rest. This was undertaken by monitoring body weight every morning and consistent monitoring of body composition. These measurements were used to alter dietary intake and ensure that energy intake matched energy expenditure (energy balance). Our results suggest that the subjects went into a slight energy surplus during the 60-day bed rest study supported by a small but statistically significant average increase in whole body fat mass (~1.0kg/~6%) in both the control and intervention groups. This highlights the challenges involved in regulating fat mass over a sustained period of time, even when body composition and RMR are measured regularly. However, the overall increase in fat mass should not have a major impact on metabolic processes relating to the muscle but may be important if we were focused on another tissue type (i.e. liver, adipocyte).

Additionally, there was a reduction in lean muscle mass (~3%) which was similar to the observed decrease in body weight (~2.35%). As with many bed rest studies we found a significant decrease in arm and leg fat free mass. The reduction in arm fat free mass was ~2.5% on average, however the reduction in leg fat free mass was ~12% following 60 days of head down tilt bed rest.

In the present study, fat-free mass significantly decreased in both the control and intervention trials and is due to muscle disuse that is independent of changes in energy balance and considered to be related to the muscles progressive loss in its ability to respond to anabolic stimuli such as

amino acids [165]. In fact muscle atrophy has been shown to be even more pronounced when there is a positive energy balance [490]. Blanc et al. [43] measured total energy expenditure using doubly labelled water (DLW) before and during 42 days of bed rest where subjects were provided food at meal times *ad libitum*. During the 42-day bed rest study, total energy expenditure and total energy intake decreased significantly while resting energy expenditure remained stable. The authors attributed this reduction in total energy expenditure to a 39% decrease in physical activity energy expenditure and not to the loss of lean body mass. This suggests that during long term bed rest, energy intake is adjusted to match or surpass total energy expenditure in order to induce a positive energy balance or maintain energy balance. In the present study, a gradual reduction in the resting metabolism rate could be attributed to the reduction in lean muscle mass.

In addition to the decrease in RMR the progressive increase in respiratory quotient (RQ) is supported by other bed rest studies [43,42,34,35]. The gradual increase in RQ suggests there was a shift in the substrate oxidation at rest, from fat to carbohydrate oxidation and this was independent of energy balance [492]. The literature, although inconclusive, suggests that the changes in oxidation could be explained by an increased proportion of glycolytic muscle fibers and a reduction in oxidative muscle fibers during prolonged bed rest [519] (see Figure 4.5 on the impact -6° HDT on people's metabolic profile). The results from animal studies suggest the shift in substrate use precedes the changes in muscle fiber type [192,443,251] so further research is required to investigate the mechanisms involved.

It is also possible that the change in substrate metabolism could be due to a preferential storage of lipid in the skeletal muscle due to the decreased energy turnover. An accumulation of intramuscular lipid species such as diacylglycerides (DAGs), ceramides and acylcarnitine and a decreased capacity to oxidize common dietary lipids, such as palmitate have previously been reported [34,125]. An increase in lipid accumulation due to a decreased capacity to oxidize fatty acids leads to a decrease in metabolic flexibility. Metabolic flexibility reflects the ability of the body to adapt to changes in metabolic or energy demand as well as the prevailing conditions or activity [188]. A disruption of this finely balanced system could explain the shift from fatty acid oxidation to carbohydrate oxidation during 60-days of bed rest. We did not measure changes in the lipid species or lipid composition in skeletal muscle in the present study but we did observe a significant increase in whole body fat mass, possibly indicating more fat is stored and less is being oxidized.

In conclusion, maintaining energy balance during bed rest is the most effective way to prevent an increase in fat mass. Such an approach accepts that a decrease in muscle mass is inevitable and

subsequently optimal countermeasures considering the importance of energy balance should be developed in order to counteract this change in particular. We found that supplementation of a micronutrient cocktail was ineffective in preventing this change in energy regulation and that these changes occur following an acute bout of bed rest (<21 days), continuing as bed rest persists (60 days).

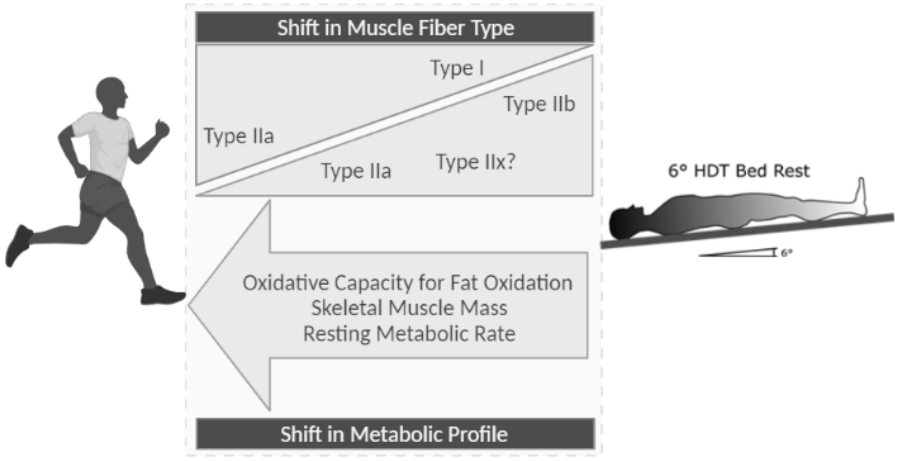

Figure 4. 5. Impact of -6°HDT Bed Rest on Metabolic Profile. Adapted from *Bergouignan et al.* [33]

Oxygen Consumption

Bed rest leads to a rapid decline in many parameters of physical fitness but particularly maximal aerobic capacity (VO_2 peak). Our results support this consistent observation, as we report reductions in VO_2 peak, peak ventilation, peak power and an increase in peak RER and heart rate. Aerobic capacity was assessed before and after 60 days of bed rest, however previous studies suggest the decline in aerobic capacity may rapidly occur in the first week of bed rest, with a more gradual decrease in subsequent weeks. This is supported by our comparison of aerobic capacity with the 21-day bed rest study which our group previously published [263]. While both studies noted a significant decline in aerobic capacity (absolute and relative) with bed rest, up to 60% of the adaptation appear to occur within the first 3-weeks (21-day BR: 16.5% decrease. 60-day BR: 27.94% decrease in VO_2 peak $ml \cdot kg^{-1} \cdot min^{-1}$). This supports the work by Capelli et al. [82] who measured aerobic capacity in subjects following 90 days of bed rest. They demonstrated that the rate of decline in aerobic capacity becomes progressively smaller as the duration of bed rest increases, underlining the capability of the body to adapt to changes in energy metabolism [191]. A comparison of peak power output (Watts) following the 21-day and 60-day bed rest study

support this further as 86% of the changes in peak power occur within the first 21-days of bed rest when compared to the results of the 60-day bed rest trial (21-day BR: 22.08% decrease. 60-day BR: 25.38% decrease in peak power output). Such results epitomize the impact of muscle disuse on muscle mass but also muscle function within the first few days of bed rest.

The decrease in aerobic capacity is indicative of the effect of prolonged bed rest on cardiac output which is linked to a reduction in plasma volume. Although we did not measure cardiac output or oxygen delivery in this study, it is well documented in the literature that both significantly decrease in parallel with a reduction in aerobic capacity following bed rest [389,82]. The Dallas Bed Rest and Training Study in 1966 was the first to demonstrate this, recording a 26% decrease in cardiac output and a 27% decrease in VO_2 peak following 3 weeks of bed rest in healthy males. They attributed this decrease to a 31% reduction in stroke volume [344], and there is increasing evidence that the initial changes in aerobic capacity occur in the first two weeks of bed rest [306]. Subsequent decreases in aerobic capacity could be explained by other adaptations of the cardiorespiratory system to bed rest.

As with peak aerobic capacity (VO_2 peak), we found a significant decrease in maximal ventilation ($L \cdot min^{-1}$) following 60 days of bed rest, consistent with the literature [494]. The decrease in ventilation could be indicative of pulmonary dysfunction but it is unlikely that the reduction in VO_2 peak was due to a decrease in maximal ventilation. At sea level, the lungs effectively saturate the arterial blood with oxygen, a system which remains consistent even during maximal exercise. There is very little difference (+1.06%) between ventilation rates ($L \cdot min^{-1}$) following 21 days of bed rest when compared to 60 days, even though aerobic capacity continues to gradually decline with the longer duration of bed rest, suggesting that a decrease in maximal cardiac output is likely to be the major factor resulting in a decreased aerobic capacity. Our results show no significant change in peak heart rate during exercise following 21 and 60 days of bed rest. However, we did find a significant increase in peak heart rate following exercise in the intervention group. Overall our results suggest no major effect of our micronutrient cocktail on aerobic fitness.

Heart rate and blood pressure where measured throughout the 60 days of bed rest in the morning and in the evening before sleep. We observed a significant increase in heart rate as an effect of time in both groups. This is a common physiological adaptation to bed rest. The increased heart rate is required to maintain cardiac output in order to meet the same workload. It also indicates that a decrease in stroke volume is the main cause of the reduced cardiac output. The factors contributing to this include a reduction in fluid volume and a decrease in oxygen demand in the vascular beds of the lower extremity while at -6°HDT. Similar studies have demonstrated a

reduction in left ventricular mass and increased cardiac atrophy, subsequently reducing the amount of blood which can be pumped from the heart around the body [389,485,548].

In addition to heart rate, there was a significant decrease in morning, but not evening, systolic and diastolic blood pressure in the control and intervention groups. The adjustments in blood pressure are consistent with other bed rest studies at -6°HDT and can be explained by decreases in fluid volume, reflected by increased heart rate, and shifts in body fluid distribution. An increase in thoracic fluid volume due to a fluid shift toward the head, results in mechanoreceptor stimulation and altered arterial baroreceptor function and reflex control [157]. This altered function is represented by a decrease in systolic and diastolic blood pressure similar to what we have observed within our bed rest model.

Changes in fluid distribution and fluid volume with -6° HDT bed rest have been recognized as factors that lead to a series of adverse cardiorespiratory effects including changes to cardiac function, exercise capacity and oxygen consumption, alterations which occur rapidly in the first weeks of bed rest and do not change much thereafter [434]. Such a response suggests that other factors, possibly at the level of the muscle, may be responsible for further decreases in aerobic capacity.

Skeletal Muscle Adaptation

In this 60-day bed rest study we report a significant reduction in whole body lean muscle mass (~-6%) and peak oxygen consumption (~-24%), both of which signify that skeletal muscle function is altered with 60 days of bed rest. The decrease in lean tissue may impact on aerobic capacity as local tissue changes may play a greater role with longer duration bed rest, given we noted short term adaptations are impacted mostly by shifts in fluid volume/distribution. In addition to the reduction in whole body fat-free mass, there is evidence of differences between the upper and lower extremities as there was a 2.6% decrease in arm fat free mass while a 12.14% decrease in leg fat-free mass. This disparity between the upper and lower extremities can be explained by the fluid shift from the lower extremities to the upper extremity due to the -6° HDT coinciding with muscle disuse [191,297,125]. MRI data from other bed rest studies support our findings, indicating a 4% reduction in quadriceps size after just 5 days of bed rest [124] and up to 26% with 90 days bed rest [439]. Measurements of maximal force production (MVP) were not taken in this study, however there is ample evidence to indicate that bed rest leads to a significant decrease in MVP particularly within the lower extremities [260,2,8].

Skeletal muscle is composed of slow-twitch (type I) and fast-twitch (type II) skeletal muscle fibers. Type I, slow-twitch, fibers are highly oxidative due to their higher number of mitochondria and subsequently have a greater oxygen consuming capacity while type II, fast-twitch have greater glycolytic capacity. Skeletal muscle fiber composition was not we measured in this study but there is evidence in both vastus lateralis (predominantly oxidative) [519] and soleus (predominantly glycolytic) [456] to suggest that bed rest leads to a shift in skeletal muscle fiber composition, from a predominantly slow myosin isoform, to a fast isoform (see Figure 4.6 for schematic representation of the shift in fiber type with bed rest) [66,536]. This reduction in type I isoform could possibly contribute to the reduction in skeletal muscle oxygen uptake.

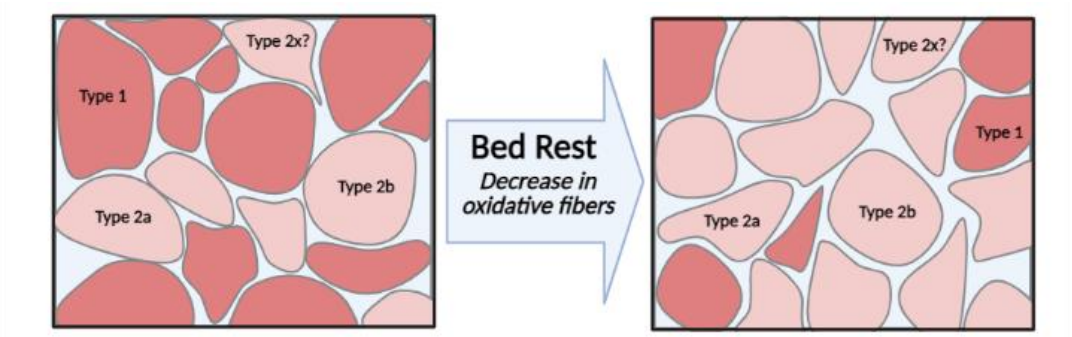

Figure 4. 6. Schematic representation of the effect bed rest has been shown to have on the expression of oxidative muscle fibers

The adaptations of the muscle to prolonged bed rest may directly impact on overall maximal oxygen consumption. With this in mind it is also important remember that these adaptations do not occur independently but are in-line with many other changes occurring within the body in response to bed rest.

Conclusion

Bed rest results in numerous adverse physiological adaptations and the findings in this study are consistent with the literature. We did not find any significant effect of the intervention on these whole body physiological changes. However, our results highlight the time-course of these adaptations by comparing the 21- and 60-day bed rest studies. Our results indicate the majority of these changes are evident in the first 3 weeks.

The most significant change we observed following bed rest is the shift in substrate metabolism from the predominant oxidation of fat at rest to carbohydrate. This modification in fuel preference has been identified as an early adaptation leading to adaptions in body composition and aerobic fitness in skeletal muscle during disuse. It is understood from transcriptomic and proteomic-wide

profiling that prolonged bed rest results in significant changes to regulators of skeletal muscle metabolism, particularly mitochondrial, which could be orchestrating some of these functional changes [145,264,403]. However, at present the exact mechanism regulating this process is unknown and studies are limited. Subsequently, further analysis of mitochondrial functional adaptations and key regulators of mitochondrial metabolism were analysed (Chapter V) following bed rest.

Chapter V: Cellular Response to Bed Rest

We hypothesized that prolonged bed rest would lead to a series of adaptations to the mitochondria which could explain some of the skeletal muscle adaptations observed in Chapter IV. We expected prolonged bed rest would result in a decrease in mitochondrial function in conjunction with a decrease in mitochondrial content. We proposed that these changes in function and content would be supported and explained by a decreased expression of regulators of mitochondrial biogenesis, dynamics and mitophagy.

Mitochondrial Content

Mitochondrial and nuclear DNA transcripts of muscle biopsies were measured using RT-qPCR as an indicator of mitochondrial content. Multiple different combinations of mitochondrial and nuclear DNA transcripts were measured, however all high resolution respirometry (HRR) data was controlled against NDUFA4:POLG ratio (NADH dehydrogenase subunit IV: Polymerase Gamma Accessory Subunit). RT-qPCR analysis identified a significant decrease in NDUFA4: POLG ratio with 60 days bed rest (p<0.0005), but no differences between groups (Figure 5.1). Changes in other targets of mitochondrial and nuclear DNA, which are in line with Figure 5.1, can be found in the Appendix (Section C).

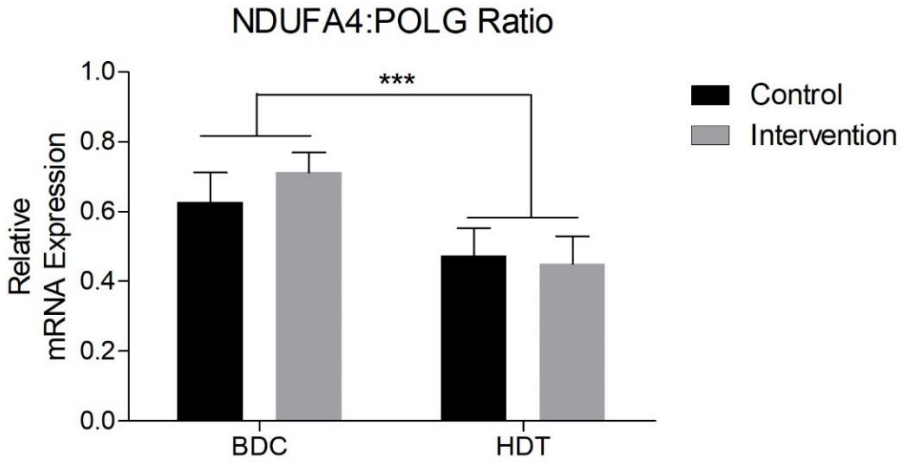

Figure 5. 1. mtDNA:nDNA ratio before & following 60 days of bed rest

(NDUFA4: POLG expression measured before and after bed rest. CONT, n=7. INT n=6 Data are presented as mean ± SE, *** significant effect of time, p<0.0005)

Mitochondrial Respiration

Samples were analysed using the substrate uncoupler inhibitor titration (SUIT) protocol for carbohydrate oxidation and represented in Figure 5.2. There were no differences in LEAK respiration (following titration of pyruvate and malate) or OXPHOS (following titration of ADP) between both groups or following bed rest ($p>0.05$). Complex IV activity (following titration of ascorbate and TMPD) was also unchanged following bed rest in both groups and there was no effect of the micronutrient cocktail. There was a significant decrease in maximal ETS cellular respiration through Complex I (following FCCP titrations), Complex I & II (with the addition of succinate) and Complex II alone (with the addition of rotenone) in both groups relative to wet muscle weight (pmol/(s*mg) ($p<0.05$) (see Figure 5.2. A). When respiration was controlled by muscle wet weight and mtDNA:nDNA ratio (Figure 5.2. B) there was no longer a significant decrease in respiration compared to baseline in either the control or intervention group. Further data controlled to other mtDNA:nDNA targets can be found in the Appendix (Section C).

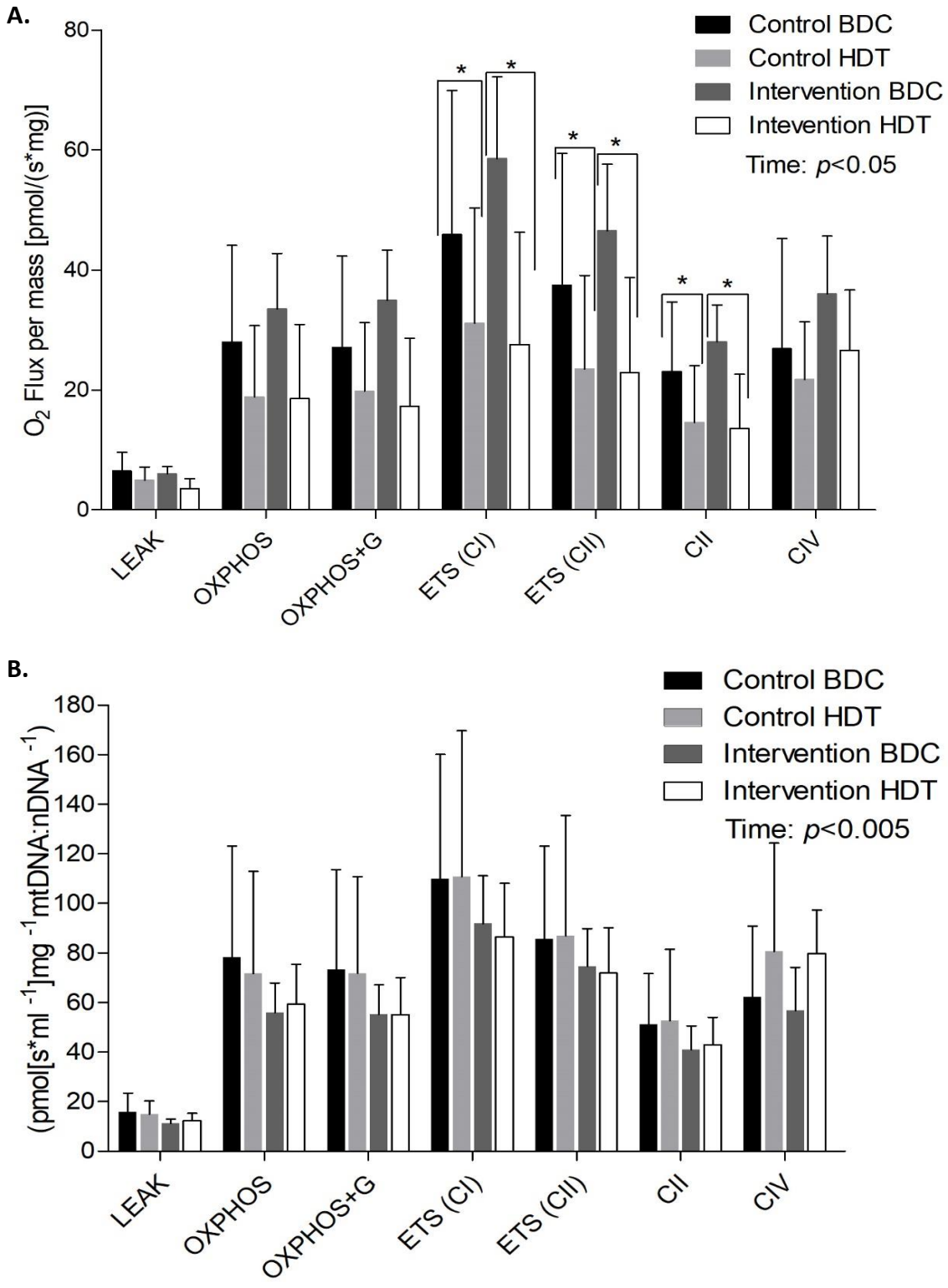

Figure 5. 2. Mitochondrial respiration before & following 60 days of bed rest

(Carbohydrate SUIT normalised to wet weight (A) (*n*=7), normalised to wet weight and mtDNA:nDNA ratio (B) (CONT *n*=7, INT *n*=6). Data are expressed as mean ± SE, *significant effect of time, *p*<0.05)

Transcriptional and Translational Targets Relating to 60 days of HDT Bed Rest

RT-qPCR and Western Blot analysis of muscle biopsy samples were conducted to measure transcriptional and translational changes in markers of mitochondrial function, morphology and cellular metabolism associated with 60 days of bed rest. All densitometry for the 60-day bed rest study can be found in the Appendix (Section D).

Expression of Markers Associated with Mitochondrial Fusion

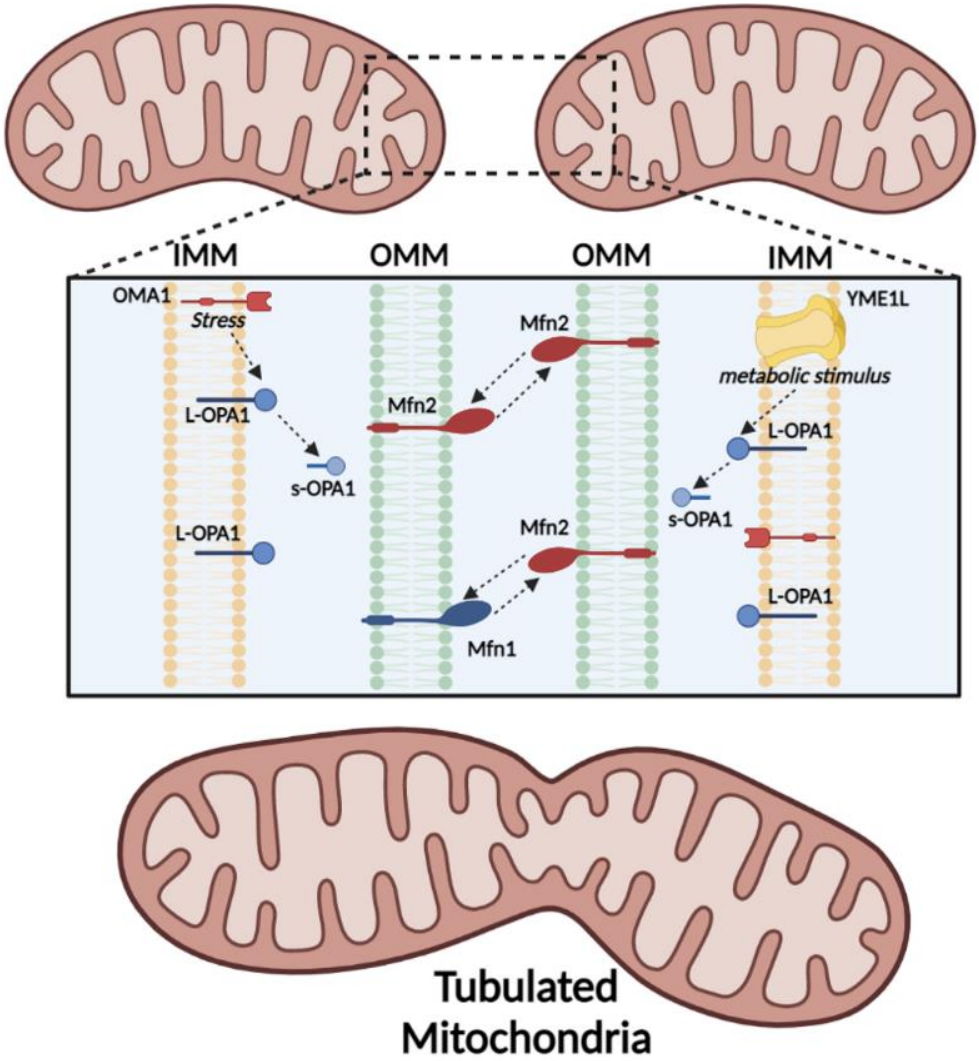

Figure 5. 3. Schematic representation of mitochondrial fusion regulated through a multifaceted process involving Mfn1, Mfn2 & OPA1. YME1L & OMA1 regulate OPA1. Adapted from *Wai & Langer,* [539]

OPA1

The mRNA (A) and protein expression (B) for OPA1 are presented in Figure 5.4. There was a significant decrease in OPA1 mRNA (A) and protein (B) expression in the control group (p<0.05) and there was a significant decrease in OPA1 mRNA expression (A) (p<0.05) but not protein expression (B) in the intervention group (p<0.05). The protein content of the long (C) and short (D) isoforms of OPA1 was decreased in the control group (p<0.05) but not the intervention group, indicating the micronutrient cocktail mitigated the decrease in OPA1. We noted there was significantly less control HDT L-OPA1 expression in comparison to the intervention HDT L-OPA1 protein expression (C) (p>0.05).

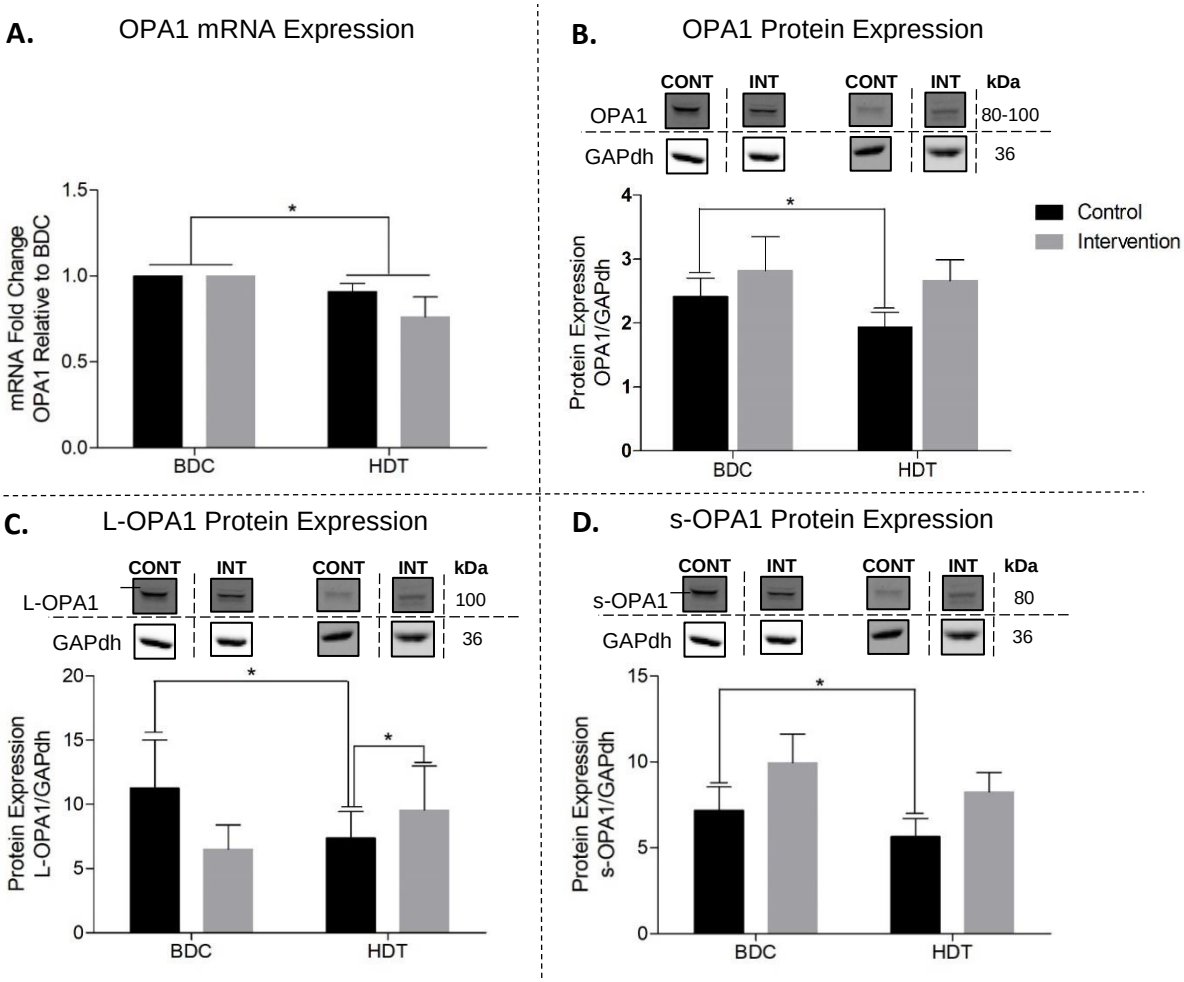

Figure 5. 4. Transcriptional and translational expression of OPA1 before & following 60 days of bed rest

(Total OPA1 mRNA expression (A) quantified by RT-qPCR (CONT, n=7, INT n=9). Total OPA1 (B) (CONT, n=9, INT, n=10), L-OPA1 (C) (CONT n=10, INT n=10) and s-OPA1 (D) (CONT, n=9, INT, n=10) protein expression quantified by western blot. OPA1 gene and protein expression were normalised against loading control (GAPdh expression) of same sample. Protein expression was normalised against loading control (GAPdh expression) of same sample. Blots presented are representative of all samples. Data is expressed as mean ±SE, * significant effect of time, p<0.05)

Other Markers of Mitochondrial Fusion - Mfn1, Mfn2, YME1L & OMA1

Protein expression of Mfn1 (A) and Mfn2 (B) are presented in Figure 5.5. There was no significant change in either Mfn1 or Mfn2 protein expression in the control or the intervention group following bed rest. The protein content of OPA1 regulators, YME1L (C) and OMA1 (D) were also analysed. There was no significant change in YME1L (C) protein expression in the control or the intervention group but we did observe a significant difference between YME1L control BDC to intervention BDC (p<0.05). We observed a significant decrease in OMA1 (B) protein expression in the control group but no change in the intervention group following 60 days of bed rest (p<0.05). These results suggest micronutrient supplementation may mitigate OMA1's cleaving of L-OPA1 to s-OPA1, resulting in a greater expression of OPA1, leading to increased potential for mitochondrial tubulation.

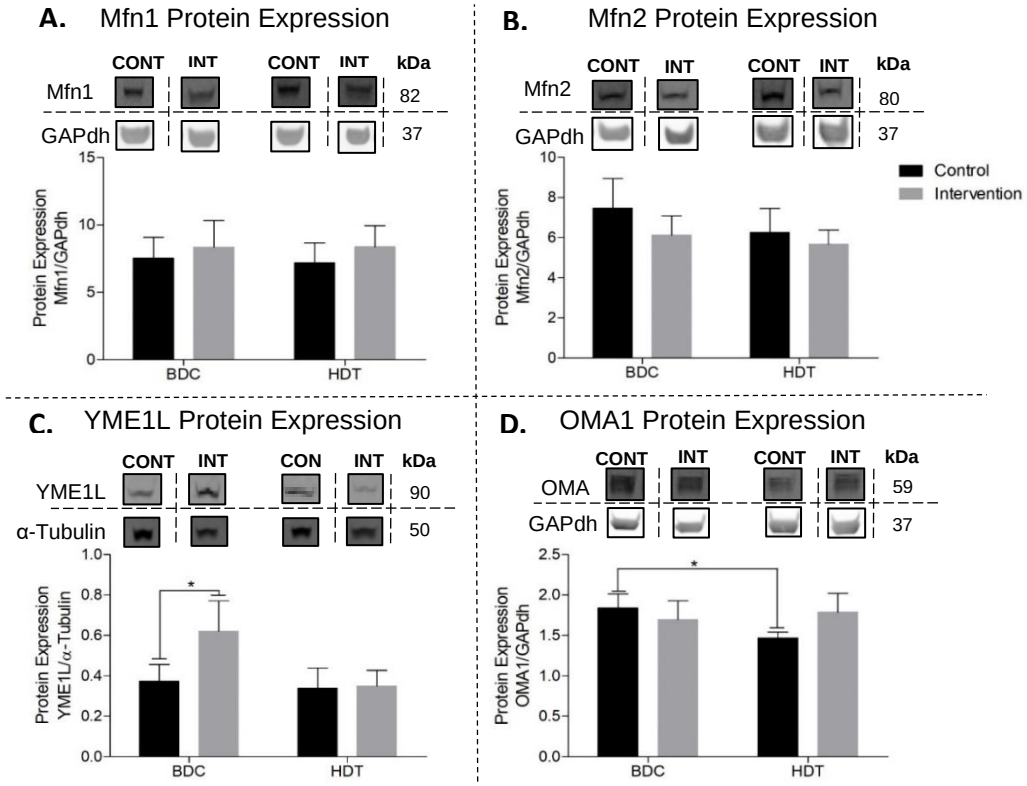

Figure 5. 5. Translational expression of other regulators of mitochondrial fusion before & following 60 days of bed rest

(Total Mfn1 (A), Mfn2 (B), YME1L (C) and OMA1 (D) protein expression quantified by western blot. (A) Mfn1 (CONT, n=10, INT n=10), (B) Mfn2 (CONT, n=10, INT n=10), (C) YME1L (CONT, n=8, INT, n=10), (D) OMA1 (CONT, n=9, INT, n=7). Protein expression were normalised against loading control (GAPdh/α-Tubulin expression) of same sample. Blots presented are representative of all samples. Data is expressed as mean ±SE, *significant effect of time, p<0.05)

Expression of Markers Associated with Mitochondrial Fission

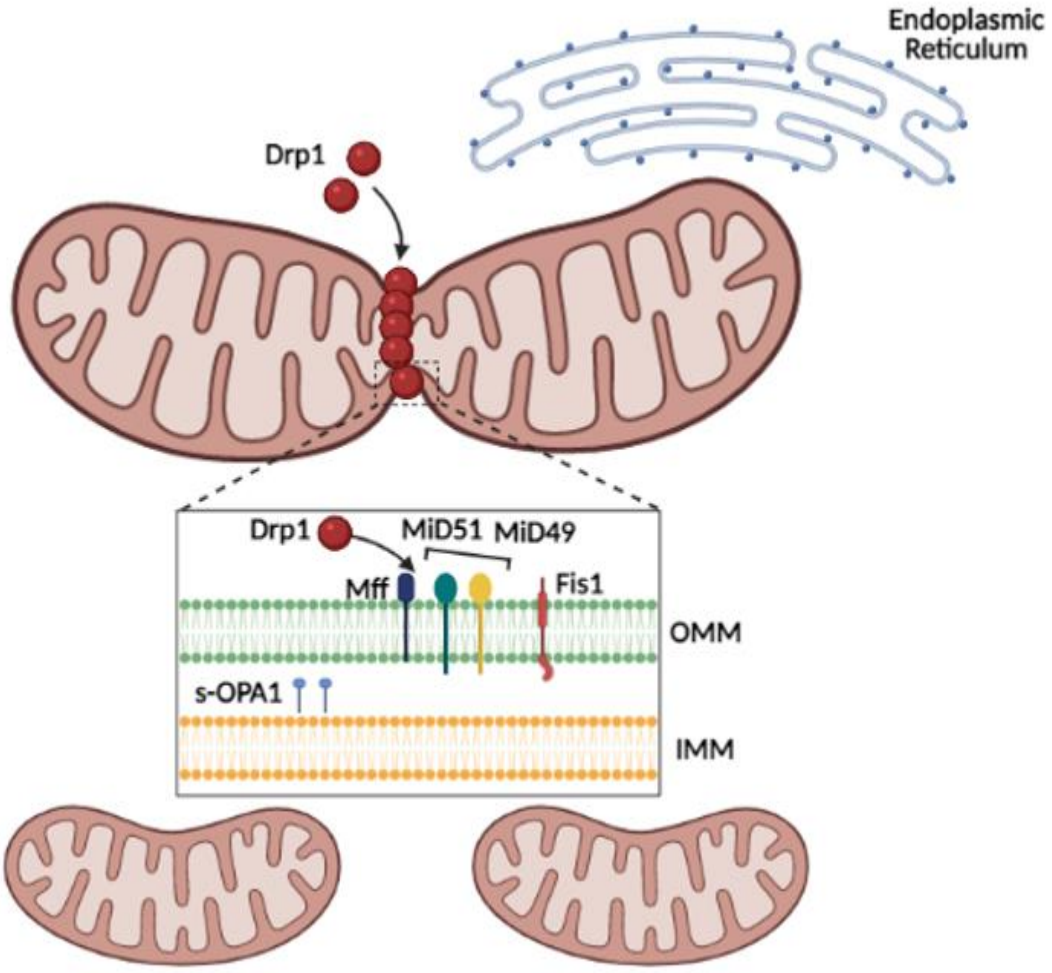

Figure 5. 6. Mitochondrial fission regulated by Drp1, Fis1, MiD49, MiD51 & ER contact sites. Adapted from *Wai & Langer,* [539]

Fission Proteins Drp1 and Fis1

The results for Drp1 and Fis1 are presented in Figure 5.7. There was a significant decrease in Drp1 protein expression (A) in the control and intervention group (p<0.005). We also noted a significant increase in pDrp1^{s616} (B) in the control and intervention group (p<0.005), suggesting an increase in mitochondrial division in both groups. We observed a significant difference between control and intervention BDC pDrp1^{s616} expression (p<0.05). There was no significant change in pDrp1^{s637} (C) in either the control or intervention groups. There was no significant change in Fis1 protein expression in either the control or the intervention group. These results suggest that the micronutrient cocktail mitigated the increase in mitochondrial division and maintained Drp1 expression.

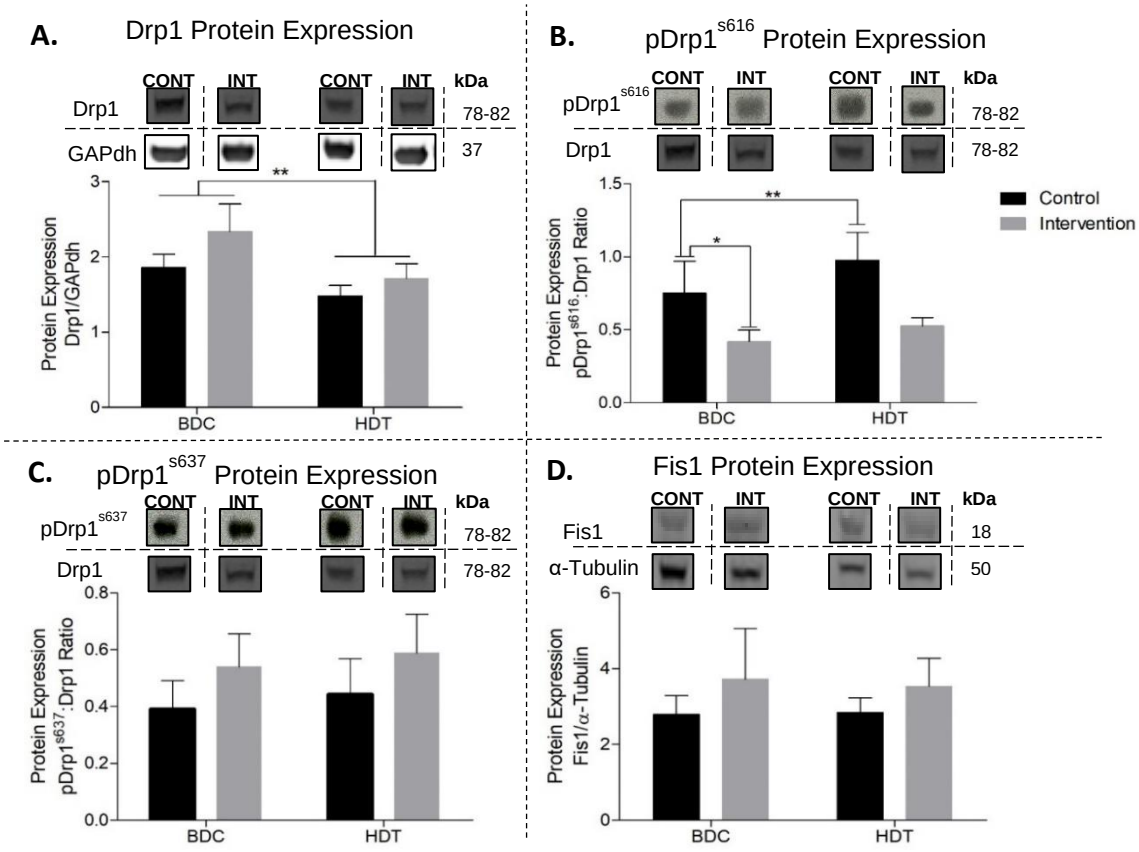

Figure 5. 7. Translational expression of markers related to mitochondrial fission before & following 60 days of bed rest

(Total Drp1 (A) (CONT, n=10, INT n=10), pDrp1^{s616} (B) (CONT, n=6, INT n=10), pDrp1^{s637} (C) (CONT, n=8, INT n=10) & Fis1 (D) (CONT, n=7, INT, n=10) protein expression was quantified by western blot. Protein expression of Drp1 (A) & Fis1 (D) were normalised against loading control (GAPdh/α-Tubulin expression) of same sample and subsequently expressed relative to BDC of same sample. pDrp1^{s616} (B) & pDrp1^{s637} (D) were normalised against Drp1 protein expression of same sample and subsequently expression relative to BDC of same sample. Blots presented are representative of all samples. Data are expressed as mean ±SE, ** significant effect of time, p<0.005)

Ratio of Mitochondrial Fusion:Fission

In order to assess for the balance between mitochondrial fusion and fission, protein expression of mitochondrial fusion marker OPA1 was controlled against protein expression of mitochondrial fission Drp1. Drp1 has been noted to directly regulate mitochondrial fission, while OPA1 regulates inner mitochondrial membrane (IMM) fusion. Mitochondrial respiration occurs along the IMM. Figure 5.8 demonstrates a significant increase in OPA1:Drp1 ratio in the intervention group (p<0.05), with no significant change in the control group. These results indicate supplementation of a micronutrient cocktail may help to increase OPA1 mediated inner mitochondrial membrane fusion due to the greater expression of OPA1 in the intervention group, thereby possibly increasing IMM CSA and curvature an adaptation which is strongly correlated with increased oxidative phosphorylation.

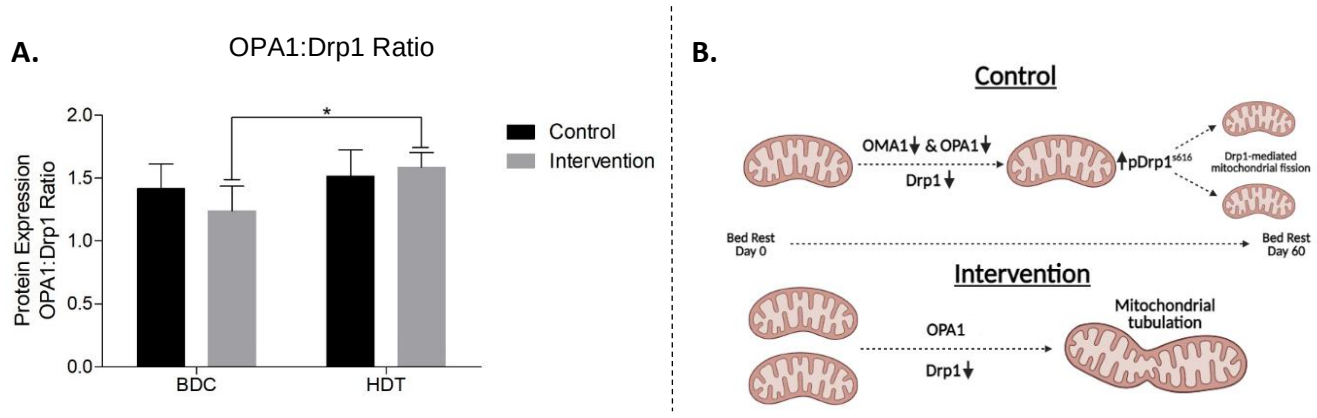

Figure 5. 8. OPA1:Drp1 Ratio before & following 60 days of bed rest

((A) OPA1:Drp1 protein expression quantified by western blot. OPA1, optic atrophy 1 was controlled against Drp1, dynamin related protein 1 protein expression (CONT, n=10, INT n=10). Both OPA1 and Drp1 protein expression were firstly normalised to their respective loading control (GAPdh). Data are expressed as mean ±SE, * significant effect of time, p<0.05. (B) Schematic highlighting the effect the intervention had on mitochondrial fusion-fission)

Expression of Markers Associated with Mitophagy

The regulators of mitochondrial breakdown (mitophagy) are presented in the below schematic.

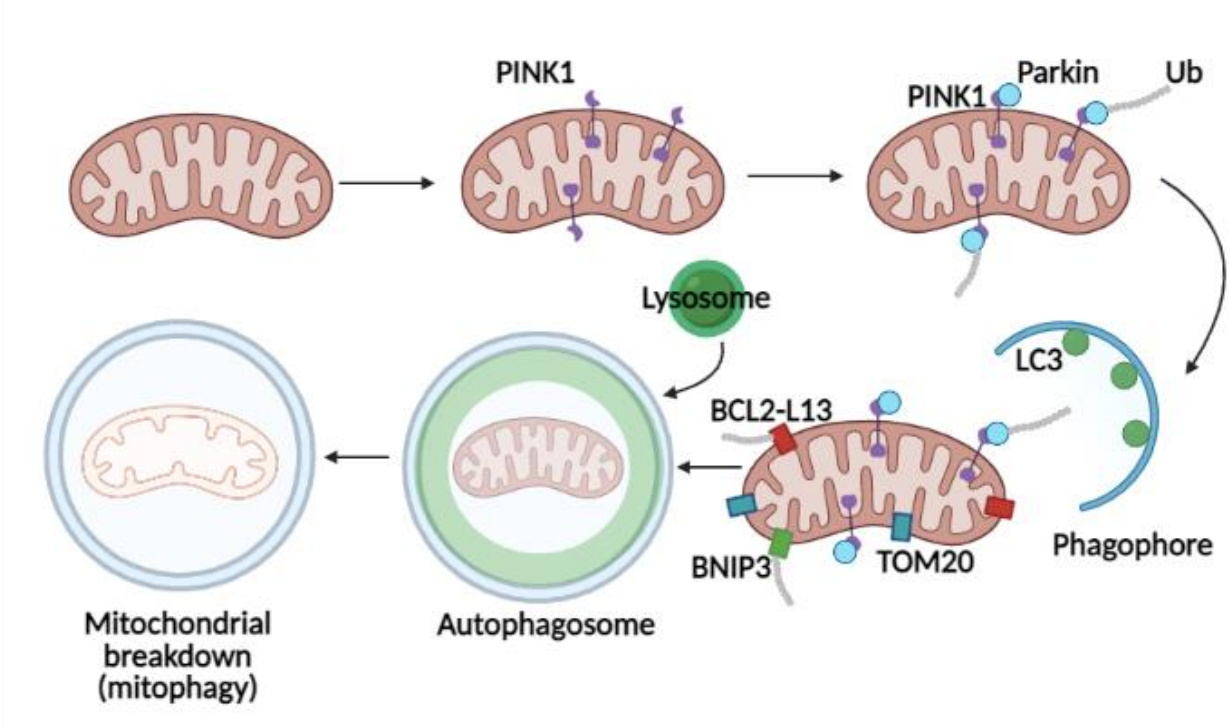

Figure 5. 9. Schematic representation of the process of mitochondrial breakdown (mitophagy)

Protein Markers Relating to Mitophagy

We observed a significant decrease in PINK1 protein expression (A) in the control group (p<0.05) but no change in the intervention group (Figure 5.10). We observed a significant difference between control and intervention BDC PINK1expression (p<0.05). There was no significant change in protein expression of any of the other mitophagy markers assessed in either groups. These results suggest that the micronutrient cocktail was capable in mitigating the adverse effects 60 days bed rest had on PINK1-mediated mitochondrial turnover.

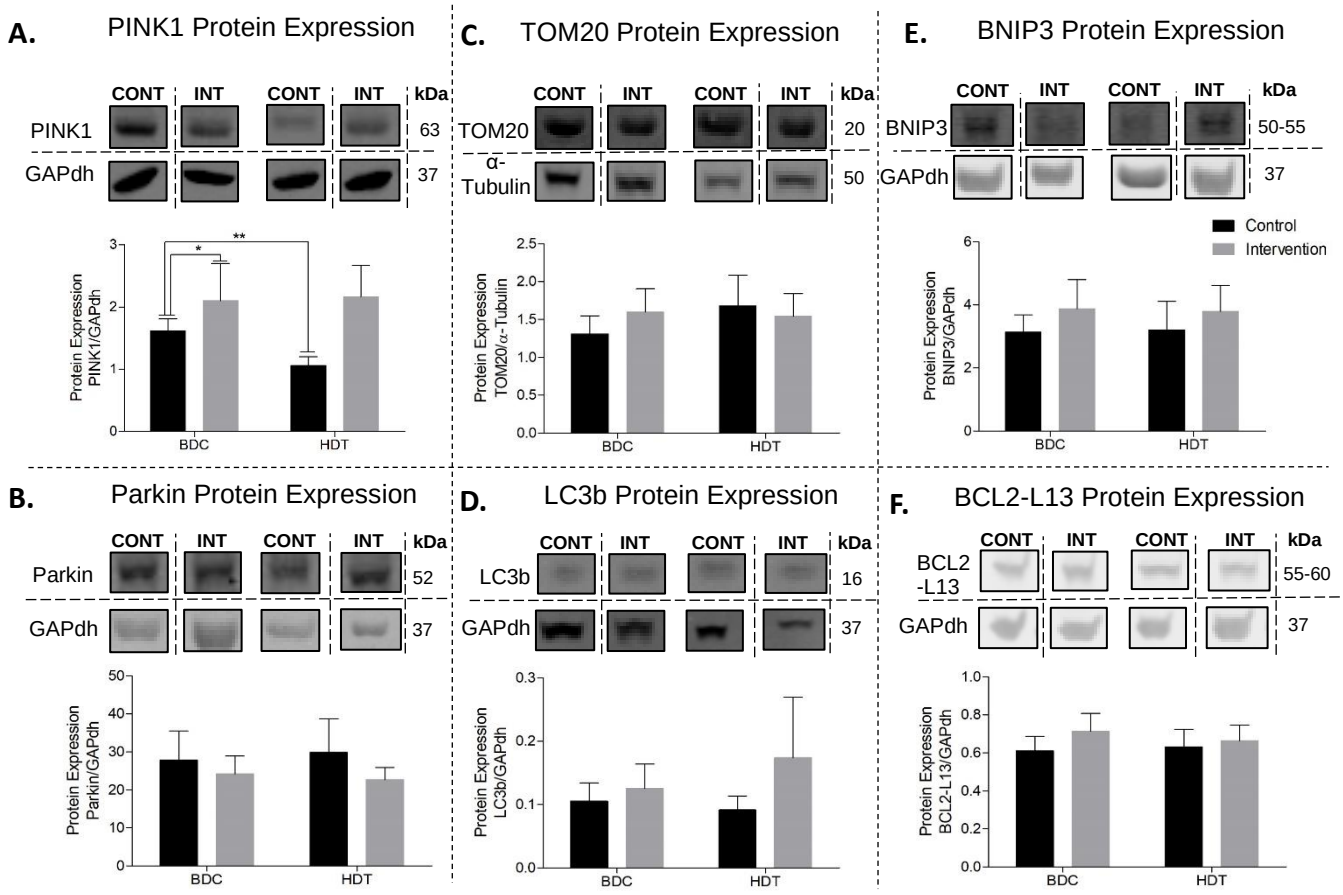

Figure 5. 10. Translational expression of markers regulating mitophagy before & following 60 days of bed rest

(PINK1 (A) (CONT, n=8, INT n=10), Parkin (B) (CONT, n=8, INT n=10), TOM20 (C) (CONT, n=7, INT, n=10), LC3b (D) (CONT, n=7, INT, n=10), BNIP3 (E) (CONT, n=7, INT n=10) & BCL2-L13 (F) (CONT, n=7, INT n=10), protein expression quantified by western blot). Protein expression was normalised against loading control (GAPdh expression) of sample. Blots presented are representative of all samples. Data is expressed as mean ±SE. **significant effect of time, p<0.005)

Regulators of Mitochondrial Biogenesis and Protein Synthesis

We found a significant increase in PGC-1α protein expression (A) in the control and intervention group following 60 days of bed rest (p<0.005) (Figure 5.11). mRNA expression (B) of PGC-1α significantly decreased in both groups (p<0.0005). There was a significant increase in SIRT1 protein (C) and mRNA (D) expression in the intervention, but not control, group following 60 days bed rest (p<0.05). We also observed a significant difference between control and intervention HDT SIRT1 mRNA expression (D) (p<0.0005). SIRT4 mRNA expression (F) significantly increased in the control (p<0.05) but not the intervention, while there was no change in mechanistic target of rapamycin (mTOR) protein expression (E) following 60 days bed rest in either the control or intervention group.

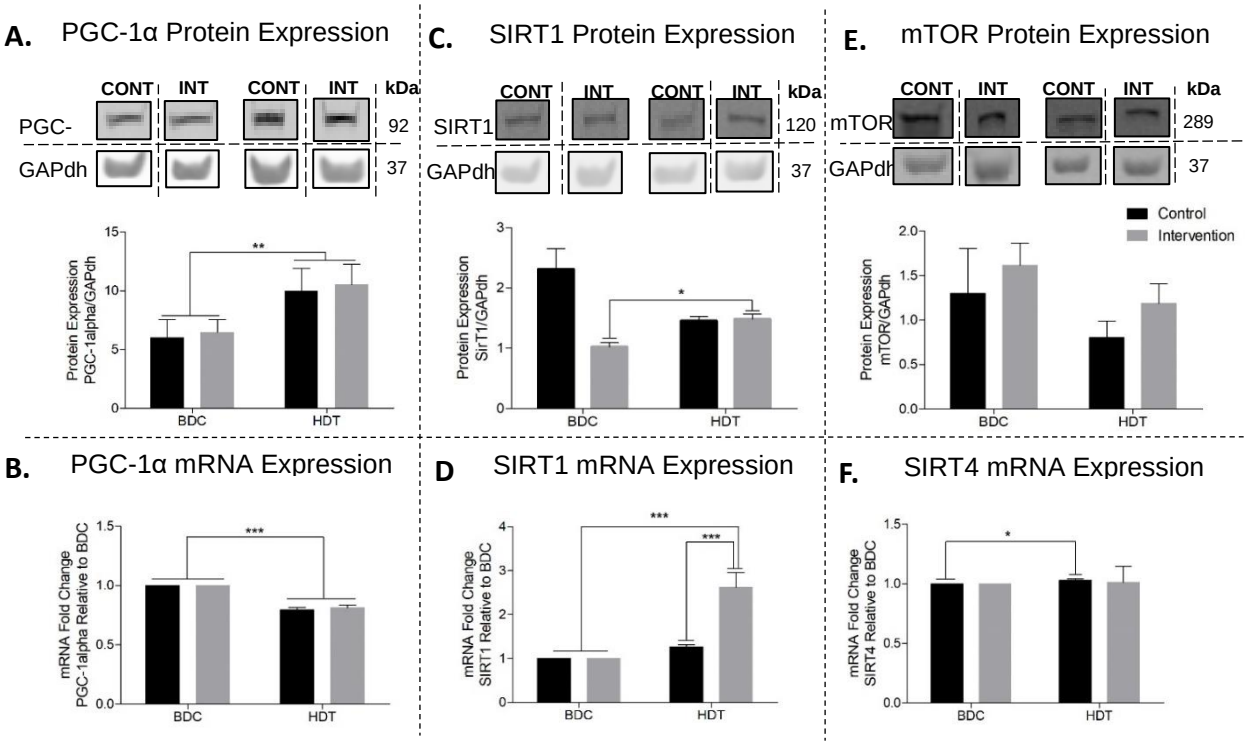

Figure 5. 11. Transcriptional and translational regulators of mitochondrial biogenesis & protein synthesis before & following 60 days of bed rest

(Total PGC-1α (A) (CONT, n=8, INT n=10), SIRT1 (C) (CONT, n=7, INT, n=7) & mTOR (E) (CONT, n=8, INT n=10) protein expression were quantified using western blot. Total PGC-1α (B) (CONT, n=8, INT n=8), SIRT1 (D) (CONT, n=8, INT n=7) & SIRT4 (F) (CONT, n=8, INT n=10) mRNA expression were quantified using RT-qPCR. Protein expression was normalised against loading control (GAPdh expression) of the same sample. Gene expression was normalised against GAPdh mRNA expression of same sample. Blots presented are representative of all samples. Data are expressed as mean ±SE. *significant effect of time, p<0.05, ***significant effect of time/treatment, p<0.0005)

Expression of Other Mitochondrial Markers

CPT1b protein (A) and mRNA (B) expression (Figure 5.12) significantly decreased in the control and intervention groups (p<0.005). While we also observed a significant difference between control and intervention HDT CPT1b mRNA expression (B) (p<0.0005). There was no change in Adenine Nucleotide Translocator 1 (ANT1) (C), Mitochondrial Calcium Uniporter (MCU) (D) or Voltage-Gated Anion Channel 1 (VDAC1) (F) protein expression following 60 days bed rest in the control or intervention group. Protein expression of Pan-Calcineurin A significantly increased in the intervention group (p<0.05) but there was no change in the control group. As CPT1b significantly decreased in protein expression following bed rest in the control group but not the intervention group, our results suggest that the micronutrient cocktail was capable of mitigating the decrease in CPT1b expression, a vital regulator in transfer of fatty acids into the mitochondria to be used for energy.

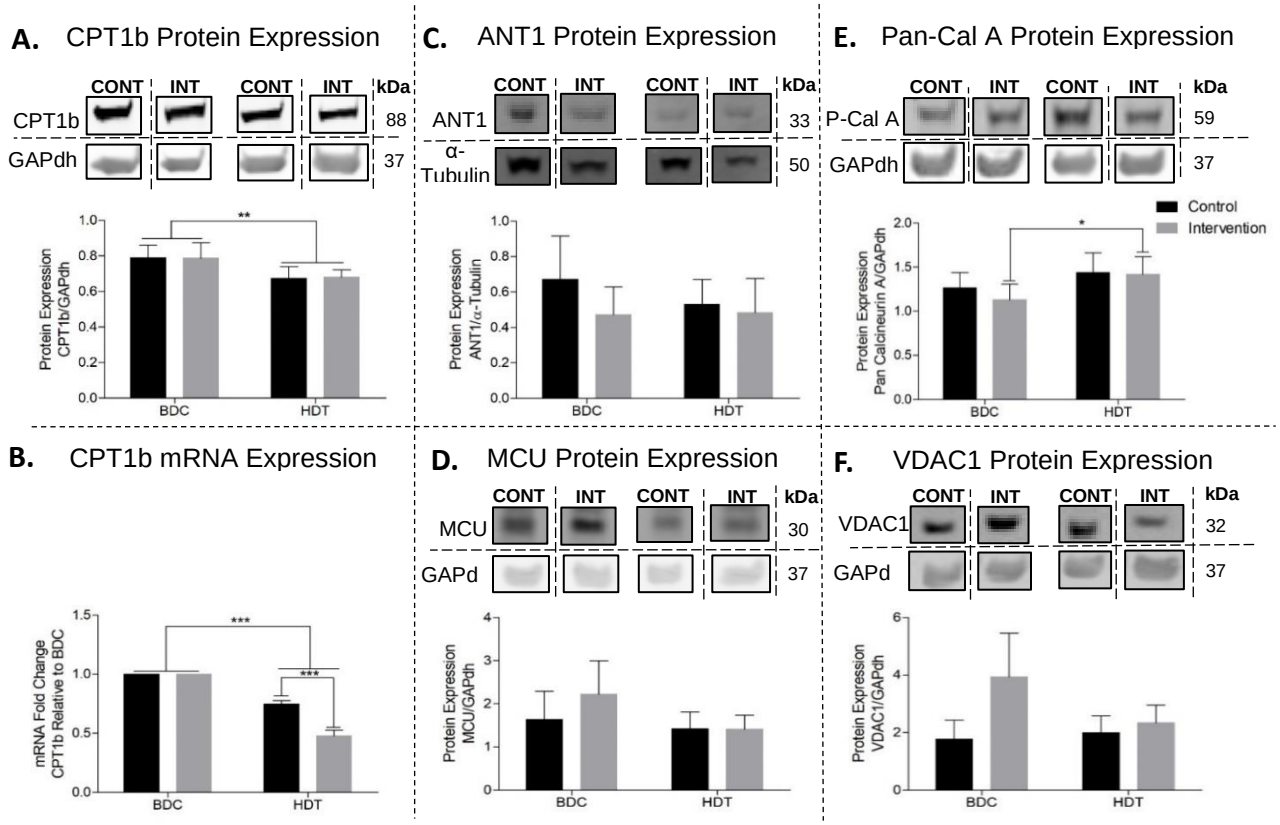

Figure 5. 12. Transcriptional and translational expression of other markers relating to mitochondrial function before & following 60 days of bed rest

(Total CPT1b mRNA expression (B) (CONT, n=8, INT n=7) quantified by RT-qPCR. Total CPT1b (A) (CONT, n=10, INT, n=7), ANT1 (C) (CONT, n=8, INT n=10), MCU (D) (CONT, n=7, INT n=10), Pan-Calcineurin A (E) (CONT, n=10, INT n=10) & VDAC1 (F) (CONT, n=7, INT n=10) protein expression quantified by western blot. Gene expression was normalised against GAPdh mRNA expression of same sample. Protein expression was normalised against loading control (GAPdh expression) of same sample. Blots presented are representative of all samples. Data are expressed as mean ±SE. *significant effect of time, p<0.05, **significant effect of time, p<0.005, ***significant effect of time/treatment, p<0.0005)

Summary of Transcriptional/Translational Markers Measured in Control/Intervention with 60-days of Bed Rest

60 days bed rest had a series of effects on multiple skeletal muscle mitochondrial transcriptional and translational markers relating to metabolism, particularly mitochondrial dynamics, biogenesis and regulators of fatty acid oxidation. It appears the micronutrient cocktail mitigated the effect 60 days bed rest on regulators of mitochondrial dynamics, increasing the mitochondrial elongation, while also maintaining PINK1-mediated mitochondrial removal keeping a healthy mitochondrial environment. Additionally, it appears that there is an attempt within the cell to counteract the effects of bed rest on mitochondrial content as represented by the increase in PGC-1α protein expression. Supplementation of a micronutrient cocktail may also mitigate the loss in regulators of free fatty acid oxidation given we noted an increase in SIRT1 protein and mRNA expression. This may coincide with the observed changes in SIRT4 and Pan-Calcineurin A expression respectively which significantly changed due to bed rest with or without our intervention respectively.

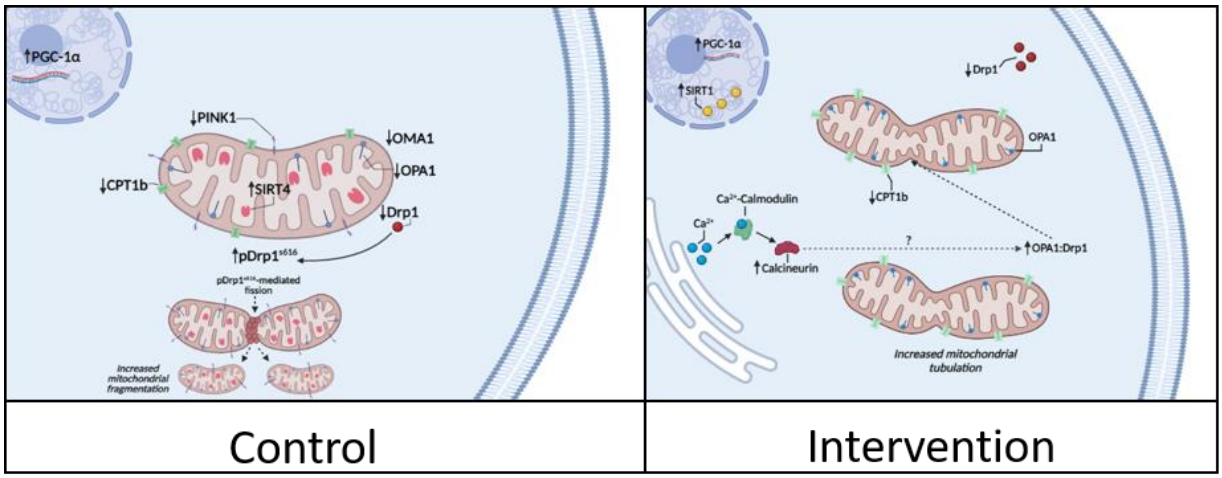

Figure 5. 13. Schematic representation of the changes occurring to regulators of mitochondrial dynamics following 60 days of bed rest in comparison to the micronutrient intervention

Table 5. 1. Summary of all transcriptional and translational changes observed with control and intervention following 60 days bed rest

Marker Measured	*Protein Expression*	*mRNA Expression*	*Direction of Change (p<0.05). Control*	*Direction of Change (p<0.05). Intervention*
OPA1	✓	✓	↓ (*)	-/↓(*)
L-OPA1	✓	-	↓ (*)	-
s-OPA1	✓	-	↓ (*)	-
Mfn1	✓	-	-	-
Mfn2	✓	-	-	-
YME1L	✓	-	-	-
OMA1	✓	-	↓ (*)	-
Drp1	✓	-	↓ (*)	↓ (*)
pDrp1^{s616}	✓	-	↑ (**)	-
pDrp1^{s637}	✓	-	-	-
Fis1	✓	-	-	-
OPA1:Drp1 Ratio	✓	-	-	↑ (*)
PINK1	✓	-	↓ (**)	-
Parkin	✓	-	-	-
TOM20	✓	-	-	-
BCL-L13	✓	-	-	-
BNIP3	✓	-	-	-
LC3b	✓	-	-	-
PGC-1α	✓	✓	↑ (**)/↓(***)	↑(**)/↓(***)
SIRT1	✓	✓	-	↑(*)/↑ (***)
SIRT4	-	✓	↑ (*)	-
mTOR	✓	-	-	-
CPT1b	✓	✓	↓(**)/↓ (***)	↓(**)/↓(***)
ANT1	✓	-	-	-
MCU	✓	-	-	-
Pan-Calcineurin A	✓	-	-	↑ (*)
VDAC1	✓	-	-	-

Comparison of 60 Day Bed Rest Protein Expression with 21 Days of Bed Rest

In order to determine if there was an effect of time on the changes in protein expression involved in mitochondrial regulation we compared our results from the control group of the 60-day bed rest trial with the control group from the 21-day bed rest study [263]. Muscle biopsies were probed for markers of mitochondrial function, morphology and cellular metabolism. All data represented is expressed as a fold change relative to relevant baseline data collection sample (BDC). Further information on the changes in protein expression along with respective densitometry within the control and the interventions used in the 21-day bed rest study can be found in Appendix (Section B).

Expression of Markers Associated with Mitochondrial Fusion

OPA1

There was a significant decrease in OPA1, L-OPA1 and s-OPA1 protein expression as an effect of time (p<0.005) but there were no significant differences between 21- and 60-days of bed rest (Figure 5.14). These results suggest that OPA1 may decrease early in response to bed rest resulting in decreased mitochondrial fusion.

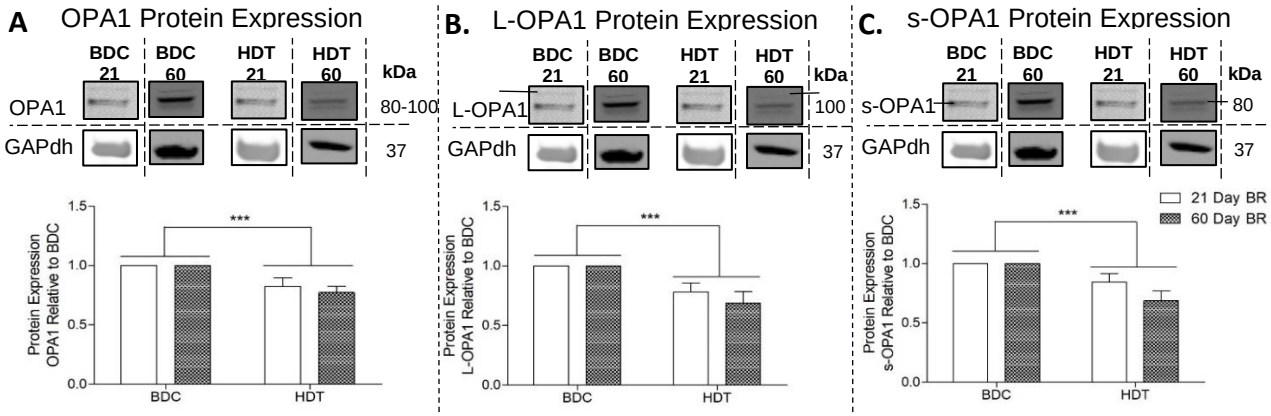

Figure 5. 14. Comparison in OPA1 expression before & following 21 & 60 days of bed rest

(OPA1 (A) (21-day BR n=9, 60-day BR n=10), L-OPA1 (B) (21-day BR n=9, 60-day BR, n=8), s-OPA1 (C) protein expression (21-day BR, n=9, 60-day BR, n=9) quantified by western blot. OPA1, L-OPA1 and s-OPA1 protein expression was normalised against loading control (GAPdh expression) of same sample and subsequently expressed relative to BDC of same sample. Blots presented are representative of all samples. Data are expressed as mean ±SE.*** significant effect of time, p<0.0005)

Other Markers of Mitochondrial Fusion - Mfn1, Mfn2, YME1L & OMA1

There was no significant change (Figure 5.15) in Mfn1 (A) or Mfn2 (B) protein expression following either 21 or 60 days bed rest (p>0.05). We further analysed the regulators of OPA1, YME1L and OMA1. There was no significant change in YME1L (C) protein expression following either 21 or 60 days bed rest (p>0.05). However, there was a significant increase in OMA1 protein expression following 21 days of bed rest (p<0.05) and a significant decrease in its protein expression with 60 days of bed rest (p<0.005). These results signal an adaptive response of OMA1 due to the duration of bed rest. The increase in OMA1 with 21 days bed rest could signal a stress response posed by bed rest acting to increase L-OPA1 cleavage to s-OPA1, decreasing mitochondrial fusion. The decreased expression with 60 days could signal an adaptive response in an attempt to maintain mitochondrial integrity.

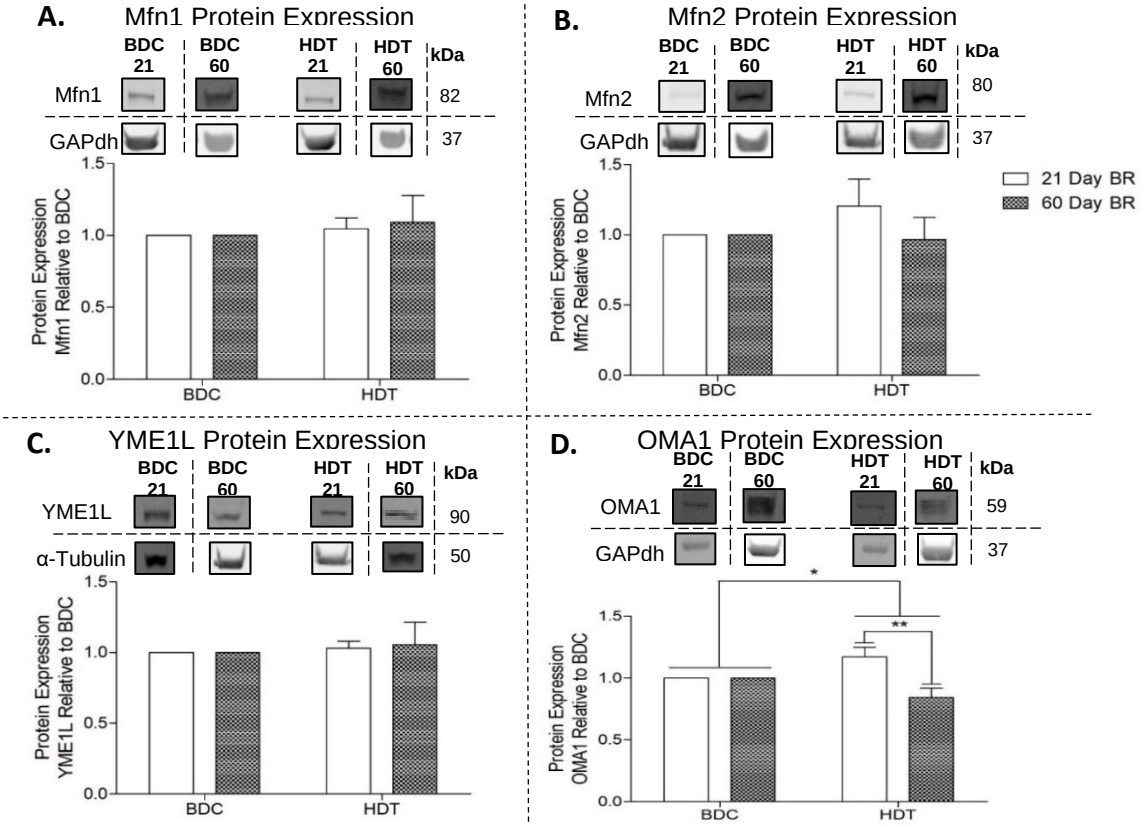

Figure 5. 15. Comparison in other regulators of mitochondrial fusion before & following 21 & 60 days of bed rest

(Mfn1 (A) (21-day BR n=10, 60-day BR n=10), Mfn2 (B) (21-day BR n=10, 60-day BR, n=10), YME1L (C) (21-day BR n=10, 60-day BR n=9) and OMA1 (D) (21-day BR n=9, 60-day BR n=9) protein expression quantified by western blot. Protein expression was normalised against loading control (GAPdh expression) of same sample and subsequently expressed relative to BDC of same sample. Blots presented are representative of all samples. Data are expressed as mean ±SE. * significant effect of time, p<0.05, ** significant effect of time, p<0.005)

Expression of Markers Associated with Mitochondrial Fission

Protein expression for Drp1 (A) significantly decreased in the 60-day bed rest (p<0.05) but not with 21 days of bed rest (Figure 5.16). There was a significant increase in pDrp1^{s616} (B) following 60 days of bed rest (p<0.005) but no change with 21 days of bed rest. There was no significant change in pDrp1^{s637} (C) or Fis1 (D) protein expression following either 21 or 60 days of bed rest. These results suggest that 60 days of bed rest decreases the expression of Drp1 but increases the activity of the protein, as represented by the increase in pDrp1^{s616}. These changes don't occur with 21 days bed rest, and therefore they may be an adaptive response to longer exposure to bed rest.

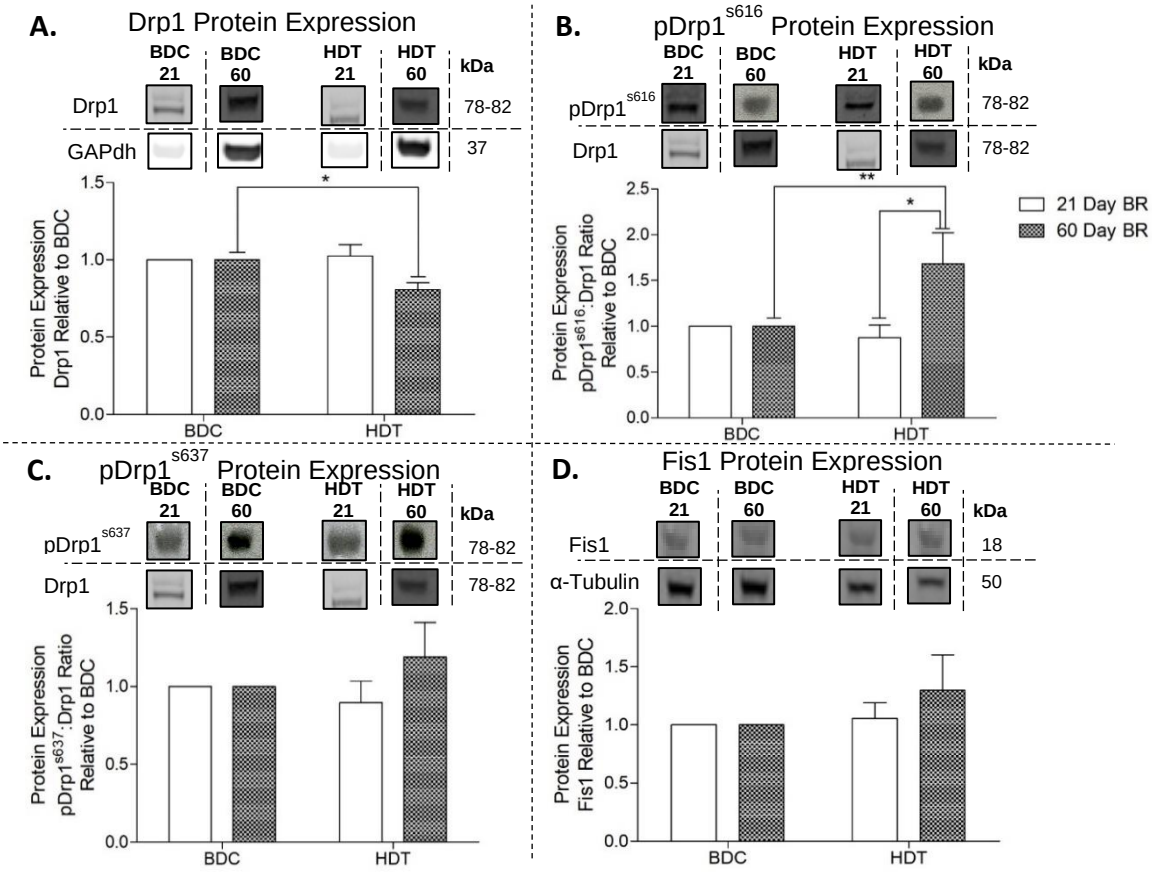

Figure 5. 16. Comparison in expression of regulators of mitochondrial fission before & following 21 & 60 days of bed rest

(Drp1 (A) (21-day BR n=10, 60-day BR n=10), pDrp1^{s616} (B) (21-day BR n=9, 60-day BR n=6), pDrp1^{s637} (C) (21-day BR n=9, 60-day BR n=8) & Fis1 (D) (21-day BR, n=10, 60-day BR, n=7) protein expression quantified by western blot. Protein expression of Drp1 (A) & Fis1 (D) were normalised against loading control (GAPdh/α-Tubulin expression) of same sample and subsequently expressed relative to BDC of same sample. pDrp1^{s616} (B) & pDrp1^{s637} (D) were normalised against Drp1 protein expression of same sample and subsequently expression relative to BDC of same sample. Blots presented are representative of all samples. Data are expressed as mean ±SE.* significant effect of time, p<0.05, ** significant effect of time, p<0.005)

Ratio of Mitochondrial Fusion:Fission

There was a significant decrease in OPA1:Drp1 ratio in the 21-day bed rest group (p<0.05) only, indicating a possible increase in Drp1 mediated mitochondrial fission due to the decrease in OPA1 protein expression with 21-days of bed rest (Figure 5.17). There was no significant change in the 60-day bed rest group, indicating a balance in Drp1 mediated mitochondrial fission and OPA1 mediated mitochondrial fusion.

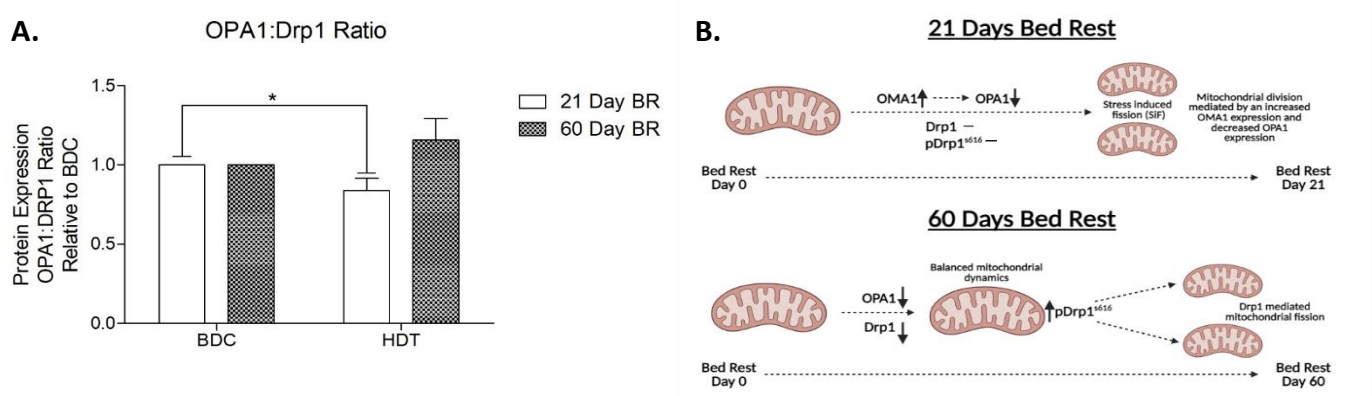

Figure 5. 17. Comparison in OPA1:Drp1 Ratio before & following 21 & 60 days of bed rest

(OPA1:Drp1 protein expression quantified by western blot (A). OPA1 was controlled against Drp1 protein expression (21-day BR n=10, 60-day BR n=10). Both OPA1 and Drp1 protein expression were firstly normalised to their respective loading control (GAPdh). Data are expressed as mean ±SE, * significant effect of time, p<0.05. (B) Schematic highlighting the effect the bed rest duration has on mitochondrial fusion-fission dynamics)

Expression of Markers Associated with Mitophagy

Protein expression for PINK1 (A) significantly decreased with 60-day bed rest (p<0.05) but not with 21 days of bed rest (Figure 5.18). There was no significant change in Parkin (B), BCL2-L13 (C) or BNIP3 (D) protein expression with 21 or 60 days of bed rest (p>0.05). This indicates that regulators of mitophagy react well to shorter bouts of bed rest, but as bed rest continues PINK1 expression decreases and increasing the availability of poorly functioning mitochondria.

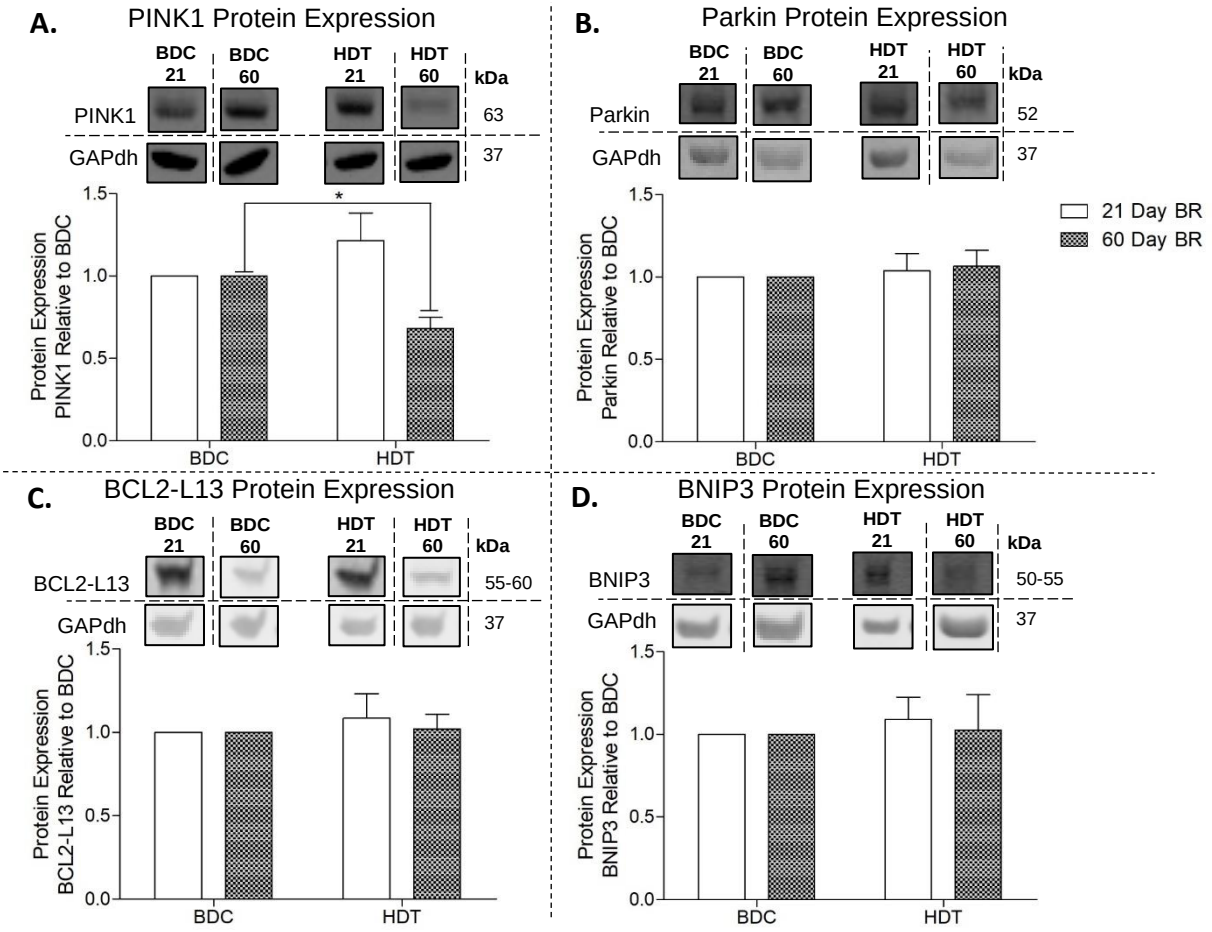

Figure 5. 18. Comparison in expression of regulators of mitophagy before & following 21 & 60 days bed rest

(PINK1 (A) (21-day BR n=10, 60-day BR n=8), Parkin (B) (21-day BR, n=10, 60-day BR, n=8), BCL2-L13 (C) (21-day BR n=10, 60-day BR n=7) & BNIP3 (D) (21-day BR, n=10, 60-day BR, n=7) protein expression quantified by western blot. Protein expression was normalised against loading control (GAPdh expression) of same sample and subsequently expressed relative to BDC of same sample. Blots presented are representative of all samples. Data are expressed as mean ±SE.* significant effect of time, p<0.05)

Expression of Markers of Mitochondrial Biogenesis

PGC-1α

We found no significant change in PGC-1α protein expression following 21 days bed rest (Figure 5.19), however PGC-1α protein expression significantly increased with 60 days of bed rest (p<0.005). PGC-1α protein expression following 21 days bed rest (HDT) was significantly different to PGC-1α protein expression following 60 days bed rest (HDT) (p<0.005). The increase in PGC-1α following 60 days of bed rest may indicate an adaptive response in the muscle to bed rest. As the cell requires mitochondria for the generation of energy, the increase in PGC-1α expression may be an attempt within the cell to generate more mitochondria to counteract against some of the detrimental effects long bouts of bed rest have on the mitochondrial environment, helping the cell meet is reduced energy demands.

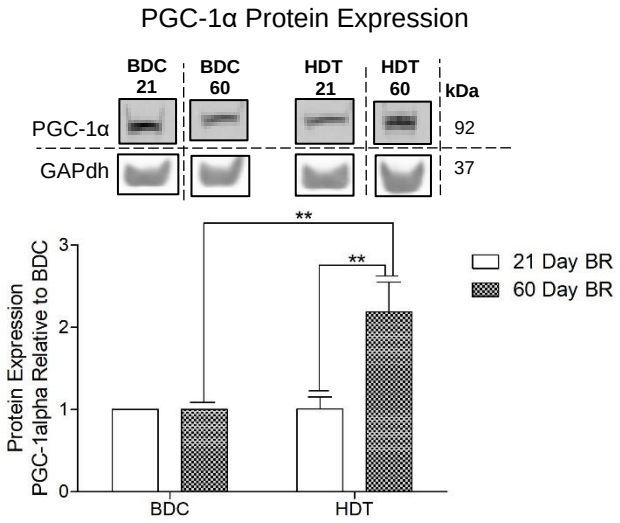

Figure 5. 19. PGC-1α expression before & following 21 & 60 days of bed rest

(PGC-1α (21-day BR n=10, 60-day BR n=8) protein expression quantified by western blot. Protein expression was normalised against loading control (GAPdh expression) of same sample and subsequently expressed relative to BDC of same sample. Data are expressed as mean ±SE.** significant effect of time, p<0.005)

Expression of Key Mitochondrial Translocators

Protein expression of CPT1b (A) and VDAC1 (C), situated on the outer mitochondrial membrane, and MCU (B), situated on the inner mitochondrial membrane respectively were analysed for protein expression with 21 and 60 days of bed rest (Figure 5.20). CPT1b (A) protein expression significantly decreased following 21 and 60 days bed rest (p<0.0005). Protein expression of MCU (B) and VDAC1 (C) did not change following 21 or 60 days bed rest. This decrease in CPT1b protein expression with 21 and 60 days bed rest supports the adverse effect prolonged bed rest has on fatty acid metabolism.

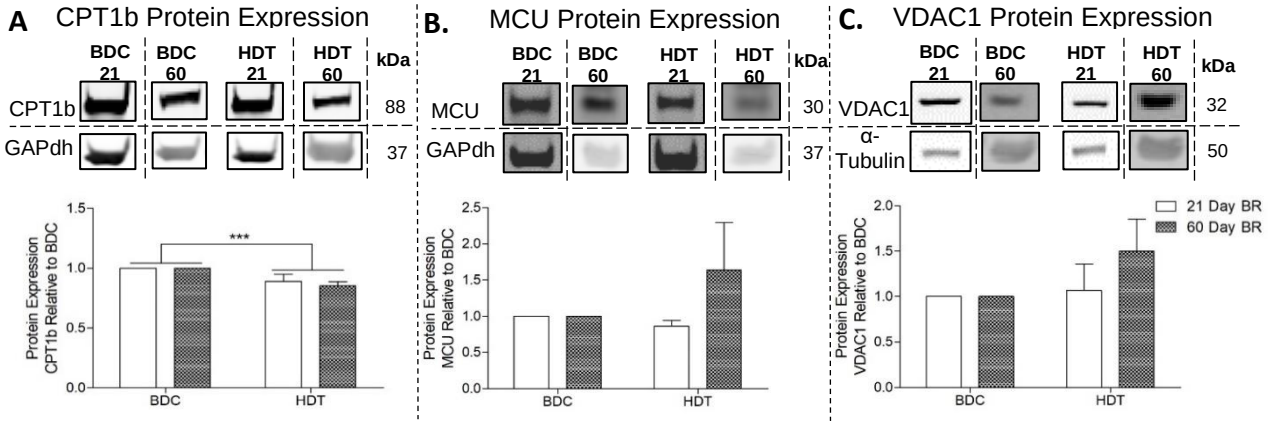

Figure 5. 20. Translational expression of key translocators before & following 21 & 60 days of bed rest

(CPT1b (A) (21-day BR, n=9, 60-day BR, n=10), MCU (B) (21-day BR n=11, 60-day BR n=7) & VDAC1 (C) (21-day BR, n=10, 60-day BR, n=7) protein expression quantified by western blot. Protein expression was normalised against loading control (GAPdh/α-Tubulin expression) of same sample and subsequently expressed relative to BDC of same sample. Data are expressed as mean ±SE, ***significant effect of time, p<0.0005)

Summary of Changes in Protein Expression in Markers Measured with 21 & 60-days of Bed Rest

Bed rest leads to significant adaptations to skeletal muscle metabolism which appear to be dictated by changes in mitochondrial function. OPA1 expression, a central regulator of mitochondrial fusion, in particular significantly decreases with both 21 and 60 days bed rest underlining its sensitivity to bed rest. Key regulators of fusion appear to adapt differently based on the duration of bed rest (i.e. OMA1), while key regulators of mitophagy and biogenesis appear to be significantly impacted by long bouts of bed rest (>21 days). These adaptations indicate that there is a decrease in the removal of dysfunctional mitochondria (PINK1) as time in bed continues, possibly leading to an increase in dysfunctional mitochondria. An increase in regulators of biogenesis (PGC-1α) may be an attempt within the cell to maintain a healthy mitochondrial content (even when low), enabling the cell meet its energy demands (even when reduced due to bed rest).

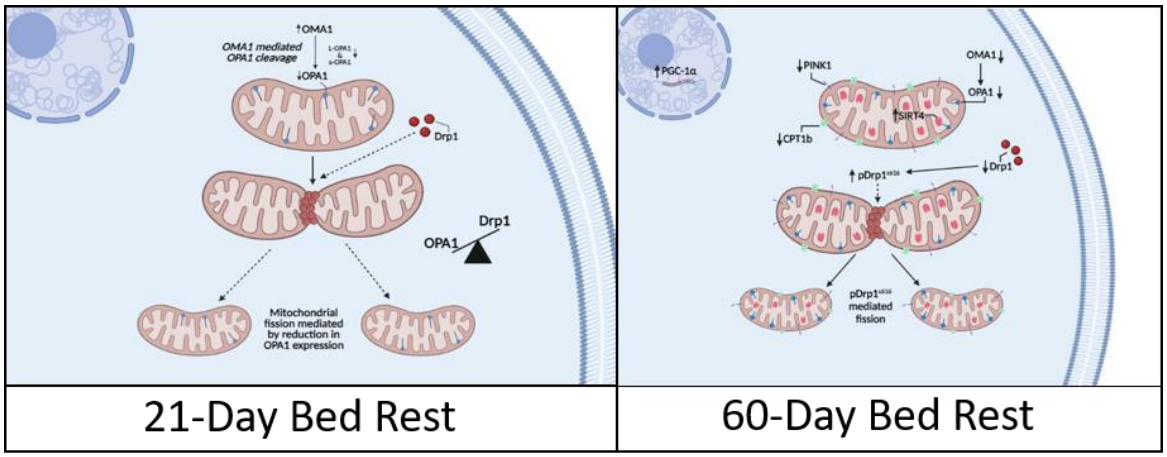

Figure 5. 21. Schematic representation of the impact 21 days of bed rest has on regulators of mitochondrial function in comparison to 60 days of bed rest

Table 5. 2. Summary of all translational changes observed following 21 and 60 days bed rest

Marker Measured	*Direction of Change. 21-day bed rest*	*p<0.05*	*Direction of Change. 60-day bed rest*	*p<0.05*
OPA1	↓	*	↓	*
L-OPA1	↓	*	↓	*
s-OPA1	↓	*	↓	*
Mfn1	-	*p*>0.05	-	*p*>0.05
Mfn2	-	*p*>0.05	-	*p*>0.05
YME1L	-	*p*>0.05	-	*p*>0.05
OMA1	↑	*	↓	*
Drp1	-	*p*>0.05	↓	*
pDrp1^{s616}	-	*p*>0.05	↑	**
pDrp1^{s637}	-	*p*>0.05	-	*p*>0.05
Fis1	-	*p*>0.05	-	*p*>0.05
OPA1:Drp1 Ratio	↓	*	-	*p*>0.05
PINK1	-	*p*>0.05	↓	*
Parkin	-	*p*>0.05	-	*p*>0.05
BCL2-L13	-	*p*>0.05	-	*p*>0.05
BNIP3	-	*p*>0.05	-	*p*>0.05
PGC-1α	-	*p*>0.05	↑	**
CPT1b	↓	*	↓	***
MCU	-	*p*>0.05	-	*p*>0.05
VDAC1	-	*p*>0.05	-	*p*>0.05

Discussion on the Cellular Response to Bed Rest

The main findings from this study were that 60 days of bed rest results in significant changes in mitochondrial function and dynamics. Bed rest resulted in a decrease in the maximal respiratory capacity of skeletal muscle that is associated with changes in mitochondrial content. At the level of mitochondrial dynamics, we found significant decreases in OPA1 and Drp1 expression. These adaptations are in conjunction with decreases in regulators of mitophagy and increased protein expression of regulators of mitochondrial biogenesis. Given the majority of these changes were only observed in the control group, the micronutrient intervention may be acting to limit these changes. Subsequently, supplementation with this micronutrient cocktail appears to be beneficial in the regulation of mitochondrial dynamics, biogenesis and mitophagy, adaptations which may be governed by NAD^+-deacetylases and ADP-ribosyltransferases, SIRT1 and SIRT4 which were shown to change in their expression in the control/intervention group respectively following 60 days of bed rest.

Comparative analysis of samples attained from a similarly completed 21-day bed rest study highlight a significant decrease in OPA1 expression with bed rest. These results signifying how OPA1-mediated mitochondrial fusion may be one of the initial adaptations in the mitochondrial phenotype during bed rest.

The Changes in Mitochondrial Content with 60 days of Bed Rest

Bed rest has been shown to lead to significant reductions in mitochondrial content and volume. As such, normalization of mitochondrial respiration to mitochondrial content is important when interpreting changes in mitochondrial function, particularly when trying to decipher the changes which occur following bed rest/muscle disuse. The gold standard method for measuring mitochondrial content in a sample is transmission electron microscopy (TEM) [193]. However, due to its inconvenience, instrument availability and cost TEM was not used. Other methods for quantifying mitochondrial content and muscle oxidative capacity include citrate synthase activity, cardiolipin content, complex I–V protein, complex I–IV activity and, as we used, mitochondrial DNA content (mtDNA). Larsen et al., [292] , was the first to validated these surrogates against a morphological measure of mitochondrial content in human muscle. This study concluded that the strongest correlation with TEM was cardiolipin, followed by citrate synthase activity and complex I activity. The well supported correlation between mitochondrial content and mtDNA:nDNA ratio was debated here by Larsen and colleagues [292]. This was surprising given the extensive evidence to support a strong correlation between mtDNA:nDNA and mitochondrial content [416,541,339].

Due to the low quantity of muscle we had available from the fasting muscle biopsy samples, we had to use insulin stimulated samples to quantify mitochondrial content. This meant that the measurement of a biomarker not impacted by insulin, requiring a low quantity of muscle and within the realistic realms of methods available to us was imperative. Citrate synthase and complex I activity are commonly used to quantify mitochondrial content but they significantly increase in response to insulin so were excluded [515,309,474,496]. Insulin also changes phospholipid metabolism, leading to fluctuations in different species of cardiolipin which ruled out this biomarker also [390,98]. Therefore, we decided the most objective measure of mitochondrial content for this study would be to use the mtDNA:nDNA ratio.

In order to be confident in our normalization procedure, we used different combinations of mtDNA:nDNA transcripts to ensure we were capturing physiologically relevant data. As with previous bed rest studies, we reported a significant decrease in mtDNA:nDNA ratio indicative of a reduction in mitochondrial content following bed rest in both groups. The reduction in mitochondrial content appears to be responsible for the decrease in mitochondrial respiration and, as with many of the changes which occur with bed rest, this adaptation appears to occur in the first 7-10 days of bed rest [125,488].

The Changes in Mitochondrial Respiration with 60 days of Bed Rest

The terms mitochondrial function and dysfunction are used widely in the field of bioenergetics. However, the exact definition of function is vague due to the different methods applied to quantify function. In its essence the main physiological function of the mitochondria is in the generation of energy in the form of ATP by oxidative phosphorylation in response to energy demands [60]. This process requires oxygen, a reactant which is consumed in the final step of the mitochondrial electron transport chain to create this ATP. Subsequently, the content and the capacity of the mitochondria to create ATP with the oxygen supply is an extremely important consideration.

Following 60 days of bed rest, we observed a decrease in many parameters of mitochondrial function when controlled to wet muscle weight, such as ETS (CI), ETS (CII) and CII. However, when normalized to mitochondrial content these changes were no longer evident and there were no differences between groups. These results indicate that even though antioxidants and anti-inflammatory's have been shown to play a beneficial role in cellular metabolism and redox balance [407,410], we did not find a difference in mitochondrial function. This does not mean that the intervention did not have a beneficial effect on oxidative stress induced by ROS/RNS production, only we did not see an effect on mitochondrial respiration. Excessive ROS has been proposed to

result in damage to important organelles and biomolecules in the cell, such as the mitochondria, while promoting cell death [407,68]. Subsequently, antioxidants and anti-inflammatories have been proposed to manage these changes by counteracting free radicals and neutralizing oxidants [214]. A decrease in mitochondrial respiration following bed rest would be indicative of mitochondrial dysfunction, while an increase would represent an increase in functional capacity. The fact we had no change in respiration in both groups when controlling for mitochondrial content, suggests they did not have an impact on mitochondrial function. However, considering we have no data on absorption, concentrations etc. we cannot know if there was a change at the level of the skeletal muscle tissue. It is also possible the respiratory experiments are not sensitive enough to detect small changes as the substrates concentrations saturate the reactions and lead to maximal responses from the mitochondria. If there were a greater number of small, poorly functioning, mitochondria they might still consume oxygen under these conditions.

There are very few studies that have measured the effect bed rest on mitochondrial function, and this is the first one to assess the impact of 60 days bed rest. Kenny et al. [263] was the first to measure mitochondrial function following 21-days bed rest and found a significant decrease in LEAK respiration. LEAK is the process whereby protons 'leak' back into the matrix of the mitochondria through alternative conductance pathways, uncoupling substrate oxidation from ATP synthesis. The free radical theory emphasises that oxidative metabolism in aerobic cells is accompanied by the production of oxygen to superoxide and other reactive oxygen species (ROS) such as hydrogen peroxide and hydroxyl radicals [210]. Given the mitochondria are both the primary source of ROS and targets of ROS damage [109], a reduction in LEAK respiration due to bed rest could potentially induce cellular damage through increased ROS production. Unlike Kenny et al. [263], we did not find a decrease in LEAK respiration following 60 days of bed rest when we controlled for mitochondrial content. One explanation for this could be that Kenny et al. [263] normalised their results to citrate synthase activity, while we normalised to mtDNA:nDNA ratio. However, a more likely reason for the difference is due to the malleability and plasticity of the mitochondria to adapt to its environment. Such adaptation may act to protect the mitochondria from further damage, for example from ROS production, during the 60 day bed rest trial [23,59].

The Effect of 60 Days of Bed Rest on Regulators of Mitochondrial Metabolism and Signalling

Skeletal muscle mitochondrial respiration was similar, in both groups, when normalised to mitochondrial content. The significant decrease in fat free mass, coupled with the decrease in mitochondrial content are most likely contributing to the decrease in whole body oxygen

consumption. At this point, we do not have causal evidence and cannot identify the main mechanistic driver but we wanted to determine if changes in mitochondrial signalling could explain some of these adverse physiological adaptations to bed rest.

Mitochondrial signalling associated with mitochondrial biogenesis, mitochondrial dynamics, mitochondrial breakdown (mitophagy) and mitochondrial substrate metabolism were analysed in the skeletal muscle samples before and after both 21 and 60 days of bed rest.

Mitochondrial Dynamics with 60 days of Bed Rest

Given the role mitochondrial dynamics has been shown to have on mitochondrial function and overall cellular homeostasis, we hypothesized that time in bed would lead to a decrease in the expression of markers relating to mitochondrial morphology which could explain some of the more descriptive physiological changes observed in Chapter IV.

We did not find any changes in the expression of outer mitochondrial membrane (OMM) fusion proteins, Mfn1 and Mfn2 following 60 days of bed rest. However, we did observe a significant decrease in the long and short isoforms of the inner mitochondrial membrane fusion protein, OPA1 in the control group and mitochondrial fission marker, Drp1 in both groups. By measuring OPA1:Drp1 ratio we could interpret if there was a shift in the mitochondrial fusion-fission balance following 60 days bed rest. Our results indicate there was no significant change in OPA1:Drp1 ratio in the control group and suggest the balance between fusion and fission was maintained during bed rest. However, total protein content does not always reflect the activity of pathways or processes in the cell.

Measuring pDrp1^{s616} and pDrp1^{s637} gave further insight to the mitochondrial dynamics and help to indicate if the mitochondria may be primed towards division (increased pDrp1^{s616}) or fusion (increased pDrp1^{s637}). Our results showed no change in pDrp1^{s637} protein expression but we did observe a significant increase in pDrp1^{s616} in the control group. This increase in phosphorylation suggests that although we have a balance in fusion and fission (OPA1:Drp1 ratio), the mitochondria are in fact primed towards division following 60 days of bed rest.

Inner mitochondrial membrane (IMM) protein, OPA1, is regulated by two proteases, OMA1 and YME1L, which cleave the IMM bound long-OPA1 to the soluble short-OPA1 [140,328,308]. OMA1 is activated by stress, while YME1L acts in response to changes in cellular ATP, given it is an ATP-dependent proteolytic complex on the inner mitochondrial membrane [539,374]. There was no change in YME1L protein expression following 60 days of bed rest, even though there was a

significant difference between BDC protein expression in both groups, indicating it may not play a role in the changes in OPA1 expression. However, we do not have YME1L activity data to support this conclusion. Interestingly, we observed a significant decrease in OMA1 protein expression in the control group. This could be as a direct result of the decreased expression of OPA1 as OMA1 requires OPA1 to cleave L-OPA1 to s-OPA1 under times of stress, reducing OPA1-mediated mitochondrial fusion. Our results infer that bed rest significantly alters pathways relating to mitochondrial fusion in an OPA1-mediated manner.

These adaptations of fission and fusion in human skeletal muscle following bed rest has not been examined to date. However, hindlimb suspension studies in mice and studies comparing exercising and sedentary individuals provide us with some insight to the possible adaptations that we observe within our prolonged bed rest study. Hindlimb suspension reduces skeletal muscle OPA1 and increases Drp1 protein expression together with a reduction in mitochondrial function [78]. Sedentary individuals, when compared with aged-matched, exercising counterparts, have a reduced expression of fusion (OPA1, Mfn1 and Mfn2) and fission (Drp1) transcripts; all of which were strongly correlated with a reduction in oxidative phosphorylation [506]. Subsequently, these changes in fusion-fission coordinate the switch in substrate metabolism at rest from fat to carbohydrate, while aiding cellular metabolism by maintaining mitochondrial content at a homeostatic level to meet the energy demands.

Interestingly, the decreases in OPA1, OMA1 and pDrp1^{s616} expression were not evident in the intervention group, indicating the micronutrient cocktail may have helped mitigate against the changes in mitochondrial dynamics. In fact, the OPA1:Drp1 ratio significantly increased in the intervention group, suggesting an increase in mitochondrial tubulation in response to the micronutrient cocktail. Little is known about the molecular mechanisms controlling mitochondrial dynamics but Pfluger et al. [395] suggested a possible regulatory role for calcineurin on Drp1 mitochondrial fission activity. Calcineurin is activated by an influx of intracellular calcium which subsequently binds to calmodulin. Calcium-calmodulin plays an important role in regulating mitochondrial function and overall cellular metabolism and is regarded as a key-signalling node in response to the environmental stimuli in the cell. It is thought to be involved in augmenting mitochondrial ATP production and possibly influencing skeletal muscle remodelling, something which is apparent following prolonged bed rest [378,152].

Pfluger et al. [395] observed that calcineurin ablation enhanced mitochondrial tubulation linked to hyper-phosphorylation of pDrp1^{s637}. We found a significant increase in Pan-Calcineurin A protein expression in the intervention group (we did not measure calcineurin B), an increased

OPA1:Drp1 ratio, a decrease in Drp1 protein content and a trending increase in pDrp1^{s637} but not pDrp1^{s616}. These data suggest that micronutrient supplementation increased mitochondrial elongation via calcium-calcineurin mediated mechanisms or that these mechanisms were subsequent to increased elongation. An increase in Pan-Calcineurin A suggests that following bed rest, there could either be an increased calcium release from the sarcoplasmic reticulum or a slower reuptake of calcium back into the sarcoplasmic reticulum of those in the intervention group, triggering an increase in calcineurin, and a subsequent activation of Drp1-mediated mitochondrial fusion (pDrp1^{s637}) [177]. Another theory could be that an increased mitochondrial surface area subsequent to more elongated mitochondria could result in an increased capacity of mitochondria to store calcium, increasing Pan-Calcineurin A. Given we didn't measure mitochondrial calcium uptake, this is still just a theory but based on our expression data our micronutrient cocktail could be regulating the balance between fission, due to the regulatory role calcineurin has on Drp1, and fusion, due to the maintenance of its expression within this cohort.

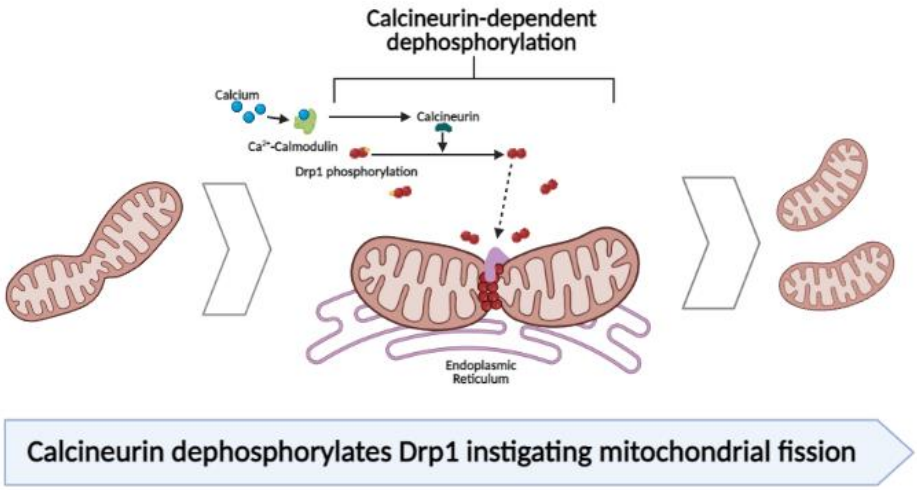

Figure 5. 22. Calcineurin-dependent dephosphorylation of Drp1. Adapted from *Giacomello et al.* [177]

Our preliminary work on this nutritional supplement [112], established that the cocktail prevented decreases in lipid oxidation and type II muscle fibers following 20 days of reduced activity. We didn't observe any differences in whole body lipid metabolism following the bed rest study and the supplement may not be sufficient to overcome the more extreme inactivity of bedrest. However, the increase in the OPA1:Drp1 ratio and the preservation of mitochondrial dynamic processes in the intervention group indicate cellular regulation that could represent an increase in mitochondrial elongation and a prevention of some changes in skeletal muscle. Elongated mitochondria have been shown to have a greater capacity to generate energy through oxidative

phosphorylation and β-oxidation over glycolysis [399,572,384,110,559]. This micronutrient cocktail was composed of multiple bioactive compounds from the diet, supported by the literature, to positively affect different physiological processes.

Polyphenols, such as resveratrol, have been shown to delay muscle degradation, although these observations have only been shown in mice [347]. Selenium appears to independently effect insulin sensitivity and secretion, while acting in conjunction with Vitamin D to protect against some of the adverse changes observed during bed rest by acting as a scavenger for ROS and RNS reducing oxidative stress [387,502,38]. Although this thesis didn't focus on these processes, we did observe a trending decrease in mTOR protein expression in both groups. mTOR is a regulator of muscle protein synthesis and decreases with inactivity. We observed a trending decrease in mTOR expression with bed rest. This, in conjunction with the significant decrease fat free mass supports that it is unlikely that the polyphenols and selenium present in our compound are having a major mechanistic impact on muscle structure but also on mitochondrial dynamics. However, it could be argued that the capacity of polyphenols and selenium in ameliorating oxidative stress enhances the capacity of the other nutritional compounds.

Vitamin E and Omega-3 fatty acids (ω-3) have a synergistic effect on lowering triglycerides (TG), raising high-density lipoproteins (HDL), protecting mitochondrial membranes from excessive oxidative damage and improving lipid metabolism [113,324,94,364,363]. Herbst et al. [219] measured skeletal muscle mitochondrial membrane phospholipid composition in young, healthy males (*n*=18) before and after 12 weeks of fish oil supplementation and demonstrate that ω-3 supplementation appeared to reorganise the composition of the mitochondrial membranes while promoting improvements in ADP sensitivity. One phospholipid known to be directly impacted by ω-3 is cardiolipin [489]. Cardiolipin is a phospholipid necessary for the formation of contact sites between inner and outer mitochondrial membranes, the stabilization of essential inner membrane proteins and respiratory complexes, increases when ω-3 is present [539,134]. As cardiolipin has a direct interaction with OPA1 at the cristae junctions, helping to give the cristae its curvature and subsequently allowing for the greater distribution of OXPHOS proteins [321,21,174], the impact of the micronutrient cocktail on mitochondrial fusion may be partially mediated by ω-3.

Given one of the first steps in lipid metabolism is the phenotypic elongation of the mitochondria, the ω-3 and Vitamin E in our intervention could be the main regulators of the increase in the OPA1:Drp1 ratio. Although unclear, this phenotypic change could indicate an initial shift in substrate oxidation from carbohydrates to fats which longer term, or higher dosed,

supplementation might emphasise to a greater extent. Unfortunately, there are no mechanistic studies examining the effect of nutrient cocktails so our interpretation of the mechanistic role is limited and further study is required.

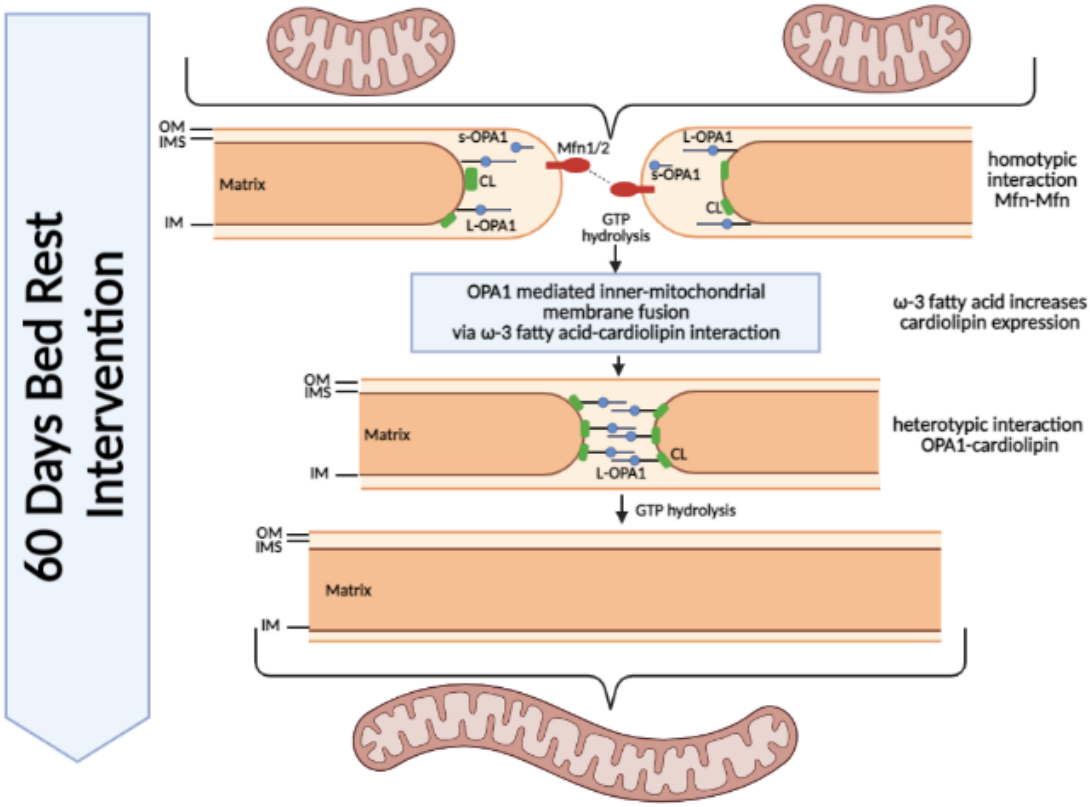

Figure 5. 23. Role Omega-3 fatty acid plays with cardiolipin to instigate an increase in OPA1-mediated mitochondrial fusion

Mitochondrial Biogenesis with 60 days of Bed Rest

There is much evidence to support the role of PGC-1α in regulating mitochondrial biogenesis by acting as a transcriptional coactivator regulating genes involved in energy metabolism. The majority of the literature demonstrates that the expression of PGC-1α decreases significantly with inactivity [6,66,238,145,488], while exercise increases PGC-1α expression in a dose-dependent manner [137,25]. We hypothesized transcriptional and translation expression of PGC-1α would significantly decrease following 60 days of bed rest. Instead we found that mRNA expression significantly decreased in both groups but protein expression of PGC-1α significantly increased in both groups. This discrepancy between transcriptional and translational markers is not uncommon and could be explained by multiple factors from post-transcriptional and post-translational modifications to a possible negative feedback loop between gene and protein expression [115]. Nevertheless, our protein expression data, which is more in-line with the

functional adaptations of the cell, suggest an upregulation of mitochondrial biogenesis following 60 days of bed rest with and without micronutrient supplementation.

Although this is in contrast to the majority of studies, there is some evidence to suggest that skeletal muscle disuse doesn't always lead to decreases in PGC-1α expression, particularly protein expression. Rittweger et al. [440] found a significant increase in PGC-1α protein expression in skeletal muscle of male astronauts following 6-months of space flight. Although, this could be indicative of the exercise measures used on-board to maintain overall health, subjects in this study had significant reductions in muscle size, architecture and strength, a phenotype frequently linked with a decrease in oxidative capacity and regulators of mitochondrial biogenesis. Ringholm et al. [435] supports our findings further, by reporting that after just 7-days of bed rest there was no significant change in PGC-1α mRNA expression, while Moriggi et al. [352] reported a slight, yet non-significant, increase in PGC-1α protein expression following 55 days of bed rest. Our data indicate that while PGC-1α expression may decrease in the short term, there may be a medium term increase to offset further loss of mitochondrial content and maintain a sufficient number of functioning mitochondria. As an increase in PGC-1α is also linked to fatty acid oxidation, in an unorthodox way the increase in PGC-1α which we observe following 60 days bed rest could also be a response to the shift in substrate oxidation (fat → carbohydrate) in an attempt to switch back the cells energy source to oxidize fatty acids.

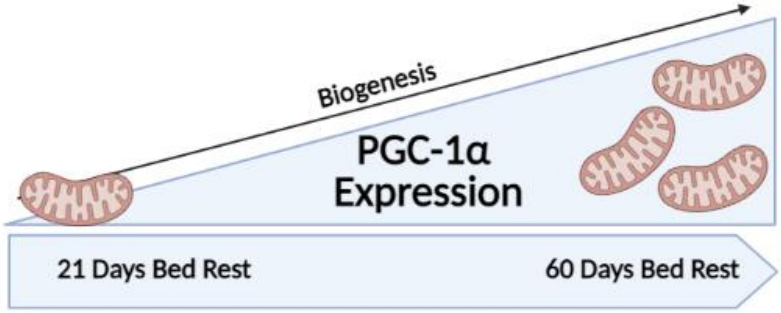

Figure 5. 24. Schematic interpretation of the adaptation of PGC-1α protein expression to prolonged bed rest

Calcium has been shown to induce an increase in mitochondrial biogenesis. In fact, Garcia-Roves et al., [170], noted that an increase in calcineurin, which is activated by increased intracellular calcium-calmodulin expression, results in a significant increase in PGC-1α expression through its regulation of myocyte enhancer factor-2 (MEF2), a transcription factor regulating muscle development and calcium-dependent gene expression [108]. Our results show that following 60 days of bed rest there is a significant increase in Pan-Calcineurin A. Subsequently, this gradual

increase in biogenesis could be linked to a gradual change in calcium homeostasis leading to an increase in fatty acid utilization. As these changes in biogenesis were not observed from a transcriptional but only a translational perspective, further research is required to examine the time-course effects of physical inactivity on mitochondrial biogenesis.

Changes in Expression of Sirtuin Family Members Following 60 days of Bed Rest

Due to the role prolonged bed rest has in altering the skeletal muscle cells substrate preference from fat to carbohydrate while at rest, emphasised by the switch from type I to type II muscle fibers and in the switch of RQ from fat oxidation to carbohydrate, some of these changes could be regulated by the sirtuin family of NAD^+-dependent deacetylases and ADP-ribosyl-transferases. The sirtuins are a family of enzymes that act to deacetylate many mitochondrial metabolic enzymes and it has been suggested that they coordinate substrate switching [542,579,557]. At least three members of this family, SIRT1, SIRT3 and SIRT4, are involved in the regulation of mitochondrial dynamics and biogenesis. SIRT1 overexpression studies demonstrate an increased PGC-1α expression, increasing mitochondrial biogenesis and resulting in an increased expression of genes related to fatty acid oxidation via an AMPK-SIRT1 signalling axis. SIRT1 knockout studies show decreased mitochondrial function, a reduction in ATP and NAD^+ and a decrease mitochondrial biogenesis [9,271,412,301].

Following bed rest, we found that SIRT1 protein and mRNA expression was significantly increased in the intervention group, closely complementing our observations in PGC-1α protein expression which significantly increased in expression. This was unexpected given SIRT1 regulates anabolic processes with hypertrophic exercise [271,420], while also extending lifespan in yeast, C. elegans and mice [41,462,88]. The increase in SIRT1 occurred against a background of bed rest induced muscle atrophy. Animal models of muscle disuse found that supplementation with resveratrol, a polyphenol known to induce the expression and activity of SIRT1, prevented the loss in muscle mass and force [242,347]. Bennett et al. [30] confirmed that resveratrol supplementation resulted in an increase in PGC-1α, SIRT1 and AMPK expression in rats following 14 days of hindlimb suspension. Although these results have not been observed in human studies, we did observe an increase in PGC-1α protein expression and a significant increase in SIRT1 mRNA and protein expression in the skeletal muscle of those supplemented with our micronutrient cocktail which was composed of polyphenols among other anti-inflammatories and antioxidants. These finding are in line with observations published from our micronutrient cocktail pilot study [112]. We illustrated in these findings how supplementation prevented the decrease in type IIa muscle fiber

CSA, and considering the observed increase in regulators strongly correlated with skeletal muscle atrophy such as SIRT1, our cocktail could provide the initial basis to preserve skeletal muscle mass.

In conjunction with the increase in PGC-1α, an increase in SIRT1 following bed rest could signify an upregulation in mitochondrial biogenesis via this AMPK-SIRT-PGC-1α axis [435,66,73]. Although shorter periods of bed rest have resulted in a significant decrease in mitochondrial biogenesis, epitomised by a reduction in both SIRT1 and PGC-1α [488], as the duration of bed rest continues, biogenesis may increase in order to compensate for the decrease in mitochondrial content. Supplementation of our micronutrient cocktail may provide a greater impetus to this regulatory pathway, managing the decrease in regulators of free fatty acid oxidation and biogenesis, both of which are strongly correlated to each other [371,230], maintaining a healthier mitochondrial environment.

SIRT4, a negative regulator of fatty acid oxidation, due to its role in regulating Malonyl-CoA decarboxylase (MCD), has also been shown to regulate mitochondrial dynamics. An increase in SIRT4 decreases fatty acid oxidation, while a decrease represents the opposite effect [366,205,342,514]. Although yet to be demonstrated in human skeletal muscle, SIRT4 has been suggested to regulate OPA1 mediated mitochondrial fusion [366,288]. We observed a slight, yet significant increase, in SIRT4 mRNA expression following 60 days bed rest in the control group only. Lang et al. [288] suggested that SIRT4 overexpression results in an increased L-OPA1 mediated mitochondrial fusion in fibroblasts and HEK293 cells. Yet our results represent an increase in SIRT4 expression as OPA1 expression decreases. No work to date has measured the impact SIRT4 on the regulation of OPA1 dynamics in skeletal muscle but due to its role in the regulation of oxidative phosphorylation and the correlation between mitochondrial elongation and changes in the preferred source of energy metabolism [421,559], SIRT4 may be an indirect regulator of OPA1 expression in skeletal muscle. The increase in SIRT4 expression in the control but not the intervention again represents the role the micronutrient intervention may have in maintaining the oxidation of free fatty acids. However, considering we only observed a subtle change in SIRT4 expression, more work is necessary here to fully elucidate if this would be functionally meaningful.

Mitophagy with 60 days of Bed Rest

Well classified markers of mitochondrial breakdown (mitophagy), PINK1, Parkin, BCL2-L13, BNIP3 and LCb3 were measured for protein expression before and following 60 days of bed rest. The literature suggests an interlink between mitophagy and mitochondrial dynamics, particularly Drp1

mediated mitochondrial fission. Mitochondrial fission has been shown to promote the segregation of damaged mitochondria and facilitate their clearance by mitophagy, whereby a fused mitochondrial network can protect mitochondria from degradation [527,14,422]. We observed a significant decrease in PINK1 protein expression following 60 days of bed rest in the control group but no change in Parkin, BNIP3, BCL2-L13 or LC3b. Similar to our study, Kang et al. [257] found a significant decrease in PINK1 expression following 3 weeks of hindlimb suspension in mice. However, this decrease was correlated with a similar decrease in BNIP3, BCL2 and an increase in LC3b expression, something we did not find. Given the subsequent decrease in PINK1 protein expression and the literature supporting the correlation in activity of PINK1-mediated mitophagy and Drp1-mediated mitochondrial fission, one could infer that following 60 days of bed rest the mitochondria adapt to their environment resulting in a decrease in fission, impacting on mitochondrial removal. Although, this remains unclear and requires further mechanistic studies to decipher the exact mechanisms at play.

Mitophagy is necessary for mitochondrial maintenance and quality control [564,565]. A decrease in mitophagy leads to an increase in damaged, dysfunctional mitochondria. It is possible that prolonged bed rest leads to an increase in damaged mitochondria as we found a decrease in PINK1 and a decrease in Drp1-mediated mitochondrial fission, coupled with an increase in PGC-1α-mediated biogenesis. There was no significant change in PINK1 protein expression in the intervention group and this may be related to the inclusion of selenium and Vitamin E. Reactive oxygen species (ROS) and reactive nitrogen species (RNS) significantly increase with inactivity and play a key role in the accelerated muscle atrophy observed during prolonged bed rest [411,409,410]. Some of the components in our micronutrient cocktail, particularly the ROS scavengers' selenium and Vitamin E have been shown to positively augment oxidative stress [231,266,387]. We did not measure ROS/RNS production following bed rest and this will require further investigation but, our intervention suggests the maintenance of a healthier mitochondrial environment, in conjunction with a more elongated phenotype.

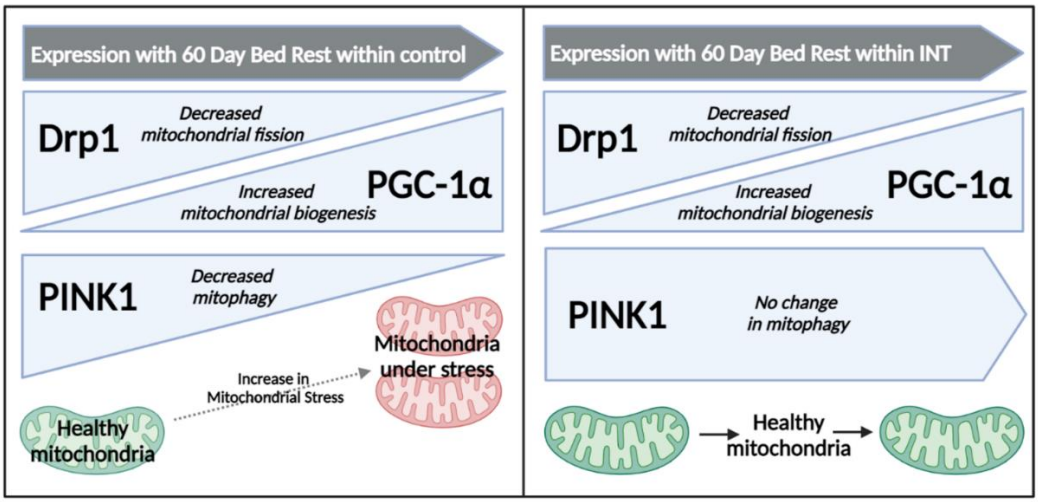

Figure 5. 25. Interpretation on the impact of 60 days bed rest on mitochondrial stress

Prolonged Bed Rest Results in Adaptations to Regulators of Substrate Oxidation

Prolonged bed rest has been shown to significantly decrease the expression of biomarkers of fatty acid oxidation such as CPT1b [33,264]. Our results support this, epitomised by the significant decrease in CPT1b protein and mRNA expression in both groups following 60 days of bed rest. CPT1b is thought to be the rate limiting enzyme in fatty acid oxidation and is inhibited by Malonyl-CoA. As SIRT4 increases Malonyl-CoA, our results showing increased SIRT4 mRNA expression and decreased CPT1b protein and mRNA expression support the switch from fat to carbohydrate oxidation we observed following bed rest [35]. Due to the limited supply of muscle sample, protein and mRNA expression could only be measured. Ideally we would look at both expression and activity to fully comprehend the changes we observed but our findings are in line with previously published literature.

Comparison of Changes in Mitochondrial Dynamics, Biogenesis and Mitophagy with 21 and 60 days Bed Rest

In order to understand the timeframe of adaptation in mitochondrial dynamics, mitophagy and biogenesis to bed rest we re-analysed samples from the control group following a 21-day bed rest study [263] and compared them to our 60-day bed rest results. Following 21 days of bed rest, the expression of both isoforms of OPA1, the L-OPA1 and s-OPA1 significantly decreased and indicates this reduction to be an early adaptation to inactivity. There was no significant change in YME1L protein expression, similar to 60 days of bed rest, but, OMA1 expression was significantly increased following 21 days of bed rest. An increase in OMA1, together with the activation of Drp1 at the mitochondrial surface is thought to lead to stress-induced fission (SiF) and a broad range of

metabolic and extracellular effects [18,539]. Given we observed a significant decrease in OMA1 expression following 60 days of bed rest, there is evidence of a transient effect on OMA1 expression whereby an initial increase in expression cleaves L-OPA1 to s-OPA1 within the first 3 weeks but subsequently decreases thereafter. These results suggest that an initial bout of bed rest (3 weeks) causes and acute stress on the mitochondria, signified by the increase in OMA1, but the muscle must adapt to longer term inactivity by maintaining the ability to fuse mitochondria.

There was no change in Drp1 expression following 21 days of bed rest, however pDrp1^{s616} significantly decreased, the opposite effect to the 60-day bed rest trial. This decrease points to a reduction in Drp1-mediated mitochondrial fission with short duration bed rest. If we compare this change to the 60-day bed rest trial, our results suggest that an acute form of bed rest (3 weeks) initiates SiF mediated by the reduction in OPA1 expression (OPA1:Drp1 ratio), linked to an increase in mitochondrial breakdown and removal supported by the trending increase in PINK1. However, as bed rest continues we have a balance in fusion-fission with mitochondria primed towards fission supported by the increase in pDrp1^{s616}.

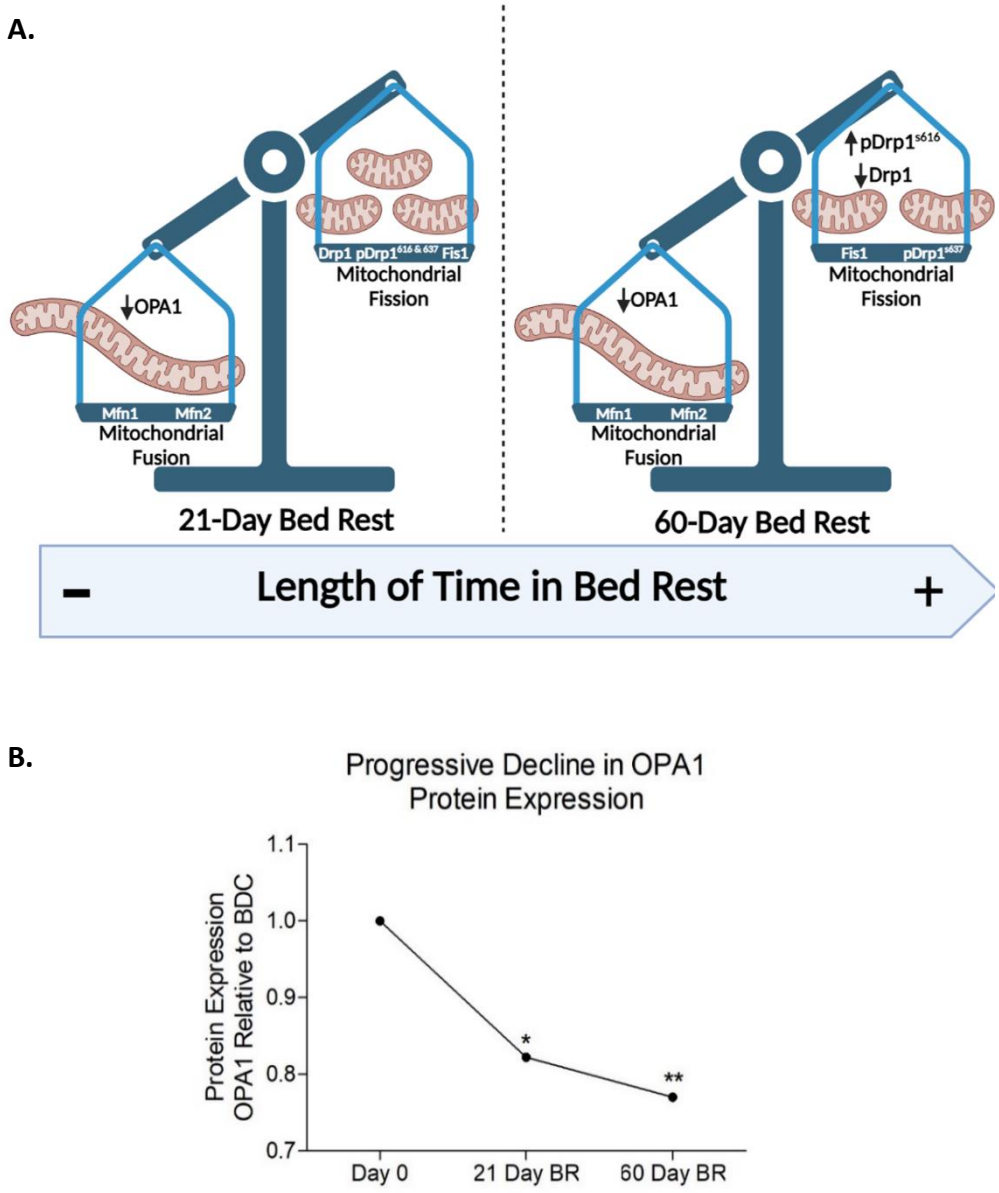

Figure 5. 26. Schematic representation of the impact length of time in bed has on regulators of mitochondrial dynamics (A) & OPA1 protein expression (B)

The change in mitochondrial dynamics could help our understanding of substrate metabolism and muscle atrophy. There is strong evidence linking the mitochondrial phenotype to substrate oxidation, with more elongated mitochondria preferring fatty acid oxidation over carbohydrate [399,572,384,110,559]. Additionally, mitochondrial fusion regulates skeletal muscle atrophy, with OPA1 overexpression/knockout significantly impacting on sarcopenia and healthy aging [531,450]. In the 21-day bed rest study we found a modest shift in RQ from fat to carbohydrate oxidation, in addition to a change from slow to fast twitch muscle fibers [263]. The accompanying decrease in OPA1-mediated mitochondrial fusion, suggests an increase in mitochondrial fragmentation. Given a shift in fuel preference is one of the primary changes to occur with inactivity and the fact that

OPA1-mediated mitochondrial fusion was one of the only factors to change following 21 days of bed rest, a change in the mitochondrial phenotype could be one of the initiating factors involved in switching fuel preference and fiber types.

Conclusion

The 21- and 60-day bed rest studies resulted in a significant decrease in OPA1 expression. Our results showed that 60 days bed rest impacted mitochondrial dynamics further, supported by the reduced expression of mitochondrial fission marker, Drp1. A balance in OPA1:Drp1 ratio following 60 days bed rest suggests an adaptive response the prolonged period of bed rest, something which was not observed following 21 days. In the first 21 days of bed rest there is an increase in fragmentation due to the decreased expression of OPA1. Although we observe a balance in OPA1 and Drp1 with 60 days bed rest, we suggest that more prolonged bed rest (>3 weeks) leads to an increase in stress induced fission (SiF) caused by an increase in $pDrp1^{s616}$. Supplementation of a micronutrient cocktail appears to curtail these changes in mitochondrial dynamics, epitomised by an increase in the OPA1:Drp1 ratio. Considering the maintenance of OPA1 protein expression within the intervention group and its relationship with cardiolipin which has been shown within the literature to increase in expression in response to ω-3, we suggest that the ω-3 component of our micronutrient cocktail is the key player in the initiation of a more elongated mitochondrial phenotype as the regulators of mitochondrial dynamics would support. As there were no changes in the expression of PINK1 in the intervention group we suggest that the other components of our cocktail, Vitamin E, selenium and the polyphenols could be integral in this regard, helping to maintain a healthier mitochondrial network. The lack of change in PINK1 could signify the normal regulation of mitophagy, a change which may be regulated by the free radical scavenging characteristics of the other components of the micronutrient cocktail, reducing mitochondrial dysfunction.

The NAD^+-deacetylase, SIRT1 mRNA and protein expression significantly increased following 60 days bed rest in the intervention group while the ADP-ribosyltransferase, SIRT4, significantly increased in expression in the control group. We suggest that the changes in mitochondrial dynamics may be regulated by these sirtuin family members, given the role SIRT1 has on regulators of mitochondrial biogenesis and substrate metabolism and the limited work to suggest SIRT4's indirect regulation of mitochondrial dynamics. Consequently, Chapter VI will attempt to elucidate the possible regulatory role SIRT4 has on mitochondrial dynamics and substrate metabolism within human skeletal muscle.

Chapter VI: SIRT4 as a Regulator of Mitochondrial Fusion

SIRT4, a member of the mammalian sirtuin family, is one of seven sirtuin nicotinamide adenine dinucleotide (NAD^+)-dependent lysine deacylases and ADP-ribosyltransferases. Alongside SIRT3 and SIRT5, SIRT4 is located within the mitochondria and is involved in the regulation of β-oxidation (Figure 6.3). SIRT4 mRNA was significantly increased following 60 days bed rest in our control group and came to our attention because of its possible regulatory role on OPA1. We hypothesised that SIRT4 regulates OPA1 mediated mitochondrial fusion, regulating free fatty acid oxidation in human skeletal muscle.

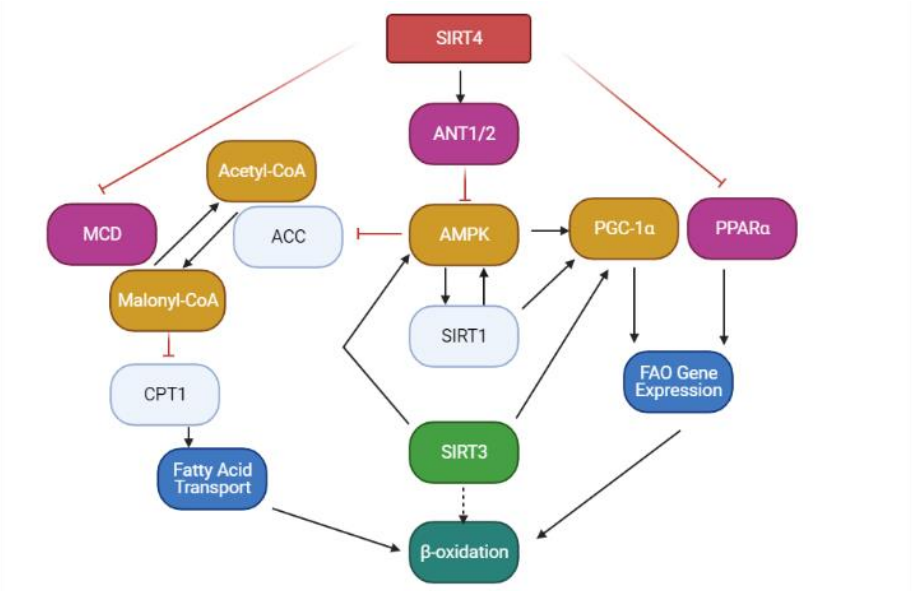

Figure 6. 1. Schematic representation of SIRT4s regulatory role on multiple cellular pathways linked to β-oxidation

Human Skeletal Muscle Myotube Characterization

Primary human skeletal muscle (HSM) myoblasts (ATCC PCS-950-010™) were subcultured in Mesenchymal Stem Cell Basal Medium (ATCC PCS-500-030™) until they reach 80-90% confluence. Myoblasts subsequently underwent differentiation using ATCC PCS-950-050™. Characterization of HSM myotubes was assessed by measurement of gene expression using RT-qPCR and morphological adaptation using microscopy techniques between day 0 and day 12 of differentiation.

Human Skeletal Muscle Myotube Morphological Adaptation

Microscopy images taken each day, using the Nikon Eclipse TS100 at 10x, of myotube differentiation, with myotube maturity indicated by elongated, large tubule structures can be seen in Figure 6.2. below. (see methods for differentiation process).

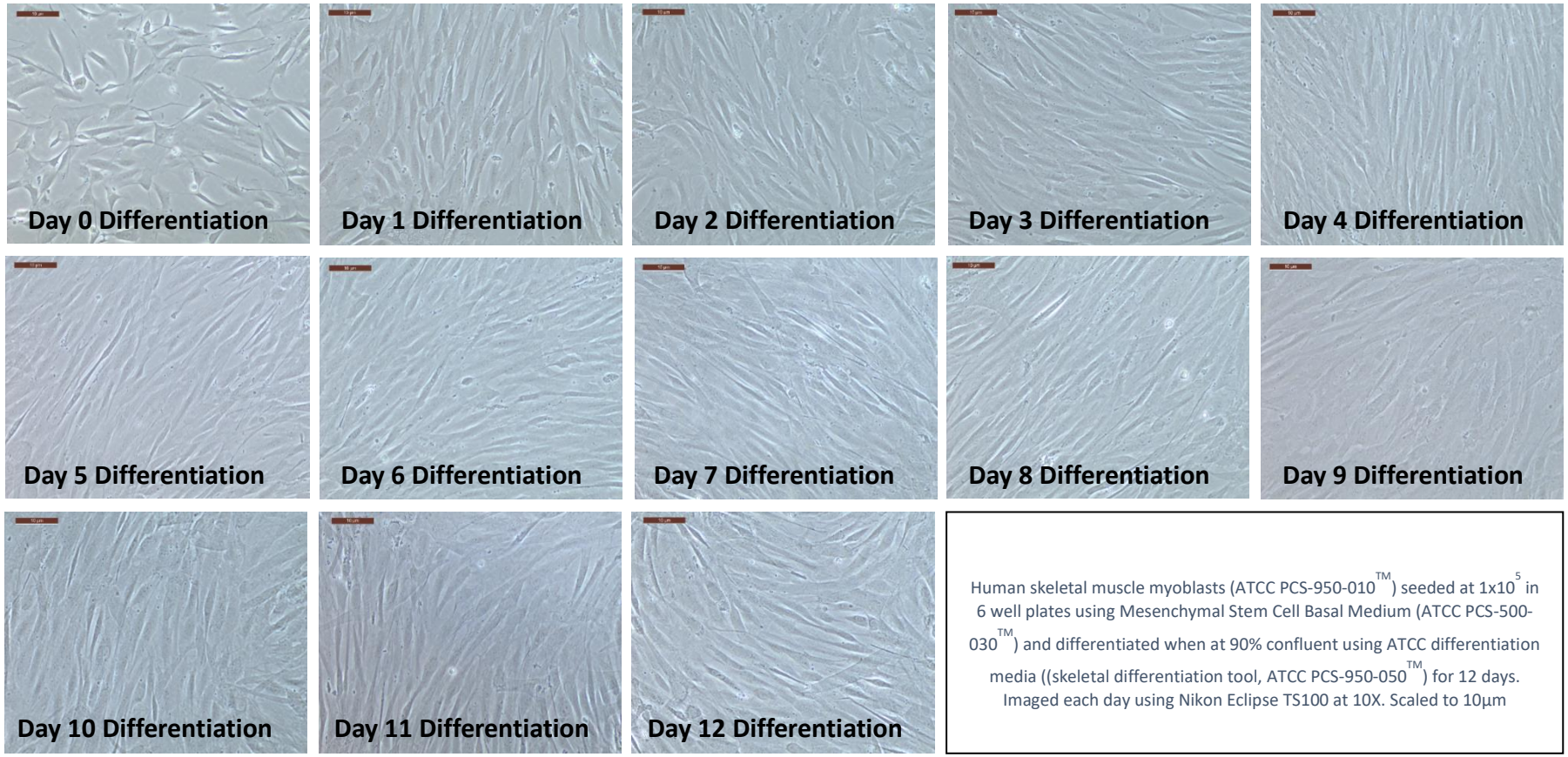

Figure 6. 2. Human skeletal muscle myoblast differentiation into myotubes over 12 days

Human Skeletal Muscle Myotube Gene Expression

Human skeletal muscle myotubes were characterized for markers of differentiation on days 0, 4, 6, 8, 10 and 12. mRNA was extracted and isolated from the cells using the referenced mRNA isolation method (referenced within methods). RT-qPCR was subsequently performed on all cDNA samples for expression of targets relating to proliferation, myoblast commitment, differentiation and maturity throughout. All targets were graphed and statistically analysed (Figure 6.3.).

There was a significant decrease in the late differentiation transcription factor Acetyl-CoA acetyltransferase 2 (ACAT2) (A) mRNA expression at day 4 in comparison to day 0 of differentiation ($p<0.05$), while there was a significant increase in Actin Alpha Cardiac Muscle 1 (ACTC1) mRNA expression at day 12 in comparison to day 0 of differentiation (B) ($p<0.05$). Creatine kinase is highly expressed in human skeletal muscle myotubes and should increase with differentiation. There was a significant increase in its mRNA expression at day 4, 6 and 12 in comparison to day 0 of differentiation (C) ($p<0.05$).

Markers of mature, enriched myotubes Myosin Heavy Chain 1 (MYH1) (D) and Myosin Heavy Chain 4 (MYH4) (E) mRNA expression significantly increased at day 4, 6 and 12 in comparison to day 0 differentiation ($p<0.05$), however there was a significant decrease in Myosin Heavy Chain 7 (MYH7) (F) mRNA expression at day 12 in comparison to day 0 ($p<0.05$). Another marker of mature myotubes, Myosin Light Chain 2 (MYL2) (G), showed no significant change in mRNA expression over 12 days of differentiation. Myoblast Determination Protein 1 (MYOD1) (H), is a myogenic transcription factor which should decrease with differentiation. We noted a significant decrease in its mRNA expression at day 4, 6 and 12 in comparison to day 0 differentiation ($p<0.05$). However, there was no significant change in Myogenin (MYOG) (I) mRNA expression, which was expected to increase over 12 days of differentiation. There was no significant change in the early transcription factor, Paired Box Protein 7 (PAX7) (J) mRNA expression over 12 days of differentiation, which would be expected to decrease with differentiation. Ras-related C3 Botulinum Toxin Substrate 1 (RAC1) mRNA (K) expression, which is expected to decrease in expression, significantly decreased at day 12 in comparison to day 0 of differentiation ($p<0.05$), while there was a significant decrease in Troponin 1 (TNN1) (L) mRNA expression at day 4 and 6 in comparison to day 0 of differentiation ($p<0.05$).

The increased expression of transcription markers of myotube maturity such as ACTC1, CKM, MYH1 and MYH4 and the significant decrease in transcription markers of myotube immaturity such as MYOD1 and RAC1 with 12 days of differentiation, positively correlated with the increase

in myotube formation as noted through our microscopy methods. Subsequently, all experimentation using these cells were conducted between days 10 and 12 of differentiation.

Human Skeletal Muscle Myotube Gene Expression over 12 Days of Differentiation

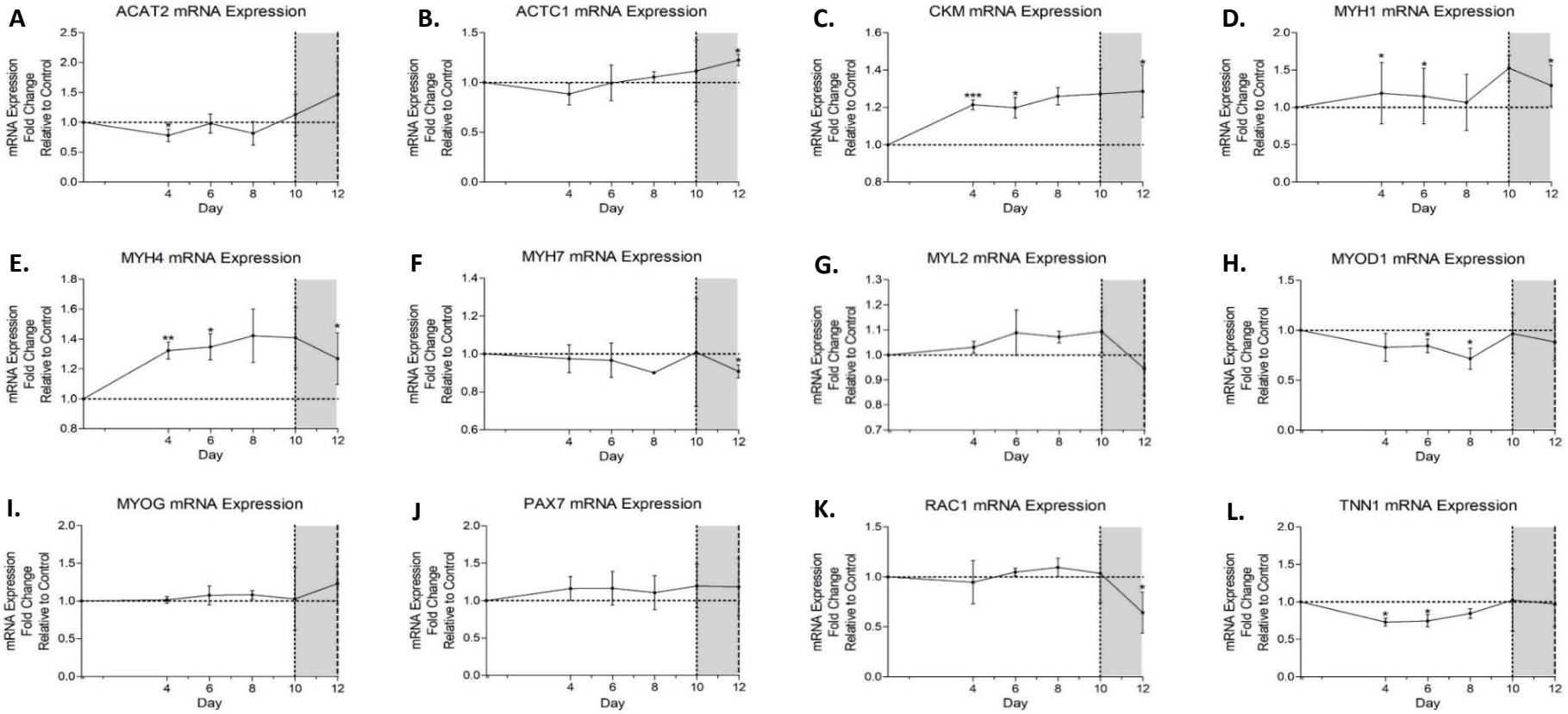

Figure 6. 3. Human skeletal muscle myotube gene expression over 12 days of differentiation

(mRNA expression of markers of commitment, proliferation, and myotube maturity throughout 12 days of differentiation. Cardiac Muscle Alpha Actin 1 (ACTC1) (A), Acetyl-CoA Acetyltransferase 2 (ACAT2) (B,) Creatine Kinase Muscle (CKM) (C), Myosin Heavy Chain 1 (MYH1) (D), Myosin Heavy Chain 4 (MYH4) (4), Myosin Heavy Chain 7 (MYH7) (F), Myosin Regulatory Light Chain 2 (MYL2) (G), Myoblast Determination Protein 1 (MYOD1) (H), Myogenin (MYOG) (I), Paired Box Protein 7 (PAX7) (J), Ras-related C3 Botulinum Toxin Substrate 1 (RAC1) (K) and Troponin I Type 1 (TNN1) (L) mRNA expression between day 0 and 12 (n=3). All data is relative to day 0 differentiation and represented as a fold change. Data are expressed as mean ± SD, *significantly different from day 0, p<0.05, **significantly different from day 0, p<0.005, ***significantly different from day 0, p<0.0005)

SIRT4 siRNA Knockdown Human Skeletal Muscle Myotubes

Following optimal characterization of human skeletal muscle myotubes, cells where differentiated for 10-12 days before knockdown SIRT4 gene and protein expression. RNA interference (RNAi) using small interfering RNAs (siRNAs) was carried out to silence specific genes that encode for SIRT4.

SIRT4 siRNA Knockdown Optimization

Optimal SIRT4 siRNA Transfection Reagent

Four separate transfection reagents were assessed to optimise siRNA SIRT4 knockdown in primary human skeletal muscle myotubes at day 10 of differentiation, MirusIT-TKO (Mirus, MIR 2154), DharmaFECT 1 (Dharmacon, T-2001-S), DharmaFECT 3 (Dharmacon, T-2003-S) and Lipofectamine 3000 (Invitrogen, L3000001). Each transfection reagent was assessed at three separate concentrations (2µl, 4µl and 6µl per 50µl Opti-MEM) in all conditions. 25nM of siRNA silencer select s23764 (siRNA 1), s23765 (siRNA 2) and silencer select siRNA negative control (4390843) (siRNA Scramble) were used for all transfection reagent conditions. The optimal transfection reagent to knockdown SIRT4 gene expression was confirmed to be 6µl of Lipofectamine 3000 (Invitrogen, L3000001) by RT-qPCR analysis (complete analysis in Appendix Section J).

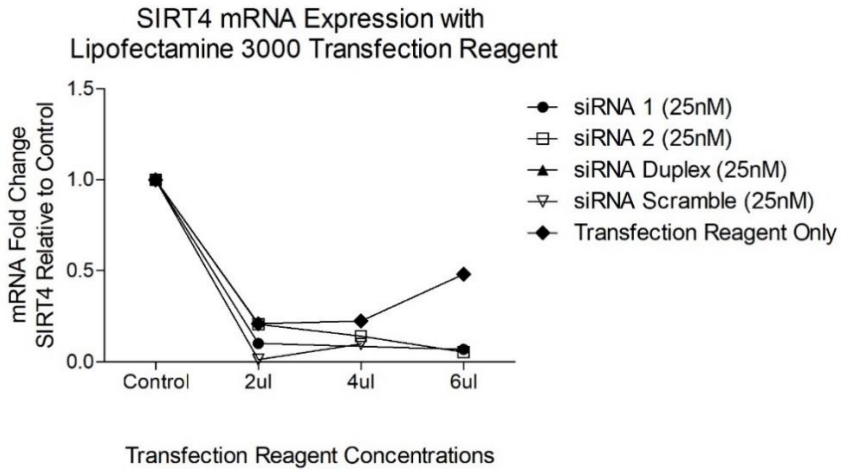

Figure 6. 4. SIRT4 mRNA expression with different concentrations of Lipofectamine 3000

(Total SIRT4 mRNA expression in HSM myotubes following 2µl, 4µl & 6µl of lipofectamine 3000 transfection reagent quantified by RT-qPCR (*n*=1). Gene expression was normalised against GAPdh mRNA expression of same sample)

Optimal SIRT4 siRNA Concentration

Four different concentrations, 25nM, 50nM, 75nM and 100nM, of siRNA silencer select were made. These four concentrations were tested on the siRNA silencer select s23764 (siRNA 1), s23765 (siRNA 2) and silencer select siRNA negative control (4390843) (siRNA Scramble). All were incubated with 6µl lipofectamine 3000 and reduced serum medium (Opti-MEM). The optimal SIRT4 siRNA concentration to knockdown SIRT4 gene expression was confirmed to be 75nM for a duplex of siRNA 1 (s23764) and 2 (s23765) by RT-qPCR analysis (complete analysis in Appendix Section L).

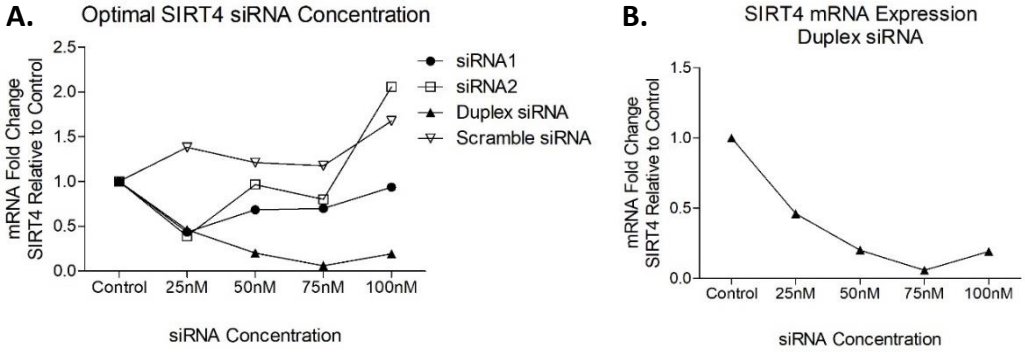

Figure 6. 5. SIRT4 mRNA expression with different concentrations of SIRT4 siRNA

(Total SIRT4 mRNA expression in HSM myotubes following incubation with 25nM, 50nM, 75nM and 100nM siRNA 1, siRNA 2, duplex siRNA and Scramble siRNA (A) duplex siRNA 1 & 2 (B) with 6µl lipofectamine 3000 transfection reagent quantified by RT- qPCR (*n*=1). Gene expression was normalised against GAPdh mRNA expression of same sample)

Optimal SIRT4 siRNA Takedown Time

Following determination of the optimal transfection reagent and concentration, the optimal incubation time to knockdown SIRT4 mRNA expression was assessed at 0 minutes, 60 minutes, 24 hours, 48 hours and 72 hours. SIRT4 mRNA expression was quantified through RT-qPCR. Results show that using a duplex siRNA (siRNA 1 and 2) at 75nM, for 24 hours incubated with 6µl Lipofectamine 3000 per well was the optimal method to knockdown SIRT4 mRNA expression in primary HSM myotubes differentiated for 10 days.

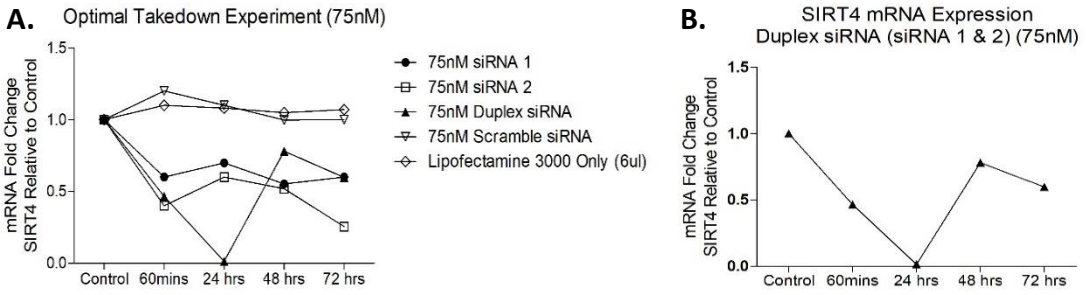

Figure 6. 6. Optimal time of incubation of SIRT4 siRNA to knockdown SIRT4

(Total SIRT4 mRNA expression in HSM myotubes following incubation with 75nM siRNA 1, 75nM siRNA 2, 75nM duplex siRNA, 75nM Scramble siRNA and lipofectamine 3000 only (A) and 75nM duplex siRNA 1 & 2 (B) with 6µl lipofectamine 3000 transfection reagent for 0 mins, 60mins, 24 hours, 48 hours and 72 hours quantified by RT-qPCR (*n*=1). Gene expression was normalised against GAPdh mRNA expression of same sample)

Morphological Impact of SIRT4 knockdown on Human Skeletal Muscle Myotubes

Human skeletal muscle myotubes differentiated for 10-12 days with 75nM Duplex SIRT4 siRNA and Lipofectamine 3000 applied for 24 hours were also assessed for the morphological impact this application can have on cell morphology. Figure 6.7 represents the impact this technique had on cell morphology (A-C) but also illustrates how a further 24 hours' incubation of cells in differentiation media leads to a reestablishment of tubule structures (D-F).

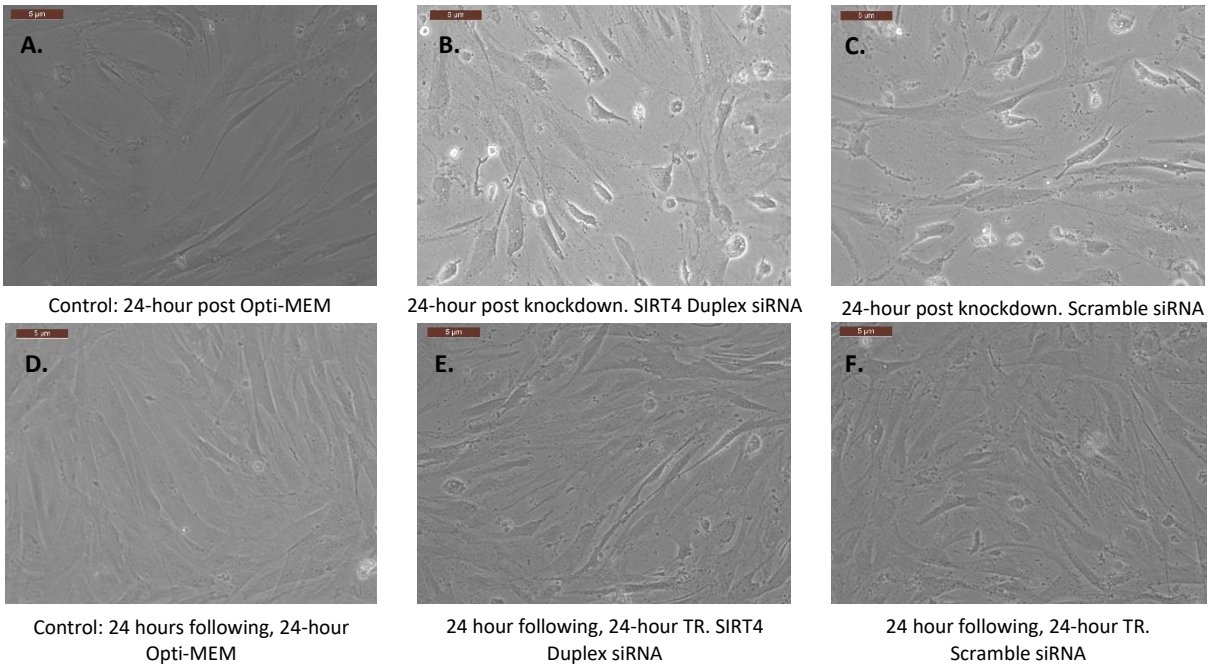

Figure 6. 7. Morphological impact of siRNA knockdown on human skeletal muscle myotubes

(Human skeletal muscle myotubes appear to contract in on themselves with siRNA transfection application. However, they appear to return to phenotypic normality when reagent is removed following transfection)

Sirtuin 4

SIRT4, the target of interest was analysed for mRNA expression using RT-qPCR and protein expression using western blot. We observed a significant decrease in mRNA (91.96%) and protein expression (72.58%) of Sirtuin 4 (SIRT4) with SIRT4 Duplex siRNA (75nM) in comparison to the control (p<0.005) and the Scramble siRNA sample (p<0.05).

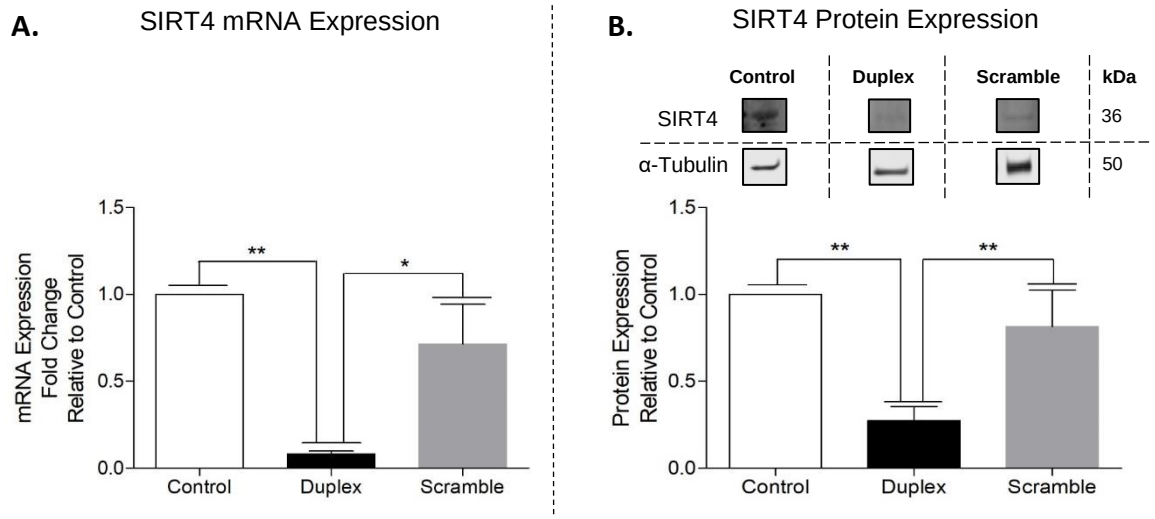

Figure 6. 8. Transcriptional and translational expression of SIRT4 following SIRT4 knockdown

(Total SIRT4 mRNA expression (A) in control, SIRT4 Duplex (75nM) siRNA and Scramble (75nM) siRNA HSM myotubes quantified by RT-qPCR (n=3). Total SIRT4 protein expression (B) in control and SIRT4 Duplex (75nM) siRNA HSM myotubes quantified by western blot (n=3). Gene expression was normalised against GAPdh mRNA expression of same sample. Protein expression was normalised against Alpha-Tubulin expression of same sample. Blots representative of all samples. Data are expressed as mean ±SD. ** significant effect of SIRT4 knockdown, p<0.005, *significant effect of SIRT4 knockdown, p<0.05)

Transcriptional and Translational Analysis of Targets Relating to SIRT4

Gene and protein expression of targets relating to mitochondrial morphology and substrate metabolism were analysed using RT-qPCR and Western Blot in SIRT4 knockdown myotubes. All transcripts and proteins analysed were normalised to a housekeeping transcript/protein (GAPdh/Alpha-Tubulin) and subsequently presented relative to the control sample. Protein expression of scramble are not represented here, however all densitometry for SIRT4 knockdown, including protein expression of scramble and analysis relative to scramble can be found in the Appendix (Section L). All mRNA analysis relative to scramble can be found in the Appendix (Section K).

Expression of Markers Associated with Mitochondrial Fusion

OPA1

There was no significant change in the mRNA expression of OPA1 following SIRT4 siRNA knockdown (Figure 6.8), however there was a significant increase in OPA1 protein expression with SIRT4 siRNA knockdown (p<0.05). There was also a significant increase in both L-OPA1 and s-OPA1 protein expression with SIRT4 siRNA in comparison to the control (p<0.05). These changes signify that SIRT4 knockout significantly increases OPA1 expression, indicative of an increase in inner mitochondrial membrane mitochondrial fusion.

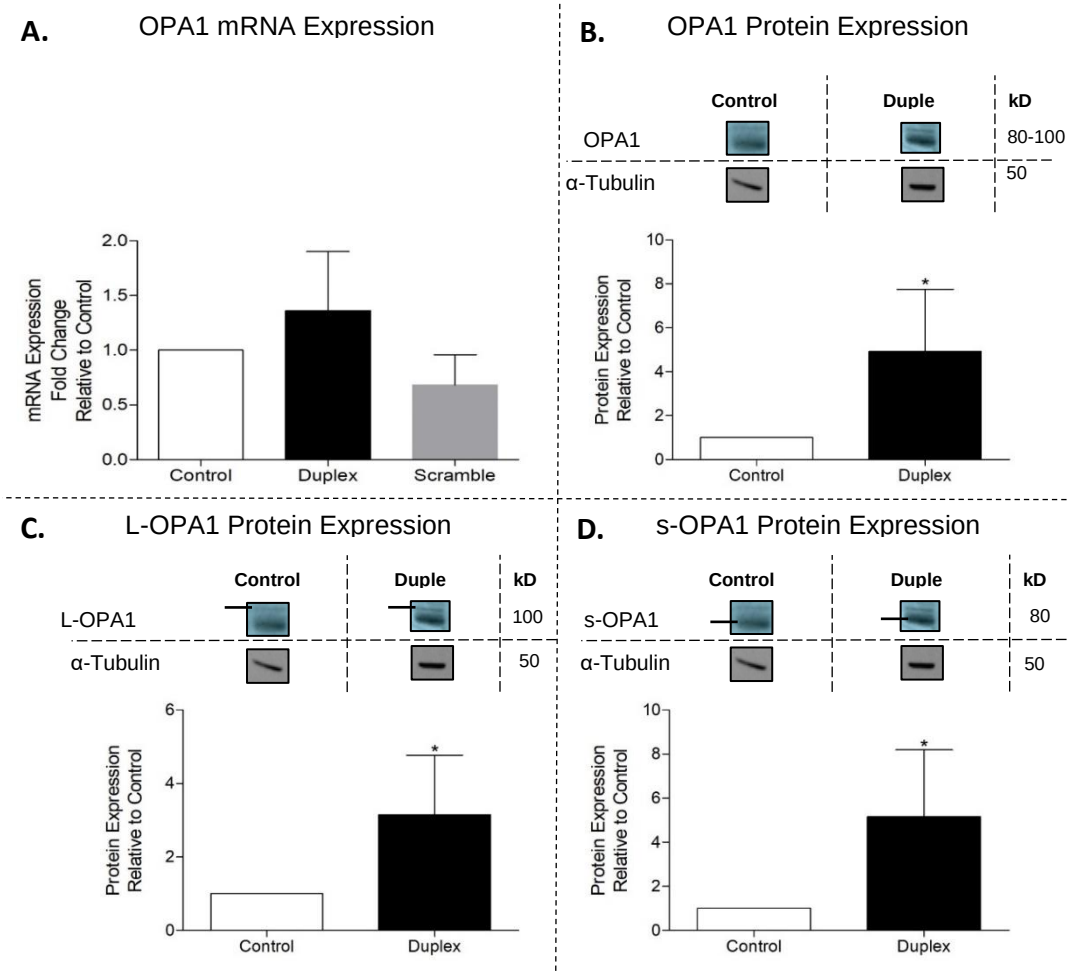

Figure 6. 9. Transcriptional and translational expression of OPA1 following SIRT4 knockdown

(Total OPA1 mRNA expression (A) in control, SIRT4 Duplex (75nM) siRNA and Scramble (75nM) siRNA HSM myotubes quantified by RT-qPCR (n=3), total OPA1 (B), L-OPA1 (C), s-OPA1 (D) protein expression in control and SIRT4 Duplex (75nM) siRNA HSM myotubes quantified by western blot (n=4). Gene expression was normalised against GAPdh mRNA expression of same sample. Protein expression was normalised against Alpha-Tubulin expression of same sample. Blots representative of all samples. Data are expressed as mean ±SD, *significant effect of SIRT4 knockdown, p<0.05)

Other markers of Mitochondrial Fusion

Mfn1 mRNA expression (C) significantly increased in SIRT4 knockdown cells (Figure 6.9) and there was a trend (p=0.052) toward increased protein expression (A). There was no significant change in Mfn2 protein (B) or mRNA expression (D) and no change in OMA1 (E) or YME1L (F) mRNA expression following SIRT4 siRNA knockdown. These results suggest SIRT4 knockdown results in an increase in targets relating to mitochondrial fusion, particularly Mfn1, suggesting an increase in outer mitochondrial membrane fusion with SIRT4 knockdown.

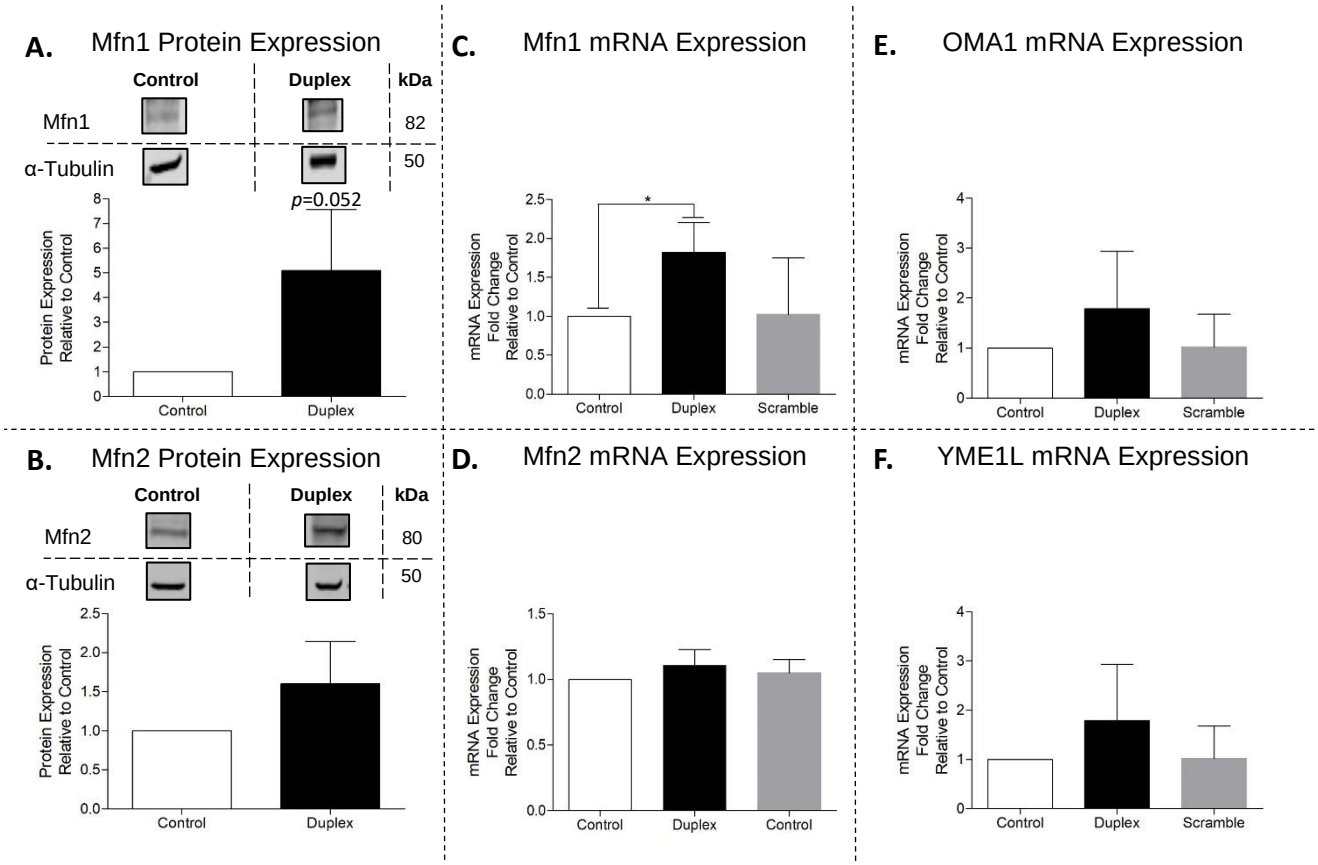

Figure 6. 10. Transcriptional and translational expression of other regulators of mitochondrial fusion following SIRT4 knockdown

(Total Mfn1 (A) and Mfn2 (B) protein expression in control and SIRT4 Duplex (75nM) siRNA HSM myotubes quantified by western blot (n=3). Total Mfn1 (C), Mfn2 (D), OMA1 (E) and YME1L (F) mRNA expression in control, SIRT4 Duplex (75nM) siRNA and Scramble siRNA (75nM) HSM myotubes quantified by RT-qPCR (n=4). Gene expression was normalised against GAPdh mRNA expression of same sample. Protein expression was normalised against Alpha-Tubulin expression of same sample. Blots representative of all samples. Data are expressed as mean ±SD, *significant effect of SIRT4 knockdown p<0.05)

Expression of Markers Associated with Mitochondrial Fission

There was no significant change in the mRNA (B) or protein expression of Drp1 (A) following SIRT4 siRNA knockdown (Figure 6.10). There was also no significant change in Fis1 (C) or MiD51 (F) mRNA expression following knockdown. mRNA expression of Mff (D) significantly increased in comparison to the control and scramble (p<0.05), while MiD49 mRNA (E) significantly increased in comparison to the control following SIRT4 knockdown (p<0.05). These results suggest that although the main mediators of mitochondrial fission, such as Drp1 and Fis1, didn't change following SIRT4 knockdown, other mediators of mitochondrial fission, Mff and MiD49 increased in expression.

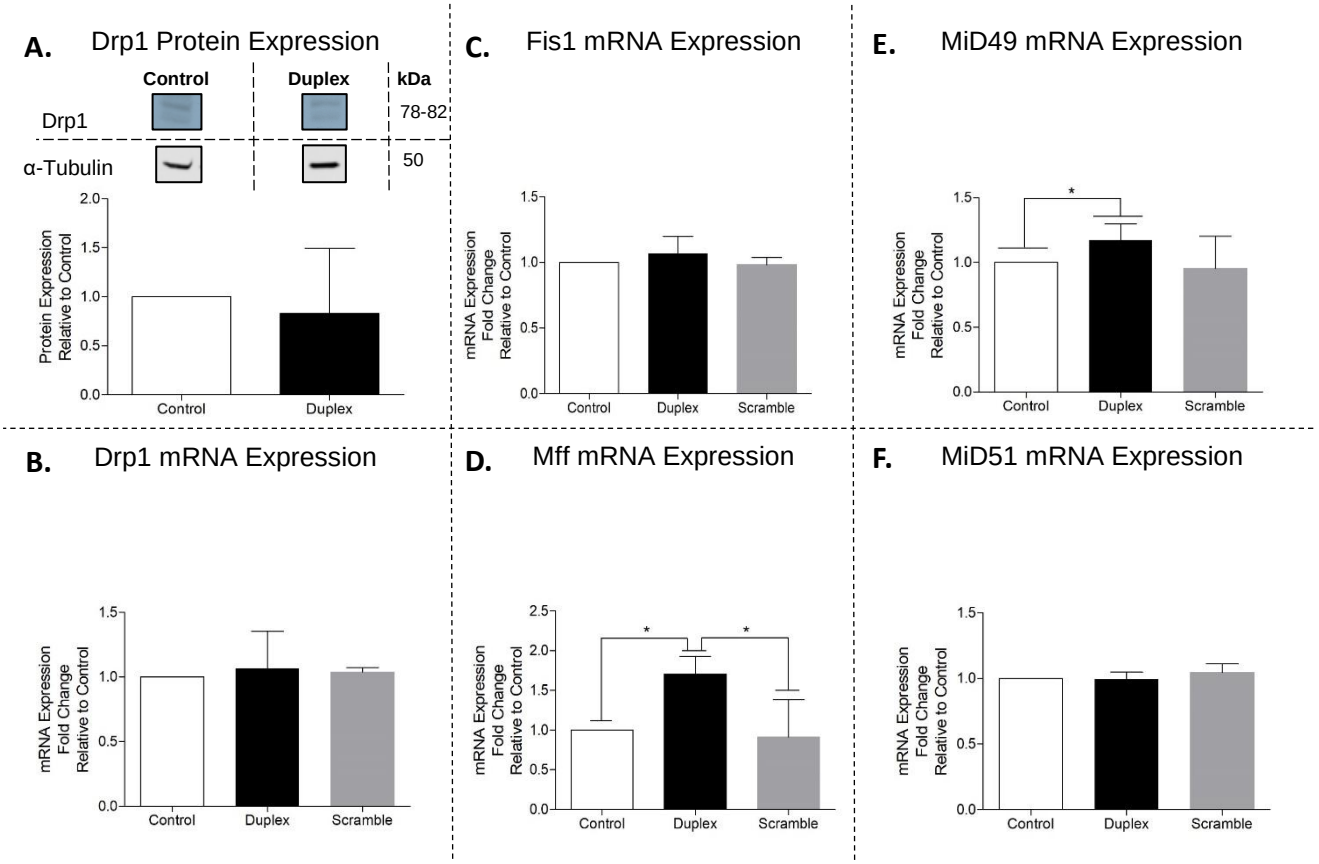

Figure 6. 11. Transcriptional and translational expression of regulators of mitochondrial fission following SIRT4 knockdown

(Total Drp1 protein expression (A) in control and SIRT4 Duplex (75nM) siRNA HSM myotubes quantified by western blot (n=3). Total Drp1 (B), Fis1 (C), Mff (D), MiD49 (E) and MiD51 (F) mRNA expression in control, SIRT4 Duplex (75nM) siRNA and Scramble (75nM) siRNA HSM myotubes quantified by RT-qPCR (n=4). Protein expression was normalised against Alpha-Tubulin expression of same sample. Gene expression was normalised against GAPdh mRNA expression of same sample. Blots representative of all samples. Data are expressed as mean ±SD, *significant effect of SIRT4 knockdown p<0.05)

Mitochondrial Fusion-Fission Balance

In order to assess for the balance between mitochondrial fusion and fission with SIRT4 siRNA knockdown, protein expression of mitochondrial fusion marker OPA1 was expressed against the mitochondrial fission Drp1 in both the control and the SIRT4 siRNA knockdown groups. Analysis illustrates a significant increase in OPA1:Drp1 ratio in the SIRT4 siRNA knockdown in comparison to the control cells (p<0.05), indicating a possible increase in OPA1 mediated mitochondrial fusion due to the significant increase in OPA1 protein expression and no change in Drp1 expression in the SIRT4 siRNA knockdown cells.

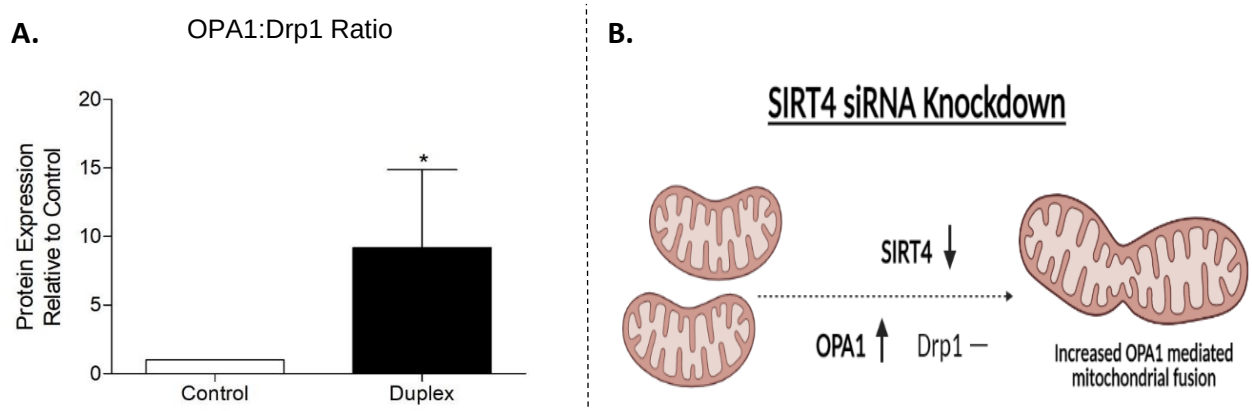

Figure 6. 12. OPA1:Drp1 Ratio following SIRT4 knockdown

(OPA1:Drp1 protein expression in control and SIRT4 Duplex (75nM) siRNA HSM myotubes quantified by western blot (A). OPA1, optic atrophy 1 was controlled against Drp1, dynamin related protein 1 protein expression (n=3). Both OPA1 and Drp1 protein expression were firstly normalised to their respective loading control (GAPdh). Data are expressed as mean ±SD, * significant effect of time, p<0.05. (B) Schematic representation of SIRT4 knockdown on mitochondrial tabulation based on OPA1:Drp1 ratio)

Expression of Adenine Nucleotide Translocators

There was a significant decrease in ANT1 (A) protein expression (p<0.0005) in the SIRT4 siRNA knockdown cells (Figure 6.12) but there was no significant change in ANT1 (B) or ANT2 (C) mRNA expression. These highlight the role SIRT4 has on ADP-ATP translocation across the inner mitochondrial membrane.

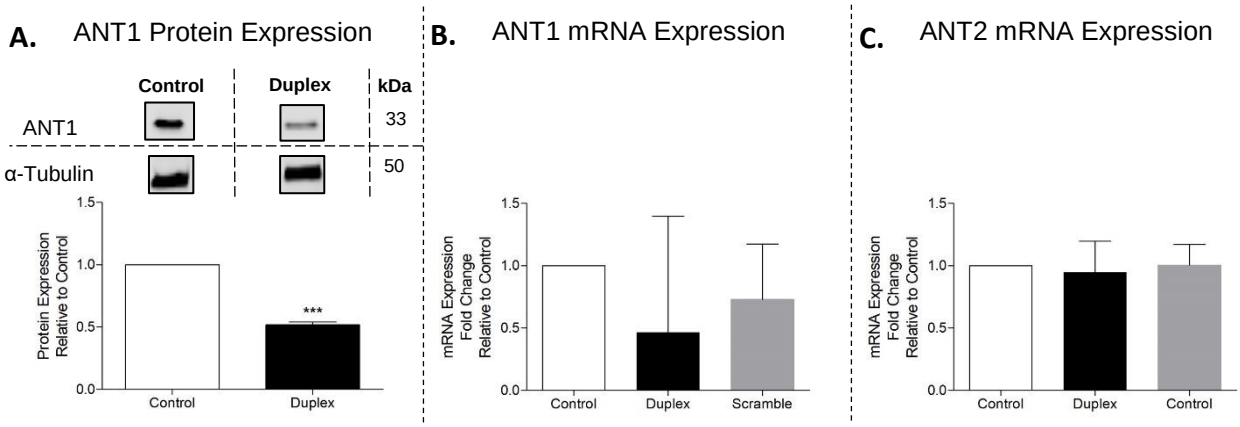

Figure 6. 13. Transcriptional and translational expression of ANT following SIRT4 knockdown

(Total ANT1 protein expression (A) in control and SIRT4 Duplex (75nM) siRNA HSM myotubes quantified by western blot (n=3). Total ANT1 (B) and ANT2 (C) mRNA expression in control, SIRT4 Duplex (75nM) siRNA and Scramble (75nM) siRNA HSM myotubes quantified by RT-qPCR (n=4). Protein expression was normalised against Alpha-Tubulin expression of same sample. Gene expression was normalised against GAPdh mRNA expression of same sample. Blots representative of all samples. Data are expressed as mean ±SD, ***significant effect of SIRT4 knockdown, p<0.0005)

Expression of Sirtuin Targets

There was a significant increase in SIRT1 protein expression (A) and a tendency for mRNA expression (p=0.054) compared to the control cells (though significantly greater than Scramble) following SIRT4 siRNA knockdown (Figure 6.13). There was no significant change in SIRT3 (B) or SIRT5 (D) mRNA expression following knockdown. However, mRNA expression of SIRT6 (E) significantly increased in comparison to the control (p<0.05) and the Scramble siRNA (p<0.005).

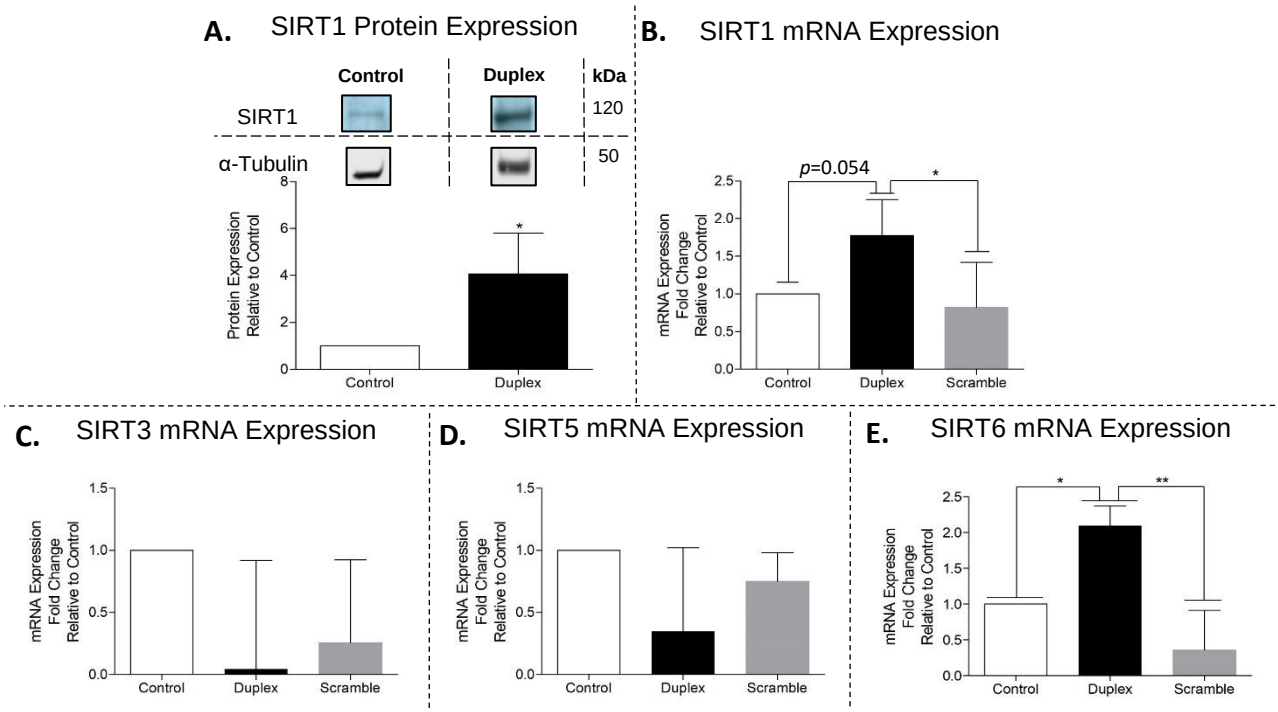

Figure 6. 14. Transcriptional and translational expression of Sirtuin members following SIRT4 knockdown

(Total SIRT1 protein expression (A) in control and SIRT4 Duplex (75nM) siRNA HSM myotubes quantified by western blot (n=4). Total SIRT1 (B), SIRT3 (C), SIRT5 (D) & SIRT6 (E) mRNA expression in control, SIRT4 Duplex (75nM) siRNA and Scramble (75nM) siRNA HSM myotubes quantified by RT-qPCR (n=4). Protein expression was normalised against Alpha-Tubulin expression of same sample. Gene expression was normalised against GAPdh mRNA expression of same sample. Blots representative of all samples. Data are expressed as mean ±SD. ** significant effect of SIRT4 knockdown, p<0.005, *significant effect of SIRT4 knockdown, p<0.05)

Expression of Markers Associated with Carbohydrate Metabolism

There was a significant increase in the protein expression of hexokinase II (A) and pyruvate dehydrogenase (B) following SIRT4 siRNA knockdown (p<0.05) but no significant change in PDHα (C) or PDHβ (D) mRNA expression, indicating an increase in Acetyl-CoA derived from glycolysis (Figure 6.14).

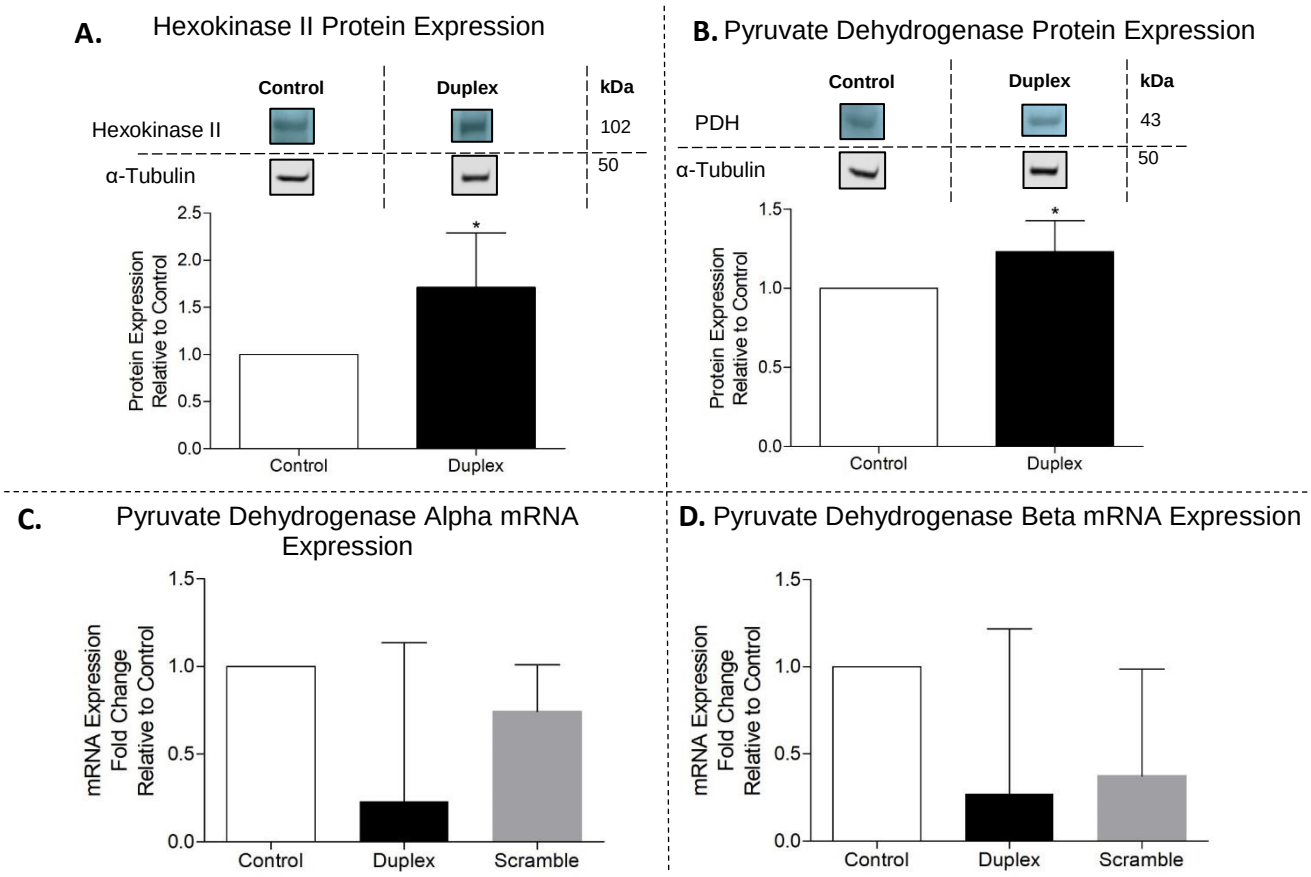

Figure 6. 15. Transcriptional and translational expression of regulators of carbohydrate metabolism following SIRT4 knockdown

(Total Hexokinase II (A) Pyruvate Dehydrogenase (B) protein expression in control and SIRT4 Duplex (75nM) siRNA HSM myotubes quantified by western blot (n=4). Total Pyruvate Dehydrogenase α (A) and Pyruvate Dehydrogenase β (B) mRNA expression in control, SIRT4 Duplex (75nM) siRNA and Scramble (75nM) siRNA HSM myotubes quantified by RT-qPCR (n=4). Protein expression was normalised against α-tubulin protein expression of same sample. Gene expression was normalised against GAPdh mRNA expression of same sample. Blots representative of all samples. Data are expressed as mean ±SD. * significant effect of SIRT4 knockdown, p<0.05)

SIRT4 as a Regulator of AMPK, ACC, CPT1b and Subsequent β-Oxidation

In order to assess to see if SIRT4 knockdown results in alterations to substrate metabolism, particularly that relating to fatty acid metabolism, mRNA and protein expression of AMP-activated protein kinase (AMPK) was analysed following SIRT4 siRNA knockdown. There was no significant change in AMPKα1 (A) or AMPKα2 (B) mRNA expression following SIRT4 siRNA knockdown (Figure 6.15). There was no significant change in pAMPK (C) with SIRT4 siRNA knockdown. Phosphorylation of Acetyl-CoA (pACC) is used as a surrogate for AMPK activity and we found a significant increase in pACC (D) following SIRT4 knockdown (p<0.05) signifying a possible increase in β-oxidation.

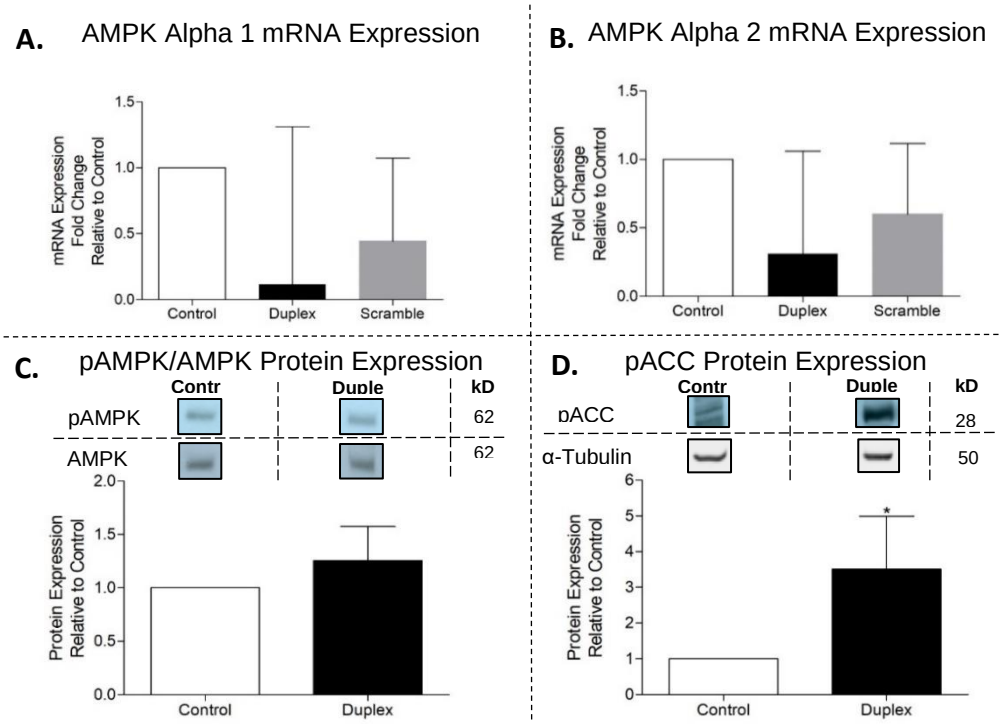

Figure 6. 16. Transcriptional and translational expression of regulators of AMPK following SIRT4 knockdown

(AMPKα1 (A) and AMPKα2 (B) mRNA expression in control, SIRT4 Duplex (75nM) siRNA and Scramble (75nM) siRNA HSM myotubes (n=4). pAMPK protein expression relative to AMPK (C) and pACC protein expression (D) relative to α-tubulin in control and SIRT4 Duplex (75nM) siRNA HSM myotubes (n=3). Gene expression was normalised against GAPdh mRNA expression of same sample. Blots representative of all samples. Data are expressed as mean ±SD, *significant effect of SIRT4 knockdown, p<0.05)

SIRT4 Regulation of Malonyl-CoA Decarboxylase, PGC-1α & CPT1b

Given the increased expression of pACC we wanted to see if SIRT4 had a significant effect on the expression of proteins associated with beta-oxidation and free fatty acid transport into the mitochondria (Figure 6.16). There was no change in Malonyl-CoA decarboxylase mRNA expression (A) following SIRT4 knockdown but PGC-1α mRNA (B) and protein (C) expression significantly increased in comparison to the control (p<0.05). CPT1b (D) protein expression also significantly increased following SIRT4 siRNA knockdown (p<0.05).

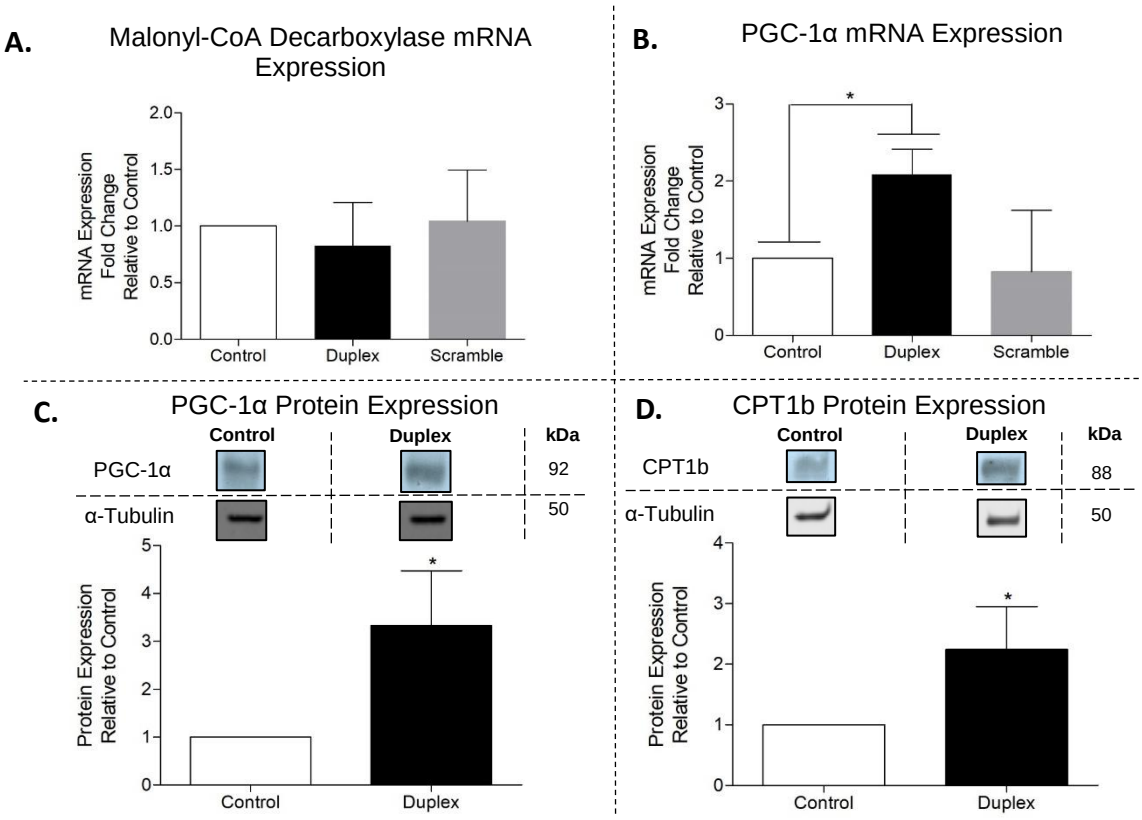

Figure 6. 17. Transcriptional and translational expression of regulators of β-oxidation following SIRT4 knockdown

(Malonyl-CoA Decarboxylase (A) and PGC-1α (B) mRNA expression in control, SIRT4 Duplex (75nM) siRNA and Scramble (75nM) siRNA HSM myotubes quantified by RT-qPCR (n=4). PGC-1α (C) and CPT1b (D) protein expression in control and SIRT4 Duplex (75nM) siRNA HSM myotubes quantified by western blot (n=3). Protein expression was normalised against α-tubulin protein expression of same sample. Gene expression was normalised against GAPdh mRNA expression of same sample. Blots representative of all samples. Data are expressed as mean ±SD, *significant effect of SIRT4 knockdown, p<0.05)

Expression of Markers Associated with Mitophagy

There was no significant change in the mRNA expression of PTEN-induced kinase 1 (PINK1) (A) and Parkin (B) with SIRT4 siRNA knockdown (Figure 6.17).

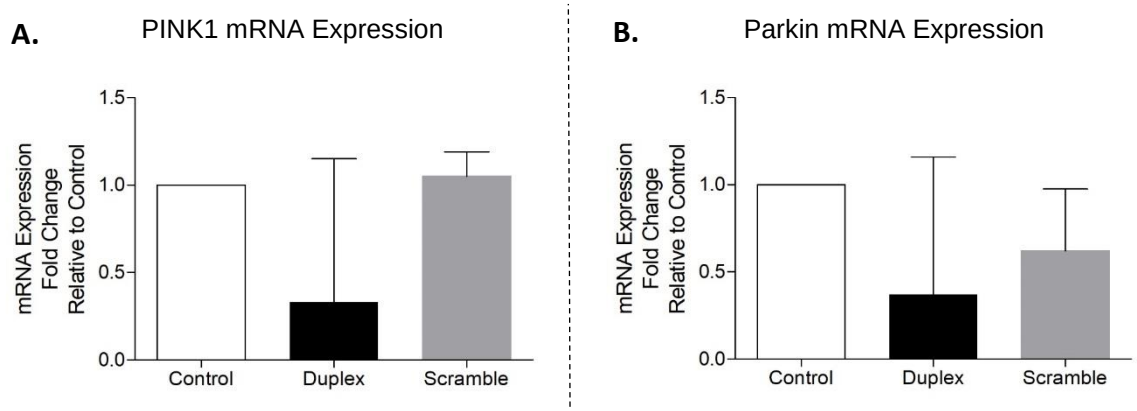

Figure 6. 18. Transcriptional expression of regulators of mitophagy following SIRT4 knockdown

(Total PINK1 (A) and Parkin (B) mRNA expression in control, SIRT4 Duplex (75nM) siRNA and Scramble (75nM) siRNA HSM myotubes quantified by RT-qPCR (*n*=4). Gene expression was normalised against GAPdh mRNA expression of same sample. Data are expressed as mean ±SD)

Expression of other Markers Relating to Cellular Metabolism

There was no significant change in protein (A) or mRNA (B) expression of mechanistic target of rapamycin (mTOR) following SIRT4 knockdown (Figure 6.18). Cyclic ADP ribose hydrolase (CD38) mRNA expression (A) did not change but there was a significant decrease in Insulin-like Growth Factor-1 (IGF-1) (B) mRNA expression in comparison to the control (p<0.05).

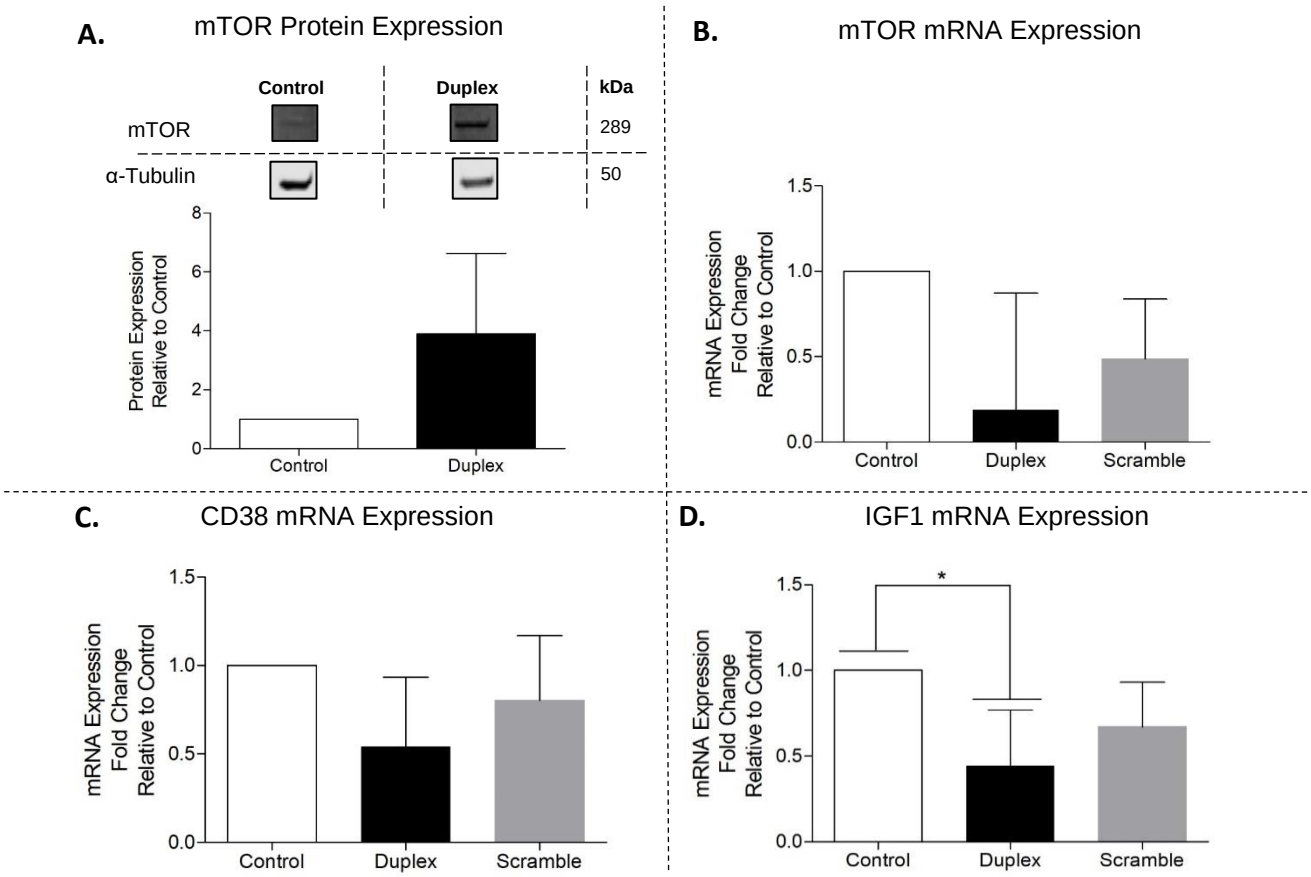

Figure 6. 19. Transcriptional and translational expression of other markers relating to cellular metbaolism following SIRT4 knockdown

(Total mTOR protein expression (B) in control and SIRT4 Duplex (75nM) siRNA HSM myotubes quantified by western blot (n=4). Total mTOR (A), CD38 (C) and IGF1 (D) mRNA expression in control, SIRT4 Duplex (75nM) siRNA and Scramble (75nM) siRNA HSM myotubes quantified by RT-qPCR (n=3). Protein expression was normalised against α-tubulin expression of same sample. Gene expression was normalised against GAPdh mRNA expression of same sample. Blots representative of all samples. Data are expressed as mean ±SD. *significant effect of SIRT4 knockdown, p<0.05)

Summary of Transcriptional & Translational Markers Measured following SIRT4 siRNA knockdown

The knockdown of SIRT4 resulted in significant transcriptional and translational changes to human skeletal muscle myotubes. In particular, SIRT4 knockdown appeared to alter markers of ADP-ATP translocation, mitochondrial dynamics and the metabolism of free fatty acids. SIRT4 knockout significantly decreased ANT1 expression, possibly decreasing mitochondrial leak respiration which could be linked to the increased expression of targets relating to the metabolism of free fatty acids such as pACC, SIRT1, PGC-1α and CPT1b. Interestingly, knockdown also resulted in a significant increase in OPA1 expression. Given we noted significant decreases in OPA1 expression following both 21 and 60 days bed rest, SIRT4 may not only regulate the metabolism of free fatty acids but also mitochondrial fusion. All changes are summarised in Table 6.1. below.

Table 6. 1. Summary of all transcriptional and translational markers measured following SIRT4 siRNA knockdown

Target Measured	*Protein/mRNA*	*Direction of Change*	*p<0.05*
SIRT4	Protein & mRNA	↓	**
OPA1	Protein & mRNA	↑	*
L-OPA1	Protein	↑	*
s-OPA1	Protein	↑	*
Mfn1	Protein & mRNA	↑	*
Mfn2	Protein & mRNA	-	*p*>0.05
OMA1	mRNA	-	*p*>0.05
YME1L	mRNA	-	*p*>0.05
Drp1	Protein & mRNA	-	*p*>0.05
Fis1	mRNA	-	*p*>0.05
Mff	mRNA	↑	*
MiD49	mRNA	↑	*
MiD51	mRNA	-	*p*>0.05
OPA1:Drp1 Ratio	Protein	↑	*
ANT1	Protein & mRNA	↓	***
ANT2	mRNA	-	*p*>0.05
SIRT1	Protein & mRNA	↑	*
SIRT3	mRNA	-	*p*>0.05
SIRT5	mRNA	-	*p*>0.05
SIRT6	mRNA	↑	*
Hexokinase II	Protein	↑	*
Pyruvate Dehydrogenase	Protein	-	*p*>0.05
PDHα	mRNA	-	*p*>0.05
PDHβ	mRNA	-	*p*>0.05
AMPKα1	mRNA	-	*p*>0.05
AMPKα2	mRNA	-	*p*>0.05
pAMPK:AMPK Ratio	Protein	-	*p*>0.05
pACC	Protein	↑	*
Malonyl-CoA Decarboxylase	mRNA	-	*p*>0.05
PGC-1α	Protein & mRNA	↑	*
CPT1b	Protein	↑	*
PINK1	mRNA	-	*p*>0.05
Parkin	mRNA	-	*p*>0.05
mTOR	Protein & mRNA	-	*p*>0.05
CD38	mRNA	-	*p*>0.05
IGF1	mRNA	↓	*

High-Resolution Respirometry

Mitochondrial function was assessed using the Oroboros Oxygraph O2k High-Resolution Respirometer (Figure 6.19). Due to the possible role SIRT4 may have on both mitochondrial morphology, but particularly beta-oxidation, following SIRT4 siRNA knockdown, HSM myotubes were extracted and assessed for their respiration stimulated by fatty acid oxidation (β-oxidation) using a fatty acid (FA) Substrate-Uncoupler-Inhibitor Titration (SUIT) protocol. LEAK respiration, as measured by the addition of palmitoylcarnitine and malate, was significantly decreased in the SIRT4 siRNA knockdown samples (p<0.05) (n=4). This may be associated with the decrease in ANT1 protein expression [263]. There was a significant increase in ADP-stimulated OXPHOS (p<0.05) indicating an enhanced rate of β-oxidation. Additional measures assessed within this SUIT protocol can be found within the Appendix (Section M).

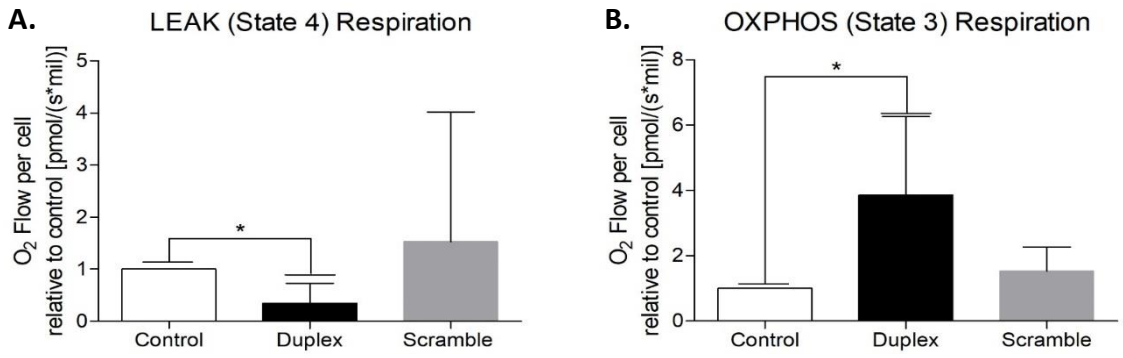

Figure 6. 20. LEAK & OXPHOS respiration following SIRT4 knockdown

(LEAK (A) and OXPHOS (B) respiration in control, SIRT4 Duplex (75nM) and Scramble (75nM) siRNA HSM myotubes quantified by HRR (n=4). Oxygen flow was normalised to cell number of the same sample. Data are expressed as mean ±SD, *significant effect of SIRT4 knockdown, p<0.05)

Confocal Microscopy

Following knockdown, HSM myotubes were probed for mitochondrial content using the MitoTraker GM (200nM) fluorescence and counter stained for nuclei content using NucBlue Live Stain (Figure 6.20). In the SIRT4 siRNA knockdown cells there is a greater amount of tubular mitochondria, particularly in comparison to the Scramble siRNA. These results support the role SIRT4 may have on mitochondrial morphology, and OPA1 in particular.

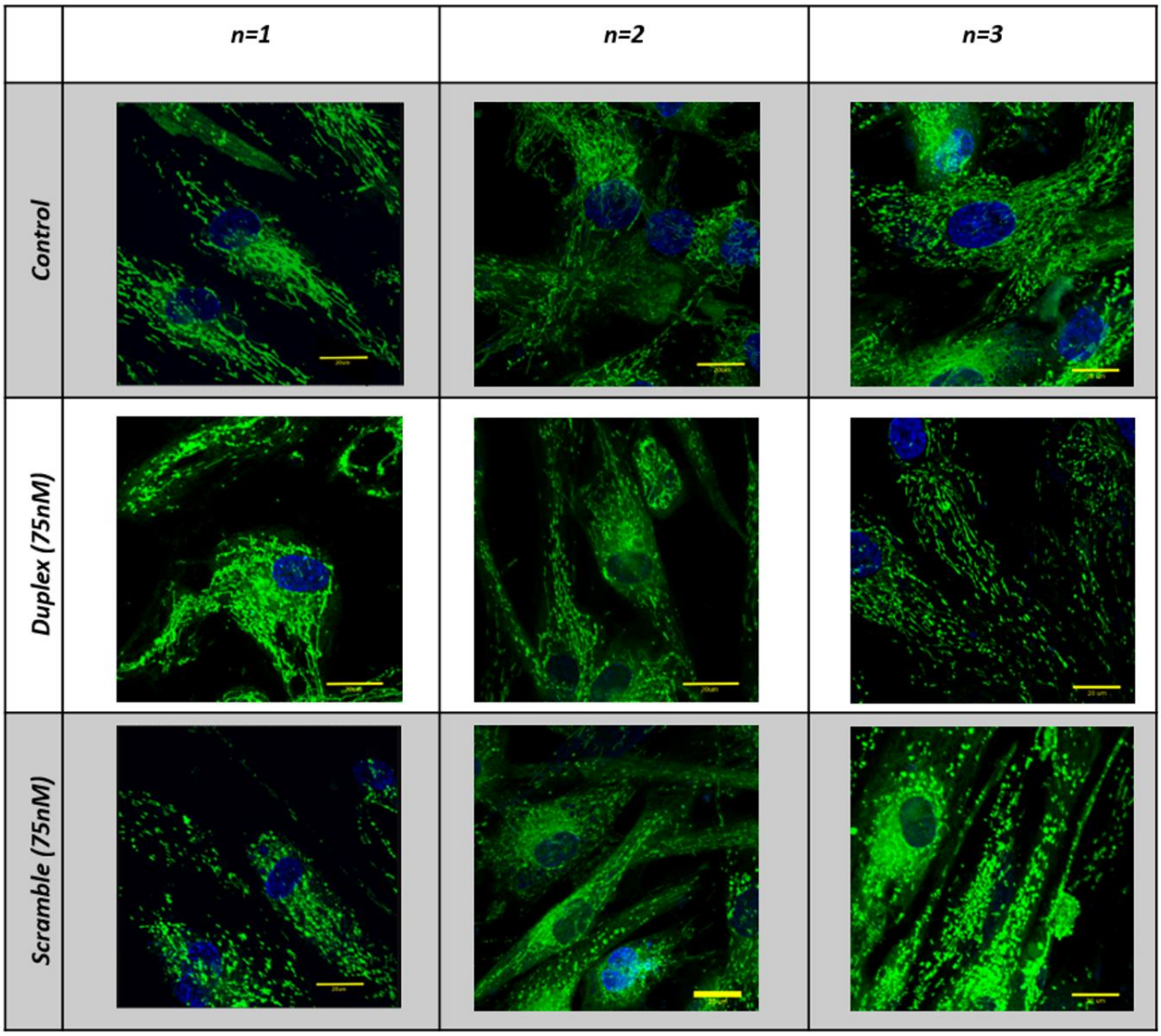

Figure 6. 21. Confocal microscopy imaging representing the effect SIRT4 knockdown had on mitochondrial elongation

(Mitochondrial content (green) and nuclei content (blue) in HSM myotubes differentiated for 10 days and imaged at 4X using Leica DM IRE2. Images scalled to 20µm. Control, Duplex SIRT4 siRNA 75nM and Scramble siRNA 75nM (*n*=3))

Mitochondrial Network Analysis (MiNA)

Following deconvolution using MetaMorph Imaging System, images were analysed for mitochondrial networks using the Mitochondrial Network Analysis (MiNA) toolset in ImageJ. For transparency of the data represented in Figure 6.23, Figure 6.22 (which is a skeletonised image of Figure 6.21, Duplex (75nM), *n*=1) has been labelled to help clarify which sections are classified as networks (branches, junction, slab and end-point pixels) and which are defined as individuals (rod, round and punctate). Only mitochondrial networks are presented in Figure 6.23.

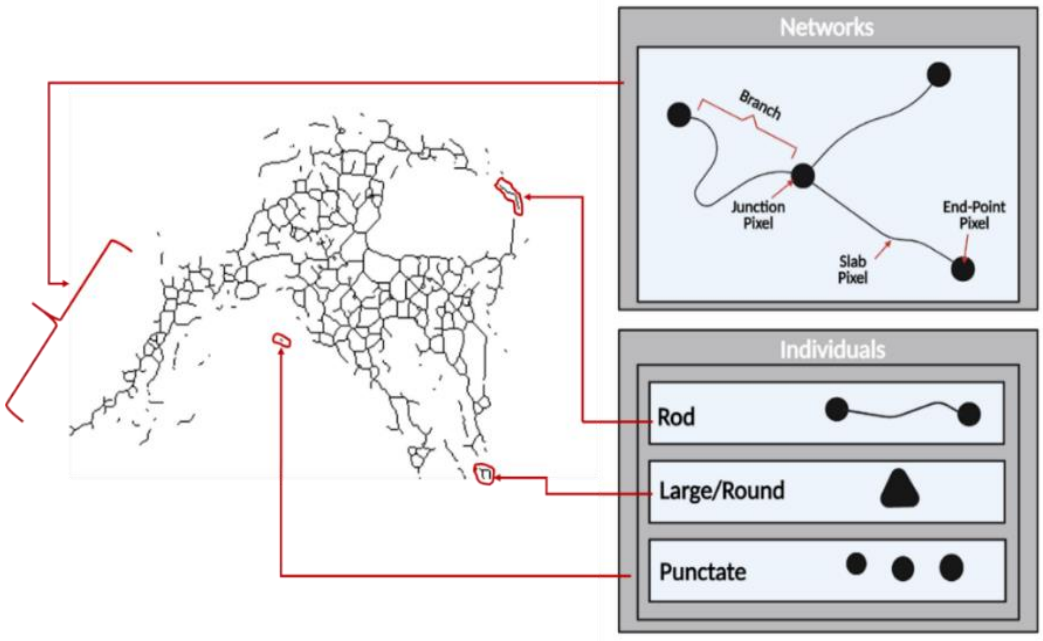

Figure 6. 22. Mitochondrial Network Analysis (MiNA) classification of mitochondrial networks and individual mitochondria

Figure 6.23 represents the output of the MiNA toolset. Results indicate that there was a significant increase in SIRT4 knockdown sample mitochondrial network branches (A), junctions (B), end-point pixels (C), number of junction pixels (D), number of slab pixels (E), number of triple points (F) and number of quadruple points (G) in comparison to both the control and the scramble samples (p<0.05), indicating an increase in mitochondrial tubulation with SIRT4 knockdown. However, there was no significant difference between average branch length (H) and maximum branch length (I) between samples.

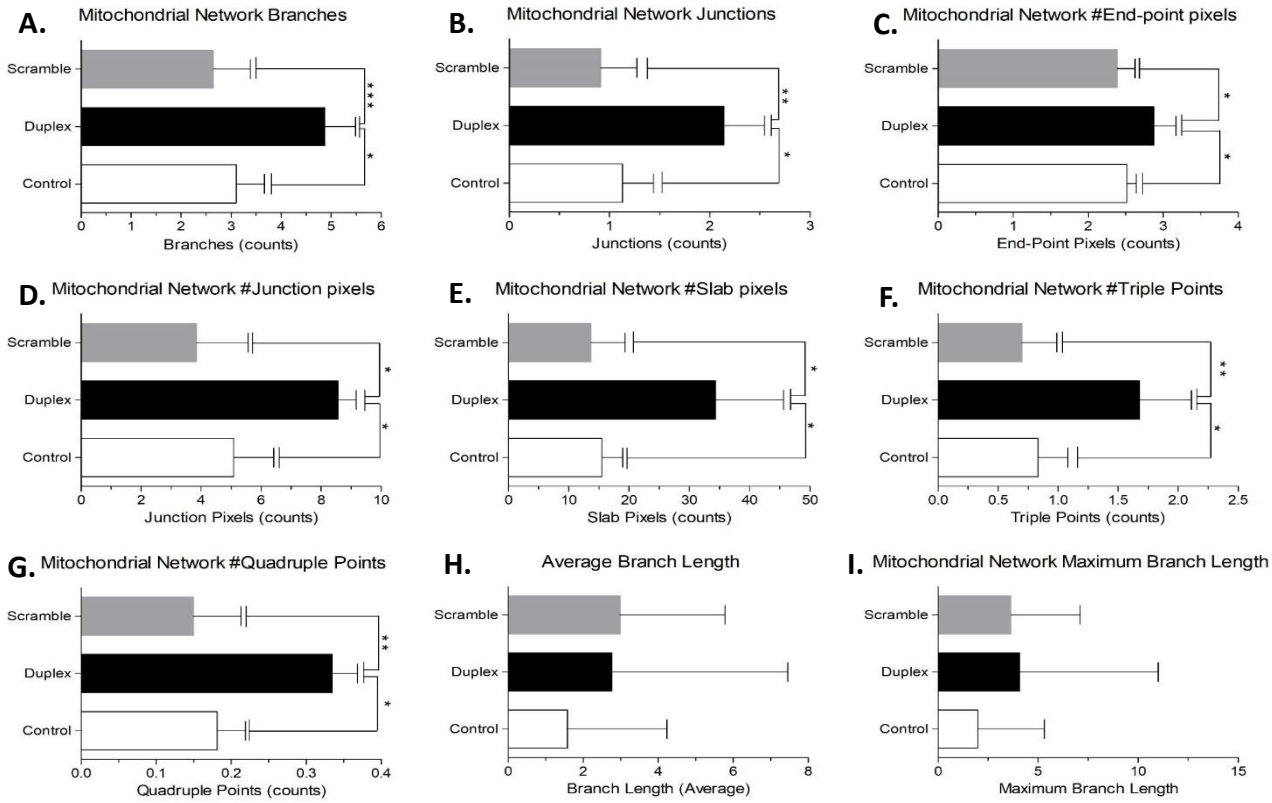

Figure 6. 23. Mitochondrial Network Analysis (MiNA) using ImageJ representing changes in mitochondrial morphology with SIRT4 knockdown

(Mitochondrial Network Analysis (MiNA) using ImageJ. Mitochondrial network branches (A), Mitochondrial network junctions (B), Mitochondrial network number of end-point pixels (C), Mitochondrial network number of junction pixels (D), Mitochondrial network slab pixels (E), Mitochondrial network number of triple points (F), Mitochondrial network number of quadruple points (G), Average branch length (H) & Mitochondrial network maximum branch length (I). Data are expressed as mean ±SD, *significant effect of SIRT4 knockdown, p<0.05, ** significant effect of SIRT4 knockdown, p<0.005, ***significant effect of SIRT4 knockdown, p<0.0005 (n=3))

Discussion on SIRT4 as a Regulator of Mitochondrial Fusion

The main findings in this chapter noted that SIRT4 regulates OPA1 mediated mitochondrial fusion, LEAK respiration through its regulation of ANT1 and ADP-stimulated oxidative phosphorylation.

We observed significant adaptations in human skeletal muscle mitochondrial dynamics with prolonged bed rest. The measurement of intricate, dynamic processes *in-vivo* is complex and often inaccurate. Subsequently, in order to measure these regulatory processes in greater detail, human skeletal muscle myoblasts were optimized and characterized for their expression of targets relating to differentiation, growth and maturity *in-vitro*. Characterization procedures helped confirm differentiation of these myoblasts to myotubes was optimal between days 10 and 12 of differentiation. Our expression analysis was supported further by microscopy depicting elongated, fused structures [381,248,197].

Our bed rest studies signified that both 21 and 60 days of bed rest resulted in the significant decrease in expression of OPA1, a change which may influence the regulation of substrate utilization. Our aim was to determine if SIRT4 is a regulator of metabolism, fatty acid oxidation and mitochondrial dynamics in skeletal muscle cells.

In SIRT4 knockdown HSM myotubes, we measured transcriptional and translational changes in markers of mitochondrial dynamics to determine if SIRT4 has a role in the regulation of this process. SIRT4 knockdown increased OPA1 protein expression as well as other markers of mitochondrial fusion such as Mfn1. This is in agreement with, and the inverse of, our bed rest data where a decrease in OPA1 was accompanied by an increase in SIRT4 expression. The balance in fusion to fission (OPA1:Drp1 ratio) allowed us to determine the impact of SIRT4 knockdown on the regulation of fusion-fission dynamics. The ratio favoured increased fusion and this was further supported by an increase in expression of regulators of free fatty acid oxidation and biogenesis such as CPT1b, pACC and PGC-1α along with the reduction in ANT1 protein expression indicative of a decrease in LEAK respiration.

Analysis of mitochondrial respiration in the SIRT4 knockdown myotubes, using a fatty acid Substrate-Uncoupler-Inhibitor Titration (SUIT) protocol, provided functional outcome support in favour of increased fat oxidation. SIRT4 knockdown resulted in a decrease in LEAK respiration and an increase in oxidative phosphorylation (β-oxidation). Confocal microscopy confirmed that SIRT4

knockdown not only increased the expression of regulators of mitochondrial fusion, increasing the mitochondria's ability to oxidize free fatty acids, but also increased mitochondrial elongation.

Human Skeletal Muscle Myotubes as a Translatable Model for our Bed Rest Study

Multiple, extensively explored immortalized rodent cell lines were available to us, such as the L6 rat cell line and C_2C_{12} murine cell line. However, immortalized cell lines often are genetically altered, and have been maintained under artificial conditions in culture for very long periods of time which can cause them to deviate from normal function, we concluded that a more translatable strategy for us would be to use primary human muscle cells [381]. Our analysis of the human bed rest biopsies provided evidence of adaptations in pathways related to mitochondrial morphology. Subsequently, primary human skeletal muscle myotubes were used to investigate one of the potential mechanisms regulating mitochondrial dynamics and function

An extensive optimization protocol was undertaken in order to understand the growth and differentiation phases, based on supported markers of immaturity and maturation. With significant increases in transcriptional markers of myotube maturation following 12 days of differentiation such as myosin heavy chain isoform (MYH) 1 and 4, ACTC1 and creatine kinase (Ckm) and decreases in markers of commitment to myoblast growth such as myoblast determination protein 1 (MYOD1) we were confident these cells represented human myotubes and that differentiation between 10-12 days was ideal to generate elongated, multinucleated myotubes. Although there is some discrepancy in the literature as to the exact length of time for differentiation of myotubes, due to some inter-individual variability, our results are in agreement with the majority of the field [1,197].

Sirtuin 4 in the Regulation of Cellular Metabolism and Mitochondrial Morphology

Due to the impact bed rest appears to have on OPA1 mediated mitochondrial fusion, and the limited research to date on the upstream regulators of OPA1 our research attempted to extend the knowledge in this area. Following SIRT4 knockdown we observed a significant increase in regulators of mitochondrial fusion, in particular, OPA1 (L-OPA1 and s-OPA1) and Mfn1. SIRT4 knockdown favours mitochondrial fusion, as indicated by the OPA1:Drp1 ratio but there was no change in mitochondrial fission markers, Drp1, Fis1 and MiD51 suggesting SIRT4 mainly acts by regulating mitochondrial fusion.

However, MiD49 and Mff significantly increased with knockdown. As eluded to within the results, mitochondrial fission factor (Mff) has been shown to regulate the activity and expression of mitochondrial fission marker Drp1 [220]. As we didn't observe a change in Drp1 but did see an increase in Mff, our results suggest Mff is not sufficient to induce fission. The increase in Mff expression could be a direct result of a greater outer mitochondrial membrane surface area as a result of the elevated expression of Mfn1 and OPA1, fusing the outer and inner mitochondrial membranes of adjacent mitochondria, increasing a mitochondrial network.

We also observed an increased expression of MiD49 with SIRT4 knockdown. Like many regulators in the cell, MiD49 (also known as MIEF2) can increase fission, but also fusion in different circumstances [578,326,449]. Subsequently, MiD49 may support Mfn1 and OPA1 to increase mitochondrial elongation with SIRT4 knockdown in human skeletal muscle.

Due to the increase in expression of OPA1 with knockdown, it was surprising to see no significant change in YME1L and OMA1, the upstream regulators of OPA1. YME1L is an ATP-dependent protease known to respond to metabolic stimuli such as changes in the ADP: ATP ratio. Given, knockdown increased oxidative phosphorylation (which will be discussed in detail further on) it could have been expected that YME1L would increase, although we did note a trending increase in its expression. Our results in this regard could be explained by the lack of change in pAMPK. Much research supports that a loss in YME1L in skeletal muscle myotubes results in the accumulation of s-OPA1 leading to an increase in mitochondrial fragmentation. Moreover, its loss is correlated with an increased expression and activity of AMPK [308].

Our data indicates that SIRT4 knockdown results in an increased expression of s-OPA1. However, we also observed an increase in L-OPA1 and mitochondrial elongation supported by microscopy data. Given the trending increase in YME1L, this ATP-dependent protease may be playing a role in this regard. Ideally we would have measured activity as well as expression to answer this question but our work was more focused on the functional outcomes. There was no change in the expression of OMA1 even though we found it significantly increased following 21 days of bed rest and decreased with 60 days of bed rest, in conjunction with an increase in SIRT4 expression. It is possible that SIRT4 knockdown may initiate other regulatory pathways of OPA1 separate to YME1L and OMA1.

Our hypothesis, that SIRT4 may regulate mitochondrial morphology by inhibiting OPA1 expression was further supported by our confocal microscopy work where we found a significant increase in mitochondrial network branches (+36% compared to the control, +45% compared to the

scramble) and junctions (+47% compared to the control, +57% compared to the scramble) in particular. The observed increase in junctions and branches suggests that that mitochondria are not isolated entities in the cell but are interconnected with each other cooperating in an organelle-organelle network, similar to how particular organs within the body actively communicate with each other [159,537]. This increased elongation has been shown to assist material exchange and signal transmission between organelles responsible for regulating metabolism, intercellular signalling and the maintenance of cellular homeostasis [537,329]. The mitofusin proteins such as Mfn1 and Mfn2 have been shown to play a critical role in this regard, acting as tethering proteins between adjacent mitochondria. Considering we observed an increase in Mfn1, this increase in junctions and branches could be initiated by Mfn1 tethering and fusing to the outer mitochondrial membrane of adjacent mitochondria, allowing for greater OPA1-mediated inner mitochondrial membrane fusion.

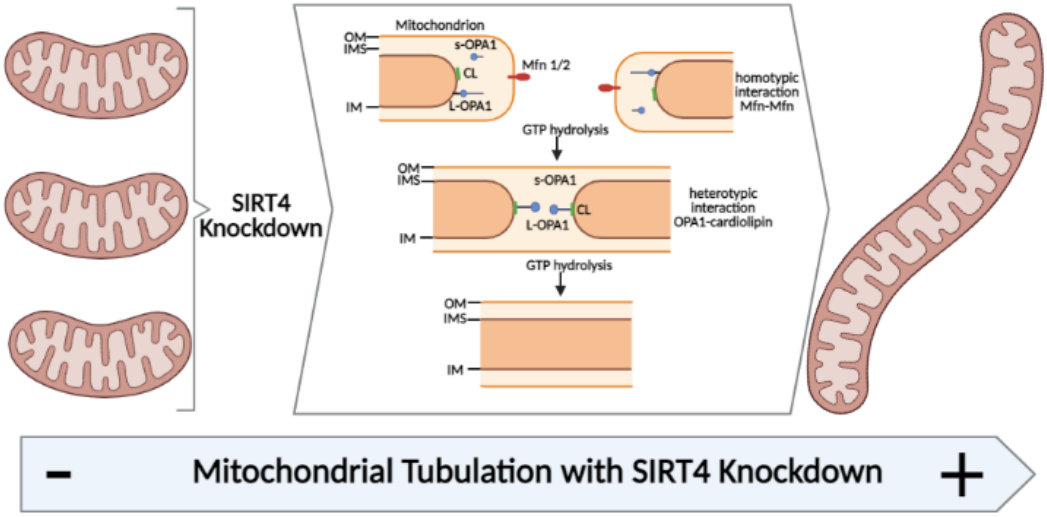

Figure 6. 24. SIRT4 Knockdown on OPA1 Function. Adapted from Liu & Chan, [321]

Our confocal work supports our transcriptional and translational data by demonstrating more elongated, fused mitochondria following knockdown in comparison to the control and scramble samples. There are very few studies that examine the SIRT4-OPA-1 axis but the evidence in fibroblasts and HEK293 cells suggests SIRT4 overexpression increases OPA1-mediated mitochondrial fusion [288]. In our primary human skeletal muscle cells, we find the opposite effect, that SIRT4 knockdown increased OPA1-mediated mitochondrial elongation. The increase in OPA1:Drp1 ratio content along with other outer mitochondrial membrane fusion proteins suggests that SIRT4 may regulate mitochondrial morphology in a tissue specific manner.

Sirtuin 4 in the Regulation of Other Members of the Sirtuin Family

SIRT4 knockdown led to a significant increase in SIRT1 and SIRT6 expression but there was no change in SIRT3 or SIRT5. SIRT6 is an ADP-ribosyltransferase, like SIRT4, but unlike SIRT4, SIRT6 is located in the nucleus and not the mitochondria. SIRT6 is a metabolic sensor connecting environmental signals to metabolic homeostasis and cellular stress [281,473]. SIRT6 overexpression has been shown to increase AMPK activity which in turn impacts on glucose metabolism by inhibiting insulin-like growth factor-1 (IGF-1) [107,447]. Our results suggest that there is a relationship between SIRT4 and SIRT6 demonstrated by the direct effect on SIRT6 mRNA and the decrease in IGF-1 expression providing indirect evidence of a role in glucose uptake, signifying an increased preference for cellular free fatty acid oxidation.

SIRT1 has been proposed to regulate AMPK activity by increasing cellular NAD^+ levels leading to deacetylation and manipulation of multiple processes in the cell [80]. As demonstrated in Chapter V, we observed a significant increase in SIRT1 in micronutrient cocktail group following 60 days of bed rest. An increase in SIRT1 has been proposed to be a key regulator of mitochondrial biogenesis and oxidative phosphorylation via a SIRT1-AMPK-PGC-1α mediated pathway [446,80,412,205]. Our results suggest SIRT4 may be having an impact on this pathway as knockdown leads to a significant increase in PGC-1α expression and previous studies have demonstrated links between the regulation of SIRT4 regulation and AMPK activity [366,221,342].

SIRT4 and the Regulation of Substrate Metabolism

Glycolysis

We observed a significant increase in hexokinase and pyruvate dehydrogenase (PDH) protein but not mRNA expression following SIRT4 knockdown. The increase in protein content indicates that SIRT4 knockdown may lead to an increase in Acetyl-CoA derived from glycolysis. Although our measurement of both hexokinase and PDH is of protein content, there is evidence in the literature to support this conclusion. The increase in hexokinase suggests SIRT4 knockdown increases production of glucose-6-phosphate which will subsequently be catalysed by PDH to increase Acetyl-CoA derived from glycolysis. There is evidence to support a regulatory role for SIRT4 on PDH, with an increased SIRT4 inhibiting PDH activity [334,514]. Subsequently, SIRT4 knockdown plays a key role in increasing Acetyl-CoA, a critical step in energy production by delivering its acetyl group to the TCA cycle for oxidation.

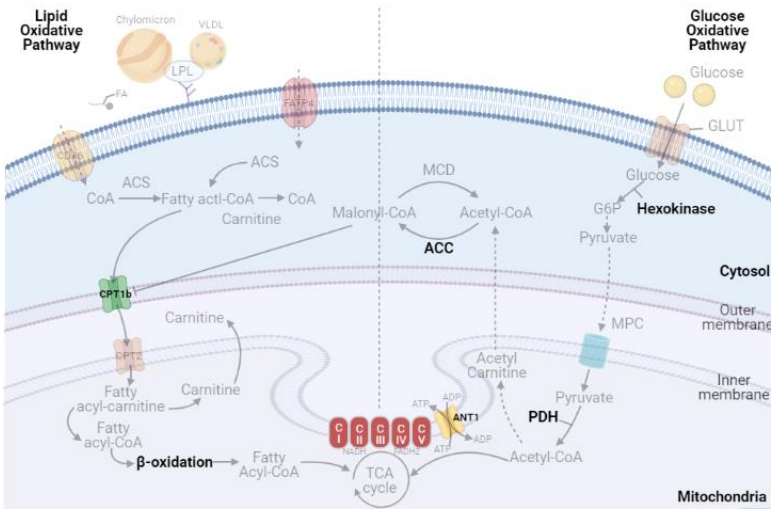

Figure 6. 25. Lipid & Glucose Oxidative Pathways. Adapted from *Fritzen et al.* [162]

Fatty Acid Oxidation – SIRT4 Regulating AMPK and Other Parameters

AMPK is an important regulator of substrate metabolism by increasing cellular energy levels in response to conditions which deplete act to deplete such energy (i.e. starvation or exercise) [171]. The activity of AMPK is dependent on the balance between ATP and ADP, with an increase in its activity associated with a decrease in ATP.

SIRT4 knockdown significantly decreased ANT1 expression and previous work from our group [263] suggests ANT1/2 is a key mediator of LEAK respiration (or uncoupling) in skeletal muscle and that a decreased in ANT1/2 expression following 21 days bed rest could explain the observed decrease in LEAK respiration. SIRT4 knockdown did not change ANT2 expression, however it has low-to-undetectable expression in skeletal muscle [493,312].

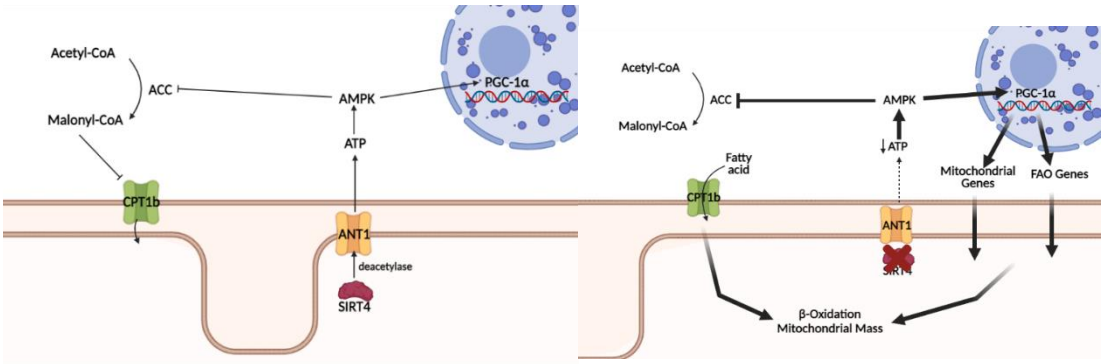

Figure 6. 26. The Role of SIRT4 on ANT1. Adapted from *Ho et al.* [221]

While SIRT4 has a direct effect on ANT1 we did not find an increase in pAMPK, despite the role of ANT1 in nucleotide translocation. As SIRT4 knockdown also increased lipid oxidation it was

surprising that pAMPK was not involved. However, pAMPK is not the most sensitive indicator of AMPK activity and we found increased pACC, a downstream target of AMPK, which has previously been reported to indicate increased AMPK activity [171,220]. pACC inactivates ACC, lowering Malonyl-CoA activity and increasing CPT1b, leading to increased lipid oxidation. We did not find a change in Malonyl-CoA decarboxylase (MCD) mRNA expression but we were unable to measure MCD activity. As we have seen an increase in pACC and CPT1b following SIRT4 knockdown we conclude AMPK is likely to play a role in this process. Leading to increased fatty acid uptake and oxidation by the mitochondria, but we cannot rule out another pathway or processes directly regulating ACC.

SIRT4 Knockdown Decreases LEAK Respiration and Increases Oxidative Phosphorylation

In order to understand the functional changes due to SIRT4 knockdown, we measured mitochondrial respiration using the fatty acid SUIT Oroboros O2k protocol. Our results show that SIRT4 knockdown significantly decreases LEAK (State 3) respiration while increasing ADP-stimulated respiration (OXPHOS). Both of these adaptations support our findings of decreased ANT1 and increased CPT1b expression. Our results also support those of Kenny et al. [263], as eluded to earlier, who reported that a reduction in ANT was indicative of a decrease in LEAK respiration. Further evidence by Ho et al., [221] recognised SIRT4's regulation of ANT, indicating that a decrease in SIRT4, decreases ANT expression and LEAK respiration. Additionally, Nasrin et al. [366] recognised how SIRT4 knockdown increased OXPHOS via an AMPK-mediated pathway. Our results are in line with these previously published studies [366,221,205], however, our data is the first to show SIRT4's regulatory role in human skeletal muscle and with accompanying data on mitochondrial dynamics and morphology.

Conclusion

There is an abundance of evidence signifying the role mitochondrial morphology plays on overall cellular metabolism. Increased mitochondrial tubulation due to either decreased mitochondrial fission or increased mitochondrial fusion has been shown to alter the preferential energy source from glycolysis to oxidative phosphorylation (OXPHOS) [399,572,384,110,559]. Our results demonstrate that SIRT4 may regulate these mitochondrial morphology pathways by interacting with OPA1 along with other mitochondrial fusion regulators such as Mfn1. Additionally, we have shown how SIRT4 is an important regulator of substrate metabolism. Our results highlight that SIRT4 knockdown decreases ANT1 expression and this may mediate the decreased LEAK

respiration subsequently increasing AMPK-mediated changes represented by increased expression of SIRT1, PGC-1α, pACC and CPT1b among others. There is also an enhancement of β-oxidation, supported by an increase in ADP-stimulated respiration with SIRT4 knockdown. Finally, SIRT4 regulates mitochondrial morphology, indicated by increased expression of regulators of mitochondrial dynamics and increased junction and branch networks, which alters the mitochondria's preferred source of substrate from carbohydrate to fatty acids.

Chapter VII: Concluding Discussion

Impact of Bed Rest and Intervention

European Space Agency standardised protocols for bed rest requires the monitoring of energy intake and expenditure in order to ensure subjects are in energy balance throughout the period of inactivity. Consequently, an increase in fat mass proportional to a decrease in muscle mass due to a decrease in energy expenditure is inevitable and something we observed within our model. However, we also observed an increase in body fat percentage following 60 days of bed rest, suggesting that the increase in fat mass may not have been proportional to the decrease in muscle mass, and subjects may have entered into a state of positive energy balance. Physical inactivity results in a switch from oxidative to glycolytic muscle fibers, and although we didn't measure skeletal muscle fiber composition, respiratory quotient (RQ) measurements using indirect calorimetry emphasise a shift from the predominant oxidation of fat to carbohydrate throughout 60 days of bed rest, supporting this probable change in skeletal muscle fiber type. This shift in substrate metabolism impacts upon body composition, increasing lipogenesis and decreasing the insulin sensitivity of tissue to glucose. Such adverse adaptations pose great stress upon the body, increasing risk in the development of chronic disease. Consequently, interventions have been developed aimed to help counteract these adverse adaptations. There were no whole body physiological differences due to the micronutrient cocktail supplement in this study but we did find subtle changes in skeletal muscle that may help to preserve metabolic function.

One of the clear outcomes was a decrease in mitochondrial content that leads to an overall reduction in respiration per gram of tissue. While the micronutrient cocktail impacted lipid metabolism during our reduced activity trial [112], it was not sufficient to overhaul the metabolic changes associated with more extreme and prolonged bed rest. We did find a switch in substrate oxidation, with greater carbohydrate oxidation at rest and a decrease in muscle mass. We propose that these changes might be explained by adaptations in mitochondrial dynamics.

After 60 days of bed rest there was a decrease in the expression of markers associated with mitochondrial fusion and fission, with reduced expression of inner mitochondrial membrane fusion protein, OPA1 (long and short isoform), and expression of mitochondrial fission marker, Drp1. A decrease in both fusion and fission respectively, indicates that although there is a decrease in OPA1 and Drp1, their ratio is maintained (OPA1:Drp1 ratio). However, an increased pDrp1^{s616},

indicates these mitochondria, although in balance, are primed to divide by stressed induced fission (SiF). We additionally observed a reduction in the protein expression of PINK1, one of the key factors in mitophagy following bed rest. These results in the control group suggest a positive relationship between mitochondrial content, dynamics and mitophagy. Although we can only speculate that a reduction in fission-fusion dynamics primed towards fission, in conjunction with a decrease in mitochondrial removal might be an attempt by the cell to offset further loss of mitochondrial content and maintain a sufficient number of functioning mitochondria. The increase in mitochondrial biogenesis transcription factor, PGC-1α could have a role in this regard. Given the reduced removal and decrease in dynamics, an increase in PGC-1α could represent an attempt by the cell to stimulate mitochondrial generation, prevent further loss of mitochondria and meet the demands for energy production.

The consequence is that mitochondria will be working harder to maintain the same level of respiration as before bed rest, increasing mitochondrial stress, as emphasised by the increase in SiF, resulting in the possibility of mitochondrial dysfunction as bed rest persists. A possible rise in mitochondrial dysfunction increases individuals risk for developing a whole host of serious chronic diseases [261,401,582,469]. As such it is imperative we develop countermeasures which might aid to mitigate some of these processes.

One aim of the bed rest was to optimize countermeasures that could mitigate the negative consequences of physical inactivity. We found that the micronutrient cocktail impacted mitochondrial dynamics, as represented by an increase in mitochondrial fusion:fission ratio, a process possibly regulated by calcium metabolism as signified by an increase in Pan-Calcineurin A. Such an increase in the fusion:fission ratio indicates this intervention may increase mitochondrial elongation, an adaptation that could increase mitochondrial oxidative phosphorylation capacity.

Our preliminary study using the micronutrient cocktail showed an increase in lipid oxidation, a decrease in lipogenesis and the maintenance of type II muscle fibers with reduced activity [112]. Although we didn't observe a change in substrate oxidation between groups, the probable mediators of this increase in mitochondrial fusion are likely to be Vitamin E and/or omega-3 fatty acid (ω-3) given their proven synergistic role in protecting mitochondrial membranes from oxidative damage and improving lipid metabolism. ω-3 in particular has been shown to directly regulate the mitochondrial membrane phospholipid, cardiolipin [219]. Cardiolipin is a necessary phospholipid for the formation of contact sites between inner and outer mitochondrial membranes, and the stabilization of essential inner membrane proteins and respiratory complexes [539,134]. Interestingly, in recent years it has emerged that cardiolipin is a direct

regulator of inner mitochondrial membrane fusion protein, OPA1 expression. This cardiolipin-OPA1 interaction has been shown to give the cristae its curvature allowing for greater distribution of oxidative phosphorylation [321,21]. As such, the ω-3 within our intervention may explain the observed increase in OPA1:Drp1 ratio following 60 days within the intervention.

We also observed no change in PINK1, the regulator of mitophagy. If we link this result with the lack of change in pDrp1^{s616} protein expression, we can speculate that our intervention is reducing SiF, and aiding the removal of dysfunctional mitochondria for quality control purposes. Bed rest was shown to significantly accelerate skeletal muscle atrophy, an effect considered to be strongly regulated by an increase in ROS and RNS, seemingly increasing mitochondrial dysfunction (the mitochondrial theory of aging) [111,119,408]. However, two compounds in our micronutrient cocktail, Vitamin E and selenium are ROS scavengers that act to decrease the impact of ROS on cellular homeostasis. We did not measure ROS/RNS production following 60 days of bed rest in either our control or intervention group. However, given mitochondrial dysfunction is inevitable with such a long period of inactivity [263,488], the lack of change in PINK1 expression in our intervention group could indicate that a micronutrient cocktail may maintain the mitochondrial quality control measures in place to keep our mitochondrial population healthy throughout bed rest.

Finally, we observed a significant increase in regulators of AMPK-mediated pathways such as SIRT1 and PGC-1α, in the intervention group following 60 days bed rest. Along with Vitamin E, selenium and ω-3 fatty acids our micronutrient cocktail was also composed of polyphenols. There is much evidence to support resveratrol as an activator of SIRT1, maintaining muscle mass during inactivity [347,30]. Unfortunately, this data is from animal models that has not translated to the human studies. However, our preliminary study noted the micronutrient cocktail prevented the decrease in type IIa fiber type CSA posed by a reduction in physical activity [112]. Given the strong negative relationship between SIRT1 and muscle atrophy, micronutrient supplementation may therefore be providing the impetus to maintain skeletal muscle mass during bed rest.

The micronutrient intervention appears capable of managing mitochondrial quality control and increasing oxidative phosphorylation capacity. As we did not find a difference in substrate oxidation between our intervention or control group, but did observe a shift in signalling pathways linked to mitochondrial dynamics, a higher dose may be required to maintain lipid oxidation at rest, therefore reducing the adverse consequence fatty acid accumulation has been shown to have on disease progression and metabolic flexibility. Further work will be needed to confirm this.

Impact of Time in Bed on Mitochondrial Dynamics

As we observed significant changes in markers of mitochondrial dynamics following 60 days of bed rest, we wanted to determine the time-course of these changes by comparing our data with samples obtained from a similar 21-day bed rest study. The expression of OPA1 significantly decreased after 21-days, however markers of fission did not change. There was a subsequent decrease in the fusion:fission ratio suggesting an increase in stress induced fragmentation (SiF) due to the initial stress bed rest initially has on the cell. This was further supported by the increase in expression of OMA1, the OPA1 regulator activated in states of increased stress.

Comparing the results of the 21 days of bed rest to the 60 days of bed rest, highlights the plasticity of OPA1 as it adopted to the changing demands of the cell. The initial shift toward fission over the first 21 days of bed rest reverted over time with decreases in both OPA1 and Drp1 and no change in the OPA1:Drp1 ratio. The mitochondria cannot continuously undergo fission and it might be that a new balance or homeostasis is reached as part of the adaptation to decreased physical activity. However, other components become active with prolonged bed rest as we found an increase in $pDrp1^{s616}$ after 60- but not 21-days.

There was no change in mitochondrial breakdown protein, PINK1 or the mitochondrial biogenesis protein, PGC-1α after 21 days of bed rest but PINK1 was decreased while PGC-1α significantly increased after 60 days. We speculate that the shorter duration bed rest results in a stress-induced increase in mitochondrial fragmentation in an attempt to reduce mitochondrial capacity to match the reduced demand of the cell. As bed rest continues a new balance is reached where there is a modest stimulus for biogenesis and a decrease in mitophagy.

While the data used for this comparison came from different studies, the control arm of ESA bed rest studies are very similar (diet, population, gender, age, location of testing). There are some differences in the participant characteristics but we do not believe they would have an impact on the muscle analysis performed.

SIRT4 as a Regulator of Mitochondrial Dynamics

Of particular interest was the increased expression of SIRT4 mRNA, an NAD^+-deacetylase, ADP-riboysltransferase, in the control group following 60 days of bed rest. SIRT4 has multiple functions in the cell but the possible regulation of OPA1 was of interest in the current study [288]. The

increase in SIRT4 mRNA, although subtle, and the decrease in OPA1 expression following bed rest, became the focus of further investigation.

For many years SIRT4 has been known to deacetylate and activate ANT 1/2, making it an important regulator of metabolism. We found that SIRT4 knockdown significantly decreased ANT1 expression, which could explain the decrease in LEAK respiration from our functional experiments. A decrease in ANT expression increases AMPK activity, as we have a decrease ATP:ADP ratio. Due to the regulatory role AMPK has on multiple cellular processes but none more so than β-oxidation, we noted that SIRT4 knockdown resulted in a significant increase in both markers and activity of lipid oxidation.

Due to this increase in oxidative phosphorylation with SIRT4 knockdown, it was no surprise that knockdown resulted in a significant increase in OPA1 expression, even though this is the opposite to work in HEK293 cells and fibroblasts [288]. An increase in mitochondrial size increases mitochondrial oxidative capacity and the increase in mitochondrial elongation was further supported by an increase in the OPA1:Drp1 ratio and our confocal microscopy work representing increased mitochondrial network branches and junctions with SIRT4 knockdown. SIRT4 appears to regulate OPA1 function and expression and the SIRT4-OPA1 axis appears to have an important role in regulating cellular metabolism. Our work has helped to unravel a novel links between mitochondrial dynamics and mitochondrial oxidative capacity.

Bed rest results in a significant switch in substrate metabolism from fat to carbohydrate, in conjunction with a shift from slow to fast twitch muscle fibers. Our results further support the role SIRT4 plays in the regulation of substrate metabolism and further work is necessary to fully elucidate the beneficial impact of targeting this protein for therapeutic purposes.

Limitations

Bed rest studies provide us with a very controlled environment but there were a few limitations which could impact the measurement outcomes. The current bed rest study used a between-patient study design. While this design has many benefits by minimising the learning effects across conditions, eliminating a washout period, to shorter subject sessions reducing chances of subject drop-out, there are limitations. Unlike a cross-over study design, where subjects are their own control, this between-patient design compared a control group of different subjects to our intervention group, resulting in natural inter-individual variability between groups.

Another limitation of this study, and one which is common to other bed rest studies, was that subject measurements during the baseline period were obtained while subjects were ambulatory. One could argue this is reflective of a free living environment, however given subjects are confined to the clinic throughout these measurements this conditional effect may be somewhat reduced. Additionally, there were multiple research teams working on the same study, meaning volunteers have to follow a strict regime of testing and there is a risk of confounding influences from the range of tests performed.

This was not a double-blind study. Subjects in the control group did not take a placebo supplement when the intervention group took their cocktail. The reason for this was due to the difficulties in finding a neutral oil to encapsulate for a placebo. Given the nature of the study therefore, subjects were aware of the group they were in. Other bed rest studies have been shown to include placebos in their study design [296,129] and given the limited effect inclusion has been shown to have we are not concerned that lack of placebo inclusion in our study will dramatically impact upon our results.

The intervention was given to the subjects at the designated times by the nurse on call within the clinic. Researchers in each team could decide if they wanted to know the subject breakdown or not. We decided not to know until samples were analysed to help best prevent bias to the results.

Muscle biopsies were taken before and after a euglycemic-hyperinsulinemic clamp before and following 60 days bed rest. We used pre-clamp muscle for the majority of measurements. However, due to limited muscle size, measurement of mitochondrial content was quantified using mtDNA:nDNA ratio from the post-clamp muscle. We are confident that mitochondrial content would not differ between pre and post clamp as changes in DNA quantity would not be influenced by glucose and insulin and not occur in this timeframe. However, this did limit our ability to directly compare with other studies we previously used citrate synthase and markers of complexes in the electron transport system.

The quantity of muscle obtained also impacted on the number of techniques we could perform. The majority of our data relates to expression (protein/mRNA) with our functional outcomes determined using mitochondrial respiration. Through measurement of more phosphorylated forms of proteins and/or more activity assays we would be able to gain a greater insight into the effects bed rest has on muscle signalling. Additionally, to coincide with the above point, supporting histology/microscopy work to represent what we observed from an expression

perspective would also aid to put clarity to the changes we observed with bed rest particularly those processes relating to mitochondrial dynamics.

We compared the 21- and 60-day bed rest studies to evaluate the effect of time on changes in protein expression. Although the European Space Agency has a standardisation protocol in place to allow for comparison between all of its studies, subject characteristics in the 21-day bed rest study were different in some respects to those in the 60-day study. Subject selection criteria were the same for both studies but due to natural inter-individual variances, differences in some of the measurements assessed could simply be down to this. This is confirmed simply by the fact that subjects within the 60-day trial had a greater body fat mass and body fat percentage in comparison to the 21-day trial. However, the trends we observed in the descriptive physiological measurements were the same. In order to minimise the variation between studies, all measurements were normalised to the same internal control.

Finally, using cell culture as a model to investigate physiological changes that we see in human models is a limitation in itself. While it does provide us with a useful model to investigate specific pathways, isolated cells in culture do not reflect the complex physiological environment of the human body. We attempted to bridge this gap by using primary human myotubes and optimizing them to best reflect the human model.

Future Directions

Bed rest allows us to study physiology in a very unique and controlled environment. While a lot of work has been completed to investigate the potential for micronutrient supplementation to mitigate the changes during bed rest, further work is needed to optimise the dose required to counteract the effects of bed rest. It is also possible that a micronutrient nutrient cocktail alone is not sufficient to mitigate these changes and combination with exercise or other nutrient countermeasures may be required.

As the micronutrient nutritional supplement was formulated as a cocktail there is limited data to determine the efficacy of individual components. As we know there is a synergistic effect of some compounds on each other (i.e. Vitamin E and Omega-3 fatty acids) this again could affect our interpretation of the results. More work examining the mechanisms at play following supplementation of nutrient compounds in combination within more systems than just the skeletal muscle is required. Some will argue that separate studies should be performed to investigate the individual aspects but this is not a practical solution for expense bed rest studies.

In addition, no single micronutrient is likely to be sufficiently effective at mitigating the range of physiological adaptations during bed rest and we need to start thinking about strategies that could more efficiently investigate nutrient combinations.

While bed rest is an ideal model to study the physiology of physical inactivity and to identify novel countermeasures to both prevent some of the adverse changes and further human exploration of space, we acknowledge that our subjects do not represent the general population, and the interpretation of the results are delimited to young active men. Therefore, to further our understanding for health related outcomes and benefits, more studies are needed on less active and older populations as well as those at-risk of developing metabolic diseases.

Antioxidant/anti-inflammatory interventions have been shown to reduce free radicals such as ROS/RNS. Such free radicals, formed within the Q cycle of the ETC, have also been argued within the literature to be the main players in skeletal muscle disuse atrophy and mitochondrial dysfunction, increasing metabolic stress. Our project did not assess the impact ROS/RNS may have in this regard. However, we could speculate it is having a positive effect in this regard. Future identification of the main players in these pathways that are adapted with supplementation during inactivity is necessary to tailor specific countermeasures and therapeutic approaches to counteract muscle atrophy.

We observed SIRT4 to be an integral regulator of mitochondrial dynamics and substrate metabolism within the human skeletal muscle myotubes. These conclusions were obtained usng gene knockdown studies in culture. Ideally, in order to fully support our findings SIRT4 overexpression studies, in conjunction with further *in-vitro* work, is necessary to fully elucidate the impact SIRT4 may be having on overall cellular metabolism and mitochondrial dynamics in human skeletal muscle along with other systems within the body.

Conclusion

Bed rest has been proven to lead to multiple adverse physiological consequences. Although whole body changes are widely reported, little is known about the mechanistic responses to physical inactivity. We observed that bed rest results in a shift in substrate metabolism, reduces skeletal muscle mass and increases fat accumulation. We considered these changes could be explained by alterations in mitochondrial function which appeared to decreased following bed rest. Interestingly however, when we normalised to mitochondrial content, these functional changes dissipated. Given the whole body adaptations persist with bed rest we subsequently hypothesised

these changes could be explained by adaptations in mitochondrial dynamics. Another aim of this study was to optimise countermeasures which could mitigate the negative consequences of bed rest. We found that supplementation with a micronutrient cocktail over 60 days of bed rest had some protective effect on regulators of mitochondrial dynamics and substrate metabolism, although these adaptations were not observed from a whole body perspective. Further work is necessary to identify appropriate dosing. Of particular interest was the observed reduction in expression of inner mitochondrial membrane fusion protein, OPA1, a change which appeared to be managed by our intervention through a possible ω-3-cardiolipin-OPA1 pathway. We explored the role OPA1 may have in greater detail, through knockdown of a novel upstream regulator of OPA1, SIRT4. SIRT4 knockdown resulted in a significant increase in OPA1 expression, an increase in mitochondrial tubulation and further increased mitochondrial oxidative capacity. Subsequently, SIRT4 may be having a similar effect as our micronutrient cocktail. Our results suggest SIRT4 has the capability to be a novel therapeutic to counteract many physiological changes associated with bed rest and metabolic disease progression. However, more work is necessary in this regard to fully elucidate this prediction.

Bibliography

[1] Abdelmoez AM, Puig LS, Smith, Jonathon A., Gabriel BM, Savikj M, Dollet L, et al. Comparative profiling of skeletal muscle models reveals heterogeneity of transcriptome and metabolism. Am J Physiol - Cell Physiol 2019. https://doi.org/10.11428/jhej1987.42.189.

[2] Adams GR, Caiozzo VJ, Baldwin KM. Skeletal muscle unweighting: Spaceflight and ground-based models. J Appl Physiol 2003;95:2185–201. https://doi.org/10.1152/japplphysiol.00346.2003.

[3] Akima H, Ushiyama JI, Kubo J, Tonosaki SI, Itoh M, Kawakami Y, et al. Resistance training during unweighting maintains muscle size and function in human calf. Med Sci Sports Exerc 2003;35:655–62. https://doi.org/10.1249/01.MSS.0000058367.66796.35.

[4] Akinwumi BC, Bordun KAM, Anderson HD. Biological activities of stilbenoids. Int J Mol Sci 2018;19:1–25. https://doi.org/10.3390/ijms19030792.

[5] Ali S, Mcstay GP. Regulation of Mitochondrial Dynamics by Proteolytic Processing and Protein Turnover. Antioxidants 2018;7:1–15. https://doi.org/10.3390/antiox7010015.

[6] Alibegovic AC, Sonne MP, Højbjerre L, Jacobsen S, Nilsson E, Færch K, et al. Insulin resistance induced by physical inactivity is associated with multiple transcriptional changes in skeletal muscle in young men. Am J Physiol - Endocrinol Metab 2010;299:752–63. https://doi.org/10.1152/ajpendo.00590.2009.

[7] Alibegovic AC, Hojbjerre L, Sonne MP, van Hall G, Stallknecht B, Dela F, et al. Impact of 9 Days of Bed Rest on Hepatic and Peripheral Insulin Action, Insulin Secretion, and Whole-Body Lipolysis in Healthy Young Male Offspring of Patients With Type 2 Diabetes. Diabetes 2009;58:2749–56. https://doi.org/10.2337/db09-0369.

[8] Alkner BA, Tesch PA. Knee extensor and plantar flexor muscle size and function following 90 days of bed rest with or without resistance exercise. Eur J Appl Physiol 2004;93:294–305. https://doi.org/10.1007/s00421-004-1172-8.

[9] Amat R, Planavila A, Chen SL, Iglesias R, Giralt M, Villarroya F. SIRT1 controls the transcription of the peroxisome proliferator-activated receptor-γ co-activator-1α(PGC-1α) gene in skeletal muscle through the PGC-1α autoregulatory loop and interaction with MyoD. J Biol Chem 2009;284:21872–80. https://doi.org/10.1074/jbc.M109.022749.

[10] Amati F, Dube JJ, Alvarez-Carnero E, Edreira MM, Chomentowski P, Coen PM, et al. Skeletal muscle triglycerides, diacylglycerols, and ceramides in insulin resistance: Another paradox in endurance-trained athletes? Diabetes 2011;60:2588–97. https://doi.org/10.2337/db10-1221.

[11] Appell HJ, Duarte JAR, Soares JMC. Supplementation of vitamin E may attenuate skeletal muscle immobilization atrophy. Int J Sports Med 1997;18:157–60. https://doi.org/10.1055/s-2007-972612.

[12] Aquilano K, Baldelli S, Barbera L La, Barbato DL, Tatulli G, Ciriolo MR. Adipose triglyceride lipase decrement affects skeletal muscle homeostasis during aging through FAs-PPARα-PGC-1α antioxidant response. Oncotarget 2016;7:23019–32. https://doi.org/10.18632/oncotarget.8552.

[13] Arribat Y, Broskey NT, Greggio C, Boutant M, Conde Alonso S, Kulkarni SS, et al. Distinct Patterns of Skeletal Muscle Mitochondria Fusion, Fission and Mitophagy upon Duration of Exercise Training. Acta Physiol 2018:e13179. https://doi.org/10.1111/apha.13179.

[14] Ashrafi G, Schwarz TL. The pathways of mitophagy for quality control and clearance of mitochondria. Cell Death Differ 2013;20:31–42. https://doi.org/10.1038/cdd.2012.81.

[15] Axelrod CL, Fealy CE, Mulya A, Kirwan JP. Exercise training remodels human skeletal muscle mitochondrial fission and fusion machinery towards a pro-elongation phenotype. Acta Physiol 2019;225:1–9. https://doi.org/10.1111/apha.13216.

[16] Bach D, Pich S, Soriano FX, Vega N, Baumgartner B, Oriola J, et al. Mitofusin-2 determines mitochondrial network architecture and mitochondrial metabolism: A novel regulatory mechanism altered in obesity. J Biol Chem 2003;278:17190–7. https://doi.org/10.1074/jbc.M212754200.

[17] Baecker N, Frings-Meuthen P, Heer M, Mester J, Liphardt AM. Effects of vibration training on bone metabolism: Results from a short-term bed rest study. Eur J Appl Physiol 2012;112:1741–50. https://doi.org/10.1007/s00421-011-2137-3.

[18] Baker MJ, Lampe PA, Stojanovski D, Korwitz A, Anand R, Tatsuta T, et al. Stress-induced OMA 1 activation and autocatalytic turnover regulate OPA1-dependent mitochondrial dynamics. EMBO J 2014;33:578–93.

[19] Balan E, Schwalm C, Naslain D, Nielens H, Francaux M, Deldicque L. Regular Endurance Exercise Promotes Fission, Mitophagy, and Oxidative Phosphorylation in Human Skeletal Muscle Independently of Age. Front Physiol 2019;10. https://doi.org/10.3389/fphys.2019.01088.

[20] Bamman MM, Clarke MSF, Feeback DL, Talmadge RJ, Stevens BR, Lieberman SA, et al. Impact of resistance exercise during bed rest on skeletal muscle sarcopenia and myosin isoform distribution. J Appl Physiol 1998;84:157–63. https://doi.org/10.1152/jappl.1998.84.1.157.

[21] Ban T, Kohno H, Ishihara T, Ishihara N. Relationship between OPA1 and cardiolipin in mitochondrial inner-membrane fusion. Biochim Biophys Acta - Bioenerg 2018;1859:951–7. https://doi.org/10.1016/j.bbabio.2018.05.016.

[22] Barbic F, Heusser K, Minonzio M, Shiffer D, Cairo B, Tank J, et al. Effects of Prolonged Head-Down Bed Rest on Cardiac and Vascular Baroreceptor Modulation and Orthostatic Tolerance in Healthy Individuals. Front Physiol 2019;10:1–9. https://doi.org/10.3389/fphys.2019.01061.

[23] Barbieri E, Sestili P. Reactive Oxygen Species in Skeletal Muscle Signaling. J Signal Transduct 2012. https://doi.org/10.1155/2012/982794.

[24] Barclay JK, Hansel M. Free radicals may contribute to oxidative skeletal muscle fatigue. Can J Physiol Pharmacol 1991;69:279–84.

[25] Barrès R, Yan J, Egan B, Treebak JT, Rasmussen M, Fritz T, et al. Acute exercise remodels promoter methylation in human skeletal muscle. Cell Metab 2012;15:405–11. https://doi.org/10.1016/j.cmet.2012.01.001.

[26] Baur JA. Resveratrol, sirtuins, and the promise of a DR mimetic. Mech Ageing Dev 2010;131:261–9. https://doi.org/10.1016/j.mad.2010.02.007.

[27] Belavý DL, Beller G, Armbrecht G, Perschel FH, Fitzner R, Bock O, et al. Evidence for an additional effect of whole-body vibration above resistive exercise alone in preventing bone

loss during prolonged bed rest. Osteoporos Int 2011;22:1581–91. https://doi.org/10.1007/s00198-010-1371-6.

[28] Belavý DL, Bock O, Börst H, Armbrecht G, Gast U, Degner C, et al. The 2nd Berlin BedRest study: Protocol and implementation. J Musculoskelet Neuronal Interact 2010;10:207–19.

[29] Beller G, Belavỳ DL, Sun L, Armbrecht G, Alexandre C, Felsenberg D. WISE-2005: Bed-rest induced changes in bone mineral density in women during 60days simulated microgravity. Bone 2011;49:858–66. https://doi.org/10.1016/j.bone.2011.06.021.

[30] Bennett BT, Mohamed JS, Alway SE. Effects of resveratrol on the recovery of muscle mass following disuse in the plantaris muscle of aged rats. PLoS One 2013;8:1–19. https://doi.org/10.1371/journal.pone.0083518.

[31] Bereiter-Hahn J. Do we age because we have mitochondria? Protoplasma 2014;251:3–23. https://doi.org/10.1007/s00709-013-0515-x.

[32] Berg HE, Larsson L, Tesch PA. Lower limb skeletal muscle function after 6 wk of bed rest. J Appl Physiol 1997;82:182–8. https://doi.org/10.1152/jappl.1997.82.1.182.

[33] Bergouignan A, Rudwill F, Simon C, Blanc S. Physical inactivity as the culprit of metabolic inflexibility: evidence from bed-rest studies. J Appl Physiol 2011;111:1201–10. https://doi.org/10.1152/japplphysiol.00698.2011.

[34] Bergouignan A, Schoeller DA, Normand S, Gauquelin-Koch G, Laville M, Shriver T, et al. Effect of Physical Inactivity on the Oxidation of Saturated and Monounsaturated Dietary Fatty Acids: Results of a Randomized Trial. PLoS Clin Trials 2006;1:e27. https://doi.org/10.1371/journal.pctr.0010027.

[35] Bergouignan A, Trudel G, Simon C, Schoeller DA, Votruba SB, Desage M, et al. Physical inactivity differentially alters dietary oleate and palmitate trafficking. Diabetes 2009;58:367–76. https://doi.org/10.2337/db08-0263.

[36] Bergouignan A, Momken I, Schoeller DA, Normand S, Zahariev A, Lescure B, et al. Regulation of energy balance during long-term physical inactivity induced by bed rest with and without exercise training. J Clin Endocrinol Metab 2010;95:1045–53. https://doi.org/10.1210/jc.2009-1005.

[37] Berman AY, Motechin RA, Wiesenfeld MY, Holz MK. The therapeutic potential of

resveratrol: a review of clinical trials. Npj Precis Oncol 2017;1. https://doi.org/10.1038/s41698-017-0038-6.

[38] Beytut E, Yilmaz S, Aksakal M, Polat S. The possible protective effects of vitamin E and selenium administration in oxidative stress caused by high doses of glucocorticoid administration in the brain of rats. J Trace Elem Med Biol 2018;45:131–5. https://doi.org/10.1016/j.jtemb.2017.10.005.

[39] Biolo G, Agostini F, Simunic B, Sturma M, Torelli L, Preiser JC, et al. Positive energy balance is associated with accelerated muscle atrophy and increased erythrocyte glutathione turnover during 5 wk. Am J Clin Nutr 2008;88:950–8.

[40] Biolo G, Ciocchi B, Stulle M, Bosutti A, Barazzoni R, Zanetti M, et al. Calorie restriction accelerates the catabolism of lean body mass during 2 wk of bed rest. Am J Clin Nutr 2007;86:366–72. https://doi.org/86/2/366 [pii].

[41] Bitterman KJ, Anderson RM, Cohen HY, Latorre-Esteves M, Sinclair DA. Inhibition of silencing and accelerated aging by nicotinamide, a putative negative regulator of yeast Sir2 and human SIRT1. J Biol Chem 2002;277:45099–107. https://doi.org/10.1074/jbc.M205670200.

[42] Blanc S, Normand S, Pachiaudi C, Fortrat J, Laville M, Gharib C. Fuel Homeostasis during Physical Inactivity Induced by Bed Rest *. J Clin Endocrinol Metab 2000;85.

[43] Blanc S, Normand S, Ritz P, Pachiaudi C, Vico L, Gharib C, et al. Energy and water metabolism, body composition, and hormonal changes induced by 42 days of enforced inactivity and simulated weightlessness. J Clin Endocrinol Metab 1998;83:4289–97. https://doi.org/10.1210/jc.83.12.4289.

[44] Blizzard RR, Young JL. Effects of whole-body vibration exercise on prevention of the negative effects of prolonged bed rest. Phys Ther Rev 2010;15:391–8. https://doi.org/10.1179/174328810X12814016179079.

[45] Blond K, Brinkløv CF, Ried-Larsen M, Crippa A, Grøntved A. Association of high amounts of physical activity with mortality risk: A systematic review and meta-analysis. Br J Sports Med 2020;54:1195–201. https://doi.org/10.1136/bjsports-2018-100393.

[46] Blottner D, Salanova M, Püttmann B, Schiffl G, Felsenberg D, Buehring B, et al. Human

skeletal muscle structure and function preserved by vibration muscle exercise following 55 days of bed rest. Eur J Appl Physiol 2006;97:261–71. https://doi.org/10.1007/s00421-006-0160-6.

[47] de Boer MD, Selby A, Atherton P, Smith K, Seynnes OR, Maganaris CN, et al. The temporal responses of protein synthesis, gene expression and cell signalling in human quadriceps muscle and patellar tendon to disuse. J Physiol 2007;585:241–51. https://doi.org/10.1113/jphysiol.2007.142828.

[48] de Boer MD, Seynnes OR, di Prampero PE, Pišot R, Mekjavić IB, Biolo G, et al. Effect of 5 weeks horizontal bed rest on human muscle thickness and architecture of weight bearing and non-weight bearing muscles. Eur J Appl Physiol 2008;104:401–7. https://doi.org/10.1007/s00421-008-0703-0.

[49] Bohé J, Low A, Wolfe RR, Rennie MJ. Human muscle protein synthesis is modulated by extracellular, not intramuscular amino acid availability: A dose-response study. J Physiol 2003;552:315–24. https://doi.org/10.1113/jphysiol.2003.050674.

[50] Bondonno CP, Yang X, Croft KD, Considine MJ, Ward NC, Rich L, et al. Flavonoid-rich apples and nitrate-rich spinach augment nitric oxide status and improve endothelial function in healthy men and women: A randomized controlled trial. Free Radic Biol Med 2012;52:95–102. https://doi.org/10.1016/j.freeradbiomed.2011.09.028.

[51] Booth FW, Laye MJ, Roberts MD. Lifetime sedentary living accelerates some aspects of secondary aging. J Appl Physiol 2011;111:1497–504. https://doi.org/10.1152/japplphysiol.00420.2011.

[52] Booth FW, Lees SJ. Fundamental questions about genes, inactivity, and chronic diseases. Physiol Genomics 2007;28:146–57. https://doi.org/10.1152/physiolgenomics.00174.2006.

[53] Bordi M, Nazio F, Campello S. The Close interconnection between mitochondrial dynamics and mitophagy in cancer. Front Oncol 2017;7:1–9. https://doi.org/10.3389/fonc.2017.00081.

[54] Borgia D, Malena A, Spinazzi M, Desbats MA, Salviati L, Russell AP, et al. Increased mitophagy in the skeletal muscle of spinal and bulbar muscular atrophy patients. Hum Mol Genet 2017;26:1087–103. https://doi.org/10.1093/hmg/ddx019.

[55] Bosquet L, Léger L, Legros P. Methods to Determine Aerobic Endurance. Sport Med 2002;32:675–700.

[56] Bouchard C, Blair SN, Katzmarzyk PT. Less sitting, more physical activity, or higher fitness? Mayo Clin Proc 2015;90:1533–40. https://doi.org/10.1016/j.mayocp.2015.08.005.

[57] Boushel R, Gnaiger E, Schjerling P, Skovbro M, Kraunsøe R, Dela F. Patients with type 2 diabetes have normal mitochondrial function in skeletal muscle. Diabetologia 2007;50:790–6. https://doi.org/10.1007/s00125-007-0594-3.

[58] Brand MD, Dunn MRC, Nutrition H, Road H, Cb C, Brand M. The efficiency and plasticity of mitochondrial energy transduction. Biochem Soc Trans 2005;33:897–904.

[59] Brand MD. Mitochondrial generation of superoxide and hydrogen peroxide as the source of mitochondrial redox signaling. Free Radic Biol Med 2016;100:14–31. https://doi.org/10.1016/j.freeradbiomed.2016.04.001.

[60] Brand MD, Nicholls DG. Assessing mitochondrial dysfunction in cells. Biochem J 2011;435:297–312. https://doi.org/10.1042/BJ20110162.

[61] Brandauer J, Andersen MA, Kellezi H, Risis S, Frøsig C, Vienberg SG, et al. AMP-activated protein kinase controls exercise training- and AICAR-induced increases in SIRT3 and MnSOD. Front Physiol 2015;6:1–16. https://doi.org/10.3389/fphys.2015.00085.

[62] Brasnyó P, Molnár GA, Mohás M, Markó L, Laczy B, Cseh J, et al. Resveratrol improves insulin sensitivity, reduces oxidative stress and activates the Akt pathway in type 2 diabetic patients. Br J Nutr 2011;106:383–9. https://doi.org/10.1017/S0007114511000316.

[63] Bravo-San Pedro JM, Kroemer G, Galluzzi L. Autophagy and Mitophagy in Cardiovascular Disease. Circ Res 2017;120:1812–24. https://doi.org/10.1161/CIRCRESAHA.117.311082.

[64] Breen DM, Sanli T, Giacca A, Tsiani E. Stimulation of muscle cell glucose uptake by resveratrol through sirtuins and AMPK. Biochem Biophys Res Commun 2008;374:117–22. https://doi.org/10.1016/j.bbrc.2008.06.104.

[65] De Brito OM, Scorrano L. Mitofusin 2 tethers endoplasmic reticulum to mitochondria. Nature 2008;456:605–10. https://doi.org/10.1038/nature07534.

[66] Brocca L, Cannavino J, Coletto L, Biolo G, Sandri M, Bottinelli R, et al. The time course of

the adaptations of human muscle proteome to bed rest and the underlying mechanisms. J Physiol 2012;590:5211–30. https://doi.org/10.1113/jphysiol.2012.240267.

[67] Brooks NE, Cadena SM, Cloutier G, Vega-López S, Roubenoff R, Castaneda-Sceppa C. Influence of exercise on the metabolic profile caused by 28 days of bed rest with energy deficit and amino acid supplementation in healthy men. Int J Med Sci 2014;11:1248–57. https://doi.org/10.7150/ijms.9694.

[68] Broome SC, Woodhead JST, Merry TL. Mitochondria-targeted antioxidants and skeletal muscle function. Antioxidants 2018;7:1–12. https://doi.org/10.3390/antiox7080107.

[69] Buler M, Aatsinki SM, Izzi V, Uusimaa J, Hakkola J. SIRT5 is under the control of PGC-1o: And AMPK and is involved in regulation of mitochondrial energy metabolism. FASEB J 2014;28:3225–37. https://doi.org/10.1096/fj.13-245241.

[70] Bull FC, Al-Ansari SS, Biddle S, Borodulin K, Buman MP, Cardon G, et al. World Health Organization 2020 guidelines on physical activity and sedentary behaviour. Br J Sports Med 2020;54:1451–62. https://doi.org/10.1136/bjsports-2020-102955.

[71] Burd NA, Tang JE, Moore DR, Phillips SM. Exercise training and protein metabolism: influences of contraction, protein intake, and sex-based differences. J Appl Physiol 2009;106:1692–701. https://doi.org/10.1152/japplphysiol.91351.2008.

[72] Burnet K, Kelsch E, Zieff G, Moore JB, Stoner L. How fitting is F.I.T.T.? A perspective on a transition from the sole use of frequency, intensity, time, and type in exercise prescription. Physiol Behav 2019;199:33–4. https://doi.org/10.1016/j.physbeh.2018.11.007.

[73] Buso A, Comelli M, Picco R, Isola M, Magnesa B, Grassi B, et al. Mitochondrial Adaptations in Elderly and Young Men Skeletal Muscle Following 2 Weeks of Bed Rest and Rehabilitation. Front Physiol 2019;10:1–18. https://doi.org/10.3389/fphys.2019.00474.

[74] Bustin SA, Benes V, Garson JA, Hellemans J, Huggett J, Kubista M, et al. The MIQE guidelines: Minimum information for publication of quantitative real-time PCR experiments. Clin Chem 2009;55:611–22. https://doi.org/10.1373/clinchem.2008.112797.

[75] Caillot-Augusseau A, Lafage-Proust MH, Soler C, Pernod J, Dubois F, Alexandre C. Bone formation and resorption biological markers in cosmonauts during and after a 180-day space flight (Euromir 95). Clin Chem 1998;44:578–85.

[76] Calder PC. Omega-3 fatty acids and inflammatory processes: From molecules to man. Biochem Soc Trans 2017;45:1105–15. https://doi.org/10.1042/BST20160474.

[77] Cannavino J, Brocca L, Sandri M, Bottinelli R, Pellegrino MA. PGC1-α over-expression prevents metabolic alterations and soleus muscle atrophy in hindlimb unloaded mice. J Physiol 2014;592:4575–89. https://doi.org/10.1113/jphysiol.2014.275545.

[78] Cannavino J, Brocca L, Sandri M, Grassi B, Bottinelli R, Pellegrino MA. The role of alterations in mitochondrial dynamics and PGC-1 α over-expression in fast muscle atrophy following hindlimb unloading. J Physiol 2015;8:1981–95. https://doi.org/10.1113/jphysiol.2014.286740.

[79] Cantó C, Auwerx J. PGC-1α, SIRT1 and AMPK, an energy sensing network that controls energy expenditure. Curr Opin Lipidol 2009;20:98–105. https://doi.org/10.1097/MOL.0b013e328328d0a4.

[80] Cantó C, Gerhart-Hines Z, Feige JN, Lagouge M, Noriega L, Milne JC, et al. AMPK regulates energy expenditure by modulating NAD+ metabolism and SIRT1 activity. Nature 2009;458:1056–60. https://doi.org/10.1038/nature07813.

[81] Canto C, Menzies KJ, Auwerx J. NAD+ metabolism and the control of energy homeostasis - a balancing act between mitochondria and the nucleus. Cell Metab 2015;22:31–53. https://doi.org/10.1016/j.cmet.2015.05.023.NAD.

[82] Capelli C, Antonutto G, Kenfack MA, Cautero M, Lador F, Moia C, et al. Factors determining the time course of V̇O2max decay during bedrest: Implications for V̇O2max limitation. Eur J Appl Physiol 2006;98:152–60. https://doi.org/10.1007/s00421-006-0252-3.

[83] Cardoso C, Afonso C, Bandarra NM. Dietary DHA and health: Cognitive function ageing. Nutr Res Rev 2016;29:281–94. https://doi.org/10.1017/S0954422416000184.

[84] Cartoni R, Léger B, Hock MB, Praz M, Crettenand A, Pich S, et al. Mitofusins 1/2 and ERRα expression are increased in human skeletal muscle after physical exercise. J Physiol 2005;567:349–58. https://doi.org/10.1113/jphysiol.2005.092031.

[85] Cescon C, Gazzoni M. Short term bed-rest reduces conduction velocity of individual motor units in leg muscles. J Electromyogr Kinesiol 2010;20:860–7. https://doi.org/10.1016/j.jelekin.2010.03.008.

[86] Chan ST, Chuang CH, Lin YC, Liao JW, Lii CK, Yeh SL. Quercetin enhances the antitumor effect of trichostatin A and suppresses muscle wasting in tumor-bearing mice. Food Funct 2018;9:871–9. https://doi.org/10.1039/c7fo01444a.

[87] Chang AR, Ferrer CM, Mostoslavsky R. SIRT6, a mammalian deacylase with multitasking abilities. Physiol Rev 2020;100:145–69. https://doi.org/10.1152/physrev.00030.2018.

[88] Chen C, Zhou M, Ge Y, Wang X. SIRT1 and aging related signaling pathways. Mech Ageing Dev 2020;187:111215. https://doi.org/10.1016/j.mad.2020.111215.

[89] Chen H, Chan DC. Mitochondrial dynamics-fusion, fission, movement, and mitophagy-in neurodegenerative diseases. Hum Mol Genet 2009;18:169–76. https://doi.org/10.1093/hmg/ddp326.

[90] Chen P, Yu Y, Tan C, Liu H, Wu F, Li H, et al. Human metabolic responses to microgravity simulated in a 45-day 6° head-down tilt bed rest (HDBR) experiment. Anal Methods 2016;8:4334–44. https://doi.org/10.1039/c6ay00644b.

[91] Chen Y, Dorn II GW. PINK1-Phosphorylated Mitofusin 2 Is a Parkin Receptor for Culling Damaged Mitochondria. Science (80-) 2013;340:471–6.

[92] Chomentowski P, Coen PM, Radiková Z, Goodpaster BH, Toledo FGS. Skeletal muscle mitochondria in insulin resistance: Differences in intermyofibrillar versus subsarcolemmal subpopulations and relationship to metabolic flexibility. J Clin Endocrinol Metab 2011;96:494–503. https://doi.org/10.1210/jc.2010-0822.

[93] Chopard A, Hillock S, Jasmin BJ. Molecular events and signalling pathways involved in skeletal muscle disuse-induced atrophy and the impact of countermeasures. J Cell Mol Med 2009;13:3032–50. https://doi.org/10.1111/j.1582-4934.2009.00864.x.

[94] Chorner Z, Barbeau PA, Castellani LC, Chorner DC, Chabowski A, Holloway GP. Dietary α-linolenic acid supplementation alters skeletal muscle plasma membrane lipid composition, sarcolemmal fat/cd36 abundance, and palmitate transport rates. Am J Physiol - Regul Integr Comp Physiol 2016;311:R1234–42. https://doi.org/10.1152/ajpregu.00346.2016.

[95] Churchward-Venne TA, Breen L, Di Donato DM, Hector AJ, Mitchell CJ, Moore DR, et al. Leucine supplementation of a low-protein mixed macronutrient beverage enhances myofibrillar protein synthesis in young men: A double-blind, randomized trial1-3. Am J Clin

Nutr 2014;99:276–86. https://doi.org/10.3945/ajcn.113.068775.

[96] Cipolat S, Rudka T, Hartmann D, Costa V, Serneels L, Craessaerts K, et al. Mitochondrial Rhomboid PARL Regulates Cytochrome c Release during Apoptosis via OPA1-Dependent Cristae Remodeling. Cell 2006;126:163–75. https://doi.org/10.1016/j.cell.2006.06.021.

[97] Cochrane DJ, Legg SJ, Hooker MJ. The Short-Term Effect of Whole-Body Vibration Training on Vertical Jump,Sprint, and Agility Performance. J Strength Cond Res 2004;18:828–32. https://doi.org/10.1519/00124278-200411000-00025.

[98] Coen PM, Menshikova E V, Distefano G, Zheng D, Tanner CJ, Standley RA, et al. Exercise and Weight Loss Improve Muscle Mitochondrial Respiration , Lipid Partitioning , and Insulin Sensitivity After Gastric Bypass Surgery. Diabetes 2015;64:3737–50. https://doi.org/10.2337/db15-0809.

[99] Cogswell AM, Stevens RJ, Hood DA. Properties of skeletal muscle mitochondria isolated from subsarcolemmal and intermyofibrillar regions. Am J Physiol - Cell Physiol 1993;264. https://doi.org/10.1152/ajpcell.1993.264.2.c383.

[100] Cohen S, Nathan JA, Goldberg AL. Muscle wasting in disease : molecular mechanisms and promising therapies. Nat Rev Drug Discov 2015;14:58–74. https://doi.org/10.1038/nrd4467.

[101] Colina-Tenorio L, Horten P, Pfanner N, Rampelt H. Shaping the mitochondrial inner membrane in health and disease. J Intern Med 2020;287:645–64. https://doi.org/10.1111/joim.13031.

[102] Connell NJ, Houtkooper RH, Schrauwen P. NAD + metabolism as a target for metabolic health: have we found the silver bullet? Diabetologia 2019;62:888–99. https://doi.org/10.1007/s00125-019-4831-3.

[103] Corpeleijn E, Saris WHM, Blaak EE. Metabolic flexibility in the development of insulin resistance and type 2 diabetes: Effects of lifestyle: Etiology and Pathophysiology. Obes Rev 2009;10:178–93. https://doi.org/10.1111/j.1467-789X.2008.00544.x.

[104] Crandall CG, Shibasaki M, Wilson TE, Cui J, Levine BD. Prolonged head-down tilt exposure reduces maximal cutaneous vasodilator and sweating capacity in humans. J Appl Physiol 2003;94:2330–6. https://doi.org/10.1152/japplphysiol.00790.2002.

[105] Cree MG, Paddon-Jones D, Newcomer BR, Ronsen O, Aarsland A, Wolfe RR, et al. Twenty-eight-day bed rest with hypercortisolemia induces peripheral insulin resistance and increases intramuscular triglycerides. Metabolism 2010;59:703–10. https://doi.org/10.1016/j.metabol.2009.09.014.

[106] Croft KD. Dietary polyphenols: Antioxidants or not? Arch Biochem Biophys 2016;595:120–4. https://doi.org/10.1016/j.abb.2015.11.014.

[107] Cui X, Yao L, Yang X, Gao Y, Fang F, Zhang J, et al. SIRT6 regulates metabolic homeostasis in skeletal muscle through activation of AMPK. Am J Physiol - Endocrinol Metab 2017;313:E493–505. https://doi.org/10.1152/ajpendo.00122.2017.

[108] Czubryt MP, McAnally J, Fishman GI, Olson EN. Regulation of peroxisome proliferator-activated receptor γ coactivator 1α (PGC-1α) and mitochondrial function by MEF2 and HDAC5. Proc Natl Acad Sci U S A 2003;100:1711–6. https://doi.org/10.1073/pnas.0337639100.

[109] Dai DF, Chiao YA, Marcinek DJ, Szeto HH, Rabinovitch PS. Mitochondrial oxidative stress in aging and healthspan. LongevHealthspan 2014;3:6.

[110] Dai W, Jiang L. Dysregulated Mitochondrial Dynamics and Metabolism in Obesity, Diabetes, and Cancer. Front Endocrinol (Lausanne) 2019;10:1–10. https://doi.org/10.3389/fendo.2019.00570.

[111] Dalla Libera L, Ravara B, Gobbo V, Tarricone E, Vitadello M, Biolo G, et al. A transient antioxidant stress response accompanies the onset of disuse atrophy in human skeletal muscle. J Appl Physiol 2009;107:549–57. https://doi.org/10.1152/japplphysiol.00280.2009.

[112] Damiot A, Demangel R, Noone J, Chery I, Zahariev A, Normand S, et al. A nutrient cocktail prevents lipid metabolism alterations induced by 20 days of daily steps reduction and fructose overfeeding : result from a randomized study. J Appl Physiol 2019;126:88–101. https://doi.org/10.1152/japplphysiol.00018.2018.

[113] Dangardt F, Chen Y, Gronowitz E, Dahlgren J, Friberg P, Strandvik B. High physiological omega-3 fatty acid supplementation affects muscle fatty acid composition and glucose and insulin homeostasis in obese adolescents. J Nutr Metab 2012;2012. https://doi.org/10.1155/2012/395757.

[114] Das S, Mitrovsky G, Vasanthi HR, Das DK. Antiaging properties of a grape-derived antioxidant are regulated by mitochondrial balance of fusion and fission leading to mitophagy triggered by a signaling network of sirt1-sirt3-foxo3-pink1-parkin. Oxid Med Cell Longev 2014;2014. https://doi.org/10.1155/2014/345105.

[115] Davies E, Stankovic B, Vian A, Wood AJ. Where has all the message gone? Plant Sci 2012;185–186:23–32. https://doi.org/10.1016/j.plantsci.2011.08.001.

[116] Davies RW, Carson BP, Jakeman PM. The effect of whey protein supplementation on the temporal recovery of muscle function following resistance training: A systematic review and meta-analysis. Nutrients 2018;10. https://doi.org/10.3390/nu10020221.

[117] Delecluse C, Roelants M, Verschueren S. Strength increase after whole-body vibration compared with resistance training. Med Sci Sports Exerc 2003;35:1033–41. https://doi.org/10.1249/01.MSS.0000069752.96438.B0.

[118] Demiryürek Ş, Babül A. Effects of vitamin E and electrical stimulation on the denervated rat gastrocnemius muscle malondialdehyde and glutathione levels. Int J Neurosci 2004;114:45–54. https://doi.org/10.1080/00207450490249374.

[119] Derbre F, Ferrando B, Gomez-Cabrera MC, Sanchis-Gomar F, Martinez-Bello VE, Olaso-Gonzalez G, et al. Inhibition of Xanthine Oxidase by Allopurinol Prevents Skeletal Muscle Atrophy: Role of p38 MAPKinase and E3 Ubiquitin Ligases. PLoS One 2012;7:1–9. https://doi.org/10.1371/journal.pone.0046668.

[120] Dickinson JM, Fry CS, Drummond MJ, Gundermann DM, Walker DK, Glynn EL, et al. Mammalian Target of Rapamycin Complex 1 Activation Is Required for the Stimulation of Human Skeletal Muscle Protein Synthesis by Essential Amino Acids. J Nutr 2011;141:856–62. https://doi.org/10.3945/jn.111.139485.

[121] Dillon EL, Sheffield-Moore M, Durham WJ, Ploutz-Snyder LL, Ryder JW, Danesi CP, et al. Efficacy of Testosterone plus NASA Exercise Countermeasures during Head-Down Bed Rest. Med Sci Sport Exerc 2018;50:1929–39.

[122] Dillon EL, Soman KV, Wiktorowicz JE, Sur R, Jupiter D, Danesi CP, et al. Proteomic investigation of human skeletal muscle before and after 70 days of head down bed rest with or without exercise and testosterone countermeasures. PLoS One 2019;14:1–38.

[123] Ding H, Jiang N, Liu H, Liu X, Liu D, Zhao F, et al. Response of mitochondrial fusion and fission protein gene expression to exercise in rat skeletal muscle. Biochim Biophys Acta - 2010;1800:250–6. https://doi.org/10.1016/j.bbagen.2009.08.007.

[124] Dirks ML, Wall BT, Snijders T, Ottenbros CLP, Verdijk LB, van Loon LJC. Neuromuscular electrical stimulation prevents muscle disuse atrophy during leg immobilization in humans. Acta Physiol 2014;210:628–41. https://doi.org/10.1111/apha.12200.

[125] Dirks ML, Wall BT, Van De Valk B, Holloway TM, Holloway GP, Chabowski A, et al. One week of bed rest leads to substantial muscle atrophy and induces whole-body insulin resistance in the absence of skeletal muscle lipid accumulation. Diabetes 2016;65:2862–75. https://doi.org/10.2337/db15-1661.

[126] Dolkas CB, Greenleaf JE. Insulin and glucose responses during bed rest with isotonic and isometric exercise. J Appl Physiol Respir Env Exerc Physiol 1977;43:1033–8.

[127] Dominy JE, Jr YL, Jedrychowski MP, Chim H, Michael J, Camporez JP, et al. The Deacetylase Sirt6 Activates the Acetyltransferase GCN5 and Suppresses Hepatic Gluconeogenesis. Mol Cells 2012;48:900–13. https://doi.org/10.1016/j.molcel.2012.09.030.The.

[128] Dorfman TA, Rosen BD, Perhonen MA, Tillery T, McColl R, Peshock RM, et al. Diastolic suction is impaired by bed rest: MRI tagging studies of diastolic untwisting. J Appl Physiol 2008;104:1037–44. https://doi.org/10.1152/japplphysiol.00858.2006.

[129] Downs ME, Scott JM, Ploutz-snyder LL, Ploutz-snyder R, Goetchius E, Buxton RE, et al. Exercise and Testosterone Countermeasures to Mitigate Metabolic Changes during Bed Rest. Life Sci Sp Res 2020;26:97–104. https://doi.org/10.1016/j.lssr.2020.03.008.

[130] Drake JC, Wilson RJ, Yan Z. Molecular mechanisms for mitochondrial adaptation to exercise training in skeletal muscle. FASEB J 2016;30:13–22. https://doi.org/10.1096/fj.15-276337.

[131] Drake LE, Springer MZ, Poole LP, Kim CJ, Macleod KF. Expanding perspectives on the significance of mitophagy in cancer. Semin Cancer Biol 2017;47:110–24. https://doi.org/10.1016/j.semcancer.2017.04.008.

[132] Drummond MJ, Dickinson JM, Fry CS, Walker DK, Gundermann DM, Reidy PT, et al. Bed rest impairs skeletal muscle amino acid transporter expression , mTORC1 signaling , and protein synthesis in response to essential amino acids in older adults. Am J Physiol

Endocrinol Metab 2012;302:1113–22. https://doi.org/10.1152/ajpendo.00603.2011.

[133] Dubé JJ, Amati F, Stefanovic-Racic M, Toledo FGS, Sauers SE, Goodpaster BH. Exercise-induced alterations in intramyocellular lipids and insulin resistance: the athlete's paradox revisited. Am J Physiol Endocrinol Metab 2008;294:882–8. https://doi.org/10.1152/ajpendo.00769.2007.

[134] Dudek J. Role of cardiolipin in mitochondrial signaling pathways. Front Cell Dev Biol 2017;5:1–17. https://doi.org/10.3389/fcell.2017.00090.

[135] Dulac M, Leduc-Gaudet JP, Reynaud O, Ayoub MB, Guérin A, Finkelchtein M, et al. Drp1 knockdown induces severe muscle atrophy and remodelling, mitochondrial dysfunction, autophagy impairment and denervation. J Physiol 2020;598:3691–710. https://doi.org/10.1113/JP279802.

[136] Dunstan DW, Healy GN, Sugiyama T, Owen N. Diabetes Prevention ' Too Much Sitting ' and Metabolic Risk – Has Modern Technology Caught Up with Us ? Eur Endocrinol 2010:1–5. https://doi.org/10.17925/EE.2010.06.00.19.

[137] Egan B, Carson BP, Garcia-Roves PM, Chibalin A V., Sarsfield FM, Barron N, et al. Exercise intensity-dependent regulation of peroxisome proliferator-activated receptor γ coactivator-1α mRNA abundance is associated with differential activation of upstream signalling kinases in human skeletal muscle. J Physiol 2010;588:1779–90. https://doi.org/10.1113/jphysiol.2010.188011.

[138] Egan B, Hawley JA, Zierath JR. SnapShot: Exercise Metabolism. Cell Metab 2016;24:342-342.e1. https://doi.org/10.1016/j.cmet.2016.07.013.

[139] Egan B, O'Connor PL, Zierath JR, O'Gorman DJ. Time Course Analysis Reveals Gene-Specific Transcript and Protein Kinetics of Adaptation to Short-Term Aerobic Exercise Training in Human Skeletal Muscle. PLoS One 2013;8. https://doi.org/10.1371/journal.pone.0074098.

[140] Ehses S, Raschke I, Mancuso G, Bernacchia A, Geimer S, Tondera D, et al. Regulation of OPA1 processing and mitochondrial fusion by m-AAA protease isoenzymes and OMA1. J Cell Biol 2009;187:1023–36. https://doi.org/10.1083/jcb.200906084.

[141] Engler MB, Engler MM. Docosahexaenoic Acid-Induced Vasorelaxation in Hypertensive Rats: Mechanisms of Action. Biol Res Nurs 2000;2:85–95.

https://doi.org/10.1177/109980040000200202.

[142] English KL, Mettler JA, Ellison JB, Mamerow MM, Arentson-Lantz E, Pattarini JM, et al. Leucine partially protects muscle mass and function during bed rest in middle-aged adults. Am J Clin Nutr 2016;103:465–73. https://doi.org/10.3945/ajcn.115.112359.

[143] FAO/WHO/UNU. Energy and protein requirements the 1985 report of the 1981 Joint FAO/WHO/UNU Expert Consultation. World Heal Organanisation Tech Rep Ser 1985:138–49. https://doi.org/10.1111/j.1467-3010.1987.tb00040.x.

[144] Fealy CE, Mulya A, Lai N, Kirwan JP. Exercise training decreases activation of the mitochondrial fission protein dynamin-related protein-1 in insulin-resistant human skeletal muscle. J Appl Physiol 2014;117:239–45. https://doi.org/10.1152/japplphysiol.01064.2013.

[145] Fernandez-Gonzalo R, Tesch PA, Lundberg TR, Alkner BA, Rullman E, Gustafsson T. Three months of bed rest induce a residual transcriptomic signature resilient to resistance exercise countermeasures. FASEB J 2020:1–12. https://doi.org/10.1096/fj.201902976R.

[146] Ferrando AA, Lane HW, Stuart CA, Davis-Street J, Wolfe RR. Prolonged bed rest decreases skeletal muscle and whole body protein synthesis. Am J Physiol - Endocrinol Metab 1996;270. https://doi.org/10.1152/ajpendo.1996.270.4.e627.

[147] Ferrando AA, Tipton KD, Bamman MM, Wolfe RR. Resistance exercise maintains skeletal muscle protein synthesis during bed rest. J Appl Physiol 1997;82:807–10. https://doi.org/10.1152/jappl.1997.82.3.807.

[148] Ferrannini E. The theoretical bases of indirect calorimetry: A review. Metabolism 1988;37:287–301. https://doi.org/10.1016/0026-0495(88)90110-2.

[149] Ferreira R, Vitorino R, Alves RMP, Appell HJ, Powers SK, Duarte JA, et al. Subsarcolemmal and intermyofibrillar mitochondria proteome differences disclose functional specializations in skeletal muscle. Proteomics 2010;10:3142–54. https://doi.org/10.1002/pmic.201000173.

[150] Fessler E, Eckl EM, Schmitt S, Mancilla IA, Meyer-Bender MF, Hanf M, et al. A pathway coordinated by DELE1 relays mitochondrial stress to the cytosol. Nature 2020;579:433–7. https://doi.org/10.1038/s41586-020-2076-4.

[151] Filichia E, Hoffer B, Qi X, Luo Y. Inhibition of Drp1 mitochondrial translocation provides neural protection in dopaminergic system in a Parkinson's disease model induced by MPTP. Sci Rep 2016;6:1–13. https://doi.org/10.1038/srep32656.

[152] Finkel T, Menazza S, Holmström KM, Parks RJ, Liu J, Sun J, et al. The Ins and Outs of Mitochondrial Calcium. Circ Res 2015;116:1810–9. https://doi.org/10.1161/CIRCRESAHA.116.305484.

[153] Fitts RH, Riley DR, Widrick JJ. Functional and structural adaptations of skeletal muscle to microgravity. J Exp Biol 2001;204:3201–8.

[154] Fletcher GF, Balady GJ, Amsterdam EA, Chaitman B, Eckel R, Fleg J, et al. Exercise Standards for Testing and Training. A Statement for Healthcare Professionals from the American Heart Association. Circulation 2001;6083:1694–740.

[155] Flis V V., Daum G. Lipid Transport between the Endoplasmic Reticulum and Mitochondria. Cold Spring Harb 2013:1–22.

[156] Floreani M, Rejc E, Taboga P, Ganzini A, Pišot R, Šimunič B, et al. Effects of 14 days of bed rest and following physical training on metabolic cost, mechanical work, and efficiency during walking in older and young healthy males. PLoS One 2018;13:1–18. https://doi.org/10.1371/journal.pone.0194291.

[157] Fortrat JO, Sigaudo D, Hughson RL, Maillet A, Yamamoto Y, Gharib C. Effect of prolonged head-down bed rest on complex cardiovascular dynamics. Auton Neurosci Basic Clin 2001;86:192–201. https://doi.org/10.1016/S1566-0702(00)00212-5.

[158] Fraga CG, Croft KD, Kennedy DO, Tomás-Barberán FA. The effects of polyphenols and other bioactives on human health. Food Funct 2019;10:514–28. https://doi.org/10.1039/c8fo01997e.

[159] Fransen M, Lismont C, Walton P. The peroxisome-mitochondria connection: How and why? Int J Mol Sci 2017;18. https://doi.org/10.3390/ijms18061126.

[160] Frayn KN. Calculation of substrate oxidation rates in vivo from gaseous exchange. J Appl Physiol 1983;55:628–34.

[161] Friedman JR, Nunnari J. Mitochondrial form and function. Nature 2014;505:335–43. https://doi.org/10.1038/nature12985.

[162] Fritzen AM, Lundsgaard AM, Kiens B. Tuning fatty acid oxidation in skeletal muscle with dietary fat and exercise. Nat Rev Endocrinol 2020;16:683–96. https://doi.org/10.1038/s41574-020-0405-1.

[163] Fu L, Dong Q, He J, Wang X, Xing J, Wang E, et al. SIRT4 inhibits malignancy progression of NSCLCs, through mitochondrial dynamics mediated by the ERK-Drp1 pathway. Oncogene 2017;36:2724–36. https://doi.org/10.1038/onc.2016.425.

[164] Fujii N, Hayashi T, Hirshman MF, Smith JT, Habinowski SA, Kaijser L, et al. Exercise induces isoform-specific increase in 5' AMP-activated protein kinase activity in human skeletal muscle. Biochem Biophys Res Commun 2000;273:1150–5. https://doi.org/10.1006/bbrc.2000.3073.

[165] Fujita S, Volpi E. Amino acids and muscle loss with aging. J Nutr 2006;136:1–8. https://doi.org/10.1093/jn/136.1.277s.

[166] Fulco M, Cen Y, Zhao P, Hoffman EP, McBurney MW, Sauve AA, et al. Glucose Restriction Inhibits Skeletal Myoblast Differentiation by Activating SIRT1 through AMPK-Mediated Regulation of Nampt. Dev Cell 2008;14:661–73. https://doi.org/10.1016/j.devcel.2008.02.004.

[167] Gambini J, Inglés M, Olaso G, Lopez-Grueso R, Bonet-Costa V, Gimeno-Mallench L, et al. Properties of Resveratrol: In Vitro and In Vivo Studies about Metabolism, Bioavailability, and Biological Effects in Animal Models and Humans. Oxid Med Cell Longev 2015;2015. https://doi.org/10.1155/2015/837042.

[168] Gao AW, Cantó C, Houtkooper RH. Mitochondrial response to nutrient availability and its role in metabolic disease. EMBO Mol Med 2014;6:580–9. https://doi.org/10.1002/emmm.201303782.

[169] Gao Y, Arfat Y, Wang H, Goswami N. Muscle Atrophy Induced by Mechanical Unloading : Mechanisms and Potential Countermeasures. Front Physiol 2018;9. https://doi.org/10.3389/fphys.2018.00235.

[170] Garcia-roves PM, Huss J, Holloszy JO, Garcia PM, Huss J, Holloszy JO. Role of calcineurin in exercise-induced mitochondrial biogenesis. Am J Physiol Endocrinol Metab 2006;290:1172–9. https://doi.org/10.1152/ajpendo.00633.2005.

[171] Garcia D, Shaw RJ. AMPK: mechanisms of cellular energy sensing and restoration of metabolic balance. Mol Cell 2017;66:789–800. https://doi.org/10.1016/j.molcel.2017.05.032.AMPK.

[172] Garman R, Rubin C, Judex S. Small oscillatory accelerations, independent of atrix deformations, increase osteoblast activity and enhance bone morphology. PLoS One 2007;2. https://doi.org/10.1371/journal.pone.0000653.

[173] Gawlowski T, Suarez J, Scott B, Torres-Gonzalez M, Wang H, Schwappacher R, et al. Modulation of dynamin-related protein 1 (DRP1) function by increased O-linked-β-N-acetylglucosamine modification (O-GlcNAc) in cardiac myocytes. J Biol Chem 2012;287:30024–34. https://doi.org/10.1074/jbc.M112.390682.

[174] Ge Y, Shi X, Boopathy S, McDonald J, Smith AW, Chao LH. Two forms of Opa1 cooperate to complete fusion of the mitochondrial inner-membrane. Elife 2019:1–14.

[175] Ghanim H, Sia CL, Abuaysheh S, Korzeniewski K, Patnaik P, Marumganti A, et al. An antiinflammatory and reactive oxygen species suppressive effects of an extract of Polygonum cuspidatum containing resveratrol. J Clin Endocrinol Metab 2010;95:1–8. https://doi.org/10.1210/jc.2010-0482.

[176] Ghanim H, Sia CL, Korzeniewski K, Lohano T, Abuaysheh S, Marumganti A, et al. A resveratrol and polyphenol preparation suppresses oxidative and inflammatory stress response to a high-fat, high-carbohydrate meal. J Clin Endocrinol Metab 2011;96:1409–14. https://doi.org/10.1210/jc.2010-1812.

[177] Giacomello M, Pyakurel A, Glytsou C, Scorrano L. The cell biology of mitochondrial membrane dynamics. Nat Rev Mol Cell Biol 2020;21:204–24. https://doi.org/10.1038/s41580-020-0210-7.

[178] Giangregorio L, Blimkie CJ. Skeletal Adaptations to Alterations in Weight-Bearing Activity. Sport Med 2002;32:459–76. https://doi.org/10.2165/00007256-200232070-00005.

[179] Gibson JNA, Halliday D, Morrison WL, Stoward PJ, Hornsby GA, Watt PW, et al. Decrease in human quadriceps muscle protein turnover consequent upon leg immobilization. Clin Sci 1987;72:503–9. https://doi.org/10.1042/cs0720503.

[180] Gibson JNA, Smith K, Rennie MJ. Prevention of Disuse Muscle Atrophy By Means of

Electrical Stimulation: Maintenance of Protein Synthesis. Lancet 1988;332:767–70. https://doi.org/10.1016/S0140-6736(88)92417-8.

[181] Giovarelli M, Zecchini S, Martini E, Garrè M, Barozzi S, Ripolone M, et al. Drp1 overexpression induces desmin disassembling and drives kinesin-1 activation promoting mitochondrial trafficking in skeletal muscle. Cell Death Differ 2020;27:2383–401. https://doi.org/10.1038/s41418-020-0510-7.

[182] Glauser L, Sonnay S, Stafa K, Moore DJ. Parkin promotes the ubiquitination and degradation of the mitochondrial fusion factor mitofusin 1. J Neurochem 2011;118:636–45. https://doi.org/10.1111/j.1471-4159.2011.07318.x.

[183] Gliemann L, Schmidt JF, Olesen J, Biensø RS, Peronard SL, Grandjean SU, et al. Resveratrol blunts the positive effects of exercise training on cardiovascular health in aged men. J Physiol 2013;591:5047–59. https://doi.org/10.1113/jphysiol.2013.258061.

[184] Glover EI, Phillips SM, Oates BR, Tang JE, Tarnopolsky MA, Selby A, et al. Immobilization induces anabolic resistance in human myofibrillar protein synthesis with low and high dose amino acid infusion. J Physiol 2008;586:6049–61. https://doi.org/10.1113/jphysiol.2008.160333.

[185] Gnaiger E. Polarographic oxygen sensors, the oxygraph and high-resolution respirometry to assess mitochondrial function. Drug-Induced Mitochondrial Dysfunct., 2008, p. 325–52.

[186] Gomes A, Fernandes E, Lima J, Mira L, Corvo M. Molecular Mechanisms of Anti-Inflammatory Activity Mediated by Flavonoids. Curr Med Chem 2008;15:1586–605. https://doi.org/10.2174/092986708784911579.

[187] Gomes LC, Benedetto G Di, Scorrano L. During autophagy mitochondria elongate, are spared from degradation and sustain cell viability. Nat Cell Biol 2011;13:589–98. https://doi.org/10.1038/ncb2220.

[188] Goodpaster BH, Sparks LM. Metabolic Flexibility in Health and Disease. Cell Metab 2017;25:1027–36. https://doi.org/10.1016/j.cmet.2017.04.015.

[189] Goodship AE, Lawes TJ, Rubin CT. Low-Magnitude High-Frequency Mechanical Signals Accelerate and Augment Endochondral Bone Repair: Preliminary Evidence of Efficacy. J Orthop Res 2009;27:922–30. https://doi.org/10.1002/jor.20824.Low-Magnitude.

[190] Gorostegi-Anduaga I, Corres P, MartinezAguirre-Betolaza A, Pérez-Asenjo J, Aispuru GR, Fryer SM, et al. Effects of different aerobic exercise programmes with nutritional intervention in sedentary adults with overweight/obesity and hypertension: EXERDIET-HTA study. Eur J Prev Cardiol 2018;25:343–53. https://doi.org/10.1177/2047487317749956.

[191] Greenleaf JE, Bernauer EM, Ertl AC, Trowbridge TS, Wade CE. Work capacity during 30 days of bed rest with isotonic and isokinetic exercise training. J Appl Physiol 1989;67:1820–6. https://doi.org/10.1152/jappl.1989.67.5.1820.

[192] Grichko VP, Heywood-Cooksey A, Kidd KR, Fitts RH. Substrate profile in rat soleus muscle fibers after hindlimb unloading and fatigue. J Appl Physiol 2000;88:473–8. https://doi.org/10.1152/jappl.2000.88.2.473.

[193] Groennebaek T, Nielsen J, Jespersen NR, Bøtker HE, Frank V. Utilization of biomarkers as predictors of skeletal muscle mitochondrial content after physiological intervention and in clinical settings. Am J Physiol - Endocrinol Metab 2020;318:886–9.

[194] Grune T, Merker K, Sandig G, Davies KJA. Selective degradation of oxidatively modified protein substrates by the proteasome. Biochem Biophys Res Commun 2003;305:709–18. https://doi.org/10.1016/S0006-291X(03)00809-X.

[195] de Guia RM, Agerholm M, Nielsen TS, Consitt LA, Søgaard D, Helge JW, et al. Aerobic and resistance exercise training reverses age-dependent decline in NAD+ salvage capacity in human skeletal muscle. Physiol Rep 2019;7:1–15. https://doi.org/10.14814/phy2.14139.

[196] Guinet P, MacNamara JP, Berry M, Larcher F, Bareille MP, Custaud MA, et al. MNX (Medium Duration Nutrition and Resistance-Vibration Exercise) Bed-Rest: Effect of Resistance Vibration Exercise Alone or Combined With Whey Protein Supplementation on Cardiovascular System in 21-Day Head-Down Bed Rest. Front Physiol 2020;11. https://doi.org/10.3389/fphys.2020.00812.

[197] Guo X, Badu-Mensah A, Thomas MC, McAleer CW, Hickman JJ. Characterization of functional human skeletal myotubes and neuromuscular junction derived-from the same induced pluripotent stem cell source. Bioengineering 2020;7:1–15. https://doi.org/10.3390/bioengineering7040133.

[198] Guo Z. Intramyocellular lipid kinetics and insulin resistance. Lipids Health Dis 2007;6:1–8. https://doi.org/10.1186/1476-511X-6-18.

[199] Guthold R, Stevens GA, Riley LM, Bull FC. Worldwide trends in insufficient physical activity from 2001 to 2016: a pooled analysis of 358 population-based surveys with 1·9 million participants. Lancet Glob Heal 2018;6:e1077–86. https://doi.org/10.1016/S2214-109X(18)30357-7.

[200] Guthold R, Stevens GA, Riley LM, Bull FC. Global trends in insufficient physical activity among adolescents: a pooled analysis of 298 population-based surveys with 1·6 million participants. Lancet Child Adolesc Heal 2020;4:23–35. https://doi.org/10.1016/S2352-4642(19)30323-2.

[201] Gutierrez-Salmean G, Ciaraldi TP, Nogueira L, Barboza J, Taub PR, Hogan MC, et al. Effects of (-)-epicatechin on molecular modulators of skeletal muscle growth and differentiation. J Nutr Biochem 2014;25:91–4. https://doi.org/10.1016/j.jnutbio.2013.09.007.

[202] Hamilton MT, Healy GN, Dunstan DW, Theodore W, Owen N. Too Little Exercise and the Need for New Recommendations on Sedentary Behavior. Curr Cardiovasc Risk Rep 2008;2:292–8. https://doi.org/10.1007/s12170-008-0054-8.Too.

[203] Han XJ, Lu YF, Li SA, Kaitsuka T, Sato Y, Tomizawa K, et al. CaM kinase Iα-induced phosphorylation of Drp1 regulates mitochondrial morphology. J Cell Biol 2008;182:573–85. https://doi.org/10.1083/jcb.200802164.

[204] Han Y, Lee H, Li H, Ryu JH. Corylifol a from psoralea corylifolia L. Enhances myogenesis and alleviates muscle atrophy. Int J Mol Sci 2020;21. https://doi.org/10.3390/ijms21051571.

[205] Han Y, Zhou S, Coetzee S, Chen A. Sirt4 and its roles in energy and redox metabolism in health, disease and during exercise. Front Physiol 2019;10. https://doi.org/10.3389/fphys.2019.01006.

[206] Handschin C. Caloric restriction and exercise “mimetics” Ready for prime time? Pharmacol Res 2016;103:158–66. https://doi.org/10.1016/j.phrs.2015.11.009.

[207] Hargens AR, Richardson S. Cardiovascular adaptations, fluid shifts, and countermeasures related to space flight. Respir Physiol Neurobiol 2009;169:30–3. https://doi.org/10.1016/j.resp.2009.07.005.

[208] Hargens AR, Vico L. Long-duration bed rest as an analog to microgravity. J Appl Physiol 2016;120:891–903. https://doi.org/10.1152/japplphysiol.00935.2015.

[209] Harman D. The Biologic Clock : The Mitochondria ? J Am Geriatr Soc 1972:145–7.

[210] Harman D. Aging: a theory based on free radical and radiation chemistry. J Gerontol 1956:298–300.

[211] Harridge SDR, Lazarus NR. Physical Activity, Aging, and Physiological Function. Physiology 2017;32:152–61. https://doi.org/10.1152/physiol.00029.2016.

[212] Hayashi T, Hirshman MF, Fujii N, Habinowski SA, Witters LA, Goodyear LJ. Metabolic Stress and Altered Glucose Transport Activation of AMP-Activated Protein Kinase as a Unifying Coupling Mechanism. Diabetes 2000;49:527–31.

[213] He J, Watkins S, Kelley DE. Skeletal muscle lipid content and oxidative enzyme activity in relation to muscle fiber type in type 2 diabetes and obesity. Diabetes 2001;50:817–23. https://doi.org/10.2337/diabetes.50.4.817.

[214] He L, He T, Farrar S, Ji L, Liu T, Ma X. Antioxidants Maintain Cellular Redox Homeostasis by Elimination of Reactive Oxygen Species. Cell Physiol Biochem 2017;44:532–53. https://doi.org/10.1159/000485089.

[215] He X, Duan Y, Yao K, Li F, Hou Y, Wu G, et al. β-Hydroxy-β-methylbutyrate, mitochondrial biogenesis, and skeletal muscle health. Amino Acids 2016;48:653–64. https://doi.org/10.1007/s00726-015-2126-7.

[216] Heiss C, Finis D, Kleinbongard P, Hoffmann A, Rassaf T, Kelm M, et al. Sustained increase in flow-mediated dilation after daily intake of high-flavanol cocoa drink over 1 week. J Cardiovasc Pharmacol 2007;49:74–80. https://doi.org/10.1097/FJC.0b013e31802d0001.

[217] Helge JW, Stallknecht B, Drachmann T, Hellgren LI, Jiménez-Jiménez R, Andersen JL, et al. Improved glucose tolerance after intensive life style intervention occurs without changes in muscle ceramide or triacylglycerol in morbidly obese subjects. Acta Physiol 2011;201:357–64. https://doi.org/10.1111/j.1748-1716.2010.02180.x.

[218] Helge JW, Tobin L, Drachmann T, Hellgren LI, Dela F, Galbo H, et al. Muscle ceramide content is similar after 3 weeks' consumption of fat or carbohydrate diet in a crossover design in patients with type 2 diabetes. Eur J Appl Physiol 2012;112:911–8. https://doi.org/10.1007/s00421-011-2041-x.

[219] Herbst EAF, Paglialunga S, Gerling C, Whitfield J, Mukai K, Chabowski A, et al. Omega-3

supplementation alters mitochondrial membrane composition and respiration kinetics in human skeletal muscle. J Physiol 2014;592:1341–52. https://doi.org/10.1113/jphysiol.2013.267336.

[220] Herzig S, Shaw RJ. AMPK: guardian of metabolism and mitochondrial homeostasis. Nat Rev Mol Cell Biol 2018;19:121–35. https://doi.org/10.1038/nrm.2017.95.AMPK.

[221] Ho L, Titus AS, Banerjee KK, George S, Lin W, Deota S, et al. SIRT4 regulates ATP homeostasis and mediates a retrograde signaling via AMPK. Aging (Albany NY) 2013;5:835–49. https://doi.org/10.18632/aging.100616.

[222] Hodgson JM, Croft KD. Tea flavonoids and cardiovascular health. Mol Aspects Med 2010;31:495–502. https://doi.org/10.1016/j.mam.2010.09.004.

[223] Hood DA, Memme JM, Oliveira AN, Triolo M. Maintenance of Skeletal Muscle Mitochondria in Health, Exercise, and Aging. Annu Rev Physiol 2019;81:19–41. https://doi.org/10.1146/annurev-physiol-020518-114310.

[224] Hoppeler H, Fluck M. Plasticity of skeletal muscle mitochondria: structure and function. Med Sci Sport Exerc 2003;35:95–104. https://doi.org/10.1249/01.MSS.0000043292.99104.12.

[225] Hortobagyi T, Dempsey L, Fraser D, Zheng D, Hamilton G, Lambert J, et al. Changes in muscle strength, muscle fibre. J Physiol 2000;524:293–304.

[226] Houtkooper RH, Pirinen E, Auwerx J. Sirtuins as regulators of metabolism and healthspan. Nat Rev Mol Cell Biol 2012;13:225–38. https://doi.org/10.1038/nrm3293.

[227] Houzelle A, Jörgensen JA, Schaart G, Daemen S, van Polanen N, Fealy CE, et al. Human skeletal muscle mitochondrial dynamics in relation to oxidative capacity and insulin sensitivity. Diabetologia 2021;64:424–36. https://doi.org/10.1007/s00125-020-05335-w.

[228] Hu C, Huang Y, Li L. Drp1-dependent mitochondrial fission plays critical roles in physiological and pathological progresses in mammals. Int J Mol Sci 2017;18. https://doi.org/10.3390/ijms18010144.

[229] Huang C, Ogawa R. Mechanotransduction in bone repair and regeneration. FASEB J 2010;24:3625–32. https://doi.org/10.1096/fj.10-157370.

[230] Huang TY, Zheng D, Houmard JA, Brault JJ, Hickner RC, Cortright RN. Overexpression of PGC-1α increases peroxisomal activity and mitochondrial fatty acid oxidation in human primary myotubes. Am J Physiol - Endocrinol Metab 2017;312:E253–63. https://doi.org/10.1152/ajpendo.00331.2016.

[231] Huey KA, Fiscus G, Richwine AF, Johnson RW, Meador BM. In vivo vitamin E administration attenuates interleukin-6 and interleukin-1β responses to an acute inflammatory insult in mouse skeletal and cardiac muscle. Exp Physiol 2008;93:1263–72. https://doi.org/10.1113/expphysiol.2008.043190.

[232] Huh JE, Shin JH, Jang ES, Park SJ, Park DR, Ko R, et al. Sirtuin 3 (SIRT3) maintains bone homeostasis by regulating AMPK-PGC-1β axis in mice. Sci Rep 2016;6:1–10. https://doi.org/10.1038/srep22511.

[233] Hwang SJ, Lublinsky S, Seo YK, Kim IS, Judex S. Extremely small-magnitude accelerations enhance bone regeneration: A preliminary study. Clin Orthop Relat Res 2009;467:1083–91. https://doi.org/10.1007/s11999-008-0552-5.

[234] Ihenacho UK, Meacham KA, Harwig MC, Widlansky ME, Hill RB. Mitochondrial Fission Protein 1: Emerging Roles in Organellar Form and Function in Health and Disease. Front Endocrinol (Lausanne) 2021;12:1–29. https://doi.org/10.3389/fendo.2021.660095.

[235] Indo HP, Majima HJ, Terada M, Suenaga S, Tomita K, Yamada S, et al. Changes in mitochondrial homeostasis and redox status in astronauts following long stays in space. Sci Rep 2016;6:1–10. https://doi.org/10.1038/srep39015.

[236] Iovino P, Chiarioni G, Bilancio G, Cirillo M, Mekjavic IB, Pisot R, et al. New Onset of Constipation during Long-Term Physical Inactivity: A Proof-of-Concept Study on the Immobility-Induced Bowel Changes. PLoS One 2013;8:1–8. https://doi.org/10.1371/journal.pone.0072608.

[237] Iqbal S, Ostojic O, Singh K, Joseph A-M, Hood DA. Expression of mitochondrial fission and fusion regulatory proteins in skeletal muscle during chronic use and disuse. Muscle Nerve 2013;48:963–70. https://doi.org/10.1002/mus.23838.

[238] Irimia JM, Guerrero M, Rodriguez-miguelez P, Cadefau JA, Tesch PA, Cussó R, et al. Metabolic adaptations in skeletal muscle after 84 days of bed rest with and without concurrent flywheel resistance exercise. J Appl Physiol 2017;122:96–103.

https://doi.org/10.1152/japplphysiol.00521.2016.

[239] Ishihara N, Fujita Y, Oka T, Mihara K. Regulation of mitochondrial morphology through proteolytic cleavage of OPA1. EMBO J 2006;25:2966–77. https://doi.org/10.1038/sj.emboj.7601184.

[240] Iwasaki KI, Zhang R, Zuckerman JH, Pawelczyk JA, Levine BD. Effect of head-down-tilt bed rest and hypovolemia on dynamic regulation of heart rate and blood pressure. Am J Physiol - Regul Integr Comp Physiol 2000;279:2189–99. https://doi.org/10.1152/ajpregu.2000.279.6.r2189.

[241] Iwasawa R, Mahul-Mellier AL, Datler C, Pazarentzos E, Grimm S. Fis1 and Bap31 bridge the mitochondria-ER interface to establish a platform for apoptosis induction. EMBO J 2011;30:556–68. https://doi.org/10.1038/emboj.2010.346.

[242] Jackson JR, Ryan MJ, Hao Y, Alway SE. Mediation of endogenous antioxidant enzymes and apoptotic signaling by resveratrol following muscle disuse in the gastrocnemius muscles of young and old rats. Am J Physiol - Regul Integr Comp Physiol 2010;299. https://doi.org/10.1152/ajpregu.00489.2010.

[243] Jäger S, Handschin C, St-Pierre J, Spiegelman BM. AMP-activated protein kinase (AMPK) action in skeletal muscle via direct phosphorylation of PGC-1α. Proc Natl Acad Sci U S A 2007;104:12017–22. https://doi.org/10.1073/pnas.0705070104.

[244] Janero DR. Therapeutic potential of vitamin E in the pathogenesis of spontaneous atherosclerosis. Free Radic Biol Med 1991;11:129–44. https://doi.org/10.1016/0891-5849(91)90193-7.

[245] Jepsen DB, Thomsen K, Hansen S, Jørgensen NR, Masud T, Ryg J. Effect of whole-body vibration exercise in preventing falls and fractures: A systematic review and meta-analysis. BMJ Open 2017;7. https://doi.org/10.1136/bmjopen-2017-018342.

[246] Jeromson S, Mackenzie I, Doherty MK, Whitfield PD, Bell G, Dick J, et al. Lipid remodeling and an altered membrane-associated proteome may drive the differential effects of EPA and DHA treatment on skeletal muscle glucose uptake and protein accretion. Am J Physiol - Endocrinol Metab 2018;314:E605–19. https://doi.org/10.1152/ajpendo.00438.2015.

[247] Jiang Q. Natural forms of vitamin E: Metabolism, antioxidant, and anti-inflammatory

activities and their role in disease prevention and therapy. Free Radic Biol Med 2014;72:76–90. https://doi.org/10.1016/j.freeradbiomed.2014.03.035.

[248] Jones JM, Player DJ, Martin NRW, Capel AJ, Lewis MP, Mudera V. An assessment of myotube morphology, matrix deformation, and myogenic mRNA expression in custom-built and commercially available engineered muscle chamber configurations. Front Physiol 2018;9:1–9. https://doi.org/10.3389/fphys.2018.00483.

[249] Jornayvaz F, Shulman G. Regulation of mitochondrial biogenesis. Essays Biochem 2010;47:69–84. https://doi.org/10.1042/bse0470069.Regulation.

[250] Judex S, Lei X, Han D, Rubin C. Low-magnitude mechanical signals that stimulate bone formation in the ovariectomized rat are dependent on the applied frequency but not on the strain magnitude. J Biomech 2007;40:1333–9. https://doi.org/10.1016/j.jbiomech.2006.05.014.

[251] Julien IB, Sephton CF, Dutchak PA. Metabolic networks influencing skeletal muscle fiber composition. Front Cell Dev Biol 2018;6:1–6. https://doi.org/10.3389/fcell.2018.00125.

[252] Kadowaki M, Kanazawa T. Amino Acids as Regulators of Proteolysis. J Nutr 2003:2052–6.

[253] Kahn BB, Flier JS, Kahn BB, Flier JS. Obesity and insulin resistance Find the latest version : Obesity and insulin resistance. J Clin Invest 2000;106:473–81. https://doi.org/10.1172/JCI10842.

[254] Kahn RC. Insulin resistance, insulin insensitivity, and insulin unresponsiveness: A necessary distinction. Metabolism 1978;27:1893–902. https://doi.org/10.1016/S0026-0495(78)80007-9.

[255] Kahn SE, Hull R., Utzschneider KM. Mechanisms Linking Obesity to Insulin Resistance and Type 2 Diabetes. Nat Insight Rev 2006;444:840–6.

[256] Kamolrat T, Gray SR. The effect of eicosapentaenoic and docosahexaenoic acid on protein synthesis and breakdown in murine C2C12 myotubes. Biochem Biophys Res Commun 2013;432:593–8. https://doi.org/10.1016/j.bbrc.2013.02.041.

[257] Kang C, Yeo D, Ji LL. Muscle immobilization activates mitophagy and disrupts mitochondrial dynamics in mice. Acta Physiol 2016:1–10. https://doi.org/10.1111/apha.12690.

[258] Karlsson HKR, Zierath JR. Insulin signaling and glucose transport in insulin resistant human skeletal muscle. Cell Biochem Biophys 2007;48:103–13. https://doi.org/10.1007/s12013-007-0030-9.

[259] Katzmarzyk PT, Janssen I. The Economic Costs Associated With Physical Inactivity and Obesity in Canada: An Update. Can J Appl Physiol 2004;29:90–115. https://doi.org/10.1139/h04-008.

[260] Kawakami Y, Akima H, Kubo K, Muraoka M, Hasegawa H, Kouzaki M, et al. Changes in muscle size , architecture , and neural activation after 20 days of bed rest with and without resistance exercise. Eur J Appl Physiol 2001;84:7–12.

[261] Kelley DE, He J, Menshikova E V., Ritov VB. Dysfunction of mitochondria in human skeletal muscle in type 2 diabetes. Diabetes 2002;51:2944–50. https://doi.org/10.2337/diabetes.51.10.2944.

[262] Kelley DE, Mandarin LJ, Mandarino LJ. Fuel selection in human skeletal muscle in insulin resistance: a reexamination. Diabetes 2000;49:677–83. https://doi.org/10.2337/diabetes.49.5.677.

[263] Kenny HC, Rudwill F, Breen L, Salanova M, Blottner D, Heise T, et al. Bed rest and resistive vibration exercise unveil novel links between skeletal muscle mitochondrial function and insulin resistance. Diabetologia 2017. https://doi.org/10.1007/s00125-017-4298-z.

[264] Kenny HC, Tascher G, Ziemianin A, Rudwill F, Zahariev A, Chery I, et al. Effectiveness of Resistive Vibration Exercise and Whey Protein Supplementation Plus Alkaline Salt on the Skeletal Muscle Proteome Following 21 Days of Bed Rest in Healthy Males. J Proteome Res 2020;19:3438–51. https://doi.org/10.1021/acs.jproteome.0c00256.

[265] Khan SR, Pearle MS, Robertson WG, Gambaro G, Canales BK, Doizi S, et al. Kidney stones. Nat Rev Dis Prim 2016;2. https://doi.org/10.1038/nrdp.2016.8.

[266] Khor SC, Abdul Karim N, Wan Ngah WZ, Mohd Yusof YA, Makpol S. Vitamin E in Sarcopenia: Current Evidences on its Role in Prevention and Treatment. Oxid Med Cell Longev 2014. https://doi.org/10.1155/2014/914853.

[267] Kim C, Hwang JK. Flavonoids: nutraceutical potential for counteracting muscle atrophy. Food Sci Biotechnol 2020;29:1619–40. https://doi.org/10.1007/s10068-020-00816-5.

[268] Kim Y, Triolo M, Hood DA. Impact of Aging and Exercise on Mitochondrial Quality Control in Skeletal Muscle. Oxid Med Cell Longev 2017;2017. https://doi.org/10.1155/2017/3165396.

[269] Kincaid B, Bossy-Wetzel E. Forever young: SIRT3 a shield against mitochondrial meltdown, aging, and neurodegeneration. Front Aging Neurosci 2013;5:1–13. https://doi.org/10.3389/fnagi.2013.00048.

[270] Kirkwood SP, Munn EA, Brooks GA. Mitochondrial reticulum in limb skeletal muscle. Am J Physiol - Cell Physiol 1986;251. https://doi.org/10.1152/ajpcell.1986.251.3.c395.

[271] Koltai E, Szabo Z, Atalay M, Boldogh I, Naito H, Goto S, et al. Exercise alters SIRT1, SIRT6, NAD and NAMPT levels in skeletal muscle of aged rats. Mech Ageing Dev 2010;131:21–8. https://doi.org/10.1016/j.mad.2009.11.002.

[272] Konda NN, Karri RS, Winnard A, Gradwell D, Velho RM, Nasser M. A comparison of exercise interventions from bed rest studies for the prevention of musculoskeletal loss. Npj Microgravity 2019;8. https://doi.org/10.1038/s41526-019-0073-4.

[273] Kondo H, Miura M, Itokawa Y. Oxidative stress in skeletal muscle atrophied by immobilization. Acta Physiol Scand 1991;142:527–8. https://doi.org/10.1111/j.1748-1716.1991.tb09191.x.

[274] Kondo H, Miura M, Kodama J, Ahmed SM, Itokawa Y. Role of iron in oxidative stress in skeletal muscle atrophied by immobilization. Pflügers Arch Eur J Physiol 1992;421:295–7. https://doi.org/10.1007/BF00374844.

[275] Kortebein P, Symons TB, Ferrando A, Paddon-Jones D, Ronsen O, Protas E, et al. Functional impact of 10 days of bed rest in healthy older adults. Journals Gerontol - Ser A Biol Sci Med Sci 2008;63:1076–81. https://doi.org/10.1093/gerona/63.10.1076.

[276] Krainski F, Hastings JL, Heinicke K, Romain N, Pacini EL, Snell PG, et al. The effect of rowing ergometry and resistive exercise on skeletal muscle structure and function during bed rest. J Appl Physiol 2014;116:1569–81. https://doi.org/10.1152/japplphysiol.00803.2013.

[277] Kramer A, Gollhofer A, Armbrecht G, Felsenberg D, Gruber M. How to prevent the detrimental effects of two months of bed-rest on muscle, bone and cardiovascular system: An RCT. Sci Rep 2017;7:1–10. https://doi.org/10.1038/s41598-017-13659-8.

[278] Kraus F, Ryan MT. The constriction and scission machineries involved in mitochondrial fission. J Cell Sci 2017;130:2953–60. https://doi.org/10.1242/jcs.199562.

[279] Kraus WE, Powell KE, Haskell WL, Janz KF, Campbell WW, Jakicic JM, et al. Physical Activity, All-Cause and Cardiovascular Mortality, and Cardiovascular Disease. Med Sci Sports Exerc 2019;51:1270–81. https://doi.org/10.1249/MSS.0000000000001939.

[280] Krishnan J, Danzer C, Simka T, Ukropec J, Walter KM, Kumpf S, et al. Dietary obesity-associated hif1α activation in adipocytes restricts fatty acid oxidation and energy expenditure via suppression of the Sirt2-NAD+ system. Genes Dev 2012;26:259–70. https://doi.org/10.1101/gad.180406.111.

[281] Kuang J, Chen L, Tang Q, Zhang J, Li Y, He J. The role of Sirt6 in obesity and diabetes. Front Physiol 2018;9:1–9. https://doi.org/10.3389/fphys.2018.00135.

[282] Kubo K, Akima H, Ushiyama J, Tabata I, Fukuoka H, Kanehisa H, et al. Effects of 20 days of bed rest on the viscoelastic properties of tendon structures in lower limb muscles. Br J Sports Med 2004;38:324–30. https://doi.org/10.1136/bjsm.2003.005595.

[283] Kühlbrandt W. Structure and function of mitochondrial membrane protein complexes. BMC Biol 2015:1–11. https://doi.org/10.1186/s12915-015-0201-x.

[284] Kumar V, Selby A, Rankin D, Patel R, Atherton P, Hildebrandt W, et al. Age-related differences in the dose-response relationship of muscle protein synthesis to resistance exercise in young and old men. J Physiol 2009;587:211–7. https://doi.org/10.1113/jphysiol.2008.164483.

[285] Kuznetsov A V., Schneeberger S, Seiler R, Brandacher G, Mark W, Steurer W, et al. Mitochondrial defects and heterogeneous cytochrome c release after cardiac cold ischemia and reperfusion. Am J Physiol - Hear Circ Physiol 2004;286:1633–41. https://doi.org/10.1152/ajpheart.00701.2003.

[286] Kuznetsov A V., Veksler V, Gellerich FN, Saks V, Margreiter R, Kunz WS. Analysis of mitochondrial function in situ in permeabilized muscle fibers, tissues and cells. Nat Protoc 2008;3:965–76. https://doi.org/10.1038/nprot.2008.61.

[287] Landstrom AP, Dobrev O, Wehrens XHT. Calcium Signaling and Cardiac Arrhythmias. Circ Res 2017;120:139–48. https://doi.org/10.1016/j.physbeh.2017.03.040.

[288] Lang A, Anand R, Altinoluk-Hambüchen S, Ezzahoini H, Stefanski A, Iram A, et al. SIRT4 interacts with OPA1 and regulates mitochondrial quality control and mitophagy. Aging (Albany NY) 2017;9:2160–86. https://doi.org/10.18632/aging.101307.

[289] Lang T, LeBlanc A, Evans H, Lu Y, Genant H, Yu A. Cortical and trabecular bone mineral loss from the spine and hip in long-duration spaceflight. J Bone Miner Res 2004;19:1006–12. https://doi.org/10.1359/JBMR.040307.

[290] Larsen S, Skaaby S, Helge JW, Dela F. Effects of exercise training on mitochondrial function in patients with type 2 diabetes. World J Diabetes 2014;5:482. https://doi.org/10.4239/wjd.v5.i4.482.

[291] Larsen S, Lundby AKM, Dandanell S, Oberholzer L, Keiser S, Andersen AB, et al. Four days of bed rest increases intrinsic mitochondrial respiratory capacity in young healthy males. Physiol Rep 2018;6:1–9. https://doi.org/10.14814/phy2.13793.

[292] Larsen S, Nielsen J, Hansen CN, Nielsen LB, Wibrand F, Schroder HD, et al. Biomarkers of mitochondrial content in skeletal muscle of healthy young human subjects. J Physiol 2012;590:3349–60. https://doi.org/10.1113/jphysiol.2012.230185.

[293] Lau E, Lee WD, Li J, Xiao A, Davies JE, Wu Q, et al. Effect of low-magnitude, high-frequency vibration on osteogenic differentiation of rat mesenchymal stromal cells. J Orthop Res 2011;29:1075–80. https://doi.org/10.1002/jor.21334.

[294] Laurent G, German NJ, Saha AK, de Boer VCJ, Davies M, Koves TR, et al. SIRT4 coordinates the balance between lipid synthesis and catabolism by repressing malonyl CoA decarboxylase. Mol Cell 2013;50:686–98. https://doi.org/10.1016/j.molcel.2013.05.012.

[295] Lavie CJ, Ozemek C, Carbone S, Katzmarzyk PT, Blair SN. Sedentary Behavior, Exercise, and Cardiovascular Health. Circ Res 2019:799–815. https://doi.org/10.1161/CIRCRESAHA.118.312669.

[296] LeBlanc AD, Driscol TB, Shackelford LC, Evans HJ, Rianon NJ, Smith SM, et al. Alendronate as an effective countermeasure to disuse induced bone loss. J Musculoskelet Neuronal Interact 2002;2:335–43.

[297] LeBlanc AD, Schneider VS, Evans HJ, Pientok C, Rowe R, Spector E. Regional changes in muscle mass following 17 weeks of bed rest. J Appl Physiol 1992;73:2172–8.

https://doi.org/10.1152/jappl.1992.73.5.2172.

[298] LeBlanc A, Schneider V, Spector E, Evans H, Rowe R, Lane H, et al. Calcium absorption, endogenous excretion, and endocrine changes during and after long-term bed rest. Bone 1995;16:4–7. https://doi.org/10.1016/S8756-3282(95)80193-6.

[299] LeBlanc AD, Evans HJ, Schneider VS, Wendt RE, Hedrick TD. Changes in IVD cross sectional area with bedrest and space flight. Spine (Phila Pa 1976) 1994;19:812–7.

[300] LeBlanc A, Schneider V, Shackelford L, West S, Oganov V, Bakulin A, et al. Bone mineral and lean tissue loss after long duration space flight. J Musculoskelet Neuronal Interact 2000;1:157–60.

[301] Lee D, Goldberg AL. SIRT1 protein, by blocking the activities of transcription factors FoxO1 and FoxO3, inhibits muscle atrophy and promotes muscle growth. J Biol Chem 2013;288:30515–26. https://doi.org/10.1074/jbc.M113.489716.

[302] Lee H, Lim JY, Choi SJ. Oleate Prevents Palmitate-Induced Atrophy via Modulation of Mitochondrial ROS Production in Skeletal Myotubes. Oxid Med Cell Longev 2017;2017. https://doi.org/10.1155/2017/2739721.

[303] Lee IM, Shiroma EJ, Lobelo F, Puska P, Blair SN, Katzmarzyk PT, et al. Effect of physical inactivity on major non-communicable diseases worldwide: An analysis of burden of disease and life expectancy. Lancet 2012;380:219–29. https://doi.org/10.1016/S0140-6736(12)61031-9.

[304] Lee IH. Mechanisms and disease implications of sirtuin-mediated autophagic regulation. Exp Mol Med 2019;51. https://doi.org/10.1038/s12276-019-0302-7.

[305] Lee JE, Westrate LM, Wu H, Page C, Voeltz GK. Multiple dynamin family members collaborate to drive mitochondrial division. Nature 2016;540:139–43. https://doi.org/10.1038/nature20555.

[306] Lee SMC, Moore AD, Everett ME, Stenger MB, Platts SH. Aerobic exercise deconditioning and countermeasures during bed rest. Aviat Sp Environ Med 2010;81:52–63. https://doi.org/10.3357/ASEM.2474.2010.

[307] Lee SMC, Schneider SM, Feiveson AH, Macias BR, Smith SM, Watenpaugh DE, et al. WISE-2005: Countermeasures to prevent muscle deconditioning during bed rest in women. J

Appl Physiol 2014;116:654–67. https://doi.org/10.1152/japplphysiol.00590.2013.

[308] Lee YJ, Hee G, Sang K, Park I, Hyun J. Down - regulation of the mitochondrial i - AAA protease Yme1L induces muscle atrophy via FoxO3a and myostatin activation. J Cell Mol Med 2019:1–11. https://doi.org/10.1111/jcmm.14799.

[309] Leek BT, Mudaliar SRD, Henry R, Mathieu-costello O, Richardson RS, Bryan T, et al. Effect of acute exercise on citrate synthase activity in untrained and trained human skeletal muscle. Am J Physiol - Regul Integr Comp Physiol 2001;280:441–7.

[310] Lembo A, Camilleri M. Chronic constipation. N Engl J Med 2003;349:1360–8. https://doi.org/10.3928/0090-4481-19871001-07.

[311] Lemos V, de Oliveira RM, Naia L, Szegö É, Ramos E, Pinho S, et al. The NAD+-dependent deacetylase SIRT2 attenuates oxidative stress and mitochondrial dysfunction and improves insulin sensitivity in hepatocytes. Hum Mol Genet 2017;26:4105–17. https://doi.org/10.1093/hmg/ddx298.

[312] Levy SE, Chen Y, Graham BH, Wallace DC. Expression and sequence analysis of the mouse adenine nucleotide translocase 1 and 2 genes. Genes (Basel) 2000;254:57–66.

[313] Li J, Wang Y, Wang Y, Wen X, Ma XN, Chen W, et al. Pharmacological activation of AMPK prevents Drp1-mediated mitochondrial fission and alleviates endoplasmic reticulum stress-associated endothelial dysfunction. J Mol Cell Cardiol 2015;86:62–74. https://doi.org/10.1016/j.yjmcc.2015.07.010.

[314] Li M, Zhao L, Liu J, Liu A, Jia C, Ma D, et al. Multi-mechanisms are involved in reactive oxygen species regulation of mTORC1 signaling. Cell Signal 2010;22:1469–76. https://doi.org/10.1016/j.cellsig.2010.05.015.

[315] Liemburg-Apers DC, Wagenaars JAL, Smeitink JAM, Willems PHGM, Koopman WJH. Acute stimulation of glucose influx upon mitoenergetic dysfunction requires LKB1, AMPK, Sirt2 and mTOR-RAPTOR. J Cell Sci 2016;129:4411–23. https://doi.org/10.1242/jcs.194480.

[316] Liesa M, Van der Bliek A, Shirihai OS. To Fis or not to Fuse? This is the question! EMBO J 2019;38:2–4. https://doi.org/10.15252/embj.2019101839.

[317] Liphardt A, Brüggemann G, Bolte V, Eckstein F. Response of thigh muscle cross-sectional area to 21-days of bed rest with exercise and nutrition countermeasures. Transl Sport Med

2019;3:93–106. https://doi.org/10.1002/tsm2.122.

[318] Lipman RL, Raskin P, Love T, Triebwasser J, Lecocq FR, Schnure JJ. Glucose intolerance during decreased physical activity in man. Diabetes 1972;21:101–7. https://doi.org/10.2337/diab.21.2.101.

[319] Lipnicki DM, Hanns-Christian G, Belavy DL, Felsenberg D. Bed Rest and Cognition: Effects on Executive Functioning and Reaction Time. Aviat Sp Environ Med 2009;80:1018–22.

[320] Liu G, Park SH, Imbesi M, Nathan WJ, Zou X, Zhu Y, et al. Loss of NAD-Dependent Protein Deacetylase Sirtuin-2 Alters Mitochondrial Protein Acetylation and Dysregulates Mitophagy. Antioxidants Redox Signal 2017;26:846–63. https://doi.org/10.1089/ars.2016.6662.

[321] Liu R, Chan DC. OPA1 and cardiolipin team up for mitochondrial fusion. Nat Cell Biol 2017;19:760–2. https://doi.org/10.1038/ncb3565.

[322] Liu YJ, McIntyre RL, Janssens GE, Houtkooper RH. Mitochondrial fission and fusion : A dynamic role in aging and potential target for age-related disease. Mech Ageing Dev 2020;186:111212. https://doi.org/10.1016/j.mad.2020.111212.

[323] Lobley GE. Species Comparisons of Tissue Protein Metabolism: Effects of Age and Hormonal Action. J Nutr 1993;123:337–43. https://doi.org/10.1093/jn/123.suppl_2.337.

[324] Logan SL, Spriet LL. Omega-3 fatty acid supplementation for 12 weeks increases resting and exercise metabolic rate in healthy community- dwelling older females. PLoS One 2015;10:1–18. https://doi.org/10.1371/journal.pone.0144828.

[325] van Loon LJC. Intramuscular triacylglycerol as a substrate source during exercise. J Appl Physiol 2004;97:1170–87. https://doi.org/10.1152/japplphysiol.00368.2004.

[326] Losón OC, Song Z, Chen H, Chan DC. Fis1, Mff, MiD49, and MiD51 mediate Drp1 recruitment in mitochondrial fission. Mol Biol Cell 2013;24:659–67. https://doi.org/10.1091/mbc.E12-10-0721.

[327] Lueken SA, Arnaud SB, Taylor AK, Baylink DJ. Changes in markers of bone formation and resorption in a bed rest model of weightlessness. J Bone Miner Res 1993;8:1433–8. https://doi.org/10.1002/jbmr.5650081204.

[328] MacVicar T, Langer T. OPA1 processing in cell death and disease - the long and short of it. J Cell Sci 2016;129:2297–306. https://doi.org/10.1242/jcs.159186.

[329] Madreiter-Sokolowski CT, Ramadani-Muja J, Ziomek G, Burgstaller S, Bischof H, Koshenov Z, et al. Tracking intra- and inter-organelle signaling of mitochondria. FEBS J 2019;286:4378–401. https://doi.org/10.1111/febs.15103.

[330] Magne H, Savary-Auzeloux I, Rémond D, Dardevet D. Nutritional strategies to counteract muscle atrophy caused by disuse and to improve recovery. Nutr Res Rev 2013;26:149–65. https://doi.org/10.1017/S0954422413000115.

[331] Mannari C, Bertelli AAE, Stiaccini G, Giovannini L. Wine, sirtuins and nephroprotection: Not only resveratrol. Med Hypotheses 2010;75:636–8. https://doi.org/10.1016/j.mehy.2010.08.004.

[332] Mao X, Zeng X, Huang Z, Wang J, Qiao S. Leptin and leucine synergistically regulate protein metabolism in C2C12 myotubes and mouse skeletal muscles. Br J Nutr 2013;110:256–64. https://doi.org/10.1017/S0007114512004849.

[333] Marzetti E, Hwang JCY, Lees HA, Wohlgemuth SE, Dupont-Versteegden EE, Carter CS, et al. Mitochondrial death effectors: Relevance to sarcopenia and disuse muscle atrophy. Biochim Biophys Acta - Gen Subj 2010;1800:235–44. https://doi.org/10.1016/j.bbagen.2009.05.007.

[334] Mathias RA, Greco TM, Oberstein A, Budayeva HG, Chakrabarti R, Rowland EA, et al. Sirtuin 4 is a lipoamidase regulating pyruvate dehydrogenase complex activity. Cell 2014;159:1615–25. https://doi.org/10.1016/j.cell.2014.11.046.

[335] Mattie S, Krols M, McBride HM. The enigma of an interconnected mitochondrial reticulum: new insights into mitochondrial fusion. Curr Opin Cell Biol 2019;59:159–66. https://doi.org/10.1016/j.ceb.2019.05.004.

[336] McGlory C, Calder PC, Nunes EA. The Influence of Omega-3 Fatty Acids on Skeletal Muscle Protein Turnover in Health, Disuse, and Disease. Front Nutr 2019;6:1–13. https://doi.org/10.3389/fnut.2019.00144.

[337] McGlory C, Gorissen SHM, Kamal M, Bahniwal R, Hector AJ, Baker SK, et al. Omega-3 fatty acid supplementation attenuates skeletal muscle disuse atrophy during two weeks of

unilateral leg immobilization in healthy young women. FASEB J 2019;33:4586–97. https://doi.org/10.1096/fj.201801857RRR.

[338] Memme JM, Slavin M, Moradi N, Hood DA. Mitochondrial bioenergetics and turnover during chronic muscle disuse. Int J Mol Sci 2021;22. https://doi.org/10.3390/ijms22105179.

[339] Menshikova E V, Ritov VB, Fairfull L, Ferrell RE, David E, Goodpaster BH. Effects of Exercise on Mitochondrial Content and Function in Aging Human Skeletal Muscle. J Gerontol 2006;61:534–40.

[340] Di Meo S, Iossa S, Venditti P. Improvement of obesity-linked skeletal muscle insulin resistance by strength and endurance training. J Endocrinol 2017;234:159–81. https://doi.org/10.1530/JOE-17-0186.

[341] Meyer JN, Leuthner TC, Luz AL. Mitochondrial fusion, fission, and mitochondrial toxicity. Toxicology 2017;391:42–53. https://doi.org/10.1016/j.tox.2017.07.019.

[342] Min Z, Gao J, Yu Y. The roles of mitochondrial SIRT4 in cellular metabolism. Front Endocrinol (Lausanne) 2019;10:1–8. https://doi.org/10.3389/fendo.2018.00783.

[343] Miquel J, Economos AC, Fleming J, Johnson JE. Mitochondrial role in cell aging. Exp Gerontol 1980;15:575–91. https://doi.org/10.1016/0531-5565(80)90010-8.

[344] Mitchell JH, Levine BD, McGuire D. The Dallas Bed Rest and Training Study. Revisited After 50 Years. Circulation 2019;140:1293–5. https://doi.org/10.1161/CIRCULATIONAHA.119.041046.

[345] Mittendorfer B, Andersen JL, Plomgaard P, Saltin B, Babraj JA, Smith K, et al. Protein synthesis rates in human muscles: Neither anatomical location nor fibre-type composition are major determinants. J Physiol 2005;563:203–11. https://doi.org/10.1113/jphysiol.2004.077180.

[346] Mizushima N, Levine B, Cuervo AM, Klionsky DJ. Autophagy fights disease through cellular. Nat Rev 2008;451:1069–75. https://doi.org/10.1038/nature06639.

[347] Momken I, Stevens L, Bergouignan a., Desplanches D, Rudwill F, Chery I, et al. Resveratrol prevents the wasting disorders of mechanical unloading by acting as a physical exercise mimetic in the rat. FASEB J 2011;25:3646–60. https://doi.org/10.1096/fj.10-177295.

[348] Montgomery MK. Mitochondrial dysfunction and diabetes: Is mitochondrial transfer a friend or foe? Biology (Basel) 2019;8. https://doi.org/10.3390/biology8020033.

[349] Moore TM, Zhou Z, Cohn W, Norheim F, Lin AJ, Kalajian N, et al. The impact of exercise on mitochondrial dynamics and the role of Drp1 in exercise performance and training adaptations in skeletal muscle. Mol Metab 2019;21:51–67. https://doi.org/10.1016/j.molmet.2018.11.012.

[350] Mootha VK, Handschin C, Arlow D, Xie X, Pierre JS, Sihag S, et al. Err alpha and Gabpa/b specify PGC-1 alpha-dependent oxidative phosphorylation gene expression that is altered in diabetic muscle. PNAS 2004;101:6570–5.

[351] Morales PE, Bucarey JL, Espinosa A. Muscle lipid metabolism: Role of lipid droplets and perilipins. J Diabetes Res 2017;2017. https://doi.org/10.1155/2017/1789395.

[352] Moriggi M, Vasso M, Fania C, Capitanio D, Bonifacio G, Salanova M, et al. Long term bed rest with and without vibration exercise countermeasures : Effects on human muscle protein dysregulation. Proteomics 2010;10:3756–74. https://doi.org/10.1002/pmic.200900817.

[353] Morigi M, Perico L, Benigni A. Sirtuins in Renal Health and Disease. J Am Soc Nephrol 2018;29:1799–809. https://doi.org/10.1681/ASN.2017111218.

[354] Morita M, Prudent J, Basu K, Goyon V, Katsumura S, Hulea L, et al. mTOR Controls Mitochondrial Dynamics and Cell Survival via MTFP1. Mol Cell 2017;67:922-935.e5. https://doi.org/10.1016/j.molcel.2017.08.013.

[355] Mortensen OH, Frandsen L, Schjerling P, Nishimura E, Grunnet N. PGC-1α and PGC-1β have both similar and distinct effects on myofiber switching toward an oxidative phenotype. Am J Physiol - Endocrinol Metab 2006;291:807–16. https://doi.org/10.1152/ajpendo.00591.2005.

[356] Mukai R, Horikawa H, Lin PY, Tsukumo N, Nikawa T, Kawamura T, et al. 8-Prenylnaringenin promotes recovery from immobilization-induced disuse muscle atrophy through activation of the Akt phosphorylation pathway in mice. Am J Physiol - Regul Integr Comp Physiol 2016;311:R1022–31. https://doi.org/10.1152/ajpregu.00521.2015.

[357] Mukai R, Nakao R, Yamamoto H, Nikawa T, Takeda E, Terao J. Quercetin prevents

unloading-derived disused muscle atrophy by attenuating the induction of ubiquitin ligases in tail-suspension mice. J Nat Prod 2010;73:1708–10. https://doi.org/10.1021/np100240y.

[358] Mulavara AP, Peters BT, Miller CA, Kofman IS, Reschke MF, Taylor LC, et al. Physiological and Functional Alterations after Spaceflight and Bed Rest. Med Sci Sports Exerc 2018;50:1961–80. https://doi.org/10.1249/MSS.0000000000001615.

[359] Mulder E, Linnarsson D, Paloski WH, Rittweger J, Wuyts FL, Zange J, et al. Effects of five days of bed rest with and without exercise countermeasure on postural stability and gait. J Musculoskelet Neuronal Interact 2014;14:359–66.

[360] Mulder ER, Horstman AM, Stegeman DF, De Haan A, Belavý DL, Miokovic T, et al. Influence of vibration resistance training on knee extensor and plantar flexor size, strength, and contractile speed characteristics after 60 days of bed rest. J Appl Physiol 2009;107:1789–98. https://doi.org/10.1152/japplphysiol.00230.2009.

[361] Murphy MP, Smith RAJ. Targeting antioxidants to mitochondria by conjugation to lipophilic cations. Annu Rev Pharmacol Toxicol 2007;47:629–56. https://doi.org/10.1146/annurev.pharmtox.47.120505.105110.

[362] Murrant CL, Reid MB. Detection of reactive oxygen and reactive nitrogen species in skeletal muscle. Microsc Res Tech 2001;55:236–48. https://doi.org/10.1002/jemt.1173.

[363] Napolitano G, Fasciolo G, Meo S Di, Venditti P. Vitamin e supplementation and mitochondria in experimental and functional hyperthyroidism: A mini-review. Nutrients 2019;11. https://doi.org/10.3390/nu11122900.

[364] Narayanankutty A, Kottekkat A, Mathew SE, Illam SP, Suseela IM, Raghavamenon AC. Vitamin E supplementation modulates the biological effects of omega-3 fatty acids in naturally aged rats. Toxicol Mech Methods 2017;27:207–14. https://doi.org/10.1080/15376516.2016.1273431.

[365] Narici M V, Boer MD De. Disuse of the musculo-skeletal system in space and on earth. Eur J Appl Physiol 2011;111:403–20. https://doi.org/10.1007/s00421-010-1556-x.

[366] Nasrin N, Wu X, Fortier E, Feng Y, Baré OC, Chen S, et al. SIRT4 regulates fatty acid oxidation and mitochondrial gene expression in liver and muscle cells. J Biol Chem 2010;285:31995–2002. https://doi.org/10.1074/jbc.M110.124164.

[367] Nemoto S, Fergusson MM, Finkel T. SIRT1 functionally interacts with the metabolic regulator and transcriptional coactivator PGC-1α. J Biol Chem 2005;280:16456–60. https://doi.org/10.1074/jbc.M501485200.

[368] Nguyen TN, Padman BS, Lazarou M. Deciphering the Molecular Signals of PINK1 / Parkin Mitophagy. Trends Cell Biol 2016;26:733–44. https://doi.org/10.1016/j.tcb.2016.05.008.

[369] Nicholls DG. Forty years of Mitchell's proton circuit: From little grey books to little grey cells. Biochim Biophys Acta - Bioenerg 2008;1777:550–6. https://doi.org/10.1016/j.bbabio.2008.03.014.

[370] Nielsen J, Suetta C, Hvid LG, Schrøder HD, Aagaard P, Ørtenblad N. Subcellular localization-dependent decrements in skeletal muscle glycogen and mitochondria content following short-term disuse in young and old men. Am J Physiol - Endocrinol Metab 2010;299:1053–60. https://doi.org/10.1152/ajpendo.00324.2010.

[371] Nikolić N, Rhedin M, Rustan AC, Storlien L, Thoresen GH, Strömstedt M. Overexpression of PGC-1α increases fatty acid oxidative capacity of human skeletal muscle cells. Biochem Res Int 2012;2012. https://doi.org/10.1155/2012/714074.

[372] O'Gorman DJ, Karlsson HKR, McQuaid S, Yousif O, Rahman Y, Gasparro D, et al. Exercise training increases insulin-stimulated glucose disposal and GLUT4 (SLC2A4) protein content in patients with type 2 diabetes. Diabetologia 2006;49:2983–92. https://doi.org/10.1007/s00125-006-0457-3.

[373] O'Leary MFN, Vainshtein A, Carter HN, Zhang Y, Hood DA. Denervation-induced mitochondrial dysfunction and autophagy in skeletal muscle of apoptosis-deficient animals. Am J Physiol - Cell Physiol 2012;303:447–54. https://doi.org/10.1152/ajpcell.00451.2011.

[374] Ohba Y, MacVicar T, Langer T. Regulation of mitochondrial plasticity by the i-AAA protease YME1L. Biol Chem 2020;401:877–90. https://doi.org/10.1515/hsz-2020-0120.

[375] Okada A, Ohshima H, Itoh Y, Yasui T, Tozawa K, Kohri K. Risk of renal stone formation induced by long-term bed rest could be decreased by premedication with bisphosphonate and increased by resistive exercise. Int J Urol 2008;15:630–5. https://doi.org/10.1111/j.1442-2042.2008.02067.x.

[376] Olesen J, Gliemann L, Biensø R, Schmidt J, Hellsten Y, Pilegaard H. Exercise training, but not resveratrol, improves metabolic and inflammatory status in skeletal muscle of aged men. J Physiol 2014;592:1873–86. https://doi.org/10.1113/jphysiol.2013.270256.

[377] De Oliveria M, Liesa M. The Role of Mitochondrial Fat Oxidation in Cancer Cell Proliferation and Survival. Cells 2020;9.

[378] Olson EN, Williams RS. Calcineurin Signaling and Muscle Remodeling. Cell 2000;101:689–92.

[379] Onoue K, Jofuku A, Ban-Ishihara R, Ishihara T, Maeda M, Koshiba T, et al. Fis1 acts as a mitochondrial recruitment factor for TBC1D15 that is involved in regulation of mitochondrial morphology. J Cell Sci 2013;126:176–85. https://doi.org/10.1242/jcs.111211.

[380] Otsuka Y, Egawa K, Kanzaki N, Izumo T, Rogi T, Shibata H. Quercetin glycosides prevent dexamethasone-induced muscle atrophy in mice. Biochem Biophys Reports 2019;18:100618. https://doi.org/10.1016/j.bbrep.2019.100618.

[381] Owens J, Moreira K, Bain G. Characterization of primary human skeletal muscle cells from multiple commercial sources. Vitr Cell Dev Biol - Anim 2013;49:695–705. https://doi.org/10.1007/s11626-013-9655-8.

[382] Palacios OM, Carmona JJ, Michan S, Chen KY, Manabe Y, Ward JL, et al. Diet and exercise signals regulate SIRT3 and activate AMPK and PGC-1alpha in skeletal muscle. Aging (Albany NY) 2009;1:771–83. https://doi.org/10.18632/aging.100075.

[383] Pannu N, Bhatnagar A. Resveratrol: from enhanced biosynthesis and bioavailability to multitargeting chronic diseases. Biomed Pharmacother 2019;109:2237–51. https://doi.org/10.1016/j.biopha.2018.11.075.

[384] Parra V, Verdejo HE, Iglewski M, Del Campo A, Troncoso R, Jones D, et al. Insulin stimulates mitochondrial fusion and function in cardiomyocytes via the AktmTOR-NFkB-Opa-1 signaling pathway. Diabetes 2014;63:75–88. https://doi.org/10.2337/db13-0340.

[385] Parry SM, Puthucheary ZA. The impact of extended bed rest on the musculoskeletal system in the critical care environment. Extrem Physiol Med 2015;4:1–8. https://doi.org/10.1186/s13728-015-0036-7.

[386] Pasqualini M, Lavet C, Elbadaoui M, Vanden-Bossche A, Laroche N, Gnyubkin V, et al. Skeletal site-specific effects of whole body vibration in mature rats: From deleterious to beneficial frequency-dependent effects. Bone 2013;55:69–77. https://doi.org/10.1016/j.bone.2013.03.013.

[387] Passerieux E, Hayot M, Jaussent A, Carnac G, Gouzi F, Pillard F, et al. Effects of vitamin C, vitamin E, zinc gluconate, and selenomethionine supplementation on muscle function and oxidative stress biomarkers in patients with facioscapulohumeral dystrophy: A double-blind randomized controlled clinical trial. Free Radic Biol Med 2015;81:158–69. https://doi.org/10.1016/j.freeradbiomed.2014.09.014.

[388] Peker N, Donipadi V, Sharma M, McFarlane C, Kambadur R. Loss of Parkin impairs mitochondrial function and leads to muscle atrophy. Am J Physiol - Cell Physiol 2018;315:C164–85. https://doi.org/10.1152/ajpcell.00064.2017.

[389] Perhonen MA, Franco F, Lane LD, Buckey JC, Blomqvist CG, Zerwekh JE, et al. Cardiac atrophy after bed rest and spaceflight. J Appl Physiol 2001;91:645–53. https://doi.org/10.1152/jappl.2001.91.2.645.

[390] Perry BMC, Tampion W, Lucy JA. The Interaction of Insulin with Phospholipids. Biochem J 1971;125:179–87.

[391] Perry CGR, Lally J, Holloway GP, Heigenhauser GJF, Bonen A, Spriet LL. Repeated transient mRNA bursts precede increases in transcriptional and mitochondrial proteins during training in human skeletal muscle. J Physiol 2010;588:4795–810. https://doi.org/10.1113/jphysiol.2010.199448.

[392] Pesta D, Gnaiger E. High-Resolution Respirometry: OXPHOS Protocols for Human Cells and Permeabilized Fibers from Small Biopsies of Human Muscle. vol. 810. 2012. https://doi.org/10.1007/978-1-61779-382-0.

[393] Petersen MC, Shulman GI. Mechanisms of Insulin Action and Insulin Resistance. Physiol Rev 2018;98:2133–223. https://doi.org/10.1152/physrev.00063.2017.

[394] Petersen N, Jaekel P, Rosenberger A, Weber T, Scott J, Castrucci F, et al. Exercise in space : the European Space Agency approach to in - flight exercise countermeasures for long - duration missions on ISS. Extrem Physiol Med 2016;5:1–13. https://doi.org/10.1186/s13728-016-0050-4.

[395] Pfluger PT, Kabra DG, Aichler M, Schriever SC, Pfuhlmann K, García VC, et al. Calcineurin Links Mitochondrial Elongation with Energy Metabolism. Cell Metab 2015;22:838–50. https://doi.org/10.1016/j.cmet.2015.08.022.

[396] Phillips SM, Glover EI, Rennie MJ. Alterations of protein turnover underlying disuse atrophy in human skeletal muscle. J Appl Physiol 2009;107:645–54. https://doi.org/10.1152/japplphysiol.00452.2009.

[397] Phillips SM, McGlory C. CrossTalk proposal: The dominant mechanism causing disuse muscle atrophy is decreased protein synthesis. J Physiol 2014;24:5341–3. https://doi.org/10.1113/jphysiol.2014.273615.

[398] Picca A, Lezza AMS, Leeuwenburgh C, Pesce V, Calvani R, Landi F, et al. Fueling inflamm-aging through mitochondrial dysfunction: Mechanisms and molecular targets. Int J Mol Sci 2017;18. https://doi.org/10.3390/ijms18050933.

[399] Pich S, Bach D, Briones P, Liesa M, Camps M, Testar X, et al. The Charcot-Marie-Tooth type 2A gene product, Mfn2, up-regulates fuel oxidation through expression of OXPHOS system. Hum Mol Genet 2005;14:1405–15. https://doi.org/10.1093/hmg/ddi149.

[400] Pickrell AM, Youle RJ. The Roles of PINK1, Parkin and Mitochondrial Fidelity in Parkinson's Disease. Neuron 2015;85:257–73. https://doi.org/10.1016/j.neuron.2014.12.007.The.

[401] Pieczenik SR, Neustadt J. Mitochondrial dysfunction and molecular pathways of disease. Exp Mol Pathol 2007;83:84–92. https://doi.org/10.1016/j.yexmp.2006.09.008.

[402] Piercy KL, Troiano RP, Ballard RM, Carlson SA, Fulton JE, Galuska DA, et al. The Physical Activity Guidelines for Americans. J Am Med Assoc 2018;320:2020–8. https://doi.org/10.1001/jama.2018.14854.

[403] Pillon NJ, Gabriel BM, Dollet L, Smith JAB, Puig LS, Botella J, et al. Transcriptomic profiling of skeletal muscle adaptations to exercise and inactivity. Nat Commun 2020;11. https://doi.org/10.1038/s41467-019-13869-w.

[404] Platts SH, Martin DS, Stenger MB, Perez SA, Ribeiro LC, Summers R, et al. Cardiovascular Adaptations to Long-Duration Head-Down Bed Rest. Aviat Space Environ Med 2009;80:A29–36. https://doi.org/10.3357/asem.br03.2009.

[405] Ploutz-Snyder LL, Downs M, Goetchius E, Crowell B, English KL, Ploutz-Snyder R, et al.

Exercise Training Mitigates Multisystem Deconditioning During Bed Rest. Med Sci Sport Exerc 2018.

[406] Polletta L, Vernucci E, Carnevale I, Arcangeli T, Rotili D, Palmerio S, et al. SIRT5 regulation of ammonia-induced autophagy and mitophagy. Autophagy 2015;11:253–70. https://doi.org/10.1080/15548627.2015.1009778.

[407] Powers SK. Can Antioxidants Protect Against Disuse Muscle Atrophy? Sport Med 2014;44:155–65. https://doi.org/10.1007/s40279-014-0255-x.

[408] Powers SK, Kavazis AN, DeRuisseau KC. Mechanisms of disuse muscle atrophy : role of oxidative stress. Am J Physiol - Regul Integr Comp Physiol 2012;288:R377–R344. https://doi.org/10.1152/ajpregu.00469.2004.

[409] Powers SK, Wiggs MP, Duarte JA, Zergeroglu MA, Demirel HA. Mitochondrial signaling contributes to disuse muscle atrophy. Am J Physiol - Endocrinol Metab 2012;303:31–9. https://doi.org/10.1152/ajpendo.00609.2011.

[410] Powers SK, Morton AB, Ahn B, Smuder AJ. Redox Control of Skeletal Muscle Atrophy. Free Radic Biol Med 2016;98:208–17. https://doi.org/10.1089/ars.2016.6782.

[411] Powers SK, Smuder AJ, Criswell DS. Mechanistic links between oxidative stress and disuse muscle atrophy. Antioxidants Redox Signal 2011;15:2519–28. https://doi.org/10.1089/ars.2011.3973.

[412] Price NL, Gomes AP, Ling AJY, Duarte F V., Martin-Montalvo A, North BJ, et al. SIRT1 is required for AMPK activation and the beneficial effects of resveratrol on mitochondrial function. Cell Metab 2012;15:675–90. https://doi.org/10.1016/j.cmet.2012.04.003.

[413] Prochaska M, Taylor E, Vaidya A, Curhan G. Low Bone Density and Bisphosphonate Use and the Risk of Kidney Stones. Clin J Am Soc Nephrol 2017;12:1284–90. https://doi.org/10.1016/j.juro.2017.09.092.

[414] Procházková D, Boušová I, Wilhelmová N. Antioxidant and prooxidant properties of flavonoids. Fitoterapia 2011;82:513–23. https://doi.org/10.1016/j.fitote.2011.01.018.

[415] Prudent J, McBride HM. Mitochondrial Dynamics: ER Actin Tightens the Drp1 Noose. Curr Biol 2016;26:R207–9. https://doi.org/10.1016/j.cub.2016.01.009.

[416] Puntschart A, Hoppeler H, Billeter R, Jostarndt K. mRNAs of enzymes involved in energy metabolism and mtDNA are increased in endurance-trained athletes. Am J Physiol Physiol 1995;269:619–25.

[417] Qiao A, Wang K, Yuan Y, Guan Y, Ren X, Li L, et al. Sirt3-mediated mitophagy protects tumor cells against apoptosis under hypoxia. Oncotarget 2016;7:43390–400. https://doi.org/10.18632/oncotarget.9717.

[418] Quirós PM, Ramsay AJ, Sala D, Fernández-Vizarra E, Rodríguez F, Peinado JR, et al. Loss of mitochondrial protease OMA1 alters processing of the GTPase OPA1 and causes obesity and defective thermogenesis in mice. EMBO J 2012;31:2117–33. https://doi.org/10.1038/emboj.2012.70.

[419] Rabøl R, Larsen S, Højberg PMV, Almdal T, Boushel R, Haugaard SB, et al. Regional anatomic differences in skeletal muscle mitochondrial respiration in type 2 diabetes and obesity. J Clin Endocrinol Metab 2010;95:857–63. https://doi.org/10.1210/jc.2009-1844.

[420] Radak Z, Suzuki K, Posa A, Petrovszky Z, Koltai E, Boldogh I. The systemic role of SIRT1 in exercise mediated adaptation. Redox Biol 2020:101467. https://doi.org/10.1016/j.redox.2020.101467.

[421] Rambold AS, Kostelecky B, Elia N, Lippincott-Schwartz J. Tubular network formation protects mitochondria from autophagosomal degradation during nutrient starvation. Proc Natl Acad Sci U S A 2011;108:10190–5. https://doi.org/10.1073/pnas.1107402108.

[422] Rana A, Oliveira MP, Khamoui A V, Aparicio R, Rera M, Rossiter HB, et al. Promoting Drp1-mediated mitochondrial fission in melanogaster. Nat Commun 2017;8:1–14. https://doi.org/10.1038/s41467-017-00525-4.

[423] Randle PJ, Garland PB, Hales CN, Newsholme EA. The Glucose Fatty-Acid Cycle: Its Role in Insulin Sensitivity and the Metabolic Disturbances of Diabetes Mellitus. Lancet 1963;281:785–9. https://doi.org/10.1016/S0140-6736(63)91500-9.

[424] Rao ZY, Wu XT, Liang BM, Wang MY, Hu W. Comparison of five equations for estimating resting energy expenditure in Chinese young, normal weight healthy adults. Eur J Med Res 2012;17:1. https://doi.org/10.1186/2047-783X-17-26.

[425] Raubenheimer E, Miniggio H, Lemmer L, van Heerden W. The Role of Bone Remodelling in

Maintaining and Restoring Bone Health: an Overview. Clin Rev Bone Miner Metab 2017;15:90–7. https://doi.org/10.1007/s12018-017-9230-z.

[426] Reddy PH. Inhibitors of Mitochondrial Fission as a Therapeutic Strategy for Diseases with Oxidative Stress and Mitochondrial Dysfunction. J Alzheimers Dis 2014;40:245–56. https://doi.org/10.3233/JAD-132060.Inhibitors.

[427] Reid MB, Haack KE, Franchek KM, Valberg PA, Kobzik L, West MS. Reactive oxygen in skeletal muscle. I. Intracellular oxidant kinetics and fatigue in vitro. J Appl Physiol 1992;73:1797–804. https://doi.org/10.1152/jappl.1992.73.5.1797.

[428] Reid MB, Shoji T, Moody MR, Entman ML. Reactive oxygen in skeletal muscle. II. Extracellular release of free radicals. J Appl Physiol 1992;73:1805–9. https://doi.org/10.1152/jappl.1992.73.5.1805.

[429] Rejc E, Floreani M, Taboga P, Botter A, Toniolo L, Cancellara L, et al. Loss of maximal explosive power of lower limbs after 2 weeks of disuse and incomplete recovery after retraining in older adults. J Physiol 2018;596:647–65. https://doi.org/10.1113/JP274772.

[430] Rejc E, di Prampero PE, Lazzer S, Grassi B, Simunic B, Pisot R, et al. Maximal explosive power of the lower limbs before and after 35 days of bed rest under different diet energy intake. Eur J Appl Physiol 2015;115:429–36. https://doi.org/10.1007/s00421-014-3024-5.

[431] Rezuş E, Burlui A, Cardoneanu A, Rezuş C, Codreanu C, Pârvu M, et al. Inactivity and Skeletal Muscle Metabolism: A Vicious Cycle in Old Age. Int J Mol Sci 2020;21:592. https://doi.org/10.3390/ijms21020592.

[432] Richter EA, Hargreaves M. Exercise, GLUT4, and skeletal muscle glucose uptake. Physiol Rev 2013;93:993–1017. https://doi.org/10.1152/physrev.00038.2012.

[433] Richter EA, Ruderman NB. AMPK and the biochemistry of exercise: Implications for human health and disease. Biochem J 2009;418:261–75. https://doi.org/10.1136/bmj.1.5388.980.

[434] Ried-Larsen M, Aarts HM, Joyner MJ. Effects of strict prolonged bed rest on cardiorespiratory fitness: Systematic review and meta-analysis. J Appl Physiol 2017;123:790–9. https://doi.org/10.1152/japplphysiol.00415.2017.

[435] Ringholm S, Biensø RS, Kiilerich K, Guadalupe-grau A, Aachmann-andersen NJ, Saltin B, et al. Bed rest reduces metabolic protein content and abolishes exercise-induced mRNA

responses in human skeletal muscle. Am J Physiol Endocrinol Metab 2011;301:649–58. https://doi.org/10.1152/ajpendo.00230.2011.

[436] Ritov VB, Menshikova E V, He J, Ferrell RE, Goodpaster BH, Kelley DE. Mitochondrial deficiency in Obesity and Type 2 Diabetes 2004;54:8–14.

[437] Rittweger J. Vibration as an exercise modality: How it may work, and what its potential might be. Eur J Appl Physiol 2010;108:877–904. https://doi.org/10.1007/s00421-009-1303-3.

[438] Rittweger J, Beller G, Felsenberg D. Acute physiological effects of exhaustive whole-body vibration exercise in man. Clin Physiol 2000;20:134–42. https://doi.org/10.1046/j.1365-2281.2000.00238.x.

[439] Rittweger J, Frost HM, Schiessl H, Ohshima H, Alkner B, Tesch P, et al. Muscle atrophy and bone loss after 90 days ' bed rest and the effects of flywheel resistive exercise and pamidronate : Results from the LTBR study. Bone 2005;36:1019–29. https://doi.org/10.1016/j.bone.2004.11.014.

[440] Rittweger J, Albracht K, Flück M, Ruoss S, Brocca L, Longa E, et al. Sarcolab pilot study into skeletal muscle's adaptation to longterm spaceflight. Npj Microgravity 2018;4. https://doi.org/10.1038/s41526-018-0052-1.

[441] Rivera-Brown AM, Frontera WR. Principles of Exercise Physiology : Responses to Acute Exercise and Long-term Adaptations to Training. PMRJ 2012;4:797–804. https://doi.org/10.1016/j.pmrj.2012.10.007.

[442] Rizzoli R, Bonjour JP. Hormones and bones. Lancet 1997;349:20–3. https://doi.org/10.1016/s0140-6736(97)90007-6.

[443] Rocchi A, Milioto C, Parodi S, Armirotti A, Borgia D, Pellegrini M, et al. Glycolytic-to-oxidative fiber-type switch and mTOR signaling activation are early-onset features of SBMA muscle modified by high-fat diet. Acta Neuropathol 2016;132:127–44. https://doi.org/10.1007/s00401-016-1550-4.

[444] Rocha AG, Franco A, Krezel AM, Rumsey JM, Alberti JM, Knight WC, et al. MFN2 agonists reverse mitochondrial defects in preclinical models of Charcot-Marie-Tooth disease type 2A. Science (80-) 2018;360:336–41. https://doi.org/10.1126/science.aao1785.

[445] Rodacki CLN, Rodacki ALF, Pereira G, Naliwaiko K, Coelho I, Pequito D, et al. Fish-oil supplementation enhances the effects of strength training in elderly women. Am J Clin Nutr 2012;95:428–36. https://doi.org/10.3945/ajcn.111.021915.

[446] Rodgers JT, Lerin C, Gerhart-Hines Z, Puigserver P. Metabolic adaptations through the PGC-1α and SIRT1 pathways. FEBS Lett 2008;582:46–53. https://doi.org/10.1016/j.febslet.2007.11.034.

[447] Roichman A, Kanfi Y, Glazz R, Naiman S, Amit U, Landa N, et al. SIRT6 overexpression improves various aspects of mouse healthspan. Journals Gerontol - Ser A Biol Sci Med Sci 2017;72:603–15. https://doi.org/10.1093/gerona/glw152.

[448] Romanello V, Guadagnin E, Gomes L, Roder I, Sandri C, Petersen Y, et al. Mitochondrial fission and remodelling contributes to muscle atrophy. EMBO J 2010;29:1774–85. https://doi.org/10.1038/emboj.2010.60.

[449] Romanello V, Sandri M. The connection between the dynamic remodeling of the mitochondrial network and the regulation of muscle mass. Cell Mol Life Sci 2021;78:1305–28. https://doi.org/10.1007/s00018-020-03662-0.

[450] Romanello V, Scalabrin M, Albiero M, Blaauw B, Scorrano L, Sandri M. Inhibition of the Fission Machinery Mitigates OPA1 Impairment in Adult Skeletal Muscles. Cells 2019;8:597. https://doi.org/10.3390/cells8060597.

[451] Rothman S. How is the balance between protein synthesis and degradation achieved ? Theor Biol Med Model 2010:1–11.

[452] Le Roux E, De Jong N, Blanc S, Simon C, Bessesen DH, Bergouignan A. Physiology of physical inactivity, sedentary behaviors and non-exercise activity: Insights from space bedrest model. J Physiol 2021;0:1–15. https://doi.org/10.1113/jp281064.

[453] Rovira-Llopis S, Bañuls C, Diaz-Morales N, Hernandez-Mijares A, Rocha M, Victor VM. Mitochondrial dynamics in type 2 diabetes: Pathophysiological implications. Redox Biol 2017;11:637–45. https://doi.org/10.1016/j.redox.2017.01.013.

[454] Rudwill F, O'Gorman D, Lefai E, Chery I, Zahariev A, Normand S, et al. Metabolic Inflexibility Is an Early Marker of Bed-Rest–Induced Glucose Intolerance Even When Fat Mass Is Stable. J Clin Endocrinol Metab 2018;103:1910–20. https://doi.org/10.1210/jc.2017-02267.

[455] Salanova M, Schiffl G, Püttmann B, Schoser BG, Blottner D. Molecular biomarkers monitoring human skeletal muscle fibres and microvasculature following long-term bed rest with and without countermeasures. J Anat 2008;212:306–18. https://doi.org/10.1111/j.1469-7580.2008.00854.x.

[456] Salanova M, Gambara G, Moriggi M, Vasso M, Ungethuem U. Vibration mechanosignals superimposed to resistive exercise result in baseline skeletal muscle transcriptome profiles following chronic disuse in bed rest. Sci Rep 2015;5:1–15. https://doi.org/10.1038/srep17027.

[457] Salem N, Litman B, Kim H, Gawrisch K. Mechanisms of Action of Docosahexaenoic Acid in the Nervous System. Lipids 2001;36:945–59. https://doi.org/10.1007/s11745-001-0805-6.

[458] Samant SA, Zhang HJ, Hong Z, Pillai VB, Sundaresan NR, Wolfgeher D, et al. SIRT3 Deacetylates and Activates OPA1 To Regulate Mitochondrial Dynamics during Stress. Mol Cell Biol 2014;34:807–19. https://doi.org/10.1128/mcb.01483-13.

[459] Sanders CE. Cardiovascular and Peripheral Vascular Diseases. Treatment by a Motorized Oscillating Bed. J Am Med Assoc 1936;106:205–7.

[460] Di Sante G, Pestell TG, Casimiro MC, Bisetto S, Powell MJ, Lisanti MP, et al. Loss of sirt1 promotes prostatic intraepithelial neoplasia, reduces mitophagy, and delays park2 translocation to mitochondria. Am J Pathol 2015;185:266–79. https://doi.org/10.1016/j.ajpath.2014.09.014.

[461] Dos Santos VOA, Browne RAV, Souza DC, Matos VAF, Macêdo GAD, Farias-Junior LF, et al. Effects of high-intensity interval and moderate-intensity continuous exercise on physical activity and sedentary behavior levels in inactive obese males: A crossover trial. J Sport Sci Med 2019;18:390–8.

[462] Satoh A, Brace CS, Rensing N, Cliften P, Wozniak DF, Herzog ED, et al. Sirt1 extends life span and delays aging in mice through the regulation of Nk2 Homeobox 1 in the DMH and LH. Cell Metab 2013;18:416–30. https://doi.org/10.1016/j.cmet.2013.07.013.

[463] Satoh M, Hamamoto T, Seo N, Kagawa Y, Endo H. Differential sublocalization of the dynamin-related protein OPA1 isoforms in mitochondria. Biochem Biophys Res Commun 2003;300:482–93. https://doi.org/10.1016/S0006-291X(02)02874-7.

[464] Schroeter H, Heiss C, Balzer J, Kleinbongard P, Keen CL, Hollenberg NK, et al. (-)-Epicatechin mediates beneficial effects of flavanol-rich cocoa on vascular function in humans. PNAS 2006;103:1024–9. https://doi.org/10.1073/pnas.0510168103.

[465] Schwalm C, Deldicque L, Francaux M. Lack of activation of mitophagy during endurance exercise in human. Med Sci Sports Exerc 2017;49:1552–61. https://doi.org/10.1249/MSS.0000000000001256.

[466] Seabright AP, Lai YC. Regulatory Roles of PINK1-Parkin and AMPK in Ubiquitin-Dependent Skeletal Muscle Mitophagy. Front Physiol 2020;11:1–11. https://doi.org/10.3389/fphys.2020.608474.

[467] Sebastián D, Palacín M, Zorzano A. Mitochondrial Dynamics : Coupling Mitochondrial Fitness with Healthy Aging. Trends Mol Med 2017;23:201–15. https://doi.org/10.1016/j.molmed.2017.01.003.

[468] Seibel MJ. Nutrition and molecular markers of bone remodelling. Curr Opin Clin Nutr Metab Care 2002;5:525–31. https://doi.org/10.1097/00075197-200209000-00011.

[469] Serasinghe MN, Chipuk JE. Mitochondrial Fission in Human Diseases. Handb Exp Pharmacol 2017;240:159–88. https://doi.org/10.1007/164.

[470] Servais S, Letexier D, Favier R, Duchamp C, Desplanches D. Prevention of unloading-induced atrophy by vitamin E supplementation: Links between oxidative stress and soleus muscle proteolysis? Free Radic Biol Med 2007;42:627–35. https://doi.org/10.1016/j.freeradbiomed.2006.12.001.

[471] Shibasaki M, Wilson TE, Cui J, Levine BD, Crandall CG. Exercise throughout 6° head-down tilt bed rest preserves thermoregulatory responses. J Appl Physiol 2003;95:1817–23. https://doi.org/10.1152/japplphysiol.00188.2003.

[472] Silva DF, Esteves AR, Oliveira CR, Cardoso SM. Mitochondrial Metabolism Power SIRT2-Dependent Deficient Traffic Causing Alzheimer's-Disease Related Pathology. Mol Neurobiol 2017;54:4021–40. https://doi.org/10.1007/s12035-016-9951-x.

[473] Singh CK, Chhabra G, Ndiaye MA, Garcia-Peterson LM, MacK NJ, Ahmad N. The Role of Sirtuins in Antioxidant and Redox Signaling. Antioxidants Redox Signal 2018;28:643–61. https://doi.org/10.1089/ars.2017.7290.

[474] Siu PM, Donley DA, Bryner RW, Alway SE, Parco M, Donley DA, et al. Citrate synthase expression and enzyme activity after endurance training in cardiac and skeletal muscles. J Appl Physiol 2003;94:555–60.

[475] Skelly LE, Gillen JB, Frankish BP, MacInnis MJ, Godkin E, Tarnopolsky MA, et al. Human Skeletal Muscle Fiber Type-Specific Responses to Sprint Interval and Moderate Intensity Continuous Exercise: Acute and Training-Induced Changes. J Appl Physiol 2021.

[476] Smith GI, Atherton P, Reeds DN, Mohammed BS, Rankin D, Rennie MJ, et al. Omega-3 polyunsaturated fatty acids augment the muscle protein anabolic response to hyperinsulinaemia-hyperaminoacidaemia in healthy young and middle-aged men and women. Clin Sci 2011;121:267–78. https://doi.org/10.1042/CS20100597.

[477] Smith GI, Atherton P, Reeds DN, Mohammed BS, Rankin D, Rennie MJ, et al. Dietary omega-3 fatty acid supplementation increases the rate of muscle protein synthesis in older adults: a randomized controlled trial. Am J Clin Nutr 2011;93:402–12. https://doi.org/10.3945/ajcn.110.005611.INTRODUCTION.

[478] Smith RAJ, Porteous CM, Gane AM, Murphy MP. Delivery of bioactive molecules to mitochondria in vivo. Proc Natl Acad Sci U S A 2003;100:5407–12. https://doi.org/10.1073/pnas.0931245100.

[479] Smith SM, Castaneda-Sceppa C, O'Brien KO, Abrams SA, Gillman P, Brooks NE, et al. Calcium kinetics during bed rest with artificial gravity and exercise countermeasures. Osteoporos Int 2014;25:2237–44. https://doi.org/10.1007/s00198-014-2754-x.

[480] Smith SM, Wastney ME, Morukov BV, Larina IM, Nyquist LE, Abrams SA, et al. Calcium metabolism before, during, and after a 3-mo spaceflight: Kinetic and biochemical changes. Am J Physiol - Regul Integr Comp Physiol 1999;277:1–10. https://doi.org/10.1152/ajpregu.1999.277.1.r1.

[481] Smith SM, Nillen JL, Leblanc A, Lipton A, Demers LM, Lane HW, et al. Collagen cross-link excretion during space flight and bed rest. J Clin Endocrinol Metab 1998;83:3584–91. https://doi.org/10.1210/jc.83.10.3584.

[482] Snowling NJ, Hopkins WG. Effects of different modes of exercise training on glucose control and risk factors for complications in type 2 diabetic patients: A meta-analysis. Diabetes Care 2006;29:2518–27. https://doi.org/10.2337/dc06-1317.

[483] Song Z, Chen H, Fiket M, Alexander C, Chan DC. OPA1 processing controls mitochondrial fusion and is regulated by mRNA splicing, membrane potential, and Yme1L. J Cell Biol 2007;178:749–55. https://doi.org/10.1083/jcb.200704110.

[484] Soriano FX, Liesa M, Bach D, Chan DC, Palacín M, Zorzano A. Evidence for a mitochondrial regulatory pathway defined by peroxisome proliferator-activated receptor-γ coactivator-1α, estrogen-related receptor-α, and mitofusin 2. Diabetes 2006;55:1783–91. https://doi.org/10.2337/db05-0509.

[485] Spaak J, Montmerle S, Sundblad P, Linnarsson D. Long-term bed rest-induced reductions in stroke volume during rest and exercise: Cardiac dysfunction vs. volume depletion. J Appl Physiol 2005;98:648–54. https://doi.org/10.1152/japplphysiol.01332.2003.

[486] Spelbrink JN. Quality matters: how does mitochondrial network dynamics and quality control impact on mtDNA integrity? Philos Trans R Soc Lond B Biol Sci 2014;369. https://doi.org/10.1098/rstb.2013.0442.

[487] Srivastava S. The mitochondrial basis of aging and age-related disorders. Genes (Basel) 2017;8. https://doi.org/10.3390/genes8120398.

[488] Standley RA, Distefano G, Trevino MB, Chen E, Narain NR, Greenwood B, et al. Skeletal muscle energetics and mitochondrial function are impaired following 10 days of bed rest in older adults. Gerontol Soc Am 2020;75:1744–53.

[489] Stanley WC, Khairallah RJ, Dabkowski ER. Update on lipids and mitochondrial function: Impact of dietary n-3 polyunsaturated fatty acids. Curr Opin Clin Nutr Metab Care 2012;15:122–6. https://doi.org/10.1097/MCO.0b013e32834fdaf7.

[490] Stein TP, Leskiw MJ, Schluter MD, Donaldson MR, Larina I. Protein kinetics during and after long-duration spaceflight on MIR. Am J Physiol - Endocrinol Metab 1999;276:1014–21. https://doi.org/10.1152/ajpendo.1999.276.6.e1014.

[491] Stein TP, Schluter MD, Galante AT, Soteropoulos P, Tolias PP, Grindeland RE, et al. Energy metabolism pathways in rat muscle under conditions of simulated microgravity. J Nutr Biochem 2002;13:471–8. https://doi.org/10.1016/S0955-2863(02)00195-X.

[492] Stein TP, Wade CE. Metabolic Consequences of Muscle Disuse Atrophy. J Nutr 2005;135:1803S-1805S. https://doi.org/10.1093/jn/135.7.1803s.

[493] Stepiens G, Torroni A, Chung AB, Hodge JA, Wallaces DC. Differential Expression of Adenine Nucleotide Translocator Isoforms in Mammalian Tissues and during Muscle Cell Differentiation *. J Biol Chem 1992;267:14592–7. https://doi.org/10.1016/S0021-9258(18)42082-0.

[494] Stremel R, Convertino VA, Bernnauer M, Greenleaf JE. Cardiorespiratory deconditioning with static and dynamic leg exercise during bed rest. J Appl Physiol 1976;41.

[495] Stuempfle KJ, Drury DG. The Physiological Consequences of Bed Rest. J Exerc Physiol 2007;6:32–41.

[496] Stump CS, Short KR, Bigelow ML, Schimke JM, Nair KS. Effect of insulin on human skeletal muscle mitochondrial ATP production , protein synthesis , and mRNA transcripts. Proc Natl Acad Sci U S A 2003;100:7996–8001.

[497] Suchankova G, Nelson LE, Gerhart-Hines Z, Kelly M, Gauthier MS, Saha AK, et al. Concurrent regulation of AMP-activated protein kinase and SIRT1 in mammalian cells. Biochem Biophys Res Commun 2009;378:836–41. https://doi.org/10.1016/j.bbrc.2008.11.130.

[498] Suetta C, Frandsen U, Jensen L, Jensen MM, Jespersen JG, Heinemeier KM, et al. Aging Affects the Transcriptional Regulation of Human Skeletal Muscle Disuse Atrophy. PLoS One 2012;7. https://doi.org/10.1371/journal.pone.0051238.

[499] Sun L, Fan G, Shan P, Qiu X, Dong S, Liao L, et al. Regulation of energy homeostasis by the ubiquitin-independent REGγ 3 proteasome. Nat Commun 2016;7. https://doi.org/10.1038/ncomms12497.

[500] Suzuki Y, Kashihara H, Takenaka K, Kawakubo K, Makita Y, Goto S, et al. Effects of daily mild supine exercise on physical performance after 20 days bed rest in young persons. Acta Astronaut 1994;33:101–11. https://doi.org/10.1016/0094-5765(94)90114-7.

[501] Sylow L, Kleinert M, Richter EA, Jensen TE. Exercise-stimulated glucose uptake — regulation and implications for glycaemic control. Nat Publ Gr 2017;13:133–48. https://doi.org/10.1038/nrendo.2016.162.

[502] Tabrizi R, Akbari M, Mosazadeh M, Lankarani KB, Tabrizi R, Samimi M, et al. The Effects of Vitamin D Supplementation on Glucose Metabolism and Lipid Profiles in Patients with Gestational Diabetes: A Systematic Review and Meta-Analysis of Randomized Controlled

Trials. Horm Metab Res 2017;49:647–53. https://doi.org/10.1055/s-0043-115225.

[503] Tanaka T, Nishimura A, Nishiyama K, Goto T, Numaga-Tomita T, Nishida M. Mitochondrial dynamics in exercise physiology. Pflugers Arch Eur J Physiol 2019;472:137–53. https://doi.org/10.1007/s00424-019-02258-3.

[504] Tandler B, Hoppel CL, Mears JA. Morphological Pathways of Mitochondrial Division. Antioxidants 2018;7:30. https://doi.org/10.3390/antiox7020030.

[505] Tascher G, Brioche T, Maes P, Chopard A, O'Gorman D, Gauquelin-Koch G, et al. Proteome-wide Adaptations of Mouse Skeletal Muscles during a Full Month in Space. J Proteome Res 2017;16:2623–38. https://doi.org/10.1021/acs.jproteome.7b00201.

[506] Tezze C, Romanello V, Desbats MA, Fadini GP, Albiero M, Favaro G, et al. Age-Associated Loss of OPA1 in Muscle Impacts Muscle Mass, Metabolic Homeostasis, Systemic Inflammation, and Epithelial Senescence. Cell Metab 2017;25:1374-1389.e6. https://doi.org/10.1016/j.cmet.2017.04.021.

[507] Theurey P, Rieusset J. Mitochondria-Associated Membranes Response to Nutrient Availability and Role in Metabolic Diseases. Trends Endocrinol Metab 2017;28:32–45. https://doi.org/10.1016/j.tem.2016.09.002.

[508] Thiele I, Swainston N, Fleming RMT, Hoppe A, Sahoo S, Aurich MK, et al. A community-driven global reconstruction of human metabolism. Nat Biotechnol 2013;31:419–25. https://doi.org/10.1038/nbt.2488.

[509] Thomas DR. Prevention and treatment of pressure ulcers. J Am Med Dir Assoc 2006;7:46–59. https://doi.org/10.1016/j.jamda.2005.10.004.

[510] Thomason DB, Biggs RB, Booth FW. Protein metabolism and β-myosin heavy-chain mRNA in unweighted soleus muscle. Am J Physiol - Regul Integr Comp Physiol 1989;257:300–5. https://doi.org/10.1152/ajpregu.1989.257.2.r300.

[511] Thomason DB, Booth FW. Atrophy of the soleus muscle by hindlimb unweighting. J Appl Physiol 1990.

[512] Thompson M, Hein N, Hanson C, Smith LM, Anderson-Berry A, Richter CK, et al. Omega-3 fatty acid intake by age, gender, and pregnancy status in the United States: National health and nutrition examination survey 2003–2014. Nutrients 2019;11:1–14.

https://doi.org/10.3390/nu11010177.

[513] Timmers S, Konings E, Bilet L, Houtkooper RH, Van De Weijer T, Goossens GH, et al. Calorie restriction-like effects of 30 days of resveratrol supplementation on energy metabolism and metabolic profile in obese humans. Cell Metab 2011;14:612–22. https://doi.org/10.1016/j.cmet.2011.10.002.

[514] Tomaselli D, Steegborn C, Mai A, Rotili D. Sirt4 : A Multifaceted Enzyme at the Crossroads of Mitochondrial Metabolism and Cancer. Front Oncol 2020;10:1–7. https://doi.org/10.3389/fonc.2020.00474.

[515] Tonkonogi M, Walsh B, Tiivel T, Saks V, Sahlin K. Mitochondrial function in human skeletal muscle is not impaired by high intensity exercise. Pflügers Arch Eur J Physiol 1999;437:562–8.

[516] Touvier T, De Palma C, Rigamonti E, Scagliola A, Incerti E, Mazelin L, et al. Muscle-specific Drp1 overexpression impairs skeletal muscle growth via translational attenuation. Cell Death Dis 2015;6:1–11. https://doi.org/10.1038/cddis.2014.595.

[517] Trappe S, Costill D, Gallagher P, Creer A, Peters JR, Evans H, et al. Exercise in space: Human skeletal muscle after 6 months aboard the International Space Station. J Appl Physiol 2009;106:1159–68. https://doi.org/10.1152/japplphysiol.91578.2008.

[518] Trappe S, Creer A, Minchev K, Slivka D, Louis E, Luden N, et al. Human soleus single muscle fiber function with exercise or nutrition countermeasures during 60 days of bed rest. Am J Physiol - Regul Integr Comp Physiol 2008;294:939–47. https://doi.org/10.1152/ajpregu.00761.2007.

[519] Trappe S, Trappe T, Gallagher P, Harber M, Alkner B, Tesch P. Human single muscle fibre function with 84 day bed-rest and resistance exercise. J Physiol 2004;557:501–13. https://doi.org/10.1113/jphysiol.2004.062166.

[520] Trappe TA, Burd NA, Louis ES, Lee GA, Trappe SW. Influence of concurrent exercise or nutrition countermeasures on thigh and calf muscle size and function during 60 days of bed rest in women. Acta Physiol 2007;191:147–59. https://doi.org/10.1111/j.1748-1716.2007.01728.x.

[521] Trappe T, Trappe S, Lee G, Widrick J, Fitts R, Costill D. Cardiorespiratory responses to

physical work during and following 17 days of bed rest and spaceflight. J Appl Physiol 2006;100:951–7. https://doi.org/10.1152/japplphysiol.01083.2005.

[522] Trevino MB, Zhang X, Standley RA, Wang M, Han X, Reis FCG, et al. Loss of mitochondrial energetics is associated with poor recovery of muscle function but not mass following disuse atrophy. Am J Physiol - Endocrinol Metab 2019;317:E899–910. https://doi.org/10.1152/ajpendo.00161.2019.

[523] Trewin AJ, Berry BJ, Wojtovich AP. Exercise and mitochondrial dynamics: Keeping in shape with ROS and AMPK. Antioxidants 2018;7. https://doi.org/10.3390/antiox7010007.

[524] Tseng AHH, Shieh SS, Wang DL. SIRT3 deacetylates FOXO3 to protect mitochondria against oxidative damage. Free Radic Biol Med 2013;63:222–34. https://doi.org/10.1016/j.freeradbiomed.2013.05.002.

[525] Turnbull PC, Longo AB, Ramos S V., Roy BD, Ward WE, Peters SJ. Increases in skeletal muscle ATGL and its inhibitor G0S2 following 8 weeks of endurance training in metabolically different rat skeletal muscles. Am J Physiol - Regul Integr Comp Physiol 2016;310:R125–33. https://doi.org/10.1152/ajpregu.00062.2015.

[526] Turner RT. Invited Review: What do we know about the effects of spaceflight on bone? J Appl Physiol 2000;89:840–7.

[527] Twig G, Elorza A, Molina AJA, Mohamed H, Wikstrom JD, Walzer G, et al. Fission and selective fusion govern mitochondrial segregation and elimination by autophagy. EMBO J 2008;27:433–46. https://doi.org/10.1038/sj.emboj.7601963.

[528] Twig G, Hyde B, Shirihai OS. Mitochondrial fusion, fission and autophagy as a quality control axis: The bioenergetic view. Biochim Biophys Acta - Bioenerg 2008;1777:1092–7. https://doi.org/10.1016/j.bbabio.2008.05.001.

[529] Twig G, Shirihai OS. The interplay between mitochondrial dynamics and mitophagy. Antioxidants Redox Signal 2011;14:1939–51. https://doi.org/10.1089/ars.2010.3779.

[530] Valente AJ, Maddalena LA, Robb EL, Moradi F, Stuart JA. A simple ImageJ macro tool for analyzing mitochondrial network morphology in mammalian cell culture. Acta Histochem 2017;119:315–26. https://doi.org/10.1016/j.acthis.2017.03.001.

[531] Varanita T, Soriano ME, Romanello V, Zaglia T, Quintana-Cabrera R, Semenzato M, et al.

The Opa1-dependent mitochondrial cristae remodeling pathway controls atrophic, apoptotic, and ischemic tissue damage. Cell Metab 2015;21:834–44. https://doi.org/10.1016/j.cmet.2015.05.007.

[532] Vargas-Ortiz K, Perez-Vazquez V, Diaz-Cisneros FJ, Figueroa A, Jiménez-Flores LM, Rodriguez-DelaRosa G, et al. Aerobic training increases expression levels of SIRT3 and PGC-1α in skeletal muscle of overweight adolescents without change in caloric intake. Pediatr Exerc Sci 2015;27:177–84. https://doi.org/10.1123/pes.2014-0112.

[533] Vasilaki A, Mansouri A, Van Remmen H, van der Meulen JH, Larkin L, Richardson AG, et al. Free radical generation by skeletal muscle of adult and old mice: Effect of contractile activity. Aging Cell 2006;5:109–17. https://doi.org/10.1111/j.1474-9726.2006.00198.x.

[534] Veksler VI, Kuznetsov A V., Sharov VG, Kapelko VI, Saks VA. Mitochondrial respiratory parameters in cardiac tissue: A novel method of assessment by using saponin-skinned fibers. BBA - Bioenerg 1987;892:191–6. https://doi.org/10.1016/0005-2728(87)90174-5.

[535] Verdin E, Hirschey MD, Finley LWS, Haigis MC. Sirtuin regulation of mitochondria: Energy production, apoptosis, and signaling. Trends Biochem Sci 2010;35:669–75. https://doi.org/10.1016/j.tibs.2010.07.003.

[536] Vikne H, Strøm V, Hugo Pripp A, Gjøvaag T. Human skeletal muscle fiber type percentage and area after reduced muscle use. A systematic review and meta-analysis. Scand J Med Sci Sports 2020:1–20. https://doi.org/10.1111/sms.13675.

[537] Vincent AE, Turnbull DM, Eisner V, Hajnóczky G, Picard M. Mitochondrial Nanotunnels. Trends Cell Biol 2017:1–13. https://doi.org/10.1016/j.tcb.2017.08.009.

[538] Wai T, García-Prieto J, Baker MJ, Merkwirth C, Benit P, Rustin P, et al. Imbalanced OPA1 processing and mitochondrial fragmentation cause heart failure in mice. Science (80-) 2015;350. https://doi.org/10.1126/science.aad0116.

[539] Wai T, Langer T. Mitochondrial Dynamics and Metabolic Regulation. Trends Endocrinol Metab 2016;27:105–17. https://doi.org/10.1016/j.tem.2015.12.001.

[540] Wang GX, Meyer JG, Cai W, Softic S, Li ME, Verdin E, et al. Regulation of UCP1 and Mitochondrial Metabolism in Brown Adipose Tissue by Reversible Succinylation. Mol Cell 2019;74:844-857.e7. https://doi.org/10.1016/j.molcel.2019.03.021.

[541] Wang H, Hiatt R, Barstow TJ. Relationships between muscle mitochondrial DNA content , mitochondrial enzyme activity and oxidative capacity in man : alterations with disease. Eur J Appl Physiol 1999;80:22–7.

[542] Wang Q, Zhang Y, Yang C, Xiong H, Lin Y. Acetylation of Metabolic Enzymes and Metabolic Flux. Science (80-) 2010;327:1004–7.

[543] Wang X, Quinn PJ. The location and function of vitamin E in membranes (Review). Mol Membr Biol 2000;17:143–56. https://doi.org/10.1080/09687680010000311.

[544] Wang X, Quinn PJ. Vitamin E and its functions in biologiccal membranes. Prog Lipid Res 1999;38:309–36.

[545] Wang X, Proud CG. The mTOR Pathway in the Control of Protein Synthesis. Physiology 2006;21:362–9.

[546] Ward K, Mulder E, Frings-Meuthen P, O'Gorman DJ, Cooper D. Fetuin-A as a Potential Biomarker of Metabolic Variability Following 60 Days of Bed Rest. Front Physiol 2020;11:1–10. https://doi.org/10.3389/fphys.2020.573581.

[547] Wells JCK, Fewtrell MS. Measuring body composition. Arch Dis Child 2006;91:612–7. https://doi.org/10.1136/adc.2005.085522.

[548] Westby CM, Martin DS, Lee SMC, Stenger MB, Platts SH. Left ventricular remodeling during and after 60 days of sedentary head-down bed rest. J Appl Physiol 2016;120:956–64. https://doi.org/10.1152/japplphysiol.00676.2015.

[549] Whedon D, Deitrick JE, Shorr E, Toscani V, Davis B, Stevens E. Modification of the effects of immobilization upon metabolic and physiologic functions of normal men by the use of an oscillating bed. Am J Med 1949;6:684–711. https://doi.org/10.1016/0002-9343(49)90306-X.

[550] Wheeler MJ, Dempsey PC, Grace MS, Ellis KA, Gardiner PA, Green DJ, et al. Sedentary behavior as a risk factor for cognitive decline ? A focus on the influence of glycemic control in brain health. Alzheimer's Dement Transl Res Clin Interv 2017;3:291–300. https://doi.org/10.1016/j.trci.2017.04.001.

[551] Wilkinson DJ, Hossain T, Hill DS, Phillips BE, Crossland H, Williams J, et al. Effects of leucine and its metabolite β-hydroxy-β-methylbutyrate on human skeletal muscle protein

metabolism. J Physiol 2013;591:2911–23. https://doi.org/10.1113/jphysiol.2013.253203.

[552] Wu D, Li Y, Zhu KS, Wang H, Zhu WG. Advances in Cellular Characterization of the Sirtuin Isoform, SIRT7. Front Endocrinol (Lausanne) 2018;9:1–13. https://doi.org/10.3389/fendo.2018.00652.

[553] Wu NN, Zhang Y, Ren J. Mitophagy, Mitochondrial Dynamics, and Homeostasis in Cardiovascular Aging. Oxid Med Cell Longev 2019;2019:10–2. https://doi.org/10.1155/2019/9825061.

[554] Yan H, Qiu C, Sun W, Gu M, Xiao F, Zou J, et al. Yap regulates gastric cancer survival and migration via SIRT1/Mfn2/mitophagy. Oncol Rep 2018;39:1671–81. https://doi.org/10.3892/or.2018.6252.

[555] Yan Z, Lira VA, Greene NP. Exercise training-induced Regulation of Mitochondrial Quality. Exerc Sport Sci Rev 2012;40:159–64. https://doi.org/10.1097/JES.0b013e3182575599.

[556] Yang JL, Mukda S, Chen S Der. Diverse roles of mitochondria in ischemic stroke. Redox Biol 2018;16:263–75. https://doi.org/10.1016/j.redox.2018.03.002.

[557] Yang L, Vaitheesvaran B, Hartil K, Robinson AJ, Hoopmann MR, Eng JK, et al. The fasted/fed mouse metabolic acetylome: N6-acetylation differences suggest acetylation coordinates organ-specific fuel switching. J Proteome Res 2011;10:4134–49. https://doi.org/10.1021/pr200313x.

[558] Yang L, Cao C, Kantor ED, Nguyen LH, Zheng X, Park Y, et al. Trends in Sedentary Behavior Among the US Population, 2001-2016. J Am Med Assoc 2019;63110:1587–97. https://doi.org/10.1001/jama.2019.3636.

[559] Yao C, Wang R, Wang Y, Kung C, Weber JD, Patti GJ, et al. Mitochondrial fusion supports increased oxidative phosphorylation during cell proliferation. Elife 2019:1–19.

[560] Yasuda N, Glover EI, Phillips SM, Isfort RJ, Tarnopolsky MA. Sex-based differences in skeletal muscle function and morphology with short-term limb immobilization. J Appl Physiol 2005;99:1085–92. https://doi.org/10.1152/japplphysiol.00247.2005.

[561] Yoo S-M, Jung Y-K. A Molecular Approach to Mitophagy and Mitochondrial Dynamics. Mol Cells 2018;41:18–26. https://doi.org/10.14348/molcells.2018.2277.

[562] Yoshioka Y, Kubota Y, Samukawa Y, Yamashita Y, Ashida H. Glabridin inhibits dexamethasone-induced muscle atrophy. Arch Biochem Biophys 2019;664:157–66. https://doi.org/10.1016/j.abb.2019.02.006.

[563] You J, Anderson GB, Dooley MS, Hornberger TA. The role of mTOR signaling in the regulation of protein synthesis and muscle mass during immobilization in mice. Dis Model Mech 2015:1059–69. https://doi.org/10.1242/dmm.019414.

[564] Youle RJ, Narendra DP. Mechanisms of mitophagy. Nat Rev Mol Cell Biol 2011;12:9–14. https://doi.org/10.1038/nrm3028.

[565] Youle RJ, Van Der Bliek AM. Mitochondrial Fission, Fusion, and Stress. Science (80-) 2012;337:1062–5. https://doi.org/10.1126/science.1219855.

[566] Yu R, Jin S, Lendahl U, Nistér M, Zhao J. Human Fis1 regulates mitochondrial dynamics through inhibition of the fusion machinery. EMBO J 2019;38:1–21. https://doi.org/10.15252/embj.201899748.

[567] Yu W, Gao B, Li N, Wang J, Qiu C, Zhang G, et al. Sirt3 deficiency exacerbates diabetic cardiac dysfunction: Role of Foxo3A-Parkin-mediated mitophagy. Biochim Biophys Acta - Mol Basis Dis 2017;1863:1973–83. https://doi.org/10.1016/j.bbadis.2016.10.021.

[568] Yu X, Jia L, Yu W, Du H. Dephosphorylation by calcineurin regulates translocation of dynamin-related protein 1 to mitochondria in hepatic ischemia reperfusion induced hippocampus injury in young mice. Brain Res 2019;1711:68–76. https://doi.org/10.1016/j.brainres.2019.01.018.

[569] Zampieri S, Mammucari C, Romanello V, Barberi L, Pietrangelo L, Fusella A, et al. Physical exercise in aging human skeletal muscle increases mitochondrial calcium uniporter expression levels and affects mitochondria dynamics. Physiol Rep 2016;4:1–15. https://doi.org/10.14814/phy2.13005.

[570] Zang M, Zuccollo A, Hou X, Nagata D, Walsh K, Herscovitz H, et al. AMP-activated protein kinase is required for the lipid-lowering effect of metformin in insulin-resistant human HepG2 cells. J Biol Chem 2004;279:47898–905. https://doi.org/10.1074/jbc.M408149200.

[571] Zange J, Mester J, Heer M, Kluge G, Liphardt AM. 20-Hz whole body vibration training fails to counteract the decrease in leg muscle volume caused by 14 days of 6° head down tilt

bed rest. Eur J Appl Physiol 2009;105:271–7. https://doi.org/10.1007/s00421-008-0899-z.

[572] Zanna C, Ghelli A, Porcelli AM, Karbowski M, Youle RJ, Schimpf S, et al. OPA1 mutations associated with dominant optic atrophy impair oxidative phosphorylation and mitochondrial fusion. Brain 2008;131:352–67. https://doi.org/10.1093/brain/awm335.

[573] Zerwekh JE, Ruml LA, Gottschalk F, Pak CYC. The effects of twelve weeks of bed rest on bone histology, biochemical markers of bone turnover, and calcium homeostasis in eleven normal subjects. J Bone Miner Res 1998;13:1594–601. https://doi.org/10.1359/jbmr.1998.13.10.1594.

[574] Zhang M, Wu J, Sun R, Tao X, Wang X, Kang Q, et al. SIRT5 deficiency suppresses mitochondrial ATP production and promotes AMPK activation in response to energy stress. PLoS One 2019;14:1–25. https://doi.org/10.1371/journal.pone.0211796.

[575] Zhang Y, Bharathi SS, Rardin MJ, Uppala R, Verdin E, Gibson BW, et al. SIRT3 and SIRT5 regulate the enzyme activity and cardiolipin binding of very long-chain Acyl-CoA dehydrogenase. PLoS One 2015;10:1–13. https://doi.org/10.1371/journal.pone.0122297.

[576] Zhang Z, Sliter DA, Bleck CKE, Ding S. Fis1 deficiencies differentially affect mitochondrial quality in skeletal muscle. Mitochondrion 2019;49:217–26. https://doi.org/10.1016/j.mito.2019.09.005.

[577] Zhang ZK, Li J, Liu J, Guo B, Leung A, Zhang G, et al. Icaritin requires Phosphatidylinositol 3 kinase (PI3K)/Akt signaling to counteract skeletal muscle atrophy following mechanical unloading. Sci Rep 2016;6:1–12. https://doi.org/10.1038/srep20300.

[578] Zhao J, Liu T, Jin S, Wang X, Qu M, Uhlén P, et al. Human MIEF1 recruits Drp1 to mitochondrial outer membranes and promotes mitochondrial fusion rather than fission. EMBO J 2011;30:2762–78. https://doi.org/10.1038/emboj.2011.198.

[579] Zhao S, Xu W, Jiang W, Yu W, Lin Y, Zhang T, et al. Regulation of Cellular Metabolism by Protein Lysine Acetylation. Science (80-) 2010;327:1000–5.

[580] Zick M, Rabl R, Reichert AS. Cristae formation — linking ultrastructure and function of mitochondria. BBA - Mol Cell Res 2009:5–19. https://doi.org/10.1016/j.bbamcr.2008.06.013.

[581] Zorzano A. Regulation of mitofusin-2 expression in skeletal muscle. Appl Physiol Nutr

Metab 2009;34:433–9. https://doi.org/10.1139/H09-049.

[582] Zorzano A, Liesa M, Palacin M. Mitochondrial dynamics as a bridge between mitochondrial dysfunction and insulin resistance. Arch Physiol Biochem 2009;115:1–12. https://doi.org/10.1080/13813450802676335.

[583] Zorzano A, Liesa M, Sebastián D, Segalés J, Palacín M. Mitochondrial fusion proteins: Dual regulators of morphology and metabolism. Semin Cell Dev Biol 2010;21:566–74. https://doi.org/10.1016/j.semcdb.2010.01.002.

Appendices

These appendices are composed of supplementary material for each of the results chapters. Data include optimisation data, additional supporting material and details relating to methods used in both our *in-vitro* and *in-vivo* studies.

Table of Contents - Appendices

Appendix A – 21-Day Bed Rest Study Supplementary

Experimental Overview of the 21-day Bed Rest Study

In order to address the issue of reduced physical activity, we participated in a European Space Agency (ESA) funded bed rest study. Bed rest studies serve as an important platform in order to prepare for future human exploration in space. Additionally, they provide us with a useful experimental design to study human physiology in the setting of extreme physical inactivity. This study was a randomized, crossover design which was conducted at the MEDES clinic, Toulouse, France from June 2012 to December 2013. A total of 9 scientific teams were involved in the study, each with their own experimental protocol. Additionally, bed rest core data were obtained. These included a selection of standardized measures that are conducted in every bed rest study. A total of 12 healthy male subjects volunteered to participate in the study. Each subject attended the clinic three times for 35 days. Each 35-day period began with a 7-day ambulatory control period (BDC: Baseline data collection). During this phase, subjects were allowed to be ambulatory during the day, remaining in the clinic at all times while undergoing baseline evaluation. This was followed by 21 days head-down tilt bed rest (-6 ˚) (HDT: head down tilt). Preventative methods, known as countermeasures have been developed to eliminate the deconditioning associated with prolonged physical inactivity. During each HDT period, subjects were allocated to one of three groups:

- Control group (CONT) which underwent bed rest only
- Resistive vibration exercise (RVE) group
- Nutrition and exercise group (NEX)

Throughout bed rest, all activities of daily living including eating, body weight measurement, energy expenditure and hygienic procedures were conducted in bed. For any measurements that were carried out in another part of the clinic, subjects were transported in their beds remaining in the head down tilt position at all times. Subjects were permitted to change position in the horizontal plane once one shoulder remained in contact with the mattress. Any muscular activity of the lower body was prohibited. Passive physical therapy was applied every 3-4 days. Adherence to all study rules were controlled by the study nurse manager. Additionally, compliance with the bed rest study requirements were monitored with 24-hour video surveillance using random real-time control. Following the bed rest and countermeasure period,

subjects were required to remain in the clinic for assessment and recovery for a further 7 days. All participants were asked to return to MEDES 14 and 28 days after each period of bed rest for follow up visits.

21-Day Bed Rest Subject Selection Criteria

Following a call for candidates via the internet on the MEDES and ESA sites and by media, 40 subjects were selected based on their application file which comprised of information on the subject's lifestyle, educational and professional experience. They also completed a medical questionnaire including personal and family medical history. The 40 potential candidates underwent a medical examination, a DEXA scan, biological tests and psychological assessment. Finally, 12 men and 2 back up subjects were selected to partake in the bed rest study. An information document was provided to each candidate and they had the opportunity to ask any questions. Once satisfied, they signed the specific Information and Consent Form. These volunteers were then notified of a selection visit at MEDES to check if they did (or did not) meet the requirements of the inclusion and non-inclusion criteria. The study was approved by the appropriate Ethics Committee (Comité de Protection des Personnes / CPP Sud – Ouest Outre-Mer I) and the French Health Authorities (Agence Française de Sécurité Sanitaire des Produits de Santé).

Appendix A. Table 1. List of inclusion and exclusion criteria for the 21-day bed rest study

Inclusion criteria	Exclusion criteria
Healthy male	Past record of orthostatic intolerance
Aged 20-45	Cardiac rhythm disorders
BMI between 20-25	Chronic back pains
Between 158-190cm in height	History of hiatus hernia or gastro-esophageal reflux
No personal nor family past record of chronic or acute disease or psychological disturbances which could affect the physiological data and/or create a risk for the subject during the experiment	History of thyroid dysfunction, renal stones, diabetes, migraines
Fitness: < 35 years: 35 ml/min./kg < VO_2max < 60ml/min/kg > 35 years: 30 ml/min./kg < VO_2max < 60ml/min/kg	Past record of thrombophlebitis, family history of thrombosis or positive response in thrombosis screening procedure
Active and free from any orthopedic, musculoskeletal and cardiovascular disorders	Abnormal result for lower limbs echo-Doppler
Non-smokers, no alcohol, no drug dependence and no medical treatment	History or active claustrophobia
Covered by a Social Security system	History of genetic muscle and bone diseases of any kind Bone mineral density: T-score ≤ -1.5
Free of any engagement during the three study planned periods	Osteosynthesis material, presence of metallic implants
	History of knee problems or joint surgery/broken leg
	Poor tolerance to blood sampling
	Having given blood (more than 8ml/kg) in a period of 8 weeks or less before the start of the experiment
	Special food diet, vegetarian or vegan
	History of intolerance to lactose or food allergy
	Positive reaction to any of the following tests: HVA IgM (hepatitis A), HBs antigen (hepatitis B), anti-HVC antibodies (hepatitis C), anti-HIV1+2 antibodies
	Echocardiography: inappropriate thoracic acoustic window
	Subject already participating or in the exclusion period of a clinical research
	Refusal to give permission to contact his general practitioner
	Incarcerated persons
	Subject who, in the judgment of the investigator, is likely to be non-compliant during the study, or unable to cooperate because of a language problem or poor mental development
	Subject who has received more than €4,500 within 12 months for being a research subject
	Subject under guardianship or trusteeship

21-Day Bed Rest Randomization

Each volunteer was randomly assigned to one of three groups during the first and second bed rest campaign and were assigned to the third group for the final and third bed rest period. The order of sequence was random. The wash out period in between the bed rest campaigns was for a minimum duration of 120 days to allow subjects to return to pre bed rest physical status.

21-Day Bed Rest Subject Baseline Measures

In total, 12 subjects volunteered to partake in the 21-day bed rest study. This study was a crossover design split into three separate campaigns. During campaign 2, subject I withdrew after the baseline testing period. During campaign 3, volunteers F, H and L withdrew from the testing. Therefore 8 subjects completed the control (CONT), resistive vibration exercise (RVE) and nutrition and exercise (NEX) protocols. The following anthropometric measurements were made at selection and were necessary to ensure each volunteer satisfied the inclusion criteria.

Appendix A. Table 2. Countermeasure group assignment/randomization

Subject	Campaign 1	Campaign 2	Campaign 3
A	RVE	NEX	CONT
B	CONT	RVE	NEX
C	RVE	NEX	CONT
D	NEX	CONT	RVE
E	NEX	CONT	RVE
G	NEX	CONT	RVE
J	RVE	NEX	CONT
K	NEX	CONT	RVE
	CONT (n=8)	*RVE (n=8)*	*NEX (n=8)*

Campaign 2 – I: withdrawal on BDC-1 (C2)

Campaign 3 – F: withdrawal on BDC-6 (C3)

H: withdrawal of C3 before the beginning of the campaign

L: withdrawal on HDT17 (C3)

21-Day Bed Rest Physiological Assessment

Anthropometrics

Height (m) was measured to the nearest centimetre using a stadiometer and body mass (kg) was measured to the nearest 0.1 kg at baseline and the first thing every morning during bedrest on a weighing trolley. This allowed them to roll from the bed to the weighing scales.

Body Composition

There were two methods applied in order to obtain body composition measurements. Subjects had DEXA scan for body composition at 5 time points throughout each study campaign (BDC-7, HDT1, HDT10, HDT20 and R+3). They also had body composition measurement using bioelectrical impedance spectroscopy (BIS) every second morning during bedrest under fasting conditions. The purpose of the BIS analysis was to closely monitor body fat mass with the aim of avoiding any major changes by adjusting the diet accordingly.

Dual Energy X-Ray Absorptiometry (DEXA)

The measurement of body composition using DEXA is achieved from the differential absorption of x-rays of two different intensities. This calculation allows for the quantification of overlying soft tissue. It is possible to obtain values for fat and fat free mass using a whole body scan and using instrument specific algorithms. DEXA was used for the purpose of analysing body composition on days -7, 1, 10 and day 20 using the Hologic DXA, QDR4500C, USA. Positioning of all subjects on the scanner platform were in accordance with the manufacturers guidelines. For the total body scan, subjects were centred and squared in the middle of the table with ankles and knees taped together and the scanner laser light was positioned 3cm above the subject's head. The scanner arm moved down over the subject's body obtaining sliced images. Fat mass and fat free mass were calculated. The radiation exposure is extremely low (0.001mSv) (www.radiologyinfo.org).

Bio Impedance analysis (BIA)

Body composition was analyzed using bioelectric impedance spectroscopy (BIS) with the bioimpedance device SFB7 (Impedimed®) every second morning throughout the bed rest study. The BIS measurement took approximately 5 minutes per subject per morning. The device utilizes Cole modeling with Hanai mixture theory to determine total body water (TBW), extracellular fluid (ECF) and intracellular fluid (ICF) from impedance data. Fat-free mass (FFM) and fat mass (FM) are then calculated on the device. Further data analysis can be undertaken using the supporting

software. Therefore, no population specific prediction equations (algorithms) were required for data analysis.

Body Composition

Body composition was measured continually during this study using dual x-ray absorptiometry (DEXA) and bioelectrical impedance (BIA). This table represents body composition before (pre) and at the end of the bed rest study (post). There was a significant reduction weight, lean muscle mass (WB FFM, kg) following 21-days of bed rest in all groups (control, RVE and NeX) (p<0.05). Due to the reduction in lean muscle mass, there was a significant increase in body fat percentage with 60 days of -6° HDT bed rest in all groups (p<0.05).

Appendix A. Table 3. Body composition changes before and after 21 days BR.

	Control (n=8)		RVE (n=8)		NEX (n=8)		
	Pre	Post	Pre	Post	Pre	Post	
Weight (kg)	73.44±3.46	70.48±3.68	73.14±3.37	70.28±3.16	71.83±3.25	70.07±3.06	**
Body Fat (%)	21.01±2.00	21.46±2.19	19.96±1.82	21.09±1.92	19.95±1.73	20.64±1.65	**
WB FFM (kg)	57.79±2.5	55.12±2.69	58.48±2.87	55.36±2.59	57.43±2.70	55.47±2.47	**
WB FM (kg)	15.65±1.97	15.36±2.13	14.66±1.60	14.92±1.64	14.41±1.57	14.61±1.52	
Arm fat (kg)	1.72 ± 0.20	1.86± 0.31	1.66 ±0.19	1.78 ± 0.22	1.68 ± 0.20	1.70 ±0.20	
Arm Lean (kg)	7.16± 0.49	7.21 ± 0.57	7.54 ± 0.57	7.30± 0.58	7.29 ± 0.53	7.16 ± 0.53	
Leg Fat (kg)	5.81 ± 1.07	4.29 ± 0.42	5.53 ± 0.74	3.96 ± 0.33	3.85 ± 0.64	5.65 ± 0.59	
Leg lean (kg)	17.45 ± 0.50	17.50 ± 0.64	17.60 ± 0.87	18.29 ± 0.67	16.48 ± 0.55	19.10 ± 0.40	

Data are presented as mean± SE. WB FFM – whole body fat free mass, WB FM – whole body fat mass. *significantly different compared to pre bed rest for each trial. **significantly different to pre bed best as an effect of time.

Resting Metabolic Rate (RMR)

Open circuit indirect calorimetry was conducted using the Deltatrac® system on days -7, 1, 5, 10, 15 and 20 for the measurement of resting metabolic rate (RMR). Upon wakening, a plastic hood with two outlets was placed over the subjects head while they remained in the lying position. The canopy consists of an inlet and an outlet valve. The subject was supplied with room air via the inlet valve at a rate of 40 L/min, while extracts of the expired air was obtained via the outlet valve. Both valves were connected to the calorimeter (Deltatrac II) via tubes. The Deltatrac II records the oxygen consumption (VO_2) and carbon dioxide production (VCO_2) from the inlet and outlet gas samples of the valves and calculates the oxygen consumption (VO_2) and carbon dioxide production (VCO_2) in ml/min by differentiation. Values for all parameters were averaged over 1 minute intervals. Subsequently, these values were used to estimate RMR using the Weir equation.

Aerobic Fitness Assessment

The assessment of aerobic capacity was performed on a cycle ergometer in upright position at selection and before and after each bed rest period. The subjects cycled for 3 minutes at 50, 100 and 150 W each followed by an increase of 25 W every 1 minute until peak exertion was reached. The exercise test took approximately 12-16 minutes to complete. Following this test, the subject pedalled the cycle ergometer at a low work rate (~25 W) in order to allow time for adequate recovery from maximal exertion. Heart rate and blood pressure were monitored continuously. Subjects wore a nose clip and were required to breathe through a respiratory valve that was connected via respiratory tubing to the metabolic cart (Oxycon Pro ™, Jegger™) for gas exchange determination in the breath by breath mode. VO_2, VCO_2 and VE were measured continuously with a metabolic cart in breath by breath mode. Arterial blood pressure was measured continuously with Finapres, Portapres or equivalent device. Percent oxygen saturation (SaO_2) was measured continuously with fingertip infrared photometry. The test continued until volitional fatigue was achieved. Oxygen uptake was considered maximal if two the following criteria were achieved: a levelling off of VO_2 max, maximal heart rate (HR) achieved was within 10 beats of age predicted HR max and /or if respiratory exchange ratio was >1.1.

Skeletal Muscle Biopsies

Skeletal muscle specimens were obtained by muscle biopsy from the vastus lateralis at 9am while subjects with in the fasted state before and after the 21-day bed rest period (BDC-1 and HDT20). An area of skin was anaesthetised (2% w/v lidocaine HCl) and a small (0.5 cm) incision was made. A sterilised Bergstrom skeletal muscle biopsy needle was inserted into the muscle and approximately 200 mg of tissue were removed while applying suction. Pressure was maintained on the wound for 10 minutes and the incision was closed with steristrip tape and wrapped tightly in a crepe bandage.

Appendix B – Cellular Response to Intervention used throughout 21 days of HDT Bed Rest

Preventative methods, known as countermeasures have been developed to eliminate the deconditioning associated with prolonged physical inactivity.

During each HDT period, subjects were allocated to one of three groups:

- Control group (CONT) which underwent bed rest only
- Resistive Vibration Exercise (RVE) group
- Nutrition and exercise group (NEX)

Skeletal muscle biopsy samples were taken from each subject's vastus lateralis using the standard Bergstrom technique before (BDC – baseline data collection) and following (HDT – head down tilt) the 21 days of bed rest. Protein expression of skeletal muscle biopsy samples was measured using Western blot techniques. Muscle samples were measured for markers of mitochondrial biogenesis, mitochondrial fusion, mitochondrial fission, mitophagy and other markers of mitochondrial and cellular metabolism.

Protein Expression of Control, RVE & NeX

Below is a comparison in protein expression for markers of mitochondrial biogenesis, fusion, fission, mitophagy and other markers of mitochondrial and cellular metabolism of all subjects which completed each trial (control, RVE and NeX).

Expression of Markers Associated with Mitochondrial Biogenesis

PGC-1α

PGC-1α, pparg coactivator-1 alpha, a well-supported regulator of mitochondrial biogenesis, was analysed for protein expression within the control, RVE and NeX groups before and after 21-days of bed rest (*n*=6). There was no significant change in PGC-1α protein expression within the any group with 21-days of bed rest (*p*>0.05).

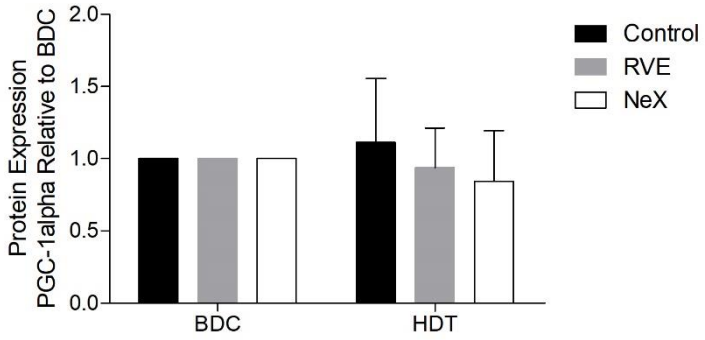

Appendix B. Figure 1. PGC-1α protein expression following 21 days bed rest with control, RVE & NeX

(PGC-1α protein expression quantified by western blot (*n*=6). PGC-1α, PPARG coactivator 1 alpha, was normalised against loading control (GAPdh expression) of same sample and subsequently expressed relative to BDC of same sample. Data are expressed as mean ±SE)

Expression of Markers Associated with Mitochondrial Fusion

OPA1

OPA1, optic atrophy 1, a regulator of mitochondrial fusion, was analysed for protein expression within the control, RVE and NeX groups before and after 21-days of bed rest (n=6). There was a significant decrease in both the control and RVE groups OPA1 protein expression following 21 days of bed rest (p<0.005), there was no significant change in NeX OPA1 protein expression (p>0.05).

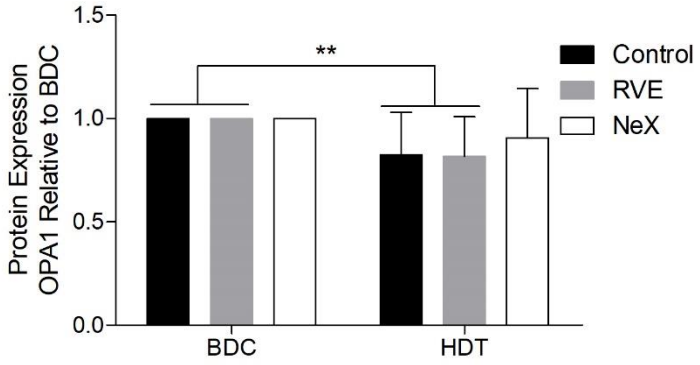

Appendix B. Figure 2. OPA1 protein expression following 21 days bed rest with control, RVE & NeX

(OPA1 protein expression quantified by western blot (n=6). OPA1, optic atrophy 1, was normalised against loading control (GAPdh expression) of same sample and subsequently expressed relative to BDC of same sample. Data are expressed as mean ±SE, ** significant effect of time, p<0.005)

L-OPA1 & s-OPA1

The long and short isoforms of OPA1, L-OPA1 (A) and s-OPA1 (B) were analysed for protein expression within the control, RVE and NeX groups before and after 21-days of bed rest (*n*=6). There was a significant decrease in both the control and RVE groups L-OPA1 and s-OPA1 protein expression following 21 days of bed rest ($p<0.005$), there was no significant change in NeX L-OPA1 and s-OPA1 protein expression ($p>0.05$).

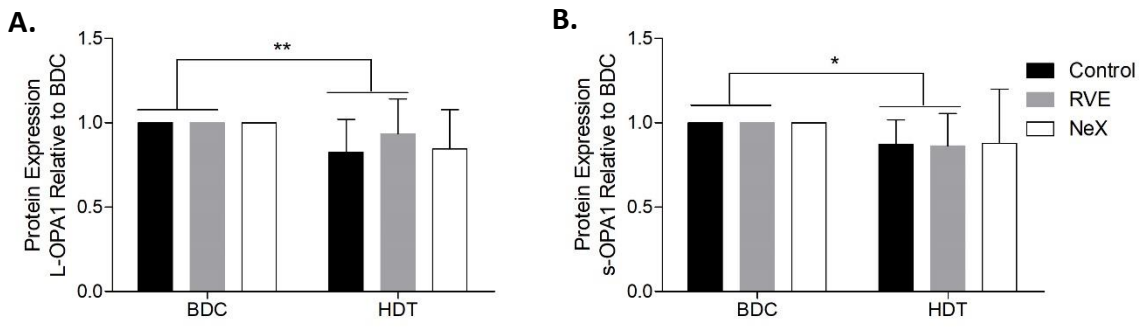

Appendix B. Figure 3. L-OPA1 & s-OPA1 protein expression following 21 days bed rest with control, RVE & NeX

(L-OPA1 (A) and s-OPA1 (B) protein expression quantified by western blot (*n*=6). L-OPA1, long isoform optic atrophy 1 and s-OPA1, short isoform optic atrophy 1, was normalised against loading control (GAPdh expression) of same sample and subsequently expressed relative to BDC of same sample. Data are expressed as mean ±SE, ** significant effect of time, $p<0.005$, *significant effect of time, $p<0.05$)

Mfn1 & Mfn2

Mitofusin-1 (Mfn1) and mitofusin-2 (Mfn2) were analysed for protein expression within the control, RVE and NeX groups before and after 21-days of bed rest (*n*=6). There was no significant change in both the Mfn1 (A) or Mfn2 (B) protein expression within any group with 21 days of bed rest (p>0.05).

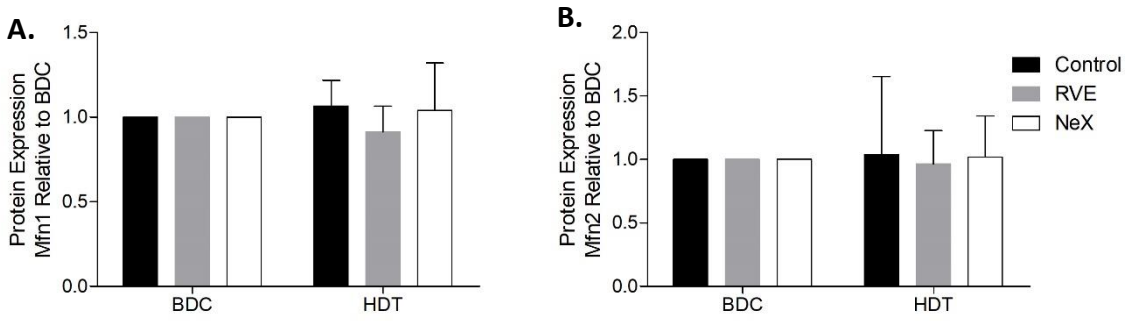

Appendix B. Figure 4. Mfn1 & Mfn2 protein expression following 21 days bed rest with control, RVE & NeX

(Mfn1 (A) and Mfn2 (B) protein expression quantified by western blot (*n*=6). Mfn1, Mitofusin-1 and Mfn2, Mitofusin-2, was normalised against loading control (GAPdh expression) of same sample and subsequently expressed relative to BDC of same sample. Data are expressed as mean ±SE)

OMA1 & YME1L

Metalloendopeptidase OMA1 (A) and ATP-dependent zinc metalloprotease YME1L (B) were analysed for protein expression within the control, RVE and NeX groups before and after 21-days of bed rest (*n*=6). There was a significant increase in OMA1 protein expression in all groups with 21-days of bed rest ($p<0.0005$). However, there was no significant change in YME1L protein expression within any group with 21 days of bed rest ($p>0.05$).

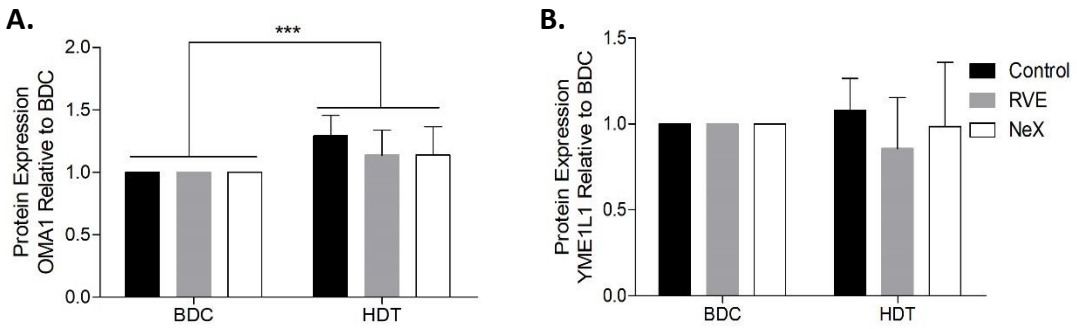

Appendix B. Figure 5. OMA1 & YME1L protein expression following 21 days bed rest with control, RVE & NeX

(OMA1 (A) and YME1L (B) protein expression quantified by western blot (*n*=6). OMA1, Metalloendopeptidase OMA1, and YME1L, ATP-dependent zinc metalloprotease YME1L, was normalised against loading control (GAPdh expression) of same sample and subsequently expressed relative to BDC of same sample. Data are expressed as mean ±SE, **significant effect of time, $p<0.0005$)

Expression of Markers Associated with Mitochondrial Fission

Drp1 & Fis1

Mitochondrial fission markers, dynamin related protein 1 (Drp1) (A) and mitochondrial fission protein 1 (Fis1) (B) were measured for protein expression within the control, RVE and NeX groups before and after 21-days of bed rest (n=6). There was a significant increase in Drp1 and Fis1 protein expression within the NeX group with 21-days of bed rest (p<0.05). However, there was no significant change in Drp1 or Fis1 protein expression within any other group following 21 days of bed rest (p>0.05).

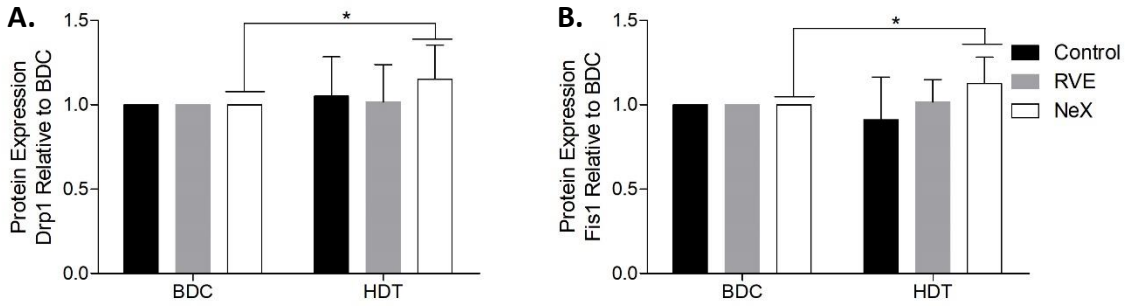

Appendix B. Figure 6. Drp1 & Fis1 protein expression following 21 days bed rest with control, RVE & NeX

(Drp1 (A) and Fis1 (B) protein expression quantified by western blot (n=6). Drp1, dynamin related protein 1, and Fis1, Mitochondrial fission protein 1, was normalised against loading control (GAPdh expression) of same sample and subsequently expressed relative to BDC of same sample. Data are expressed as mean ±SE, *significant effect of time, p<0.05)

Ratio of Mitochondrial Fusion:Fission

In order to assess for the balance between mitochondrial fusion and fission with RVE, NeX or without an intervention (control) following 21 days of -6° head down tilt bed rest, protein expression of mitochondrial fusion marker, OPA1 was controlled against protein expression of mitochondrial fission marker, Drp1.

OPA1:Drp1 Ratio

There was a significant decrease in OPA1:Drp1 ratio in all groups following 21-days of bed rest (p<0.005). This result indicates that following 21-days of bed rest there was a possible increase in Drp1 mediated mitochondrial fission due to the possible decrease in OPA1 mediated mitochondrial fusion in all groups.

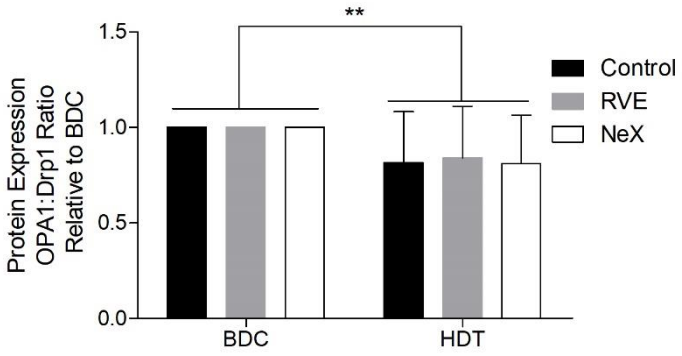

Appendix B. Figure 7. OPA1:Drp1 Ratio following 21 days bed rest with control, RVE & NeX

(OPA1:Drp1 protein expression quantified by western blot. OPA1, optic atrophy 1 was controlled against Drp1, dynamin related protein 1, protein expression (n=6). Both OPA1 and Drp1 protein expression were firstly normalised to their respective loading control (GAPdh) and subsequently expressed relative to BDC of same sample. Data are expressed as mean ±SE, ** significant effect of time, p<0.005)

Expression of Markers Associated with Mitophagy

PINK1 & Parkin

Mitochondrial breakdown (mitophagy) markers, PTEN-induced kinase 1 (PINK1) (A) and Parkin (B) were measured for protein expression within the control, RVE and NeX groups before and after 21-days of bed rest (*n*=6). There was no significant change in PINK1 or Parkin protein expression following 21-days of bed rest in any of the groups assessed ($p>0.05$).

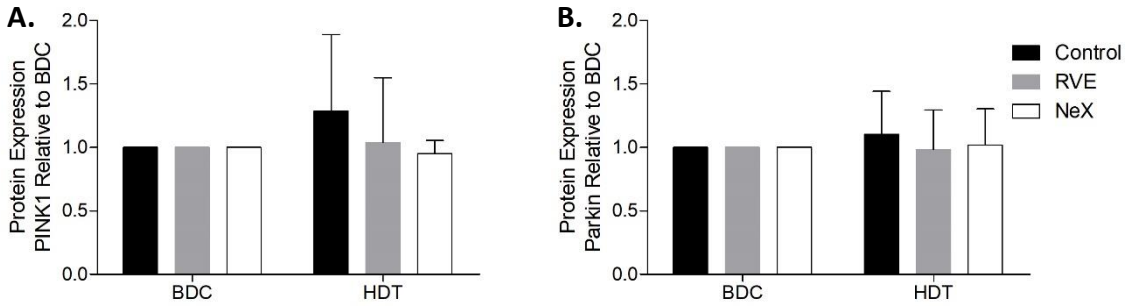

Appendix B. Figure 8. PINK1 & Parkin protein expression following 21 days bed rest with control, RVE & NeX

(PINK1 (A) and Parkin (B) protein expression quantified by western blot (*n*=6). PINK1, PTEN-induced kinase 1, and Parkin were normalised against loading control (GAPdh expression) of same sample and subsequently expressed relative to BDC of same sample. Data are expressed as mean ±SE)

BNIP3 & BCL2-L13

BCL2/adenovirus E1B 19 kDa protein-interacting protein 3 (BNIP3) (A) and Bcl-2-like protein 13 (BDC2-L13) (B) protein expression was measured within the control, RVE and NeX groups before and after 21-days of bed rest (*n*=6). There was a significant decrease in BNIP3 and BCL2-L13 protein expression within the RVE group ($p<0.05$), however there was no significant change in BNIP3 or BCL2-L13 protein expression within the control or NeX groups ($p>0.05$).

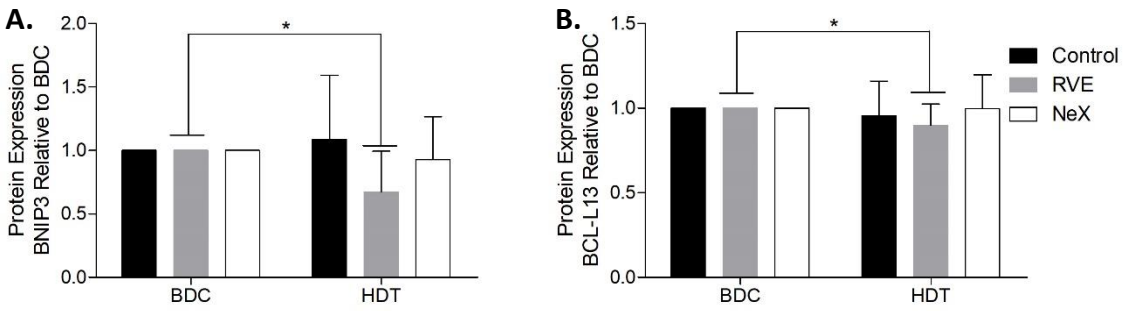

Appendix B. Figure 9. BNIP3 & BCL2-L13 protein expression following 21 days bed rest with control, RVE & NeX

(BNIP3 (A) and BCL-L13 (B) protein expression quantified by western blot (*n*=6). BNIP3, BCL2/adenovirus E1B 19 kDa protein-interacting protein 3, and BCL-L13, Bcl-2-like protein 13, were normalised against loading control (GAPdh expression) of same sample and subsequently expressed relative to BDC of same sample. Data are expressed as mean ±SE, * significant effect of time, $p<0.05$)

Expression of Other Mitochondrial Markers

MCU & VDAC1

Mitochondrial calcium uniporter (MCU) (A) and voltage-dependent anion channel 1 (VDAC1) (B) protein expression was measured within the control, RVE and NeX groups before and after 21-days of bed rest (*n*=6). There was no significant change in MCU or and VDAC1 protein expression within any group following 21-days of bed rest ($p>0.05$).

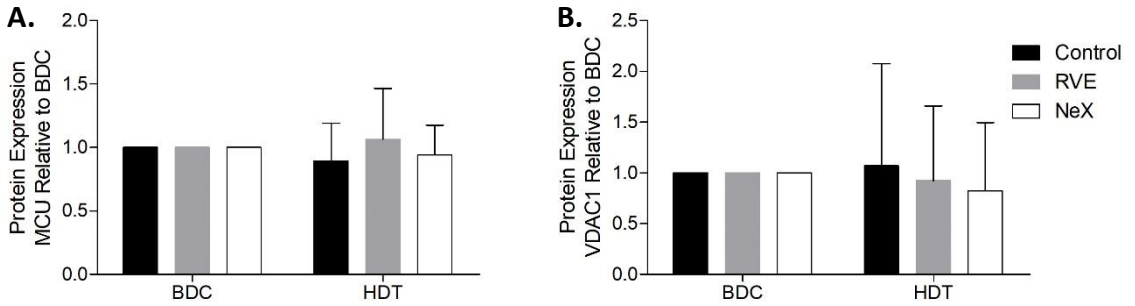

Appendix B. Figure 10. MCU & VDAC1 protein expression following 21 days bed rest with control, RVE & NeX

(MCU (A) and VDAC1 (B) protein expression quantified by western blot (*n*=6). MCU, Mitochondrial Calcium Uniporter, and VDAC1, Voltage-dependent anion-selective channel 1, were normalised against loading control (GAPdh expression) of same sample and subsequently expressed relative to BDC of same sample. Data are expressed as mean ±SE)

Resistive Vibration Exercise (RVE)

The training was performed two times per week with 3 to 4-day intervals (HDT 2, 5, 12, 16, 21). All training was performed on an integrated training device (Novotec Medical, Pforzheim, Germany). This device is a combination of two systems already used in bed rest studies. The vibration system (Vibration training device including monitoring function and data recording) combined with a system designed to exercise in the -6˚ orientation. Subjects were told to wear flat soled, non-cushioned training shoes to protect their feet. Subjects underwent two familiarization sessions during the 7-day baseline data collection period with the second familiarization session being scheduled at least 5 days before the onset of bed rest. The first exercise session during the bed rest period was on the second day. Each session comprised of the following components:

Warm up: Bilateral squats from 10° to 90° knee angle; timing: 8 seconds (4 down, 4 up) controlled by metronome; number of repetitions: 8; load: 50% of the one repetition maximum (1-RM); vibration parameters: 8 mm peak-to-peak amplitude and 24 Hz vibration frequency.

Squatting exercise: Bilateral squats from 10° to 90° knee angle; timing: 8 seconds (4 down, 4 up) controlled by metronome; number of repetitions: 10; load at study commencement: 75% of the 1-RM during study commencement; progression: 5% load increase when more than 10 repetitions are possible; 5% load decrease when 6 or fewer repetitions are possible; vibration parameters: 8 mm peak-to peak and 24 Hz.

Single leg heel raises: From maximal dorsiflexion to maximal plantar flexion; heel contact with footplate is avoided by a bar under the forefoot; timing: as fast as possible; number of repetitions: unto exhaustion; load at study commencement: 1.3 times body weight; progression: 5% load increase when more than 50 seconds are possible, 5% load decrease when 30 seconds or less are possible; vibration parameters: 8 mm peak to peak and 26 Hz.

Bilateral heel raises: From maximal dorsiflexion to maximal plantar flexion; heel contact with footplate is avoided by a bar under the forefoot; timing: as fast as possible; number of repetitions: unto exhaustion; load at study commencement: 1.8 times body weight; progression: 5% load increase when more than 55 seconds are possible, 5% load decrease when 40 seconds or less are possible; vibration parameters: 8 mm peak to peak and 26 Hz.

Protein Expression of RVE only

Below is a comparison in protein expression before (BDC) and after (HDT) 21 days of bed rest for markers of mitochondrial biogenesis, fusion, fission, mitophagy and other markers of mitochondrial and cellular metabolism in subjects who completed the resistive vibration exercise (RVE) trial only.

Expression of Markers Associated with Mitochondrial Biogenesis

PGC-1α

PGC-1α, pparg coactivator-1 alpha, a well-supported regulator of mitochondrial biogenesis, was analysed for protein expression before and after 21-days of bed rest in those within the RVE trial (*n*=11). There was no significant change in PGC-1α protein expression in those completing the RVE trial following 21-days of bed rest ($p>0.05$).

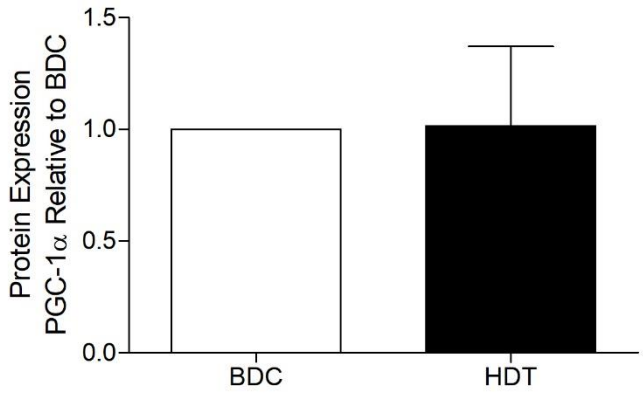

Appendix B. Figure 11. PGC-1α protein expression following 21 days bed rest with control & RVE

(PGC-1α protein expression quantified by western blot (*n*=11). PGC-1α, PPARG coactivator 1 alpha, was normalised against loading control (GAPdh expression) of same sample and subsequently expressed relative to BDC of same sample. Data are expressed as mean ±SE)

Expression of Markers Associated with Mitochondrial Fusion

OPA1

OPA1, optic atrophy 1, a regulator of mitochondrial fusion, was analysed for protein expression before and after 21-days of bed rest in those within the RVE trial (*n*=11). There was no significant change in OPA1 protein expression in those completing the RVE trial following 21-days of bed rest (*p*>0.05).

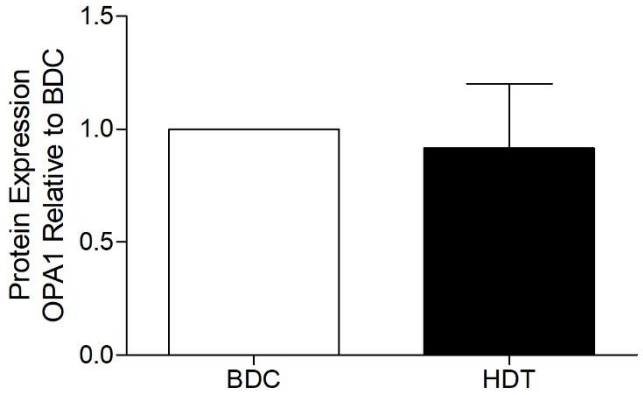

Appendix B. Figure 12. OPA1 protein expression following 21 days bed rest with control & RVE

(OPA1 protein expression quantified by western blot (*n*=11). OPA1, optic atrophy 1, was normalised against loading control (GAPdh expression) of same sample and subsequently expressed relative to BDC of same sample. Data are expressed as mean ±SE)

L-OPA1 & s-OPA1

The long and short isoforms of OPA1 were analysed for protein expression before and after 21-days of bed rest in those within the RVE trial (*n*=11). There was no significant change in either L-OPA1 (A) or s-OPA1 (B) protein expression in those completing the RVE trial following 21-days of bed rest (*p*>0.05).

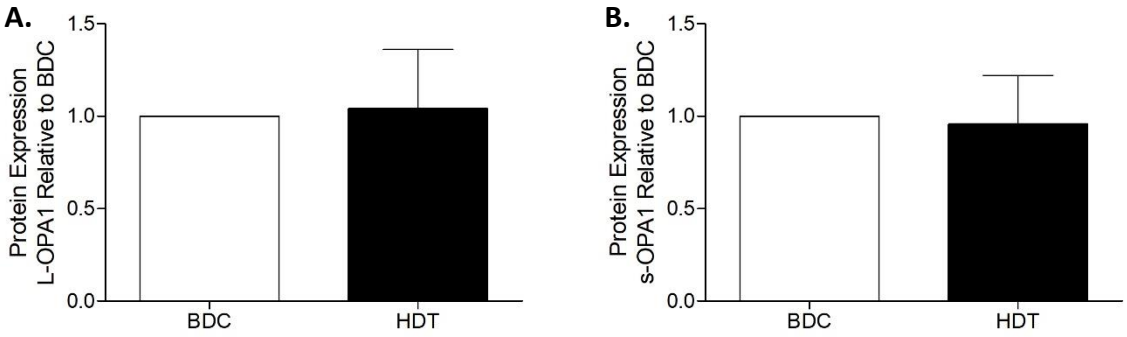

Appendix B. Figure 13. L-OPA1 & s-OPA1 protein expression following 21 days bed rest with control & RVE

(L-OPA1 (A) & s-OPA1 (B) protein expression quantified by western blot (*n*=11). L-OPA1, long isoform optic atrophy 1 & s-OPA1, short isoform optic atrophy 1, were normalised against loading control (GAPdh expression) of same sample and subsequently expressed relative to BDC of same sample. Data are expressed as mean ±SE)

Mfn1 & Mfn2

Mitofusin-1 (Mfn1) (A) and mitofusin-2 (Mfn2) (B) were analysed for protein expression before and after 21-days of bed rest in those within the RVE trial (*n*=11). There was no significant change in either Mfn1 (A) or Mfn2 (B) protein expression in those completing the RVE trial following 21-days of bed rest (*p*>0.05).

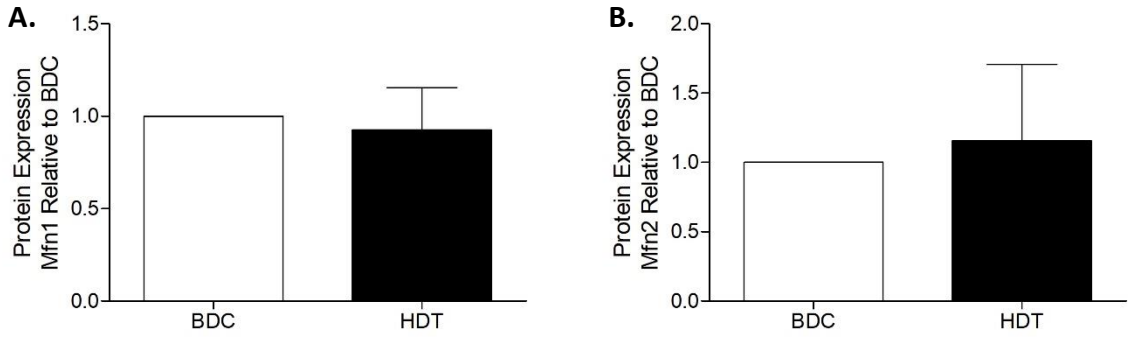

Appendix B. Figure 14. Mfn1 & Mfn2 protein expression following 21 days bed rest with control & RVE

(Mfn1 (A) & Mfn2 (B) protein expression quantified by western blot (*n*=11). Mfn1, Mitofusin-1, & Mfn2, Mitofusin-2, were normalised against loading control (GAPdh expression) of same sample and subsequently expressed relative to BDC of same sample. Data are expressed as mean ±SE)

OMA1 & YME1L

Metalloendopeptidase OMA1 (A) and ATP-dependent zinc metalloprotease YME1L (B) were analysed for protein expression before and after 21-days of bed rest in those within the RVE trial (*n*=11). There was an increase in OMA1 protein expression following 21-days of bed rest within the RVE trial ($p<0.05$). There was no significant change in YME1L protein expression following 21-days of bed rest within the RVE trial ($p>0.05$).

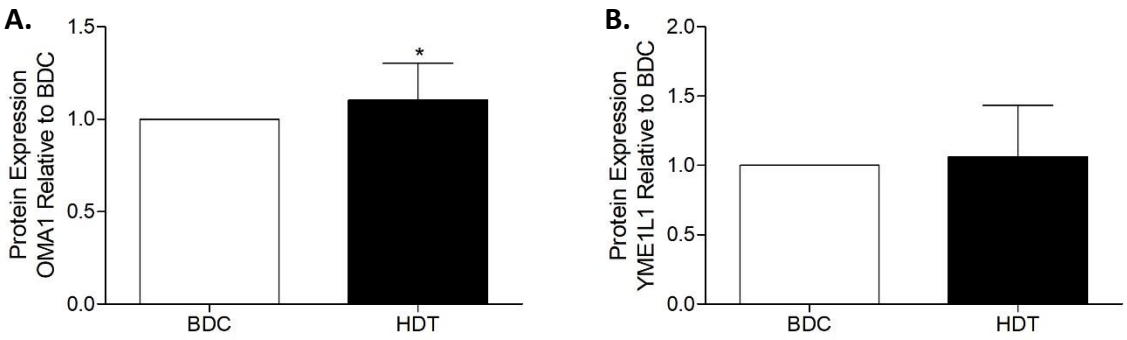

Appendix B. Figure 15. OMA1 & YME1L protein expression following 21 days bed rest with control & RVE

(OMA1 (A) & YME1L (B) protein expression quantified by western blot (*n*=11 (A) & n=8 (B)). OMA1, Metalloendopeptidase OMA1, & YME1L, ATP-dependent metalloprotease YME1L, were normalised against loading control (GAPdh expression) of same sample and subsequently expressed relative to BDC of same sample. Data are expressed as mean ±SE, * significant effect of time, $p<0.05$)

Expression of Markers Associated with Mitochondrial Fission

Drp1 & Fis1

Markers of mitochondrial fission, dynamin related protein 1 (Drp1) (A) and mitochondrial fission protein 1 (Fis1) (B) were analysed for protein expression before and after 21-days of bed rest in those within the RVE trial (n=11). There was no significant change in Drp1 protein expression following 21-days of bed rest within the RVE trial (p>0.05). However, there was a significant increase in Fis1 protein expression following 21-days of bed rest within the RVE trial (p<0.05).

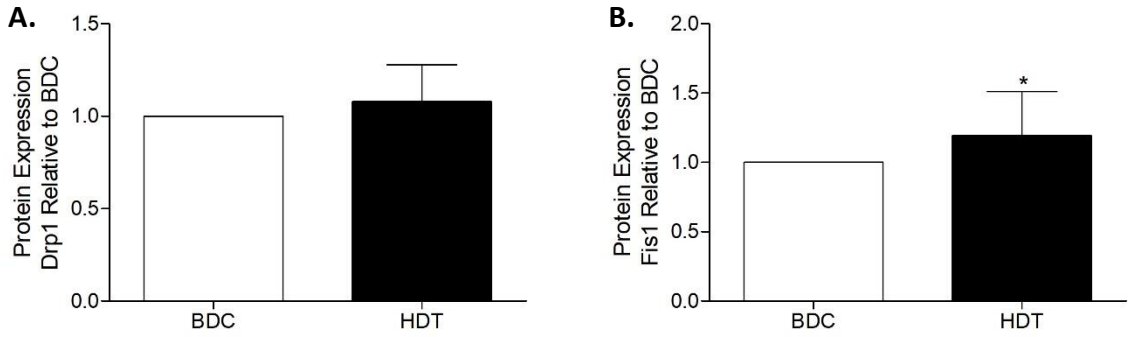

Appendix B. Figure 16. Drp1 & Fis1 protein expression following 21 days bed rest with control & RVE

(Drp1 (A) & Fis1 (B) protein expression quantified by western blot (n=11). Drp1, dynamin related protein 1, & Fis1, mitochondrial fission protein 1, were normalised against loading control (GAPdh expression) of same sample and subsequently expressed relative to BDC of same sample. Data are expressed as mean ±SE, * significant effect of time, p<0.05)

Ratio of Mitochondrial Fusion:Fission (RVE)

In order to assess for the balance between mitochondrial fusion and fission with RVE following 21 days of -6° head down tilt bed rest, protein expression of mitochondrial fusion marker, OPA1 was controlled against protein expression of mitochondrial fission marker, Drp1.

OPA1:Drp1 Ratio

There was a significant decrease in OPA1:Drp1 ratio within the RVE group following 21-days of bed rest (p<0.05). This result indicates that following 21-days of bed rest with RVE there was a possible increase in Drp1 mediated mitochondrial fission (yet not significant) due to the possible decrease in OPA1 mediated mitochondrial fusion (yet not significant) within this group.

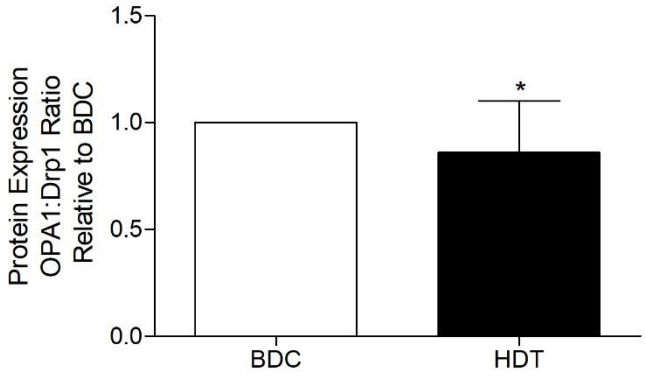

Appendix B. Figure 17. OPA1:Drp1 Ratio following 21 days bed rest with control & RVE

(OPA1:Drp1 protein expression quantified by western blot. OPA1, optic atrophy 1 was controlled against Drp1, dynamin related protein 1, protein expression (n=11). Both OPA1 and Drp1 protein expression were firstly normalised to their respective loading control (GAPdh) and subsequently expressed relative to BDC of same sample. Data are expressed as mean ±SE, * significant effect of time, p<0.05)

Expression of Markers Associated with Mitophagy

PINK1 & Parkin

Markers of mitophagy, PTEN-induced kinase 1 (PINK1) (A) and Parkin (B) were analysed for protein expression before and after 21-days of bed rest in those within the RVE trial (*n*=11). There was no significant change in either PINK1 or Parkin protein expression following 21-days of bed rest within the RVE trial ($p>0.05$).

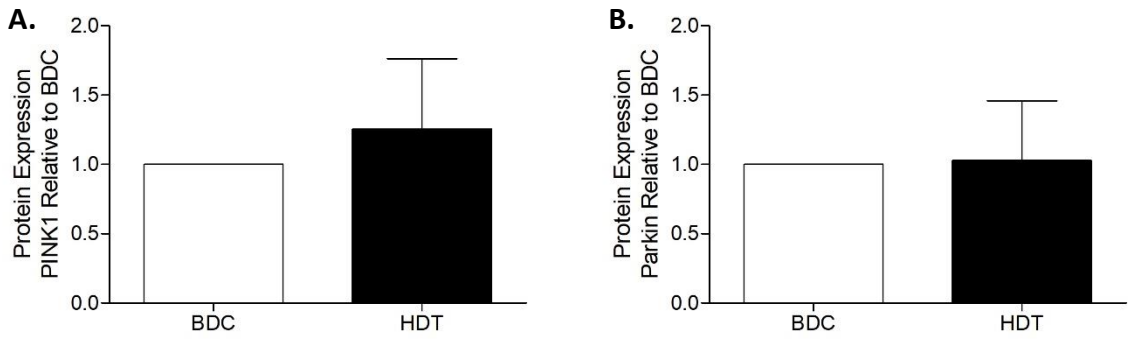

Appendix B. Figure 18. PINK1 & Parkin protein expression following 21 days bed rest with control & RVE

(PINK1 (A) & Parkin (B) protein expression quantified by western blot (*n*=11). PINK1, PTEN-induced kinase 1, & Parkin were normalised against loading control (GAPdh expression) of same sample and subsequently expressed relative to BDC of same sample. Data are expressed as mean ±SE)

BNIP3 & BCL2-L13

BCL2/adenovirus E1B 19 kDa protein-interacting protein 3 (BNIP3) (A) and Bcl-2-like protein 13 (BCL2-L13) (B) were analysed for protein expression before and after 21-days of bed rest in those within the RVE trial (*n*=11). There was a significant decrease in BNIP3 protein expression in those within the RVE group following 21-days of bed rest ($p<0.005$). There was no significant change in BCL2-L13 protein expression within the RVE group following 21-days of bed rest ($p>0.05$).

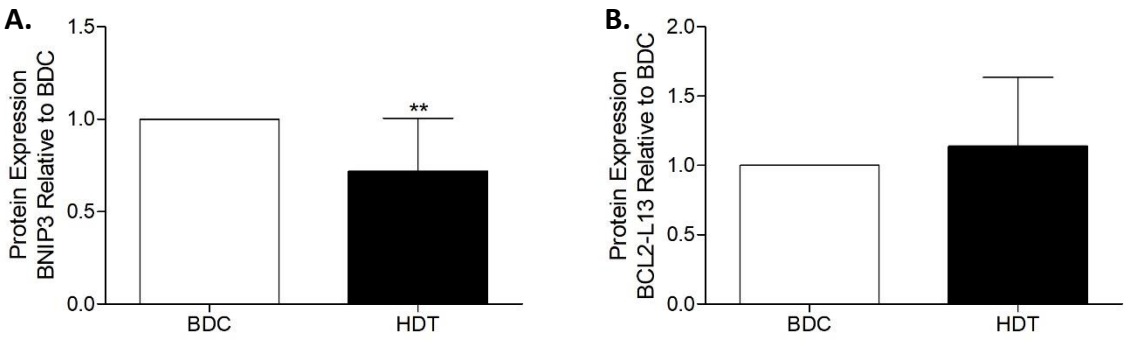

Appendix B. Figure 19. BNIP3 & BCL2-L13 protein expression following 21 days bed rest with control & RVE

(BNIP3 (A) & BCL2-L13 (B) protein expression quantified by western blot (*n*=11). BNIP3, BCL2/adenovirus E1B 19 kDa protein-interacting protein 3, & BCL2-L13, Bcl-2-like protein 13, were normalised against loading control (GAPdh expression) of same sample and subsequently expressed relative to BDC of same sample. Data are expressed as mean ±SE, * significant effect of time, $p<0.05$)

Expression of Other Mitochondrial Markers

MCU & VDAC1

Mitochondrial calcium uniporter (MCU) (A) and voltage-dependent anion channel 1 (VDAC1) (B) were analysed for protein expression before and after 21-days of bed rest in those within the RVE trial (*n*=11). There was no significant change in either MCU or VDAC1 protein expression within the RVE group following 21-days of bed rest ($p>0.05$).

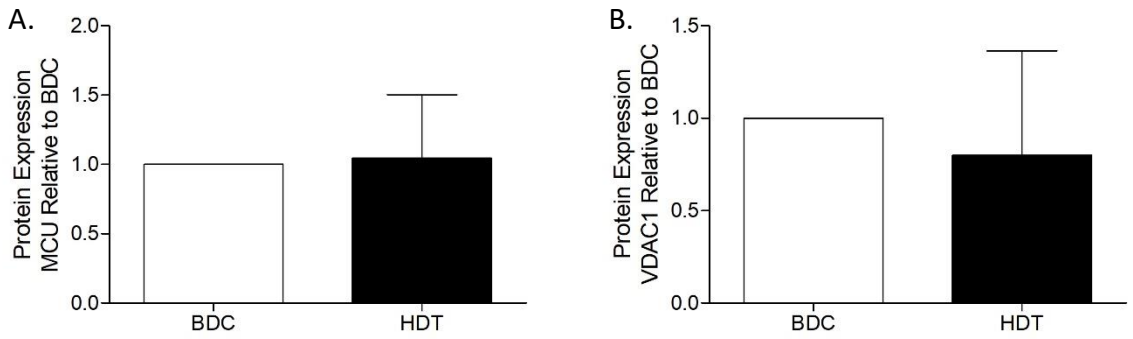

Appendix B. Figure 20. MCU & VDAC1 protein expression following 21 days bed rest with control & RVE

(MCU (A) & VDAC1 (B) protein expression quantified by western blot (*n*=11). MCU, mitochondrial calcium uniporter, & VDAC1, Voltage-dependent anion-selective channel 1, were normalised against loading control (GAPdh expression) of same sample and subsequently expressed relative to BDC of same sample. Data are expressed as mean ±SE)

Nutrition and exercise group (NEX)

For all ESA bed rest studies, the aim is to maintain fat mass while accepting the fat free mass is likely to decrease. Fat mass is clamped by ensuring the total energy intake matches energy expenditure. This is achieved by measuring resting metabolic rate and adjusting the diet accordingly. This way, we see no change in fat mass (kg) and a reduction in lean muscle mass (kg). This is important in order to isolate the effects of bed rest and the countermeasures. If fat mass increased, we could not then attribute any changes that we see to bed rest or countermeasures as increased fat mass would be a confounding variable.

Subjects in the exercise and nutrition group (NEX) were given a whey protein supplement in addition to partaking in the resistive exercise vibration protocol (section 3.3.1). An isocaloric supplementation of whey protein (0.6 g/kg body weight/day) was given to the volunteers in the NEX group bringing the total protein intake to 1.8 g/kg body weight/day. Protein supplementation was given every day. On days without exercise, the supplement was applied in equal amounts with main meals. On days with exercise, half of the daily amount was given in a timeframe of 30 minutes after exercise and the other halve equally distributed with main meals. The product was Diaprotein®, a powder supplied by Nephrologische Präparate Dr. Volker Steudle (Linden, Allemagne).

The composition was the following:

- Diaprotein® 100 g Powder
- Calorie intake 1573 kJ (370 kcal)
- Proteins 90 g
- Fat 0.2 g
- Lactose 2.5 g
- Sodium < 300 mg
- Potassium < 650 mg
- Calcium < 400 mg
- Phosphorus < 250 mg
- Relation Phosphorus/protein < 3 mg/g

As one disadvantage of high protein intake along with low dietary alkalinity (characterized by low potassium intake) is that this may exacerbate bone loss. For this reason and since whey protein adds a certain acid load to the diet, supplementation of 90 mmol KHCO3 per day was applied in 6

portions (with main meals and snacks) and compensated for that. Effervescent tablets of potassium bicarbonate were provided by Krüger GmbH & Co (Bergisch Gladbach, Germany).

Protein Expression of NeX only

Below is a comparison in protein expression before (BDC) and after (HDT) 21 days of bed rest for markers of mitochondrial biogenesis, fusion, fission, mitophagy and other markers of mitochondrial and cellular metabolism in subjects who completed the nutrition and exercise (NeX) trial only.

Expression of Markers Associated with Mitochondrial Biogenesis

PGC-1α

PGC-1α, pparg coactivator-1 alpha, a well-supported regulator of mitochondrial biogenesis, was analysed for protein expression before and after 21-days of bed rest in those within the NeX trial (*n*=7). There was a significant decrease in PGC-1α protein expression in those who completed the NeX trial following 21-days of bed rest ($p<0.005$).

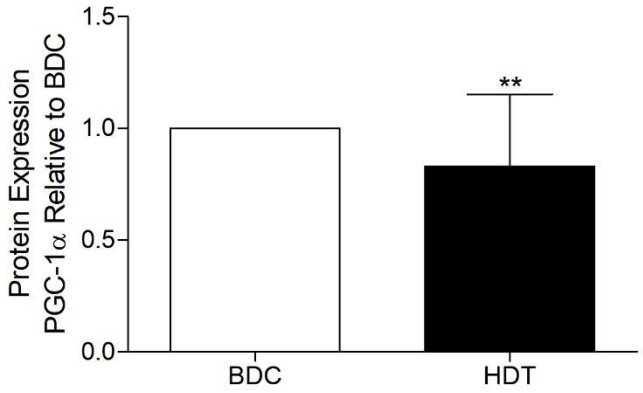

Appendix B. Figure 21. PGC-1α protein expression following 21 days bed rest with control & NeX

(PGC-1α protein expression quantified by western blot (*n*=7). PGC-1α, PPARG coactivator 1 alpha, was normalised against loading control (GAPdh expression) of same sample and subsequently expressed relative to BDC of same sample and subsequently expressed relative to BDC of same sample. Data are expressed as mean ±SE, ** significant effect of time, $p<0.005$)

Expression of Markers Associated with Mitochondrial Fusion

OPA1

OPA1, optic atrophy 1, a regulator of mitochondrial fusion, was analysed for protein expression before and after 21-days of bed rest in those within the NeX trial (*n*=7). There was no significant change in OPA1 protein expression in those who completed the NeX trial following 21-days of bed rest ($p>0.05$).

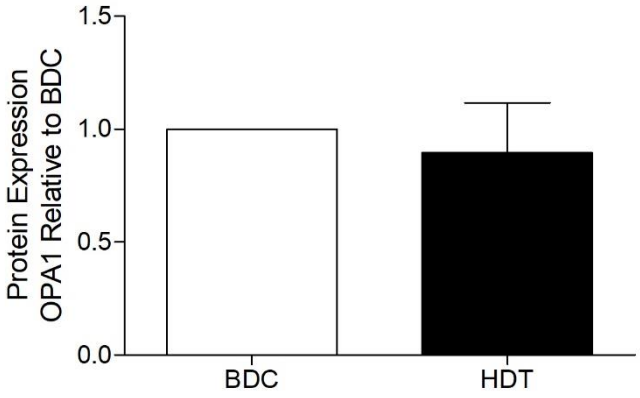

Appendix B. Figure 22. OPA1 protein expression following 21 days bed rest with control & NeX

(OPA1 protein expression quantified by western blot (*n*=7). OPA1, optic atrophy 1, was normalised against loading control (GAPdh expression) of same sample and subsequently expressed relative to BDC of same sample. Data are expressed as mean ±SE)

L-OPA1 & s-OPA1

The long and short isoforms of OPA1were analysed for protein expression before and after 21-days of bed rest in those within the NeX trial (*n*=7). There was a significant decrease in L-OPA1 (A) protein expression in those who completed the NeX trial ($p<0.05$), however there was no significant change in s-OPA1 (B) protein expression in those who completed the NeX trial following 21-days of bed rest ($p>0.05$).

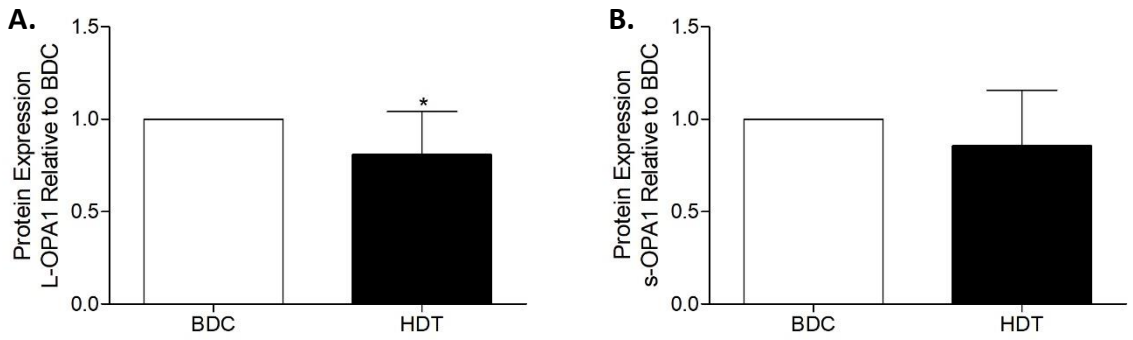

Appendix B. Figure 23. L-OPA1 & s-OPA1 protein expression following 21 days bed rest with control & NeX

(L-OPA1 (A) & s-OPA1 (B) protein expression quantified by western blot (*n*=7). L-OPA1, long isoform optic atrophy 1 & s-OPA1, short isoform optic atrophy 1, were normalised against loading control (GAPdh expression) of same sample and subsequently expressed relative to BDC of same sample. Data are expressed as mean ±SE, * significant effect of time, $p<0.05$)

Mfn1 & Mfn2

Mitofusin-1 (Mfn1) and mitofusin-2 (Mfn2) were analysed for protein expression before and after 21-days of bed rest in those within the NeX trial (*n*=7). There was no significant change in either Mfn1 or Mfn2 protein expression in those who completed the NeX trial following 21-days of bed rest ($p>0.05$).

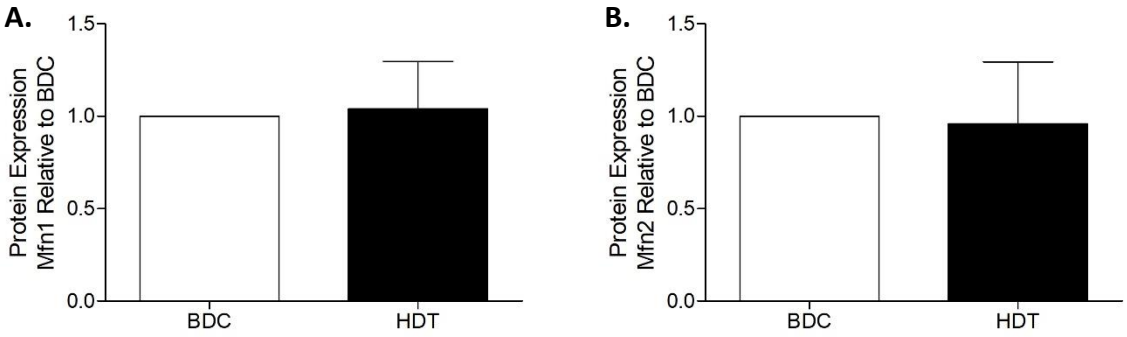

Appendix B. Figure 24. Mfn1 & Mfn2 protein expression following 21 days bed rest with control & NeX

(Mfn1 (A) & Mfn2 (B) protein expression quantified by western blot (*n*=7). Mfn1, Mitofusin-1, & Mfn2, Mitofusin-2, were normalised against loading control (GAPdh expression) of same sample and subsequently expressed relative to BDC of same sample. Data are expressed as mean ±SE)

OMA1 & YME1L

Metalloendopeptidase OMA1 (A) and ATP-dependent zinc metalloprotease YME1L (B) were analysed for protein expression before and after 21-days of bed rest in those within the NeX trial (*n*=7). There was no significant change in either OMA1 or YME1L protein expression in those who completed the NeX trial following 21-days of bed rest ($p>0.05$).

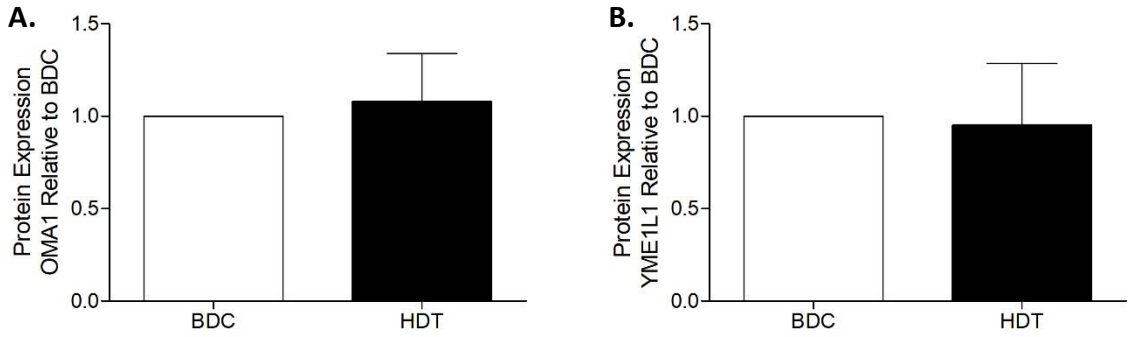

Appendix B. Figure 25. OMA1 & YME1L protein expression following 21 days bed rest with control & NeX

(OMA1 (A) & YME1L (B) protein expression quantified by western blot (*n*=7 (A) & n=5 (B)). OMA1, Metalloendopeptidase OMA1, & YME1L, ATP-dependent metalloprotease YME1L, were normalised against loading control (GAPdh expression) of same sample and subsequently expressed relative to BDC of same sample. Data are expressed as mean ±SE, * significant effect of time, $p<0.05$)

Expression of Markers Associated with Mitochondrial Fission

Drp1 & Fis1

Markers of mitochondrial fission, dynamin related protein 1 (Drp1) (A) and mitochondrial fission protein 1 (Fis1) (B) were analysed for protein expression before and after 21-days of bed rest in those within the NeX trial (*n*=7). There was a significant increase in Drp1 protein expression in those who completed the NeX trial following 21-days of bed rest ($p<0.05$). There was no significant change in Fis1 protein expression in those who completed the NeX trial following 21-days of bed rest ($p>0.05$).

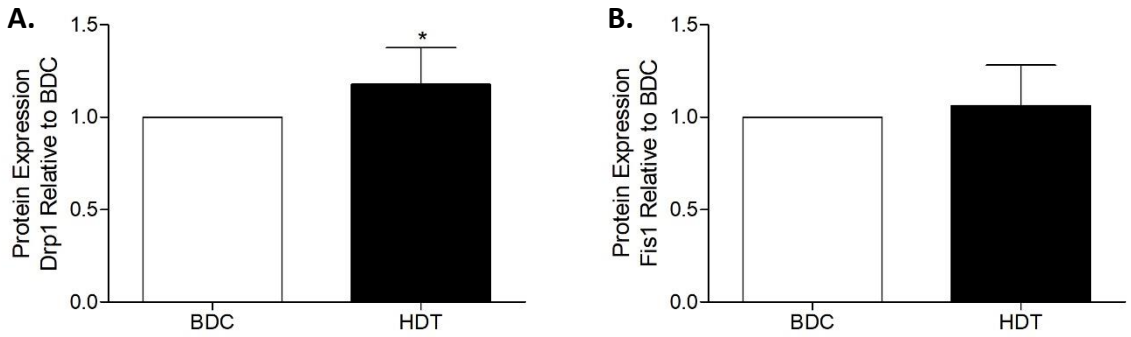

Appendix B. Figure 26. Drp1 & Fis1 protein expression following 21 days bed rest with control & NeX

(Drp1 (A) & Fis1 (B) protein expression quantified by western blot (*n*=7). Drp1, dynamin related protein 1, & Fis1, mitochondrial fission protein 1, were normalised against loading control (GAPdh expression) of same sample and subsequently expressed relative to BDC of same sample. Data are expressed as mean ±SE, * significant effect of time, $p<0.05$)

Ratio of Mitochondrial Fusion:Fission (NeX)

In order to assess for the balance between mitochondrial fusion and fission with NeX following 21 days of -6° head down tilt bed rest, protein expression of mitochondrial fusion marker, OPA1 was controlled against protein expression of mitochondrial fission marker, Drp1.

OPA1:Drp1 Ratio

There was a significant decrease in OPA1:Drp1 ratio within the NeX group following 21-days of bed rest (p<0.05). This result indicates that following 21-days of bed rest with NeX there was an increase in Drp1 mediated mitochondrial fission due to the lack of change in OPA1 protein expression within the NeX group.

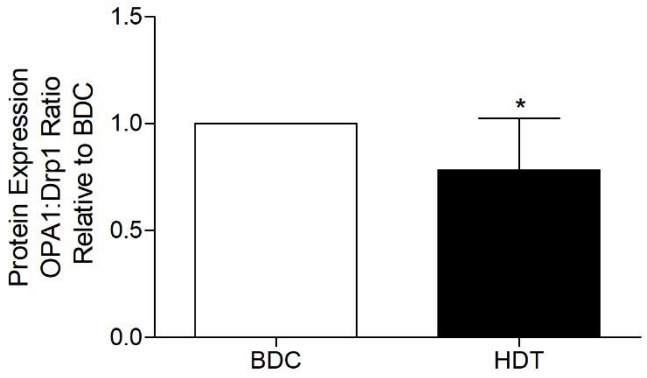

Appendix B. Figure 27. OPA1:Drp1 Ratio following 21 days bed rest with control & NeX

(OPA1:Drp1 protein expression quantified by western blot. OPA1, optic atrophy 1 was controlled against Drp1, dynamin related protein 1, protein expression (n=7). Both OPA1 and Drp1 protein expression were firstly normalised to their respective loading control (GAPdh) and subsequently expressed relative to BDC of same sample. Data are expressed as mean ±SE, * significant effect of time, p<0.05)

Expression of Markers Associated with Mitophagy

PINK1 & Parkin

Markers of mitophagy, PTEN-induced kinase 1 (PINK1) (A) and Parkin (B) were analysed for protein expression before and after 21-days of bed rest in those within the NeX trial (n=7). There was a significant increase in PINK1 protein expression in those who completed the NeX trial following 21-days of bed rest (p<0.05). There was no significant change in Parkin protein expression in those who completed the NeX trial following 21-days of bed rest (p>0.05).

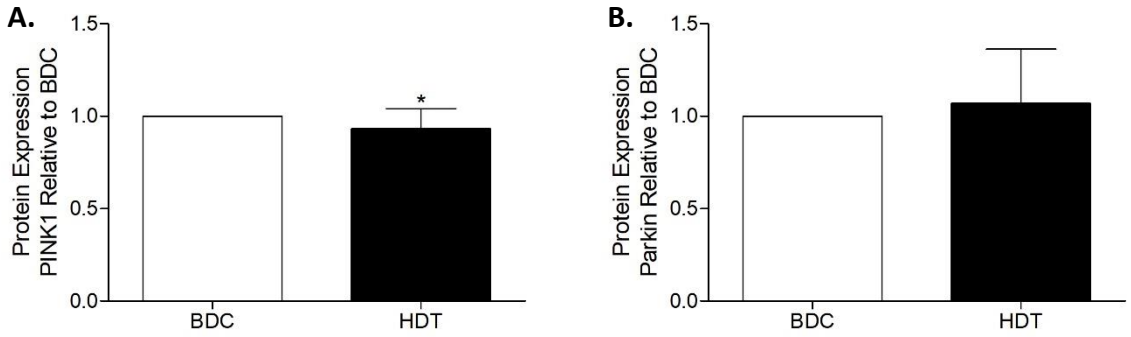

Appendix B. Figure 28. PINK1 & Parkin protein expression following 21 days bed rest with control & NeX

(PINK1 (A) & Parkin (B) protein expression quantified by western blot (n=7). PINK1, PTEN-induced kinase 1, & Parkin were normalised against loading control (GAPdh expression) of same sample and subsequently expressed relative to BDC of same sample. Data are expressed as mean ±SE, * significant effect of time, p<0.05)

BNIP3 & BCL2-L13

BCL2/adenovirus E1B 19 kDa protein-interacting protein 3 (BNIP3) (A) and Bcl-2-like protein 13 (BCL2-L13) (B) protein expression were analysed before and after 21-days of bed rest in those within the NeX trial (*n*=7). There was no significant change in either BNIP3 or BCL2-L13 protein expression in those who completed the NeX trial following 21-days of bed rest (*p*>0.05).

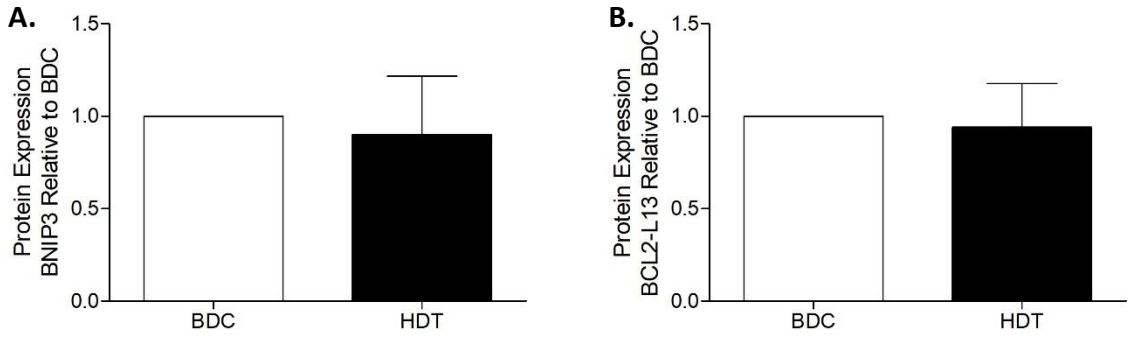

Appendix B. Figure 29. BNIP3 & BCL2-L13 protein expression following 21 days bed rest with control & NeX

(BNIP3 (A) & BCL2-L13 (B) protein expression quantified by western blot (*n*=7). BNIP3, BCL2/adenovirus E1B 19 kDa protein-interacting protein 3, & BCL2-L13, Bcl-2-like protein 13, were normalised against loading control (GAPdh expression) of same sample and subsequently expressed relative to BDC of same sample. Data are expressed as mean ±SE)

Expression of Other Mitochondrial Markers

MCU & VDAC1

Mitochondrial calcium uniporter (MCU) (A) and voltage-dependent anion channel 1 (VDAC1) (B) protein expression were analysed before and after 21-days of bed rest in those within the NeX trial (*n*=7). There was no significant change in either MCU or VDAC1 protein expression in those who completed the NeX trial following 21-days of bed rest ($p>0.05$).

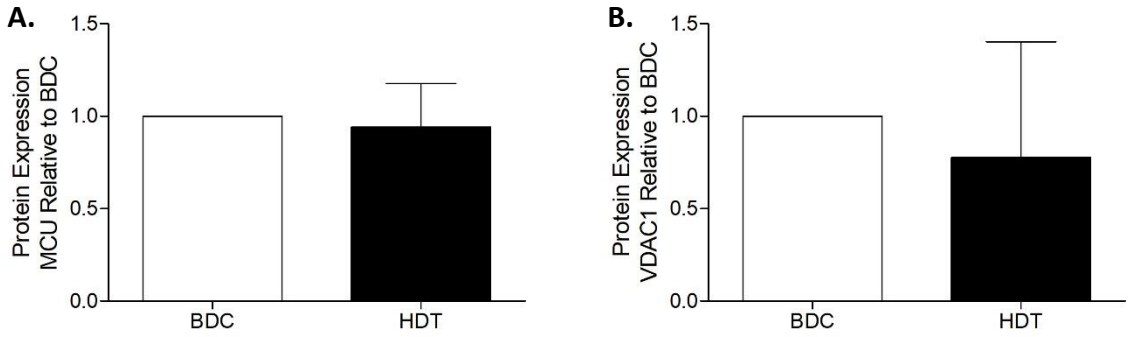

Appendix B. Figure 30. MCU & VDAC1 protein expression following 21 days bed rest with control & NeX

(MCU (A) & VDAC1 (B) protein expression quantified by western blot (*n*=7). MCU, mitochondrial calcium uniporter, & VDAC1, Voltage-dependent anion-selective channel 1, were normalised against loading control (GAPdh expression) of same sample and subsequently expressed relative to BDC of same sample. Data are expressed as mean ±SE)

Ponceau Blots 21-Day Bed Rest Study

All blots were incubated in neat ponceau for 30 seconds following transfer of protein onto nitrocellulose membrane. Ponceau was subsequently removed by washing in TBS-t. Phosphorylated proteins and those transferred onto PVDF membranes were not incubated in ponceau. Subsequently, not all proteins have representative ponceau images. Below are representative ponceau blots for used to assess for expression of proteins.

Ponceau Blot for Markers of Mitochondrial Biogenesis

PGC-1α

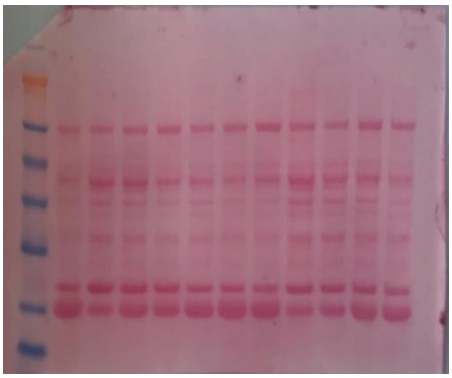

Appendix B. Figure 31. Ponceau blot example - PGC-1α

Ponceau Blot for Markers of Mitochondrial Fusion

OPA1

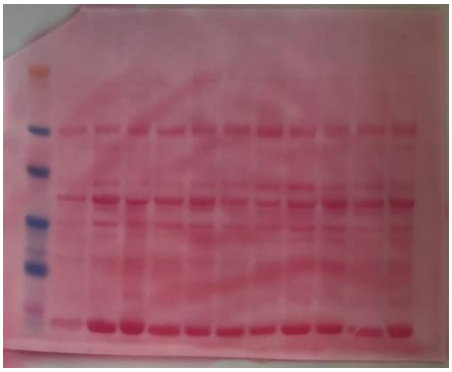

Appendix B. Figure 32. Ponceau blot example - OPA1

Mfn1 & Mfn2

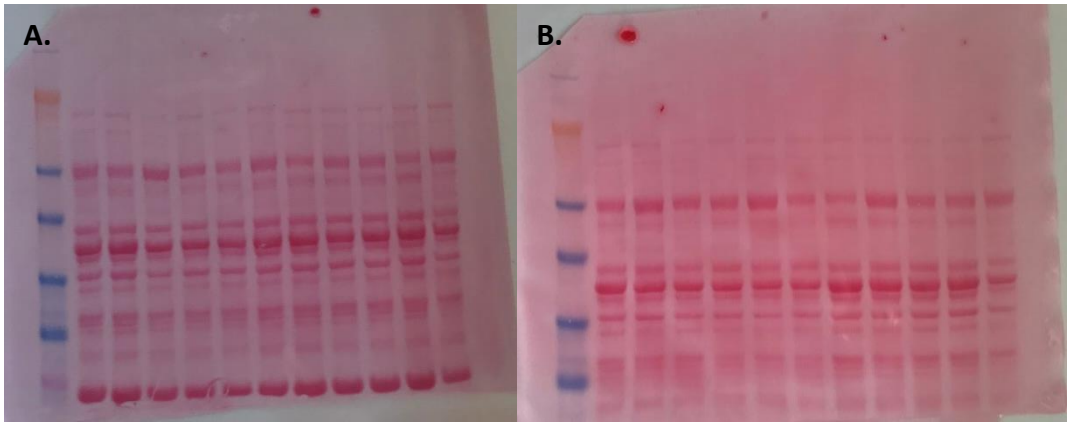

Appendix B. Figure 33. Ponceau Blot. Mfn1 (A). Ponceau blot Mfn2 (B)

OMA1 & YME1L

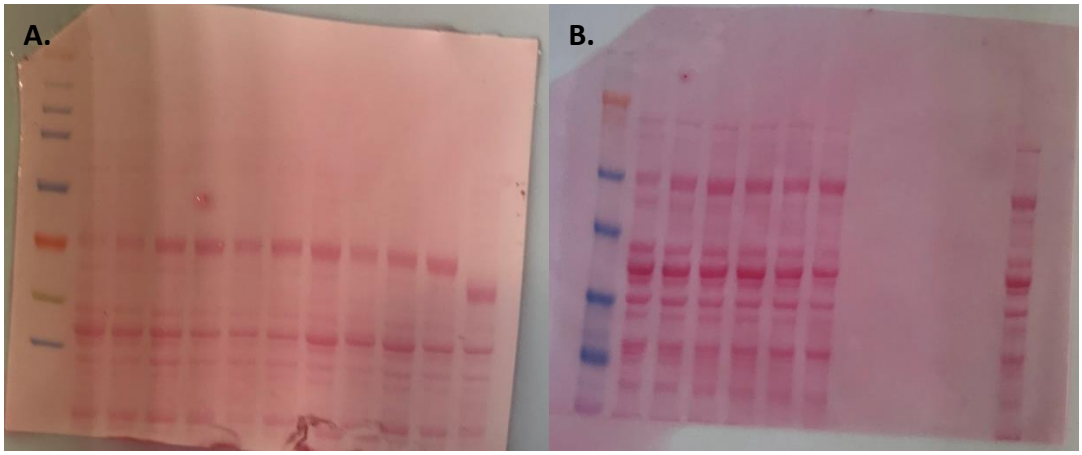

Appendix B. Figure 34. Ponceau Blot. OMA1 (A). Ponceau blot YME1L (B)

Ponceau Blot for Markers of Mitochondrial Fission

Drp1 & Fis1

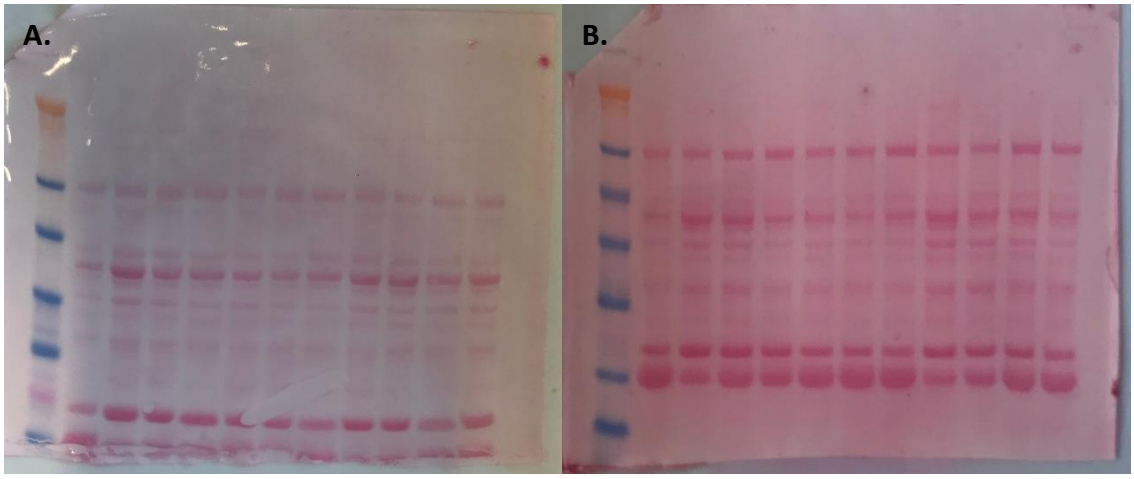

Appendix B. Figure 35. Ponceau Blot. Drp1 (A). Ponceau blot Fis1 (B)

Ponceau Blot for Markers of Mitophagy

PINK1 & Parkin

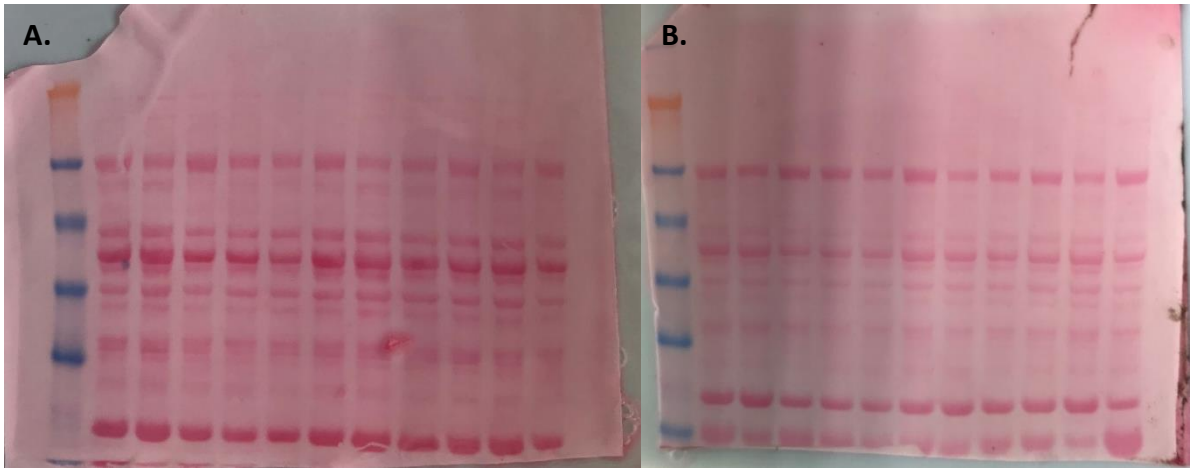

Appendix B. Figure 36. Ponceau Blot. PINK1 (A). Ponceau blot Parkin (B)

BNIP3 & BCL2-L13

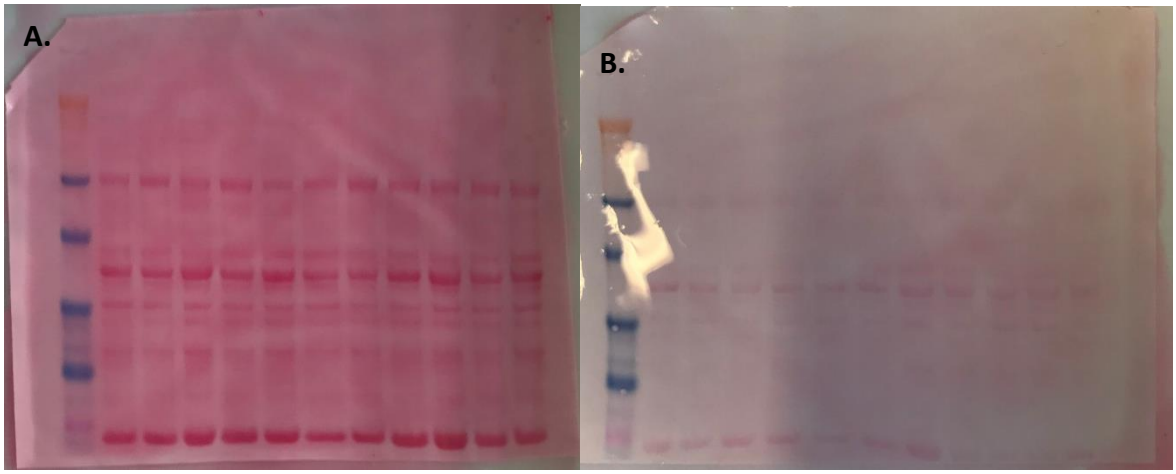

Appendix B. Figure 37. Ponceau Blot. BNIP3 (A). Ponceau blot BCL2-L13 (B)

Ponceau Blot for Other Mitochondrial Markers

MCU & VDAC1

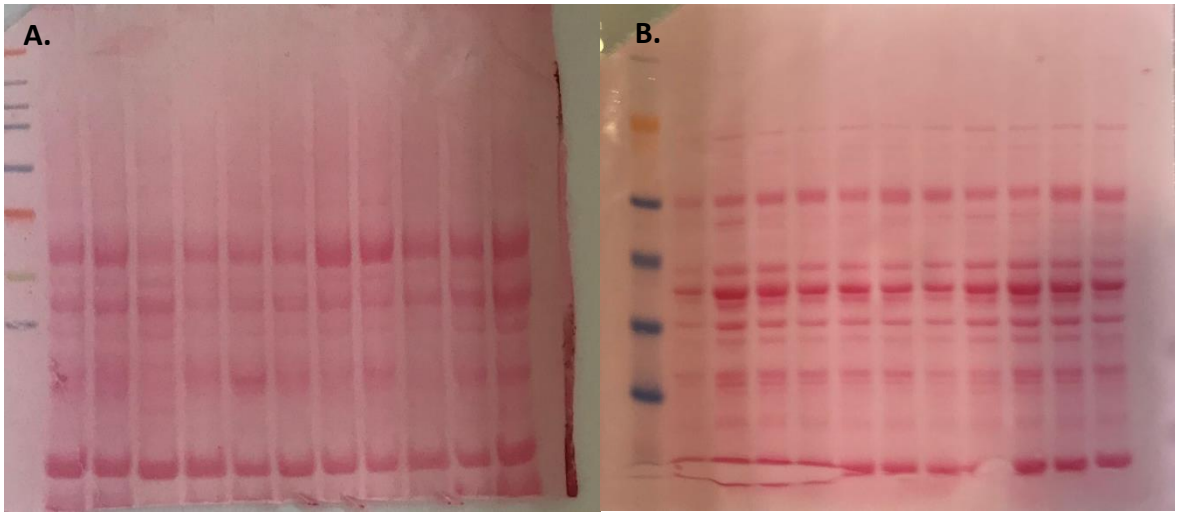

Appendix B. Figure 38. Ponceau Blot. MCU (A). Ponceau blot VDAC1 (B)

Densitometry Blots – 21 Day Bed Rest Study

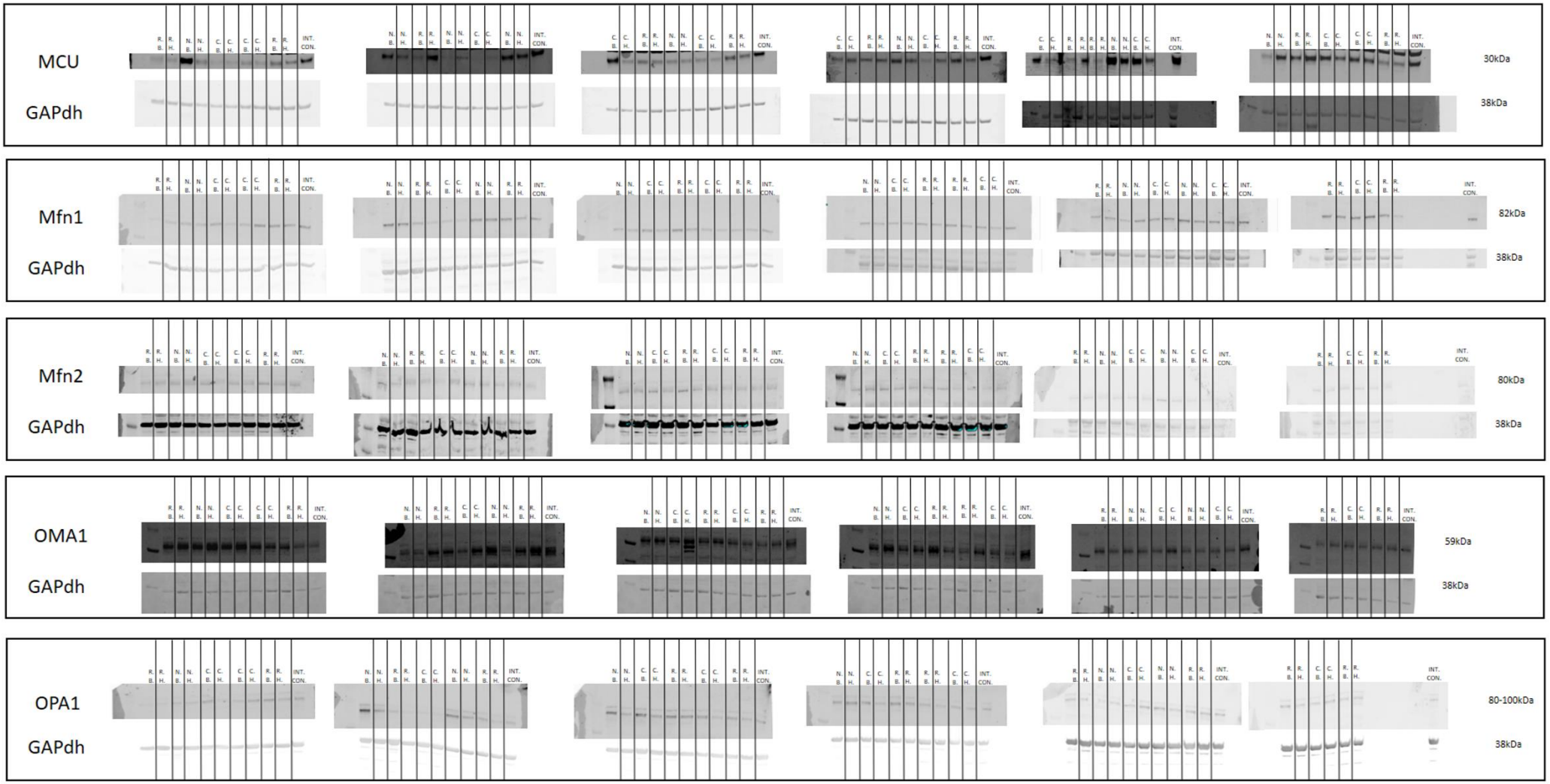

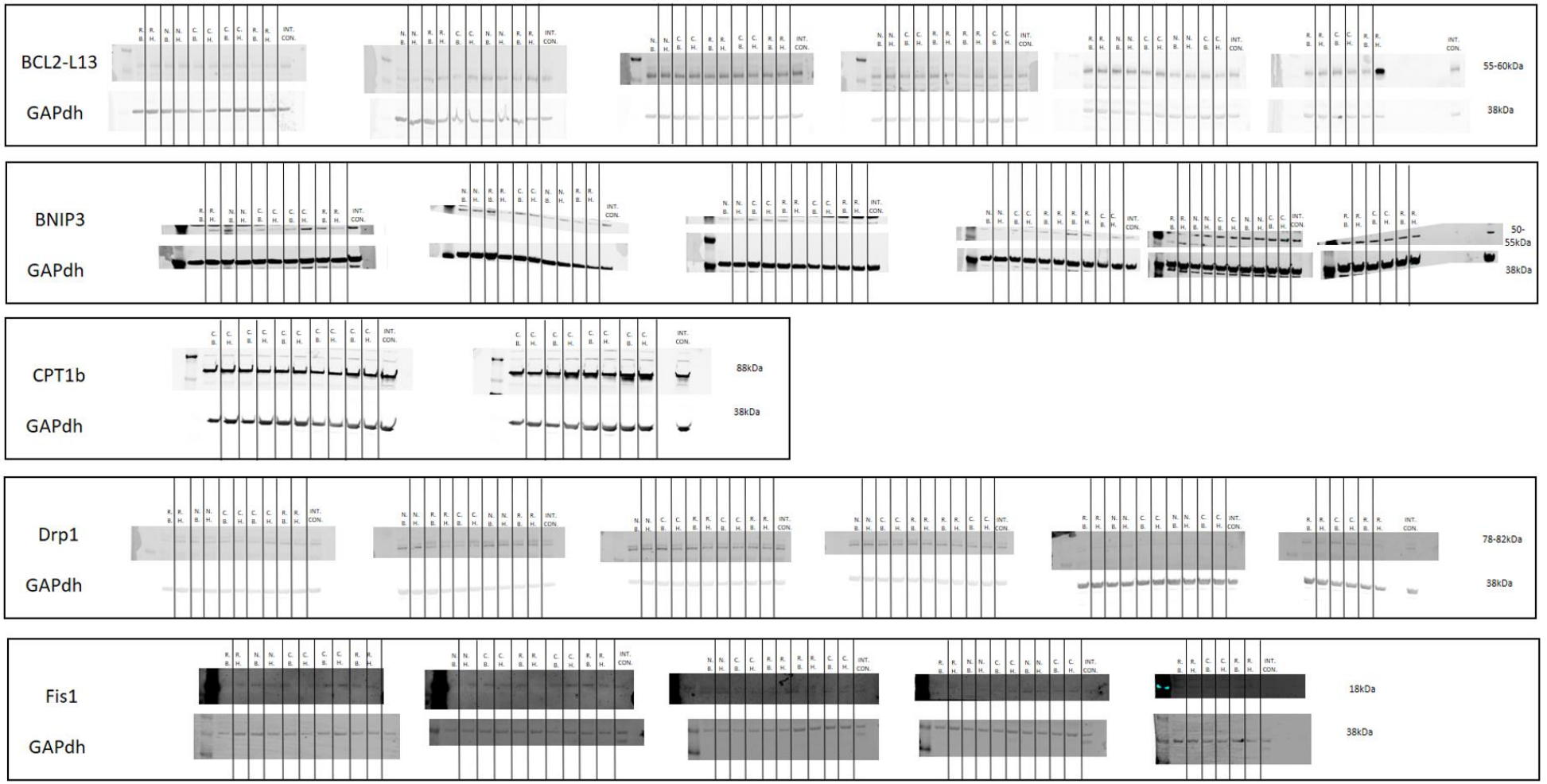
BCL2-L13
GAPdh
55-60kDa
38kDa
BNIP3
GAPdh
50-55kDa
38kDa
CPT1b
GAPdh
88kDa
38kDa
Drp1
GAPdh
78-82kDa
38kDa
Fis1
GAPdh
18kDa
38kDa

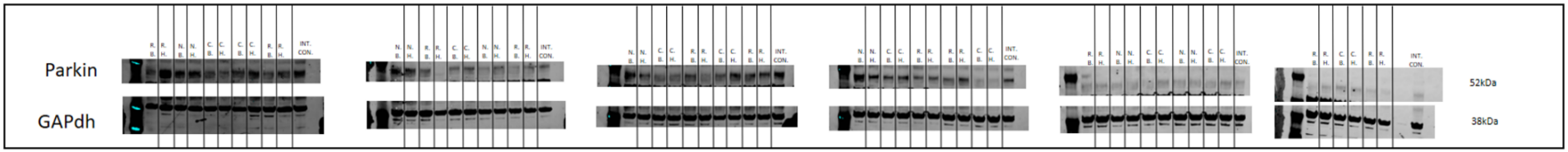
Parkin
GAPdh
52kDa
38kDa

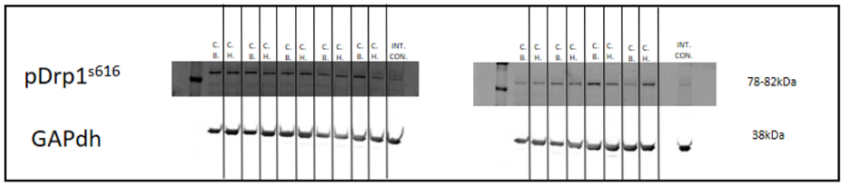
pDrp1s616
GAPdh
78-82kDa
38kDa

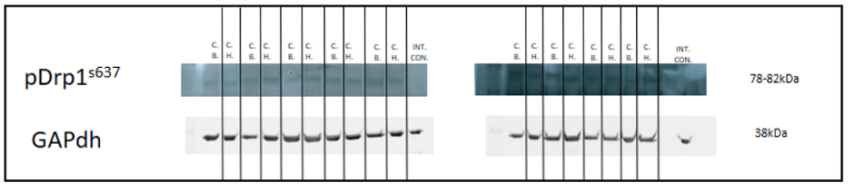
pDrp1s637
GAPdh
78-82kDa
38kDa

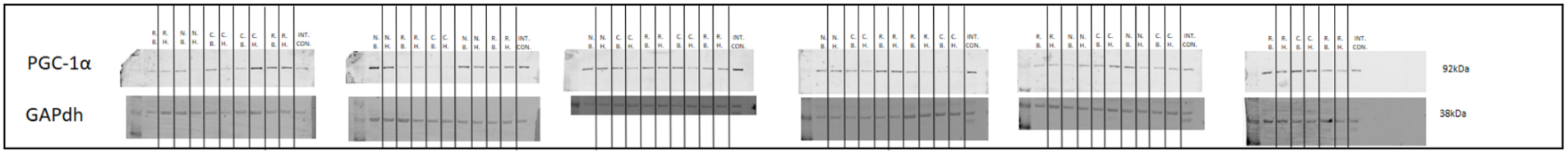
PGC-1α
GAPdh
92kDa
38kDa

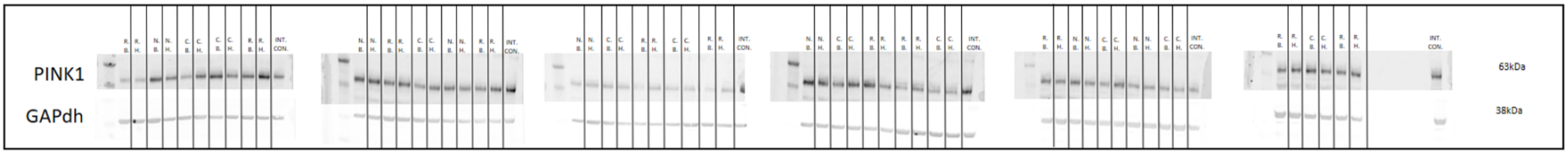
PINK1
GAPdh
63kDa
38kDa

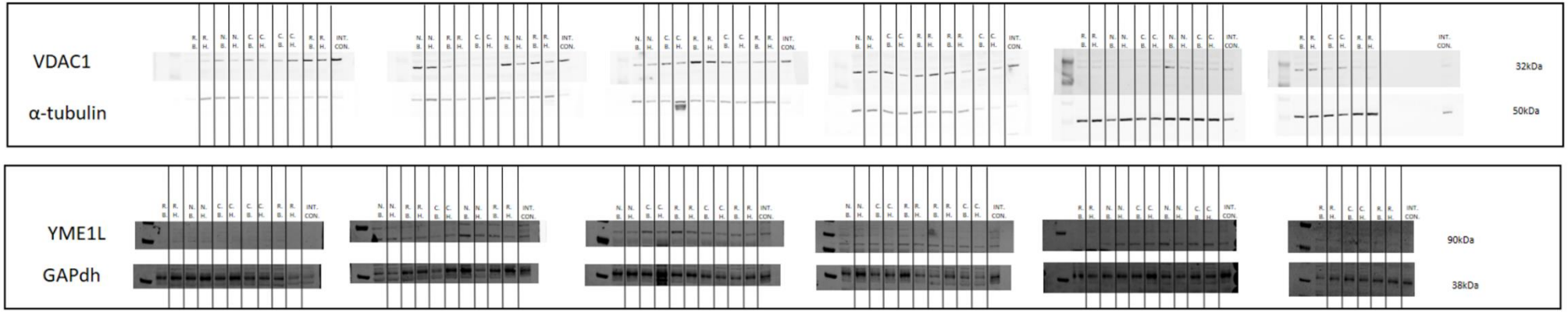

Appendix B. Figure 39. 21-day bed rest study densitometry

Legend:

- C.B. → Control BDC
- C.H. → Control HDT
- N.B. → Nutrition & Exercise Group BDC
- N.H. → Nutrition & Exercise Group HDT
- R.B. → Resistance Vibration Exercise Group BDC
- R.H. → Resistance Vibration Exercise Group HDT

Appendix C - 60 Day Bed Rest – High Resolution Respirometry (HRR)

Mitochondrial Content – mtDNA:nDNA ratio

60-day BDC and HDT HRR data was controlled for changes in mitochondrial content using mtDNA:nDNA ratio before and after bed rest. mtDNA and nDNA transcripts were measured using RT-qPCR. The mitochondrial DNA transcripts measured were:

- MT_ATP6: ATP synthase membrane subunit 6
- NDUFA4: NADH dehydrogenase subunit 4

The following nuclear DNA transcripts measured were:

- POLG: Polymerase γ Accessory Subunit
- COXIV: Cytochrome C Oxidase Subunit 4 nuclear
- MT_CO4: Cytochrome C Oxidase Subunit 4 nuclear

Multiple different combinations were compared against each other in order to quantity mtDNA:nDNA ratio in the skeletal muscle biopsies before and after 60 days of bed rest.

- MT_ATP6:COXIV
- MT_ATP6:MT_CO4
- MT_ATP6:POLG
- NDUFA4:COXIV
- NDUFA4:MT_CO4
- NDUFA4:POLG

MT_ATP6: COXIV Ratio

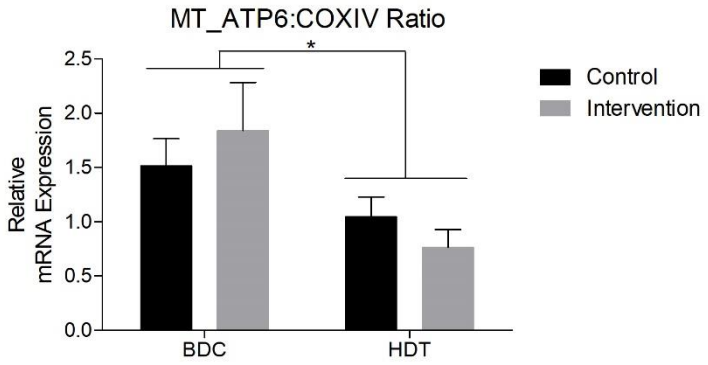

Appendix C. Figure 1. MT_ATP6:COXIV Ratio

(MT_ATP6:COXIV mtDNA:nDNA expression measured before and after bed rest. CON, *n*=7. INT *n*=6 Data are presented as mean ± SE, * significant effect of time, $p<0.05$)

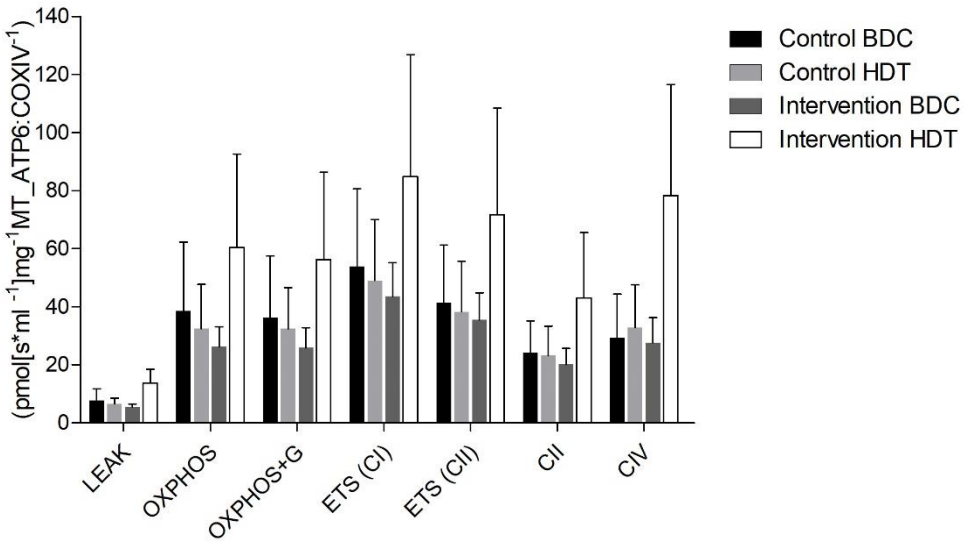

Appendix C. Figure 2. Carbohydrate SUIT normalised to wet weight & MT_ATP:COXIV Ratio

(Carbohydrate SUIT normalized to wet weight and MT_ATP6:COXIV (mtDNA:nDNA) ratio (CON *n*=7, INT *n*=6). Data are expressed as mean ± SE)

MT_ATP6:MT_CO4 Ratio

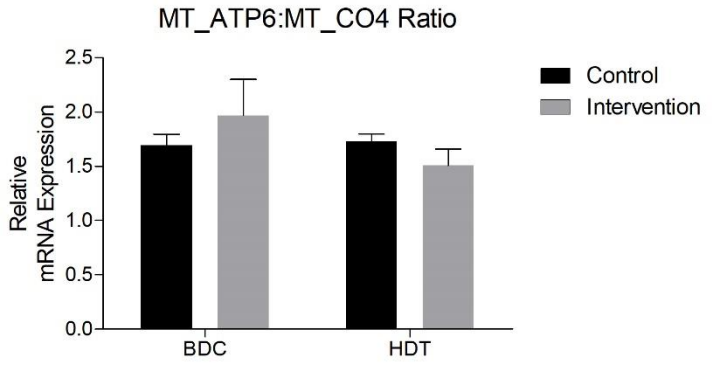

Appendix C. Figure 3. MT_ATP6:MT_CO4 Ratio

(MT_ATP6:MT_CO4 mtDNA:nDNA expression measured before and after bed rest. CON, *n*=7. INT *n*=6 Data are presented as mean ± SE)

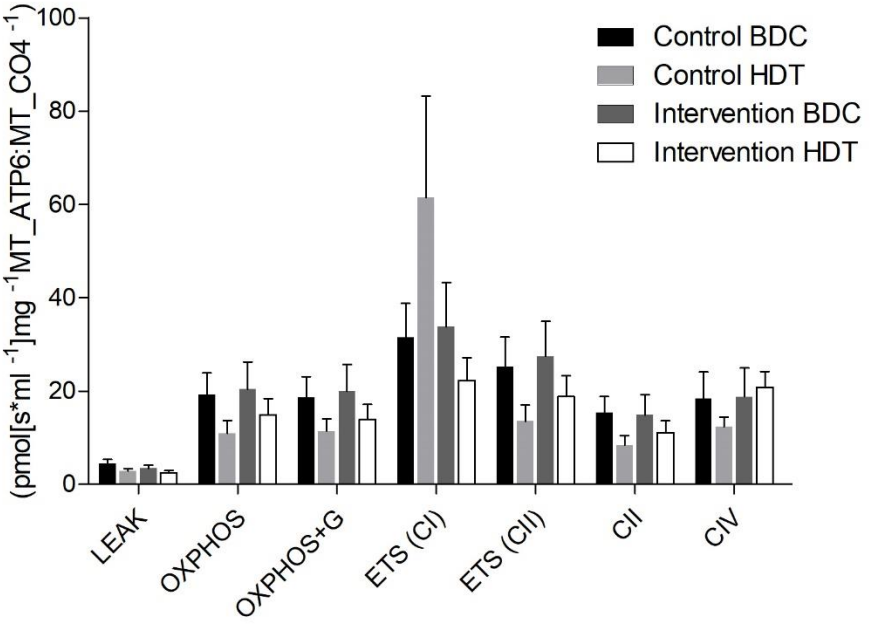

Appendix C. Figure 4. Carbohydrate SUIT normalised to wet weight & MT_ATP6:MT_CO4 Ratio

(Carbohydrate SUIT normalized to wet weight and MT_ATP6:MT_CO4 (mtDNA:nDNA) ratio (CON *n*=7, INT *n*=6). Data are expressed as mean ± SE)

MT_ATP6:POLG Ratio

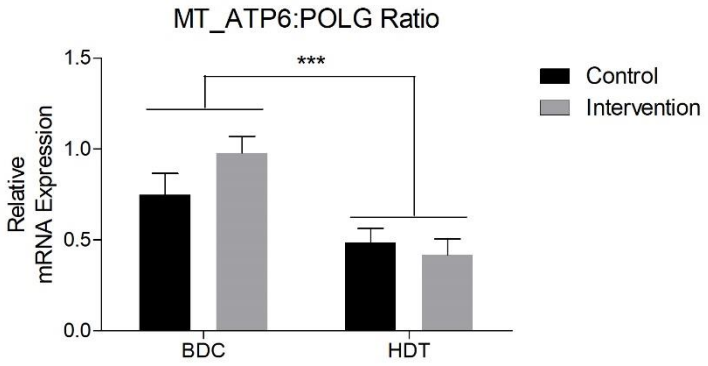

Appendix C. Figure 5. MT_ATP6:POLG Ratio

(ATP6:POLG mtDNA:nDNA expression measured before and after bed rest. CON, *n*=7. INT *n*=6 Data are presented as mean ± SE, *** significant effect of time, *p*<0.0005)

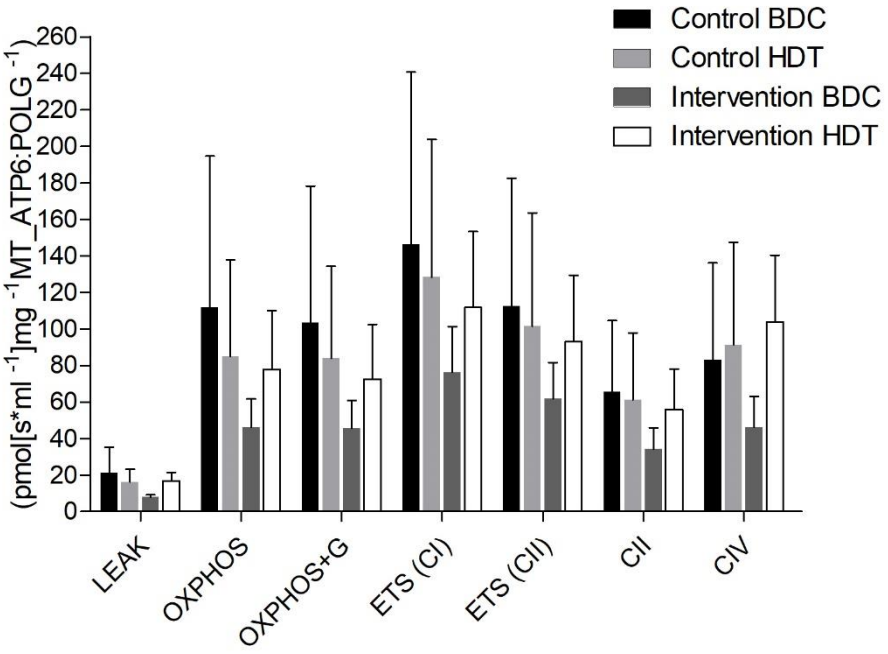

Appendix C. Figure 6. Carbohydrate SUIT normalised to wet weight & MT_ATP6:POLG Ratio

(Carbohydrate SUIT normalized to wet weight and MT_ATP6:POLG (mtDNA:nDNA) ratio (CON *n*=7, INT *n*=6). Data are expressed as mean ± SE)

NDUFA4: COXIV Ratio

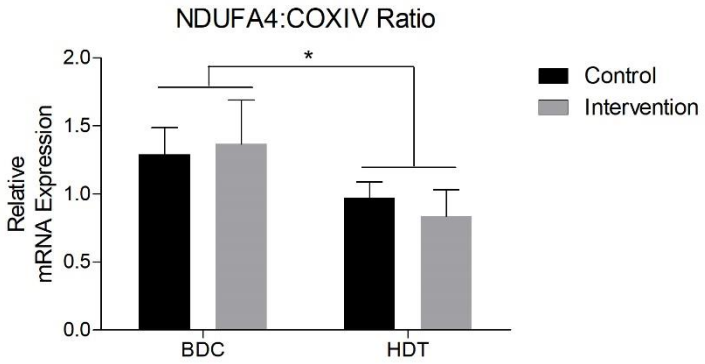

Appendix C. Figure 7. NDUFA4:COXIV Ratio

(NDUFA4: COXIV mtDNA:nDNA expression measured before and after bed rest. CON, *n*=7. INT *n*=6 Data are presented as mean ± SE, *significant effect of time, *p*<0.05)

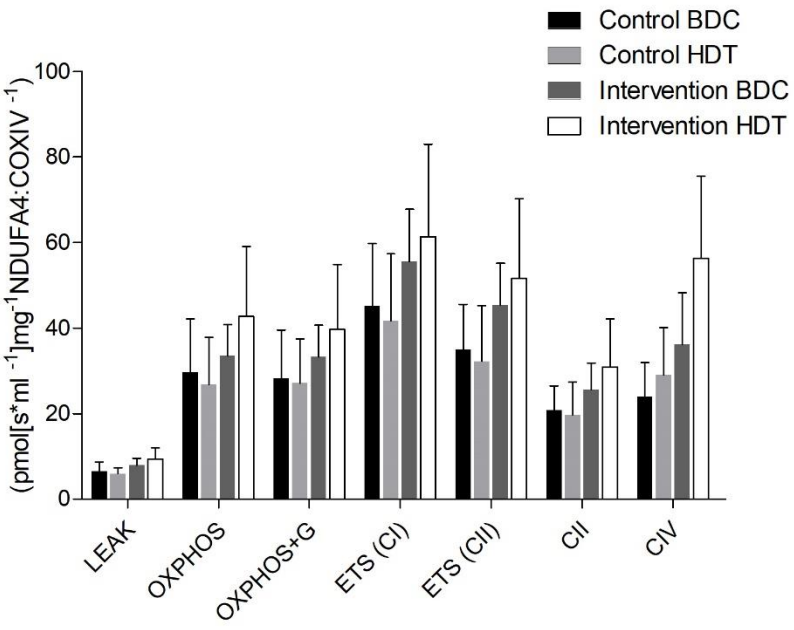

Appendix C. Figure 8. Carbohydrate SUIT normalised to wet weight & NDUFA4:COXIV Ratio

(Carbohydrate SUIT normalized to wet weight and NDUFA4: COXIV (mtDNA:nDNA) ratio (CON *n*=7, INT *n*=6). Data are expressed as mean ± SE)

NDUFA4:MT_CO4 Ratio

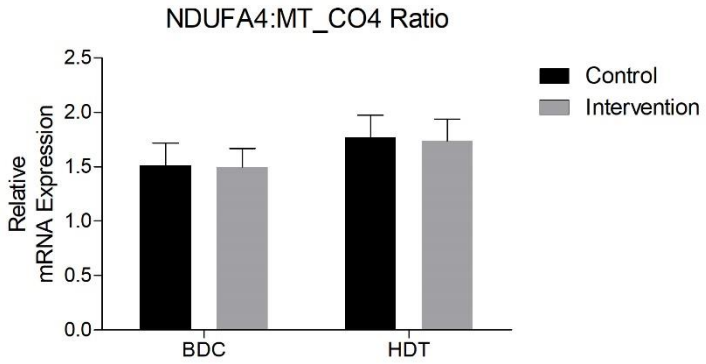

Appendix C. Figure 9. NDUFA4:MT_CO4 Ratio

(NDUFA4: MT_CO4 mtDNA:nDNA expression measured before and after bed rest. CON, *n*=7. INT *n*=6 Data are presented as mean ± SE)

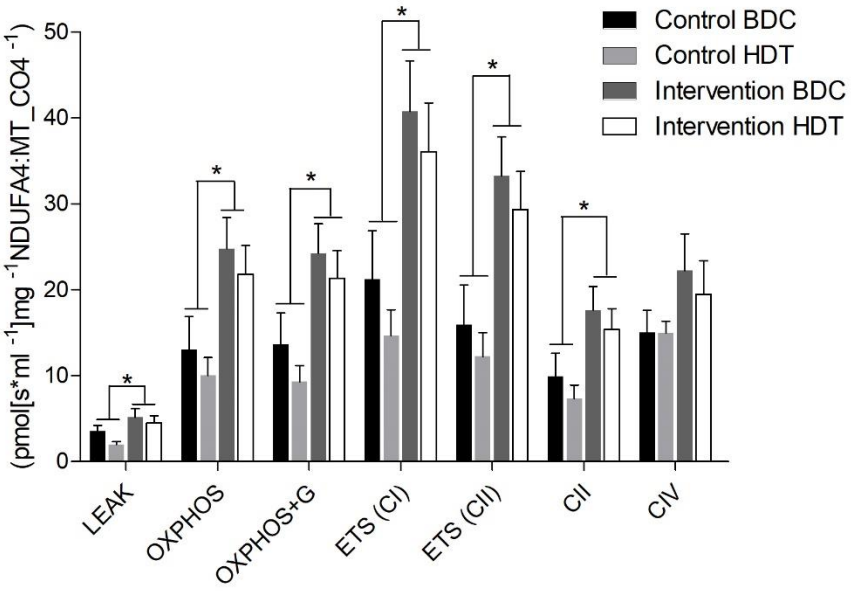

Appendix C. Figure 10. Carbohydrate SUIT normalised to wet weight & NDUFA4:MT_CO4 Ratio

(Carbohydrate SUIT normalized to wet weight and NDUFA4: MT_CO4 (mtDNA:nDNA) ratio (CON *n*=7, INT *n*=6). Data are expressed as mean ± SE, *significant effect of treatment, $p<0.05$)

Appendix D – Cellular Response to 60 days of HDT Bed Rest: Protein Expression

Ponceau Blots 60-Day Bed Rest Study

All blots were incubated in neat ponceau for 30 seconds following transfer of protein onto nitrocellulose membrane. Ponceau was subsequently removed by washing in TBS-t. Phosphorylated proteins and those transferred onto PVDF membranes were not incubated in ponceau. Subsequently, not all proteins have representative ponceau images. Below are representative ponceau blots for used to assess for expression of proteins.

Ponceau Blot for Markers of Mitochondrial Biogenesis

PGC-1α

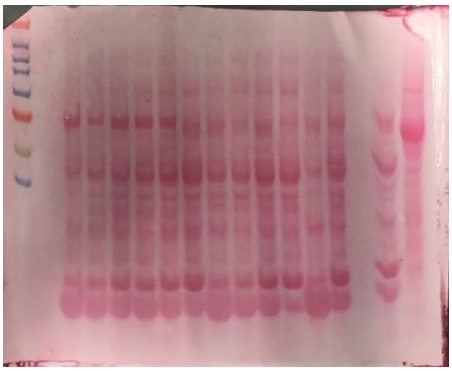

Appendix D. Figure 1. Ponceau blot example – PGC-1α

Ponceau Blot for Markers of Mitochondrial Fusion

OPA1

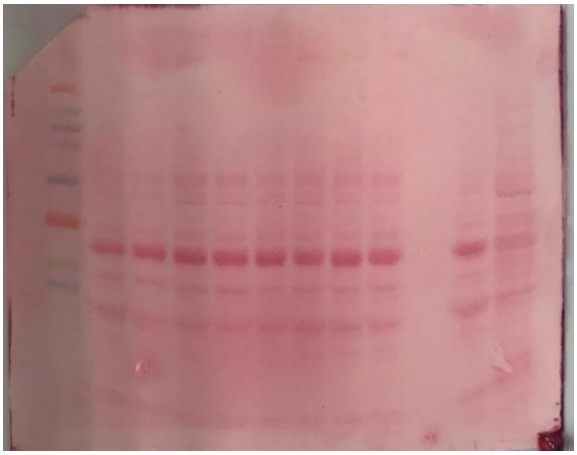

Appendix D. Figure 2. Ponceau blot example – OPA1

Mfn1 & Mfn2

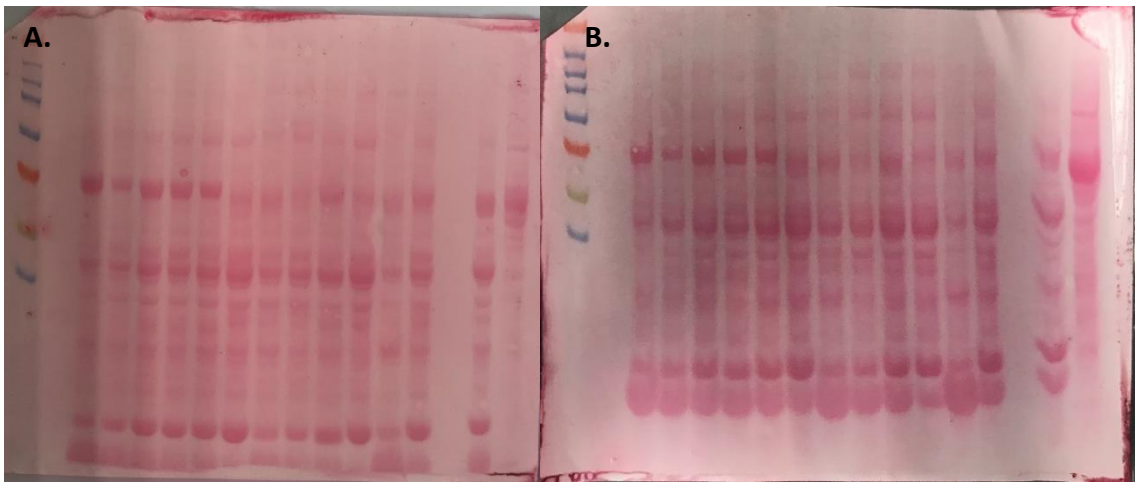

Appendix D. Figure 3. Ponceau blot examples. Mfn1 (A) & Mfn2 (B)

YME1L

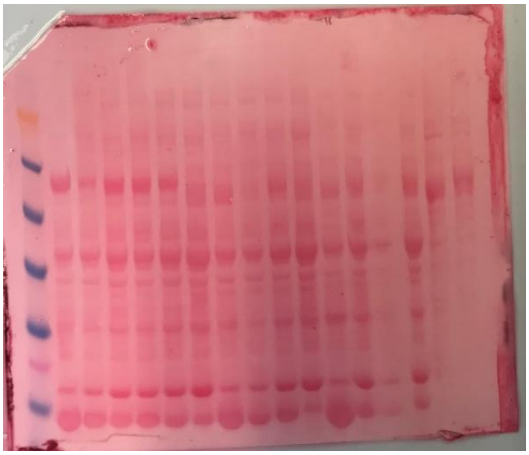

Appendix D. Figure 4. Ponceau blot example – YME1L

Ponceau Blot for Markers of Mitochondrial Fission

Drp1

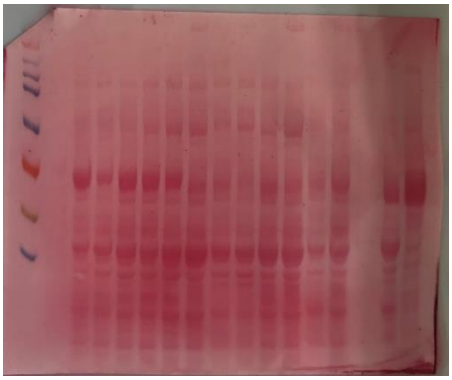

Appendix D. Figure 5. Ponceau blot example – Drp1

pDrp1^{s616} & pDrp1^{s637}

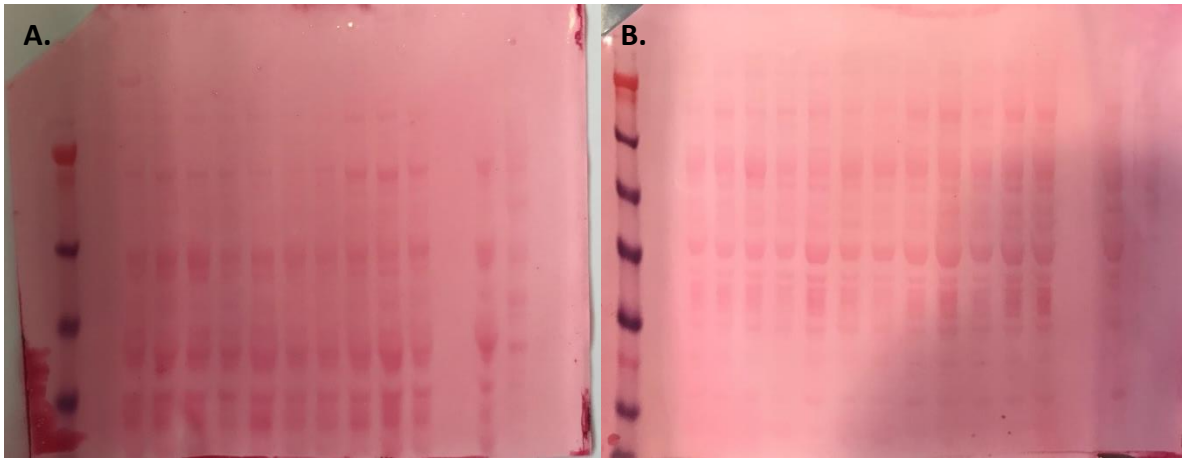

Appendix D. Figure 6. Ponceau blot examples. pDrp1^{s616} (A) & pDrp1^{s637} (B)

Ponceau Blot for Markers of Mitophagy

PINK1

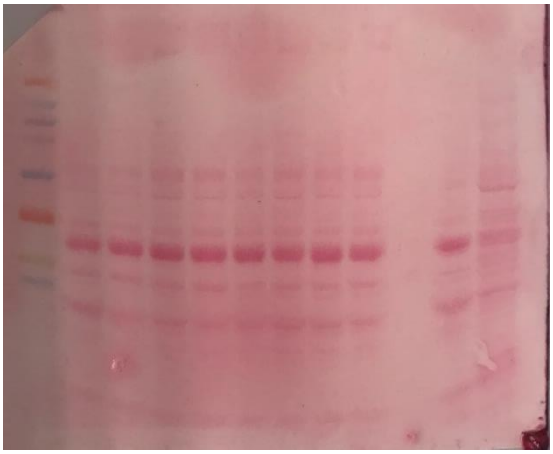

Appendix D. Figure 7. Ponceau blot example – PINK1

BNIP3 & BCL2-L13

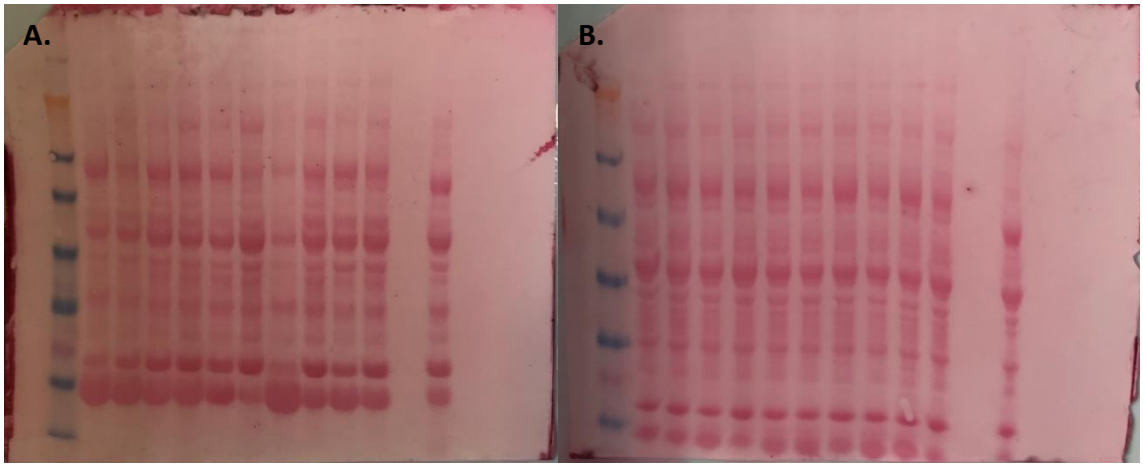

Appendix D. Figure 8. Ponceau blot examples. BNIP3 (A) & BCL2-L13 (B)

Ponceau Blot for Other Mitochondrial Markers

MCU & VDAC1

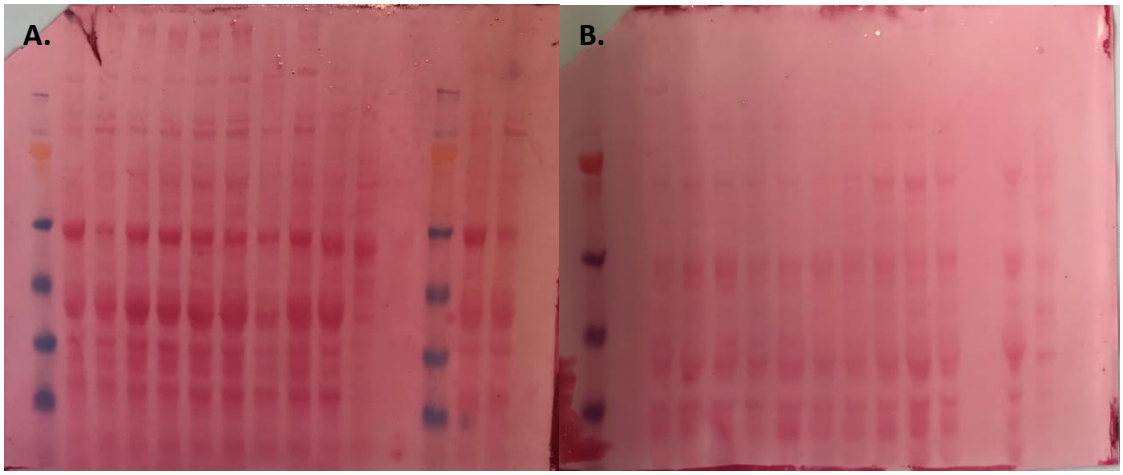

Appendix D. Figure 9. Ponceau blot examples. MCU (A) & VDAC1 (B)

SIRT1 & Pan-Calcineurin A

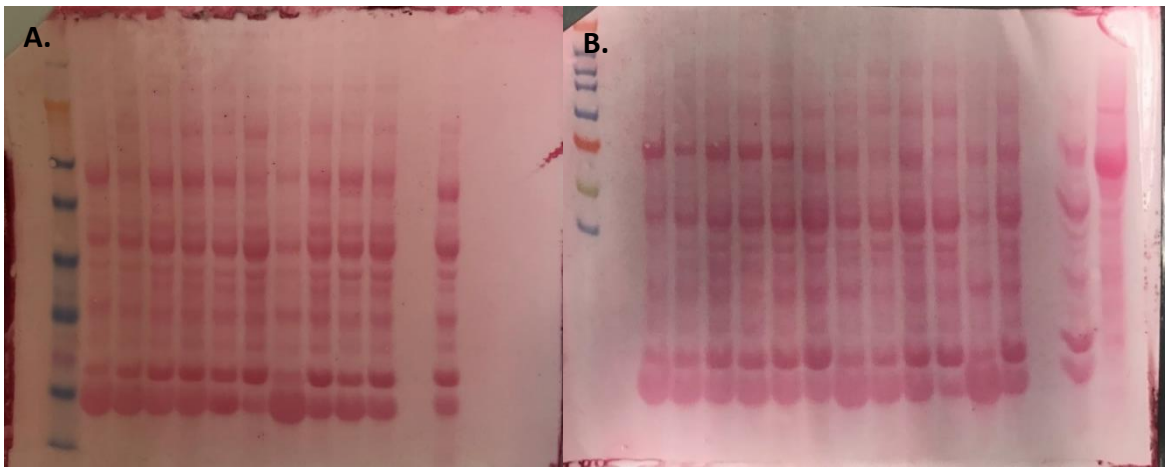

Appendix D. Figure 10. Ponceau blot examples. SIRT1 (A) & Pan-Calcineurin A (B)

Densitometry Blots – 60 Day Bed Rest

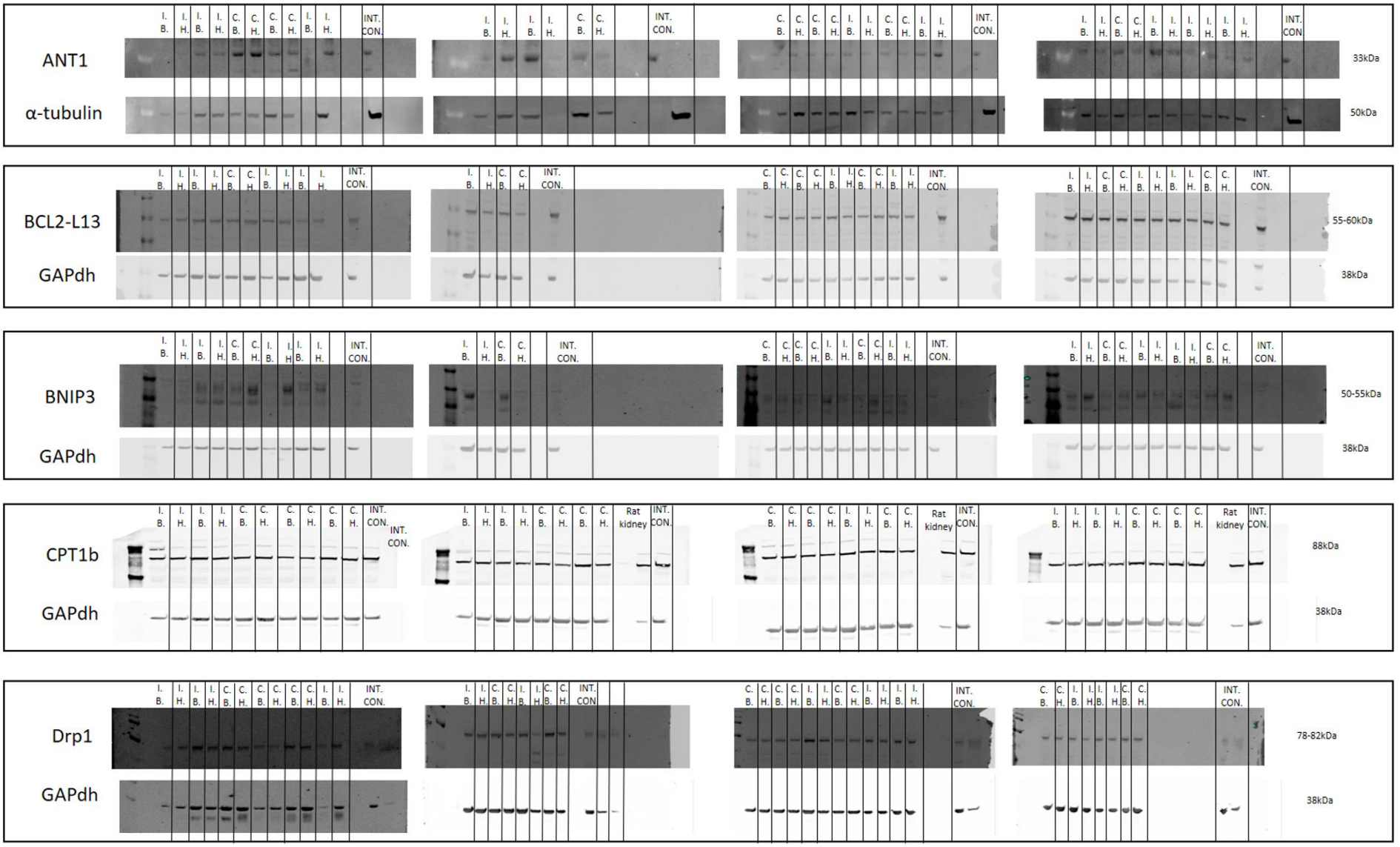

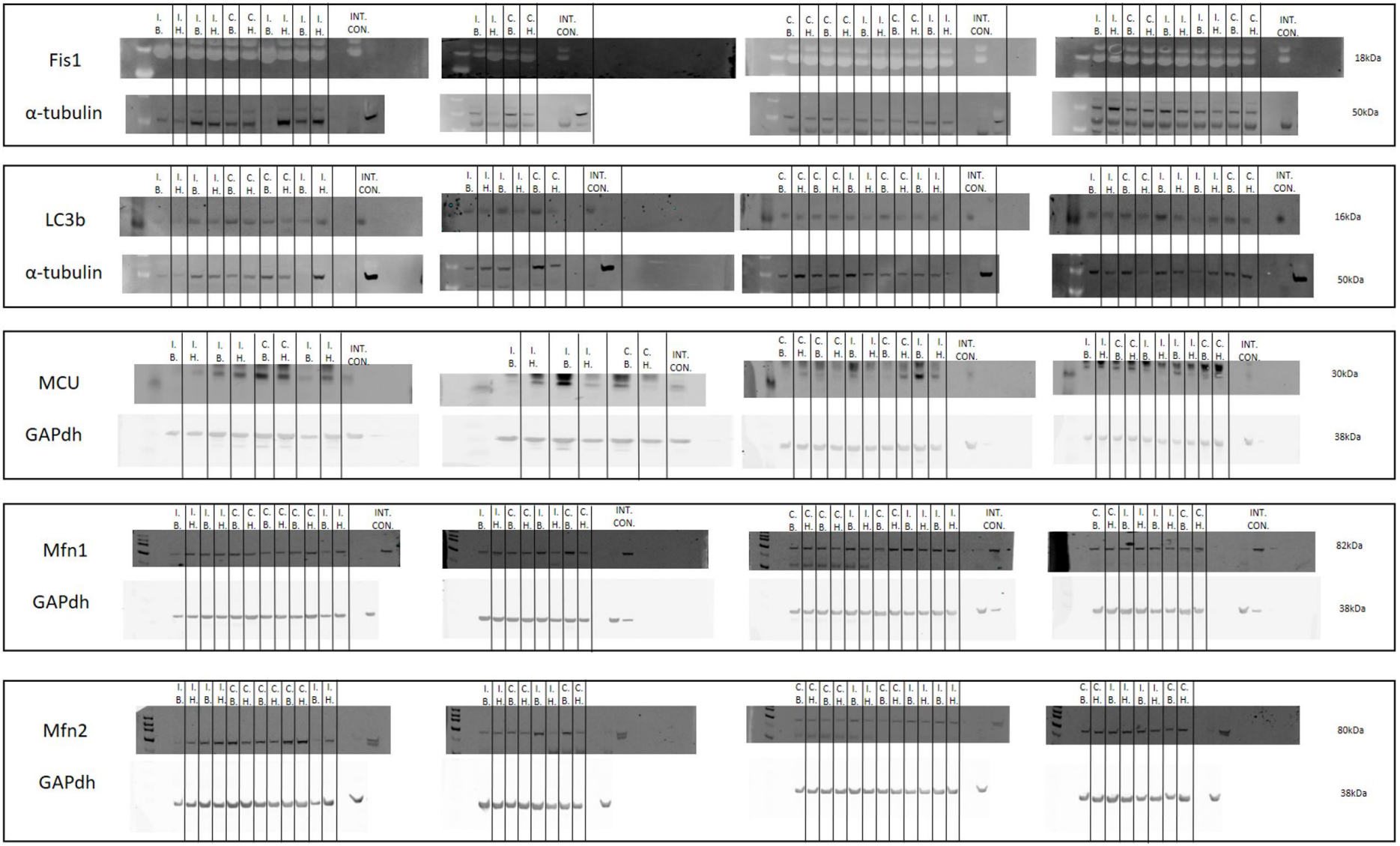
Fis1
α-tubulin
18kDa
50kDa
LC3b
α-tubulin
16kDa
50kDa
MCU
GAPdh
30kDa
38kDa
Mfn1
GAPdh
82kDa
38kDa
Mfn2
GAPdh
80kDa
38kDa

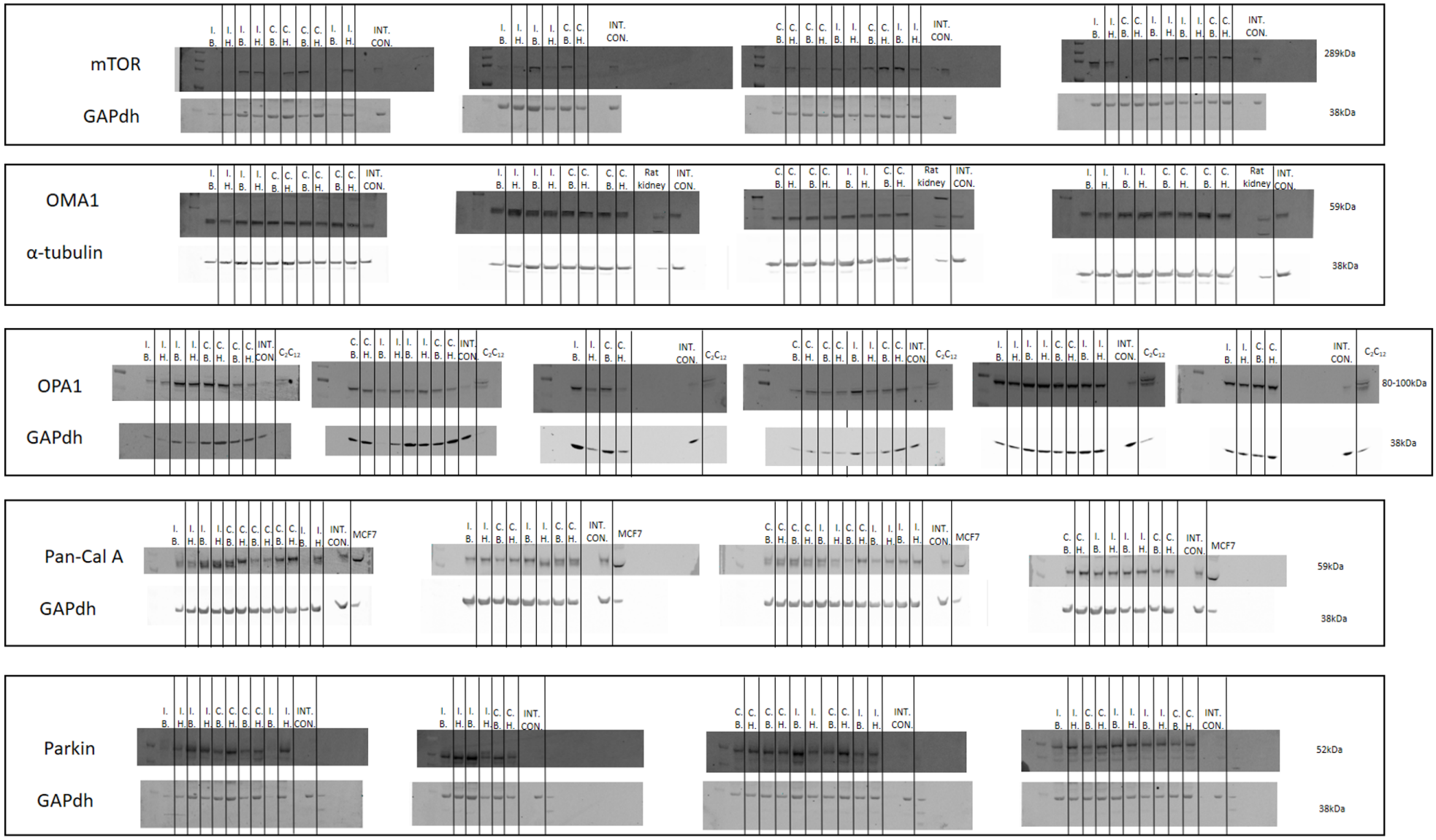
mTOR
GAPdh
289kDa
38kDa
OMA1
α-tubulin
59kDa
38kDa
OPA1
GAPdh
80-100kDa
38kDa
Pan-Cal A
GAPdh
59kDa
38kDa
Parkin
GAPdh
52kDa
38kDa

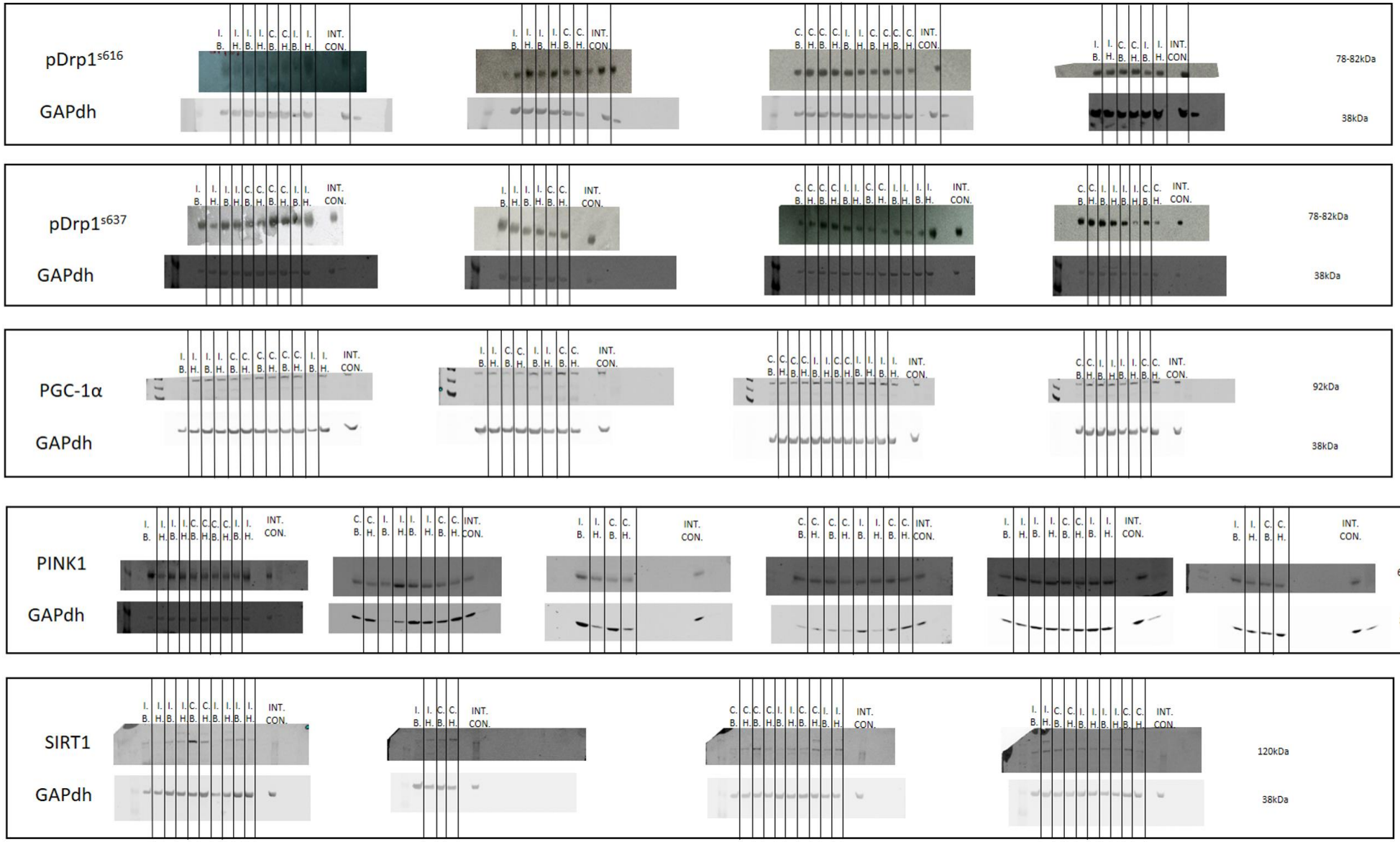
pDrp1s616
GAPdh
78-82kDa
38kDa
pDrp1s637
GAPdh
78-82kDa
38kDa
PGC-1α
GAPdh
92kDa
38kDa
PINK1
GAPdh
63kDa
38kDa
SIRT1
GAPdh
120kDa
38kDa

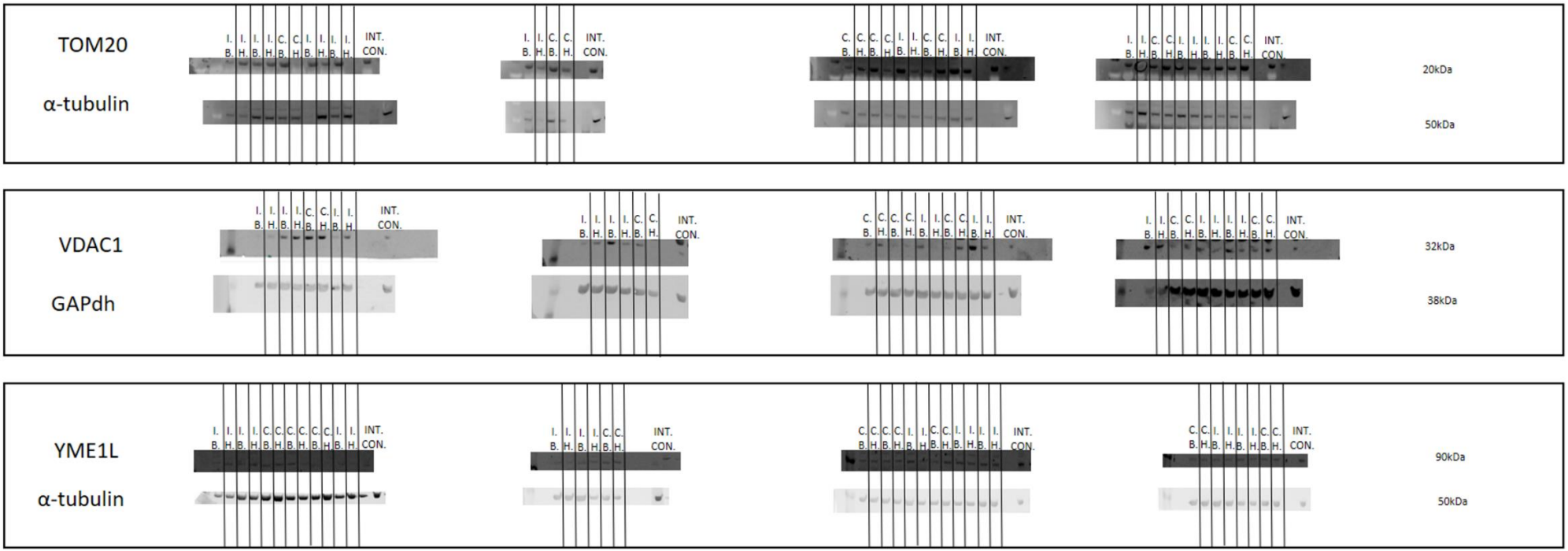

Appendix D. Figure 11. 60-day bed rest study densitometry

Legend:

- C.B. → Control BDC
- I.B. → Intervention BDC
- C.H. → Control HDT
- I.H. → Intervention HDT

Appendix E – Supplementary Cell Culture

Media for Growth of Cell Lines

C_2C_{12}

C_2C_{12} mouse cells – a murine skeletal muscle cell line and L6 rat cells – were used during this project in training. Dulbeco's Modified Eagle's Media (DMEM) (D5671, Sigma-Aldrich) substituted with 2% L-Glutamine and 10 % Fetal Bovine Serum (FBS) was used to grow C_2C_{12} myoblasts. Media was heated to 37^{o}C for 15 minutes prior to use. C_2C_{12} myoblasts were passaged once grown to 60-70% confluent.

L6

α-minimum essential medium (α-MEM) (Life technologies, #12571-063 substituted with 10% Fetal Bovine Serum (FBS) and 1% Antibiotic/Antimycotic (AB) (Life technologies, #15240-062) was used to grow L6 myoblasts. Media was heated to 37°C for 15 minutes prior to use. L6 myoblasts were passaged once grown to 60-70% confluent.

Subculture of the L6 and C_2C_{12} cells

Cells were maintained in the conditions outlined above and sub-cultured every 3-4 days (80-90% confluence) to maintain them in mid-exponential phase of their growth cycle. Culture media was removed from the flask (T25, T75, T175) and discarded in a glass waste bottle which was then autoclaved. The flask was rinsed with 1 ml trypsin to remove any residual media. Then, 1-2 ml of trypsin was added to flask, which was then incubated at 37^{o}C until almost all the cells had detached from the bottom of the flask (approximately 2-5 minutes). The detachment of cells was monitored under a microscope to prevent over-exposure to trypsin, which can be cytotoxic. Once the cells were detached, a volume of growth media equivalent to that of trypsin was added to the flask, and the media, trypsin and cellular solution was transferred to a 20 ml sterile universal and centrifuged at 1,000 rpm for 5 minutes. The supernatant was discarded, and the pellet was suspended in 2 ml of growth media. Cells where then counted using a cell viability assay as mentioned in paragraph 3.1.4. C_2C_{12} myoblasts where seeded at $1x10^5$ per T25, T75, and T125 and per well of a 6 well plate. An extra 5, 10 or 20ml of fresh media was added to the T25, T75 or T125 flask respectively following seeding and an extra 2ml of growth media was added per well of a 6 well plate.

Cell Culture Media for Differentiation Skeletal Muscle of cell lines

Dulbeco's Modified Eagle's Media (DMEM) (D5671, Sigma-Aldrich) substituted with 2% L-Glutamine and 2% Horse Serum (HS) was used to differentiate C_2C_{12} myoblasts to myotubes when myoblasts reached confluence. Media was heated to 37°C for 15 minutes prior to use.

α-minimum essential medium (α-MEM) (Life technologies, #12571-063) substituted with 2% Fetal Bovine Serum (FBS) and 1% Antibiotic/Antimycotic (AB) (Life technologies #15240-062) was used to differentiate L6 myoblasts to myotubes when myoblasts reached confluence. Media was heated to 37°C for 15 minutes prior to use

C_2C_{12} Differentiation

Once a 6 well plate reached 80-90% confluence, growth media was removed and discarded into waste. Cells were washed with phosphate buffered saline (PBS). C_2C_{12} myoblasts were then incubated in differentiation media (e.g. 2ml per well of a 6 well plate). Cells where differentiated for 5 days with media changing occurring on day 3. Media change consisted of removing current media from plates and discarding it into waste, washing each well with PBS before incubating once again in differentiation media.

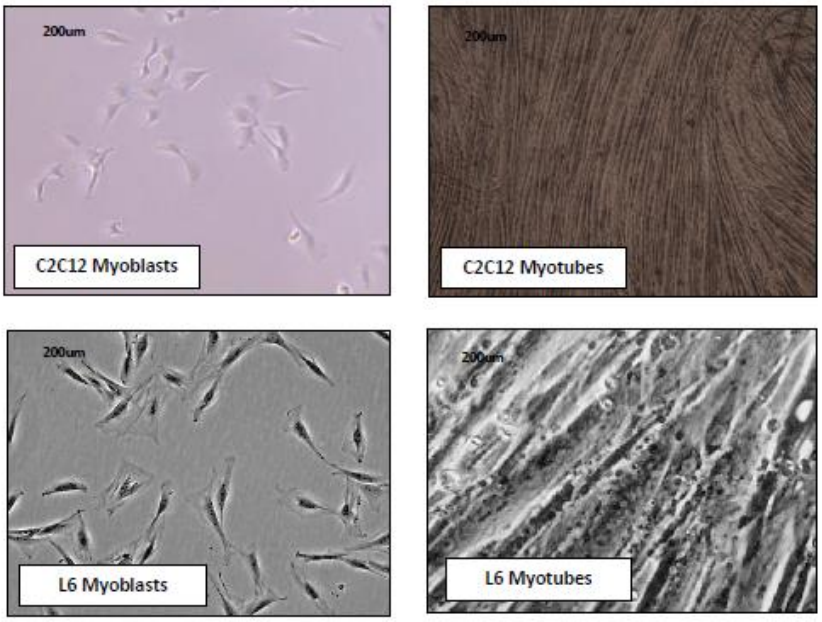

Appendix E. Figure 1. C_2C_{12} & L6 myoblasts & myotubes

Cryopreservation

Freezing Working Stocks

C_2C_{12} Myoblast Cryopreservation

To allow long term storage of cell lines stocks, cells were frozen down to -196°C in liquid nitrogen employing the commonly-used cryo-protectant dimethyl sulphoxide (DMSO, Sigma-Aldrich, D5879-M). Due to its toxicity at warm temperatures, a 2x freezing solution containing 10% DMSO in growth media was prepared and kept on ice until required. A final concentration of 5% DMSO and 5% FBS was used to freeze the cells.

Cells in the middle of the exponential phase were trypsinized and re-suspended in 5 ml growth media. An equal volume of the 2x freezing solution was added to the cell suspension and the final solution was aliquoted in 1ml pre-chilled and labelled cryovials (Greiner Bio-one, 121278). These where immediately placed at the top of a liquid nitrogen tank for 2 hours, after which, the vials were lowered into the liquid nitrogen for storage. All C_2C_{12} myoblasts where counted and a viability assay was complete before they were frozen. C_2C_{12} myoblasts where frozen at $5x10^5$ per cryovial.

Appendix F- Protein Target Positive Controls

The following cell lines were grown to assist in the probing of protein targets of interest using western blot.

HEK293 cells

The HEK293 cell line is a cell line derived from human embryonic kidney cells which acted as a positive control for AMPK (5' AMP-activated protein kinase, CST, 23A3 #2603, monoclonal, rabbit, 62kDa) and pACC Ser79 (Phospho-Acetyl-CoA Carboxylase Serine79, CST, 3661, monoclonal, rabbit, 280kDa).

HEK293t cells

The HEK293t cell line derived from human embryonic kidney cells that expresses a mutant version of the SV40 large T antigen. The HEK293t cell line acted as a positive control for mitochondrial fusion target, Mfn2 (Mitofusin-2, CST, 9482, monoclonal, rabbit, 80kDa) and mitophagy target, PINK1 (PTEN-induced kinase 1, CST, D8G3, 6946, monoclonal, rabbit, 50 & 60 kDa).

HeLa cells

The HeLa cell line is a human cell line derived from cervical cancer cells. This cell line acted as a positive control for BNIP3 (BCL2/adenovirus E1B 19 kDa protein-interacting protein 3, CST, D7U1T, 44060, rabbit, polyclonal, 22-28 & 50-55 kDa), Drp1 (dynamin-related protein 1, CST, D6C7, 8570, rabbit, monoclonal, 78-82 kDa), Hexokinase II (CST, C64G5 #2867, rabbit, monoclonal, 102kDa), LC3b (Autophagy marker Light Chain 3b, CST, 2775, rabbit, monoclonal, 14 & 16kDa), Mfn1 (Mitofusin-1, CST, D6E2S, 14739, rabbit, monoclonal, 82kDa), OPA1 (optic atrophy 1, CST, 80471, rabbit, monoclonal, 80-100kDa), pDrp1s616 (Phospho-Dynamin related protein 1, Serine 616, CST, 3455, rabbit, monoclonal, 78-82kDa) and SIRT1 (sirtuin 1, CST, 9475, rabbit, monoclonal, 120kDa).

HepG2 cells

The HepG2 cell line is a human liver cancer cell line which acts as a positive control for ANT1 (Adenosine nucleotide translocase 1, Abcam, ab180715, rabbit, polyclonal, 33kDa), PDH (Pyruvate dehydrogenase, CST, C54G1, #3205S, rabbit, monoclonal, 43 kDa) and YME1L (ATP-dependent zinc metalloprotease YME1L, Abcam, ab170123, rabbit, polyclonal, 90kDa).

MCF7 cells

The MCF7 cell line is a human breast cancer cell line which acted as a positive control for Pan-Calcineurin A (CST, 2614, rabbit, monoclonal, 59kDa).

Panc-1 cells

The Panc-1 cell line is a human pancreatic cancer cell line isolated from a pancreatic carcinoma of ductal cell origin. The Panc-1 cell line acted as a positive control for MCU (Mitochondrial Calcium Uniporter, CST, 14997S, rabbit, monoclonal, 30kDa).

Raji B cells

The Raji B cell line is a cell line derived from human B-lymphocytes which acts as a positive control for TOM20 (Mitochondrial import receptor subunit TOM20 homolog, Santa Cruz, F-10. SC-17764, mouse, monoclonal, 20kDa).

SK-RB-3 cells

The SK-RB-3 cell line is a human breast cancer cell line which acts as a positive control for mitochondrial fission target, Fis1 (Mitochondrial fission protein 1) (Santa Cruz, B-5, SC-376447, monoclonal, mouse, 18kDa).

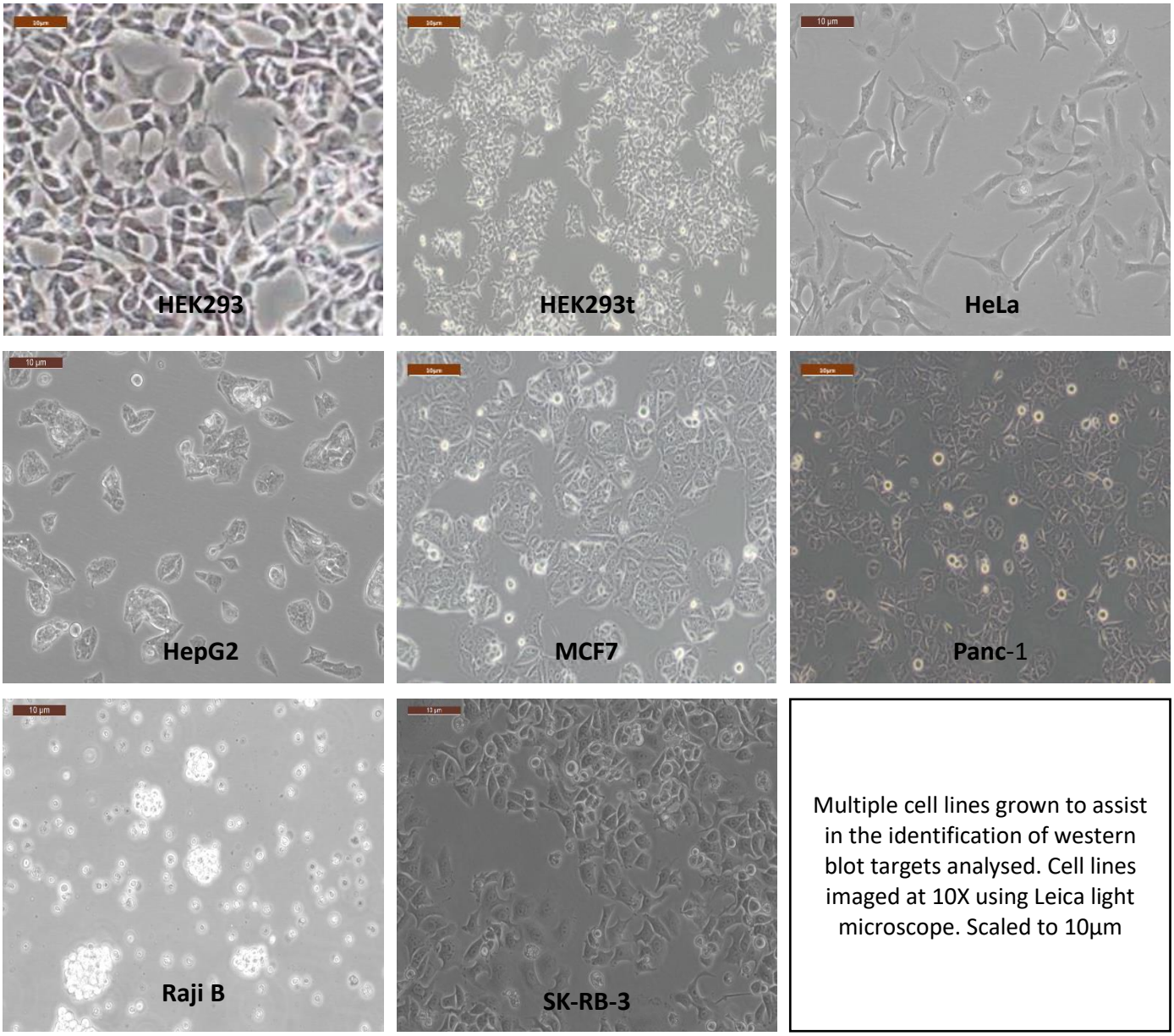

Appendix F. Figure 1. Multiple cell lines grown to assist in the identification of western blot targets

Appendix G – Microscopy

The Leica SP8 STED microscope, the Leica DM IRE2 confocal, the Nikon Eclipse Ti time-lapse microscope and the Leica DFC 500 fluorescent microscopes were used for microscopy in this work. Standard operating procedures based on user guidelines were adhered to following expertise training on their use.

Appendix G. Figure 1. Microscopy methods used for imaging

((A) Leica SP8 STED. (B) Nikon Eclipse Ti-Time-Lapse microscope. (C) Leica DM IRE2 confocal microscope. (D) Leica DFC 500 fluorescent microscope)

Mitochondrial Content & Nuclear Content Probing Assays

Mitochondrial Content Staining

Following preparation of 1mM MitoTraker Green FM (Invitrogen, M7514, MW:671.88), as per manufacturer's instructions, optimization of an ideal concentration to measure mitochondrial content was addressed. Optimal concentration of MitoTraker Green FM was addressed on C_2C_{12} myoblasts and myotubes to assist in the analysis of mitochondrial content in primary human skeletal muscle myotubes.

Cells were prepared for this assay in 24 and 96 well plates. Once cells had grown/differentiated cell media was removed, cells were washed with PBS twice, and cells were incubated in prepared Mitotraker Green FM media at 37°C, 0.5% CO_2 in darkness. Following incubation of MitoTraker Green FM at a concentration of 50nM, 100nM, 150nM or 200nM, media was removed and cells were washed with PBS twice before analysis. Optimal concentration and probing time (15-30 minutes) were addressed using a fluorescent microscope (Leica DFC 500) and reading fluorescence on a plate reader (BioTek Synergy HT).

Optimal mitochondrial Content Probing – Fluorescent Microscopy

C_2C_{12} myotubes were probed for mitochondrial content using MitoTraker Green FM which is a green-fluorescent mitochondrial stain. Myoblasts were grown in growth media in 24 well plates until 60-70% confluent. Following this, cells were differentiated using differentiation media for 5 days. On day 5 cells were incubated in 50nm, 100nm, 150nm, and 200nm MitoTraker Green FM. All concentrations of MitoTraker were tested between 15 minutes (recommended minimum) and 30 minutes (recommended maximum) at 37°C, 0.5% CO_2 before being viewed for optimal signal via fluorescent microscopy and fluorescence on the plate reader (BioTek Synergy HT plate reader).

15 minutes' incubation (50nM, 100nM, 150nM & 200nM)

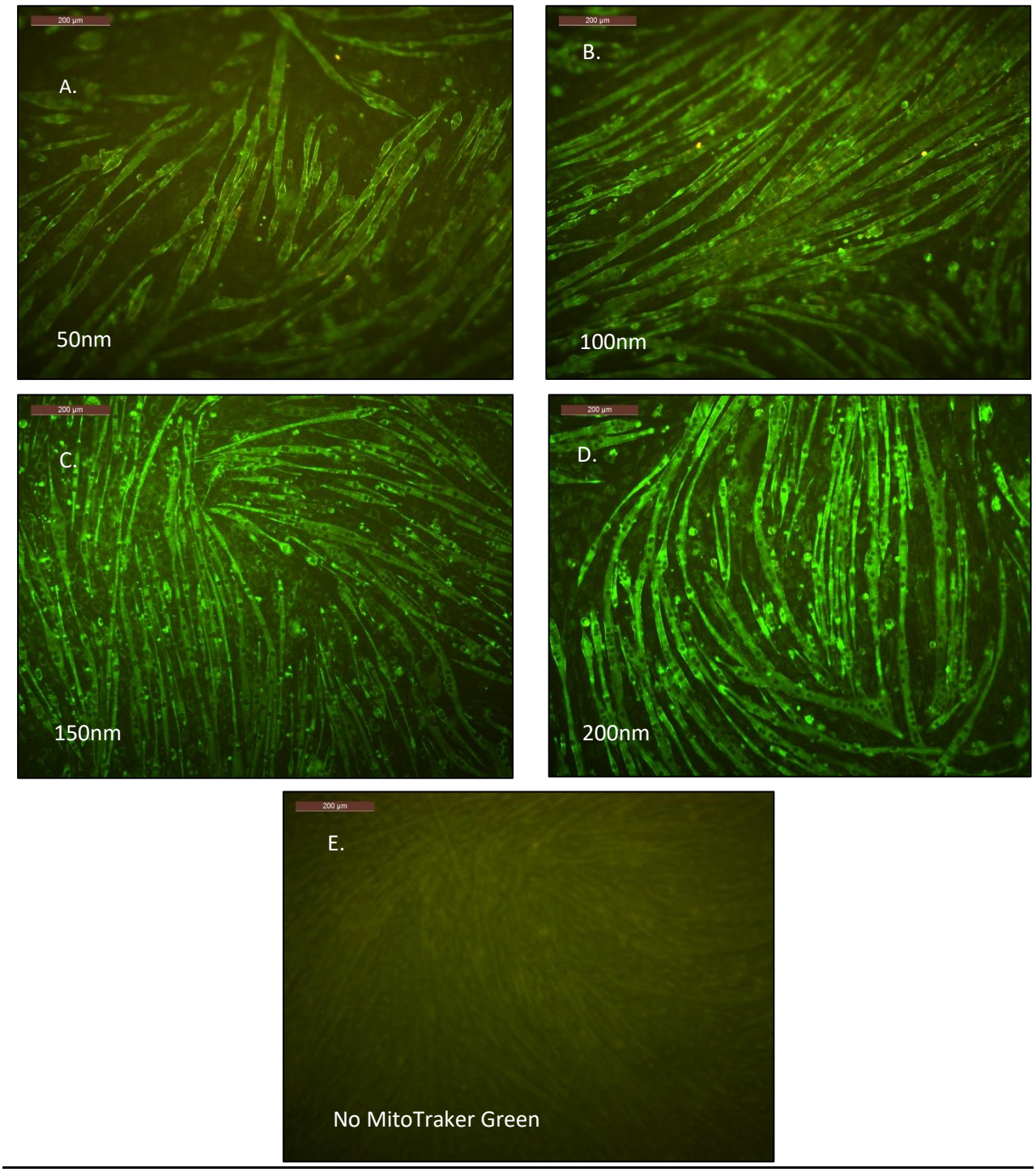

Appendix G. Figure 2. Fluorescent images representing MitoTraker Green FM probing of C_2C_{12} myotubes with 15mins incubation

(Fluorescent images representing MitoTraker Green FM probing of C_2C_{12} myotubes with 15-minute incubation times at concentrations between 50 and 200nm (A-D) against myotubes without probing (E). All images viewed under a 10X lens using the Leica DFC 500 fluorescent microscope, *n*=3)

30 minutes' incubation (50nM, 100nM, 150nM & 200nM)

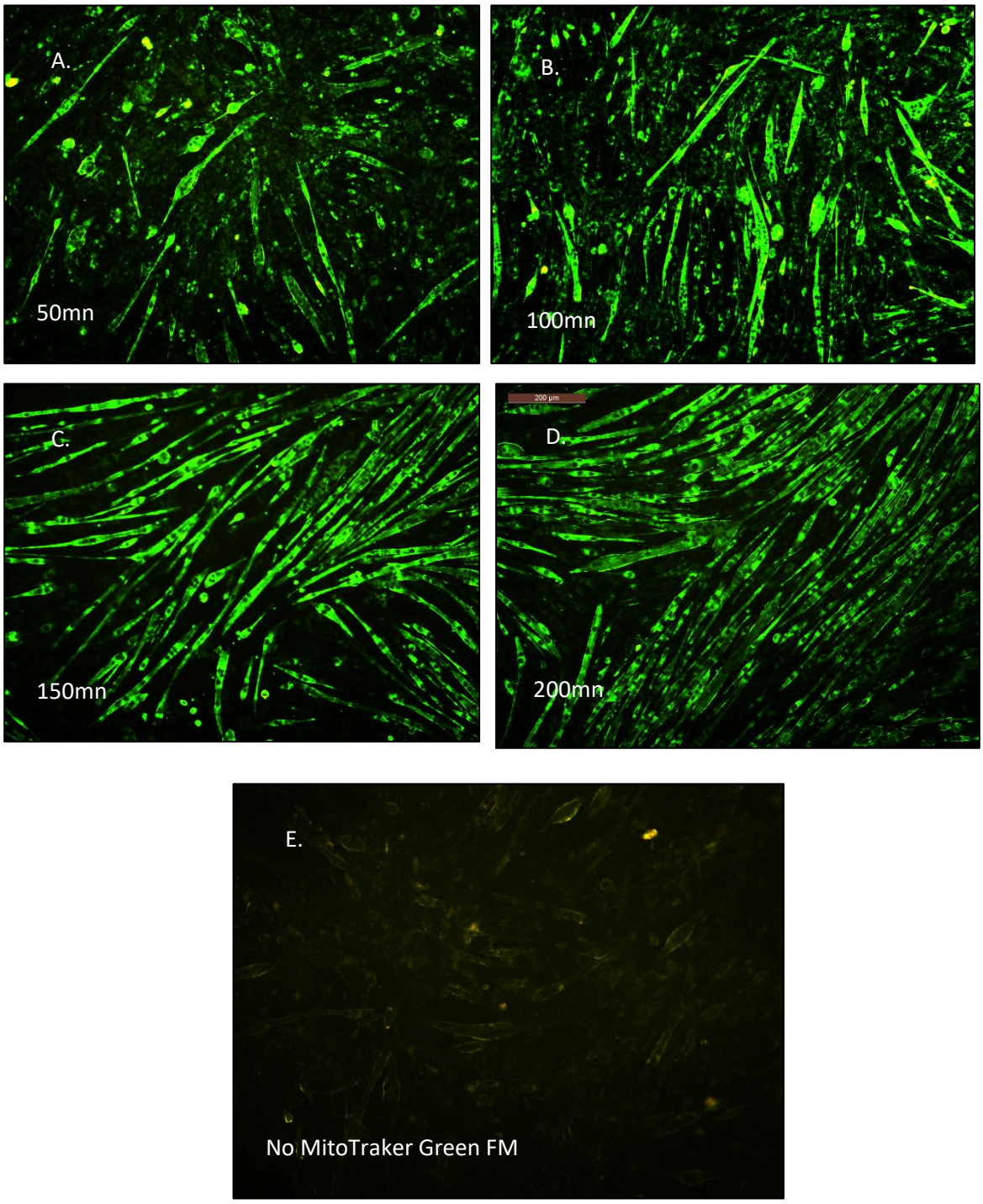

Appendix G. Figure 3. Fluorescent images representing MitoTraker Green FM probing of C_2C_{12} myotubes with 30mins incubation

(Fluorescent images representing MitoTraker Green FM probing of C_2C_{12} myotubes with 30-minute incubation times at concentrations between 50 and 200nm (A-D) against myotubes without probing (E). All images viewed under a 10X lens using the Leica DFC 500 fluorescent microscope, *n*=3)

Nuclear Staining

Dapi FluoroPure^{TM} stain (Invitrogen, D21490) was applied to C_2C_{12} myoblasts and myotubes to act as a counter stain for MitoTraker Green FM (Invitrogen, M7514). Nuclear staining using Dapi was optimized in these cells in order to assist in nuclear staining of primary human skeletal muscle myotubes. Prior to staining, media was removed from cells and cells were washed with PBS. Dapi was made to 1:5000 in PBS. This solution was reincubated onto cells for 10 minutes at room temperature away from the light. Following incubation PBS was once again removed from cells and cells were washed with fresh PBS before reincubation in relevant cell media. Cells were then assessed for nuclear staining using fluorescent microscopy (Leica DFC 500).

Optimal mitochondrial and nuclear staining of C_2C_{12} myotubes

Following optimization of MitoTraker Green FM on C_2C_{12} myotubes, myotubes were dual stained for both mitochondrial content using 200nM MitoTraker Green FM and Dapi for nuclei expression. The table below represents staining of C_2C_{12} myotubes mitochondrial and nucleus on their own and when the channels are merged together. Images were taken using a Leica DFC 500 fluorescent microscope at 10X (*n*=3).

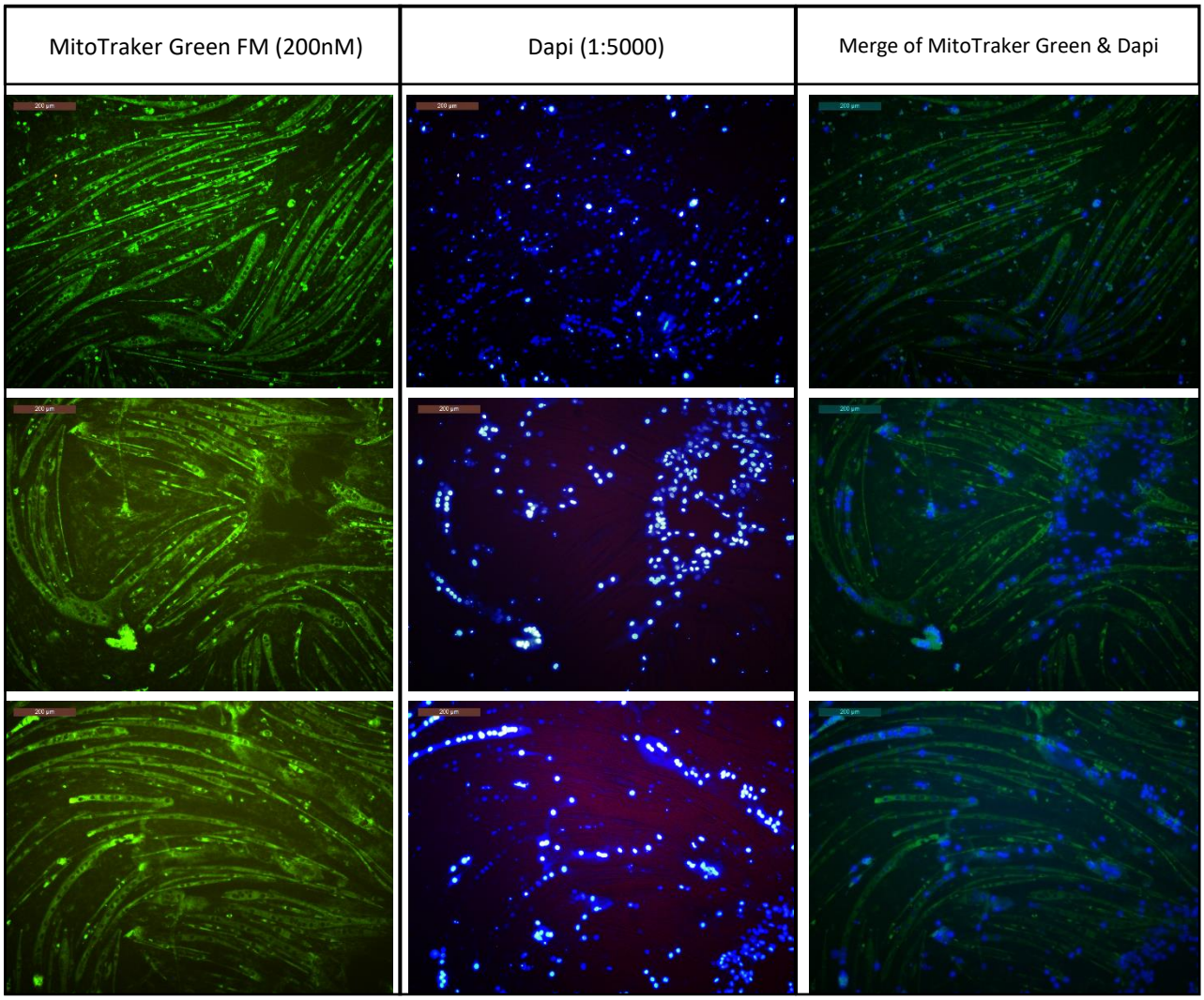

Appendix G. Figure 4. C_2C_{12} myotube MitoTraker Green & Dapi staining optimisation

(C_2C_{12} myotubes, MitoTraker Green, Dapi and merged MitoTraker Green & Dapi staining merged. *n*=3)

Summary Mitochondrial Content Analysis

The recommended incubation time of C_2C_{12} myotubes with MitoTraker Green FM is a minimum of 15 minutes. Our results a slight difference between a 15 minute and a 30-minute incubation time, with 30 minutes of incubation proving to produce a clearer image of mitochondrial content. Additionally, recommended concentration of MitoTraker Green FM is between 50-200nm which is a large difference. Our optimization protocols appear to suggest that at a higher concentration of Mitotraker Green FM (between 150-200nM) for up to 30 minutes' results in an ideal staining for mitochondrial content in C_2C_{12} skeletal muscle myotubes.

MitoTraker Green FM Fluorescent Intensity Time Course

C_2C_{12} myoblasts were grown at a cell density of $1x10^4$ and $1x15^4$ per well until confluent in black 96 well plates. Once confluent cells were differentiated for 5 days. On day 5 cells were probed for MitoTraker Green FM to assess for change in mitochondrial content fluorescence over 24 hours. Cells were assessed for fluorescence after 30 minutes (minimum recommended time), 4 hours and 24 hours in order to assess for optimal reading time on the fluorescent plate reader (BioTek Synergy HT).

MitoTraker Green FM Fluorescent Intensity

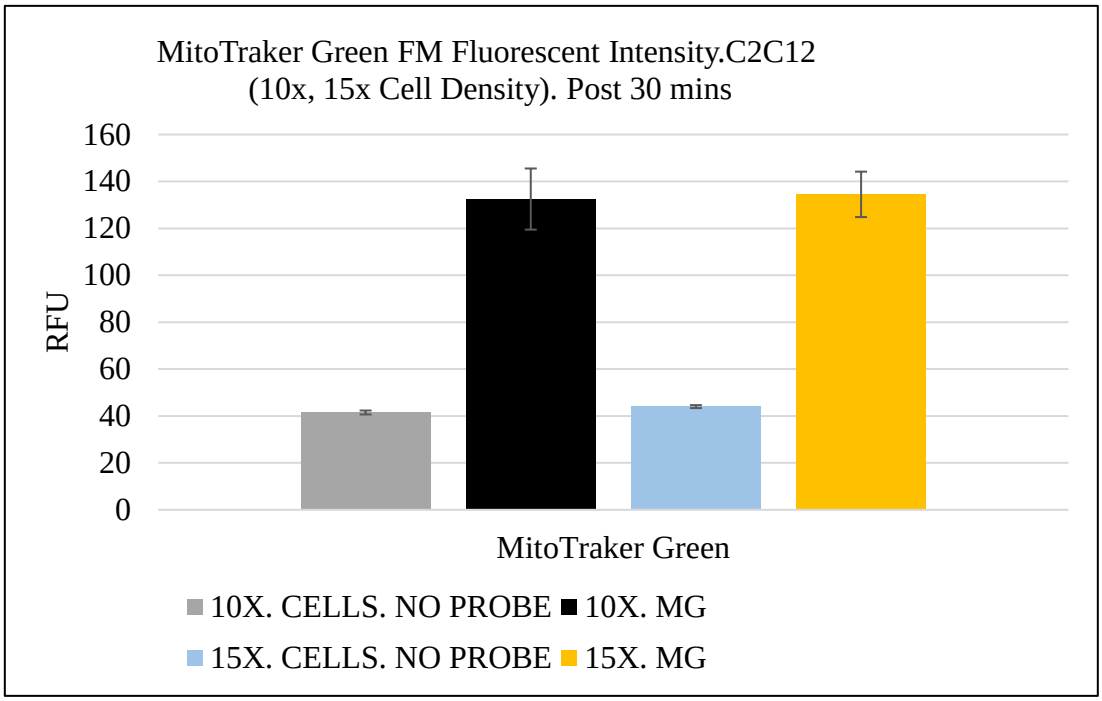

Appendix G. Figure 5. MitoTraker Green Fluorescent Intensity post 30mins incubation

(Identifying the effect of MitoTraker Green FM probing 30 minutes' post incubation at $1x10^4$ and $1x15^4$, increased fluorescence following 30mins of MitoTraker incubation $p<0.05$, $n=3$)

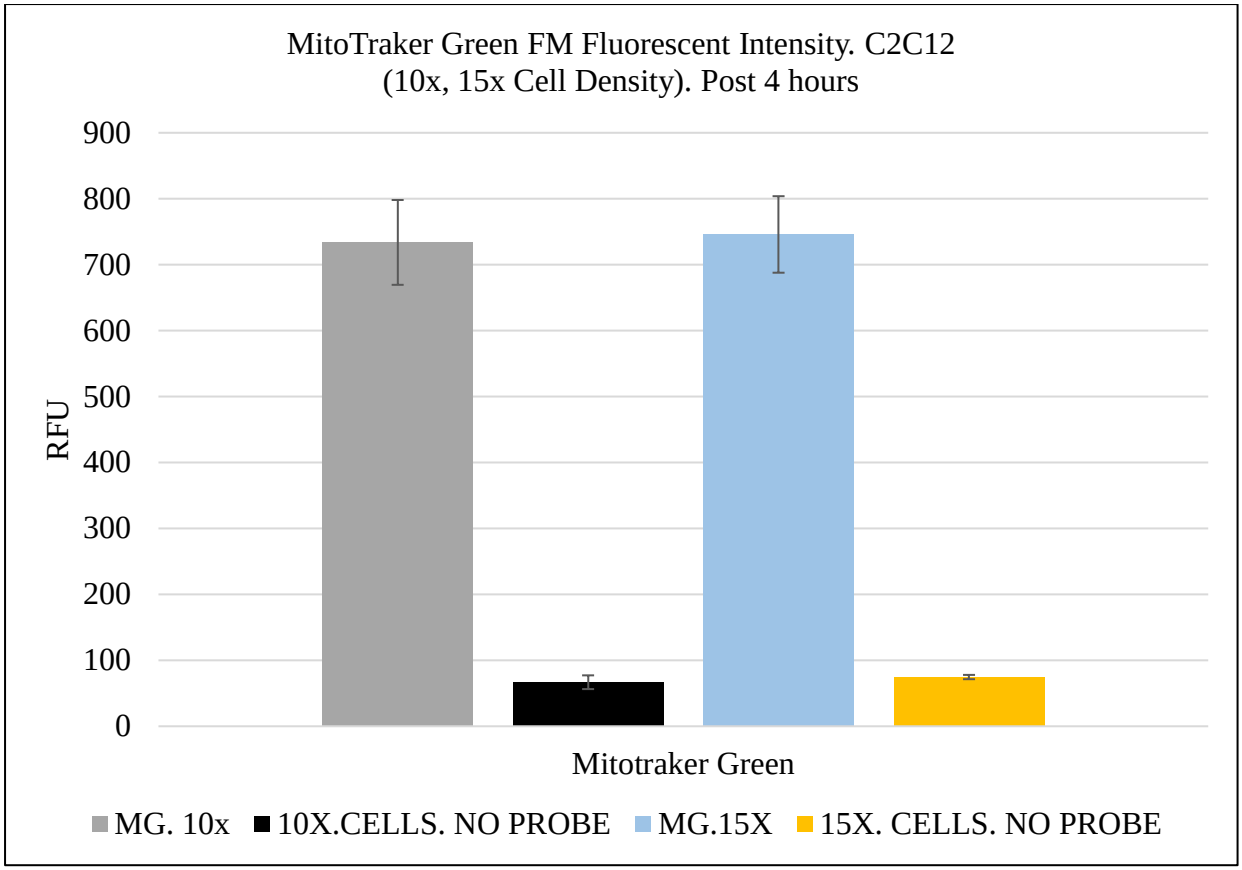

Appendix G. Figure 6. MitoTraker Green Fluorescent Intensity post 4 hours' incubation

(Identifying the effect of MitoTraker Green FM probing 4 hours post incubation at $1x10^4$ and $1x15^4$, increased fluorescence following 4 hours of MitoTraker incubation $p<0.05$, $n=3$)

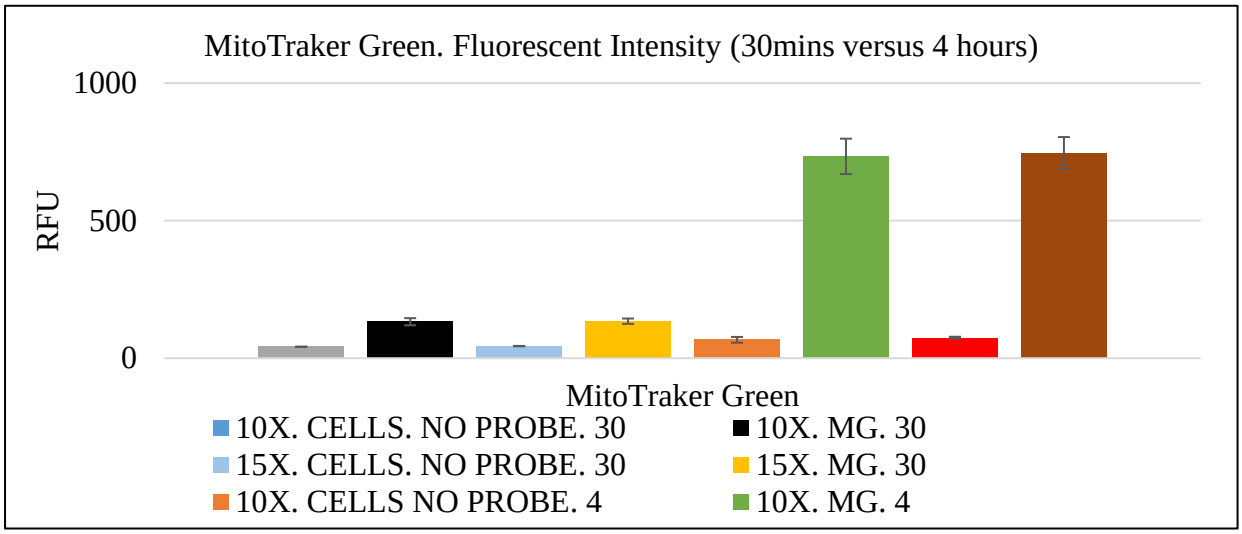

Appendix G. Figure 7. MitoTraker Green Fluorescent Intensity post 30 minutes v 4 hours incubation

(Identifying the effect of MitoTraker Green FM probing 30 minutes' post incubation versus 4 hours post incubation at $1x10^4$ and $1x15^4$, significant difference in fluorescence between 30 minutes and 4 hours of viewing, $p<0.05$, $n=3$)

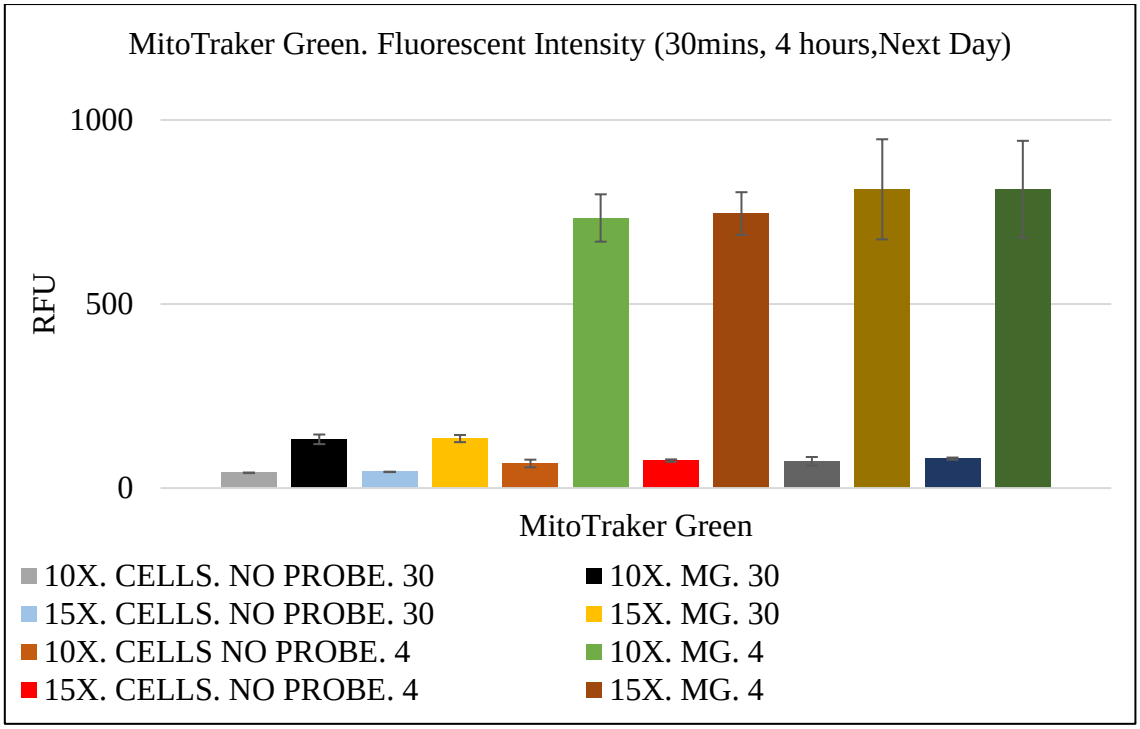

Appendix G. Figure 8. MitoTraker Green Fluorescent Intensity post 30mins, 4 hours and 24 hours' incubation

(Identifying the effect of MitoTraker Green FM probing 30 minutes, 4 hours and 24 hours post incubation at $1x10^4$ and $1x15^4$, significant effect of time on assessment, with a significant increase in fluorescence between 30 minutes and 4 hours, 4 hours and 24 hours, $p<0.05$, $n=3$)

Summary Mitochondrial Content Fluorescence

Results indicate a significant change in mitochondrial content fluorescence between 30 minutes and 24 hours of assessment ($p<0.05$). There is a clear, significant effect of the dye in comparison to the control in all samples while there is a gradual increase in fluorescence over time. These results don't suggest that mitochondrial content increases but do suggest the significant impact of time. Supporting that all C_2C_{12} myotubes should be assessed at the same time following incubation of MitoTraker Green FM due to the dramatic effect of time on the fluorescence in mitochondrial content in these cells.

Mitochondrial Membrane Potential Assay

JC-1 (5,5',6,6'-tetrachloro-1,1',3,3'-tetraethylbenzimodazolcarbocynanine iodine) (Invitrogen, Molecular Probes T3168) was used for preliminary work to assess for alterations in mitochondrial membrane potential (Ψm) (the movement of protons into/out of the mitochondria). C_2C_{12} myoblasts were grown and differentiated on glass covered slides coated in polylysine. 200µm JC-1 was prepared from 10mM stock in differentiation media. Differentiation media was removed from C_2C_{12} myotubes and cells were washed in PBS twice. Prepared 200µm JC-1 media was pipette onto cells and incubated for 30 minutes at 37°C. Following incubation media was removed, cells were washed with PBS twice and cells were fixed. Fixing was complete using 4% formaldehyde (Sigma Aldrich, 252549) (prepared in differentiation media) for 15 minutes at ambient temperature. Cells were then washed twice with PBS and permeabilized using 0.1% Triton X-100 (Sigma Aldrich, 106K0177) for 10 minutes. Cells were then washed with PBS once again. Antifade prolong gold (Thermo Fischer Scientific, P10144) was used as a mountant to ensure lasting fluorescence and placed onto glass slide. Slides where viewed for fluorescence using a fluorescent microscope in darkness before stored at 4°C for future viewing if necessary. JC-1 fluorescence was also assessed within black 96 well plates where myotubes were incubated in JC-1 dye and read for fluorescent intensity using the BioTek plate reader (BioTek Synergy HT). To assess for change in mitochondrial membrane potential (ΔΨm) cells should have been incubated in 5µM FCCP however this was not done. Inclusive to this the pH gradient was not assessed which is key for assessment of mitochondrial membrane potential.

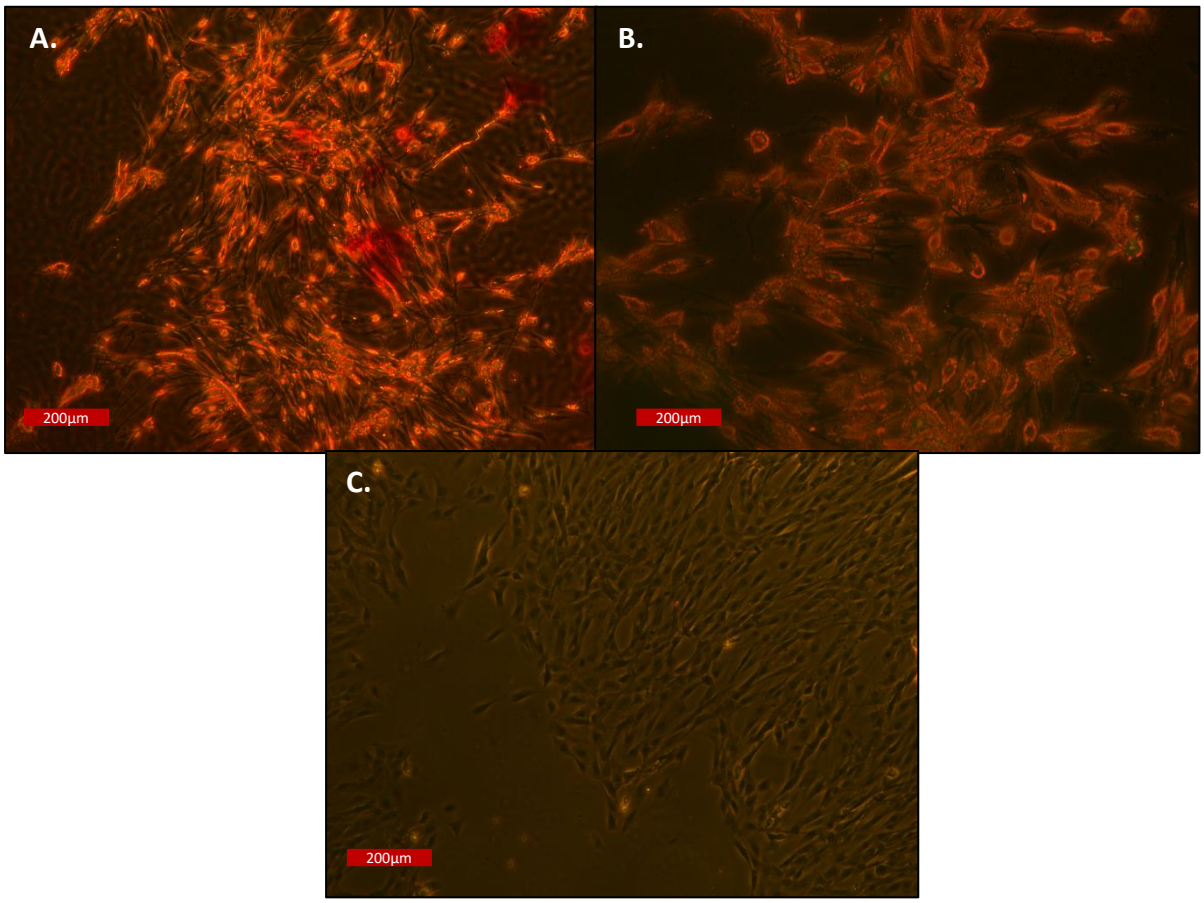

Appendix G. Figure 9. JC-1 mitochondrial potential fluorescent images, C_2C_{12} myotubes

(Fluorescent images representing JC-1 at 200µm probing of C_2C_{12} myotubes grown on coverslips with 30-minute incubation time (A & B) against myotubes without probing (C). All images viewed using the Leica DFC 500 fluorescent microscope (10X), *n*=1)

Summary JC-1 Mitochondrial Membrane Potential - Microscopy

C_2C_{12} myotubes didn't look healthy while growing on coverslips while following assessment it was apparent that the JC-1 dye had crystalized and bound to the cells creating a larger fluorescence than should have. In addition to this FCCP was not added to assess for change in membrane potential as would be the case when usually looking at mitochondrial membrane potential dyes.

JC-1 Membrane Potential Fluorescent Intensity Time Course (Plate Reader)

C_2C_{12} myoblasts were grown at a cell density of $1x10^4$ and $1x15^4$ per well until confluent in black 96 well plates (Analab, 353219). Once confluent cells were differentiated for 5 days. On day 5 cells were probed for JC-1 to assess for change in mitochondrial membrane potential fluorescence over 24 hours. Cells were assessed for fluorescence after 30 minutes (minimum recommended time), 4 hours and 24 hours in order to assess for optimal reading time on the fluorescent plate reader (BioTek Synergy HT).

JC-1 Fluorescent Intensity

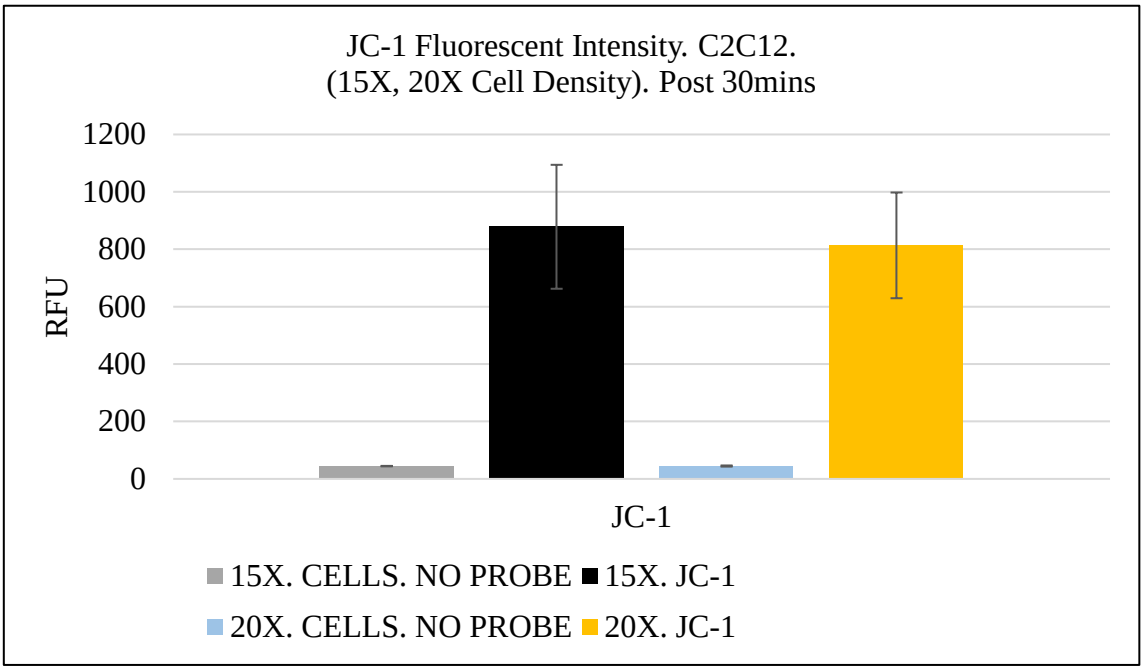

Appendix G. Figure 10. JC-1 Fluorescent Intensity post 30mins incubation

(Identifying the effect of JC-1 probing 30 minutes' post incubation at $1x10^4$ and $1x15^4$, significant difference in fluorescence between 30 minutes' incubation and control, $p<0.05$, $n=3$)

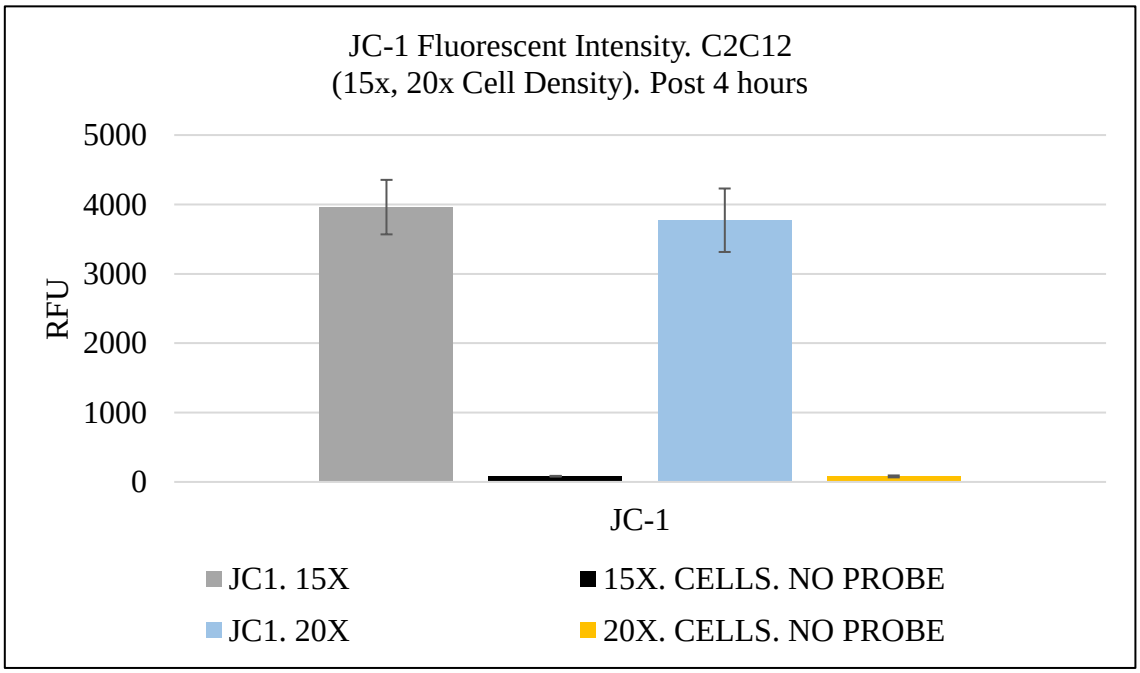

Appendix G. Figure 11. JC-1 Fluorescent Intensity post 4 hours' incubation

(The effect of JC-1 probing 4 hours post incubation at $1x10^4$ and $1x15^4$, significant difference between 4 hours following incubation and control, $p<0.05$, $n=3$)

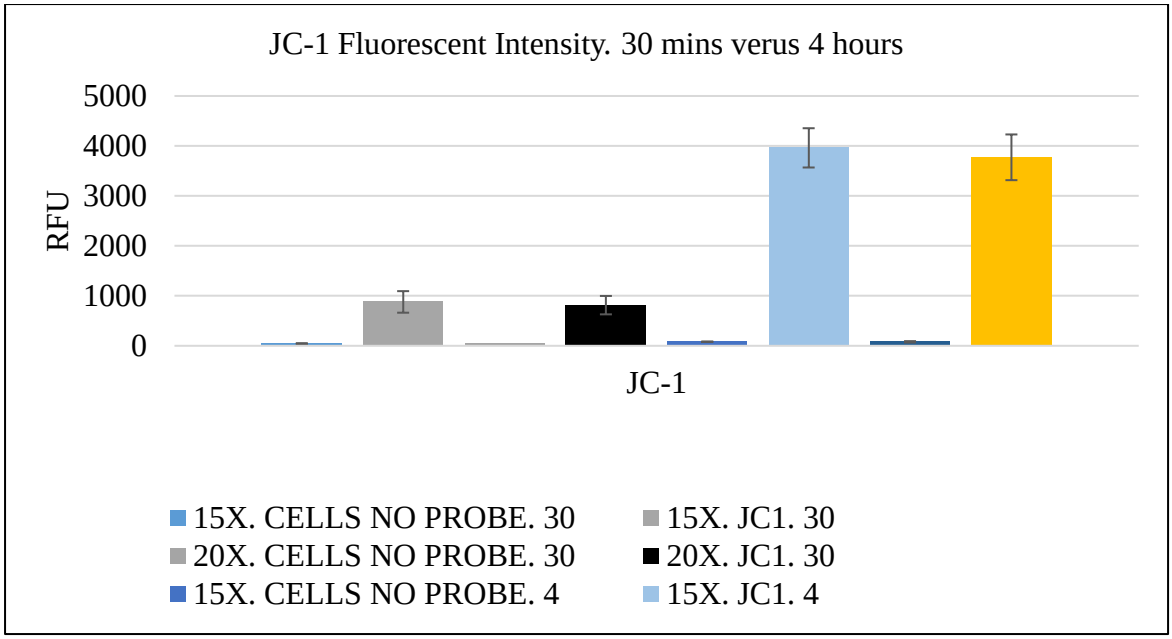

Appendix G. Figure 12. JC-1 Fluorescent Intensity post 30 minutes' v 4 hours' incubation

(The effect of JC-1 probing 30 minutes' post incubation versus 4 hours post incubation at $1x10^4$ and $1x15^4$, significant difference in fluorescence between 30 minutes and 4 hours of viewing, $p<0.05$, $n=3$)

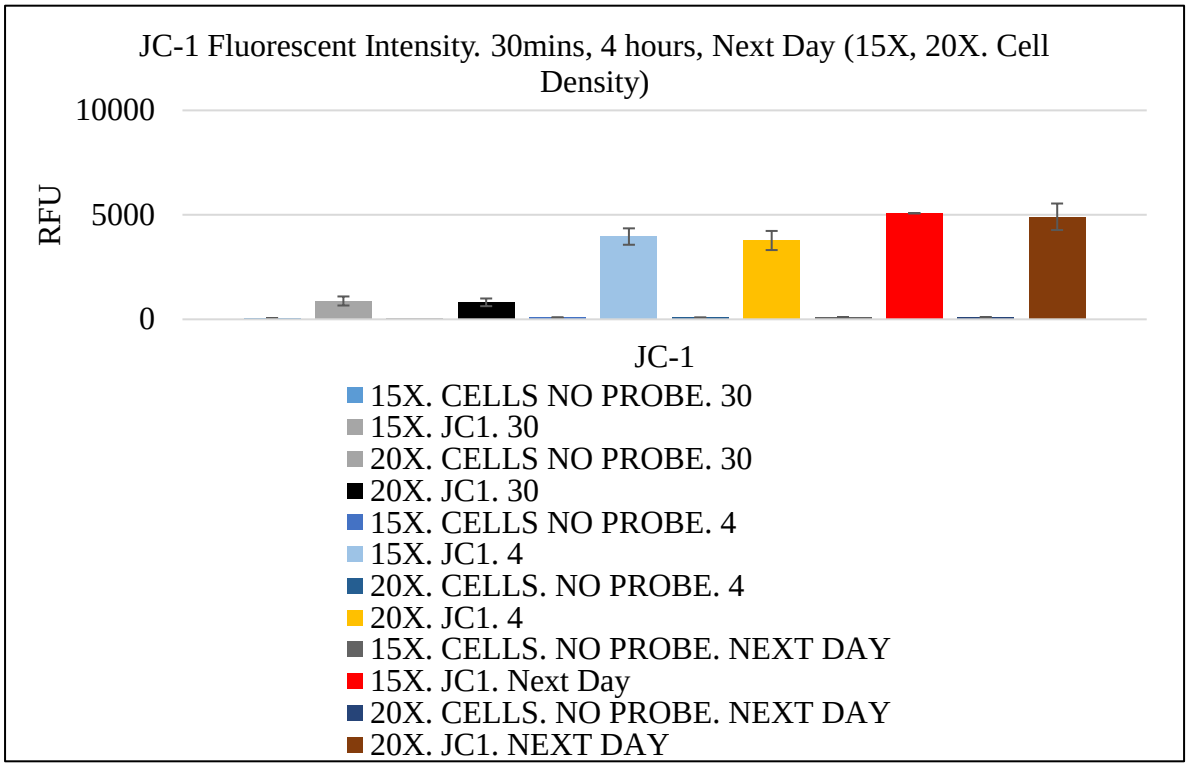

Appendix G. Figure 13. JC-1 Fluorescent Intensity post 30 minutes, 4 hours & 24 hours post incubation

(The effect of JC-1 probing 30 minutes, 4 hours and 24 hours post incubation at $1x10^4$ and $1x15^4$, with a significant increase in fluorescence between 30 minutes and 4 hours, 4 hours and 24 hours, $p<0.05$, $n=3$)

Summary Mitochondrial Membrane Potential Fluorescence

Results indicate a significant change in mitochondrial membrane potential fluorescence between 30 minutes and 24 hours of assessment. There is a clear significant effect of the dye in comparison to the control in all samples while there is a gradual increase in fluorescence over time. From these results it supports that all samples should be assessed at the same time following incubation of JC-1 due to the dramatic effect of time on the fluorescence in membrane potential in these cells. Ideally the use of this dye should be in combination with FCCP (to induce a reaction) and with the calculation of the pH gradient. In addition to these points JC-1 has been proven as a poor probe for mitochondrial membrane potential and the optimal dye being tetramethylrhodamin-methylester (TMRM+). TMRM+ is now in our collection of probes and will be used for mitochondrial membrane potential in combination with FCCP and pH calculation in future experiments of this nature.

Appendix H - Primary Human Skeletal Muscle Certificate of Analysis Information

The following relevant information was given to us upon purchase of these primary human skeletal muscle cells from ATCC.

ATCC Number: PCS-950-010

Lot Number: 81129171

Name: Primary Skeletal Muscle Cells, Normal, Human (Homo Sapiens)

Manufacture Date: Dec 2017

Fill Volume: 1.0 ml

Passage Number: 3

Donor Tissue Source: Thigh

Donor Gender: Female

Donor Age: Neonate

Donor Race: Caucasian

Appendix I - Human Skeletal Muscle Primer Optimization

Primers were optimised as depicted within the Methods. Along with insuring only one melt and one amplification curve through RT-qPCR, specificity and base pair size was also confirmed by measuring band expression using agarose gels with a 100bp DNA ladder (ThermoScientific, 15628019) Below is an example of an agarose gel ran for 1 hour at 100 volts following RT-qPCR to confirm primer specificity:

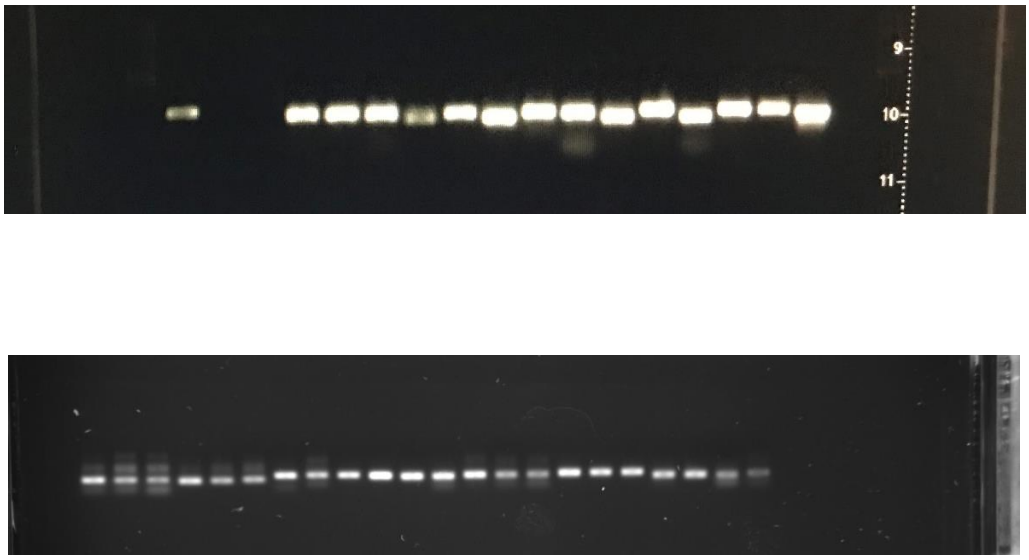

Appendix I. Figure 1. Agarose gels used to confirm optimisation results of RT-qPCR for primer design

Primer Efficiency

Already amplified gene using Lightcycler 96 RT-qPCR reaction (12µl) was diluted in nuclease free water (1:1000). A serial dilution (1:10) of this 1:1000 amplified primer was conducted to measure the efficiency of the primer at lower concentrations. Each dilution was made up into a mastermix for PCR reaction using the Lightcycler 96.

Primer Amplification Curves

Drp1

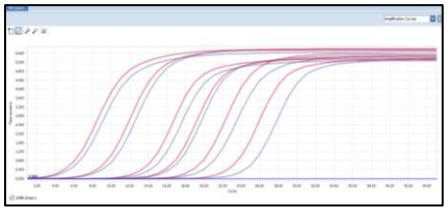

Fis1

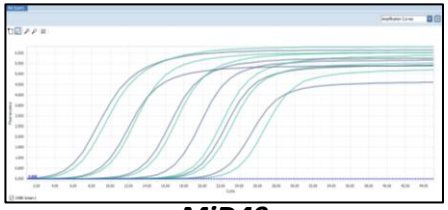

Mff

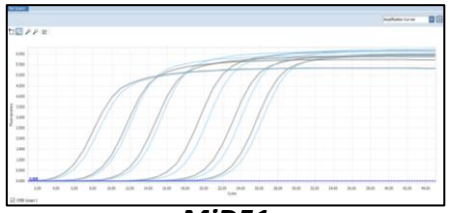

Mfn1

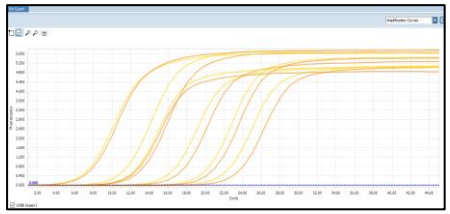

Mfn2

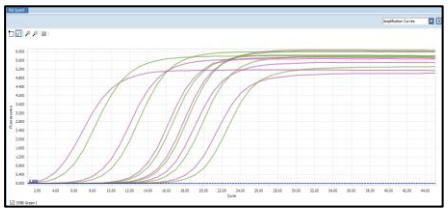

MiD49

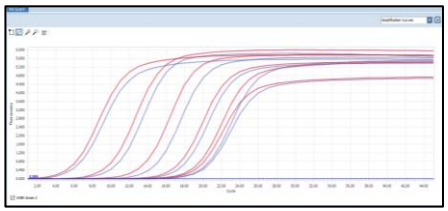

MiD51

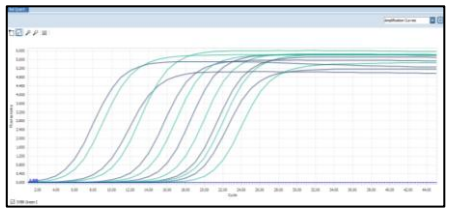

OMA1

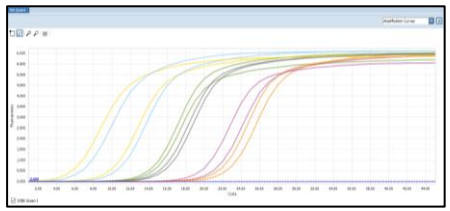

OPA1

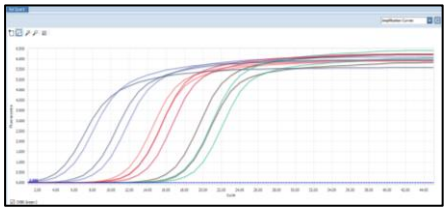

YME1L

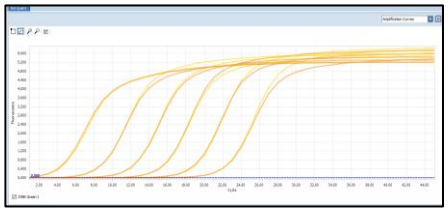

PGC-1α

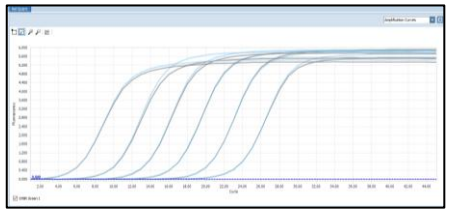

Parkin

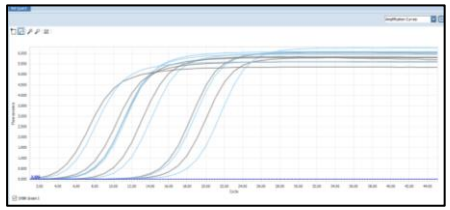

PINK1

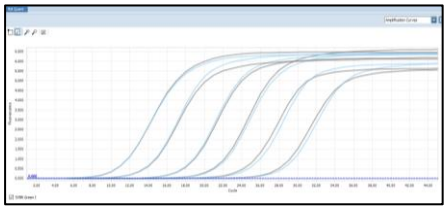

AMPKα1

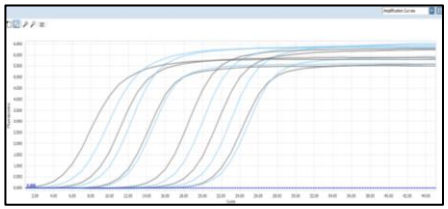

AMPKα2

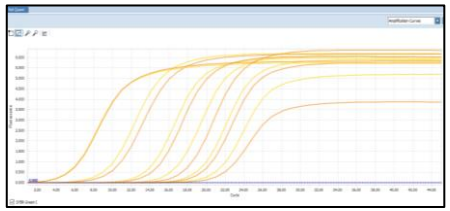

ANT1

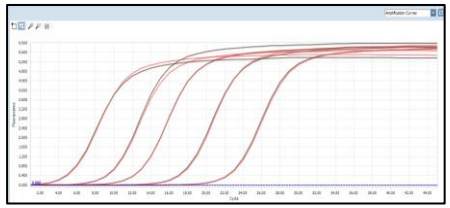

ANT2

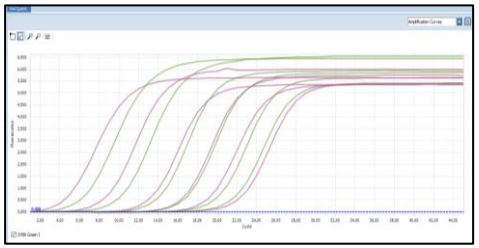

CAMK2α

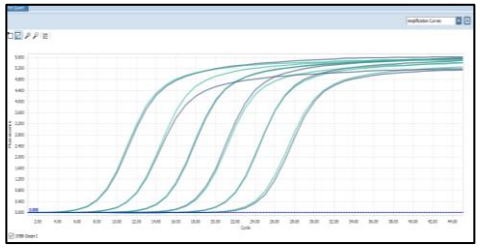

Glucose-6-Phosphate

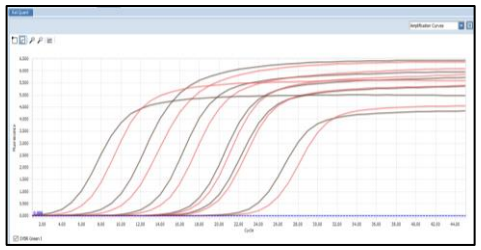

mTOR

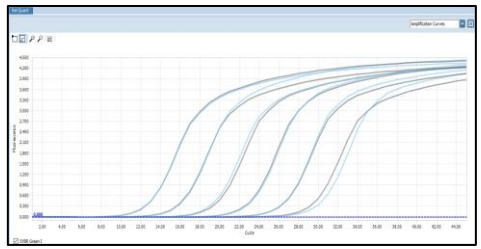

Pyruvate Dehydrogenase α1

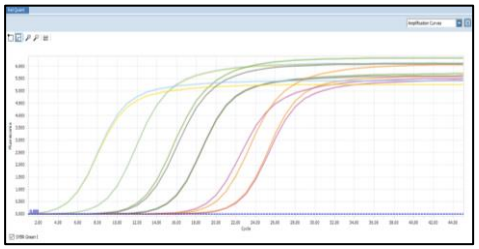

Pyruvate Dehydrogenase β1

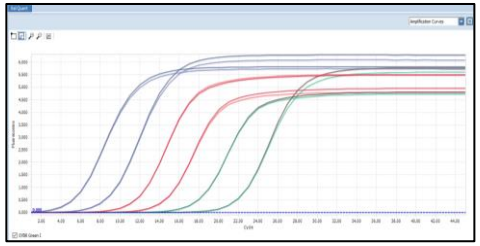

ACC

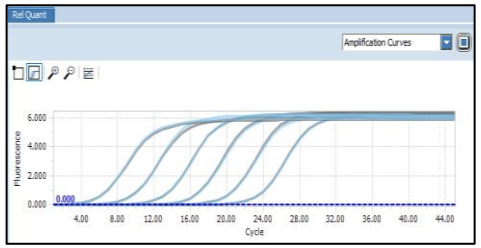

CPT1b

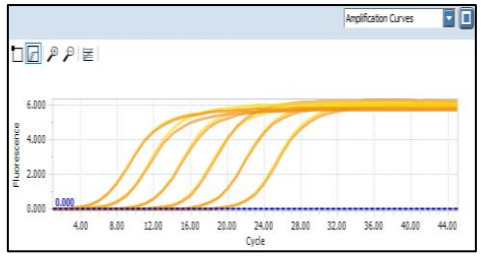

SIRT1

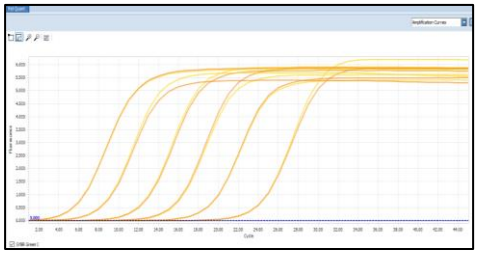

SIRT3

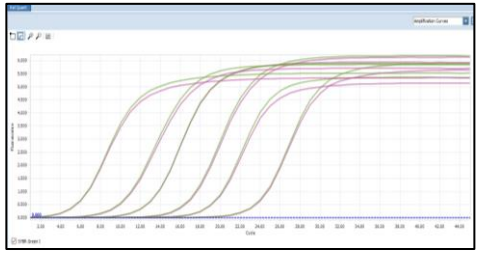

SIRT4

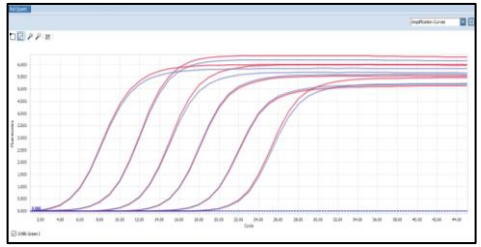

SIRT5

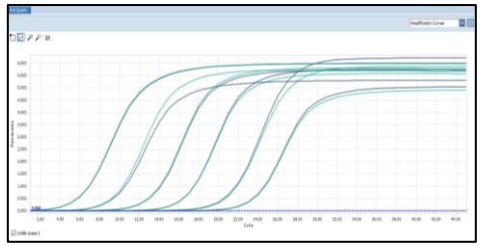

SIRT6

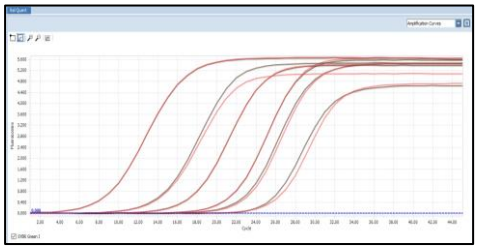

ACTC1

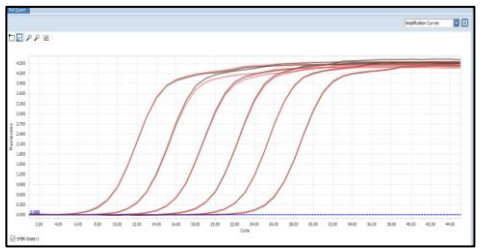

ACAT2

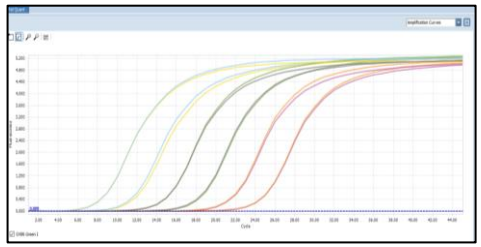

CKM

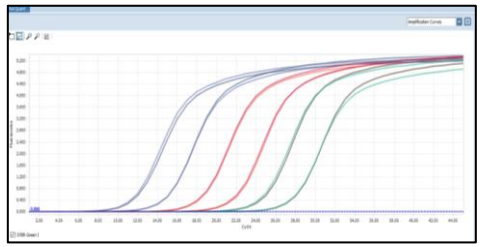

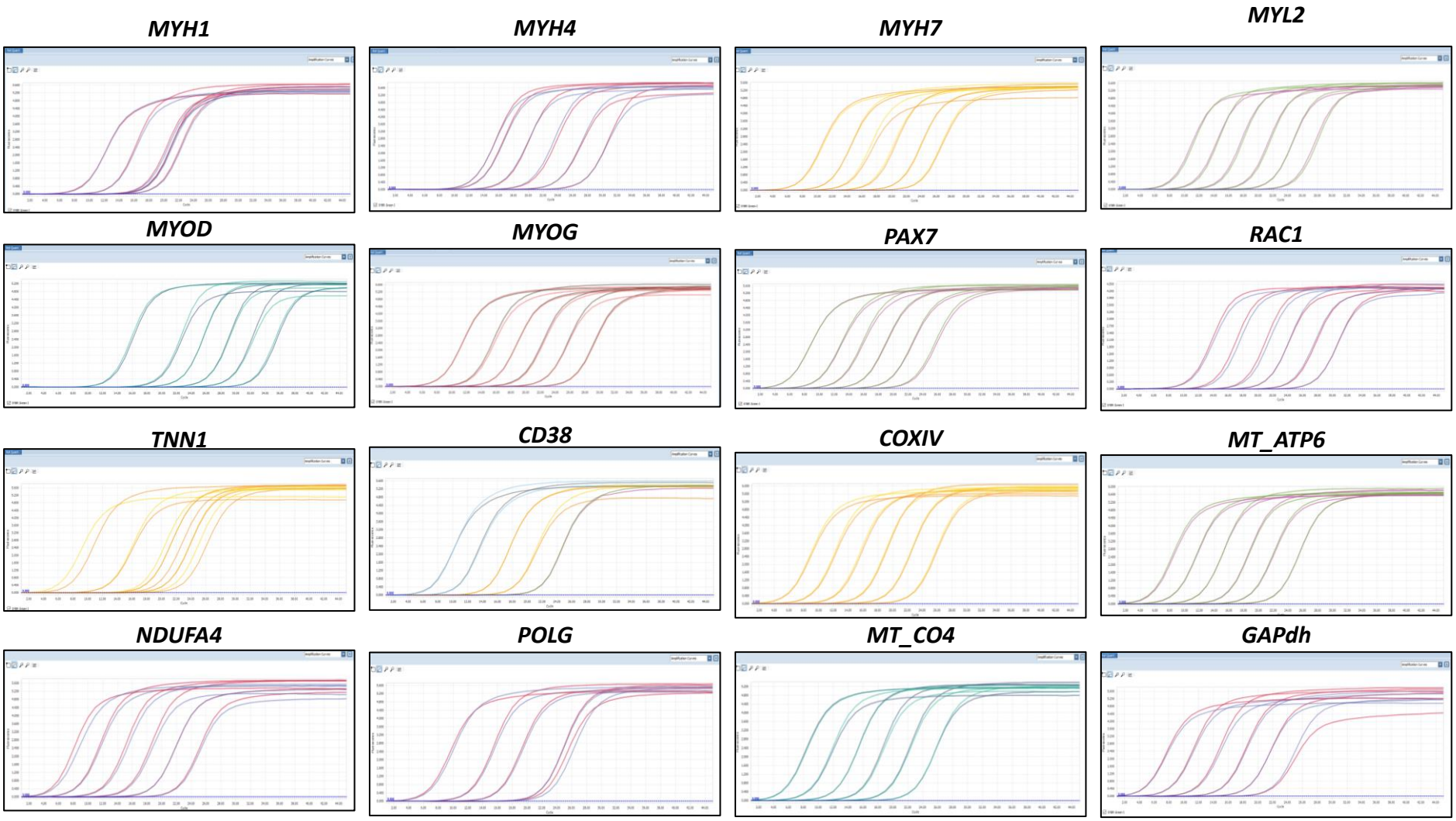

Appendix I. Figure 2. Primer efficiency amplification curves

Primer Melt Curves

Drp1

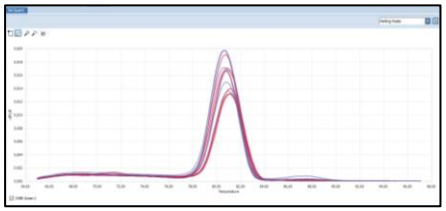

Fis1

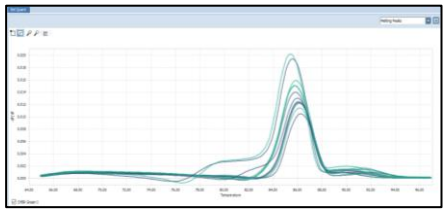

Mff

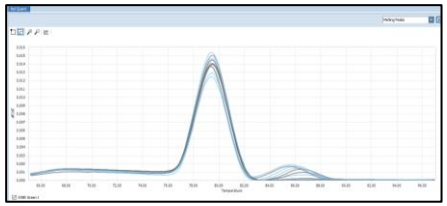

Mfn1

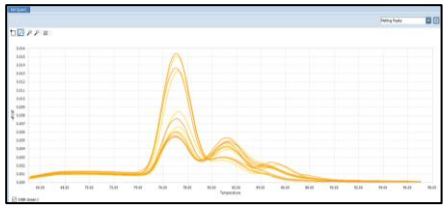

Mfn2

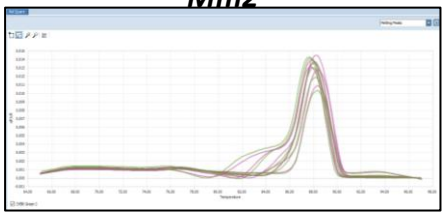

MiD49

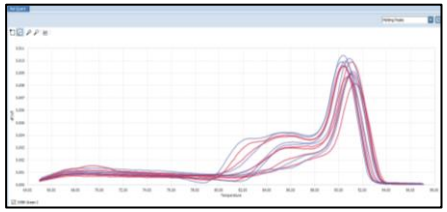

MiD51

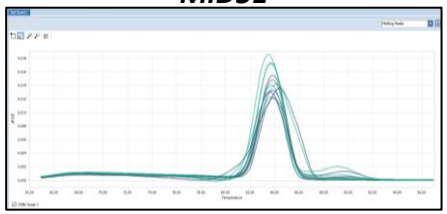

OMA1

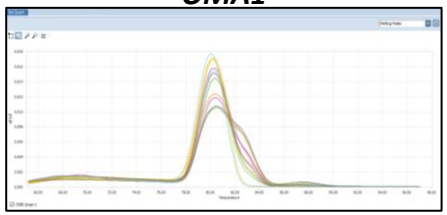

OPA1

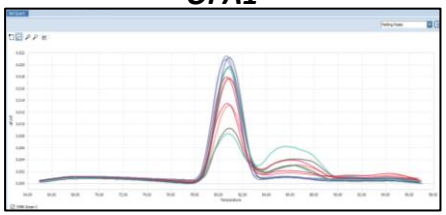

YME1L

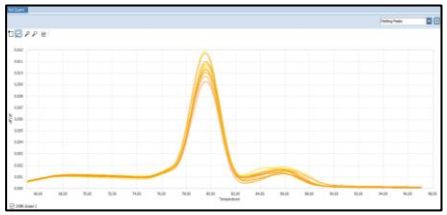

PGC-1α

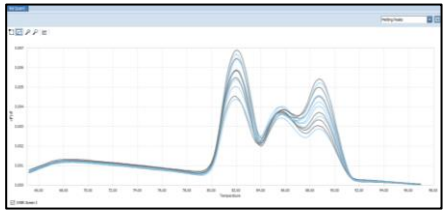

Parkin

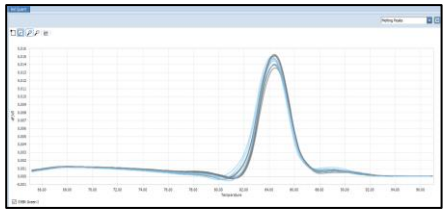

PINK1

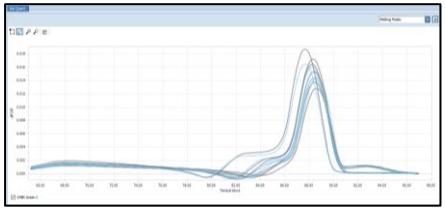

AMPKα1

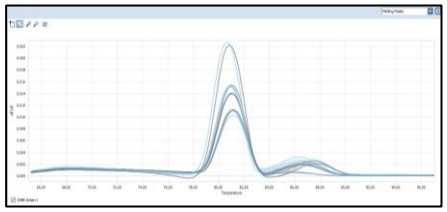

AMPKα2

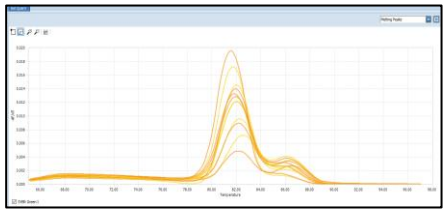

ANT1

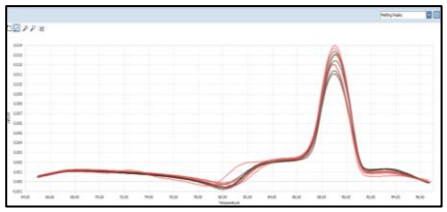

ANT2

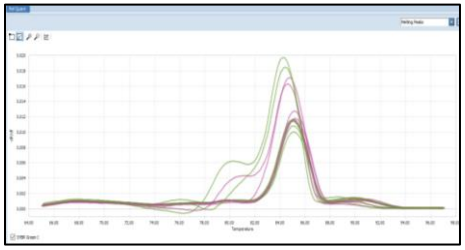

CAMK2α

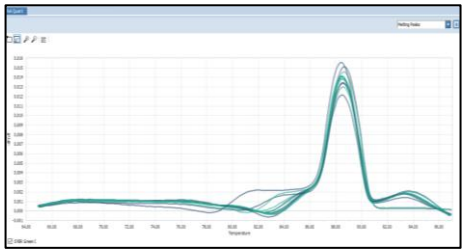

Glucose-6-Phosphate

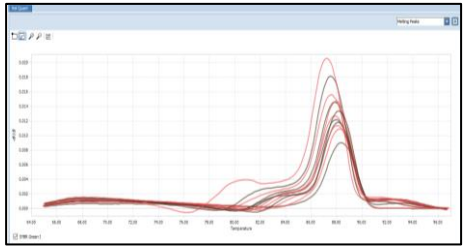

mTOR

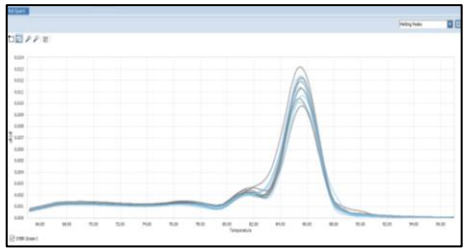

Pyruvate Dehydrogenase α1

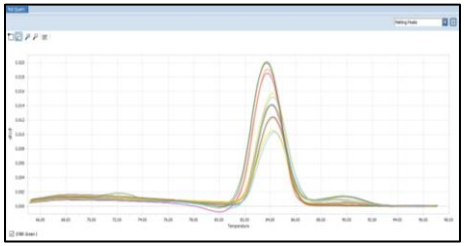

Pyruvate Dehydrogenase β1

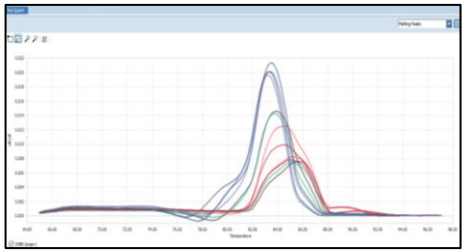

ACC

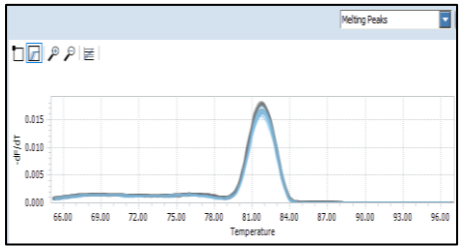

CPT1b

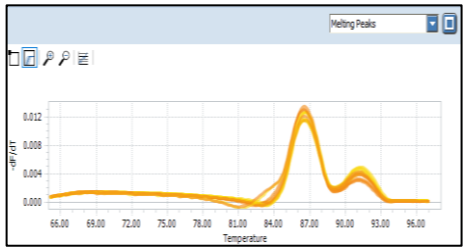

SIRT1

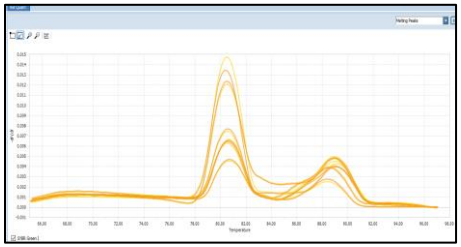

SIRT3

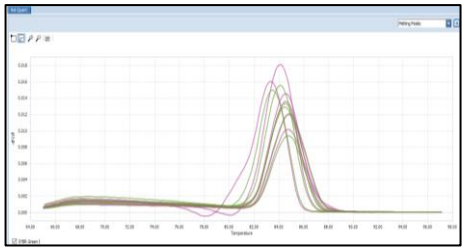

SIRT4

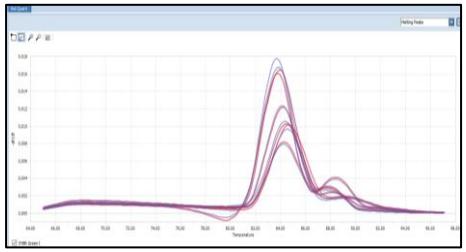

SIRT5

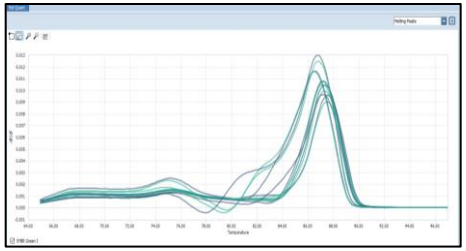

SIRT6

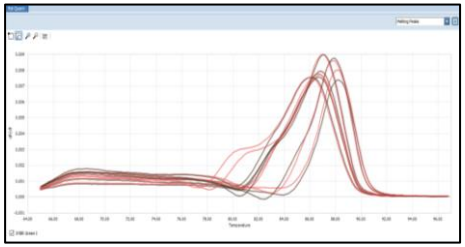

ACTC1

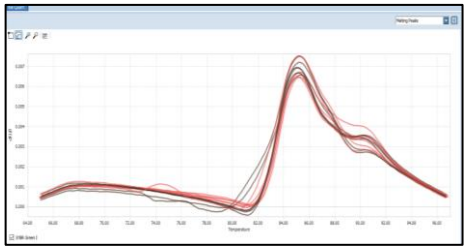

ACAT2

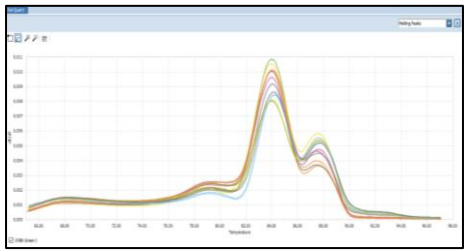

CKM

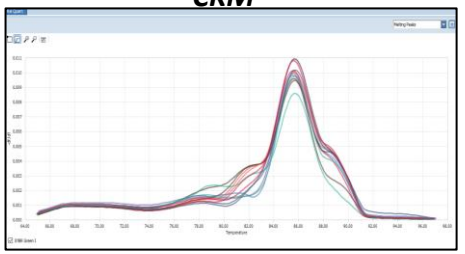

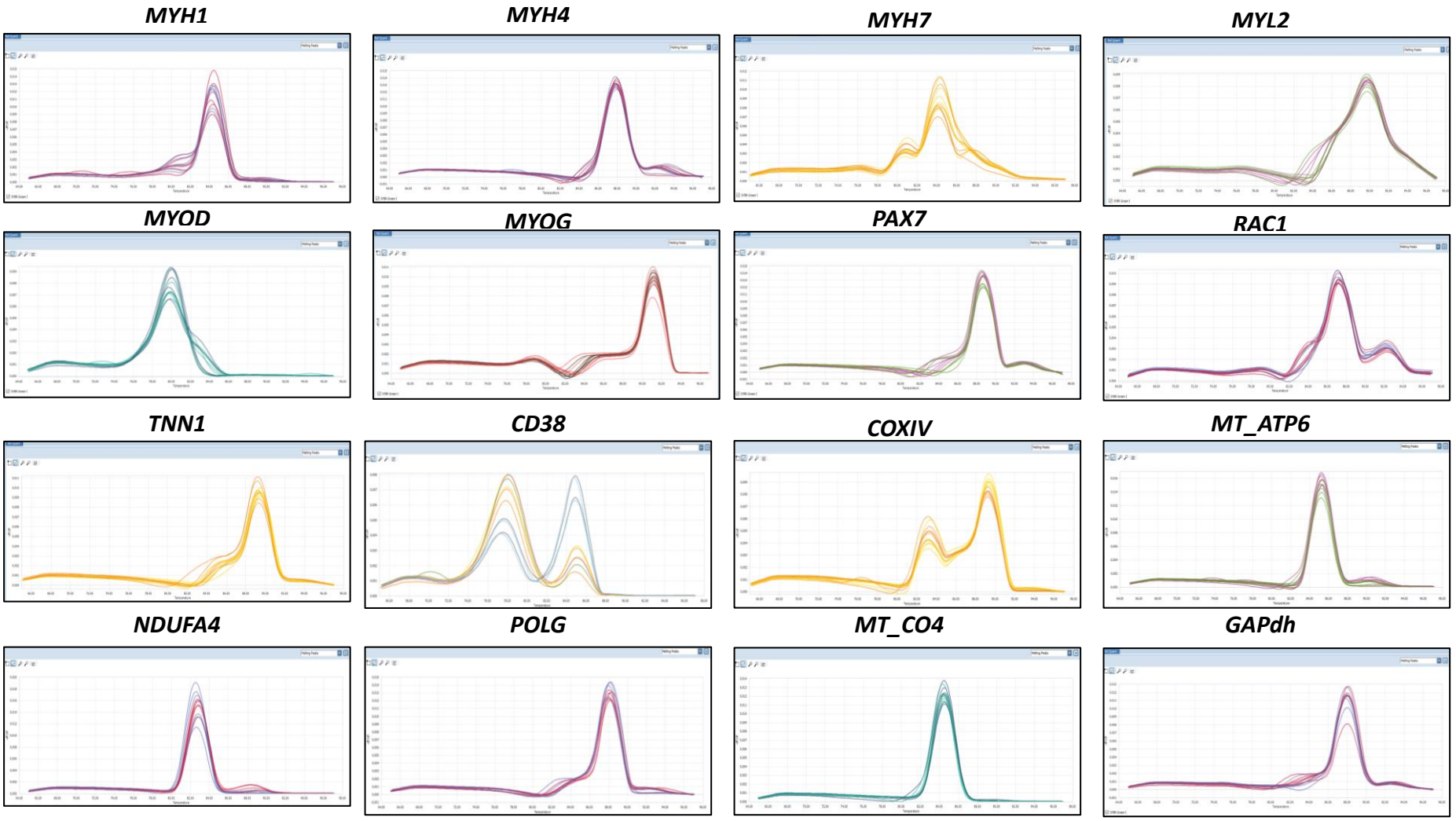

Appendix I. Figure 3. Primer efficiency melt curves

Primer Efficiency Curves

Drp1

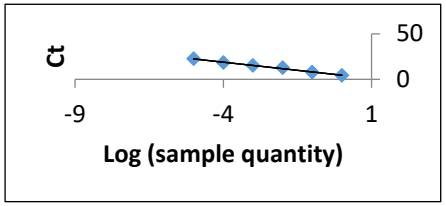

Fis1

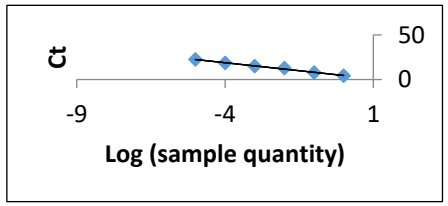

Mff

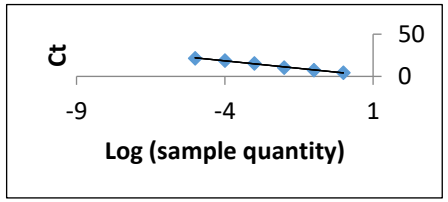

Mfn1

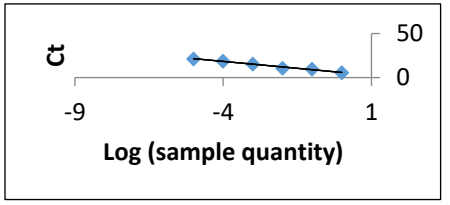

Mfn2

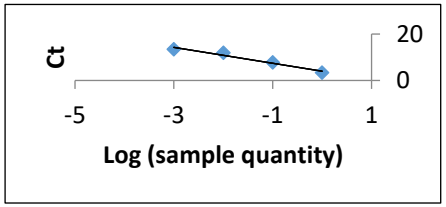

MiD49

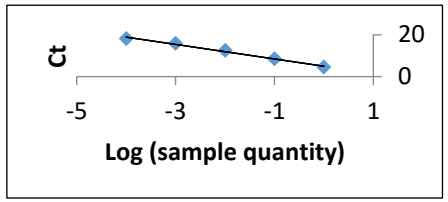

MiD51

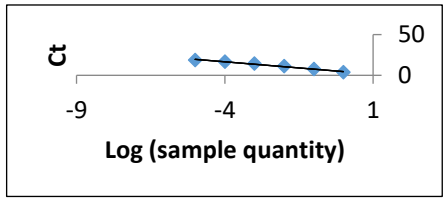

OMA1

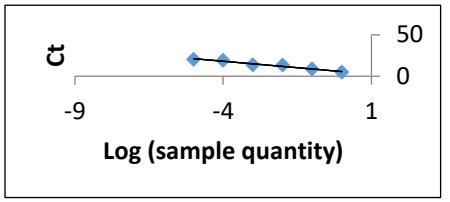

OPA1

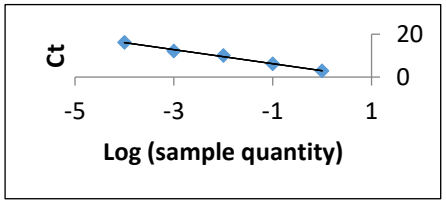

YME1L

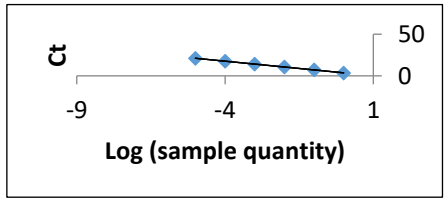

PGC-1α

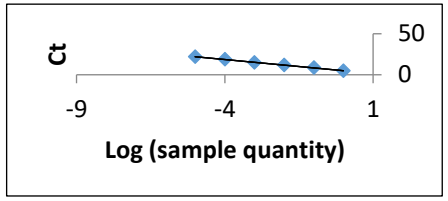

Parkin

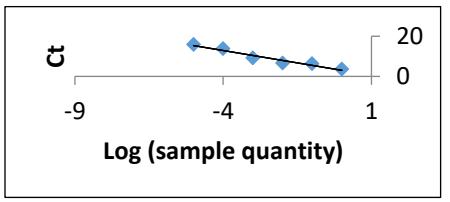

PINK1

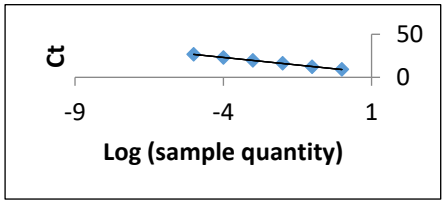

AMPKα1

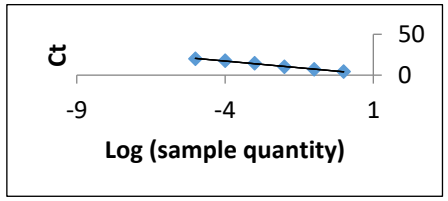

AMPKα2

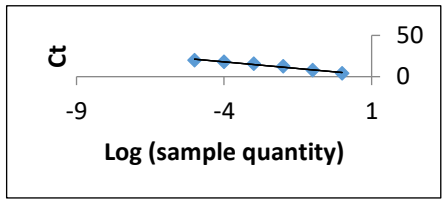

ANT1

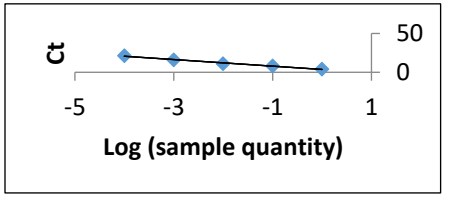

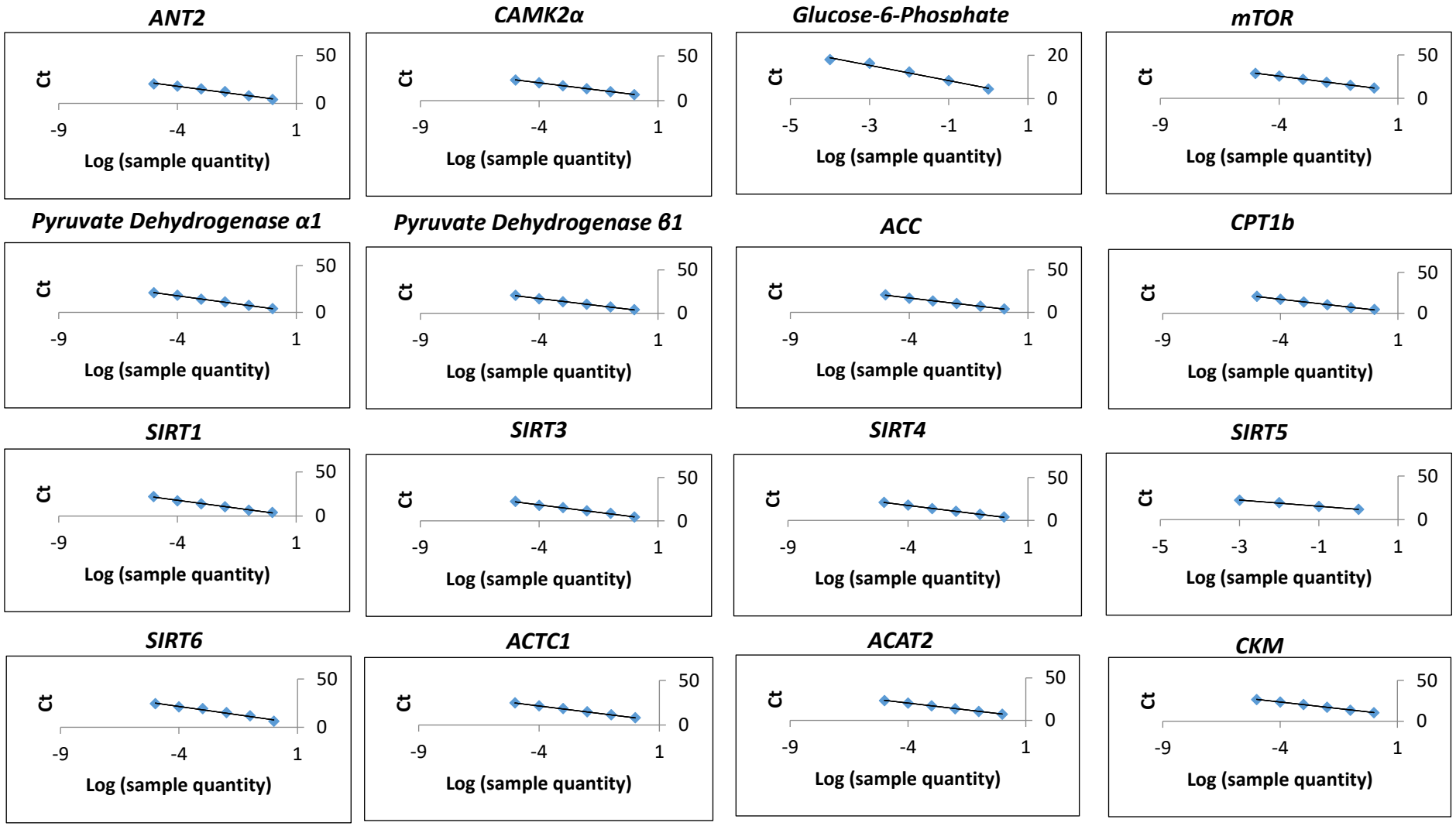
ANT2
CAMK2α
Glucose-6-Phosphate
mTOR
Pyruvate Dehydrogenase α1
Pyruvate Dehydrogenase β1
ACC
CPT1b
SIRT1
SIRT3
SIRT4
SIRT5
SIRT6
ACTC1
ACAT2
CKM
Ct
Log (sample quantity)

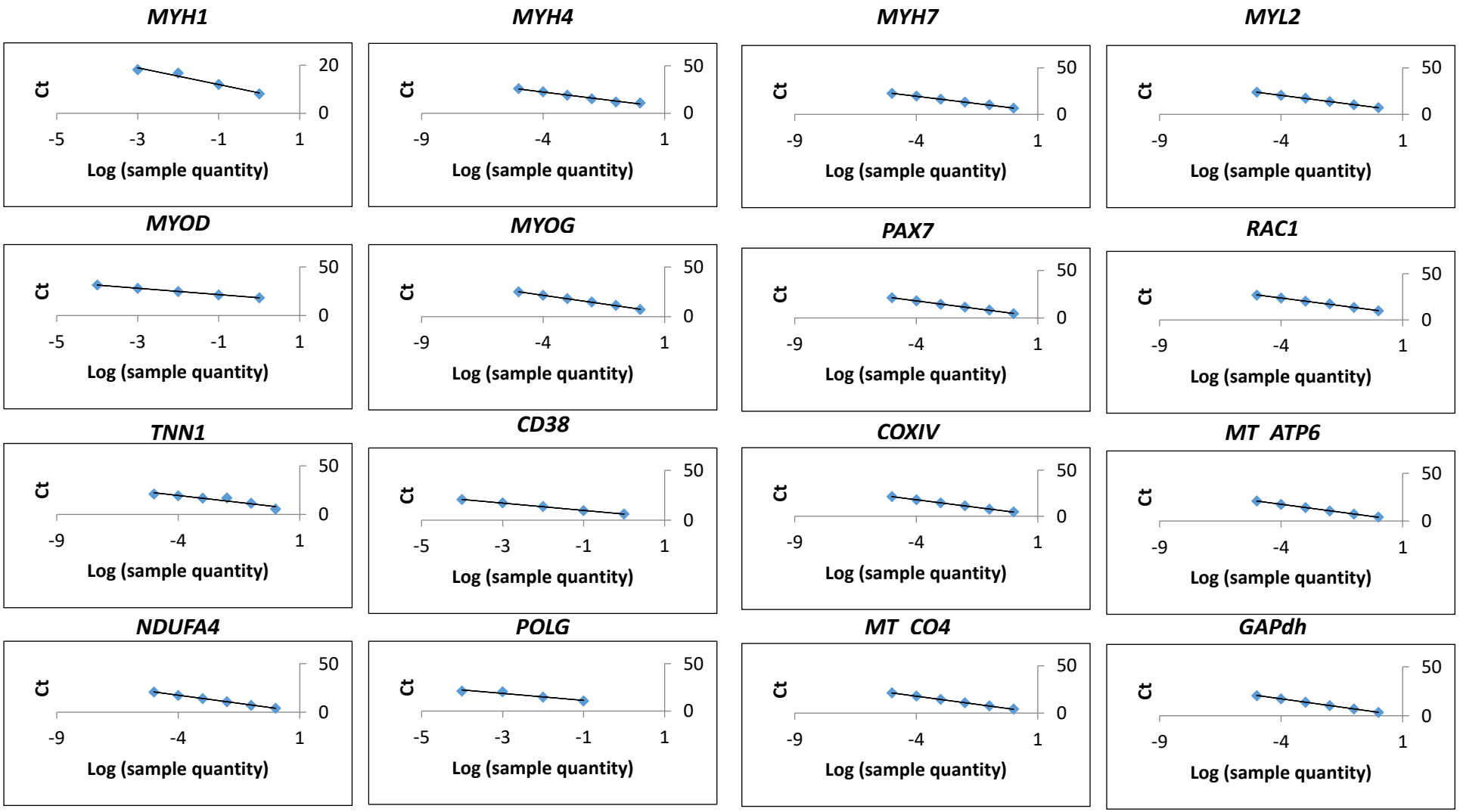

Appendix I. Figure 4. Primer efficiency curves

Appendix J - SIRT4 siRNA Optimization

Optimal Transfection Reagent

In order to understand the optimal transfection reagent and concentration to knockdown SIRT4 mRNA expression in primary human skeletal muscle myotubes four separate transfection reagents were assessed. Myotubes were grown and differentiated for 10 days. The following transfection reagents were used to assess for SIRT4 knockdown (*n*=1):

- MirusIT-TKO (Mirus, MIR 2154)
- DharmaFECT 1 (Dharmacon, T-2001-S)
- DharmaFECT 3 (Dharmacon, T-2003-S)
- Lipofectamine 3000 (Invitrogen, L3000001)

Each transfection reagent was assessed at three separate concentrations (2µl, 4µl and 6µl per 50µl Opti-MEM) in all conditions. 25nM of siRNA silencer select s23764, s23765 and silencer select siRNA negative control (4390843) were used for all transfection reagent conditions. Further details discussed in Chapter III Methodology, Cell Culture Methods, Primary Human Skeletal Muscle Myotube siRNA Transfection. Optimal transfection reagent to knockdown SIRT4 gene expression was confirmed through RT-qPCR analysis which highlighted Lipofectamine 3000 to be the most ideal method to knockdown SIRT4 gene expression (*n*=1).

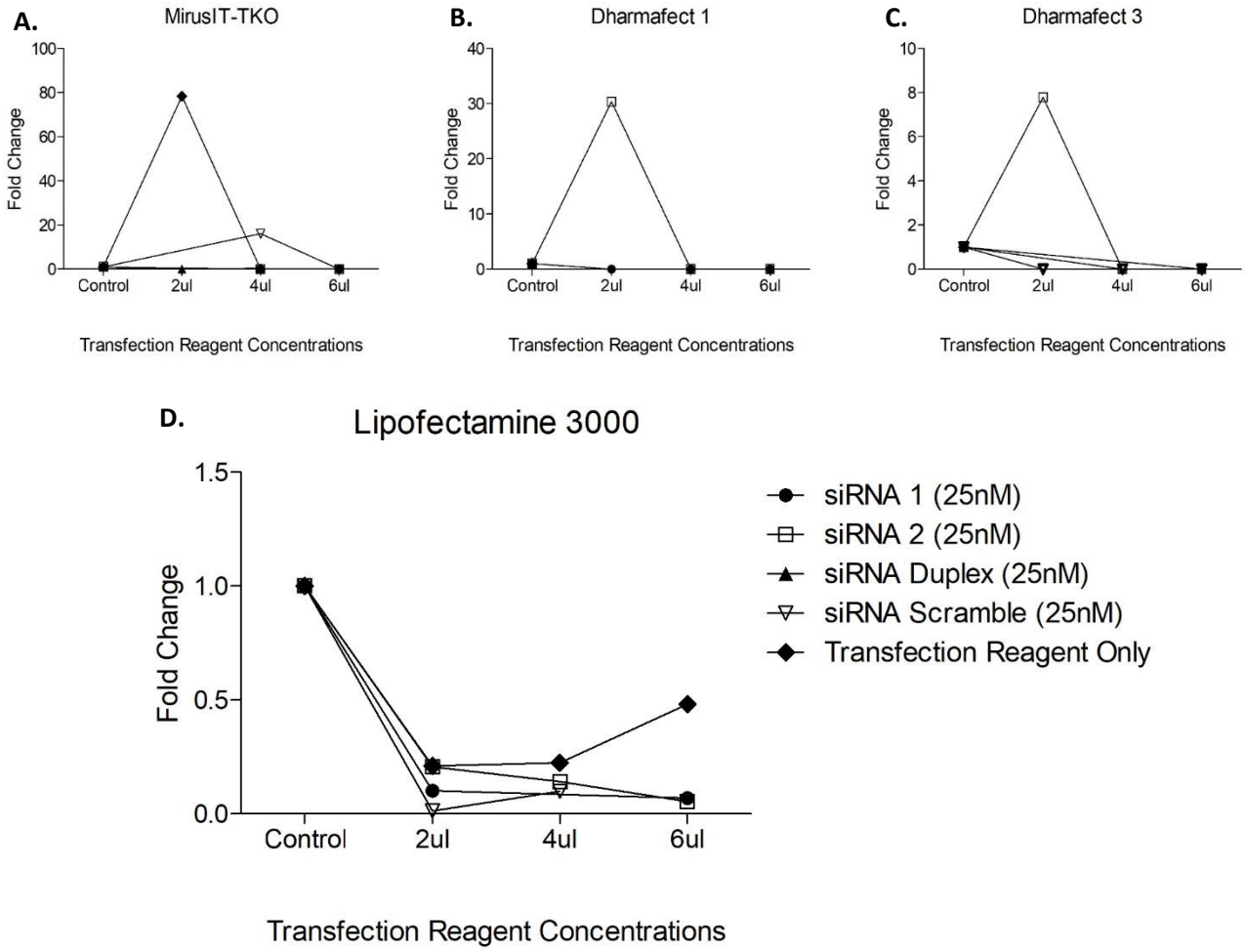

Appendix J. Figure 1. SIRT4 mRNA expression with transfection optimisation

(Total SIRT4 mRNA expression in HSM myotubes following 2µl, 4µl & 6µl of (A) MirusIT-TKO, (B) Dharmafect 1, (C) Dharmafect 3 and (D) Lipofectamine 3000 transfection reagent quantified by RT-qPCR (*n*=1). Gene expression was normalised against GAPdh mRNA expression of same sample before being normalised to the control sample)

Optimal siRNA Concentration

Four different concentrations, 25nM, 50nM, 75nM and 100nM, of siRNA silencer select were made. These four concentrations were tested on the siRNA silencer select s23764 (siRNA 1), s23765 (siRNA 2) and silencer select siRNA negative control (4390843) (siRNA Scramble). These were all incubated with 6µl lipofectamine 3000 and reduced serum medium (Opti-MEM). Optimal SIRT4 siRNA concentration to knockdown SIRT4 gene expression was confirmed through RT-qPCR analysis (*n*=1). SIRT4 mRNA expression following incubation of 6µl Lipofectamine 3000 only was also measured. Such analysis confirmed the optimal SIRT4 siRNA concentration to knockdown SIRT4 to be 6µl of Lipofectamine 3000 (Invitrogen, L3000001), with a duplex of siRNA 1 and 2 at a concentration of 75nM.

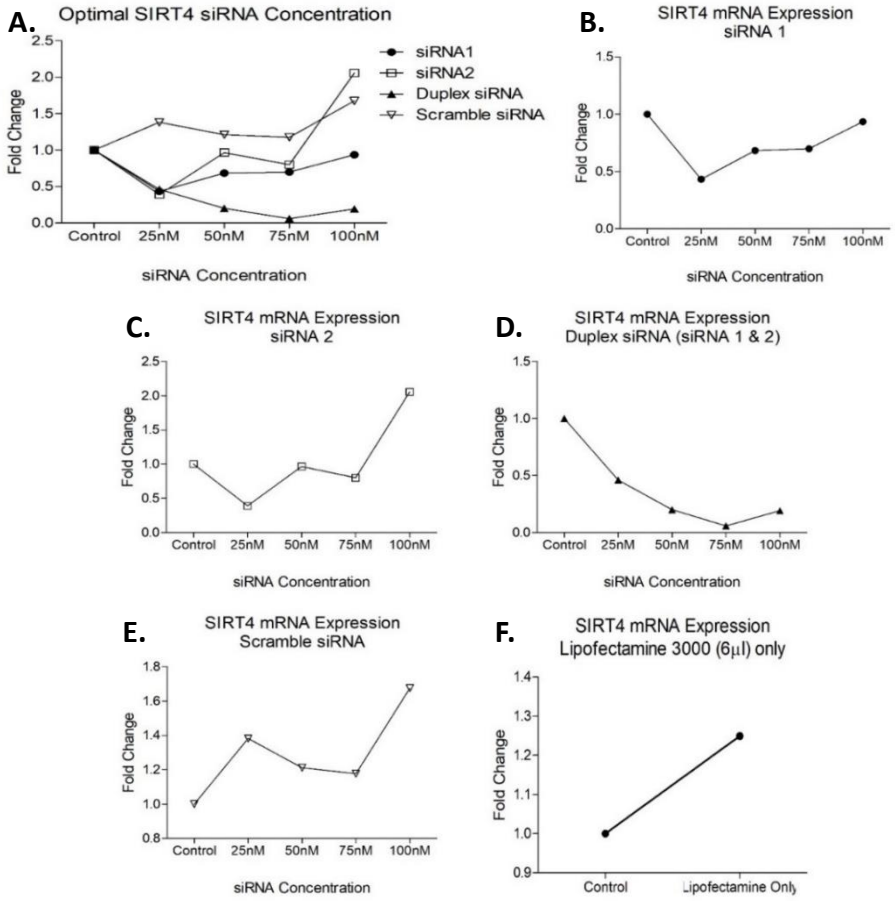

Appendix J. Figure 2. SIRT4 mRNA expression with SIRT4 siRNA optimisation

(Total SIRT4 mRNA expression in HSM myotubes following incubation with 25nM, 50nM, 75nM and 100nM siRNA 1, siRNA 2, duplex siRNA and Scramble siRNA (A), siRNA 1 (B), siRNA 2 (C), duplex siRNA 1 & 2 (D), Scramble siRNA (E) with 6µl lipofectamine 3000 transfection reagent and SIRT4 mRNA expression following incubation with 6µl Lipofectamine 3000 only (F) quantified by RT-qPCR (*n*=1). Gene expression was normalised against GAPdh mRNA expression of same sample before being normalised to the control sample)

Optimal Takedown Experiment (75nM)

Once an understanding was made on the optimal transfection reagent, concentration and SIRT4 siRNA concentration and combination, optimal incubation time to knockdown SIRT4 was assessed at 0 minutes, 60 minutes, 24 hours, 48 hours and 72 hours. SIRT4 mRNA expression was assessed through RT-qPCR (*n*=1).

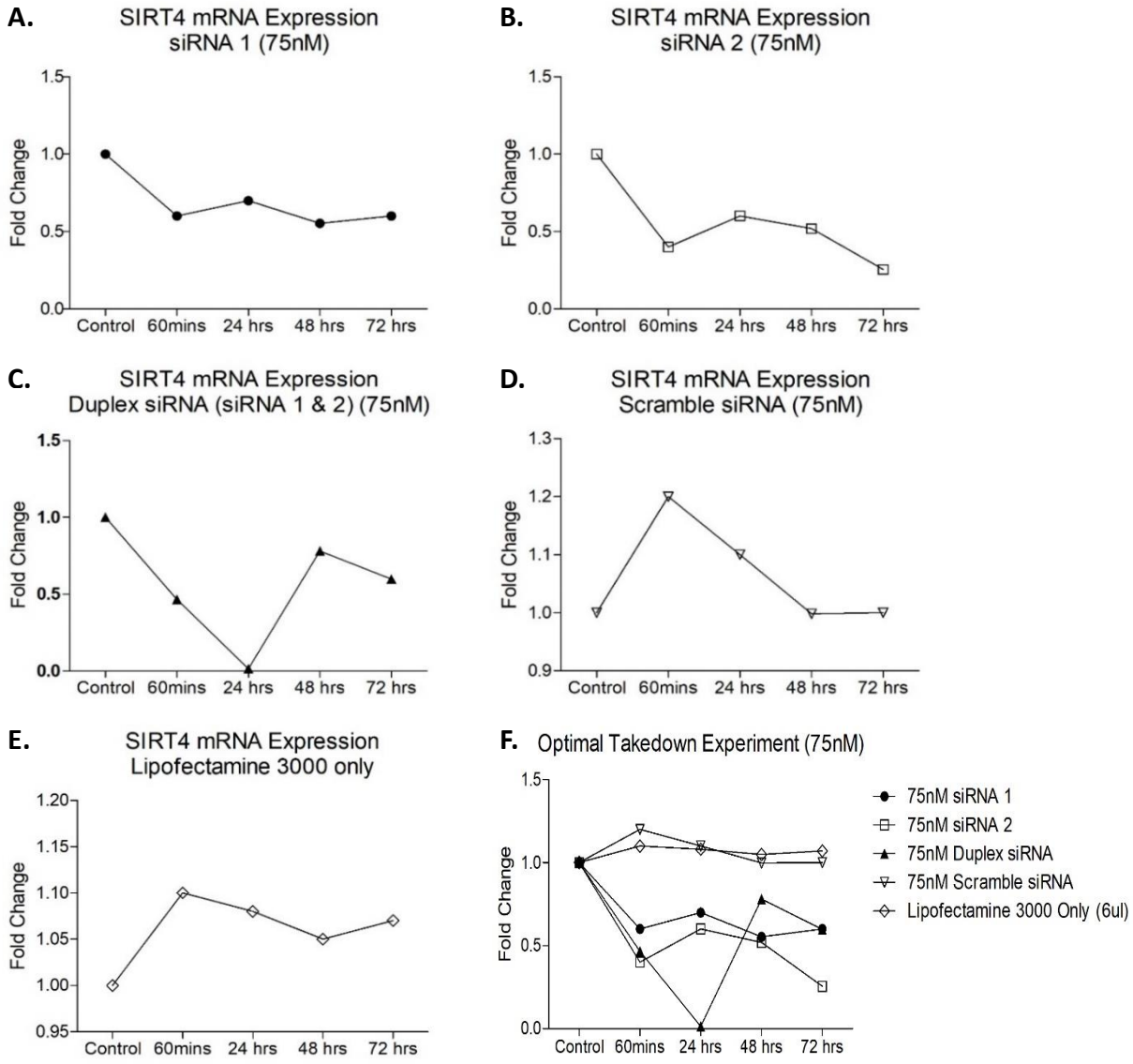

Appendix J. Figure 3. Optimal time of takedown following SIRT4 siRNA (75nM)

(Total SIRT4 mRNA expression in HSM myotubes following incubation with 75nM siRNA 1 (A), 75nM siRNA 2 (B), 75nM duplex siRNA (C), 75nM Scramble siRNA (D), SIRT4 mRNA expression with 6µl lipofectamine 3000 transfection reagent only (E), and all of the above (F) quantified by RT-qPCR (*n*=1). Gene expression was normalised against GAPdh mRNA expression of same sample before being normalised to the control sample)

Optimal Takedown Experiment (50nM)

In order to be confident that 75nM duplex siRNA 1 and 2 was the optimal concentration to knockdown SIRT4 mRNA expression, the same experiment was developed using a concentration of 50nM duplex siRNA 1 and 2. Optimal incubation time with 50nM duplex siRNA 1 and 2 was assessed at 0 minutes, 60 minutes, 24 hours, 48 hours and 72 hours. SIRT4 mRNA expression was assessed through RT-qPCR (*n*=1).

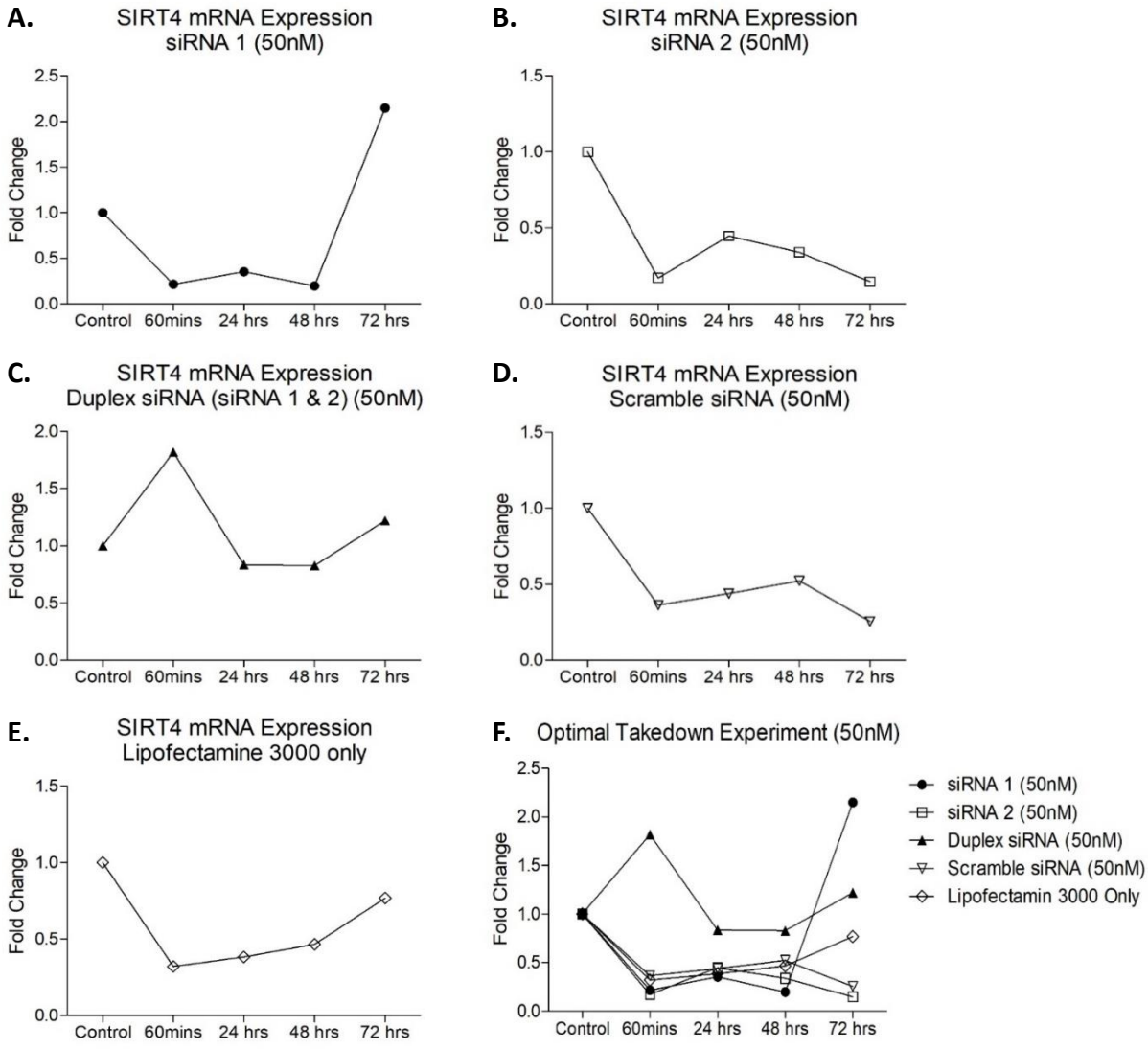

Appendix J. Figure 4. Optimal time of takedown following SIRT4 siRNA (50nM)

(Total SIRT4 mRNA expression in HSM myotubes following incubation with 50nM siRNA 1 (A), 50nM siRNA 2 (B), 50nM duplex siRNA (C), 50nM Scramble siRNA (D), SIRT4 mRNA expression with 6µl lipofectamine 3000 transfection reagent only (E), and all of the above (F) quantified by RT-qPCR (*n*=1). Gene expression was normalised against GAPdh mRNA expression of same sample before being normalised to the control sample)

Appendix K - SIRT4 siRNA Knockdown Transcriptional Expression Relative to the Scramble

Transcriptional expression of SIRT4

SIRT4, the target of interest and a nicotinamide adenine dinucleotide (NAD+)-dependent lysine deacylases was analysed for mRNA expression using RT-qPCR and expressed below relative to the Scramble siRNA (75nM). There was a significant decrease in the mRNA expression of Sirtuin 4 (SIRT4) with SIRT4 Duplex siRNA (75nM) in comparison to the Scramble siRNA (p<0.05) and the control samples (p<0.05) (n=3).

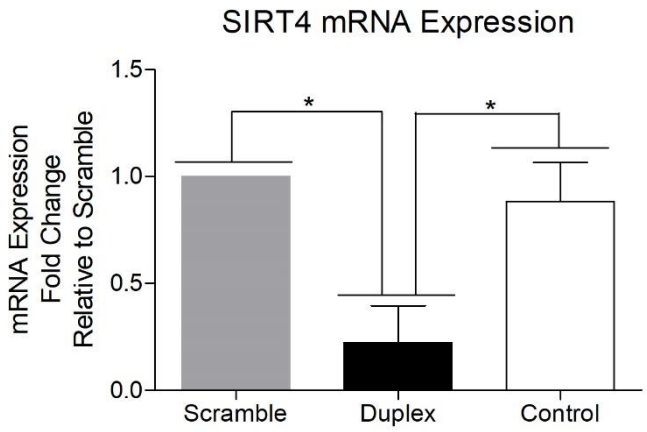

Appendix K. Figure 1. SIRT4 mRNA expression following SIRT4 knockdown

(Total SIRT4 mRNA expression in Scramble siRNA (75nM), SIRT4 Duplex (75nM) siRNA and Control HSM myotubes quantified by RT-qPCR (n=4). Gene expression was normalised against GAPdh mRNA expression of same sample. Data are expressed as mean ±SD. *significant effect of SIRT4 knockdown, p<0.05)

Transcriptional expression of other Sirtuin Targets

SIRT1, SIRT3, SIRT5 & SIRT6

The other members of the sirtuin family, SIRT1 (located within the nucleus and the cytoplasm), SIRT3 (located within the mitochondria, cytoplasm and nucleus), SIRT5 (located within the mitochondria) and SIRT6 (located within the nucleus) were analysed for mRNA expression following the successful knockdown of SIRT4. Results show that there was no significant change in mRNA expression of Sirtuin 1 (SIRT1) (A), Sirtuin 3 (SIRT3) (B), Sirtuin 5 (SIRT5) (C) or Sirtuin 6 (SIRT6) (D) mRNA expression with SIRT4 knockdown (p>0.05) (n=4).

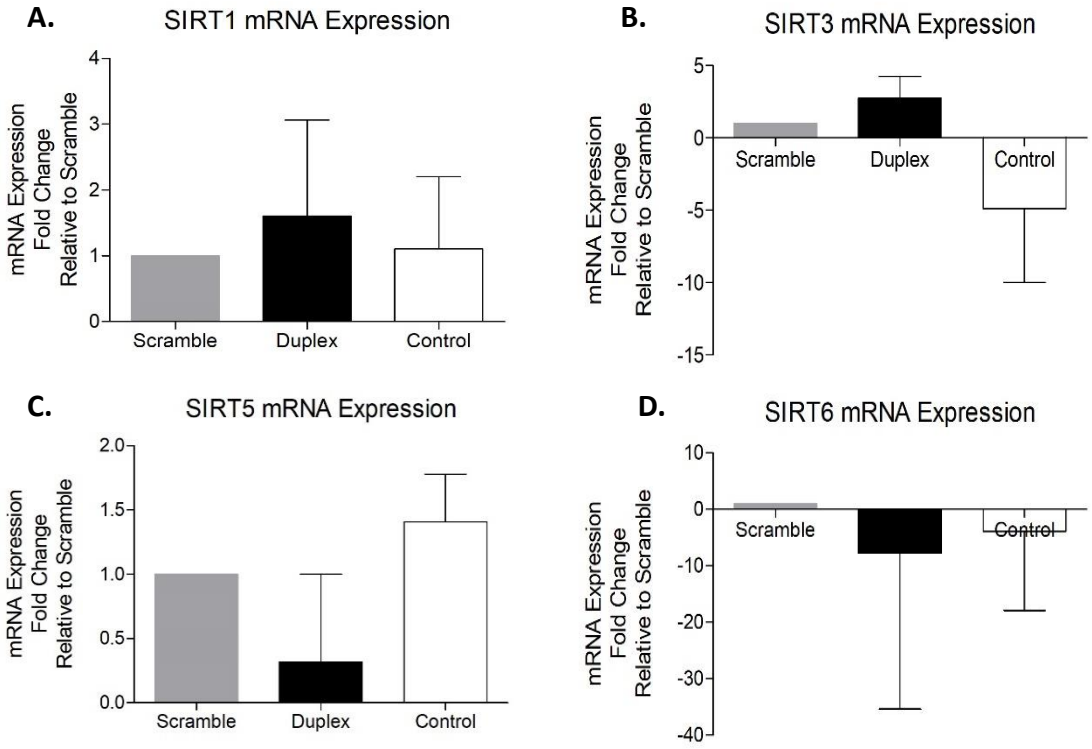

Appendix K. Figure 2. Transcriptional expression of targets in the Sirtuin family following SIRT4 siRNA knockdown

(Total SIRT1 (A), SIRT3 (B), SIRT5 (C) and SIRT6 (D) mRNA expression in Scramble siRNA (75nM), SIRT4 Duplex (75nM) siRNA, Control HSM myotubes quantified by RT-qPCR (n=4). Gene expression was normalised against GAPdh mRNA expression of same sample. Data are expressed as mean ±SD)

Transcriptional Expression of Markers Associated with Mitochondrial Biogenesis

PGC-1α

PGC-1α, a stimulator of mitochondrial biogenesis, was assessed for mRNA expression following SIRT4 knockdown using RT-qPCR. There was no significant change in the mRNA expression of PPARG coactivator-1 alpha (PGC-1α) with SIRT4 siRNA knockdown (75nM) (p>0.05) (n=3).

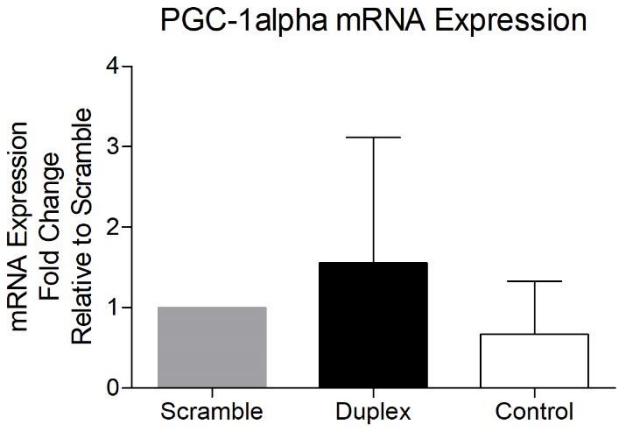

Appendix K. Figure 3. Transcriptional expression PGC-1α following SIRT4 siRNA knockdown

(Total PGC-1α mRNA expression in Scramble siRNA (75nM), SIRT4 Duplex (75nM) siRNA and Control HSM myotubes quantified by RT-qPCR (n=3). Gene expression was normalised against GAPdh mRNA expression of same sample. Data are expressed as mean ±SD)

Transcriptional Expression of Markers Associated with Mitochondrial Fusion

OPA1

OPA1, optic atrophy 1, a marker of mitochondrial fusion was analysed for mRNA expression following SIRT4 knockdown using RT-qPCR. There was no significant change in the mRNA expression of Optic atrophy 1 (OPA1) with SIRT4 siRNA knockdown (75nM) (p>0.05) (n=4).

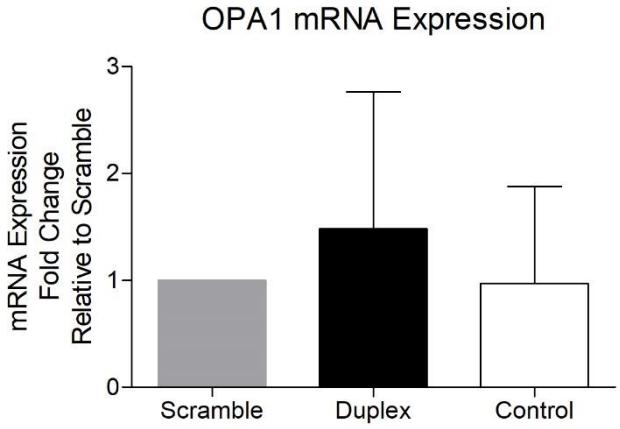

Appendix K. Figure 4. Transcriptional expression OPA1 following SIRT4 siRNA knockdown

(Total OPA1 mRNA expression in Scramble siRNA (75nM), SIRT4 Duplex (75nM) siRNA and Control HSM myotubes quantified by RT-qPCR (n=4). Gene expression was normalised against GAPdh mRNA expression of same sample. Data are expressed as mean ±SD)

Mfn1 & Mfn2

Mitofusin-1 and mitofusin-2, markers of mitochondrial fusion, were analysed for mRNA expression following SIRT4 knockdown. There was no significant change in the mRNA expression of Mitofusin-1 (Mfn1) (A) and Mitofusin-2 (Mfn2) (B) with SIRT4 siRNA knockdown (75nM) (p>0.05) (n=4).

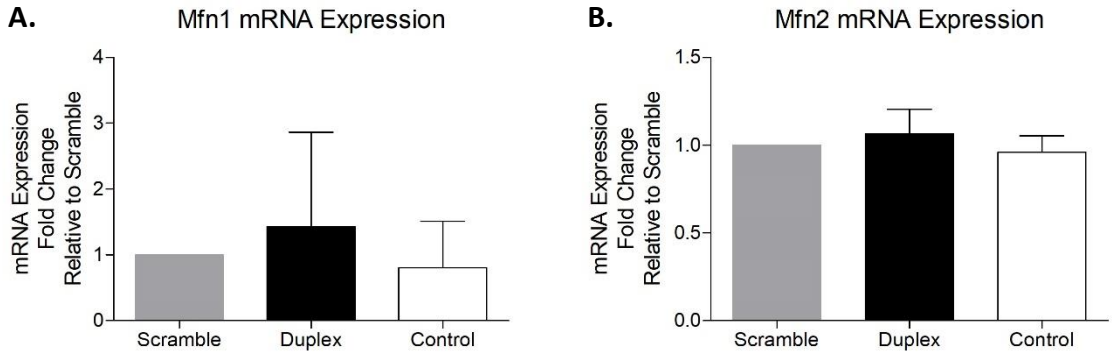

Appendix K. Figure 5. Transcriptional expression of Mfn1 & Mfn2 following SIRT4 siRNA knockdown

(Total Mfn1 (A) and Mfn2 (B) mRNA expression in Scramble siRNA (75nM), SIRT4 Duplex (75nM) siRNA and Control HSM myotubes quantified by RT-qPCR (n=4). Gene expression was normalised against GAPdh mRNA expression of same sample. Data are expressed as mean ±SD)

OMA1 & YME1L

Regulators of OPA1 expression, OMA1, metalloendopeptidase OMA1 and YME1L, ATP-dependent zinc metalloprotease YME1L, were measured for mRNA expression following SIRT4 knockdown. There was no significant change in the mRNA expression of metalloendopetidase OMA1 (OMA1) (A) and ATP-dependent metalloprotease (YME1L) (B) with SIRT4 siRNA knockdown (75nM) (p>0.05) (n=4).

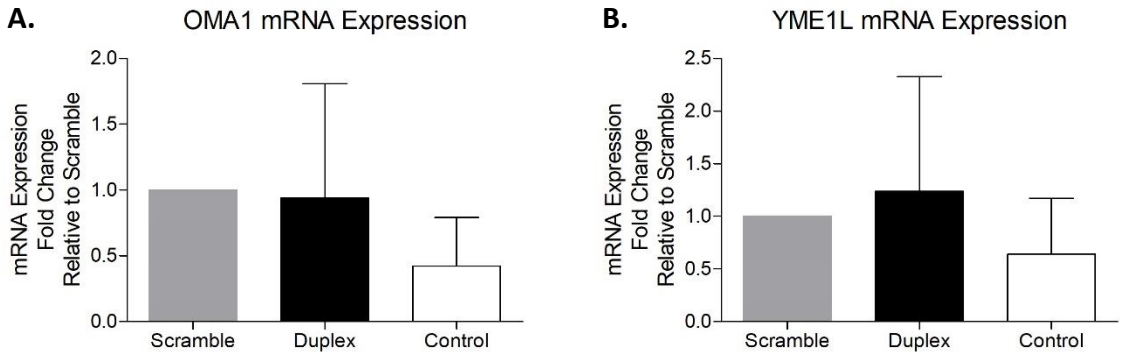

Appendix K. Figure 6. Transcriptional expression of OMA1 & YME1L following SIRT4 siRNA knockdown

(Total OMA1 (A) and YME1L (B) mRNA expression in Scramble siRNA (75nM), SIRT4 Duplex (75nM) siRNA and Control HSM myotubes quantified by RT-qPCR (n=4). Gene expression was normalised against GAPdh mRNA expression of same sample. Data are expressed as mean ±SD)

Transcriptional Expression of Markers Associated with Mitochondrial Fission

Drp1 & Fis1

Regulators of mitochondrial fission, dynamin related protein 1 (Drp1) and mitochondrial fission protein 1 (Fis1) were analysed for mRNA expression following SIRT4 knockdown. There was no significant change in the mRNA expression of Dynamin related protein 1 (Drp1) (A) and Mitochondrial Fission 1 (Fis1) (B) with SIRT4 siRNA knockdown (75nM) (p>0.05) (n=4).

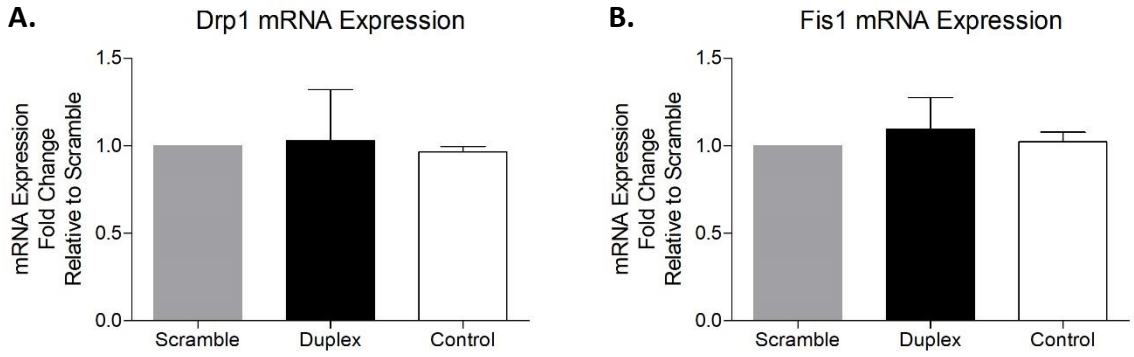

Appendix K. Figure 7. Transcriptional expression of Drp1 & Fis1 following SIRT4 siRNA knockdown

(Total Drp1 (A) and Fis1 (B) mRNA expression in Scramble siRNA (75nM), SIRT4 Duplex (75nM) siRNA and Control HSM myotubes quantified by RT-qPCR (n=4). Gene expression was normalised against GAPdh mRNA expression of same sample. Data are expressed as mean ±SD)

Mff, MiD49 & MiD51

Promoters of mitochondrial fission, Mitochondrial fission factor (Mff), Mitochondrial dynamics protein MiD49 (MiD49) and Mitochondrial dynamics protein MID51 (MiD51) were analysed for mRNA expression following SIRT4 knockdown using RT-qPCR. There was no significant change in the mRNA expression of Mitochondrial fission factor (Mff) (A), Mitochondrial dynamics protein 49 (MiD49) (B) or Mitochondrial dynamics protein 51 (MiD51) (C) with SIRT4 siRNA knockdown (75nM) (p>0.05) (n=4).

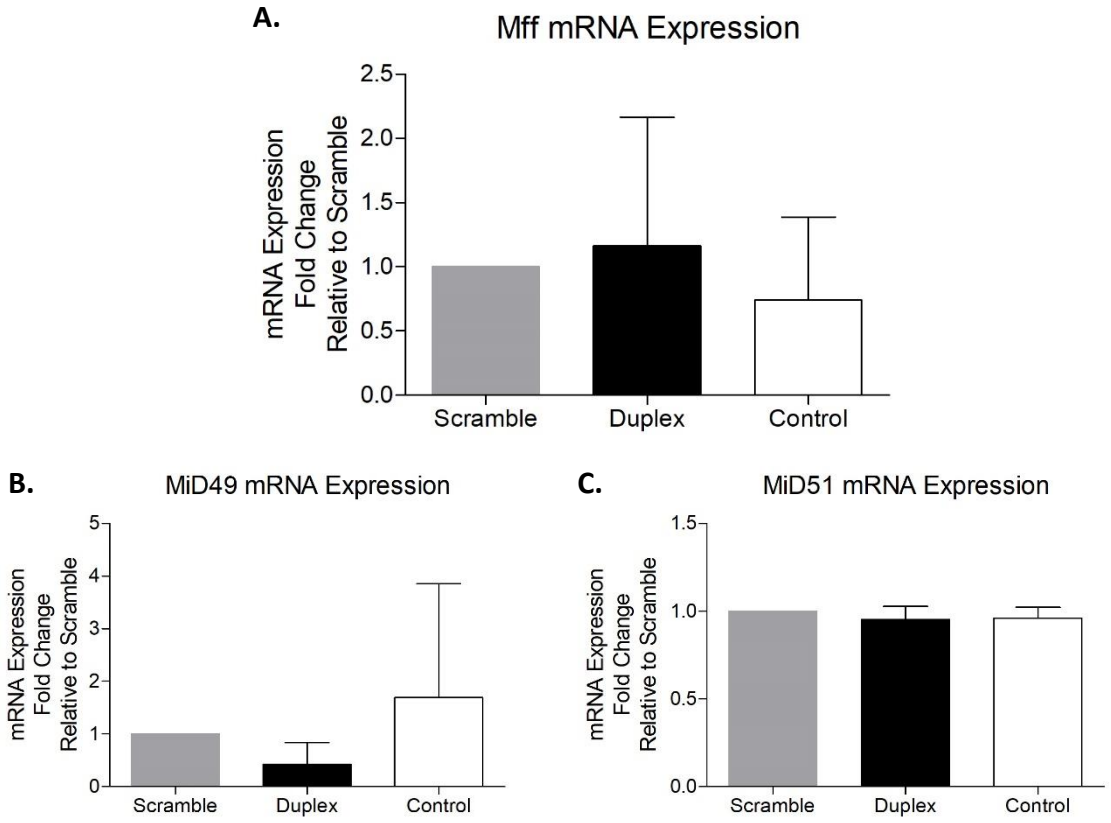

Appendix K. Figure 8. Transcriptional expression of Mff, MiD49 & MiD51 following SIRT4 siRNA knockdown

(Total Mff (A), MiD49 (B) and MiD51 (C) mRNA expression in Scramble siRNA (75nM), SIRT4 Duplex (75nM) siRNA and Control siRNA HSM myotubes quantified by RT-qPCR (n=4). Gene expression was normalised against GAPdh mRNA expression of same sample. Data are expressed as mean ±SD, *significant effect of SIRT4 knockdown, p<0.05)

Transcriptional Expression of Markers Associated with Mitophagy

PINK1 & Parkin

Markers of mitochondrial breakdown (mitophagy), PTEN-induced kinase 1 (PINK1) and Parkin were analysed for mRNA expression using RT-qPCR following SIRT4 knockdown. There was no significant change in the mRNA expression of PTEN-induced kinase 1 (PINK1) (A) and Parkin (B) with SIRT4 siRNA knockdown (75nM) (p>0.05) (n=4).

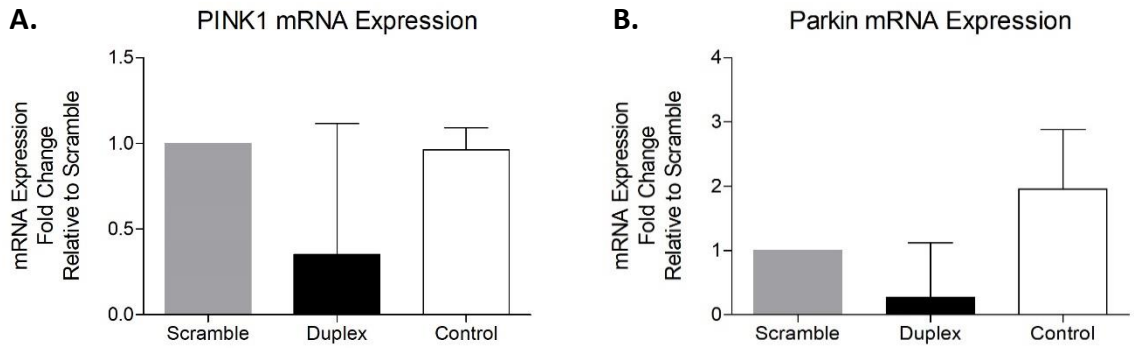

Appendix K. Figure 9. Transcriptional expression of PINK1 & Parkin following SIRT4 siRNA knockdown

(Total PINK1 (A) and Parkin (B) mRNA expression in Scramble siRNA (75nM), SIRT4 Duplex (75nM) siRNA and Control HSM myotubes quantified by RT-qPCR (n=4). Gene expression was normalised against GAPdh mRNA expression of same sample. Data are expressed as mean ±SD)

Transcriptional Expression of Other Mitochondrial Markers

ANT1, ANT2, AMPKα1, AMPKα2, MNA, Nampt, PDHα & PDHβ

Expression of Adenine nucleotide translocase 1 and 2 (ANT1 and ANT2), the two isoforms of AMP-activated protein kinase, alpha 1 and alpha 2 (AMPKα1 and AMPKα2), malonyl coa decarboxylase (MNA), Nicotinamide phosphoribosyltransferase (Nampt) and the two isoforms of pyruvate dehydrogenase (PDHα and PDHβ) were analysed for mRNA expression following SIRT4 knockdown using RT-qPCR. There was no significant change in the mRNA expression of Adenine Nucleotide Translocator 1 (ANT1) (A), Adenine Nucleotide Translocator 2 (ANT2) (B), 5'-AMP-activated protein kinase catalytic subunit alpha-1 (AMPKα1) (C), 5'-AMP-activated protein kinase catalytic subunit alpha-2 (AMPKα2) (D), MNA (Malonyl-CoA Dehydrogenase) (E), Nicotinamide Phosphoribosyltransferase (Nampt) (F), Pyruvate Dehydrogenase-α (PDHα) (G) and Pyruvate Dehydrogenase-β (PDHβ)(H) with SIRT4 siRNA knockdown (75nM) (p>0.05) (n=4).

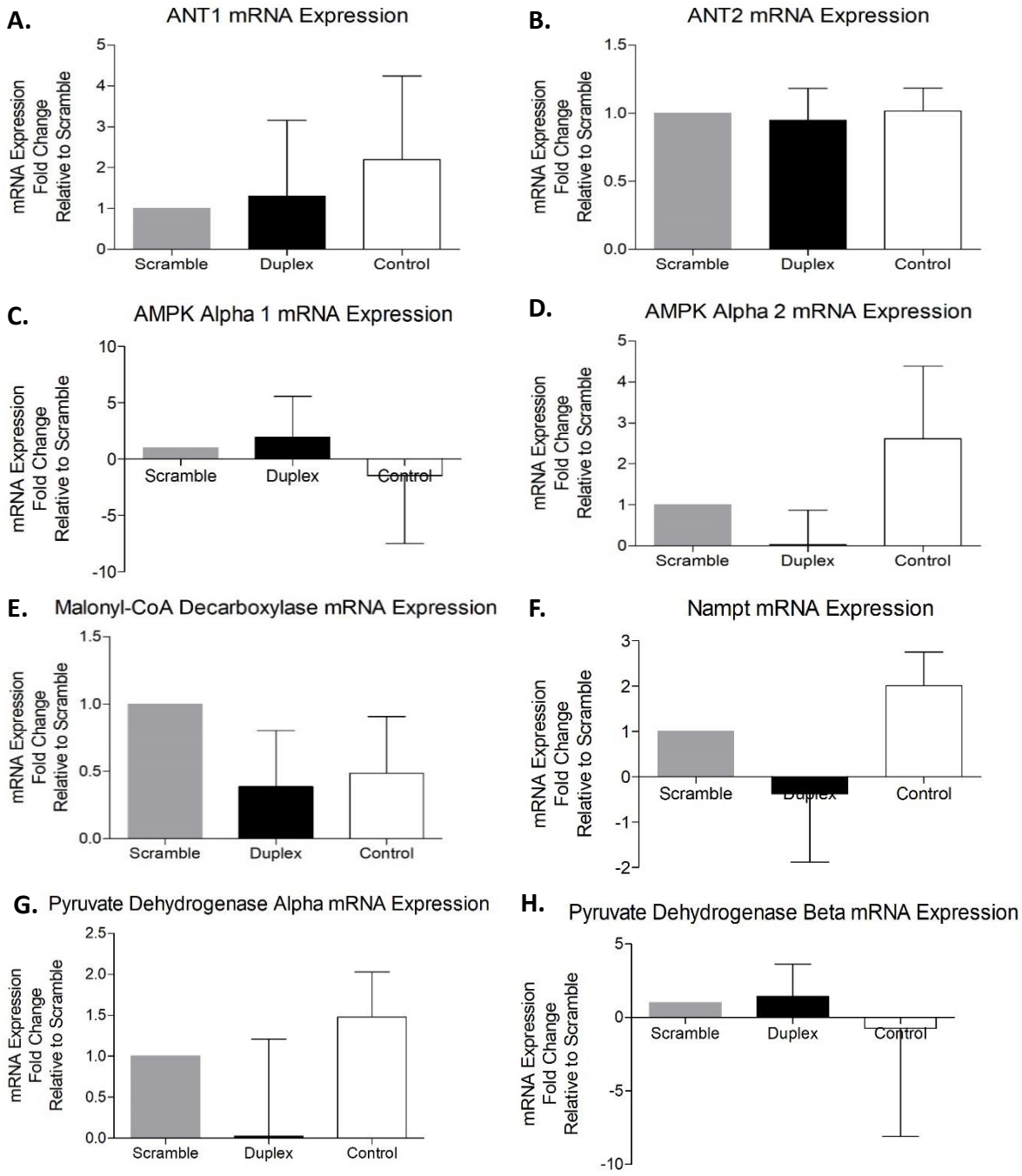

Appendix K. Figure 10. Transcriptional expression of other mitochondrial markers following SIRT4 knockdown

(Total ANT1 (A), ANT2 (B), AMPKα1 (C), AMPKα2 (D), Malonyl-CoA Decarboxylase (E), Nampt (F), Pyruvate Dehydrogenase α (G) and Pyruvate Dehydrogenase β (H) mRNA expression in Scramble siRNA (75nM), SIRT4 Duplex (75nM) siRNA and Control HSM myotubes quantified by RT-qPCR (*n*=4). Gene expression was normalised against GAPdh mRNA expression of same sample. Data are expressed as mean ±SD)

Transcriptional Expression of Other Markers Relating to Cellular Metabolism

CD38, IGF1 & mTOR

Expression of cyclic ADP ribose hydrolase (CD38), insulin-like growth factor 1 (IGF1) and mechanistic target of rapamycin (mTOR) mRNA expression were analysed following SIRT4 knockdown using RT-qPCR. There was no significant change in mRNA expression of Cluster Differentiation 38 (CD38) (A), Insulin-like Growth Factor-1 (IGF-1) (B) or mechanistic target of rapamycin (mTOR) (C) (p>0.05) (n=3).

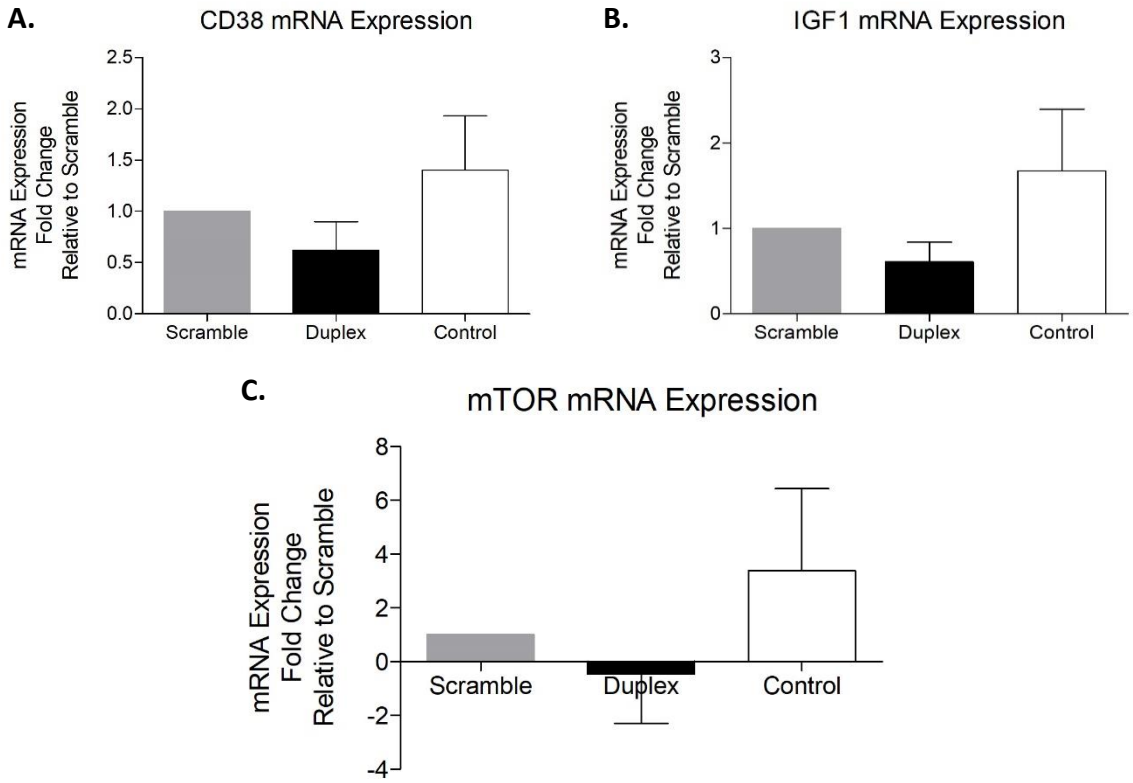

Appendix K. Figure 11. Expression of other markers relating to cellular metabolism following SIRT4 knockdown

(Total CD38 (A), IGF1 (B) and mTOR (C) mRNA expression in Scramble siRNA (75nM), SIRT4 Duplex (75nM) siRNA and Control HSM myotubes quantified by RT-qPCR (n=3). Gene expression was normalised against GAPdh mRNA expression of same sample. Data are expressed as mean ±SD, *significant effect of SIRT4 knockdown, p<0.05)

Appendix L - SIRT4 siRNA knockdown Protein Expression (inclusion of Scramble)

Densitometry Blots – SIRT4 siRNA Knockdown Experiments

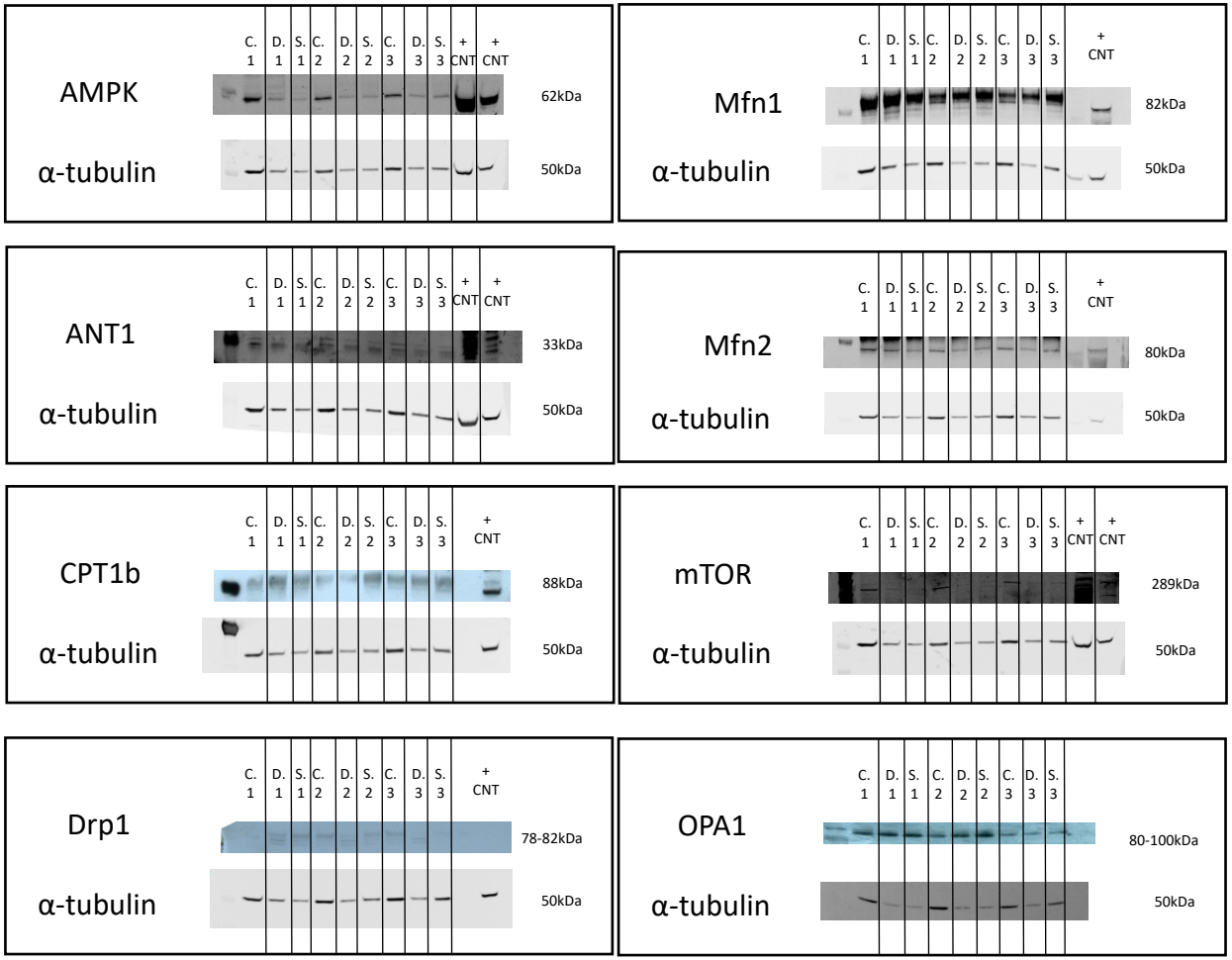

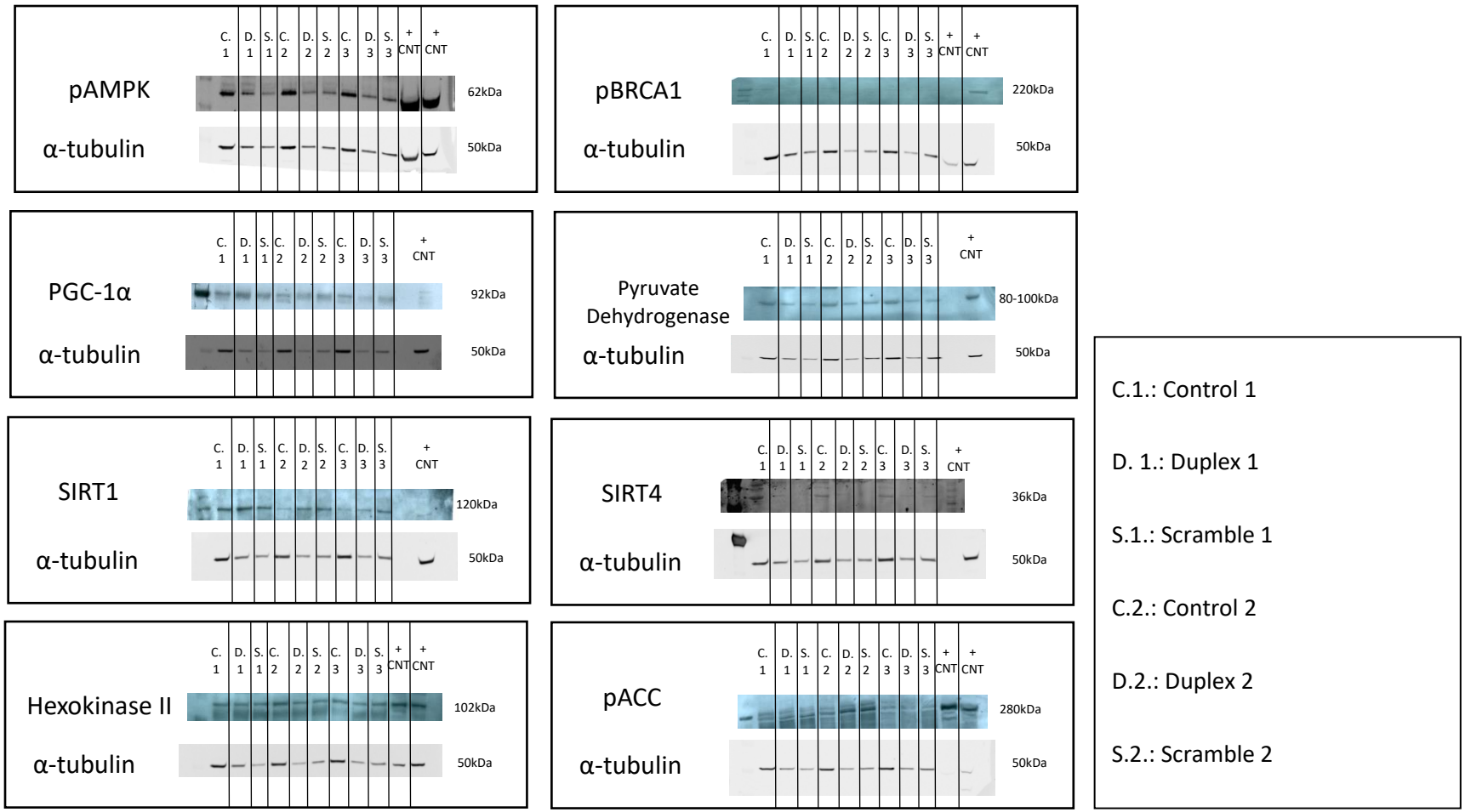

Appendix L. Figure 1. SIRT4 siRNA knockdown densitometry

Normalised to Control Sample

Following knockdown, HSM myotube protein lysates were extracted and analysed for protein expression of targets relating to mitochondrial morphology and substrate metabolism using western blot. All targets analysed were normalised against a housekeeping protein of either GAPdh or α-Tubulin and subsequently presented relative to the control sample (*n*=4).

Expression of Markers Associated with Mitochondrial Biogenesis

PGC-1α

PGC-1α, a marker of mitochondrial biogenesis, was analysed for protein expression following the knockdown of SIRT4. Results indicate a significant increase in PGC-1α protein expression in both the Duplex siRNA (75nM) and the Scramble siRNA (75nM) ($p>0.005$) (*n*=4).

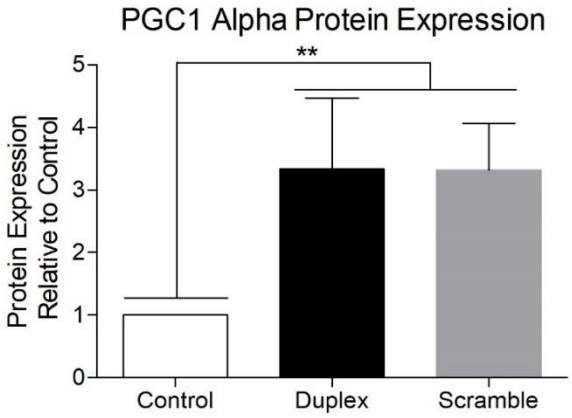

Appendix L. Figure 2. Protein expression of markers relating to biogenesis relative to control following SIRT4 knockdown

(PGC-1α protein expression in control, SIRT4 Duplex (75nM) siRNA and Scramble (75nM) siRNA HSM myotubes quantified by western blot (*n*=4). Protein expression was normalised against α-tubulin protein expression of same sample. Data are expressed as mean ±SD, **significant effect of treatment, $p<0.005$)

Expression of Markers Associated with Mitochondrial Fusion

OPA1

OPA1, a marker of mitochondrial fusion, was analysed for protein expression following the knockdown of SIRT4. Results indicate a significant increase in OPA1 protein expression within the Duplex siRNA (75nM) samples only (p<0.05) and not within the Scramble siRNA samples (75nM) (p>0.05) (n=4).

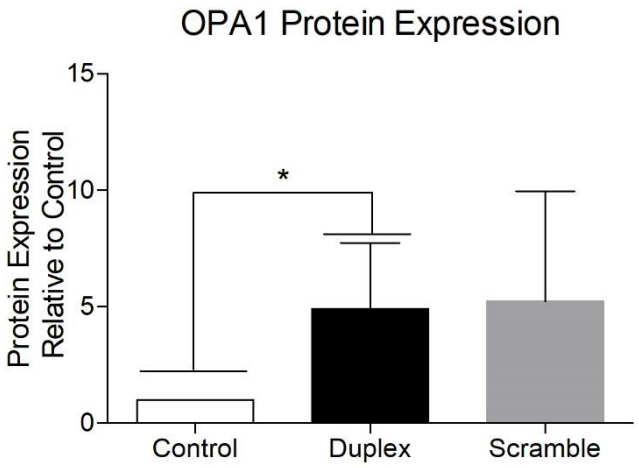

Appendix L. Figure 3. OPA1 protein expression relative to control following SIRT4 knockdown

(OPA1 protein expression in control and SIRT4 Duplex (75nM) siRNA and Scramble (75nM) siRNA HSM myotubes quantified by western blot (n=4). Protein expression was normalised against α-tubulin protein expression of same sample. Data are expressed as mean ±SD, *significant effect of treatment, p<0.05)

L-OPA1 & s-OPA1

The long and short isoforms of OPA1 were analysed for protein expression following the knockdown of SIRT4. Results indicate a significant increase in L-OPA1 (A) and s-OPA1 (B) protein expression within the Duplex siRNA (75nM) samples only (p<0.05) and not within the Scramble siRNA samples (75nM) (p>0.05) (n=4).

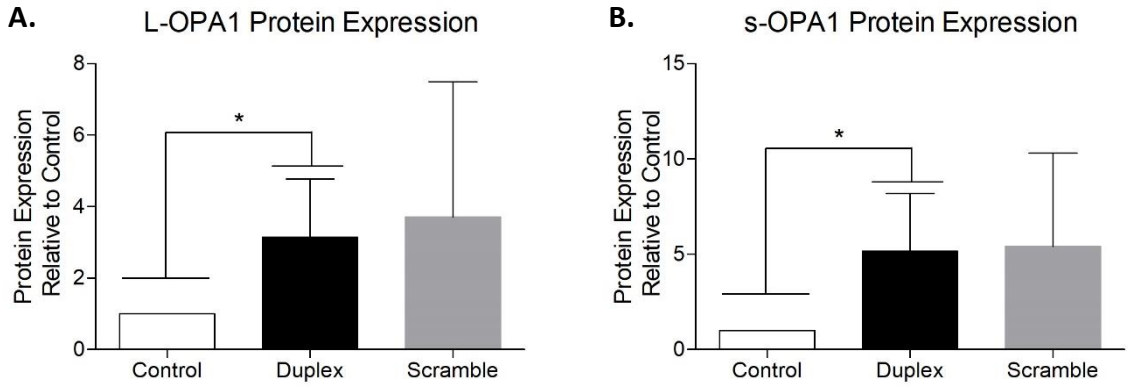

Appendix L. Figure 4. L-OPA1 & s-OPA1 protein expression relative to control following SIRT4 knockdown

(L-OPA1 (A) and s-OPA1 (B) protein expression in control, SIRT4 Duplex (75nM) siRNA and Scramble (75nM) siRNA HSM myotubes quantified by western blot (n=4). Protein expression was normalised against α-tubulin protein expression of same sample. Data are expressed as mean ±SD, *significant effect of treatment, p<0.05)

Mfn1 & Mfn2

Mitofusin-1 (Mfn1) (A) and Mitofusin-2 (B) were analysed for protein expression following the knockdown of SIRT4. Results indicate no significant change in either Mfn1 and Mfn2 protein expression within the Duplex siRNA (75nM) samples or the Scramble siRNA samples (75nM) (p>0.05) (n=3).

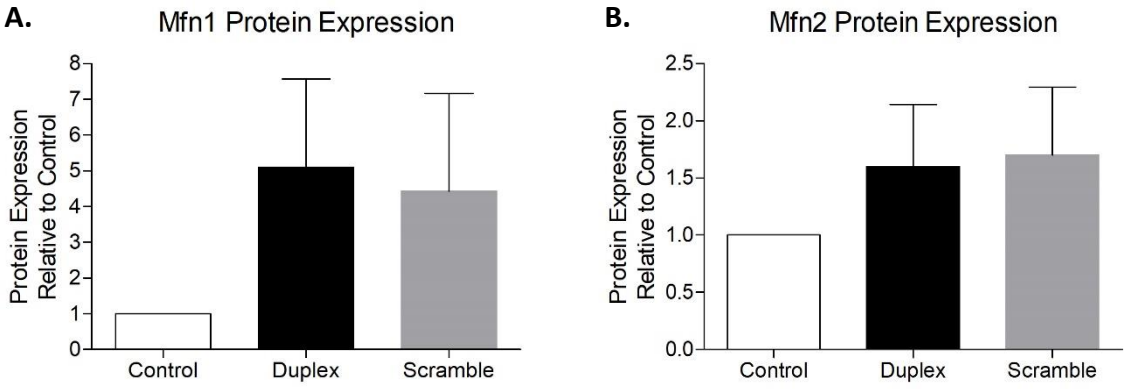

Appendix L. Figure 5. Mfn1 & Mfn2 protein expression relative to control following SIRT4 knockdown

(Mfn1 (A) and Mfn2 (B) protein expression in control, SIRT4 Duplex siRNA (75nM), and Scramble (75nM) siRNA HSM myotubes quantified by western blot (n=3). Protein expression was normalised against α-tubulin protein expression of same sample. Data are expressed as mean ±SD)

Expression of Markers Associated with Mitochondrial Fission

Drp1

The marker of mitochondrial fission, dynamin related protein 1 (Drp1), was analysed for protein expression following the knockdown of SIRT4. Results indicate no significant change in Drp1 protein expression within the Duplex siRNA (75nM) samples or the Scramble siRNA samples (75nM) (p>0.05) (n=3).

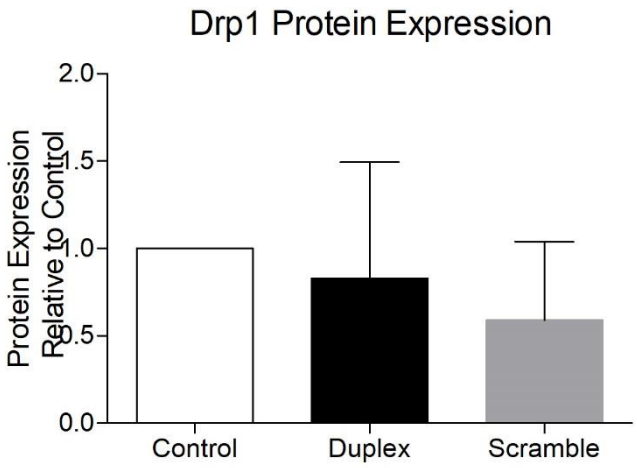

Appendix L. Figure 6. Drp1 protein expression relative to control following SIRT4 knockdown

(Drp1 protein expression in control, SIRT4 Duplex (75nM) siRNA and Scramble siRNA (75nM) HSM myotubes quantified by western blot (n=3). Protein expression was normalised against α-tubulin protein expression of same sample. Data are expressed as mean ±SD)

Ratio of Mitochondrial Fusion:Fission

In order to assess for the balance between mitochondrial fusion and fission within the Duplex SIRT4 siRNA (75nM) or the Scramble siRNA (75nM), protein expression of mitochondrial fusion marker, OPA1 was controlled against protein expression of mitochondrial fission marker, Drp1.

OPA1:Drp1 Ratio

There was a significant increase in OPA1:Drp1 ratio within both the SIRT4 duplex siRNA (75nM) and Scramble siRNA (75nM) protein samples. This result indicates that with SIRT4 knockdown we have a possible decrease in Drp1 mediated mitochondrial fission and an increase in OPA1 mediated mitochondrial fusion leading to a possible increase in mitochondrial tubulation (*n*=3).

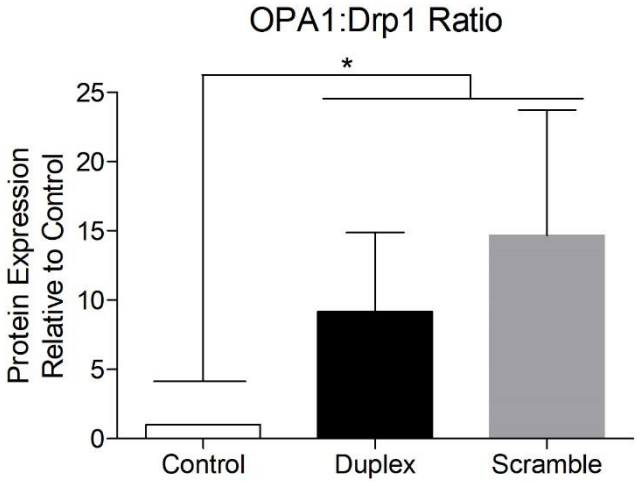

Appendix L. Figure 7. OPA1:Drp1 Ratio relative to control following SIRT4 knockdown

(OPA1:Drp1 protein expression in control, SIRT4 Duplex (75nM) siRNA and Scramble (75nM) siRNA HSM myotubes quantified by western blot. OPA1, optic atrophy 1 was controlled against Drp1, dynamin related protein 1 protein expression (*n*=3). Both OPA1 and Drp1 protein expression were firstly normalised to their respective loading control (GAPdh). Data are expressed as mean ±SD, * significant effect of time, $p<0.05$)

Expression of Other Mitochondrial Markers Relating to Fatty Acid Metabolism

pAMPK & AMPK

Phosphorylated AMP-activated protein kinase (pAMPK) (A) and AMP-activated protein kinase (AMPK) (B) were analysed for protein expression following the knockdown of SIRT4. Results indicate a significant decrease in pAMPK and AMPK protein expression within the Duplex siRNA (75nM) samples (p>0.05) but not the Scramble siRNA samples (75nM) (p>0.05) (n=3).

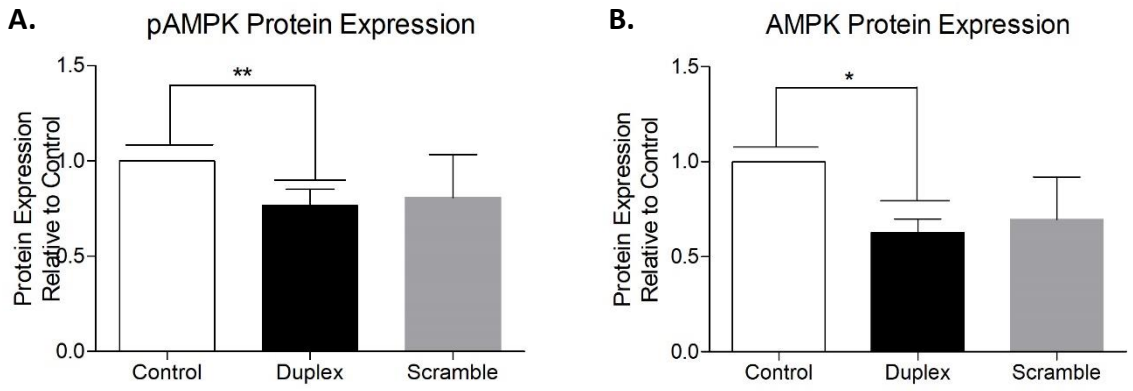

Appendix L. Figure 8. pAMPK & AMPK protein expression relative to control following SIRT4 knockdown

(pAMPK (A) and AMPK (B) protein expression in control, SIRT4 Duplex (75nM) siRNA and Scramble siRNA (75nM) HSM myotubes quantified by western blot (n=3). Protein expression was normalised against α-tubulin protein expression of same sample. Data are expressed as mean ±SD, *significant effect of treatment, p<0.05, **significant treatment)

pAMPK:AMPK

Phospho-AMPK protein expression was controlled against AMPK protein expression to assess to see if there is an increase in AMPK activity with SIRT4 knockdown. Results indicate there is no significant change in AMPK activity with knockdown, either within the SIRT4 duplex siRNA (75nM) group or the scramble siRNA (75nM) group (p>0.05) (n=3).

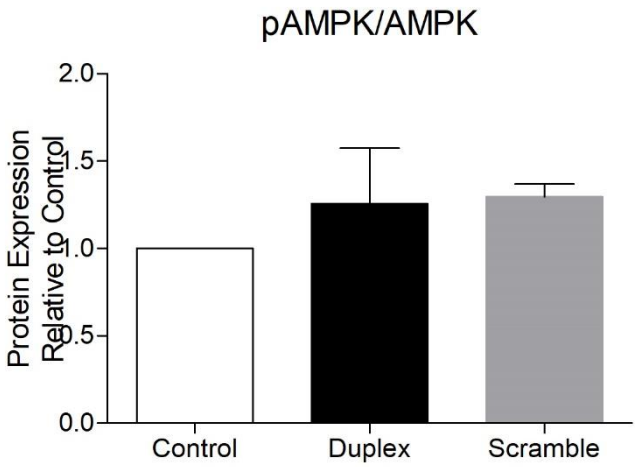

Appendix L. Figure 9. pAMPK:AMPK protein expression relative to control following SIRT4 knockdown

(pAMPK protein expression relative to AMPK protein expression in control, SIRT4 Duplex (75nM) siRNA and Scramble (75nM) siRNA HSM myotubes quantified by western blot (n=3). Protein expression was normalised against α-tubulin protein expression of same sample. Data are expressed as mean ±SD)

pACC

Phosphorylated Acetyl-CoA protein expression was measured using western blot following the knockdown of SIRT4. Results indicate a significant increase in pACC protein expression within the Duplex siRNA (75nM) samples (p<0.05) but not the Scramble siRNA samples (75nM) (p>0.05) (n=3). These results indicate a possible increase in free fatty acid oxidation with SIRT4 knockdown.

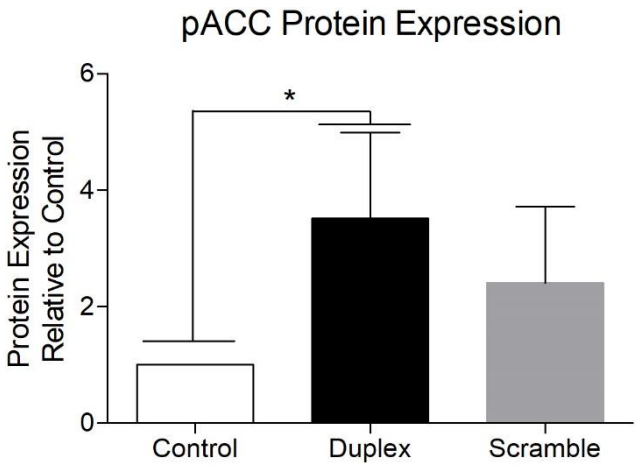

Appendix L. Figure 10. pACC protein expression relative to control following SIRT4 knockdown

(pACC protein expression in control, SIRT4 Duplex (75nM) siRNA and Scramble (75nM) siRNA HSM myotubes quantified by western blot (n=3). Protein expression was normalised against α-tubulin protein expression of same sample. Data are expressed as mean ±SD, *significant effect of treatment, p<0.05)

ANT1 & CPT1b

Adenine Nucleotide Translocator 1 (ANT1) (A) and Carnitine Palmitoyltransferase 1b (CPT1b) (B) were analysed for protein expression following the knockdown of SIRT4. Results indicate a significant decrease in ANT1 within the Duplex siRNA (75nM) samples (p<0.0005) but not the Scramble siRNA samples (75nM) (p>0.05) and a significant increase in CPT1b protein expression in both the Duplex siRNA (75nM) and Scramble siRNA (75nM) samples (p<0.05) (n=3).

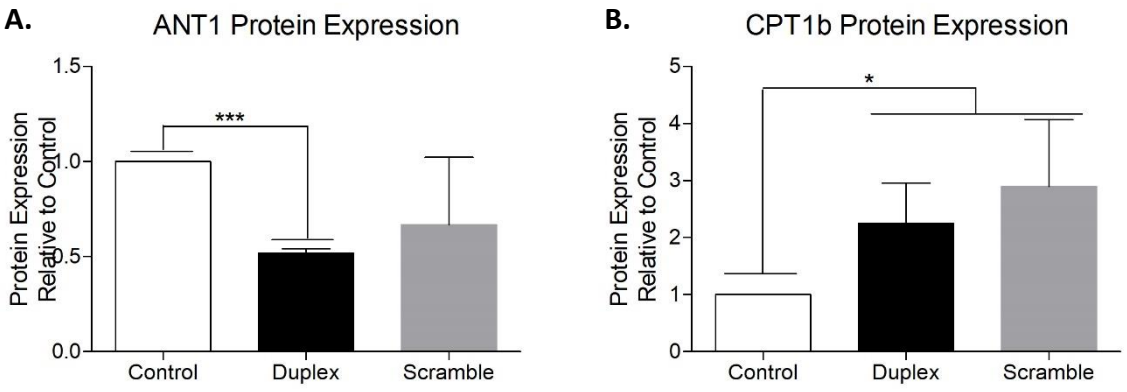

Appendix L. Figure 11. ANT1 & CPT1b protein expression relative to control following SIRT4 knockdown

(ANT1 (A) and CPT1b (B) protein expression in control, SIRT4 Duplex (75nM) siRNA and Scramble (75nM) siRNA HSM myotubes quantified by western blot (n=3). Protein expression was normalised against α-tubulin protein expression of same sample. Data are expressed as mean ±SD,***significant effect of treatment, p<0.0005,*significant effect of treatment, p<0.05)

Expression of Relating to Carbohydrate Metabolism

Hexokinase II & Pyruvate Dehydrogenase

Hexokinase II (A) and Pyruvate dehydrogenase (B) were analysed for protein expression following the knockdown of SIRT4. Results indicate a significant increase in Hexokinase II and Pyruvate dehydrogenase within the Duplex siRNA (75nM) samples (p<0.05) but not the Scramble siRNA samples (75nM) (p>0.05) (n=4).

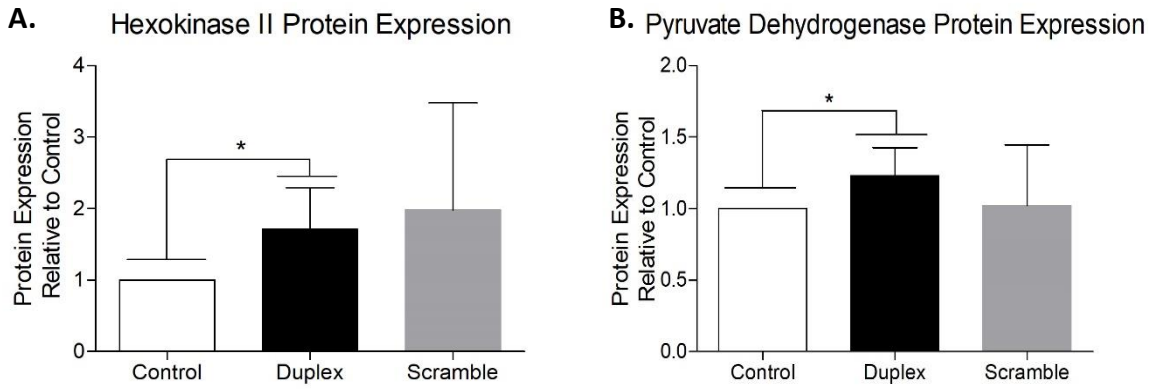

Appendix L. Figure 12. Protein expression of markers relating to carbohydrate metabolism relative to control following SIRT4 knockdown

(Hexokinase II (A) and Pyruvate Dehydrogenase (B) protein expression in control, SIRT4 Duplex (75nM) siRNA and Scramble (75nM) siRNA HSM myotubes quantified by western blot (n=4). Protein expression was normalised against α-tubulin protein expression of same sample. Data are expressed as mean ±SD, *significant effect of treatment, p<0.05)

Expression of Markers Relating to Cellular Metabolism

mTOR & SIRT1

The mechanistic target of rapamycin (mTOR) (A) and Sirtuin 1 (SIRT1) (B) were analysed for protein expression following the knockdown of SIRT4. Results indicate a significant increase in SIRT1 protein expression within the Duplex siRNA (75nM) and the Scramble siRNA samples (75nM) (p<0.05). However, there was no significant changes noted in mTOR protein expression within either the Duplex siRNA (75nM) or the Scramble siRNA (75nM) samples (p>0.05) (n=4).

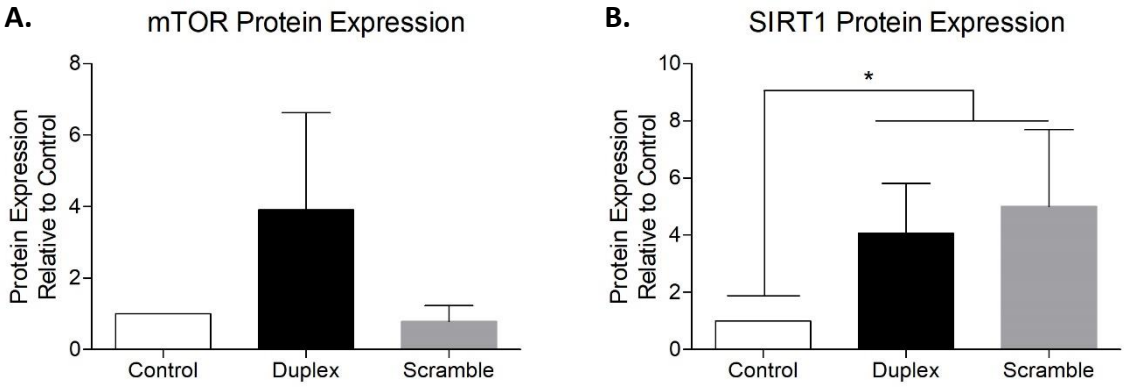

Appendix L. Figure 13. Protein expression of other markers relating to cellular metabolism relative to control following SIRT4 knockdown

(mTOR (A) and SIRT1 (B) protein expression in control, SIRT4 Duplex (75nM) siRNA and Scramble (75nM) siRNA HSM myotubes quantified by western blot (n=4). Protein expression was normalised against α-tubulin protein expression of same sample. Data are expressed as mean ±SD, *significant effect of treatment, p<0.05)

Normalised to Scramble Sample

Following knockdown, HSM myotube protein lysates were extracted and analysed for protein expression of targets relating to mitochondrial morphology and substrate metabolism using western blot. All targets analysed were normalised against a housekeeping protein of either GAPdh or α-Tubulin and subsequently presented relative to the scramble sample (*n*=4).

Expression of Markers Associated with Mitochondrial Biogenesis

PGC-1α

PGC-1α, a marker of mitochondrial biogenesis, was analysed for protein expression following the knockdown of SIRT4. Results, which are expressed relative to the Scramble siRNA (75nM), indicate a significant decrease in PGC-1α protein expression within control samples only ($p<0.005$) and not within the Duplex siRNA (75nM) samples ($p>0.05$) ($n=4$).

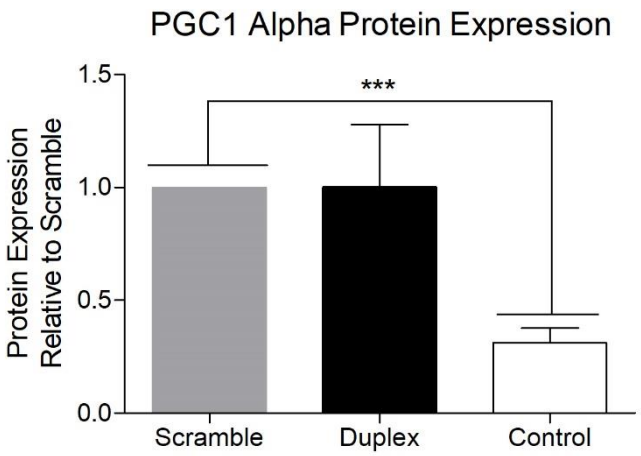

Appendix L. Figure 14. Protein expression of other markers relating to mitochondrial biogenesis relative to scramble following SIRT4 knockdown

(PGC-1α protein expression in Scramble (75nM) siRNA, SIRT4 Duplex (75nM) siRNA and Control HSM myotubes quantified by western blot (*n*=4). Protein expression was normalised against α-tubulin protein expression of same sample. Data are expressed as mean ±SD, ***significant effect of treatment, $p<0.0005$)

Expression of Markers Associated with Mitochondrial Fusion

OPA1

OPA1, a marker of mitochondrial fusion, was analysed for protein expression following the knockdown of SIRT4. Results, which are expressed relative to the Scramble siRNA (75nM), indicate a significant difference between the scramble data and the control data and the duplex data and the control data (p<0.005) (n=4).

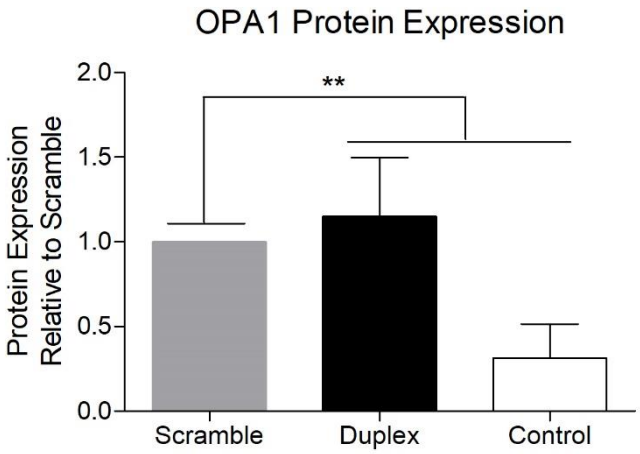

Appendix L. Figure 15. OPA1 protein expression relative to scramble following SIRT4 knockdown

(OPA1 protein expression in Scramble siRNA (75nM), SIRT4 Duplex (75nM) siRNA and Control HSM myotubes quantified by western blot (n=4). Protein expression was normalised against α-tubulin protein expression of same sample. Data are expressed as mean ±SD, **significant effect of treatment, p<0.005)

L-OPA1 & s-OPA1

The long and short isoforms of OPA1 were analysed for protein expression following the knockdown of SIRT4. Results, which are expressed relative to the Scramble siRNA (75nM), indicate a significant increase in L-OPA1 (A) within Duplex siRNA (75nM) (p<0.05) only. While results of s-OPA1 protein expression (B) indicate that there was a significant difference between the Scramble siRNA (75nM) and the control samples (p<0.005) and the Duplex siRNA (75nM) and the control samples (p<0.005) (n=4).

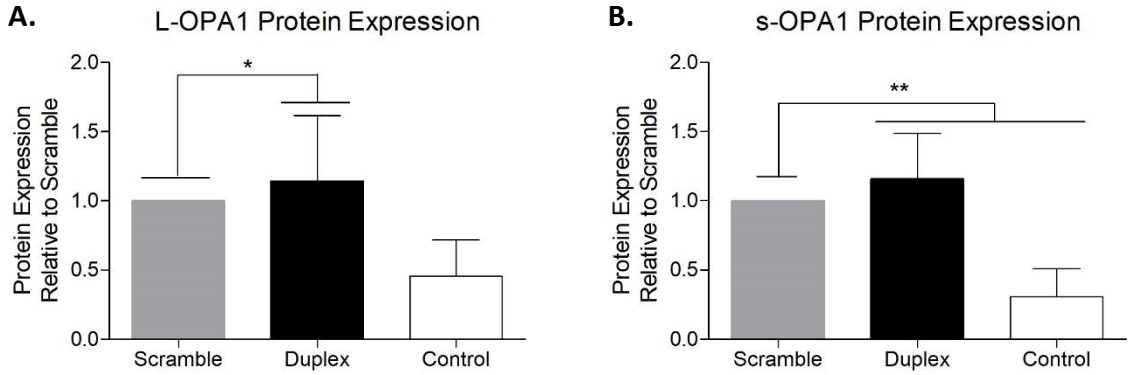

Appendix L. Figure 16. L-OPA1 & s-OPA1 protein expression relative to scramble following SIRT4 knockdown

(L-OPA1 (A) and s-OPA1 (B) protein expression in Scramble siRNA (75nM), SIRT4 Duplex (75nM) siRNA and Control HSM myotubes quantified by western blot (n=4). Protein expression was normalised against α-tubulin protein expression of same sample. Data are expressed as mean ±SD, *significant effect of treatment, p<0.05)

Mfn1 & Mfn2

Mitofusin-1 (Mfn1) (A) and mitofusin-2 (Mfn2) (B) were analysed for protein expression following the knockdown of SIRT4. Results, which are expressed relative to the Scramble siRNA (75nM), indicate a significant increase in Mfn1 protein expression within Duplex siRNA (75nM) (p<0.05) only. While results of Mfn2 protein expression indicate that there were no significant differences between groups (p>0.05) (n=3).

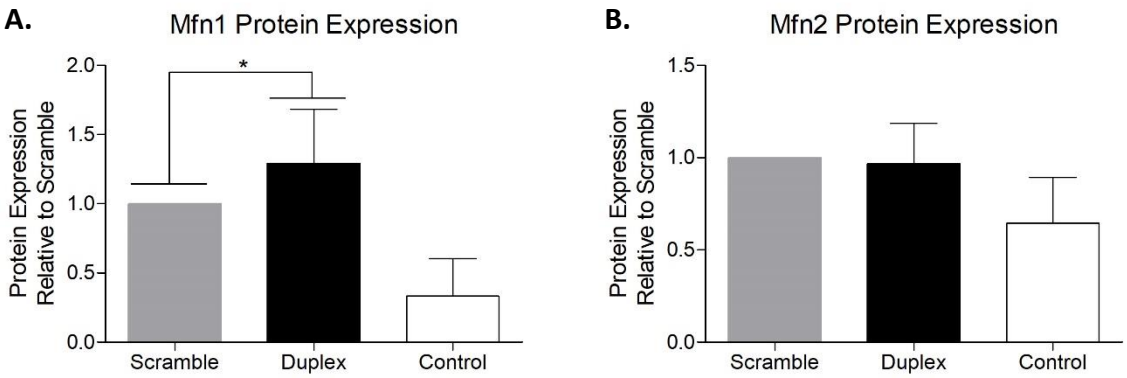

Appendix L. Figure 17. Mfn1 & Mfn2 protein expression relative to scramble following SIRT4 knockdown

(Mfn1 (A) and Mfn2 (B) protein expression in Scramble siRNA (75nM), SIRT4 Duplex siRNA (75nM), and Control HSM myotubes quantified by western blot (n=3). Protein expression was normalised against α-tubulin protein expression of same sample. Data are expressed as mean ±SD, *significant effect of treatment, p<0.05)

Expression of Markers Associated with Mitochondrial Fission

Drp1

Dynamin related protein 1 (Drp1) was analysed for protein expression following the knockdown of SIRT4. Results, which are expressed relative to the Scramble siRNA (75nM), indicate no significant differences between groups in Drp1 protein expression (p>0.05) (n=3).

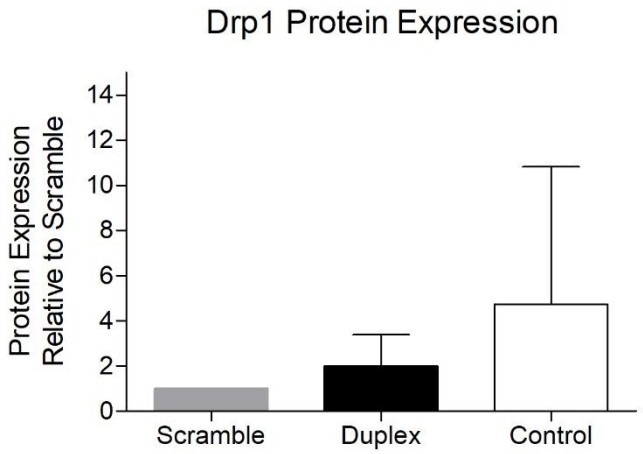

Appendix L. Figure 18. Drp1 protein expression relative to scramble following SIRT4 knockdown

(Drp1 protein expression in Scramble siRNA (75nM), SIRT4 Duplex (75nM) siRNA and Control HSM myotubes quantified by western blot (n=3). Protein expression was normalised against α-tubulin protein expression of same sample. Data are expressed as mean ±SD)

Ratio of Mitochondrial Fusion:Fission

In order to assess for the balance between mitochondrial fusion and fission within the Duplex SIRT4 siRNA (75nM) or the Scramble siRNA (75nM), protein expression of mitochondrial fusion marker, OPA1 was controlled against protein expression of mitochondrial fission marker, Drp1.

OPA1:Drp1 Ratio

There was a significant decrease in OPA1:Drp1 ratio within the control samples (p<0.0005). This decrease was significantly different to both the Scramble siRNA (75nM), to which the data presented was relative to, and the Duplex siRNA (75nM) samples. This result indicates that with SIRT4 knockdown we have a possible decrease in Drp1 mediated mitochondrial fission and an increase in OPA1 mediated mitochondrial fusion leading to a possible increase in mitochondrial tubulation (n=3).

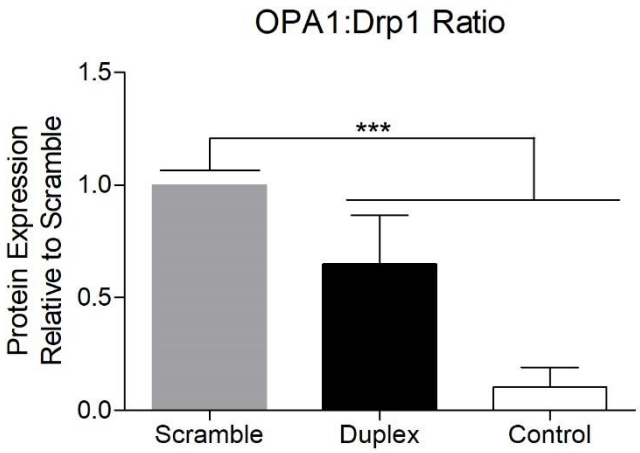

Appendix L. Figure 19. OPA1:Drp1 protein expression relative to scramble following SIRT4 knockdown

(OPA1:Drp1 protein expression in Scramble siRNA (75nM), SIRT4 Duplex (75nM) siRNA and Control HSM myotubes quantified by western blot. OPA1, optic atrophy 1 was controlled against Drp1, dynamin related protein 1 protein expression (n=3). Both OPA1 and Drp1 protein expression were firstly normalised to their respective loading control (GAPdh). Data are expressed as mean ±SD, *** significant effect of time, p<0.0005)

Expression of Other Mitochondrial Markers Relating to Fatty Acid Metabolism

pAMPK & AMPK

Phosphorylated AMP-activated protein kinase (pAMPK) (A) and AMP-activated protein kinase (B) protein expression were analysed following the knockdown of SIRT4. Results, which are expressed relative to the Scramble siRNA (75nM), indicate a significant increase in pAMPK protein expression within the control samples (p<0.05) only. While results of AMPK protein expression indicate that there were no significant differences between groups (p>0.05) (n=3).

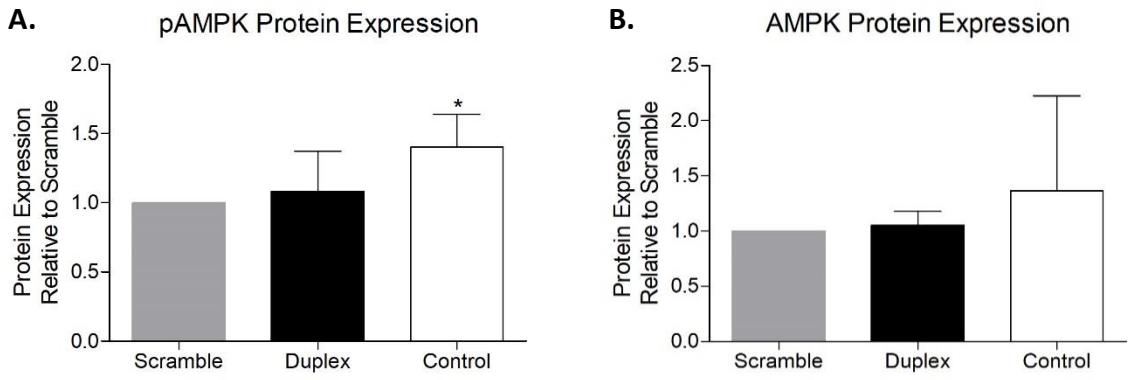

Appendix L. Figure 20. pAMPK & AMPK protein expression relative to scramble following SIRT4 knockdown

(pAMPK (A) and AMPK (B) protein expression in Scramble siRNA (75nM), SIRT4 Duplex (75nM) siRNA and Control HSM myotubes quantified by western blot (n=3). Protein expression was normalised against α-tubulin protein expression of same sample. Data are expressed as mean ±SD, *significant effect of treatment, p<0.05)

pAMPK:AMPK

Phospho-AMPK protein expression was controlled against AMPK protein expression to assess to see if there is an increase in AMPK activity with SIRT4 knockdown. Results, which are expressed relative to the Scramble siRNA (75nM), indicate there is no significant change in AMPK activity with knockdown, either within the SIRT4 duplex siRNA (75nM) group or the control samples (p>0.05) (n=3).

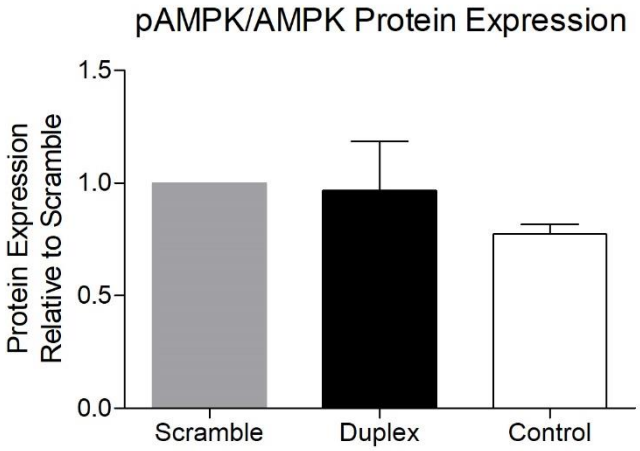

Appendix L. Figure 21. pAMPK:AMPK protein expression relative to scramble following SIRT4 knockdown

(pAMPK protein expression relative to AMPK protein expression in Scramble siRNA (75nM), SIRT4 Duplex (75nM) siRNA and Control HSM myotubes quantified by western blot (n=3). Protein expression was normalised against α-tubulin protein expression of same sample. Data are expressed as mean ±SD)

pACC

Phosphorylated Acetyl-CoA protein expression was measured using western blot following the knockdown of SIRT4. Results, which are expressed relative to Scramble siRNA (75nM), indicate a significant decrease in pACC protein expression within the control samples (p<0.05). No significant difference was noted within the Duplex siRNA (75nM) samples (p>0.05) (n=3).

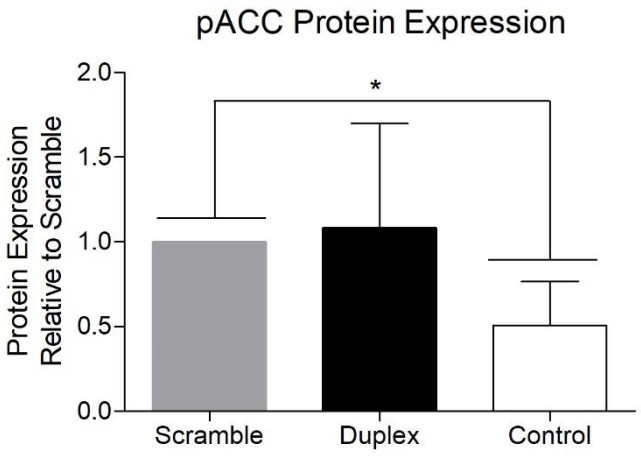

Appendix L. Figure 22. pACC protein expression relative to scramble following SIRT4 knockdown

(pACC protein expression in Scramble siRNA (75nM), SIRT4 Duplex (75nM) siRNA and control HSM myotubes quantified by western blot (n=3). Protein expression was normalised against α-tubulin protein expression of same sample. Data are expressed as mean ±SD, *significant effect of treatment, p<0.05)

ANT1 & CPT1b

Adenine Nucleotide Translocator 1 (ANT1) (A) and Carnitine Palmitoyltransferase 1B (CPT1b) (B) protein expression were analysed following the knockdown of SIRT4. Results, which are expressed relative to the Scramble siRNA (75nM), indicate no significant changes in ANT1 protein expression in either the Duplex siRNA (75nM) or control samples (p>0.05). While there was a noted decrease in CPT1b protein expression within the control samples relative to the Scramble siRNA (75nM) and the Duplex siRNA (75nM) (p<0.005) (n=3).

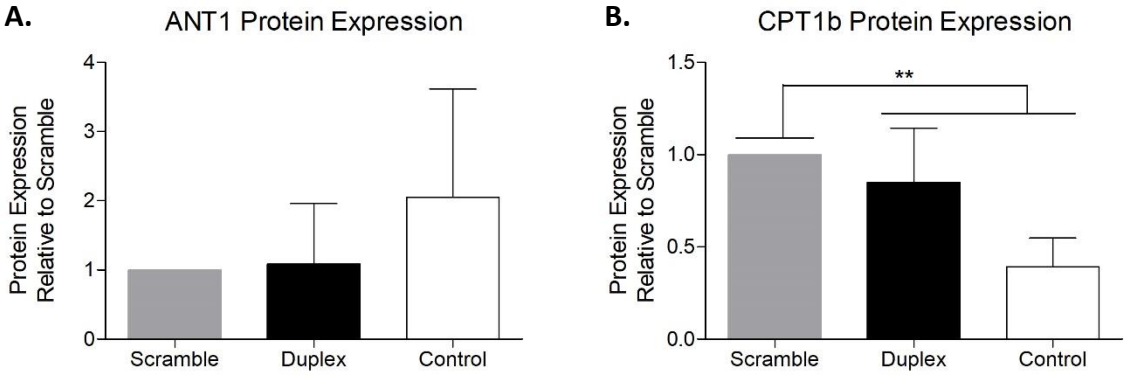

Appendix L. Figure 23. ANT1 & CPT1b protein expression relative to scramble following SIRT4 knockdown

(ANT1 (A) and CPT1b (B) protein expression in Scramble siRNA (75nM), SIRT4 Duplex (75nM) siRNA and Control HSM myotubes quantified by western blot (n=3). Protein expression was normalised against α-tubulin protein expression of same sample. Data are expressed as mean ±SD,**significant effect of treatment, p<0.005)

Expression of Markers Relating to Carbohydrate Metabolism

Hexokinase II & Pyruvate Dehydrogenase

Hexokinase II (A) and Pyruvate dehydrogenase (B) protein expression were analysed following the knockdown of SIRT4. Results, which are expressed relative to the Scramble siRNA (75nM), indicate no significant changes in Hexokinase II or Pyruvate dehydrogenase protein expression in either the Duplex siRNA (75nM) or control samples (p>0.05) (n=4).

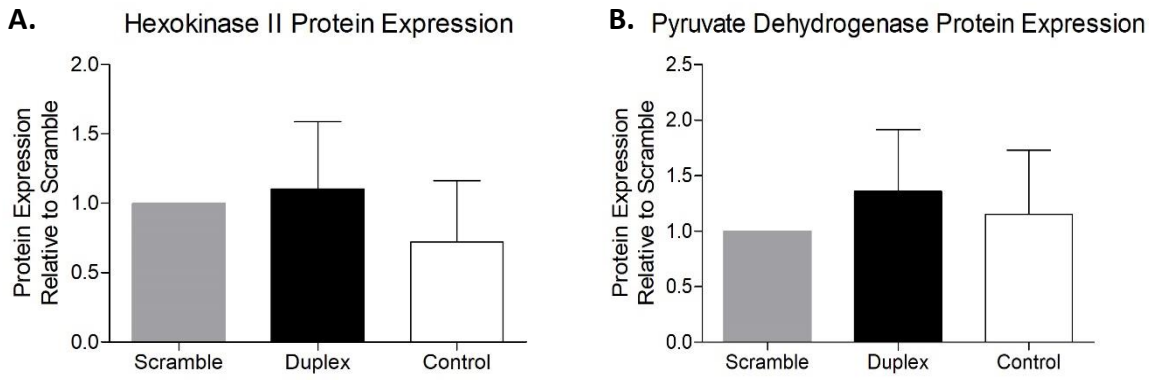

Appendix L. Figure 24. Protein expression of markers relating to carbohydrate metabolism

(Hexokinase II (A) and Pyruvate Dehydrogenase (B) protein expression in Scramble siRNA (75nM), SIRT4 Duplex (75nM) siRNA and Control HSM myotubes quantified by western blot (n=4). Protein expression was normalised against α-tubulin protein expression of same sample. Data are expressed as mean ±SD)

Expression of Markers Relating to Cellular Metabolism

mTOR & SIRT1

Protein expression of the mechanistic target of rapamycin (mTOR) (A) and Sirtuin 1 (SIRT1) (B) were analysed following the knockdown of SIRT4. Results, which are expressed relative to the Scramble siRNA (75nM), indicate no significant changes in mTOR protein expression in either the Duplex siRNA (75nM) or control samples (p>0.05) (n=4). However, there was a significant decrease in SIRT1 protein expression in the control samples relative to both the Scramble siRNA (75nM) and the Duplex siRNA (75nM) (p<0.005) (n=4).

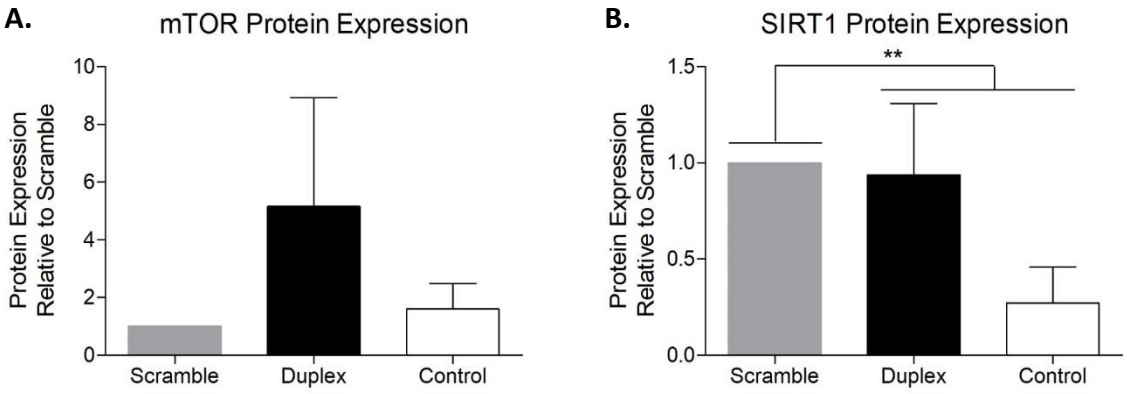

Appendix L. Figure 25. Protein expression of other markers relating to cellular metabolism

(mTOR (A) and SIRT1 (B) protein expression in Scramble siRNA (75nM), SIRT4 Duplex (75nM) siRNA and control HSM myotubes quantified by western blot (n=4). Protein expression was normalised against α-tubulin protein expression of same sample. Data are expressed as mean ±SD, **significant effect of treatment, p<0.005)

Appendix M - High-Resolution Respirometry (additional points of interest) SIRT4 siRNA knockdown

Membrane Integrity

The integrity of the outer mitochondrial membrane was assessed with the addition of 10mM Cytochrome C in the FA SUIT following the measurement of ADP stimulated respiration. There was no significant change in the level of respiration after the addition of cytochrome C, although it did increase (to be expected with the application of transfection reagent) ensuring the permeabilization did not compromise the integrity of the outer mitochondrial membrane (p>0.05) (n=4).

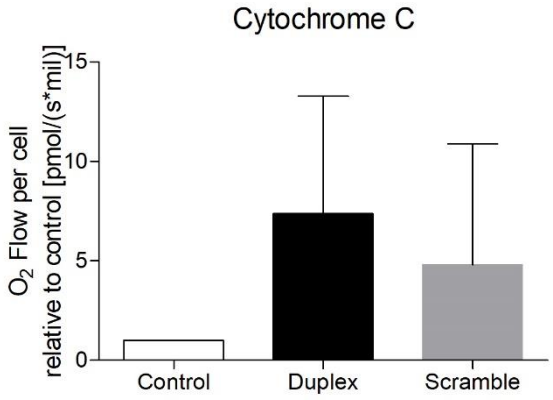

Appendix M. Figure 1. Respiration following cytochrome C with SIRT4 knockdown relative to control

(Membrane integrity as measured through addition of cytochrome C in control, SIRT4 Duplex (75nM) and Scramble (75nM) siRNA HSM myotubes quantified by HRR (n=4). Oxygen flow was normalised to cell number of the same sample. Data are expressed as mean ±SD)

Octanoylcarnitine

There was a slight, yet insignificant increase in respiration with SIRT4 knockdown (duplex) and scramble following the addition of the medium chain fatty acid, octanoylcarnitine (p>0.05) (n=4).

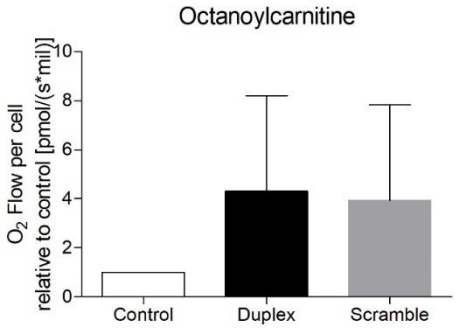

Appendix M. Figure 2. Respiration following octanoylcarnitine with SIRT4 knockdown relative to control

(Respiration following addition of medium chain fatty acid, octanoylcarnitine, control, SIRT4 Duplex (75nM) and Scramble (75nM) siRNA HSM myotubes quantified by HRR (n=4). Oxygen flow was normalised to cell number of the same sample. Data are expressed as mean ±SD)

Uncoupling of the Electron Transport Chain (ETS) (FCCP)

With the addition of the uncoupler, Carbonyl cyanide-p-trifluoromethoxyphenylhydrazone (FCCP), we measured complex I linked electron transport system (ETC) capacity. There was no significant decrease in complex I linked ETS with SIRT4 knockdown or scramble (p>0.05) (n=4).

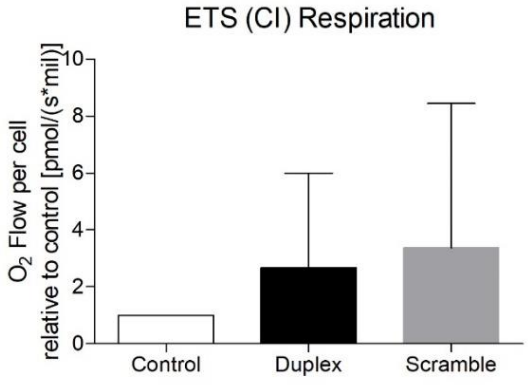

Appendix M. Figure 3. ETS (CI) respiration following SIRT4 knockdown relative to control

(ETS (CI) mediated respiration in control, SIRT4 Duplex (75nM) and Scramble (75nM) siRNA HSM myotubes quantified by HRR (n=4). Oxygen flow was normalised to cell number of the same sample. Data are expressed as mean ±SD)

Succinate Driven Respiration (ETS)

Respiration driven by succinate for complex II following FCCP titrations is a measure of complex I and II linked ETS (maximal ETS). There was no significant change in succinate driven respiration with SIRT4 knockdown or scramble (p>0.05) (n=4).

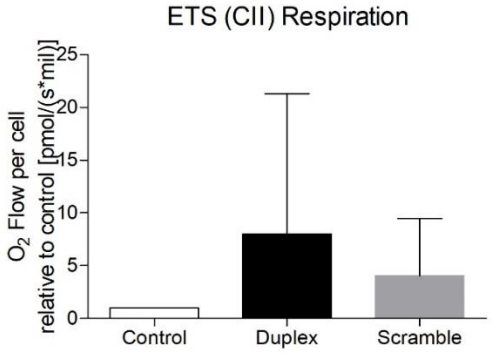

Appendix M. Figure 4. ETS (CII) respiration following SIRT4 knockdown relative to control

(ETS (CII) mediated respiration in control, SIRT4 Duplex (75nM) and Scramble (75nM) siRNA HSM myotubes quantified by HRR (n=4). Oxygen flow was normalised to cell number of the same sample. Data are expressed as mean ±SD)

Rotenone Complex I Inhibitor → Complex II Activity

Inhibition of complex I with the addition of rotenone allowed us to assess respiratory flux through complex II. There was a significant increase in complex II respiration following SIRT4 knockdown (p<0.05) but no significant change in complex II respiration within the scramble group (n=4).

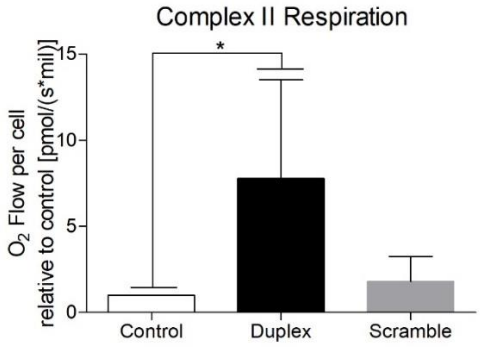

Appendix M. Figure 5. Complex II respiration following SIRT4 knockdown relative to control

(Complex II respiration in control, SIRT4 Duplex (75nM) and Scramble (75nM) siRNA HSM myotubes quantified by HRR (n=4). Oxygen flow was normalised to cell number of the same sample. Data are expressed as mean ±SD, *significant effect of SIRT4 knockdown, p<0.05)